

2014

“Clickable” glycoconjugates – a new approach to the synthesis of bioconjugates

Consulato James Cara
University of Wollongong, cjc373@uowmail.edu.au

Follow this and additional works at: <https://ro.uow.edu.au/theses>

University of Wollongong

Copyright Warning

You may print or download ONE copy of this document for the purpose of your own research or study. The University does not authorise you to copy, communicate or otherwise make available electronically to any other person any copyright material contained on this site.

You are reminded of the following: This work is copyright. Apart from any use permitted under the Copyright Act 1968, no part of this work may be reproduced by any process, nor may any other exclusive right be exercised, without the permission of the author. Copyright owners are entitled to take legal action against persons who infringe their copyright. A reproduction of material that is protected by copyright may be a copyright infringement. A court may impose penalties and award damages in relation to offences and infringements relating to copyright material.

Higher penalties may apply, and higher damages may be awarded, for offences and infringements involving the conversion of material into digital or electronic form.

Unless otherwise indicated, the views expressed in this thesis are those of the author and do not necessarily represent the views of the University of Wollongong.

Recommended Citation

Cara, Consulato James, “Clickable” glycoconjugates – a new approach to the synthesis of bioconjugates, Doctor of Philosophy thesis, School of Chemistry, University of Wollongong, 2014. <https://ro.uow.edu.au/theses/4313>

Research Online is the open access institutional repository for the University of Wollongong. For further information contact the UOW Library: research-pubs@uow.edu.au



“Clickable” Glycoconjugates – A New Approach to the Synthesis of Bioconjugates

A thesis submitted in fulfilment of the requirements

for the award of the degree

Doctor of Philosophy

By

Consulato James Cara

Bachelor of Medicinal Chemistry Advanced (Hons.)

School of Chemistry, Faculty of Science, Medicine and Health

July 2014

for Meghan

Thesis Declaration

I, Consulato James Cara, declare that the work described in this thesis, submitted in fulfilment of the requirements of the award of Doctor of Philosophy, in the School of Chemistry at the University of Wollongong is wholly my own work unless otherwise acknowledged or referenced. The research described in this thesis was completed at the University of Wollongong, and has not been submitted for any qualifications at any other academic institution.

Consulato James Cara

July 18, 2014

Table of Contents

Thesis Declaration.....	i
List of Figures	vi
List of Schemes	ix
List of Tables.....	xiii
List of Abbreviations.....	xiv
Publications Arising from this Thesis (To Date).....	xxii
Acknowledgements	xxiv
Abstract	xxv
Chapter 1 : Introduction	1
1.1 Carbohydrates – Definition and Structural Diversity	1
1.2 Roles of Carbohydrates in Biological Systems	3
1.2.1 Structural Roles of Carbohydrates	3
1.2.2 Carbohydrates in Cellular Signalling, Recognition and Growth	5
1.2.3 Carbohydrates in Energy Usage, Storage and Metabolism	8
1.3 Carbohydrates in Medicinal Chemistry	12
1.4 Carbohydrates in Nuclear Imaging.....	14
1.4.1 ¹⁸ F-Fluorodeoxyglucose ([¹⁸ F]-FDG).....	16
1.4.2 Peptide Imaging Agents.....	17
1.5 The Copper Assisted Azide-Alkyne [3 + 2] Huisgen Cycloaddition (CuAAC). ..	26
1.5.1 Background and Mechanism	26
1.5.2 Utilization of the CuAAC “Click” Reaction with Carbohydrates	28
1.5.3 Fluorine-18 Labelling of Carbohydrates utilizing the CuAAC “Click” Reaction	33
1.5.4 Fluorine-18 Labelled Glycoconjugates Synthesised using the CuAAC “Click” Reaction	35
1.5.5 Alternative Strategies for the Fluorine-18 Labelling of Glycoconjugates using the CuAAC “Click” Reaction.....	40
1.6 Project Aims.....	43

Chapter 2 : Synthesis and Functionalization of Serine, Lysine and α-Amino Linked “Clickable” Glycoconjugates.	46
2.1 Synthetic Rationale.....	46
2.2 Initial Synthetic Targets	48
2.2.1 Conjugate Criteria.....	48
2.2.2 Synthetic Approaches	50
2.3 Synthesis of <i>Glc</i> - and <i>Gal</i> -Sugar Azido Acids.....	54
2.3.1 Synthesis of 1-Azido-2,3,4-tri- <i>O</i> -acetyl- β -D-glucuronic acid (60)	54
2.3.2 Synthesis of 1-Azido-2,3,4-tri- <i>O</i> -acetyl- β -D-galacturonic acid (65)	61
2.4 Synthesis of “Clickable” Glycoconjugates	67
2.4.1 Synthesis of Sidechain-linked Derivatives (66-69)	67
2.4.2 Synthesis of Leucine, Methionine and Glutamine α -Amino linked Derivatives (70-73)	74
2.5 Synthesis of Functionalized Glycoconjugates.....	78
2.5.1 Optimisation of CuAAC “Click” Reaction Conditions	78
2.5.2 Synthesis of Functionalized Glycoconjugates (78-87)	81
2.6 Towards the Synthesis and Functionalization of “Clickable” Glycopeptides.....	85
2.6.1 Synthesis of Sugar Azido Acid-Ac.Lys-Pro-Val.NH ₂	85
 Chapter 3 : Synthesis and Functionalization of Sidechain-Linked “Clickable” Glycoconjugates	 91
3.1 Synthetic Rationale.....	91
3.2 Synthetic Approach	92
3.3 - Synthesis and Functionalization of Anomeric-linked “Clickable” Glycoconjugates	93
3.3.1 Synthesis of Key β -Azidoglycosylamine Intermediate 103	95
3.3.2 Synthesis of Boc-protected Amino Acids 108 and 109.....	102
3.3.3 Synthesis of Sidechain Carboxyl-linked “Clickable” Glycoconjugates 110 & 111	104
3.3.4 Synthesis of Functionalized Sidechain Carboxyl-linked Glycoconjugates 112 & 113	106

Chapter 4 : Synthesis and Functionalization of Thioether-linked “Clickable” Glycoconjugates	110
4.1 Synthetic Rationale.....	110
4.2 Initial Synthetic Approach.....	111
4.3 Attempted Synthesis of 6-Thioether-linked “Clickable” Glycoconjugates	113
4.3.1 Synthesis of 6-Iodo-2,3,4-tri- <i>O</i> -acetyl- β -D-glucosyl azide (117)	113
4.3.2 Synthesis of Thiol-bearing Amino Acid Boc.HCys.OtBu (120).....	116
4.3.3 Attempted Alkylation of 6-Iodo-2,3,4-tri- <i>O</i> -acetyl- β -D-glucosyl azide (117)	117
4.4 Synthesis of Anomeric Thioether-linked “Clickable” Glycoconjugate 131	121
4.4.1 Synthesis of 6-Azido-2,3,4-tri- <i>O</i> -acetyl- α -D-glucopyranosyl trichloroacetimidate (127)	122
4.4.2 Synthesis of Fmoc.HCys.OMe (130).....	125
4.4.3 Synthesis of Thioether-Linked “Clickable” Glycoconjugate 131	126
4.5 Synthesis of Thioether-linked “Clickable” Glycoconjugate 138 Using a “Click” Thiol-ene Approach.....	132
4.5.1 Synthesis of Maleimide-Sugar Azido Acid-linked Derivative 136	135
4.5.2 Thiol-ene “Click” Reaction of Maleimide-linked Derivative 136 and Fmoc.HCys.OMe (130).	138
4.6 Functionalization of Thioether-linked “Clickable” Glycoconjugate 137.....	140
 Chapter 5 : Strategies Towards the Synthesis and Functionalization of “Clickable” Neoglycopeptides.....	143
5.1 Synthetic Rationale.....	143
5.2 Initial Synthetic Strategy	148
5.2.1 Synthetic Criteria	148
5.3 Synthesis of Orthogonally-protected Glycoconjugates	152
5.3.1 Initial Pathway Towards 4-Protected Sugar Azido Acids	152
5.3.2. Improved Pathway Towards 4-Protected Sugar Azido Acids	160
5.3.3 Synthesis of 4-Orthogonally Protected Intermediate 165	166
5.3.4 Synthesis of the 3-Orthogonally Protected Intermediate 170.....	171

Chapter 6 : Conclusions and Future Directions.....	181
6.1 Conclusions	181
6.1.1 “Clickable” Glycoconjugates.....	181
6.1.2 Functionalized Neoglycopeptides.....	184
6.2 Future Directions	185
6.2.1 Improved Access to Sugar Azido Acids From Protected Derivatives.....	185
6.2.2 Extension of the Synthesis of “Clickable” Glycoconjugates to Carboxyl and Thiol-containing Peptides	186
6.2.3 Synthesis of “Clickable” Neoglycopeptides	188
6.2.4 Development and Synthesis of Radiolabelled Glycoconjugates Using the CuAAC “Click” Reaction.....	190
 Chapter 7 : Experimental.....	 194
7.1 Chemical Procedures	194
7.1.1 General Experimental	194
7.1.2 Chromatography	195
7.1.3 Nuclear Magnetic Resonance (NMR) Spectroscopy	195
7.1.4 Mass Spectrometry	196
7.1.5 Chemical and Spectral Illustrations/Calculations	197
7.2 Chapter 2 Experimental Data:	198
7.3 Chapter 3 Experimental Data:	233
7.4 Chapter 4 Experimental Data:	245
7.5 Chapter 5 Experimental Data:	264
 Chapter 8 : References.....	 283

List of Figures

Figure 1.1: Examples of non-reducing (D-fructose, A) and reducing (D-glucose, B) linear carbohydrates, which in solution cyclize to form furan (C) and pyran (D) glycosides respectively.	1
Figure 1.2: Pyran-based isomers of chemical formula $C_6H_{12}O_6$	2
Figure 1.3: Cellulose (1), xylan (2), chitin (3) and murein (4) – important polysaccharides that maintain the cellular structure of plant (A), algal (B), fungal (C) and bacterial (D) species. ^{14–16}	4
Figure 1.4: Roles of carbohydrate-bearing macromolecules in cellular signaling, recognition and growth. A: Ig binds disaccharide (Gal(α 1->3)Gal) antigens (Fab region) and requires glycosylation to bind pathogens (Fc region), B: Influenza viruses utilize carbohydrate-binding glycoproteins hemagglutinin and neuraminidase for viral entry and release. ³⁹	7
Figure 1.5: Roles of carbohydrates in cellular turnover and growth. A – Induction of phagocytosis of red blood cells (RBCs) following cleavage of neuraminic acid residues from the cell surface. B - Structure of erythropoietin, bearing heavily glycosylated chains provide structural stability. ⁴⁸	8
Figure 1.6: Carbohydrate-based therapeutic agents used as antibiotics (5 and 6), and in the treatment of influenza (7 and 8) and diabetes (9 and 10).....	12
Figure 1.7: Heparan sulphate mimetic PI-88 (11) and pentavalent conjugate vaccine 12, bearing antigens for tumour-upregulated glycoproteins (MUC-1 – Tn, TF, STn), glycolipids (Globo-H) and gangliosides (GM2), agents under evaluation for their treatment of malignancies.	13
Figure 1.8: Iodine-125 radiolabelled glycoconjugate imaging agents, based on the cyclo-RGD (14) and octreotide (15 and 16) peptide scaffolds. ^{99,101–104}	20
Figure 1.9: Fluorine-18 radiolabelled imaging agents 18 and 19 based on the cyclo-RGD and octreotide peptide scaffolds, with both agents glycosylated and labelled at lysine. ^{76,109}	22
Figure 1.10: [^{18}F]-Containing prosthetic groups utilized in the synthesis of ^{18}F -radiolabelled probes. ¹⁰⁶	23
Figure 1.11: ^{18}F -containing glycopeptides radiolabelled using 39 and the CuAAC “click” reaction. ^{139–143}	38
Figure 1.12: Threonine-linked derivatives 50 and 51, examples of “clickable” glycosylamino acids. ^{144,145}	42
Figure 2.1: Examples of sugar azido acids previously reported in the literature. ^{149–151} ..	50
Figure 2.2: Heat of formation (ΔH_f) of the α - and β - anomers of 56 and 61, calculated using ChemBio3D 11.0.....	62
Figure 2.3: The gCOSY (left) and NOESY (right) 2D 1H NMR spectral plots for 64..	66
Figure 2.4: 1H NMR spectrum of 68, highlighting the pseudo 6-membered ring formed through hydrogen bonding, inducing rigidity at the C4 position.....	72

Figure 2.5: ^1H NMR spectrum of 69, highlighting the chemical equivalence of the two protons bound to C^6 , allowing for bond rotation at the C5 position.	73
Figure 2.6: ^1H NMR spectra of leucine-based “clickable” glycoconjugates 70 and 71, highlighting the deshielded amide nitrogen and proton of the α -carbon of leucine	76
Figure 2.7: ^{13}C NMR spectrum of methionine-based “clickable” glycoconjugate 72, highlighting the shielded carbonyl signal resulting from amide bond formation.	77
Figure 2.8: ^{13}C NMR spectrum of glutamine-based “clickable” glycoconjugate 73, highlighting the shielded signal resulting from amide bond formation in comparison to the sidechain amide bond carbonyl.	78
Figure 2.9: ^1H NMR spectrum of the functionalized triazole-bearing glycoconjugate 74.	80
Figure 2.10: ^1H NMR spectrum of the functionalized glycoconjugate 86, highlighting the formation of the triazole ring.	84
Figure 2.11: Primary structure of α -melanocortin stimulating hormone (α -MSH), and N^{α} -acetyl lysine-proline-valinamide (Ac.KPV.NH ₂), a tripeptide analogue of the C-terminus of α -MSH	86
Figure 2.12: ^1H NMR spectrum of the <i>glc</i> -Ac.KPV.NH ₂ -based “clickable” glycopeptide 88, highlighting the pseudo 6-membered ring formed through hydrogen bonding, and three-bond coupling correlation.	87
Figure 2.13: 2D ^1H NMR gCOSY experiment of the <i>glc</i> -Ac.KPV.NH ₂ -based “clickable” glycopeptide 88, highlighting the pseudo 6-membered ring formed through hydrogen bonding, and three-bond coupling correlation.	88
Figure 3.1: ^1H NMR spectrum of 6-azido-1,2-isopropylidene- α -D-glucofuranose (96).97	
Figure 3.3: A: ^1H NMR spectrum of 101, highlighting signals indicating H1 and H3, B: ^{13}C NMR spectrum of 101, highlighting the downfield C1 carbon.	99
Figure 3.4: NOESY 2D ^1H NMR experiment of 101, showing weak H1/H5 correlation.	100
Figure 3.5: ^{13}C NMR spectra of 102 and 103, highlighting the deprotection of the anomeric enamine.	102
Figure 3.6: ^1H NMR spectrum (A) and gCOSY 2D ^1H NMR experiment (B) of the sidechain carboxyl-linked “clickable” glycoconjugate 110, highlighting the correlation between the H1 and NH resulting from amide bond formation.	105
Figure 3.7: ^1H NMR spectrum (4.0 ppm – 8.0 ppm) of functionalized glycoconjugate 112, highlighting the formation of a 1,4-substituted triazole.	107
Figure 4.1: Comparison of the ^1H NMR spectrums of 117 (A), Boc.HCys.OtBu (120, B) and the crude alkylation reaction mixture (C), highlighting reformation of (Boc.HCys.OtBu) ₂ (119) and the <i>glc</i> hex-5-enopyranoside 121 (D).	119
Figure 4.2: ^1H NMR spectrum of 127, highlighting the small coupling constant ($J = 3.7$ Hz) between the H1 and H2 protons, indicative of the α -stereochemistry present in 127.	124
Figure 4.3: ^1H NMR spectra for both α - and β -anomers (A and B) of the thioether-linked “clickable” glycoconjugate 131.	127

Figure 4.4: Proposed hydrogen bonding between the amino acid H ^γ methylene protons and neighbouring acetate group of 131, resulting in different chemical environments for the two H ^γ protons in the ¹ H NMR spectrum (CDCl ₃ , 25°C) of 131.	128
Figure 4.5: Comparison between the chemical shift for H ^β protons in the ¹ H NMR spectra of 136 and 137, highlighting the effect of planarity in the maleimide of 136 versus the succinimide of 137.	140
Figure 5.1: Leu-Enkephalin neoglycopeptide analogues 139 and 140, containing sugar amino acids (in red) -mimicking a Gly-Gly dipeptide motif. ¹⁵⁴	144
Figure 5.2: Conformations induced by differing substitution patterns of various sugar amino acids embedded into cyclic peptides. ¹⁵⁴	145
Figure 5.3: Cyclic neoglycopeptide derivatives 141, 142 and 143, as sugar amino acid (red) containing analogues of somatostatin. ^{154,210,212}	146
Figure 5.4: Sugar diamino acids (SDAs) reported by Wittmann <i>et al.</i> and Gervay-Hague <i>et al.</i> ^{214–216}	148
Figure 5.5: 2D NOESY experiment highlighting correlations between the acetal CH, and H4 and H6 in 150.	155
Figure 5.6: Comparison of the ¹ H NMR spectra of 154 (A) and 161 (B), highlighting the loss of two protons (A – H6/H6') through oxidation, resulting in the sugar azido acid (B).	164
Figure 5.7: ¹ H NMR experiment (A) and 2D gCOSY experiment (B) of glycoconjugate 164.	168
Figure 5.8: Comparison of the ¹ H NMR spectra of 164 (A) and 165 (B), highlighting the deshielding effect on the H4 of 165 through TBS-protection.	170
Figure 5.9: ¹ H (A) and ¹³ C (B) NMR spectra of the crude 6,3-lactone 166, highlighting the presence of 2 acetyl protecting groups at the 2- and 4- positions.	176
Figure 5.10: ¹ H and ¹³ C NMR spectra of the 3-OH glycoconjugate 169, highlighting the formation of an bond resulting from the nucleophilic ring-opening of 164 by H.Ala.OMe.HCl.	178

List of Schemes

Scheme 1.1: Glycolysis, a key metabolic pathway in the production of free energy from carbohydrates. ⁵	9
Scheme 1.2: Pathways for the production and storage of free glucose, highlighting its production via gluconeogenesis or glycogenolysis, or its storage as the polysaccharide glycogen. ⁵	10
Scheme 1.3: Xenobiotic metabolism, a key process in the metabolism and removal of foreign substances, including pharmacologically active species. ⁵³	11
Scheme 1.4: Injection of [¹⁸ F]FDG into a patient and analysis using Positron Emission Tomography (PET), allowing for the 3D visualization of the size, shape and distribution of malignancies.	16
Scheme 1.5: Oxime-linkage method for the synthesis of ¹⁸ F-radiolabelled glycoconjugates developed by Li and O'Hagan. ^{114–116}	25
Scheme 1.6: Regioselective comparison of the Huisgen 1,3-dipolar azide-alkyne cycloaddition to the copper-assisted and ruthenium-assisted azide-alkyne cycloadditions (CuAAC and RuAAC). ^{118,120,121}	26
Scheme 1.7: Proposed mechanism for the formation of 1,4-substituted-1,2,3-triazoles via the CuAAC “click” reaction. ¹²²	28
Scheme 1.8: Synthesis of carbonic anhydrase inhibitors by Poulsen and co-workers, utilizing the CuAAC “click” reaction. ^{128–130}	29
Scheme 1.9: Synthesis of triazole-containing glycosylamino acids via the CuAAC “click” reaction. ¹³¹	30
Scheme 1.10: <i>In vivo</i> CuAAC “click” reaction of Chinese hamster ovary (CHO) cells fed 33, allowing for their visualization under fluorescence microscopy. ¹³³	31
Scheme 1.11: <i>In vivo</i> strain-promoted Cu-free “click” reaction of mouse tumour cells fed an azidogalactosamine, allowing for their visualization under fluorescence microscopy. ¹³⁵	32
Scheme 1.12: Synthesis of ¹⁸ F-radiolabelled glucose derivative 36 from direct radiofluorination of a triazole-containing derivative 35. ¹³⁶	33
Scheme 1.13: Synthesis of ¹⁸ F-radiolabelled glucose derivative 36 from CuAAC “click” reaction of azido sugar 37 with a ¹⁸ F-fluorinated alkyne. ¹³⁶	34
Scheme 1.14: Synthesis of ¹⁸ F-radiolabelled triazole-containing glycosylamino acid 40 in 60% radiochemical yield via the CuAAC “click” reaction. ¹³⁸	36
Scheme 1.15: Synthesis of 2-OTf-containing derivative 38 from D-mannose, a key precursor in the synthesis of 2-[¹⁸ F]fluoro-2-deoxy-β-D-glucopyranosyl azide (39). ¹³⁸	39
Scheme 1.16: Comparison of methods that may be used to produce ¹⁸ F-radiolabelled glycosylamino acids using the CuAAC “click” reaction. A: Previously described strategy developed by Prante and co-workers, B: Postulated method using “clickable” glycosylamino acids radiolabelled by a [¹⁸ F]-fluoroalkyne using the CuAAC “click” reaction.	41

Scheme 1.17: General scope of the synthesis and functionalization of “clickable” glycoconjugates performed in this project.	44
Scheme 2.1: Proposed scheme for the synthesis of "clickable" glycoconjugates.	48
Scheme 2.2: Key design principles required in the synthesis of "clickable" glycoconjugates, utilizing a uronic acid precursor.	49
Scheme 2.3: Three potential pathways <i>en route</i> to the synthesis of sugar azido acids based on the <i>Glc</i> scaffold. ^{154–156}	52
Scheme 2.4: Synthesis of peracetylated glucuronic acid allyl ester 57 from D-glucuronic acid.	54
Scheme 2.5: Synthetic pathways towards the production of the protected sugar azido acid 59.	55
Scheme 2.6: Alternative mechanistic pathway for the synthesis of 1-azido-2,3,4-tri- <i>O</i> -acetyl-β-D-glucuronic acid allyl ester (59).	56
Scheme 2.7: Mechanism for the SnCl ₄ -catalyzed azidonation that formed 59. ¹⁴⁹	57
Scheme 2.8: Catalytic cycle for the deprotection of allyl esters. ¹⁶⁰	59
Scheme 2.9: Synthesis of 1-azido-2,3,4-tri- <i>O</i> -acetyl-β-D-glucuronic acid 60.	59
Scheme 2.10: Proposed mechanism of the Staudinger reduction that occurs in the synthesis of 60.	60
Scheme 2.11: Synthesis of peracetylated allyl ester 62 from D-galacturonic acid monohydrate.	62
Scheme 2.12: Mechanism for the synthesis of 64 from 62 in the presence of SnCl ₄ . ¹⁶³ 64	
Scheme 2.13: Synthesis of 1-azido-2,3,4-tri- <i>O</i> -acetyl-β-D-galacturonic acid (65).	65
Scheme 2.14: Synthesis of serine-based “clickable” glycoconjugates 66 and 67.	67
Scheme 2.15: Mechanism of the synthesis of esters using a Steglich DCC/DMAP coupling approach.	68
Scheme 2.16: Mechanism of the synthesis of amides using a DCC/HOBt coupling approach.	71
Scheme 2.17: Synthesis of leucine-based “clickable” glycoconjugates 70 and 71	75
Scheme 2.18: Synthesis of “clickable” glycoconjugates 72 and 73.	77
Scheme 2.19: Synthesis of triazole-bearing functionalized glycoconjugates 75-77.	81
Scheme 2.20: Synthesis of triazole-bearing functionalized glycoconjugates 78-83.	82
Scheme 2.21: Synthesis of triazole-bearing functionalized glycoconjugates 84 and 85 83	
Scheme 2.22: Synthesis of triazole-bearing functionalized glycoconjugates 86 and 87 84	
Scheme 2.23: Synthesis of Ac.KPV.NH ₂ -based “clickable” glycopeptide 88	86
Scheme 2.24: Postulated synthesis of the <i>glc</i> -Ac.KPV.NH ₂ -based functionalized glycopeptide 89	89
Scheme 3.1: Proposed synthesis of sidechain carboxyl-linked "clickable" glycoconjugates.	92
Scheme 3.2: Further derivatization of an azidoglucosylamine (90) previously described by Garcia Fernandez and Co-workers. ¹⁸⁶	94
Scheme 3.3: Approach towards the synthesis of amide-linked “clickable” glycoconjugates linked at the anomeric position.	95

Scheme 3.4: Synthesis of 6-azido-1,2-isopropylidene- α -D-glucofuranose (96).....	96
Scheme 3.5: Proposed mechanism for the production of 99 utilizing an NH_4HCO_3 -promoted anomeric amination.....	98
Scheme 3.6: Synthesis of enamine-protected 6-azido- β -D-glucopyranosylamine 101. .	99
Scheme 3.7: Synthesis of the 6-azido-2,3,4-tri- <i>O</i> - β -D-glucopyranosylamine hydrobromide salt 103.....	100
Scheme 3.8: Proposed mechanism for the formation of 103 through enamine cleavage mediated by wet Br_2	101
Scheme 3.9: Synthesis of Boc.Asp.OMe (108) and Boc.Glu.OMe (109).	103
Scheme 3.10: Synthesis of sidechain carboxyl-linked “clickable” glycoconjugates 110 and 111.	104
Scheme 3.11: Synthesis of functionalized sidechain carboxyl-linked “clickable” glycoconjugates 112 and 113 through the CuAAC “click” reaction.	106
Scheme 4.1: Proposed synthesis of thioether-linked "clickable" glycoconjugates.	111
Scheme 4.2: Pathways towards the synthesis of thioether-linked “clickable” glycoconjugates.....	112
Scheme 4.3: Synthesis of 6-iodo-2,3,4,tri- <i>O</i> -acetyl- β -D-glucopyranosyl azide (117). ¹⁹⁴	115
Scheme 4.4: Synthesis of Boc.HCys.OtBu (120) from L,L-homocystine. ^{176,195}	116
Scheme 4.5: Proposed mechanism for the elimination of hydrogen iodide from 121-123 in the presence of a non-nucleophilic base.	117
Scheme 4.6: Synthesis of 6-azido-6-deoxy-1,2,3,4-tetra- <i>O</i> -acetyl-D-glucose 125.	122
Scheme 4.7: Synthesis of α -trichloroacetimidate bearing azidosugar 127. ¹⁴⁴	124
Scheme 4.8: Synthesis of Fmoc.HCys.OMe (130) from L,L-homocystine. ²⁰¹	125
Scheme 4.9: Synthesis of thioether-linked “clickable” glycoconjugate 131 from anomeric acetate 125.....	126
Scheme 4.10: Proposed mechanism for the stereoselective formation of β -glycosides from an α -trichloroacetimidate.....	129
Scheme 4.11: Synthesis of azido- β -thioglycoside 132 performed by Gouin and co-workers. ²⁰⁵	130
Scheme 4.12: Synthesis of thioether-linked “clickable: glycoconjugate 131 from α -trichloroacetimidate 127.	131
Scheme 4.13: Ionic (A) and radical (B) mechanisms for the synthesis of thioethers via the thiol-ene reaction. ²⁰⁶	133
Scheme 4.14: Approach towards the synthesis and functionalization of thioether-linked “clickable” glycoconjugates utilizing the thiol-ene “click” reaction.	135
Scheme 4.15: Synthesis of ethylenediamine maleimide 135.	136
Scheme 4.16: Synthesis of maleimide-SAA linked derivative 136.	137
Scheme 4.17: Synthesis of thioether-linked “clickable” glycoconjugate 137 by “click” thiol-ene reaction of 136 and Fmoc.HCys.OMe (130).	138
Scheme 4.18: Synthesis of the functionalized maleimide-linked glycoconjugate 136.	141

Scheme 5.1: Proposed approach towards the synthesis of "clickable" neoglycopeptides.	147
Scheme 5.2: Key strategy towards the development of "clickable" neoglycopeptides.	151
Scheme 5.3: Synthesis of 2,3,4,6-tetra- <i>O</i> - β -D-glucopyranosyl azide (148) from D-glucose.	152
Scheme 5.4: Synthesis of 4,6-benzylidene- β -D-glucopyranosyl azide (150). ^{156,223}	153
Scheme 5.5: Mechanism for the acid catalysed formation of the 4,6-benzylidene acetal 150.	154
Scheme 5.6: Synthesis of 2,3-protected-4,6-diol derivatives 153 and 154.	156
Scheme 5.7: Synthesis of 6-protected glycosides 155 and 156.	158
Scheme 5.8: ¹ H NMR spectrum of 156, highlighting overlapping signals at 3.77 and 3.80 ppm that indicates the PMB and MMTr-methoxy groups, respectively.	159
Scheme 5.9: Original synthetic pathway highlighting additional synthetic steps from 156 required to produce the desired sugar azido acid target.	160
Scheme 5.10: Synthesis of 1-azido-2,3- <i>O</i> -benzoyl- β -D-glucuronic acid methyl ester (158) from phenyl-4,6-benzylidene-1-thio- β -D-glucopyranoside (157) published by Bera and Linhardt. ²²⁴	161
Scheme 5.11: Examples of selective oxidation of a primary alcohol present on a pyran-based glycoside previously described by Van Den Bos and coworkers. ²²⁶	162
Scheme 5.12: TEMPO/BAIB-mediated oxidation of diol 154 to form the sugar azido acid 161.	163
Scheme 5.13: Proposed mechanism for the oxidation of primary alcohols to carboxylic acids utilizing the TEMPO/PhI(OAc) ₂ oxidation protocol.	165
Scheme 5.14: Synthesis of previously reported glucuronic acid methyl ester 162. ²²⁴	166
Scheme 5.15: Synthesis of L-alanine methyl ester hydrochloride (163). ^{234,235}	167
Scheme 5.16: Synthesis of alanine-sugar azido acid glycoconjugate 164 via amide coupling.	167
Scheme 5.17: Synthesis of the orthogonally-protected glyconjugate 165.	169
Scheme 5.18: Conversion of 1-azido-2,3,4-tri- <i>O</i> -acetyl- β -D-glucuronic acid methyl ester (53) to the 6,3-lactone 166 reported by Tosin <i>et al.</i> ^{155,236}	172
Scheme 5.19: Mechanism for the formation of 6,3-lactone 53 from 166, utilizing saponification and chair conformation interconversion.	172
Scheme 5.20: Nucleophilic substitution of the 6,3-lactone 164, resulting in the ester and amide derivatives 167 and 168 that bear unprotected 3-OH groups. ^{155,237}	173
Scheme 5.21: Proposed synthesis of glycoconjugates bearing a free 3-OH group from the 6,3-lactone 166, towards the synthesis of "clickable" neoglycopeptides.	174
Scheme 5.22: Synthesis of 1,2,3,4-tetra- <i>O</i> -acetyl- β -D-glucuronic acid methyl ester (52) from glucuronolactone.	175
Scheme 5.23: Synthesis of 1-azido-2,3,4-tri- <i>O</i> -acetyl- β -D-glucuronic acid methyl ester (53). ¹⁵⁴	175
Scheme 5.24: Synthesis of 3-OH bearing glycoconjugate 169 via ring-opening of the 6,3-lactone 166.	177

Scheme 5.25: Synthesis of the orthogonally-protected glycoconjugate 170.	179
Scheme 6.1: The diversity of “clickable” glycoconjugates synthesised from azidosugars, and functionalized using the CuAAC “click” reaction that have been described in the current study.....	182
Scheme 6.2: The synthesis of orthogonally-protected glycoconjugates 165 and 170 from simple precursors (D-glucose; 165, and glucuronolactone; 170).....	184
Scheme 6.3: The tripeptides Fibronectin Binding Motif (LDV; 171) and reduced-Glutathione (172), potential model peptides in the synthesis of amide and thioether-linked “clickable” glycopeptides.....	188
Scheme 6.4: Proposed synthetic strategy for the synthesis of Type A and B “clickable” neoglycopeptides from 164 and 169.	190
Scheme 6.5: Synthesis of fluorinated glycoconjugates 173 and 174.	191

List of Tables

Table 1.1: Native peptides upregulated in various cancers and their mimics used as diagnostic probes in nuclear imaging. ⁸⁸	18
Table 1.2: Efficiency of prosthetic groups commonly used in the radiolabelling of peptides and glycoconjugates with fluorine-18. ¹⁰⁶	24
Table 2.1: Reaction conditions for the synthesis of lysine-based “clickable” glycoconjugates 68 and 69	70
Table 2.2: Optimization of CuAAC “Click” reaction conditions, producing the triazole-bearing functionalized glycoconjugate 74.	79
Table 4.1: Attempted alkylation of 6-iodo-2,3,4-tri- <i>O</i> -acetyl- β -D-glucopyranosyl azide (117) by Boc.HCys.OtBu (120).	118

List of Abbreviations

δ	Chemical shift
Ac	Acetyl
AcOH	Acetic acid
ADP	Adenosine-5'-diphosphate
Ala	Alanine
<i>Allo</i>	Allose
AM1	Austin model 1 semi-empirical theory
Aq.	Aqueous
ArC	Aromatic Carbon
ArH	Aromatic Hydrogen
ASCT	Anti-neutral amino acid transporter
Asp	Aspartic acid
ATP	Adenosine-5'-triphosphate
B.p	Boiling point
Bs	Broad Singlet
Boc	<i>N</i> - <i>tert</i> butoxycarbonyl
Bz	Benzoyl

CA	Carbonic Anhydrase
CHO	Chinese hamster ovaries
CuAAC	Copper-assisted azide-alkyne cycloaddition
Cys	Cysteine
d	Doublet
D	Dextrorotatory
dd	Doublet of doublets
DBU	1,8-Diazabicyclo[5.4.0]undec-7-ene
DCC	<i>N,N'</i> -1,3-dicyclohexylcarbodiimide
DIC	<i>N,N'</i> -1,3-diisopropylcarbodiimide
DIPEA	<i>N,N'</i> -diisopropylethylamine
DMAP	<i>N,N'</i> -dimethylaminopyridine
DMF	<i>N,N'</i> -dimethylformamide
dt	Doublet of triplets
<i>E</i>	<i>Trans</i> configuration
EDCI	1-(3-dimethylaminopropyl)-3-ethylcarbodiimide
EPO	Erythropoietin
Eq.	Equivalents

Et ₂ O	Diethyl ether
EtOAc	Ethyl acetate
EtOH	Ethanol
Fab	Fragment antigen binding region
Fc	Fragment crystallizable region
FDG	Fluorodeoxyglucose
FDR	Fluorodeoxyribose
Fmoc	<i>N</i> -fluorenylmethyloxycarbonyl
<i>Gal</i>	Galactose
GAG	Glycosylaminoglycan
<i>g</i> COSY	Gradient correlation spectroscopy
<i>g</i> HMBC	Gradient heteronuclear multiple bond correlation
<i>g</i> HSQC	Gradient heteronuclear single quantum correlation
<i>Glc</i>	Glucose
Gln	Glutamine
Glu	Glutamic acid
h	Hours

HBTU	<i>N,N,N',N'</i> -Tetramethyl- <i>O</i> -(1 <i>H</i> -benzotriazol-1-yl)
	uronium Hexafluorophosphate
HCys	Homocysteine
ΔH_f	Heat of formation
HOBt	1-Hydroxybenzotriazole
Hpg	Homopropargylglycine
HPLC	High Performance Liquid Chromatography
HR-ESIMS	High Resolution Electrospray Ionisation Mass Spectroscopy
IC ₅₀	Concentration required to inhibit 50% of the population
<i>J</i>	Spin-spin coupling constant (NMR)
KLH	Keyhole Limpet Hemocyanin
KPV	Lysine-Proline-Valine
L	Levorotatory
LAT	Large amino acid Transoporter
LDV	Leucine-Aspartic acid-Valine
Leu	Leucine
Lit.	Literature data

LR-ESIMS	Low Resolution Electrospray Ionisation Mass Spectroscopy
Lys	Lysine
m	Multiplet
M	Molar
[M ⁺]	Molecular ion
<i>Manno</i>	Mannose
MeOH	Methanol
Met	Methionine
min.	Minutes
MMTr	4-methoxytriphenylmethyl
M.p	Melting point
MS	Mass spectroscopy
α -MSH	Alpha-Melanocortin Stimulating Hormone
MUC	Cell surface associated Mucin
<i>m/z</i>	Mass to charge ratio
N ₂	Nitrogen gas
NH ₃	Ammonia

NMR	Nuclear Magnetic Resonance Spectroscopy
NAG	<i>N</i> -acetylglucosamine
NAM	<i>N</i> -acetylmuramic acid
NADH	Nicotinalmide adenine dinucleotide
NST	Neurotensin receptor
NOESY	Nuclear Overhauser Effect Spectroscopy
OMe	Methoxy
OTs	<i>p</i> -Toluenesulfonyl
<i>p</i>	para
PAI-2	Plasminogen Activation Inhibitor 2
PET	Positron Emission Tomography
Pfp	Pentafluorophenyl
<i>p</i> Ka	Logarithmic acid dissociation constant
PMB	<i>p</i> -methoxybenzyl
ppm	parts per million
Pro	Proline
PyBOP	(benzotriazol-1-yl)-tripyrrolidinophosphonium
	hexafluorophosphate

R _f	Retardation factor
RBC	Red Blood Cells
RCY	Radiochemical Yield
RGD	Arginine-Glycine-Aspartic acid
ROS	Reactive Oxygen Species
RT	Room Temperature
SAA	Sugar Amino Acid
sat.	Saturated
sst	Somatostatin Receptors
SDA	Sugar Diamino Acid
Ser	Serine
S _N ²	Second Order Nucleophilic Substitution Reaction
SPECT	Single Photon Emission Computerised Tomography
t	Triplet
TACA	Tumour Associated Carbohydrate Antigens
TBAF	Tetrabutylammonium fluoride
TBDPS	<i>Tert</i> butyldiphenylsilyl
TBS	<i>Tert</i> butyldimethylsilyl

TBTA	Tris((1-benzyl-1 <i>H</i> -1,2,3-triazol-4-yl)methyl)amine
TBTU	<i>N,N,N',N'</i> -Tetramethyl- <i>O</i> -(1 <i>H</i> -benzotriazol-1-yl)uranium tetrafluoroborate
<i>t</i> Bu	<i>tert</i> -Butyl
TCA	Tricarboxylic acid
TEMPO	2,2,6,6-Tetramethylpiperidin-1-yl)oxy Radical
TFA	Trifluoroacetic acid
THF	Tetrahydrofuran
TLC	Thin Layer Chromatpography
Trt	Triphenylmethyl
Val	Valine
<i>Z</i>	<i>Cis</i> Configuration

Publications Arising from this Thesis (To Date)

Journal Articles Arising from this Work

1. **Cara, C.J** and Skropeta, D., Synthesis and Functionalization of “Clickable” Glycoconjugates, *Manuscript in Preparation*

Conference Seminar and Poster Abstracts

2. **Cara, C.J**; Katsifis, A. and Skropeta, D., Design and Synthesis of Novel Glycopeptide Imaging Agents, *School of Chemistry, University of Wollongong*, Wollongong, New South Wales, Australia (June 24, 2010) (Oral Seminar).
3. **Skropeta, D.**; Katsifis, A.; Thilikan, M.; **Cara, C.J.** and Sarowi, S, M, Synthesis and Radiolabelling of Novel Sugar Diamino Acids: Potential Applications in the Development of Anticancer Imaging Agents, *RACI Connect*, Melbourne, Victoria, Australia (July 4, 2010) (Oral Seminar).
4. **Cara, C.J**; Katsifis, A. and Skropeta, D., Novel Sugar Amino Acid Derivatives for Glycopeptide Synthesis, *RACI Organic Chemistry Group 31st Annual One Day Symposium*, Wollongong, New South Wales, Australia (December 1, 2010) (Poster).
5. **Cara, C.J**; Katsifis, A. and Skropeta, D., “Click”-Glycoconjugates – A Novel Method for the Development of Radilabelled Glycopeptides, *CRC-BID Annual Meeting*, Melbourne, Victoria, Australia, (May 5, 2011) (Oral Seminar).

6. **Cara, C.J.**; Katsifis, A. and Skropeta, D., Diagnostic Approaches Targetting Cancer's Sweet Spot, *Trailblazer UOW Innovation Competition*, Wollongong, New South Wales, Australia (August 4, 2011) (Oral Seminar).
7. **Cara, C.J.**; Katsifis, A. and Skropeta, D., Diagnostic Approaches Targetting Cancer's Sweet Spot, *Trailblazer National Innovation Competition*, Brisbane, Queensland, Australia (August 16, 2011) (Oral Seminar).
8. **Cara, C.J.**; Katsifis, A. and Skropeta, D., "Click"-Glycoconjugates –Novel Methods for the Development of Radilabelled Glycopeptides, *School of Chemistry and IPRI Annual Conference*, Nowra, New South Wales, Australia (November 2, 2011) (Oral Seminar).
9. **Cara, C.J.**; Katsifis, A. and Skropeta, D., "Click"-Glycoconjugates – Novel Methods for the Development of Radilabelled Glycopeptides, *RACI Biomolecular Conference*, Torquay, Victoria, Australia (December 2, 2011) (Poster).
10. **Cara, C.J.**; Katsifis, A. and Skropeta, D., Glycosylated L-Methionine and L-Glutamine – Towards Molecular Probes for Amino Acid Transport, *IUPAC 19th International Congress on Organic Synthesis*, Melbourne, Victoria, Australia (July 1-6, 2012) (Poster).
11. **Cara, C.J.**; and Skropeta, D., Synthesis and Functionalization of "Clickable" Glycoconjugates, *RACI Biomolecular Conference*, Leura, New South Wales, Australia (July 14-17, 2013) (Poster).

Acknowledgements

There are a number of people I would like to thank and acknowledge for their encouragement, help and support in the completion of my PhD. Firstly, I would like to thank Dr. Danielle Skropeta for her formal supervision and support during my candidature. Your guidance and advice over the past 5 years have been instrumental in the direction of my PhD project. Also, I'd like to acknowledge Dr. Andrew Katsifis for his initial contributions to the direction of my PhD project, and the technical staff in the School of Chemistry for their technical expertise in accessing and using a wide variety of equipment within the school.

A big warm-hearted thank you is due for Assoc. Prof. Paul Keller, Dr Michael Kelso, Dr. Simon Bedford, Dr. Glennys O'Brien and Prof. Stephen Pyne for their mentorship, suggestions and general synthetic know-how during my candidature, particularly during Danielle's absences. I'd also like to thank them for providing me with the opportunity to teach, an important part of the PhD process. Additionally, I'd like to thank all members past and present of the Keller, Kelso and Skropeta research groups for their input and discussion on a range of chemistry-related topics.

I'd like to extend my appreciation to those who have provided me with emotional support in the completion of this work. Akash, Ben, Holly, Lloyd, Reece, Luke, Ander, Aaron, Cass and Leighton, your mateship and vigorous discussion of a variety of topics, often over a coffee or beer and not always chemistry related, helped maintain my sanity throughout the completion of this project. For that, I am forever thankful.

Many thanks are due for the Cara and Jones families, for their incredible love and support during the completion of this work. Mum, Dad, Yvonne and Peter, your endless encouragement over the last 5 years has helped me soldier on and focus on the end goal of this work, teaching me the greater importance of a well-rounded education. Finally, a massive thank is reserved for my better half, Meghan. You experienced the difficult times I endured in the completion of this work, and were nothing short of amazing in encouraging and supporting me through those times. Your love and support kept me going, and words can't adequately describe how much it meant to me. I dedicate this work to you, and hope that you are as proud of it as I am.

Abstract

Carbohydrates have been heavily exploited in the development of new therapeutic agents. Extensively utilized in nuclear medicine, derivatives such as [^{18}F]-FDG (**13**) have gained broad usage in the diagnosis of malignancies. Displaying high selectivity and favourable pharmacokinetics, carbohydrates have subsequently been incorporated into peptide-based imaging agents, producing diagnostic probes with greatly improved physicochemical properties. The efficient radiolabelling of glycoconjugate-based imaging agents however represents a significant challenge, with many glycoconjugates prone to degradation under current radiolabelling conditions.

Compatible techniques such as the copper-assisted azide-alkyne cycloaddition (CuAAC) “click” reaction have found usage in the synthesis of radiolabelled glycoconjugates, linking [^{18}F]-radiolabelled glycosyl azides to alkyne-containing peptides. The wider application of this approach in the labelling of glycoconjugates though has been limited by the incongruity of this process with native amino acids, and peptides or proteins. In this thesis, a methodology for the synthesis of glycoconjugates amenable to functionalization by the CuAAC “click” reaction is illustrated.

The concise, 5-step production of *glc*- and *gal*-sugar azido acids **60** and **65** allowed for the formation of “clickable” glycoconjugates **66-73** in 64-96% yield, linked to serine, lysine and α -amino containing (Leu, Met, Gln) amino acids. Possessing β -azides at the anomeric position, the CuAAC “click” reaction of these with alkyne donors produced the functionalized glycoconjugates **78-87** in 52-85% yield, representing the first examples of glycosides linked to an amino acid, and derivatized using the CuAAC “click” reaction. Conjugation of *glc*-sugar azido acid **60** to the

tripeptide Ac.KPV.NH₂ resulted in the glycoconjugate (**88**), which may be functionalized by the CuAAC “click” reaction, thus broadening the scope of this methodology to the labelling of biologically-relevant substrates.

Extension of this methodology to the formation of linkages with carboxyl-containing amino acids was also investigated, with the key synthon 6-azido-6-deoxy-1-amino-2,3,4-tri-*O*-acetyl- β -D-glucose hydrobromide (**103**) successfully produced in 8 steps from 1,2;5,6-diisopropylidene- α -D-glucofuranose (**93**). Amide coupling at the anomeric amine of **103** by sidechain carboxyl-containing (Asp, Glu) amino acids produced the “clickable” glycoconjugates **110** and **111** in 60-70% yield. Subsequent CuAAC “click” reaction with 4-pentyn-1-ol yielded the functionalized glycoconjugates **112** and **113** in 62-70% yield, the first examples of functionalized glycoconjugates formed from carboxyl containing amino acids.

Using 6-*p*-toluenesulfonyl-1,2,3,4-tetra-*O*-acetyl-D-glucose (**114**) as a key synthon, thioether-linked glycoconjugates bearing an anomeric or 6-azido group were also evaluated. Alkylation of the anomeric azide 6-iodo-6-deoxy-1,2,3-tri-*O*-acetyl- β -D-glucosyl azide (**117**; 40% yield in 3 steps from **114**), by the thiol-containing amino acid (HCys) **120** did not yield the desired glycoconjugate (**124**). Alternatively, glycosylation of the HCys derivative **130** by the glycosyl donors 6-azido-6-deoxy-1,2,3,4-tetra-*O*-acetyl-D-glucose (**125**) and 6-azido-6-deoxy-1,2,3-tri-*O*-acetyl- α ,D-glucosyl trichloroacetimidate (**127**) yielded the thioether-linked “clickable” glycoconjugate **131**, however this was present as an anomeric mixture.

Subsequently, an efficient method for the formation of thioether-linked glycoconjugates utilizing the “click” thiol-ene reaction was developed. The maleimide-

sugar azido acid conjugate **136** was produced from **60** (66% yield), with “click” thiol-ene reaction with Fmoc.HCys.OMe (**130**) producing the functionalized derivative **137** (62% yield). CuAAC “click” reaction resulted in the functionalized thioether-linked glycoconjugates **138**, which together with amide-linked examples demonstrated the versatility of azidosugars in the formation of functionalizable glycoconjugates.

Beyond “clickable” glycoconjugates, a strategy for the formation of orthogonally-protected Type A and B “clickable” neoglycopeptides was also developed. Orthogonal protection of the 4-position of a *glc*-based glycoside yielded the β -azides **155** and **156** (7 steps). Containing bulky protecting groups (Trt, MMTrt, PMB) though, the development of a superior atom-economical approach was sought, with subsequent selective TEMPO/PhI(OAc)₂ oxidation of the 2,3-OBz diol **154** producing the orthogonally-protected sugar azido acid **161** (88% yield). Consequently, amide coupling (**164**, 50% yield) and 4-OTBS protection (**165**, 36% yield) yielded key intermediates for the production of Types A and B “clickable” neoglycopeptides.

The scope of this strategy was subsequently broadened to those bearing orthogonal protection at the 3-position. Formation of the 6,3-lactone intermediate **166** from 1-azido-1-deoxy-2,3,4-tri-*O*-acetyl- β -D-glucuronic acid methyl ester (**53**) and nucleophilic ring opening, produced the 3-OH glycoconjugate **169** (42% over 3 steps). Subsequent 3-OTBS protection (66% yield) yielded the orthogonally protected derivative **170**, which alongside **169** represent key intermediates for the production of Types A and B “clickable” neoglycopeptides. In conjunction with the developed “clickable” glycoconjugates, these derivatives provide a solid platform for the broader utilization of the CuAAC “click” reaction in the formation and functionalization of bioconjugates encompassing carbohydrates.

Chapter 1 : Introduction

1.1 Carbohydrates – Definition and Structural Diversity

Carbohydrates, synonymously known as saccharides, are a structurally rich class of complex molecules. Comprising carbon, hydrogen and oxygen atoms, carbohydrates exist in many different forms, ranging from linear non-reducing (ketose) and reducing (aldose) species (Figure 1.1, A and B) consisting of three to nine carbons, to cyclic hemiacetal-containing species forming five (pentose - furan) or six (hexose - pyran) membered ring systems (Figure 1.1, C and D).¹

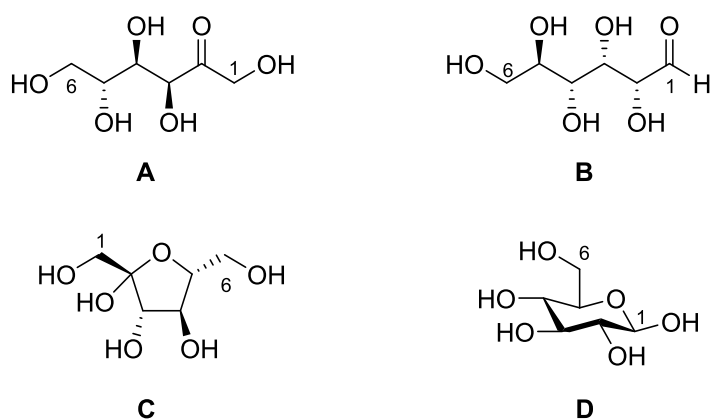


Figure 1.1: Examples of non-reducing (D-fructose, A) and reducing (D-glucose, B) linear carbohydrates, which in solution cyclize to form furan (C) and pyran (D) glycosides respectively.

Bearing multiple hydroxyl groups, carbohydrates form a variety of structural isomers. For example, cyclic hexoses such as glucose, mannose, allose, galactose, idose and talose are structural isomers with the chemical formula $C_6H_{12}O_6$, resulting from the

alternating stereochemistry of their hydroxyl groups (Figure 1.2). Some examples such as glucose (*glc*) and galactose (*gal*) can be further classified as epimers of each other, with these isomers bearing at only one position of the molecule (e.g. C4 in *glc/gal*, Figure 1.2).¹ Likewise, isomers may also have epimers at multiple stereocentres, with mannose (C2), allose (C3) and idose (C5) also epimers of glucose (Figure 1.2)

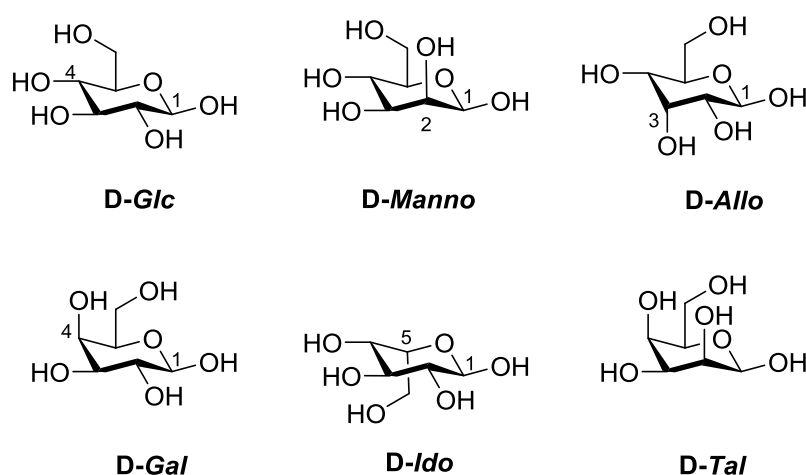


Figure 1.2: Pyran-based isomers of chemical formula $C_6H_{12}O_6$.

Formed by the conversion of linear aldoses to cyclic pentoses and hexoses, epimers of individual isomers including glucose and galactose, may also be produced. Occurring at the carbon participating in cyclization (or C1), this is known as the anomeric carbon, with epimers at this position specifically known as anomers.^{1,2} Differing in the configuration of the proton linked to the anomeric carbon, the stereochemical assignment of a glycoside is directly relative to its absolute configuration. In hexose sugars such as D-glucose, the stereochemistry of both the C1 and C5 carbon defines the assignment, with an axial proton at the C5 and an equatorial proton at the C1 denoting an α -anomer, whilst axial proton at both C1 and C5 carbons denote a β -anomer.² The anomeric configuration of many carbohydrates is of great

importance, as many carbohydrates exist as multimers of individual saccharides, including di-, tri-, tetra- and oligosaccharides.³ This can produce isomers of saccharides conjugated to each other at the same position, such as maltose and cellobiose, which represent α - and β -isomers of a (1 \rightarrow 4) linked disaccharide respectively.² Additionally, saccharides can form linkages at a variety of different positions and can also form glycosidic linkages with a number of different C-, O-, S- and N-acceptors. Hence, considering the array of structural permutations that carbohydrates may embody, it is of little surprise that carbohydrates are amongst the most analysed chemical entities, with their roles in biological systems widely studied.^{3,4}

1.2 Roles of Carbohydrates in Biological Systems

1.2.1 Structural Roles of Carbohydrates

The structural diversity of carbohydrates underlies their importance in a number of biological functions. Generally speaking, these roles can be divided into three main categories – structural; cellular signalling and recognition; and energy usage metabolism.⁵ In plant, algal, fungal and bacterial species, polysaccharides play an important role in maintaining cellular structure.⁶ In green plants and algae, the β (1 \rightarrow 4) glucose polysaccharide cellulose (Figure 1.3, **1**) forms a key component of the cell wall, with chains of cellulose forming large hydrogen bonding networks that provide strength and stability.^{7,8} These fibrils of cellulose are often reinforced with other polysaccharide units, including pectins (Figure 1.3, **2**), which are rich in poly-galacturonic acids, and hemicelluloses such as xylan, which are rich in D-xylose and pentose glycosides.^{6,9}

In fungi, their cell walls consists of the $\beta(1\rightarrow4)$ -linked *N*-acetyl-D-glucosamine polysaccharide chitin (Figure 1.3, **3**).¹⁰ Aligned in fibrils akin to cellulose, chitin provides many fungi with strength and flexibility. Interestingly, chitin is also present in the shells and exoskeletons of many arthropods - including crustacea and insects,¹¹ with crosslinking by calcium species (primarily CaCO_3) in these structures producing chitin that is much harder and stronger than that in fungal species.^{10,12} In bacterial species, peptidoglycan (or murien) forms the principle component of the organism's cell wall.¹³ Consisting of polymeric residues of *N*-acetylglucosamine and *N*-acetylmuramic acid (NAM), peptide chains linked to NAM residues allow for inter-strand cross-linking, producing a matrix that maintains the strength of the cell wall (Figure 1.3, **4**).¹³

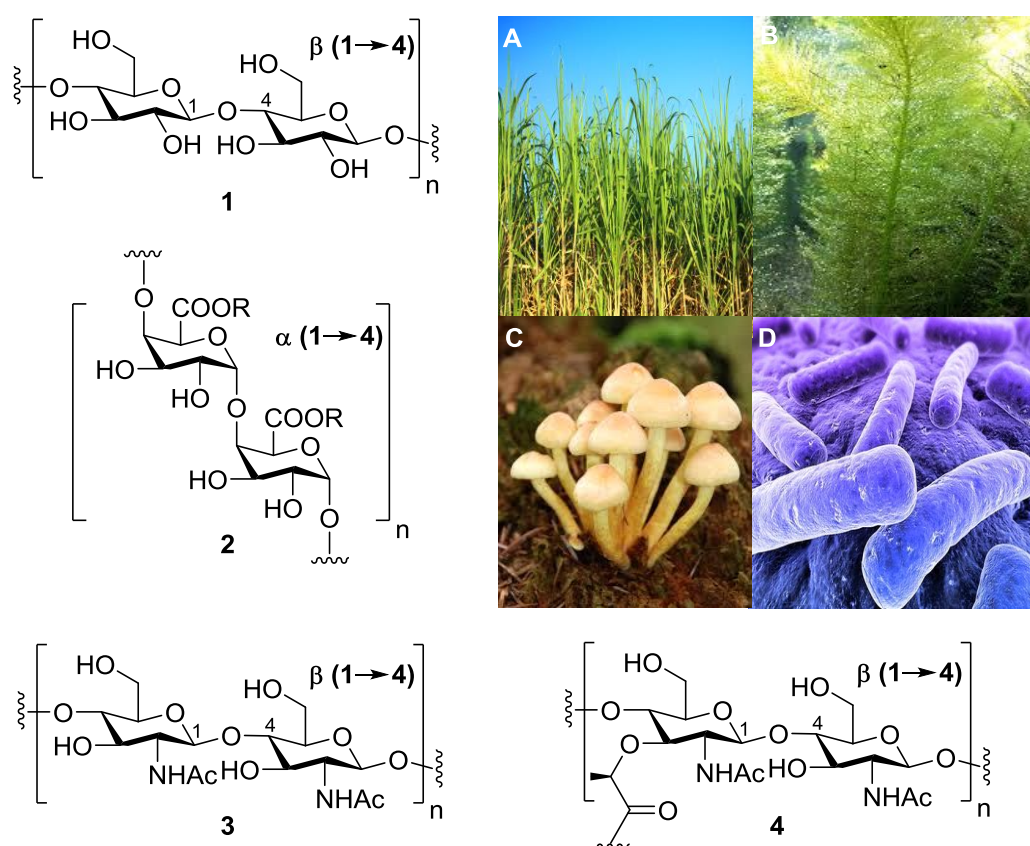


Figure 1.3: Cellulose (1), xylan (2), chitin (3) and murein (4) – important polysaccharides that maintain the cellular structure of plant (A), algal (B), fungal (C) and bacterial (D) species.^{14–16}

In mammalian species, the extracellular matrix that lies between individual cells is composed of a variety of different glycosylaminoglycans (GAG's), including hyaluronic acid and chondroitin sulphate, in addition to dermatan sulphate and keratan sulphate.^{3,17} These negatively charged unbranched polysaccharides are constituents of proteoglycans, core proteins that are heavily glycosylated with polysaccharides.^{6,18} GAG's display an uncanny ability to coordinate water molecules, producing a matrix that can compress and flex when pressure is applied to them.⁶ Displaying such flexibility, it is of no surprise that GAG's form the basis for tissues under constant loading and stress, including bone cartilage.^{6,19,20}

1.2.2 Carbohydrates in Cellular Signalling, Recognition and Growth

Many carbohydrate-bearing entities hold key positions in the mediation of cell-cell recognition processes.²¹ Glycoconjugates are species where one or multiple glycosides are linked to a biological molecule via a glycosidic bond,²² such as glycoproteins and glycolipids, which are the most abundant forms of glycoconjugates found in nature.²³ Linked to one or multiple glycans (short oligosaccharides of ~3-9 units), glycoproteins play important roles in a number of cellular functions, including the lubrication and protection of epithelial tissues,²⁴ immunological responses and defences, cell-cell attachment, and cellular growth and development.²⁵⁻²⁸

Mucins, a class of 19 highly glycosylated glycoproteins secreted on the surfaces of epithelial cells, form a major constituent of important bodily lubricants such as saliva and mucous.²⁹ High in molecular weight (~250-500 kDa), mucins are composed of oligosaccharide chains attached via *O*-linked amino acid residues including serine and

threonine, and to a lesser degree via *N*-linked asparagine residues.^{24,29} Mucins are integral to the body's defence against external pathogens and key to their role is their capacity for gelation, whereby they can expand and coat cell surfaces, providing a physical barrier that both lubricates and protects the cell from pathogens.^{24,29}

Immunoglobins, large Y-shaped proteins that are produced by the immune system (B cells) to detect and nullify potential pathogens, utilize carbohydrates in their protective functions.³⁰ Containing two light and heavy polypeptide chains across two regions (Fab and Fc), the Fc region of an antibody interacts with the Fc receptor of immune cells - including B lymphocytes, natural killer cells and antigen presenting cells, eliciting an immune response (Figure 1.4, A), with glycosylation of the Fc region by D-fucose, in addition to *N*-acetylglucosamine and neuraminic acid residues essential for immune activity (Figure 1.4, A).³⁰⁻³² In contrast, the Fab region of an antibody binds to a number of different antigens (including pathogens), stimulating an immune response upon immune cell attachment. Once again glycosylation is important, with the Fab regions of many natural antibodies having affinity for the disaccharide motif Gal-(α 1->3)-Gal expressed in a number of bacteria and enveloped viruses, thereby providing immunity against such pathogens and protecting cells from infection (Figure 1.4, A).^{33,34}

Interestingly, many pathogens also exploit the carbohydrate binding affinity of cell surface proteins to avoid detection by the immune system, using cell surface proteins that bind specific carbohydrate motifs, known as lectins.⁶ The influenza viral envelope is coated with membrane-bound glycoproteins including haemagglutinin and neuraminidase that are crucial in viral entry and propagation (Figure 1.4, B).^{35,36}

Displaying a high affinity for neuraminic acid residues on the exterior of cell-surface membranes, influenza haemagglutinin binds to these residues, bringing the viral envelope within close proximity of a host cell (Figure 1.4, B). Membrane fusion with the viral envelope induces endocytosis, resulting in viral uptake. Following viral replication, neuraminidases present on the surface of newly produced virions aid in their expulsion from the cell. Targeting neuraminic acid residues bound to hemagglutinin and other cell-surface glycoproteins, cleavage of these residues by neuraminidase triggers exocytosis, resulting in the release of viral particles that may infect other host cells.^{37,38}

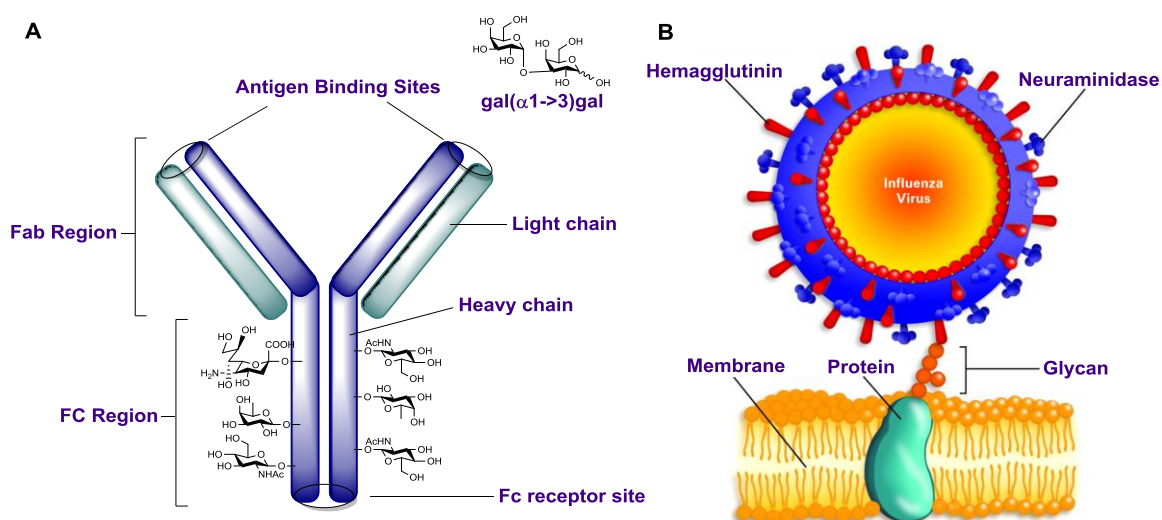


Figure 1.4: Roles of carbohydrate-bearing macromolecules in cellular signaling, recognition and growth. A: Ig binds disaccharide (Gal(α1-3)Gal) antigens (Fab region) and requires glycosylation to bind pathogens (Fc region), B: Influenza viruses utilize carbohydrate-binding glycoproteins hemagglutinin and neuraminidase for viral entry and release.³⁹

Neuraminic acid residues are also key mediators of cell turnover, coating the outer surface of red blood cells (RBCs)^{40,41} and other cells present in the circulatory system (thrombocytes, leukocytes and hepatocytes, etc.).⁴²⁻⁴⁴ Cleavage of these residues either by serum neuraminidases or by chemical hydrolysis, unmask galactose residues

underneath the neuraminic acid. As a marker of cellular aging, these residues attract the attention of macrophages, which attach to the cells at these residues and subsequently induce phagocytosis (Figure 1.5, A).^{45,46} Additionally to cellular clearance, carbohydrates also play important roles in cellular growth, with glycoprotein hormones such as erythropoietin (EPO) pivotal to the production of red blood cells.⁴⁷ Heavily glycosylated with branched saccharide chains, these chains stabilize the protein structure of EPO, allowing it to bind to the erythropoietin receptor and stimulate the growth of red blood cells in the bone marrow (Figure 1.5, B).⁴⁷

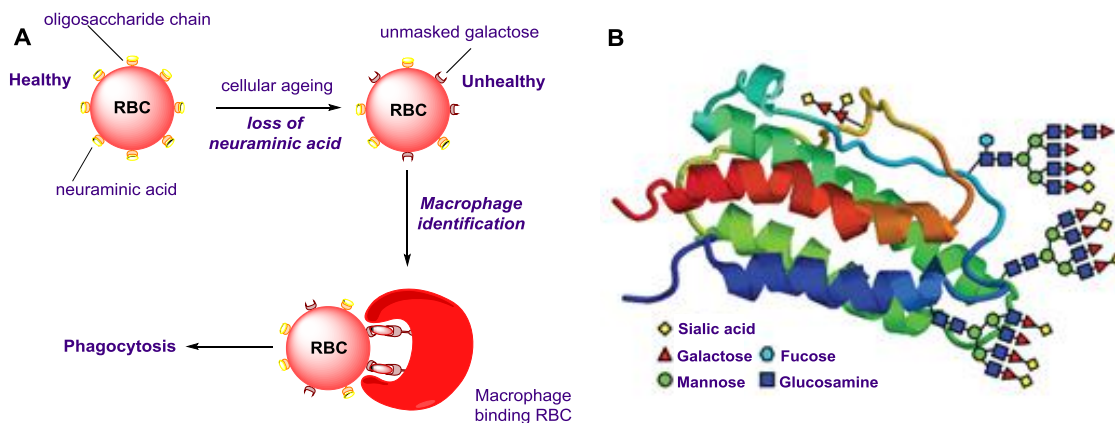
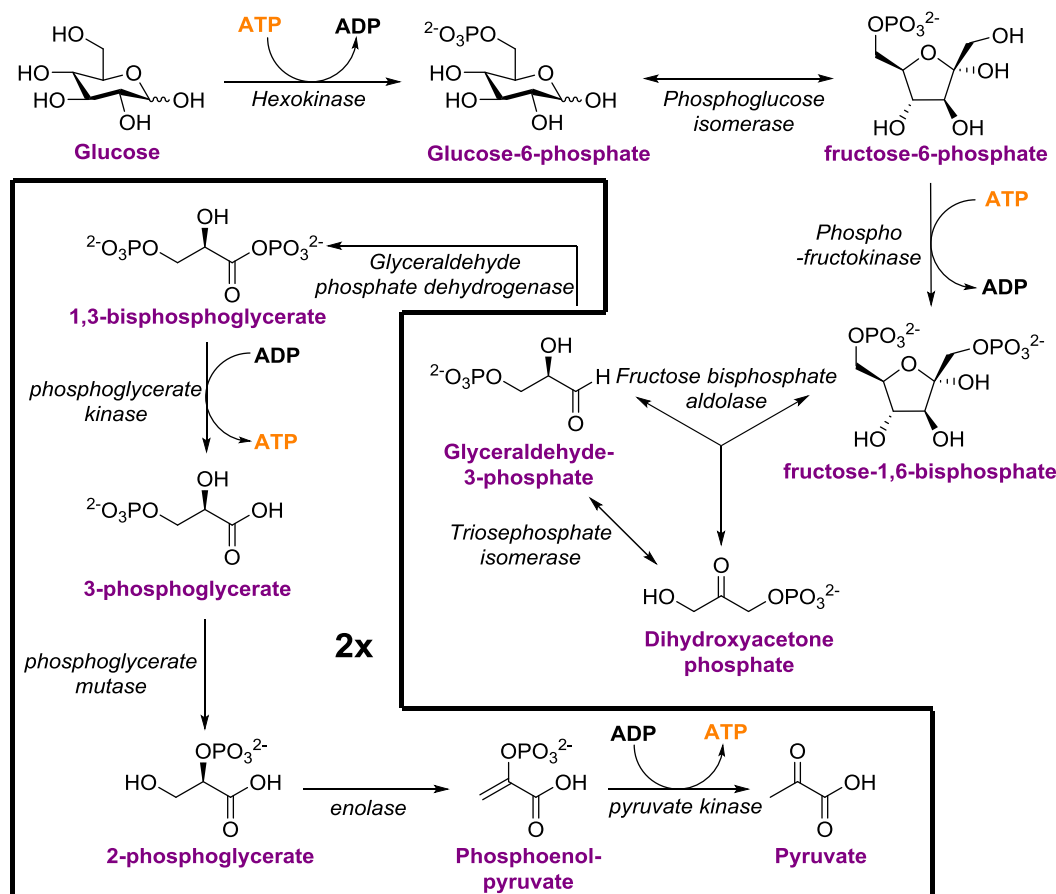


Figure 1.5: Roles of carbohydrates in cellular turnover and growth. A – Induction of phagocytosis of red blood cells (RBCs) following cleavage of neuraminic acid residues from the cell surface. B - Structure of erythropoietin, bearing heavily glycosylated chains provide structural stability.⁴⁸

1.2.3 Carbohydrates in Energy Usage, Storage and Metabolism

The central role of carbohydrates in the regulation of cell structure, recognition and protection, is matched by their importance in the production and storage of energy. Glycolysis, a key metabolic process that exists in all organisms, converts glycosides

into the metabolite pyruvate (Scheme 1.1).⁵ Enzymatically driven and readily occurring in the cytosol of cells, glycolysis directly produces two molecules of adenosine triphosphate (ATP) and reduced nicotinamide adenine dinucleotide (NADH).⁵

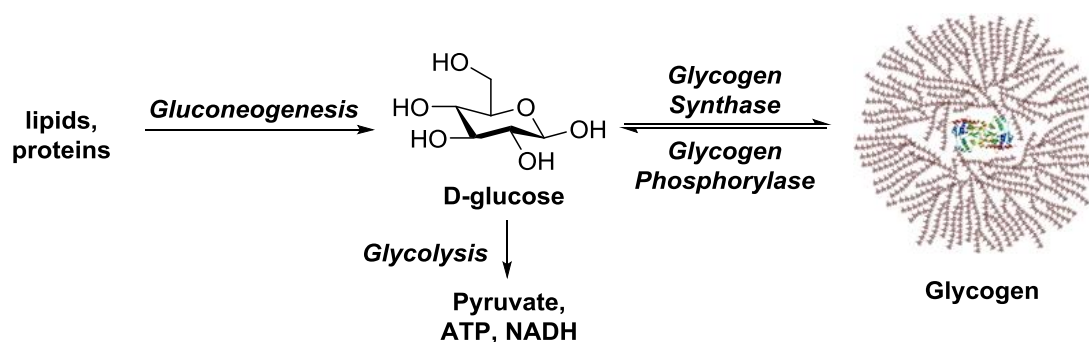


Scheme 1.1: Glycolysis, a key metabolic pathway in the production of free energy from carbohydrates.⁵

Both high energy coenzyme molecules, ATP and NADH are the main providers of chemical energy within a cell.⁵ In addition, pyruvate molecules produced as a by-product of glycolysis can be directly fed into the tricarboxylic acid (TCA) cycle in aerobic organisms, which following enzymatic conversion to oxaloacetate and citrate,

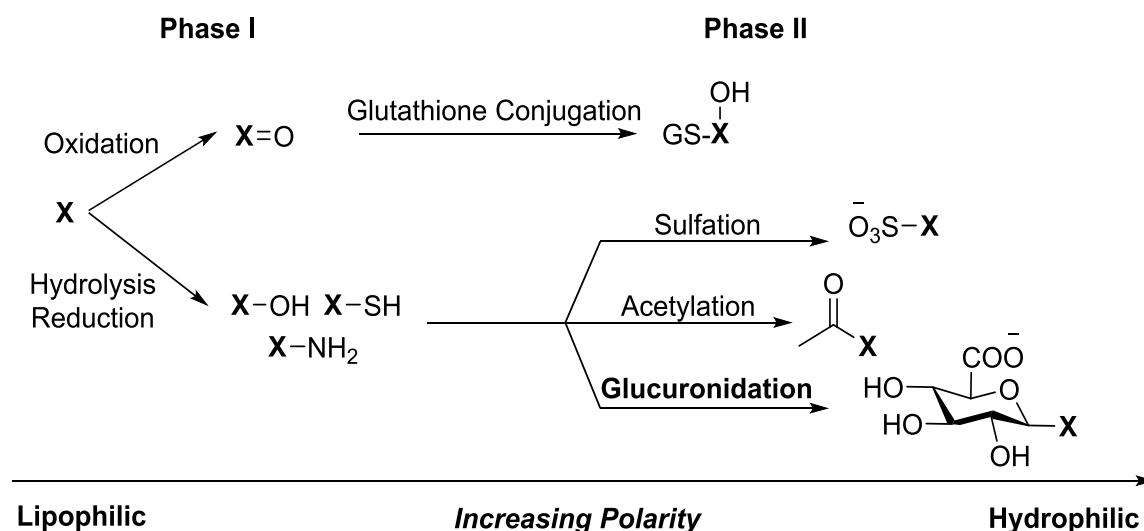
(in addition to other key intermediate molecules) results in the production of an additional ~34 molecules of ATP per hexose sugar consumed. Hence the utilization of carbohydrates provides the most readily accessible source of energy to cells.^{49,50}

In the absence of available glucose, proteins and lipids may also be converted to glucose in order to meet energy requirements via gluconeogenesis. However, the catabolism of lipid and protein reserves is energy intensive, with the production of glucose from these sources resulting in a 33% decrease in available energy.⁵¹ Therefore, a readily accessible stored form of glucose, known as glycogen is utilized. Glycogen, which is present in muscle tissue and the liver as a network of branched glucose polysaccharides, is readily formed by the action of the enzyme glycogen synthase.⁵ In times of high blood glucose (e.g., postprandial), glycogen synthase can store glucose as glycogen via chain addition (Scheme 1.2). In contrast, glycogenolysis – the breakdown of glycogen, can be enacted by the enzyme glycogen phosphorylase, liberating glucose to curtail low blood glucose levels (Scheme 1.2).⁵ It is this enzyme in addition to the hormones insulin and glucagon that modulate the secretion, storage and concentration of blood glucose.⁵



Scheme 1.2: Pathways for the production and storage of free glucose, highlighting its production via gluconeogenesis or glycogenolysis, or its storage as the polysaccharide glycogen.⁵

Beyond the production of free energy from the metabolism of glucose, carbohydrates play key roles in other metabolic functions. Processes such as xenobiotic metabolism utilize glucuronidation in the breakdown and excretion of substances that are foreign to an organism.^{52,53} The 6-carboxyl derivative of glucose, glucuronic acid is conjugated to xenobiotic substances in the liver that have been processed by Phase I metabolism, with glucuronidation representing the most common detoxifying transformation that takes place under Phase II metabolism (Scheme 1.3).⁵⁴ Ionisable at physiological pH, substitution of molecules linked to glucuronic acid following reaction with uridine diphosphate glucuronate - a carrier of glucuronic acid, produces metabolites that are significantly more polar, allowing for their excretion in urine or bile.⁵⁵ The importance of this process is exemplified in drug metabolism, where the rate of clearance may have a pronounced influence on the effectiveness of a dosage.^{53,55}



Scheme 1.3: Xenobiotic metabolism, a key process in the metabolism and removal of foreign substances, including pharmacologically active species.⁵³

1.3 Carbohydrates in Medicinal Chemistry

The integral role of carbohydrates in such a vast array of biological systems has attracted the attention of researchers keen to exploit their therapeutic potential. Whilst beyond the scope of the current discussion, the range of conditions and diseases that are targeted by carbohydrate-based or containing entities is truly diverse (Figure 1.6). These range from aminoglycoside and glycopeptide antibiotics such as streptomycin and vancomycin (**5** and **6**)^{56–58} through to cardiac glycosides for the treatment of heart failure such as digoxin,⁵⁹ and glycosidase inhibitors for the treatment of influenza (e.g. Zanamivir (Relenza[®])⁶⁰ **7** and Oseltamivir (Tamiflu[®]) (**8**))⁶¹ and also for diabetes (e.g. Miglitol (**9**) and Voglibose (**10**)).^{62,63}

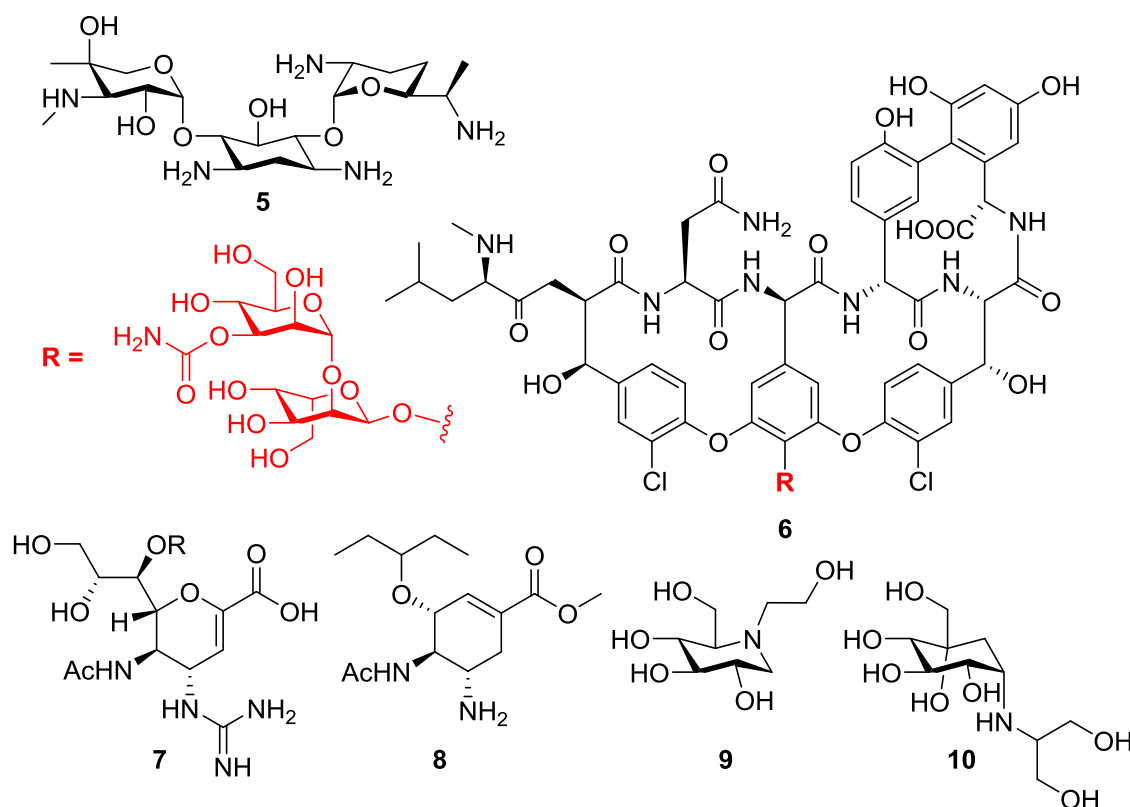


Figure 1.6: Carbohydrate-based therapeutic agents used as antibiotics (**5** and **6**), and in the treatment of influenza (**7** and **8**) and diabetes (**9** and **10**).

In addition to treating the above conditions, carbohydrate-containing species have also displayed potential in the treatment of a number of malignancies, targeting glycoproteins upregulated by metastatic cells. Many of these play important roles in cellular structure and growth, with examples such as the heparan sulphate mimetic PI-88 (Muparfostat, **11**) that inhibits angiogenesis, reaching phase III clinical trials for the treatment of post-resectional hepatocellular carcinoma (Figure 1.7).^{64,65}

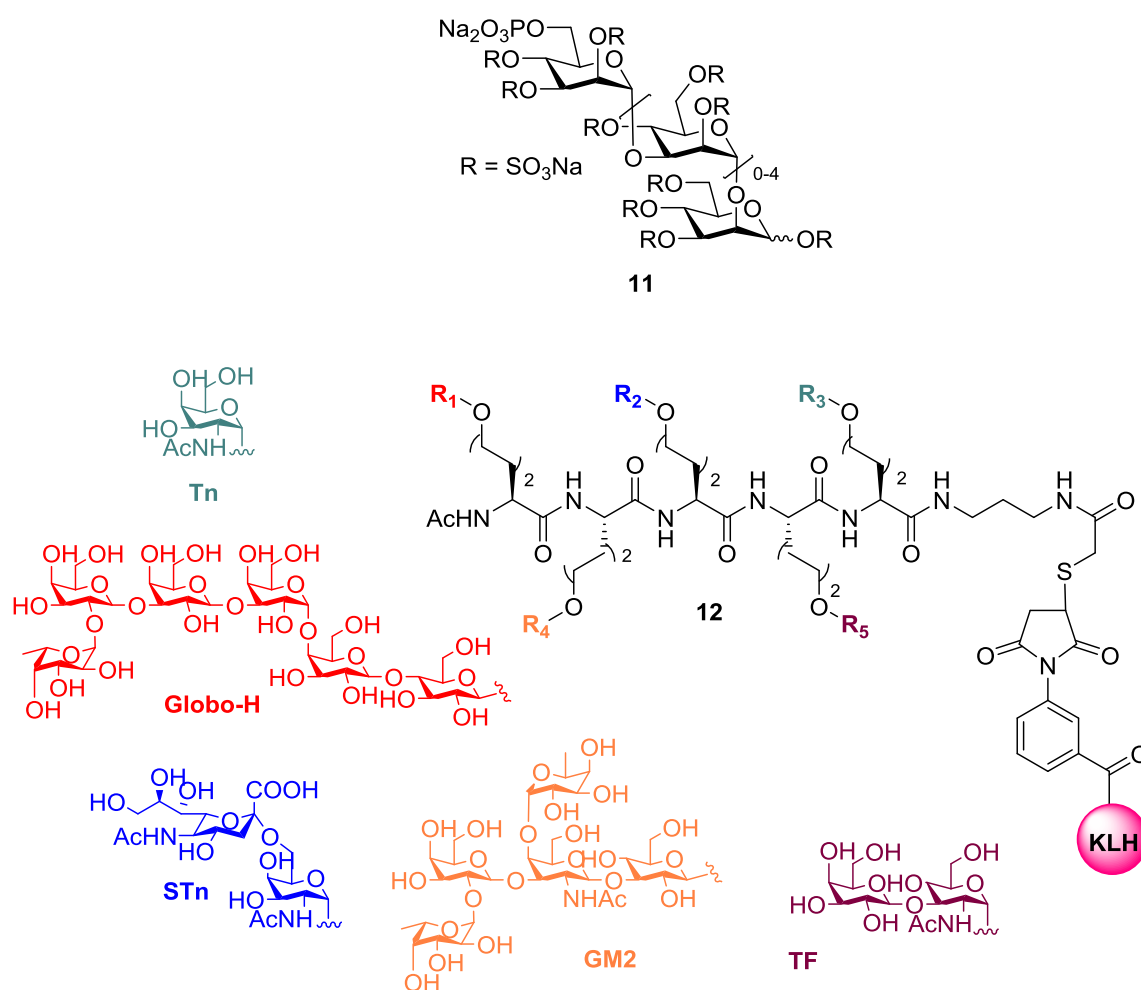


Figure 1.7: Heparan sulphate mimetic PI-88 (**11**) and pentavalent conjugate vaccine **12**, bearing antigens for tumour-upregulated glycoproteins (MUC-1 – Tn, TF, STn), glycolipids (Globo-H) and gangliosides (GM2), agents under evaluation for their treatment of malignancies.

Furthermore, a number of other heavily glycosylated glycoproteins are over-expressed in tumour cells, including a number of mucins.⁶⁶ MUC-1 is a mucin glycoprotein that is bound to the apical surface of epithelial cells present in the tissues of the lungs, stomach and intestines, and represents an excellent tumour marker, with the targeting of mucins and other markers using tumour associated carbohydrate antigens (TACAs) representing a promising strategy towards the development of new anticancer vaccines.^{66–68} A number of vaccines bearing these antigens have been developed, with many bearing multiple carbohydrate-based antigens targeting MUC-1 (e.g Tn, TF and STn). Additionally, many of these vaccines also target glycolipids (e.g Globo-H), glycophospholipids and gangliosides (e.g, GM2), which are also overexpressed on the surfaces of a range of cells.⁶⁸ This work has been pioneered by Danishefsky and co-workers, who have developed a number of mono, tri and pentavalent cancer vaccines.^{69,70} Linked to an immunogenic protein such as keyhole limphet haemocyanin (KLH),⁷¹ pentavalent vaccines such as **12** (Figure 1.7) have displayed great promise in providing targeted, selective treatment to specific metastases, reaching Phase I clinical trials.^{69,70}

1.4 Carbohydrates in Nuclear Imaging

Whilst carbohydrate-based medicines have been developed for the treatment of a variety of different illnesses, their greatest impact has been in the diagnosis of a number of different malignancies. In Australia, cancer is a leading cause of mortality and morbidity accounting for around 30% of deaths in 2011, with approximately 1 in 2 men, and 1 in 3 women expected to be diagnosed with cancer by the age of 85.⁷² However,

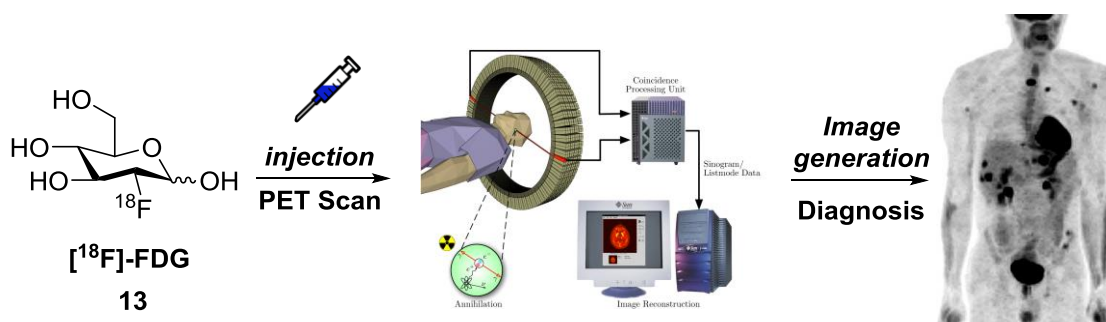
whilst a major cause of death in Australia, the actual rate of morbidity from cancer has decreased over the last thirty years, with 16% fewer people dying from cancer today as opposed to thirty years ago.⁷² The survival rate for sufferers of the most common cancers has also improved dramatically, with 30% more people surviving cancer than twenty years ago, and the survival rate for sufferers five years after diagnosis rising by 60%.⁷² Beyond the development of new and improved cancer therapies, the improvement in cancer survival can be attributed to three main factors:

- A push towards earlier detection of malignancies
- The development of tumour-targeting diagnostic probes/imaging agents
- More accurate means of detecting malignancies (PET/SPECT)

Greater public awareness of the warning signs and symptoms of particular cancer types have dramatically decreased the time between occurrence and diagnosis, resulting in the treatment of cancer in the early stages and limiting the spread and proliferation of tumours to other tissues.⁷² However, it can be equally said that the development of new molecular probes that specifically target tumours has had a profound impact on the diagnosis of malignancies.⁷³ Incorporating radionuclides linked to a probe that targets specific features of different malignancies, these probes are delivered to, and accumulate in the targeted tumour.⁷³ When coupled with techniques that quantify the radiation emitted by the attached radionuclide, such as Positron Emission Tomography (PET) or Single Photon Emission Computerized Tomography (SPECT),^{74,75} the use of diagnostic probes provides an accurate 3D depiction of the size, shape and distribution of metastases, allowing for their treatment or removal.⁷⁶

1.4.1 ^{18}F -Fluorodeoxyglucose (^{18}F -FDG)

Of the diagnostic probes developed over the last 40 years, the radiolabelled glucose derivative [^{18}F]-fluorodeoxyglucose (^{18}F -FDG, **13**, Figure 1.11) is by far the most widely used and regarded, revolutionizing the diagnosis of metastatic tumours.⁷⁷ First described in 1969,⁷⁸ and developed for nuclear imaging in 1976 at the Brookhaven National Laboratory,⁷⁹ [^{18}F]-FDG is fluorinated at the 2-position with radioactive fluorine-18 ($T_{1/2} = 109$ minutes), a positron-emitting radionuclide.⁸⁰ Taken up by tissues that maintain a high rate of glucose metabolism, the 2-fluoro group prevents the initial metabolism by glycolysis, with eventual radioactive decay of fluorine-18 to oxygen-18 allowing for the fast metabolism and clearance of **13** identical to that of naturally occurring hexoses.⁸¹ As metastatic tissues require high quantities of glucose to maintain their growth, and [^{18}F]-FDG is not metabolised until radioactive decay occurs, the localization of [^{18}F]-FDG in these tissues ensues. Using PET/SPECT methods, contrast differences of tissues containing [^{18}F]-FDG to those that don't (signal to noise ratio) are quantified to highlight the presence of high glucose-metabolizing tissues, which are subsequently used to diagnose the presence of malignancies (Scheme 1.4).⁸¹



Scheme 1.4: Injection of [^{18}F]-FDG into a patient and analysis using Positron Emission Tomography (PET), allowing for the 3D visualization of the size, shape and distribution of malignancies.

Whilst the use of [^{18}F]-FDG has significantly improved the diagnosis of a number of cancer types, for some its use has been rather problematic. As [^{18}F]-FDG exploits the high glucose metabolism of metastatic tissues, a lack of target selectivity has been encountered, with this phenomenon primarily observed in tissues that would normally exhibit a high rate of glucose metabolism.⁸² This particularly relates to neuroendocrine tumours of the brain,^{83,84} gastrointestinal tract⁸⁵ and pancreas,⁸⁶ where the presence of metastatic tissues in close proximity to naturally high glucose-metabolizing tissues has made accurate diagnosis difficult, leading in some cases to false positives and misdiagnosis.⁸⁵ Though the use of [^{18}F]-FDG in the diagnosis of metastases at these sites still bears some clinical significance, efforts have been made to develop more selective means of tumour diagnosis in these tissues.⁸⁷

1.4.2 Peptide Imaging Agents

In addition to the exploitation of high glucose metabolism by [^{18}F]-FDG in the diagnosis of malignancies, a large number of non-carbohydrate imaging agents have also been developed.⁸⁷ Accompanying the upregulation of cell surface glycans in tumour cells, a number of different cell-membrane receptors are also upregulated that promote tumour growth and proliferation.⁸⁷ Appearing in much larger numbers in tumour cells compared to healthy cells, these receptors represent good diagnostic markers for defining the presence and spread of malignancies.⁸⁷ Consequently, a number of peptide imaging agents have been developed that target receptors associated with one or multiple forms of cancer.⁸⁸ These peptides include mimetics of the endogenous peptides somatostatin,^{89,90} α -melanocortin stimulating hormone (α -MSH)⁹¹

and neuropeptide-Y,⁹² which are associated with, and whose receptors are upregulated in neuroendocrine, skin and breast cancers respectively (Table 1.1, Entries 1-3).

Table 1.1: Native peptides upregulated in various cancers and their mimics used as diagnostic probes in nuclear imaging.⁸⁸

Native Peptide	Tumour/Cancer Type	Probes
Somatostatin	Neuroendocrine, melanoma, breast	Octreoscan®
α -MSH	Melanoma	[¹¹¹ In]DOTA-NAPamide
Neuropeptide Y	Breast	(Cu/DOTA) ⁴]BVD-15
Bombesin/GRP	Lung, colon, glioblastoma, prostate	[^{99m} Tc]Bombesin

These also include derivatives of exogenous peptides such as Bombesin (Table 1.1, Entry 4), which is derived from the toad *Bombina bombina*.⁹³ A homologue of the mammalian Gastrin-releasing Peptide (GRP), Bombesin binds to GRP receptors, which are overexpressed in lung, colon and prostate cancer.^{94,95} Peptide imaging agents targeting overexpressed receptors have been highly beneficial as diagnostic tools. Radiolabelled cyclic peptides including In-111-Octreotide (Octreoscan®, Mallinckrodt), an octapeptide derivative of somatostatin-14 that shows high affinity for somatostatin receptors (sst) upregulated in neuroendocrine tumours, has found broad clinical use.⁹⁶ However, despite such promise the clinical utility of these imaging agents has been fraught with a number of challenges. A common problem encountered with their use is *in vivo* degradation, with many peptide imaging agents susceptible to the actions of intracellular proteases.⁷³ Additionally, the reabsorption of small peptides by glomerular filtration in the kidneys often limits the quantity of

radiotracer that reaches the desired target, thereby exposing the kidneys to potential nephrotoxicity, and large doses of radiation.⁹⁷ Finally, if the utilized imaging agent does indeed reach the desired target they often suffer from poor tumour retention, which has the effect of reducing the quality of the diagnostic scan performed by reducing the signal to noise ratio.⁹⁸ Considering these issues, in addition to those encountered in the use of [¹⁸F]-FDG, it is evident that their problems with both selectivity and clearance are balanced by their opposing properties. The high selectivity for metastatic tissues possessed by peptide imaging agents, in addition to the high tumour retention and clearance exhibited by [¹⁸F]-FDG together impart properties that would be ideal for a diagnostic agent. Thus, a number of researchers have worked to develop strategies that would combine these properties of peptide imaging agents and [¹⁸F]-FDG.

1.4.3 Glycoconjugation – Improving the Pharmacokinetics of Peptide Imaging Agents

1.4.3.1 Iodine-125 Radiolabelled Imaging Agents

As a result of their complimentary properties, a number of carbohydrate-containing peptide imaging agents have been developed. These include cyclic glycoconjugates bearing the peptide motif RGD (Arg-Gly-Asp), that display a high affinity for the $\alpha_v\beta_3$ integrin.⁹⁹ A heterodimeric transmembrane glycoprotein that mediates cell to cell matrix interactions, $\alpha_v\beta_3$ is upregulated in metastatic tissues and is an important mediator of tumour invasion and angiogenesis.¹⁰⁰ Initial derivatives of RGD developed by Wester and co-workers incorporated a cyclic pentapeptide also

bearing (Lys; K) and tyrosine (Tyr; Y) residues, with the presence of a sugar on the sidechain ϵNH_2 of the lysine modulating the peptides' lipophilicity.⁹⁹ The presence of the tyrosine residue allowed for radioiodination with iodine-125, producing the radiolabelled glycosylated RGD derivative **14** (Figure 1.8).⁹⁹

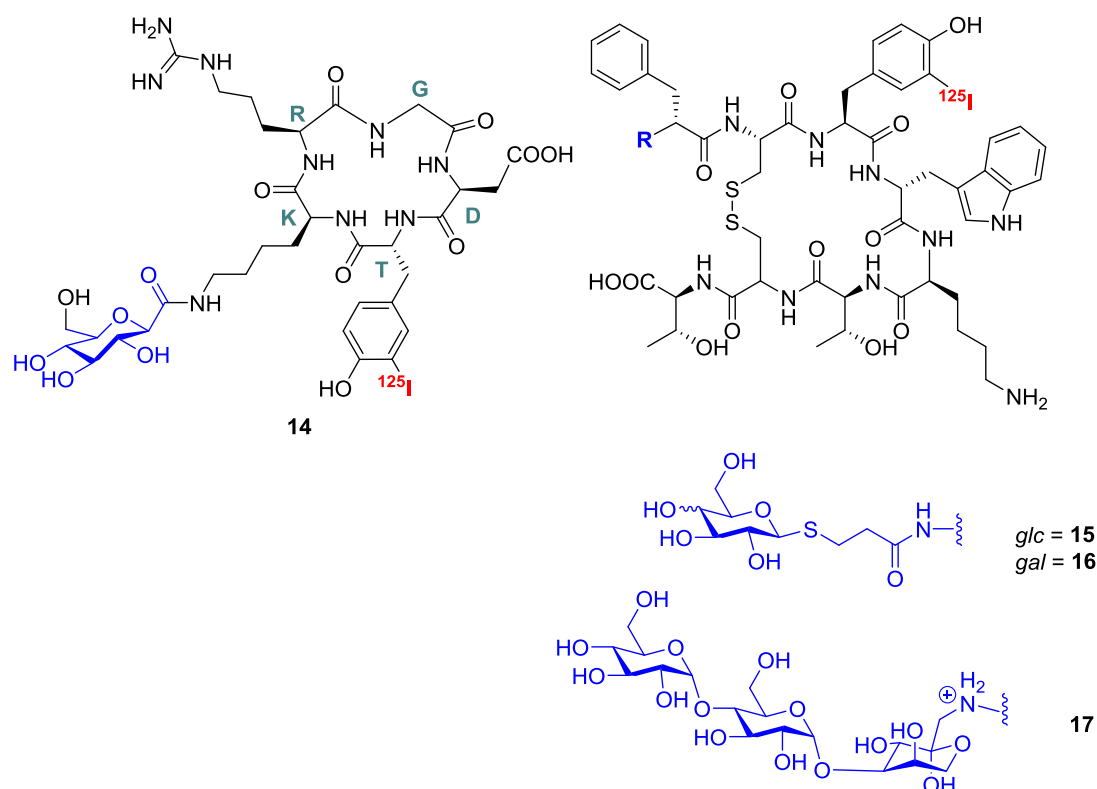


Figure 1.8: Iodine-125 radiolabelled glycoconjugate imaging agents, based on the cyclo-RGD (14**) and octreotide (**15** and **16**) peptide scaffolds.**^{99,101–104}

The marked reduction in lipophilicity of **14** compared to the non-glycosylated derivatives inspired the translation of this approach to other diagnostically relevant peptides. This is demonstrated by the [^{125}I]-labelled derivatives **15** and **16**, and the maltotriose-containing derivative **17**, which incorporate the octapeptide somatostatin derivative Octreotide (Figure 1.8).¹⁰² Whilst the lipophilicity of $\alpha_v\beta_3$ and sst-targeting

imaging agents **14-17** has been significantly decreased by glycosylation, the use of iodine-125 as a radionuclide for labelling in these examples limits their usability, with the long-half life ($T_{1/2} = 59.4$ days) and requirement of a tyrosine residue for introduction being limiting factors.¹⁰⁵

1.4.3.2 Fluorine-18 Radiolabelled Imaging Agents

To overcome these hurdles, Wester and co-workers developed a strategy that allowed for the glycosylation and radiolabelling of peptides with fluorine-18¹⁰⁶. Utilizing a galacturonic acid-derivative linked via the terminal lysine NH_2 of the cyclic peptide (-RGDFK-), acylation with *p*-nitrophenyl-2- ^{18}F fluoropropionate (^{18}F -NPFP) resulted in the ^{18}F -radiolabelled glycoconjugate **18**, which is more commonly known as ^{18}F GalactoRGD (Figure 1.9).^{99,107-109} Radiolabelled on the carbohydrate as opposed to the peptide chain, the shorter half-life of fluorine-18 has led to an increase in the translation of cyclic-RGD derivatives to the clinic, with ^{18}F GalactoRGD considered the “gold standard” for the detection and diagnosis of angiogenesis.¹⁰⁸ Furthermore, the use of the 2- ^{18}F fluoropropionate method essentially allows for the introduction of fluorine-18 at any site bearing a free amino group. As a direct result of the success of ^{18}F GalactoRGD, *p*-nitrophenyl-2-[2- ^{18}F]fluoropropionate has also been used to introduce fluorine-18 into octreotide derivatives, resulting in the ^{18}F -radiolabelled derivative **19** (Figure 1.9).⁷⁶

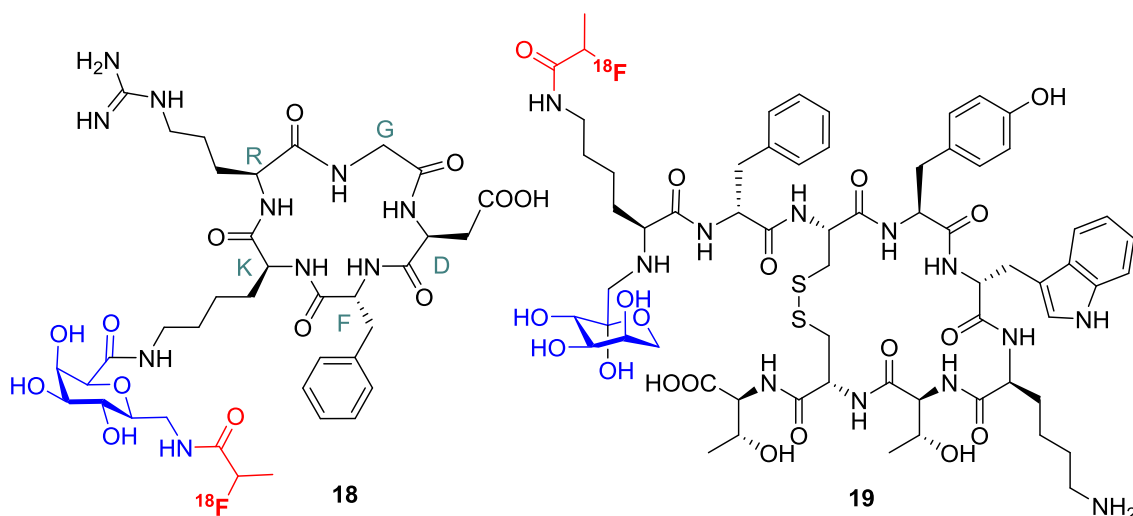


Figure 1.9: Fluorine-18 radiolabelled imaging agents 18 and 19 based on the cyclo-RGD and octreotide peptide scaffolds, with both agents glycosylated and labelled at lysine.^{76,109}

1.4.3.3 Alternative Methods for the Introduction of Fluorine-18

A variety of different radiofluorination methods exist in addition to the use of *p*-nitrophenyl-2-[¹⁸F]fluoropropionate (**20**). For the introduction of fluorine-18 into derivatives such as **18** and **19**, this includes the use of different prosthetic groups (akin to [¹⁸F]-NPFP), and electrophilic and nucleophilic fluorination methods.¹¹⁰ Introducing a fluorine-18 atom to a respective amine through acylation, the actions of [¹⁸F]-NPFP have been mirrored by other [¹⁸F]-bearing prosthetic groups, such as *N*-succinimidyl-4-[¹⁸F]fluorobenzoate ([¹⁸F]-SFB; Figure 1.10, **21**). Additionally, prosthetic groups that label via a different ligation method have also been used, with imidation and alkylation by 3-[¹⁸F]fluoro-5-nitrobenzimidate ([¹⁸F]-NFB; Figure 1.10, **22**) and 4-[¹⁸F]fluorophenacyl bromide ([¹⁸F]-FPB; Figure 1.10, **23**) are also common.^{77,106}

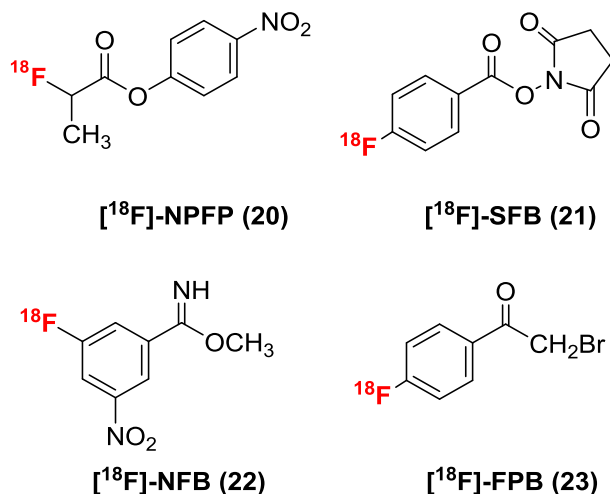


Figure 1.10: [^{18}F]-Containing prosthetic groups utilized in the synthesis of ^{18}F -radiolabelled probes.¹⁰⁶

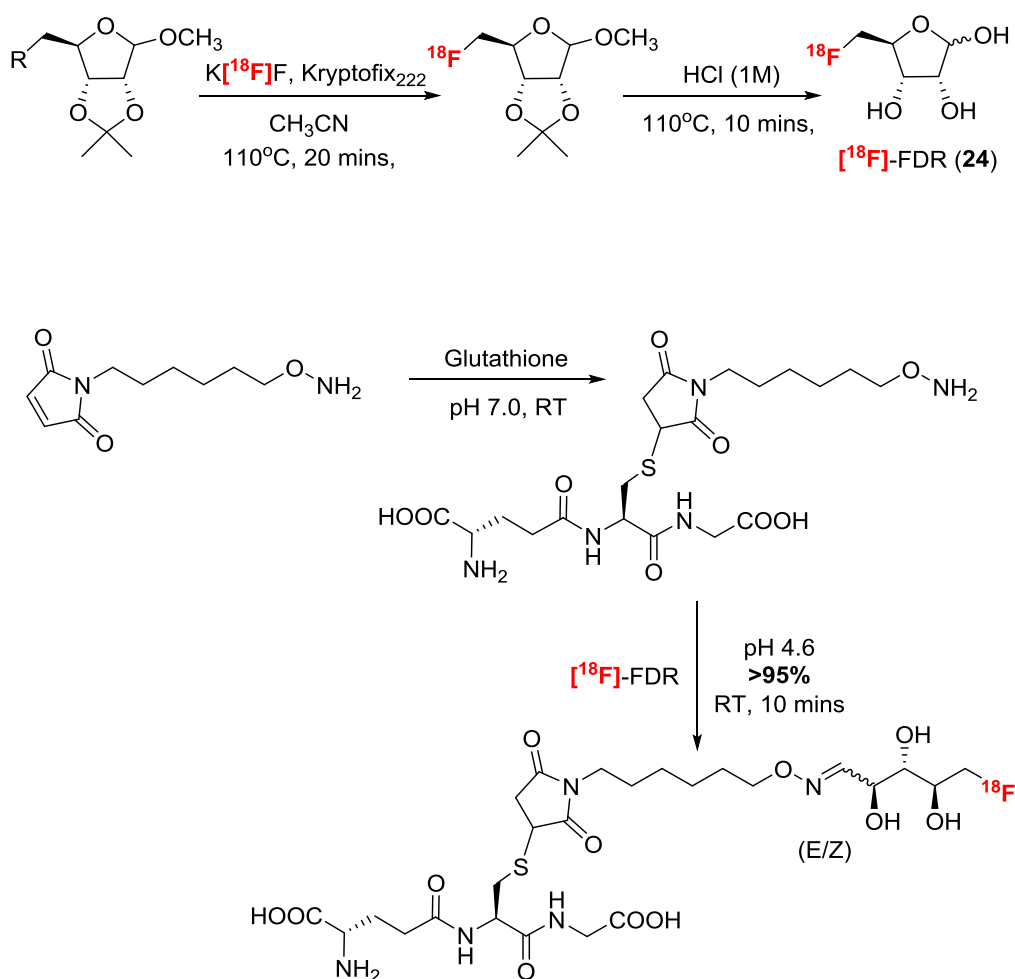
The exploitation of these prosthetic groups and their respective conjugative techniques provides a means for utilizing fluorine-18 in the radiolabelling of peptides and proteins. However, a major disadvantage of these methods is their synthetic complexity, with the prosthetic groups described requiring numerous synthetic steps and long reaction times for their production. Often, these factors result in the isolation of prosthetic groups containing fluorine-18 in yields much lower than what could be expected based on the initial amount of radionuclide available, which is also known as radiochemical yield (Table 1.2).¹⁰⁶ Additionally, bar a small number of examples,^{111–113} the use of nucleophilic and electrophilic radiofluorination methods have largely been avoided in the development of radiofluorinated peptides. The diversity of reactive groups present on a peptide limit the use of nucleophilic radiofluorination methods, with electrophilic radiofluorination also limited by the need for the use of carriers with agents such as [^{18}F]- F_2 .¹⁰⁶

Table 1.2: Efficiency of prosthetic groups commonly used in the radiolabelling of peptides and glycoconjugates with fluorine-18.¹⁰⁶

Method	¹⁸ F Labelling Agent	# Steps	Time (min)	RCY(%)
Acylation	4-nitrophenyl-2-[¹⁸ F]fluoropropionate	3	90	60
	<i>N</i> -succinimidyl-4-[¹⁸ F]fluorobenzoate	3	30-35	18
Imidation	3- [¹⁸ F]fluoro-5-nitrobenzimidate	3	45	20-33
Alkylation	4- [¹⁸ F]fluorophenacyl bromide	3	75	28-40
	<i>N</i> -(<i>p</i> -[¹⁸ F]fluorophenyl)maleimide	4	100	15

Hence, considerable research has been undertaken into the further development of more efficient labelling methods for glycopeptide imaging agents. One method that has emerged is the labelling of peptides using [¹⁸F]-5-fluoro-5-deoxyribose ([¹⁸F]-FDR, **24**) through oxime linkages. Developed by Xiang-Guo Li and David O'Hagan from the University of St Andrews, [¹⁸F]-FDR is synthesised from a tosylated, protected furanoside by nucleophilic radiofluorination and deprotection (Scheme 1.5).¹¹⁴ Isolated in high purity, **24** can be incorporated into peptides bearing an oxime via furan ring opening, with 95% conversion of **24** to an oxime-linked ¹⁸F-radiolabelled glycopeptide observed (Scheme 1.5).¹¹⁴ Directly labelling the glycoside used prior to peptide conjugation, this method provides an alternative to the use of prosthetic groups, limiting the exposure of the radiolabelled glycoconjugate to harsh reaction conditions. One issue that remains with this method though is the potential formation of cis and trans (*E/Z*) isomers from peptide conjugation, a result of labelling via ring opening at the anomeric carbon of **24**.^{115,116} A relatively minor issue though, the promise of this strategy has

supported its wider usage in the fluorine-18 radiolabelling of peptides. Beyond this example though, significant attention is still being paid to approaches that could be utilized in the production of radiolabelled glycoconjugates encompassing fluorine-18 and other radiolabels commonly used in nuclear medicine.

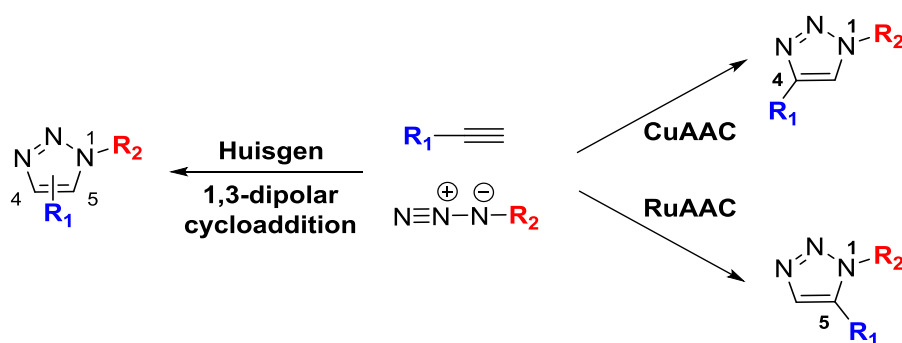


Scheme 1.5: Oxime-linkage method for the synthesis of ^{18}F -radiolabelled glycoconjugates developed by Li and O'Hagan.^{114–116}

1.5 The Copper Assisted Azide-Alkyne [3 + 2] Huisgen Cycloaddition (CuAAC).

1.5.1 Background and Mechanism

One method that has been widely exploited for its labelling potential is the copper-assisted azide-alkyne [3 + 2] cycloaddition (CuAAC). Initially reported separately in 2001 by the groups of Barry Sharpless and Valery Folkin from the Scripps Research Institute, and Morten Meldal from the Carlsberg Laboratory,^{117–119} the CuAAC reaction builds on the Huisgen 1,3-dipolar cycloaddition developed by Rolf Huisgen in 1961 to produce 1,2,3-triazoles from azide and alkyne precursors.¹²⁰ The catalysis of this reaction by Cu(I) species results in the selective production of 1,2,3-triazoles bearing a 1,4-substitution pattern (Scheme 1.6), allowing for the preparation of complex molecules from fairly simple synthons. The CuAAC reaction is often discussed alongside other modular ligation methods, with this field of reactions referred to collectively as “click chemistry”. Subsequently, as the CuAAC is the most popular of these reactions, it is often described as the quintessential “click” reaction.¹¹⁷

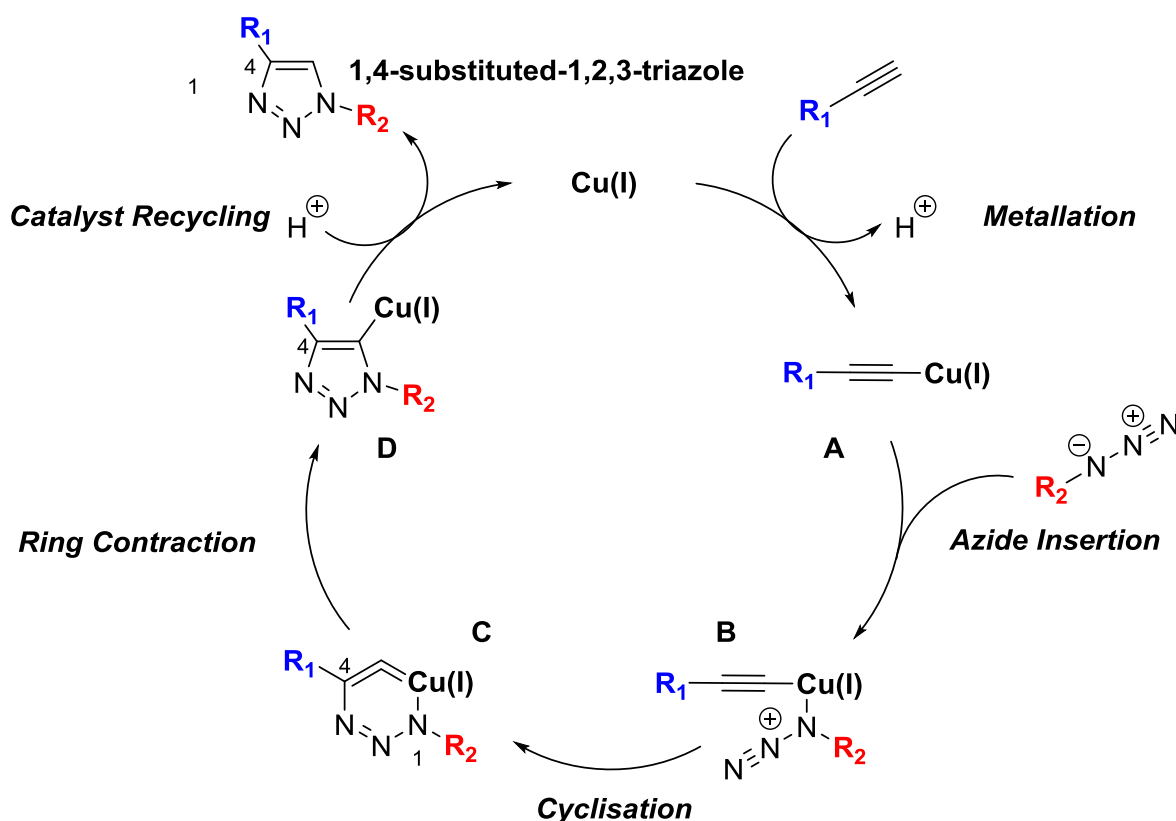


Scheme 1.6: Regioselective comparison of the Huisgen 1,3-dipolar azide-alkyne cycloaddition to the copper-assisted and ruthenium-assisted azide-alkyne cycloadditions (CuAAC and RuAAC).^{118,120,121}

Mechanistically, metallation of an alkyne by Cu(I) ions, results in the Cu-alkyne intermediate A and the release of a proton (Scheme 1.7). Next, the dissociation of ligands associated with the Cu(I) ion (not shown) and secondary metallation of an azide-bearing group to the copper ion via the proximal nitrogen of the azide, result in the formation of the alkyne-Cu-azide intermediate B (Scheme 1.7). Within close proximity to each other, the distal nitrogen of the azide group of B undergoes intramolecular attack of the distal carbon (C2) of the alkyne, resulting in the unusual six-membered ring intermediate C (Scheme 1.7). Under immense steric strain, a rearrangement occurs whereby the six-membered ring undergoes ring contraction, resulting in a 5-membered triazole ring with the Cu(I) bound to the 5-position (D, Scheme 1.7). Subsequently, exchange between the Cu(I) ion and a proton results in the formation of a 1,4-substituted-1,2,3-triazole, with recycling of the Cu(I) species into the catalytic cycle allowing for the propagation of the reaction (Scheme 1.7).¹²²

Alternatively to the CuAAC reaction, the selective formation of 1,5-substituted-1,2,3-triazoles may also be achieved, with ruthenium complexes such as pentamethylcyclopentadienylbis(triphenylphosphine)ruthenium(II) chloride $[\text{Cp}^*\text{RuCl}(\text{PPh}_3)_2]$.¹²¹ This variation of the Huisgen 1,3-dipolar cycloaddition is known as the ruthenium-catalysed azide-alkyne cycloaddition (RuAAC, Scheme 1.6).¹²¹ The rate-limiting steps in both the CuAAC and RuAAC reactions are the specific formation of the triazole ring, with the transformation of 6-membered energetically unfavourable metallocycles resulting in a significant increase in reaction kinetics compared to the Huisgen 1,3-dipolar cycloaddition. In particular, the CuAAC reaction experiences a 10^7 to 10^8 -fold increase in the overall rate of reaction at room temperature compared to the uncatalysed reaction.¹²² Considering that the CuAAC “click” reaction utilizes a catalytic

quantity of Cu(I) ions, and is susceptible to further rate enhancements through the modulation of catalyst loading (1-10%) and temperature, the CuAAC “click” reaction represents a flexible, efficient and quick method for the conjugation of different chemical entities.¹²²

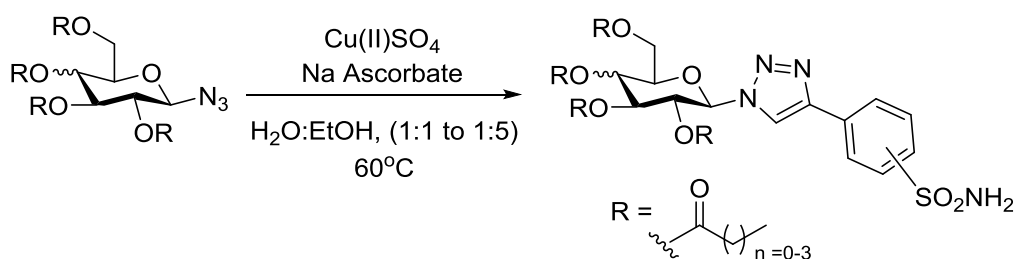


Scheme 1.7: Proposed mechanism for the formation of 1,4-substituted-1,2,3-triazoles via the CuAAC “click” reaction.¹²²

1.5.2 Utilization of the CuAAC “Click” Reaction with Carbohydrates

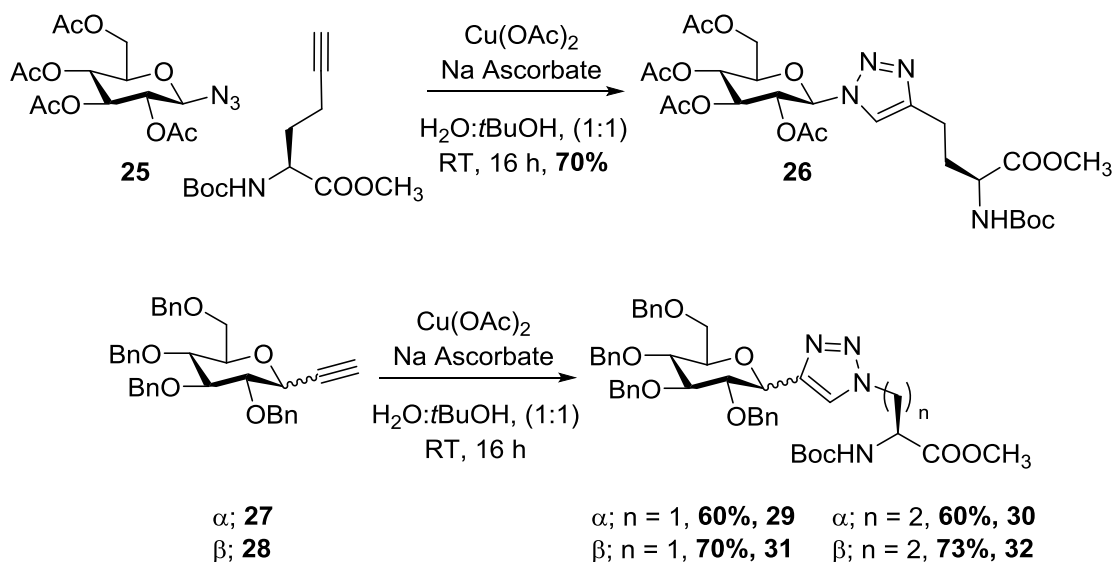
As a result of the convenience of the CuAAC “click” reaction in the conjugation of small molecules, its use in the development of new carbohydrate-containing entities

has been extensive.^{123–125} Azides are widely used in carbohydrate chemistry, with the first examples of glycosyl azides (glycosides bearing azides at the anomeric position) produced in 1930, pre-dating both the discovery of the CuAAC “click” reaction and the Huisgen 1,3-dipolar cycloaddition.¹²⁶ Subsequently, glycosyl azides comprise the bulk of the literature utilizing the CuAAC “click” reaction in carbohydrate chemistry, with their ease of access through anomeric azidation allowing for their efficient derivatization with a plethora of alkyne-containing molecules.¹²⁷ The ability to efficiently produce diverse libraries has supported their use in medicinal chemistry, where the utility of this reaction has enabled the production of diverse libraries of biologically active compounds. This has been illustrated previously by those such as Poulsen and co-workers, who successfully demonstrated the utility of the CuAAC “click” reaction in the generation of multiple libraries of sulphonamide-containing glycoconjugates.^{128–130} Utilizing CuSO₄ and sodium ascorbate to generate Cu(I) from Cu(II) *in situ* for catalysis of the “click” reaction, the synthesised glycoconjugates inhibit cancer-associated carbonic anhydrase (CA) enzymes at nanomolar concentrations (Scheme 1.8).^{128,129}



Scheme 1.8: Synthesis of carbonic anhydrase inhibitors by Poulsen and co-workers, utilizing the CuAAC “click” reaction.^{128–130}

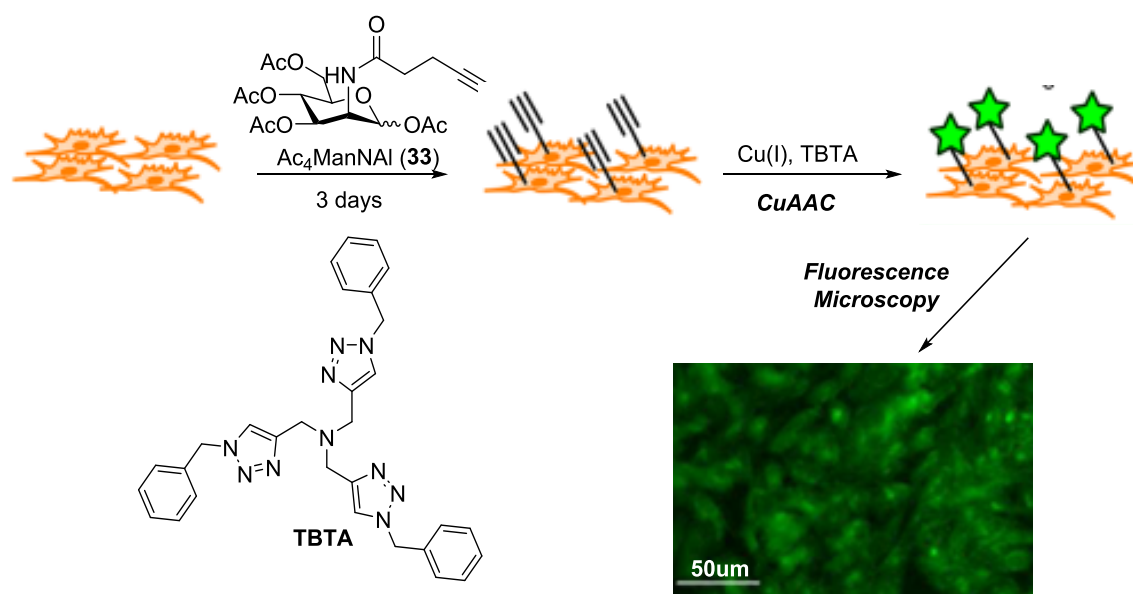
Moreover, the use of glycosyl azides and the CuAAC “click” reaction has been investigated in the development of new glycoconjugation methods with biologically relevant molecules, including amino acids. Rutjes and co-workers have illustrated the versatility of glycoconjugates in mimicking linkages found in nature. Linking glycosyl azide (**25**) and alkyne-containing amino acids/dipeptides together using the CuAAC “click” reaction, they have produced triazole-linked glycosylamino acids and glycopeptides such as **26** (Scheme 1.9).¹³¹ Alternatively, triazole-linked glycosylamino acids utilizing glycosides bearing C-linked alkynes at the anomeric centre have also been developed. These include the α - and β -acetylenic glucose derivatives **27** and **28**, which were linked to azide-bearing amino acids to produce the triazole-linked glycosylamino acids **29-32** (Scheme 1.9).¹³¹



Scheme 1.9: Synthesis of triazole-containing glycosylamino acids via the CuAAC “click” reaction.¹³¹

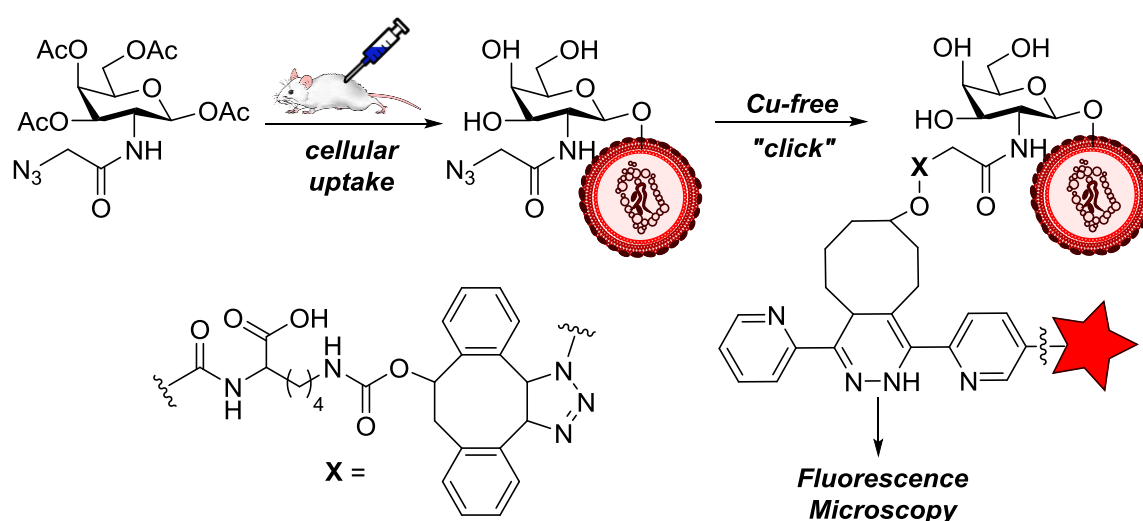
In addition to these methods that utilize carbohydrates bearing azides or alkynes directly conjugated to the sugar backbone, a number of examples have been produced

where these moieties are linked to a respective carbohydrate via a prosthetic group. This ligation strategy has found particular use in cellular imaging, where glycosides may be fed to an organism (or cells) and subsequently expressed in cell surface glycoproteins.¹³² This work has been pioneered by Carolyn Bertozzi and co-workers, who have utilized acetylated mannosamine derivatives bearing a 2-linked pentynoyl group (such as **33**) to label Chinese hamster ovary (CHO) cells.¹³³ Taken up by these cells and converted to alkynylneuraminic acid, these alkynyl-containing species are incorporated into cell-surface glycoproteins (Scheme 1.10). When cells bearing these groups are washed with Cu(I) species, a chelating ligand that specifically stabilizes the Cu(I) oxidation state (TBTA, Tris[(1-benzyl-1*H*-1,2,3-triazol-4-yl)methyl]amine) and an azide-bearing fluorescein, the CuAAC “click” reaction ensues. This reaction produces cells labelled by triazole-linked fluorosceins, that can be visualized using fluorescence microscopy (Scheme 1.10).¹³³



Scheme 1.10: *In vivo* CuAAC “click” reaction of Chinese hamster ovary (CHO) cells fed **33**, allowing for their visualization under fluorescence microscopy.¹³³

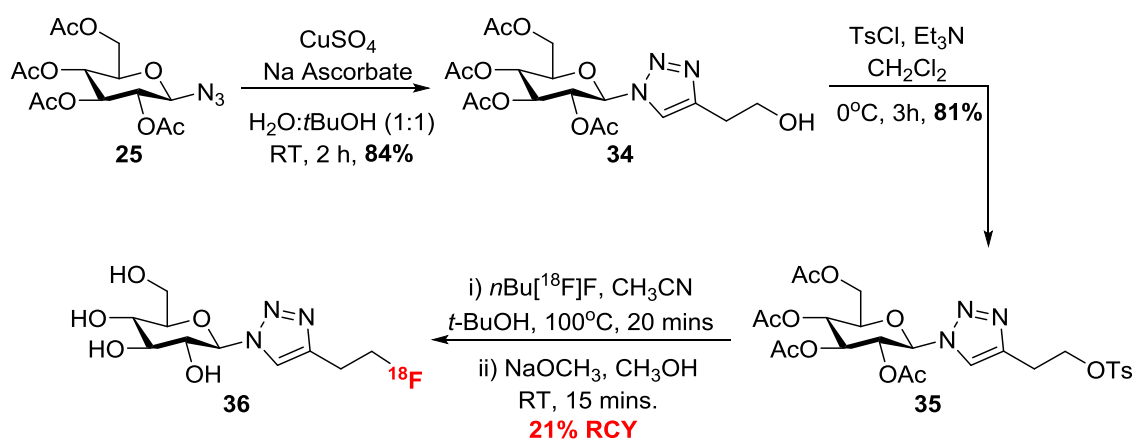
A consideration in the usage of this method, is the impact of Cu toxicity to the organism, resulting from the potential generation of reactive oxygen species (ROS).¹³⁴ Accordingly, methods that limit the need for the use of copper catalysis in the formation of triazoles have been investigated, with the most well known utilizing strained alkynes in the formation of triazole-linked glycoconjugates. Again pioneered by Carolyn Bertozzi and co-workers, this approach has been widely used in the labelling of cell surface glycoproteins.¹³⁵ The utility of these synthons is exemplified by the work of Kevin Brindle and co-workers at the University of Cambridge, who have used a strain-promoted “click” approach to label mouse tumour cells.¹³⁶ Following the injection of a galactosamine derivative bearing an azide group into live mice, incubation of the mice and cellular uptake of the probe, resulted in incorporation and externalization of it in cell-surface glycoproteins.¹³⁶ Subsequent injection of a strained cyclooctyne derivative resulted in Cu-free triazole formation, which upon further conjugation allowed for the visualization of labelled tumour cells by fluorescence microscopy (Scheme 1.11).¹³⁶



Scheme 1.11: *In vivo* strain-promoted Cu-free “click” reaction of mouse tumour cells fed an azidogalactosamine, allowing for their visualization under fluorescence microscopy.¹³⁶

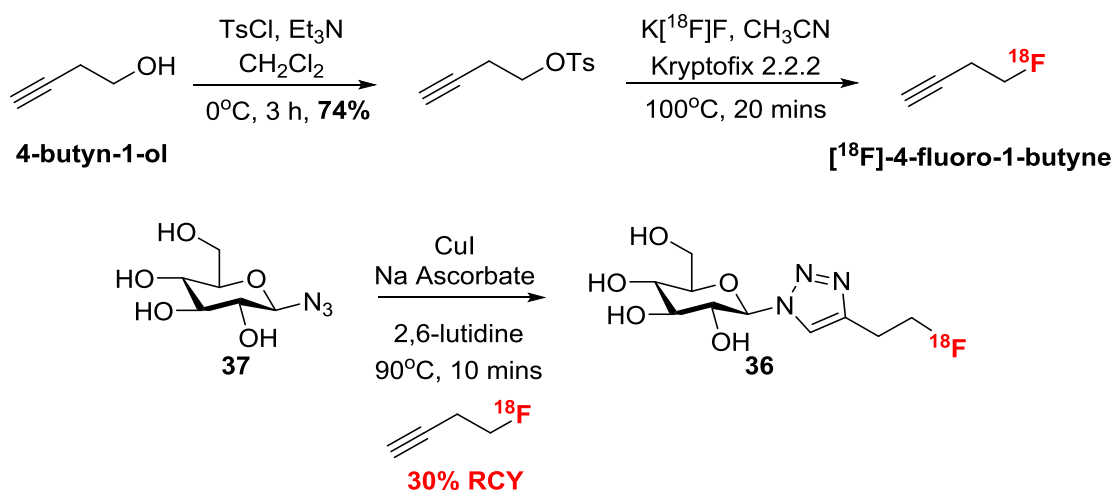
1.5.3 Fluorine-18 Labelling of Carbohydrates utilizing the CuAAC “Click” Reaction

Based on the utility of the CuAAC “click” reaction in the synthesis of glycoconjugates, the potential of this method to develop biologically-relevant probes labelled with fluorine-18 has been evaluated. Initial work in this area by Kim and co-workers focussed on the production of ^{18}F -radiolabelled derivatives of D-glucose.¹³⁷ Starting from 2,3,4,6-tetra-*O*-acetyl- β -D glucopyranosyl azide (**25**), a CuAAC “click” reaction with 3-butyn-1-ol was performed, resulting in the 1,4-triazole containing glycoside **34**. Subsequent tosylation of the primary alcohol group (**35**), radiofluorination using $n\text{Bu}_4\text{N}[^{18}\text{F}]\text{F}$ and Zemplén deacetylation resulted in the ^{18}F -radiolabelled triazole-bearing glycoside **36** in 21% radiochemical yield from **25** (Scheme 1.12).¹³⁷



Scheme 1.12: Synthesis of ^{18}F -radiolabelled glucose derivative **36** from direct radiofluorination of a triazole-containing derivative **35**.¹³⁷

Using S_N^2 nucleophilic displacement of a tosylate group to introduce fluorine-18, the synthesis of **36** directly from β -D-glucopyranosyl azide (**37**) has also been performed, with the CuAAC “click” reaction of [^{18}F]-4-fluoro-1-butyne (produced from 4-butyne-1-ol, Scheme 1.13) and **37** resulting in the ^{18}F -radiolabelled triazole-bearing glycoside **36** in 30% radiochemical yield (Scheme 1.13).¹³⁷ This efficiency of the CuAAC “click” radiofluorination has also been replicated in our research group, using 2-deoxy-2-*N*-acetyl-3,4,6-tri-*O*-acetyl- β -D-glucopyranosyl azide and [^{18}F]-4-fluoro-1-butyne, resulting in the isolation of the desired radiolabelled glycoside in 22% radiochemical yield (unoptimised).¹³⁸ In comparison to the acylation and imidation methods previously described, the radiochemical yield gained for **36** represents a decrease from those previously observed, with the high volatility of [^{18}F]-4-fluoro-1-butyne (b.p 45°C) believed to be a major contributor to these results. Thus, the use of less volatile alkynes is key to the utilization of this methodology for ^{18}F -radiolabelling.

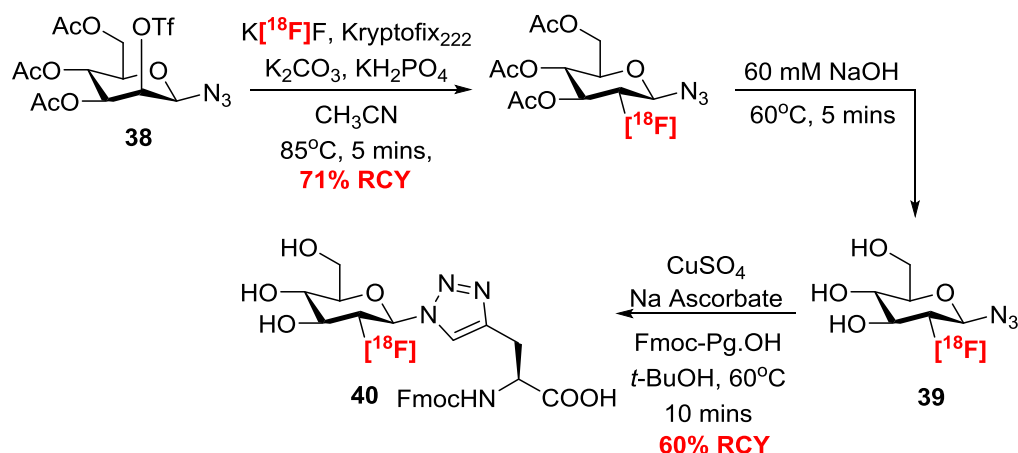


Scheme 1.13: Synthesis of ^{18}F -radiolabelled glucose derivative **36** from CuAAC “click” reaction of azido sugar **37** with a ^{18}F -fluorinated alkyne.¹³⁷

The strategy described above allows the labelling of sugar molecules, but is not amenable to the ^{18}F -radiolabelling of peptide-based molecular probes. Furthermore, the efficiency of this method in the ^{18}F -radiolabelling of the protected azido sugar **25** or unprotected azido sugar **37** is much lower than that observed in the production of [^{18}F]FDG (~50% RCY).⁷⁹ Because of this, alternative methods that utilize the CuAAC “click” reaction in the synthesis of ^{18}F -radiolabelled glycoconjugates for use as molecular probes have been evaluated.

1.5.4 Fluorine-18 Labelled Glycoconjugates Synthesised using the CuAAC “Click” Reaction

Following in the footsteps of probes such as [^{18}F]FDG, in which fluorine-18 is introduced by nucleophilic displacement of a mannosyl triflate, methods that utilize glycosides radiolabelled in this way have been investigated.¹³⁹ The versatility of the CuAAC “click” reaction as a ligation method has resulted in the development of [^{18}F]-radiolabelled glycoconjugates linked via a triazole at the anomeric centre of the glycoside. Initially developed by Olaf Prante and co-workers, preliminary nucleophilic radiofluorination of 2-trifluoromethanesulfonyl-3,4,6-tri-*O*-acetyl- β -D-mannopyranosyl azide (**38**) using $\text{K}[^{18}\text{F}]\text{F}$ and Kryptofix 2.2.2 resulted in the production of 2-[^{18}F]-2-deoxy- β -D-glucopyranosyl azide (**39**) in 71% radiochemical yield (Scheme 1.14).¹³⁹ An azide-bearing derivative of [^{18}F]FDG, deprotection of the acetyl groups followed by CuAAC “click” reaction with an Fmoc-protected L-propargylglycine resulted in the production of the ^{18}F -radiolabelled glycosylamino acid **40** in 60% radiochemical yield from **39** (Scheme 1.14).¹³⁹



Scheme 1.14: Synthesis of ^{18}F -radiolabelled triazole-containing glycosylamino acid **40** in 60% radiochemical yield via the CuAAC “click” reaction.¹³⁹

The production of **39** and its subsequent conjugation via the CuAAC “click” reaction provided impetus for the further utilization of this methodology in the synthesis of $[^{18}F]$ -labelled glycoconjugate probes. Building on this work, Prante and co-workers utilized **39** to glycosylate and radiolabel a propargylglycine-bearing cyclic RGD-containing peptide, producing the radiolabelled derivative **41**, which in addition to other $[^{18}F]$ -glycosylated derivatives have been evaluated for their diagnostic potential in the quantification of angiogenesis (Figure 1.11).^{140,141} In addition, this methodology has been extended to the development of probes targeting neurotensin receptor 1 (NST1), a G-protein coupled receptor upregulated in a number of tumour types, including those of the breast, lung, pancreas and prostate.¹⁴² Examples of probes developed include those containing both peptidic and non-peptidic scaffolds, with the non-peptidic derivative **42** (Figure 1.11) displaying low nanomolar affinity for NST1, and 70-fold selectivity for this receptor over the related neurotensin receptor 2 (NST2).¹⁴²

Such has been the worth of this method in the development of radiolabelled glycoconjugates, that it has been adopted by researchers investigating other biological

targets. Schibli and co-workers have utilized **39** and the CuAAC “click” reaction to target the folate receptor.¹⁴³ A membrane-anchored protein that binds folic acid as its natural substrate, the folate receptor is upregulated in a variety of different tumour types in addition to a number of autoimmune and inflammatory diseases, positioning it well as a diagnostic target.¹⁴³ Subsequently, the CuAAC “Click” reaction of **39** with a propargylglycine-bearing folate derivative, resulted in the [¹⁸F]-glycosylated derivative **43** (Figure 1.11), which showed high affinity for the folate receptor.

Beyond the production of diagnostic probes (such as **43**), the CuAAC “click” reaction has also been used in the evaluation and analysis of glycoprotein interactions. This is exemplified by the group of Benjamin Davis at the University of Oxford, who have selectively synthesised proteins bearing fluorosugars. Incorporating non-natural amino acids (such as L-homopropargylglycine (Hpg)) into proteins,¹⁴⁴ these residues may participate in the CuAAC “click” reaction in mild conditions, with linkage at these sites providing a mechanism for the production of [¹⁸F]-radilabelled glycoproteins. This is illustrated by the triazole-linked glycoprotein **44**, that was formed by the CuAAC “click” reaction of **39** and the protein SsβG, a beta-glycosidase derived from the hyperthermophilic bacteria *Sulfolobus solfataricus* (Figure 1.11).¹⁴⁴

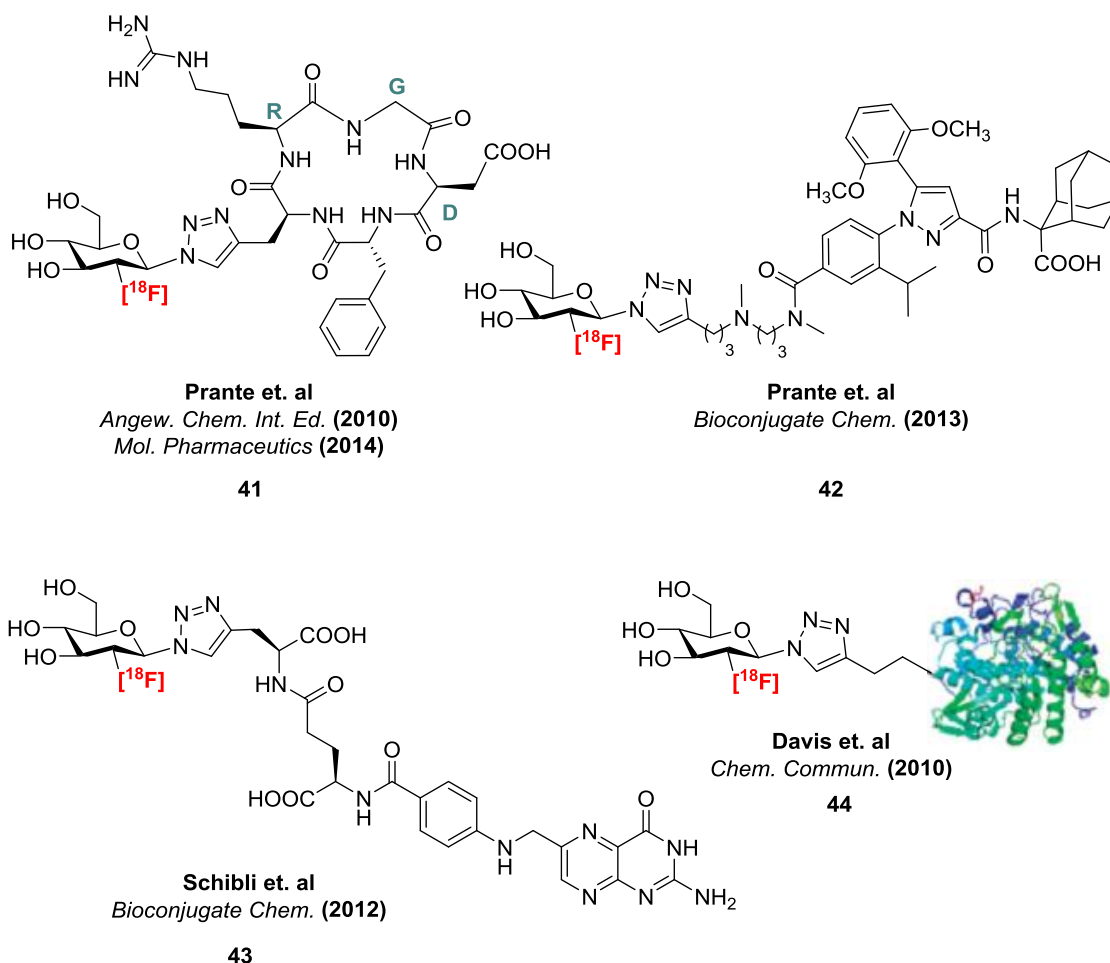
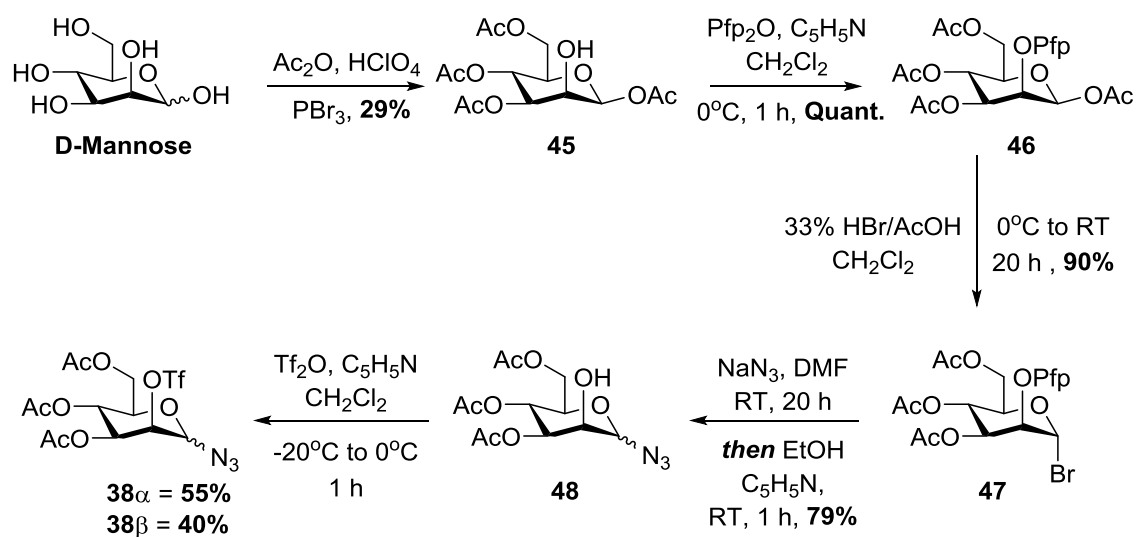


Figure 1.11: ^{18}F -containing glycopeptides radiolabelled using 39 and the CuAAC “click” reaction.^{140–144}

The utilization of azide-bearing [^{18}F]-labelled sugars such as 39 have resulted in the development of diagnostically-relevant [^{18}F]-labelled glycoconjugate probes. However, the current methodology for the synthesis of the required fluorosugars (39), and ligation to the desired peptide or protein using the CuAAC “click” reaction, present some challenges. Firstly, access to 39 from a commercially-available starting material in high yield is difficult, with the production of the precursor 38(β -anomer) from D-mannose yielding only 8.2% yield over 5 synthetic steps (Scheme 1.15).¹³⁹ Much of this is due to the need for the use of an orthogonal protection strategy, allowing for the

selective conversion of the mannosyl triflate derivative **38**(β -anomer) into the glucosyl fluoride.¹³⁹ Also, the requirement of a β -azide that can undergo the CuAAC “click” reaction significantly lowers the efficiency of this process, with the presence of a pentafluorophenyl (Pfp) group in **46** and **47** prior to azidonation significantly decreasing the selectivity of this reaction, producing both α - and β -anomers of **48** (Scheme 1.15).



Scheme 1.15: Synthesis of 2-OTf-containing derivative **38** from D-mannose, a key precursor in the synthesis of 2-[¹⁸F]fluoro-2-deoxy- β -D-glucopyranosyl azide (**39**).¹³⁹

However, one of the largest issues with the current methodology is the need for an alkyne group in the macromolecule or peptide to be labelled. Whilst in the previously described examples **41-43** this approach is used efficiently, it isn't really appropriate for use in the synthesis of larger peptides and proteins. As illustrated by the work of Davis and co-workers (**44**), in order to introduce an alkyne-bearing amino acid changes to the peptide or protein of interest at specific positions in the amino acid sequence are required.¹⁴⁴ This represents both a synthetic and structural challenge, as the introduction

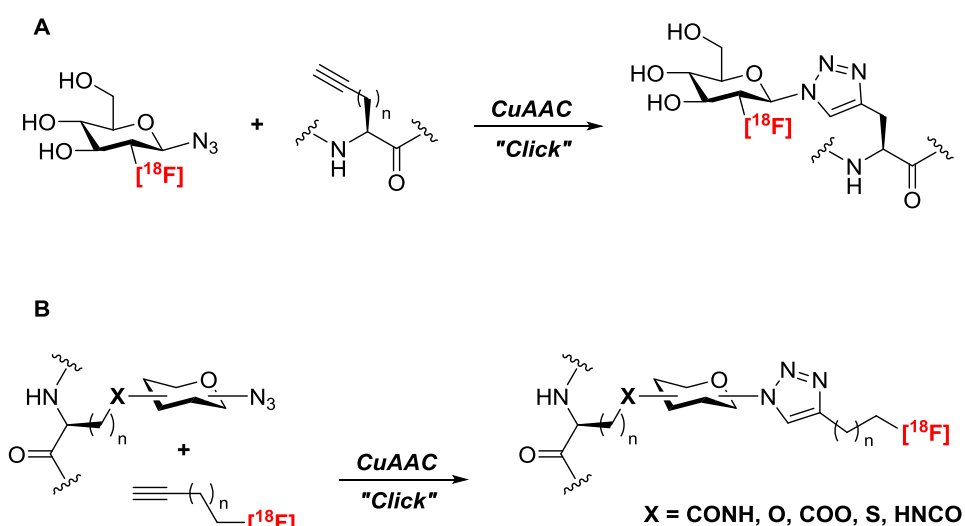
of the required alkyne-containing amino acid must be performed in a way that is synthetically efficient. Also, it is important that the modifications made do not alter the structural characteristics of the peptide or protein in question, maintaining the biological activity of the probe.

1.5.5 Alternative Strategies for the Fluorine-18 Labelling of Glycoconjugates using the CuAAC “Click” Reaction

Considering the potential complications of this approach and how these may affect the broader utilization of this strategy, the development of an alternative method to the labelling of glycoconjugates via the CuAAC “click” reaction is warranted. We propose that an alternative methodology that utilizes azide-bearing glycosides that can be readily conjugated to proteinogenic amino acids would be advantageous. Containing an azide group, these glycosides would by definition be azidosugars. If a number of azidosugars were produced that contained different functional groups forming linkages with amino acids (such as carboxylic acids, amines, leaving groups, etc), these could be incorporated into peptides or conjugates (Scheme 1.16). The use of a protecting group strategy utilizing acetyl protecting groups would allow for the installation of the required azide groups, in addition to amino acid coupling. Simple and easily installed, these groups also have the benefit of being easily cleaved in the cellular environment, due to pH and the presence of intracellular esterases.¹⁴⁵

These glycoconjugates could thus be described as being “clickable,” with the corresponding free azide group of the glycoside available for use in the CuAAC “Click”

reaction. In conjunction with alkynes akin to the previously discussed [^{18}F]-4-fluoro-1-butyne, this could be utilized to produce ^{18}F -radiolabelled glycoconjugates (Scheme 1.16).¹³⁷ This represents a methodology that allows for the introduction of fluorine-18 into a glycoconjugate in the final step, an important feature when working with radioisotopes with short half lives. Also, as non-proteinogenic amino acids are not required, it allows for the use of unmodified native peptides and proteins that may display ideal radiopharmaceutical properties, thus limiting the need for the installation of prosthetic groups (such as alkynes) for conjugation (Scheme 1.16).



Scheme 1.16: Comparison of methods that may be used to produce ^{18}F -radiolabelled glycosylamino acids using the CuAAC “click” reaction. **A:** Previously described strategy developed by Prante and co-workers, **B:** Postulated method using “clickable” glycosylamino acids radiolabelled by a [^{18}F]-fluoroalkyne using the CuAAC “click” reaction.

Therefore, in order to produce ^{18}F -radiolabelled glycoconjugates of this form, “clickable” glycosylamino acids consisting of an azidosugar linked to an amino acid

must be produced. However, an evaluation of the relevant literature has highlighted a clear lack of structures of this form. Of those previously synthesised, many are ether-linked conjugates between azidosugars and hydroxyl-containing amino acids, including serine, threonine, tyrosine and hydroxyproline, and as demonstrated by the threonine-linked derivatives **49** and **50** (Figure 1.12).^{146,147}

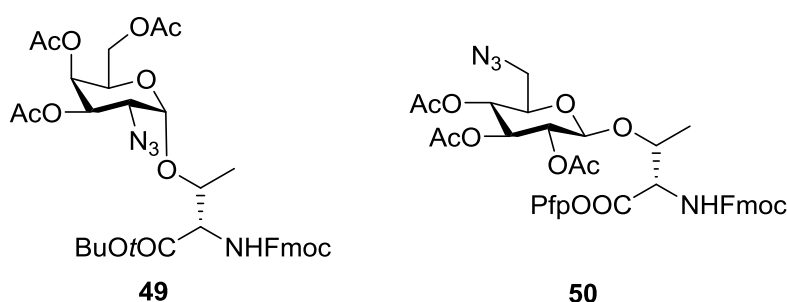


Figure 1.12: Threonine-linked derivatives 50 and 51, examples of “clickable” glycosylamino acids.^{146,147}

Interestingly, the formation of glycoconjugates between azidosugars and other amino acids used in the synthesis of glycoconjugates, including serine (Ser; via ester linkages), lysine (Lys), aspartic acid (Asp), glutamic acid (Glu) and cysteine (Cys) be performed. Also, the majority of “clickable” glycoconjugates previously synthesized either pre-date the development of the CuAAC “click” reaction, or instead have been used as precursors in the synthesis of other glycoconjugates, including *N*-acetylglycosylamino acids.^{146,147} Thus, there lies the opportunity to develop and synthesise a host of “clickable” glycosylamino acids and demonstrate the applicability of the CuAAC “click” reaction in their further derivatization. Conjugated together via ester linkages initially, before being utilized in the formation of conjugates formed through more stable amide and thioether linkages, the synthesis of these derivatives could then be extended to other glycopeptides, neoglycopeptides and glycoconjugates.

The development of this approach would further expand the use of the CuAAC “click” reaction in the production ^{18}F -radiolabelled glycoconjugates for nuclear imaging.

1.6 Project Aims

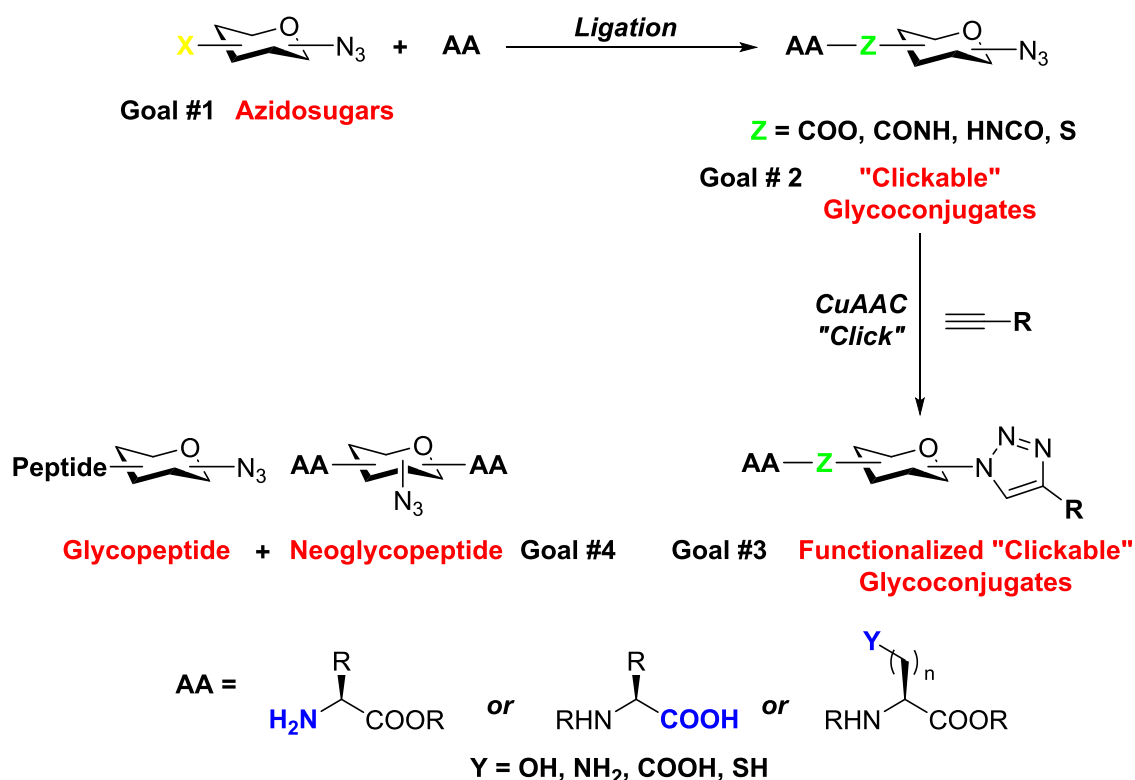
The CuAAC “click” reaction represents a useful method for the synthesis of ^{18}F -radiolabelled glycoconjugates. Utilizing “clickable” glycosylamino acids and glycopeptides, this method would allow for the efficient production of a range of ^{18}F -radiolabelled diagnostic probes. In order to evaluate this approach, azidosugars that can ligate to a number of different proteinogenic amino acids must be developed and optimised (Scheme 1.17). Subsequent ligation would produce the desired “clickable” glycoconjugates, which would be open to evaluation with the CuAAC “click” reaction (Scheme 1.17). The success of this process may then be ported to the synthesis of “clickable” glycopeptides and neoglycopeptides, paving the way for the development of ^{18}F -radiolabelled glycoconjugates for use as probes in nuclear imaging (Scheme 1.17).

Therefore, the specific aims of this project were:

1. To synthesise a range of different azidosugars (sugar azido acids and azidoglucopyranosyl amines) that could form linkages with proteinogenic amino acids commonly used in bioconjugation (serine, lysine, aspartic/glutamic acid, homocysteine, etc.) (Goal 1, Scheme 1.17).
2. To synthesise a range of “clickable” glycoconjugates bearing ester, amide and thioether linkages to various amino acid residues (Goal 2, Scheme 1.17).

3. To demonstrate the utility of the synthesised glycoconjugates in the CuAAC “click” reaction (Goal 3, Scheme 1.17).
4. To extend this methodology towards the synthesis of glycopeptides and neoglycopeptides that may be functionalized via the CuAAC “click” reaction (Goal 4, Scheme 1.17).

In Chapter 2, 3 and 4, the synthesis and functionalization of “clickable” glycoconjugates will be discussed. These chapters will focus on examples linked to serine, lysine and α -amino groups (Chapter 2), aspartic acid and glutamic acid (Chapter 3) and homocysteine (Chapter 4). In Chapter 5, the development of methods toward the synthesis and functionalization of “clickable” neoglycopeptides will also be discussed.



Scheme 1.17: General scope of the synthesis and functionalization of “clickable” glycoconjugates performed in this project.

Chapter 2 : Synthesis and Functionalization of Serine, Lysine and α -Amino Linked “Clickable” Glycoconjugates.

Carbohydrates that can be incorporated into peptides and functionalized using the CuAAC “click” reaction have a wide range of potential applications. In the following chapter, the synthesis and functionalization of serine, lysine and α -amino linked “clickable” glycoconjugates will be described. Conjugates of sugar azido acids linked to proteinogenic amino acids are useful compounds that can be incorporated into peptides and are also freely available for functionalization using the CuAAC “click” reaction.

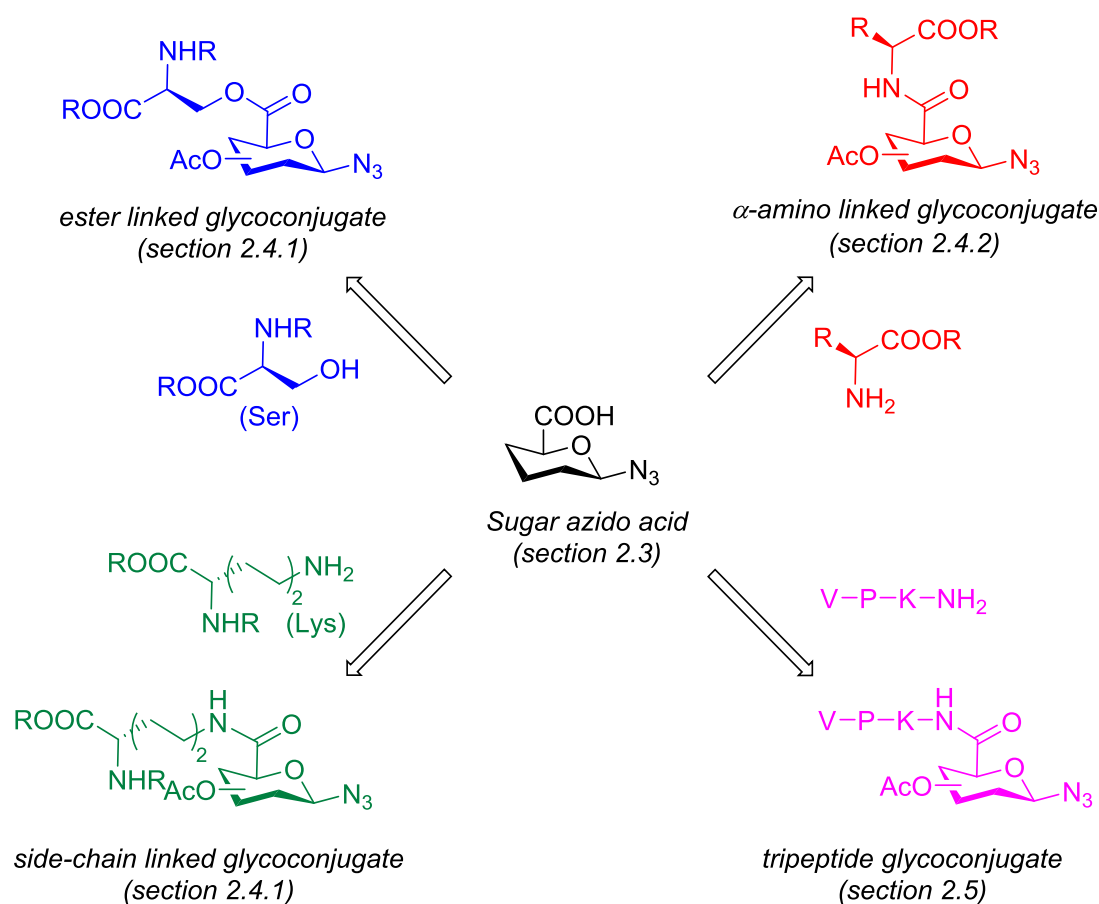
2.1 Synthetic Rationale

Azidosugars are highly amenable to the CuAAC “click” reaction. If the same azidosugars could also be coupled to amino acid residues then they would have great potential for use in the synthesis and labeling of glycopeptides.¹³⁹ However, currently there is limited literature precedence on the development of azidosugars that can both couple to amino acids or peptides, and also be free to undergo the CuAAC “click” reaction. Hence, a methodology that provides a comprehensive, wide-ranging approach

towards the introduction (and labeling) of carbohydrates into linear and/or cyclic peptides would be highly advantageous.

Previously in our research group, work had been performed towards the development of acid-labile cytotoxic isatin prodrug models for conjugation to the cancer relevant protein plasminogen activator inhibitor-2 (PAI-2), whereby the acid-labile prodrug was tethered by a carboxylic acid group to a N^α /C-protected lysine residue.^{148,149} Conjugates that are tethered together through an amide linkage hold a distinct advantage over those formed through other methods, particularly due to their strength and chemical resistance under a wide variety of conditions, and ease of synthesis through peptide coupling conditions.¹⁵⁰ Whilst conjugates to lysine may be linked via its N^ϵ -sidechain, it could be envisaged that amino acid residues containing chemically inert sidechains may also form amide linkages, through coupling to carboxylic acid containing moieties through their terminal α -amino group (Scheme 2.1). Moreover, using this coupling strategy could result in conjugates with other amino acid residues commonly used as linkers in peptide conjugation and labeling, including ester linkages when coupled to the amino acids serine or threonine.

Therefore, if a glycosyl coupling partner that included a carboxylic acid group (uronic acid); such as a sugar azido acid was employed, and coupled to a variety of different proteinogenic amino acids, this could produce a library of “clickable” glycoconjugates that could be employed in the CuAAC “click” reaction (Scheme 2.1). The synthesis and functionalization of conjugates of this type would provide further insight into the feasibility of this approach in producing glycoconjugates that could find future utility in the synthesis and labeling of glycopeptides (Scheme 2.1).



Scheme 2.1: Proposed scheme for the synthesis of "clickable" glycoconjugates.

2.2 Initial Synthetic Targets

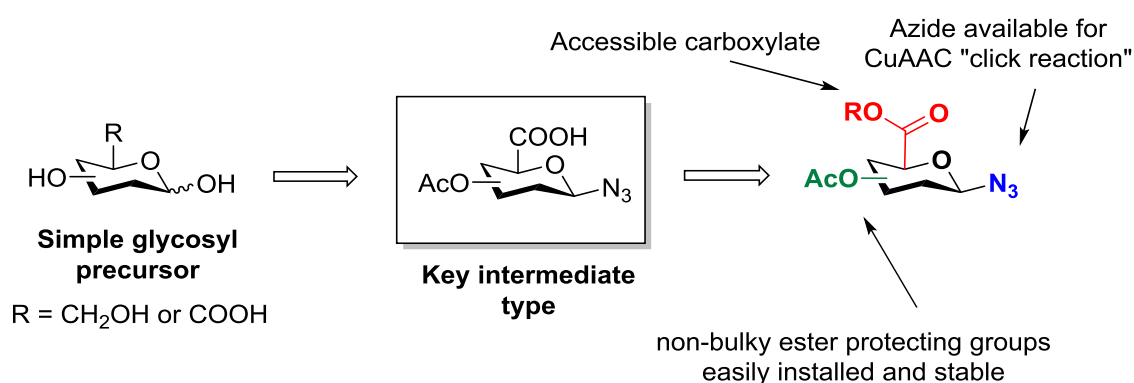
2.2.1 Conjugate Criteria

In order to synthesize a library of diverse “clickable” glycoconjugates, it was recognized that a few key design principles were required. The synthetic approach undertaken should be:

- Divergent in nature, allowing for the production of a variety of different “clickable” glycosyl-amino acids from one or two precursor molecules, and;

- Synthetically efficient, with easy installation and access to the azide and carboxylic acid functional groups required for coupling and the CuAAC reaction.

Whilst not a definitive requirement, it was also decided that the glycosides used would be pyran-based (6-membered ring). By using a pyran ring as a scaffold, it would ultimately leave the 6-position as the most synthetically viable site for the introduction of the required carboxyl group. This is an attractive option, allowing the carboxyl group to be introduced via oxidation of a 6-OH group. Alternatively, it would be highly advantageous to utilize uronic acid precursors in which the carboxylic acid is already installed if possible. If the azido group of the sugar azido acid was installed at the anomeric centre, and ester protecting groups such as acetyl (OAc) groups were utilized, this would provide a versatile, stereoselective method for the synthesis of sugar azido acids. Additionally, this methodology would be portable, and hence could be used in the synthesis of sugar azido acids based on different glycosyl isomers (Scheme 2.2).



Scheme 2.2: Key design principles required in the synthesis of "clickable" glycoconjugates, utilizing a uronic acid precursor.

2.2.2 Synthetic Approaches

Based on the criteria described in section 2.2.1, a review of sugar azido acids reported in the literature was undertaken. To date, all sugar azido acids previously synthesized can be classified into one of four different stereochemical isomer classes; *glc*,¹⁵¹ *gal*,¹⁵² *manno*¹⁵³ or *allo*¹⁵³ (Figure 2.1), with a β -configuration at the anomeric position the most common. Of these, sugar azido acids based on D-glucuronic acid were the most prominent, with multiple methods previously used in the synthesis of D-glucuronic acid based derivatives with either α - or β -stereochemistry present at the anomeric centre. Hence, commercially available D-glucuronic acid was employed as the scaffold for the synthesis of the sugar azido acids described herein.

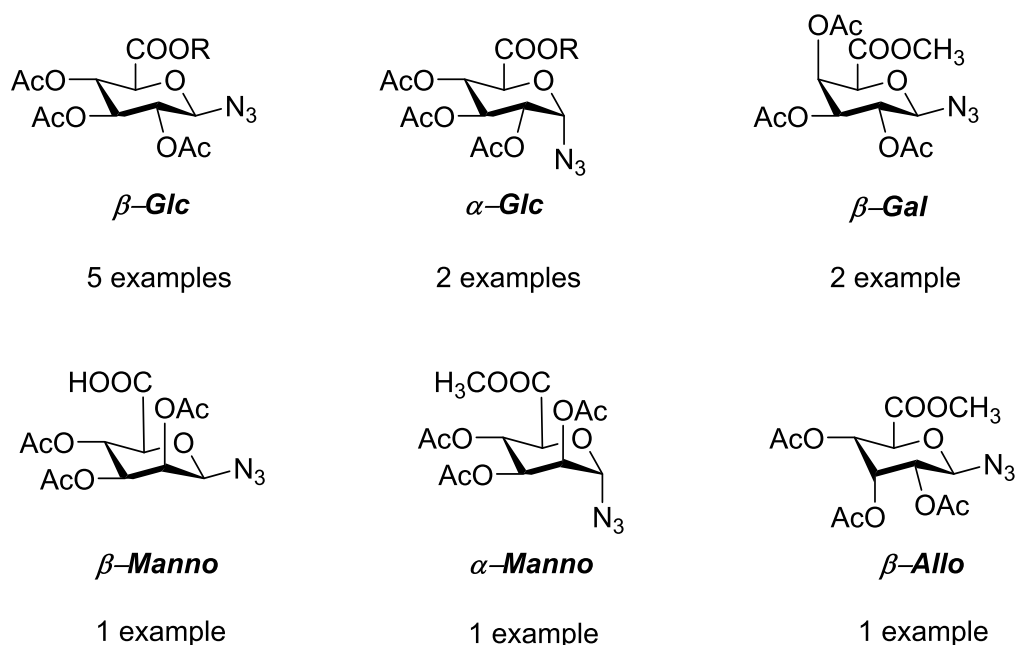


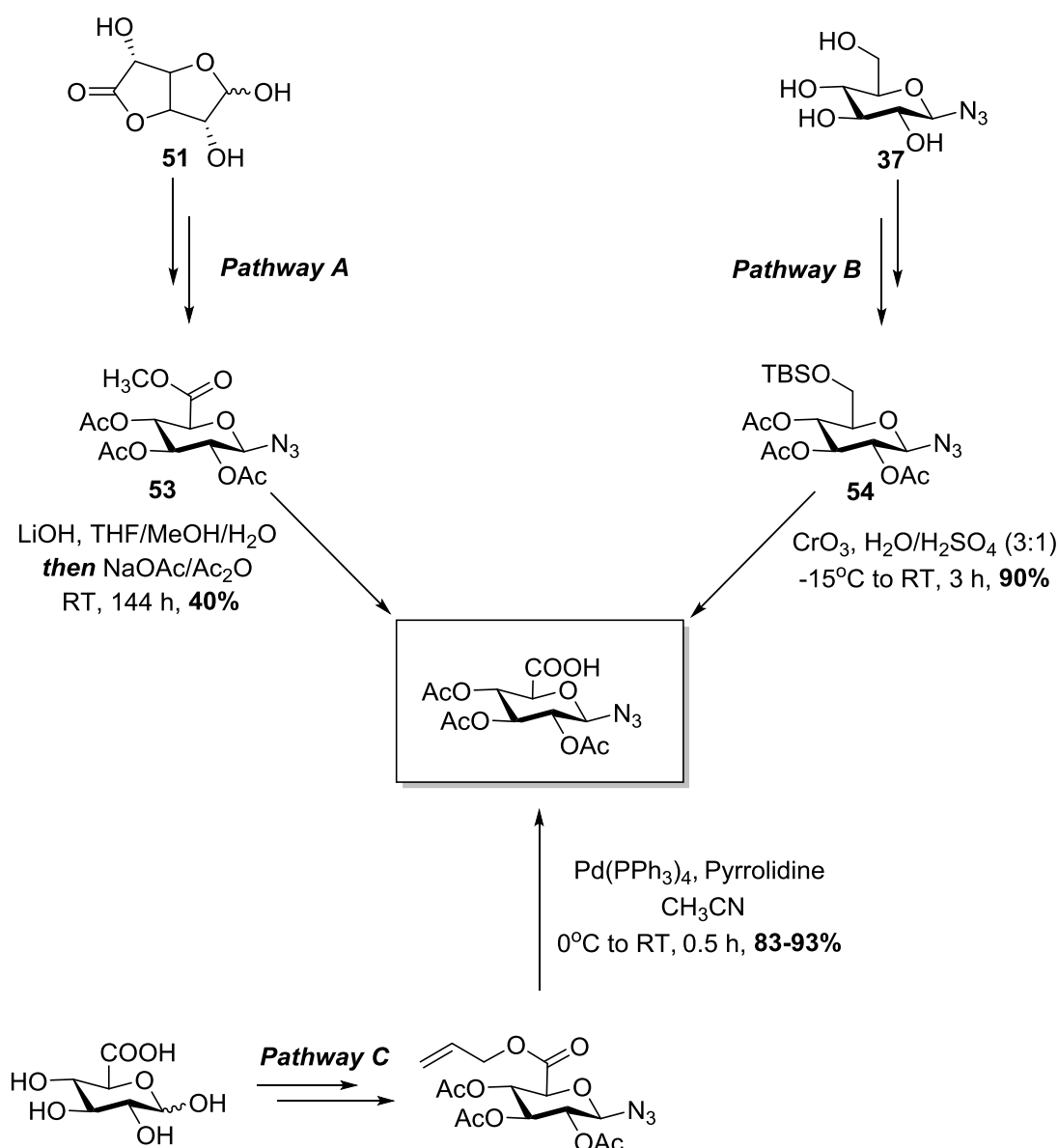
Figure 2.1: Examples of sugar azido acids previously reported in the literature.^{151–153}

The selection of D-glucuronic acid-based derivatives was further rationalized by the prominent role of D-glucuronic acid in living systems, such as glucuronidation described in Chapter 1.⁵³ D-Glucuronic acid is also present as a constituent in a number of different biologically relevant glycosaminoglycans, including hyaluronic acid and chondroitin sulfate, where they are important constituents in connective tissues such as cartilage.¹⁹

D-Galacturonic was chosen as a second scaffold for the synthesis of sugar azido acids. Varying only by the axial stereochemistry of the hydroxyl group attached to the C4 position of the pyran ring, D-galacturonic was selected as it was thought that this distinction would not affect the further functionalization of the molecule, but would impart a stereochemical difference into the “clickable” glycoconjugates. Furthermore, akin to D-glucuronic acid, D-galacturonic acid displays a variety of roles in nature, particularly as a structural element of plant gums such as pectin.¹⁵⁴ D-Galacturonic acid is present in many different food stuffs, thus it is likely that conjugates containing D-galacturonic acid would be well tolerated if used in nuclear imaging agents in the future.¹⁵⁵ In addition to D-glucuronic acid and D-galacturonic acid, D-mannuronic acid was also considered as a sugar azido acid scaffold. However, the axial stereochemistry at the C2 position on the pyran ring increased the potential risk of side reactions due to the closer proximity of the C2 hydroxyl group to the carboxylate group. Hence no SAAs based on mannuronic acid were synthesized herein.

In selecting an approach for the synthesis of the required *glc*- and *gal*- sugar azido acids, three potential methodologies were considered (Scheme 2.3). The first of these, described by Von Roedern *et al.*,¹⁵⁶ was the synthesis of 1-azido-2,3,4-tri-*O*-acetyl- β -D-glucuronic acid methyl ester (**53**) from the corresponding 1,2,3,4-tri-*O*-

acetyl- β -D glucuronic acid methyl ester (**52**) (Pathway A, Figure 2.4). Utilizing glucuronolactone (**51**) as a precursor, this pathway was deemed not suitable in this instance due to the long duration/low yielding nature of the process. Also, this method would not be able to be ported to the synthesis of a *gal*-based sugar azido acid.



Scheme 2.3: Three potential pathways *en route* to the synthesis of sugar azido acids based on the *Glc* scaffold.^{156–158}

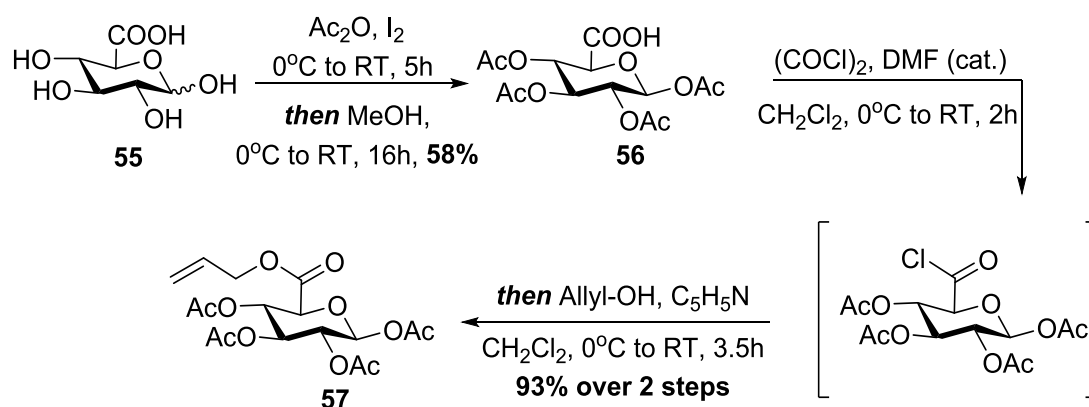
An alternate strategy previously developed by D’Onofrio *et al.*,¹⁵⁸ that was considered also commenced from a previously synthesized precursor, β -D-glucopyranosyl azide (**37**, Scheme 2.3 Pathway 2), where selective protection of the primary 6-OH, peracetylation of the remaining 2-,3- and 4-OH groups (**54**), followed by the one pot selective deprotection of a silyl ether and oxidation of the primary 6-OH, resulted in the required SAA. However, the utilization of the $\text{CrO}_3/\text{H}_2\text{SO}_4$ reaction cocktail in the one-pot deprotection/oxidation of **54** posed some safety concerns,¹⁵⁸ reducing the scalability of the synthesis considerably.

Instead, a strategy whereby the target SAAs were synthesized from D-glucuronic/or galacturonic starting materials was employed (Scheme 2.3, Pathway 3). Utilizing cheap, readily available precursor molecules of D-glucuronic and D-galacturonic acid, this methodology would allow for the stereoselective introduction of an azido group at the anomeric position, with β -stereochemistry. Furthermore, this concise four step synthesis allows for the utilization of a number of different protecting groups for the 6-carboxyl group, including the methyl protecting group utilized by Von Roedern *et al.*,¹⁵⁶ and other commonly used protecting groups such as the ethyl, allyl, *tert*-butyl or benzyl groups;¹⁵⁹ providing versatility in the deprotection procedure that would yield the required sugar azido acids.

2.3 Synthesis of *Glc*- and *Gal*-Sugar Azido Acids.

2.3.1 Synthesis of 1-Azido-2,3,4-tri-*O*-acetyl- β -D-glucuronic acid (**60**)

For the production of *glc*- and *gal*- sugar azido acids, protection of both the secondary hydroxyl groups and the carboxylic acid was required. Based on the protocol reported by Bergeon *et al.*,¹⁶⁰ D-glucuronic acid (**55**) was peracetylated using I_2 as a Lewis acid, with slow, cold addition of methanol resulting in the cleavage of the intermediate anhydride, which after recrystallization produced **56** in 58% yield (Scheme 2.4).

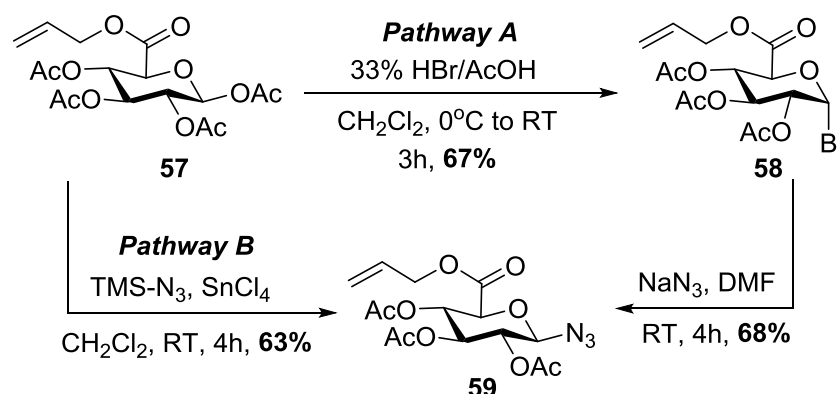


Scheme 2.4: Synthesis of peracetylated glucuronic acid allyl ester **57** from D-glucuronic acid.

Analysis of the 1H NMR spectrum highlighted the β -configuration of the OAc group at the anomeric centre, with a doublet at 5.79 ppm ($J = 7.6$ Hz) indicative of a shielded proton of α - or axial anomeric configuration. Subsequently, the free carboxylic acid of **56** was protected using the method of Tosin *et al.* to form an allyl ester.¹⁵⁷ The allyl ester was chosen over other options due to its stability under both acidic and basic conditions. Furthermore, the selective deprotection of an allyl ester in the presence of an azido group would allow for the efficient production of the required *glc*- sugar azido

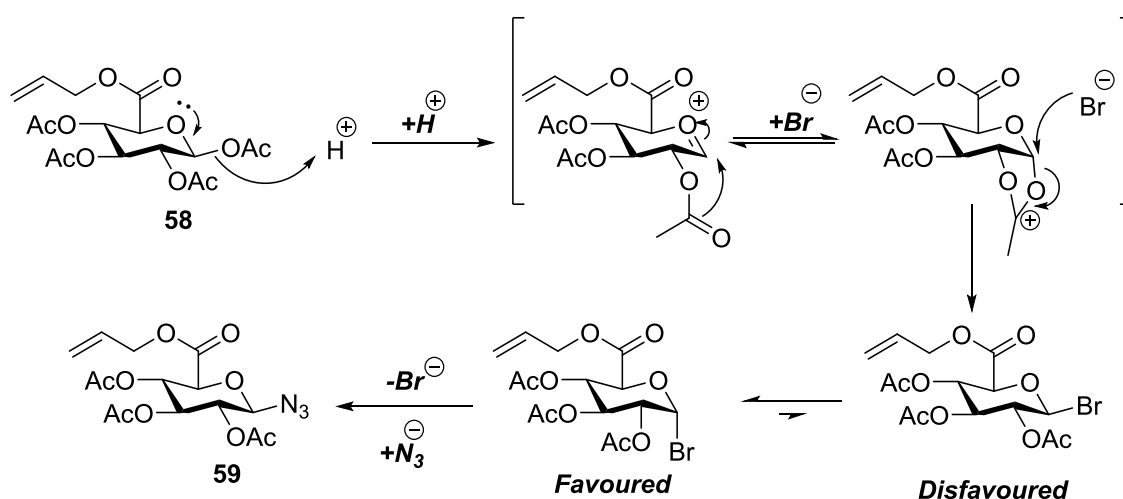
acid. Installation of the allyl ester began with the formation of a glucuronyl chloride from **56**, utilizing oxalyl chloride and catalytic DMF. Substitution of the glucuronyl chloride with allyl alcohol, followed by scavenging of the alcohol proton by pyridine, resulted in the peracetylated glucuronic acid allyl ester **57** in 93% yield over two steps (Scheme 2.4).¹⁵⁷ In the ^1H NMR spectrum, multiplets at 5.89 ppm and 5.37 ppm integrating for one and two protons respectively, and a doublet at 4.61 ppm ($J = 6.1$ Hz) integrating for two protons were consistent with the allyl group in **57**.

Accordingly, with **57** in hand the synthesis of the β -azidosugar **59** was investigated. In comparison to tin (IV) chloride-catalyzed azidonation reactions presented in the literature in the formation of the previously described β -azide **25**,¹⁵⁷ it was identified that variations in the coordinating group at the C6 position of the protected glycoside (OAc group versus COOMe) could result in a noticeable decrease in the yield of product. Therefore, an alternate strategy employing a two-step process was initially used. Firstly, acid-catalyzed bromination of the anomeric centre of **57** using 33% HBr in acetic acid, produced the α -brominated compound **58** in 67% yield (Scheme 2.5).



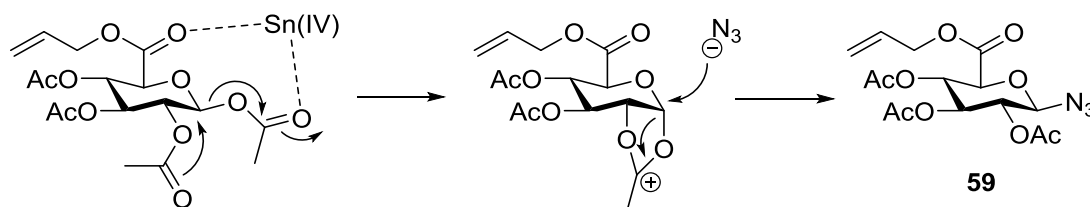
Scheme 2.5: Synthetic pathways towards the production of the protected sugar azido acid **59**.

In the following reaction in dichloromethane, the anomeric OAc group of **57** dissociates, producing an oxocarbenium intermediate (Scheme 2.6). Stabilization of this intermediate produces an anomeric-centred carbocation, which in the presence of a bromide undergoes nucleophilic substitution. Formation of the α -bromo compound **58** is highly favoured, due to hyperconjugation resulting from the orbital overlap present between the lone pair of electrons of the ring oxygen, and the anti-bonding orbital of the anomeric carbon (Scheme 2.6). α -Bromo compound **58** was then subjected to nucleophilic substitution at the anomeric centre employing NaN_3 , producing the sugar azido acid **59** in 68% yield (Scheme 2.5). The use of a polar aprotic solvent such as DMF allowed the nucleophilic substitution to proceed smoothly without the formation of potentially hazardous side products. This is in contrast to the use of CH_2Cl_2 , which when used with ionic azides is known to result in the production of diazidomethane – a highly unstable, shock sensitive species.¹⁶¹ To this end, the use of NaN_3 in chlorinated solvents during azidation reactions was completely avoided in this work.



Scheme 2.6: Proposed alternative mechanistic pathway for the synthesis of 1-azido-2,3,4-tri-O-acetyl- β -D-glucuronic acid allyl ester (**59**).

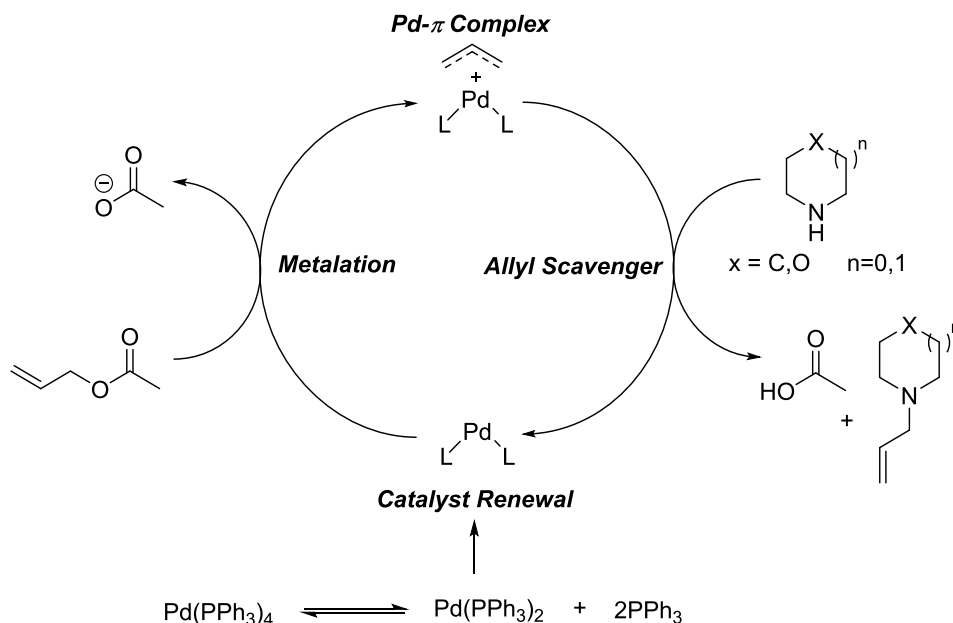
Whilst this methodology produced the required protected sugar azido acid **59**, the yield for this product proved to be significantly less than that expected (44% versus ~70% as described in the literature).¹⁵⁷ Furthermore, the sensitivity of the intermediate α -bromo compound **58** to degradation hindered the scalability of this process. Hence, the procedure of Tosin *et al.* was utilized (Scheme 2.5, pathway B), where the azido group was directly introduced to **57**, using TMSN₃ as a soft azide donor and catalyzed by tin(IV) chloride (Figure 2.8).¹⁵⁷ Workup and subsequent recrystallization generated the fully protected sugar azido acid **59** in 63% yield (Scheme 2.5). Mechanistically, tin(IV) chloride forms a coordinate complex with the carbonyl oxygen of the carboxylic acid and that of the anomeric OAc group. This coordination induced neighbouring-group participation from the carbonyl of the OAc group attached to the C2 of the pyran ring results in the formation of a carbocation-containing acetal intermediate, and the release of an acetate ion (Scheme 2.7). The axial stereochemistry of the acetal intermediate allowed for the S_N² nucleophilic substitution at the anomeric centre with the azide anion, forming the required β -sugar azido-acid **59**.



Scheme 2.7: Mechanism for the SnCl₄-catalyzed azidation that formed **59**.¹⁵¹

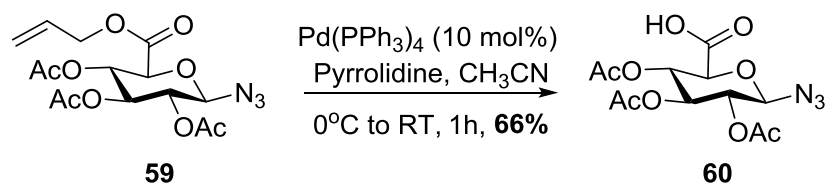
The ^1H and ^{13}C NMR spectra of **59** highlight the distinct difference in electron density surrounding the anomeric centre, with a doublet ($J = 9.1$ Hz) in the ^1H NMR at 4.71 ppm and a singlet in the ^{13}C NMR at 88.3 ppm respectively, with the correlation of these signals confirmed by a 2D gHSQC NMR experiment. These appear noticeably upfield from those signals for the peracetylated precursor **57** (5.79 ppm and 91.6 ppm respectively), and are indicative of the inductive electron-withdrawing effects of the anomeric OAc group in **59**, which deshields the nuclei of H1 and C1. Even further upfield from the H1 doublet in the ^1H NMR spectrum of **59** is a doublet representing the H5 proton (4.14 ppm, $J = 9.8$ Hz). The difference between these protons (~ 0.6 ppm) and their relative positions was a consistent feature of the ^1H NMR spectra of all derivatized sugar azido acids synthesised in this project.

The protected sugar azido acid **59**, was then subjected to deprotection, in order to yield the required 1-azido-2,3,4-tri-*O*-acetyl- β -D-glucuronic acid (**60**). The utilization of the allyl ester allowed for the selective “unmasking” of the carboxylic acid through mild palladium(0)-catalyzed deallylation. Mechanistically, when in the presence of Pd(0) catalysts such as $\text{Pd}(\text{PPh}_3)_4$ the allyl ester is cleaved, forming a free carboxylate and Pd- π complex between the catalyst and the liberated allene. In the presence of a “scavenger” molecule such as pyrrolidine, piperidine or morpholine, the allene is sequestered from the catalyst, which is reintegrated into the catalytic cycle, producing the free carboxylic acid product (Scheme 2.8).¹⁵⁷



Scheme 2.8: Catalytic cycle for the deprotection of allyl esters.¹⁶²

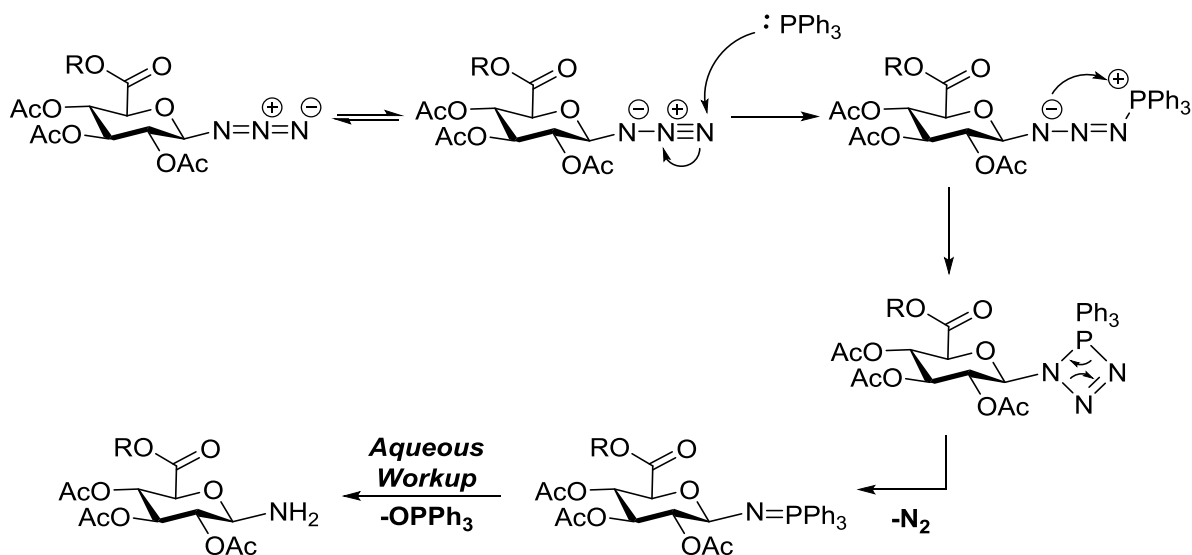
Hence, using this approach and the methodology of Tosin and co-workers, the allyl ester of **59** was deprotected, to form the target sugar azido acid **60**. Utilizing $\text{Pd(PPh}_3)_4$ as a catalyst and pyrrolidine as an allyl scavenger, **60** was synthesized in 66% yield (Scheme 2.9).¹⁵⁷



Scheme 2.9: Synthesis of 1-azido-2,3,4-tri-*O*-acetyl- β -D-glucuronic acid **60**.

In comparison to the literature, this yield was somewhat less than that previously achieved (83-93%) when performed on the same scale.^{151,157} Furthermore, this yield proved inconsistent when synthesized on larger scales, with yields ranging from

49-66%. Considering the catalyst ($\text{Pd}(\text{PPh}_3)_4$) used, the high loading of catalyst (10 mol%) and the proposed mechanism of this reaction, one likely reason for these variances is the potential side reaction of the starting material with triphenylphosphine (PPh_3) leached from the catalyst. In the presence of PPh_3 , the azide at the anomeric centre of **59** can undergo a Staudinger reduction, resulting in the release of N_2 gas and upon aqueous work-up the formation of triphenylphosphine oxide and a sugar amino acid derivative (Scheme 2.10).



Scheme 2.10: Proposed mechanism of the Staudinger reduction that occurs in the synthesis of **60**.

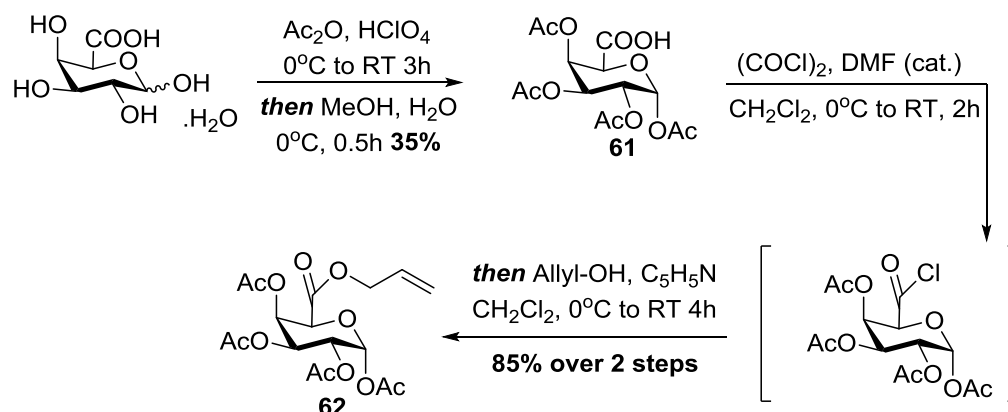
The leaching of PPh_3 from the catalyst is supported by the presence of signals in both the ^1H and ^{13}C NMR spectrum between 7.40 and 7.80 ppm, respectively in a number of the crude reaction samples of **60**, which are indicative of the presence of an aromatic ring, of which PPh_3 or O=PPh_3 are the only potential contributors in this protocol. In addition, signals of m/z 301 present in the low resolution electrospray ionization mass spectrum (LR-ESIMS) of the reaction mixture are indicative of $\text{O=PPh}_3 + \text{Na}$. To combat the potential interference of PPh_3 in this reaction, freshly

recrystallized $\text{Pd}(\text{PPh}_3)_4$ was used, and removal of the catalyst was performed via filtration over a thick pad of celite, to prevent any leaching. Whilst no amine formation was detected in the worked-up solution, the following approach to the use of catalyst resulted in generally higher yields of **60**, compared to when no recrystallization of the catalyst was performed. In this manner, starting initially from D-glucuronic acid, 1-azido-2,3,4-tri-*O*-acetyl- β -D-glucuronic acid (**60**) was successfully synthesized in a total yield of 23% over four steps.

2.3.2 Synthesis of 1-Azido-2,3,4-tri-*O*-acetyl- β -D-galacturonic acid (**65**)

Based on the convenient synthesis of **60** from D-glucuronic acid, it was envisaged that this methodology would prove quite useful in the synthesis of 1-azido-2,3,4-tri-*O*-acetyl- β -D-galacturonic acid (**65**). Hence, the synthesis of this sugar azido acid initiated with the peracetylation of commercially available D-galacturonic monohydrate. Utilizing the protocol developed by Vogel and co-workers, acetic anhydride and perchloric acid were employed to produce 1,2,3,4-tetra-*O*-acetyl- α -D-galacturonic acid (**61**) in 35% yield (Scheme 2.11).¹⁶³ Mechanistically, the perchloric acid-catalyzed protocol proceeds in a comparable manner to the use of I_2 in the acetylation of D-glucuronic acid, with an in depth examination of the literature illustrating the similarities in yield when either method is used to synthesise **61**.¹⁶⁴ The α -stereochemistry of the anomeric centre is highlighted by the ^1H NMR spectrum of **61**, where a doublet integrating to one proton at 6.47 ppm indicates the deshielded, equatorial nature of H1. Furthermore, the small coupling constant of $J = 2.9$ Hz

emphasizes the small dihedral angle that exists between H1 and H2 when H1 is in the equatorial position.



Scheme 2.11: Synthesis of peracetylated allyl ester **62** from D-galacturonic acid monohydrate.

The presence of α -stereochemistry at the anomeric centre of **61** is in stark contrast to the β -stereochemistry present in the D-glucuronic acid derivative **56**. To understand and reason this difference further, a brief conformational analysis was undertaken using the molecular modeling program ChemBio3D 11. Using the AM1 semi-empirical level of theory, the heat of formation (ΔH_f) for both α - and β -anomers of **56** and **61** was calculated (Figure 2.2).

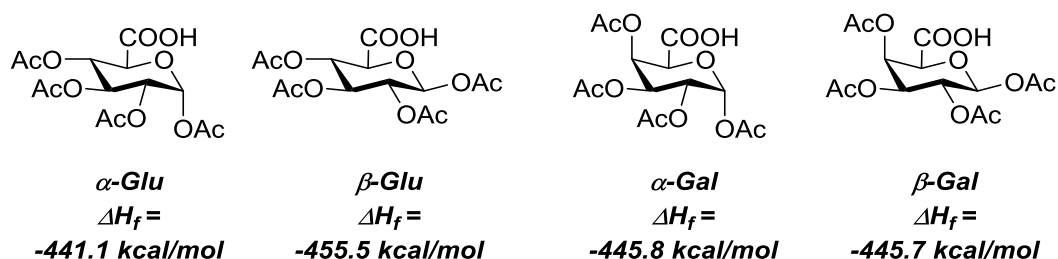


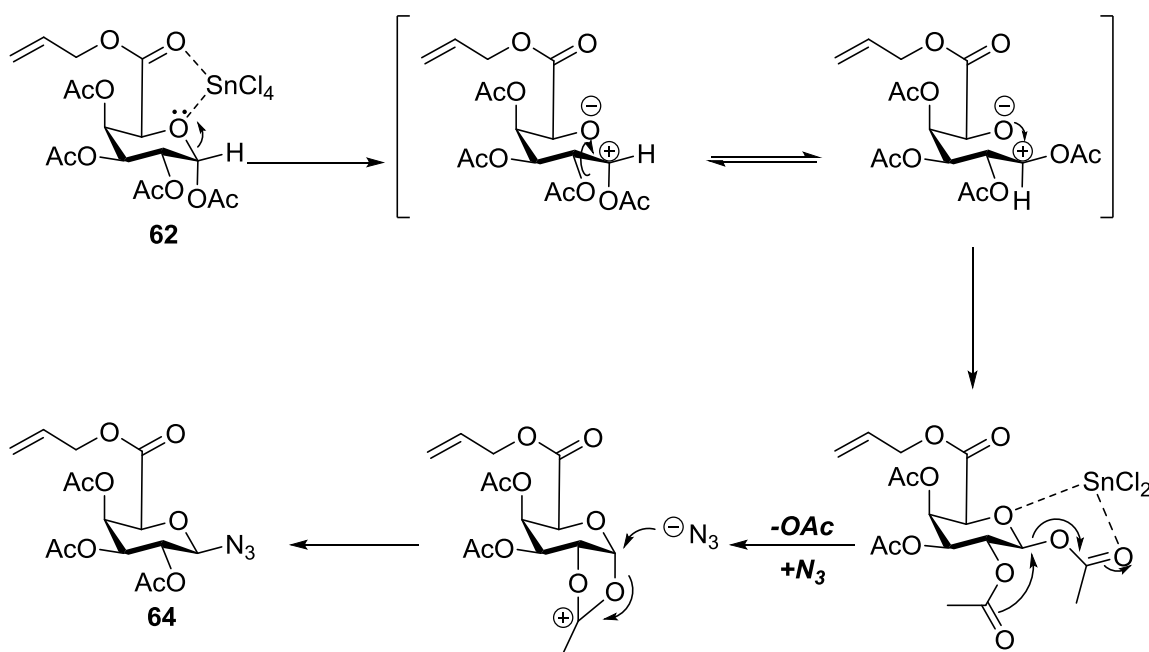
Figure 2.2: Heat of formation (ΔH_f) of the α - and β - anomers of **56** and **61**, calculated using ChemBio3D 11.0.

Interestingly, there were noticeable differences between the different uronic acids, with the β -anomer of **56** calculated to have a ΔH_f 11.4 kcal/mol less than its counterpart α -anomer. This is indicative of the greater stability of the β -anomer, as seen by the resulting ratio of the β -anomer of **56**. In contrast, the calculated ΔH_f values for the respective anomers of **61** show negligible differences between them (0.1 kcal/mol, Figure 2.2), suggesting an even likelihood of the formation of both α - and β -anomers. Considering the low yield of **61** and the use of recrystallization in its isolation, it is entirely possible that the production of the β -anomer of **61** could have occurred in equal quantities to the isolated α -anomer.

With **61** in hand, the free carboxylic acid could be protected. Utilizing the protocol optimised in the synthesis of **57**, the peracetylated galacturonic acid allyl ester derivative **62** was synthesized via the acid chloride intermediate in 85% yield (Scheme 2.11). Similarly to the previously synthesized **57**, signals in the ^1H NMR spectrum at 5.75 ppm (1H), 5.15 ppm (2H) and 4.70 ppm (2H) were indicative of the presence of the allyl ester. Subsequently, **62** was subjected to azidation at the anomeric centre. Based, on the experience gained during the synthesis of **59**, the peracetylated galacturonic acid allyl ester **62** was subjected to reaction under $\text{TMSN}_3/\text{SnCl}_4$ conditions. Interestingly though, compared to the moderate yielding synthesis of **59**, an initial reaction attempted over 4 hours yielded the anticipated product **64** in only 18% yield. Increasing reaction time to 20 hours only mildly increased the yield of product (29%), with no further gains in yield observed after 72 hours of reaction time.

Mechanistically, the α -stereochemistry of the parent molecule appeared to impede the kinetics of this reaction, as a result of the large distance between the OAc

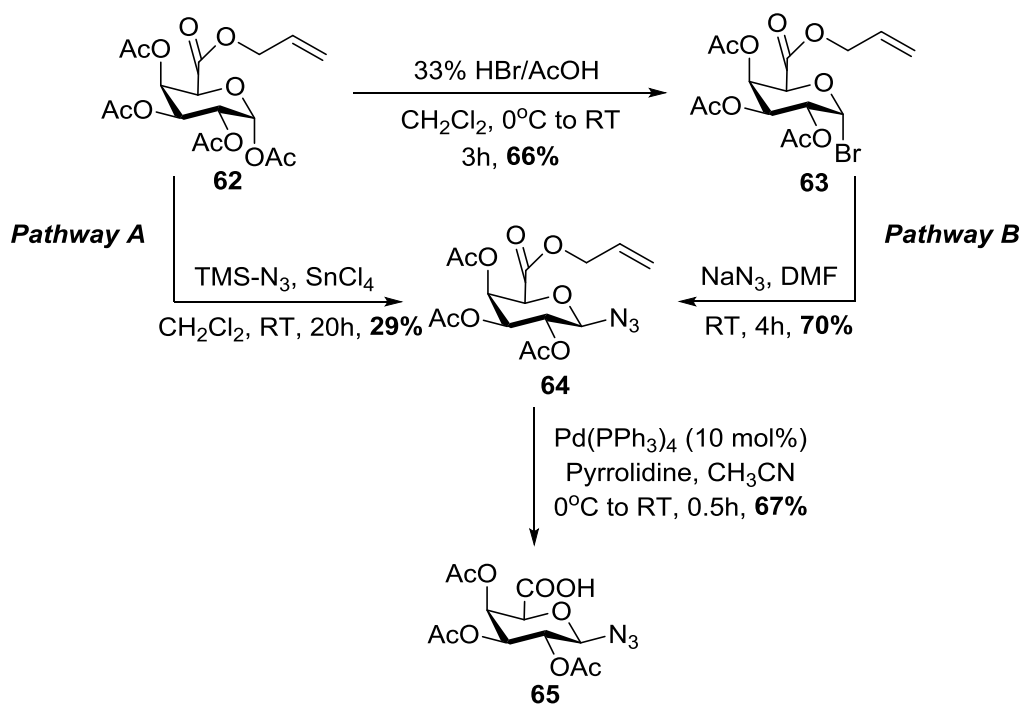
group at the C1 position, and the carbonyl group of the allyl ester (Scheme 2.12). Hence, when SnCl_4 is dissolved in dichloromethane and in the presence of **62**, it instead preferentially forms an interaction between the carbonyl group of the allyl ester, and the oxygen of the pyran ring. This interaction can destabilize the pyran ring, leading to ring-opening at the anomeric centre, resulting in the formation of a C1-centred carbocation intermediate. Mutarotation of the C-C bond between C1 and C2, and subsequent ring closing of this intermediate results in the formation of the β -anomer of **62**, which can undergo OAc elimination, neighbouring group participation and nucleophilic substitution to form the protected sugar azido acid **64** (Scheme 2.12).¹⁵¹



Scheme 2.12: Mechanism for the synthesis of **64** from **62** in the presence of SnCl_4 .¹⁶⁵

As a consequence of the inefficiencies present in this process, it was determined that the synthesis of the α -bromo intermediate *en route* to **64** would provide the most

viable procedure towards the synthesis of 1-azido-2,3,4-tri-*O*-acetyl- β -D-galacturonic acid (see Scheme 2.6). Furthermore, the oxocarbenium transition state is formed independent of the stereochemistry present at the anomeric centre.



Scheme 2.13: Synthesis of 1-azido-2,3,4-tri-*O*-acetyl- β -D-galacturonic acid (**65**)

Hence, the peracetylated allyl ester **62** was subject to bromination utilizing the conditions developed in the preparation of **58** (33% HBr/Acetic acid in dichloromethane), resulting in the α -bromo compound **63** in 66% yield. Next, **63** was subjected to NaN_3 azidation, producing the β -azide derivative **64** in 70% yield (Scheme 2.13, pathway B). The structure of **64** was confirmed using 2D NMR spectroscopy, with the gCOSY spectral plot displaying correlations between the H5 and H4, H4 and H3, and H2 and H1 (Figure 2.3). The axial stereochemistry of the proton at the anomeric centre of **64** was identified using the NOESY spectral plot, where through-

space correlations between the H1 and H3 of **64** were detected. Hence, the azido group present at the anomeric centre possessed β -stereochemistry (Figure 2.3).

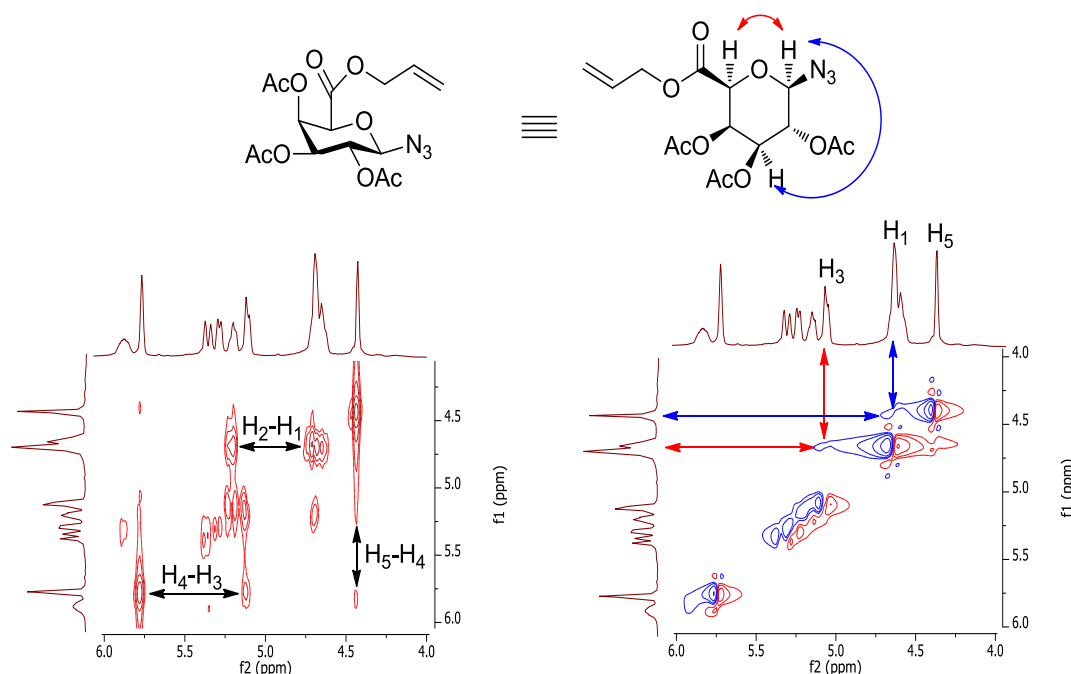


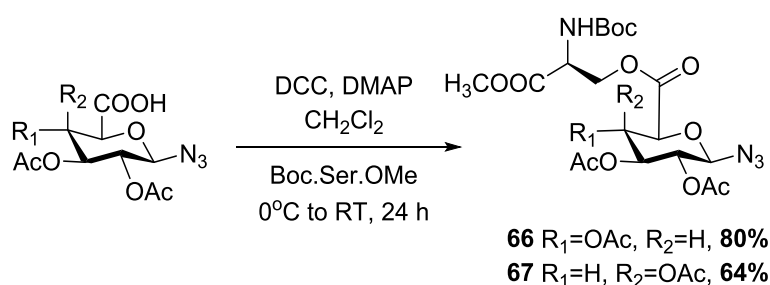
Figure 2.3: The gCOSY (left) and NOESY (right) 2D ^1H NMR spectral plots for **64**.

Subsequently, the carboxylic acid group was unmasked through the Pd-catalyzed deprotection of the allyl ester of **64**, producing 1-azido-2,3,4-tri-*O*-acetyl- β -D-galacturonic acid (**65**) in 67% yield (Scheme 2.13).¹⁵⁷ This was evident by the ^1H and ^{13}C NMR spectra of **65**, where the disappearance of signals from the allyl group of **64** highlighted the deallylation. Therefore, the novel, target sugar azido acid **65** was synthesized from D-galacturonic acid monohydrate in 9% over 5 steps. Comparable in yield to the synthesis of the *glc* sugar azido acid **60**, this synthesis allowed for the timely, scalable synthesis of SAAs without the need of chromatography. Thus, sufficient material for the synthesis of a library of “clickable” glycoconjugates was procured.

2.4 Synthesis of “Clickable” Glycoconjugates

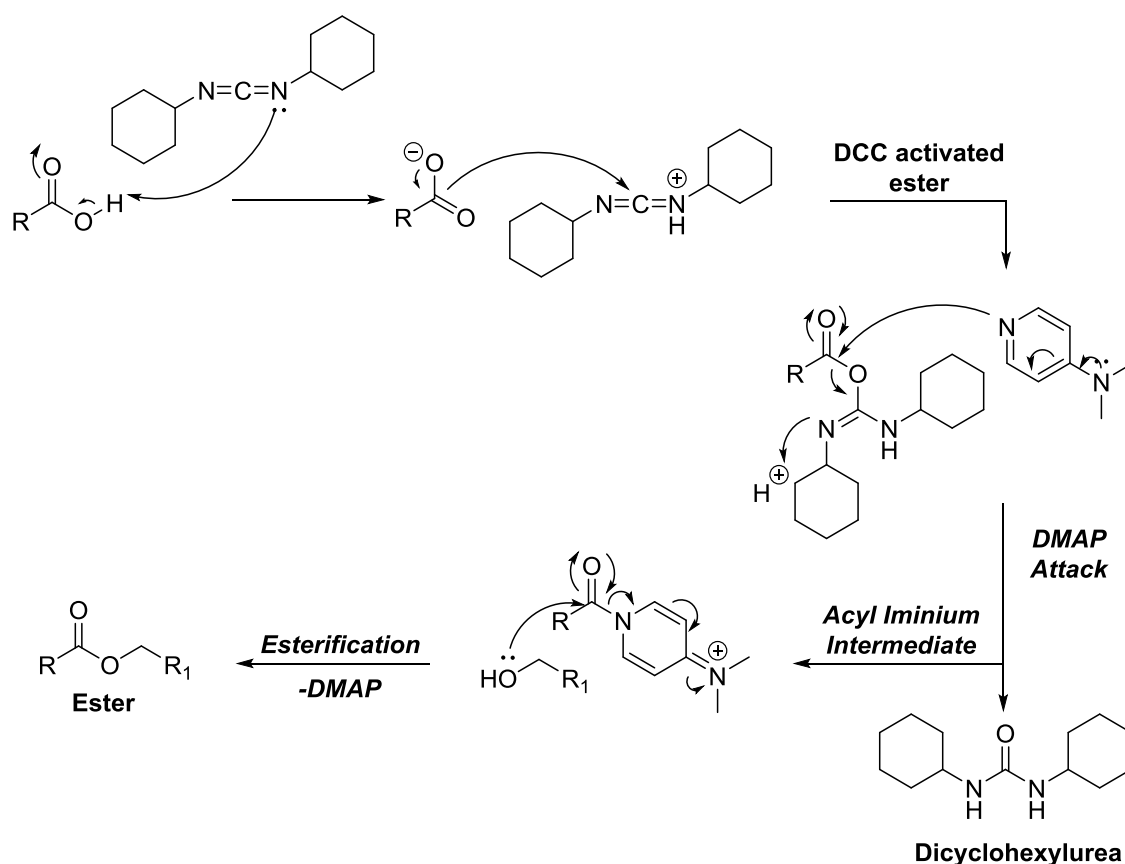
2.4.1 Synthesis of Sidechain-linked Derivatives (66-69)

With the key *glc*- and *gal*- sugar azido acids **60** and **65** in hand, our attention turned to the synthesis of “clickable” glycosyl amino acids. Initially, the synthesis of conjugates formed through the coupling of our synthesized sugar azido acids with serine was targeted, with Boc.Ser.OMe selected as the protected serine donor. The general reactivity of primary alcohols in peptide coupling conditions, positioned serine ideally as a coupling amino acid in the development of “clickable” glycoconjugates. The formation of serine-linked glycoconjugates was also validated by the importance and prevalence of serine glycosylation in the production of biologically important glycoconjugates.¹⁶⁶ Hence, utilizing a classical Steglich *N,N'*-1,3-dicyclohexylcarbodiimide (DCC)-based esterification protocol, Boc.Ser.OMe was coupled to the *glc*- sugar azido acid **60**, successfully producing the novel serine-based “clickable” glycosyl amino acid **66** in 80% yield (Scheme 2.14).¹⁶⁷



Scheme 2.14: Synthesis of serine-based “clickable” glycoconjugates **66** and **67**.

Mechanistically, in the presence of a non-nucleophilic base such as DMAP, the free carboxylic acid of **66** reacts with the carbodiimide of DCC to form an activated ester (Scheme 2.15). Driven by electron donation into the pyridine ring, DMAP can subsequently attack the activated ester resulting in the acyl iminium intermediate and the displacement of dicyclohexylurea as a by-product. Relatively unstable, the acyl iminium intermediate is subsequently prone to nucleophilic substitution by the hydroxyl group of the Boc.Ser.OMe sidechain, resulting in the formation of desired ester product **66** (Scheme 2.15). Subsequently, the success of this procedure was mirrored by its use in the synthesis of the novel *gal*-based sugar azido acid **67**, which was produced from Boc.Ser.OMe and **65** in 64% yield (Scheme 2.14).



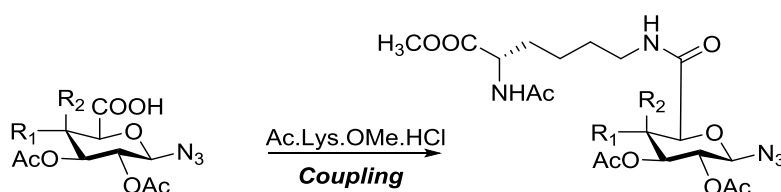
Scheme 2.15: Mechanism of the synthesis of esters using a Steglich DCC/DMAP coupling approach.

The ^1H NMR spectra of both **66** and **67** highlighted the presence of signals each integrating for 2 protons at 4.58 and 4.47 ppm, respectively, with both of these indicative of the CH_2 protons adjacent to the ester on serine. This is in comparison to the corresponding protons in the parent amino acid (Boc.Ser.OMe, 3.80 - 3.95 ppm), which are more shielded due to the presence of the adjacent hydroxyl group. In addition, the ^{13}C NMR spectra of **66** and **67** highlighted the formation of the esters in each, with signals at 173.2 and 167.8 ppm in **60** and **65** replaced by signals at 165.9 and 165.0 ppm in **66** and **67**. Furthermore, the LR-ESIMS of both **66** and **67** highlighted signals at m/z 639, indicative of a $[\text{M} + \text{Na}]^+$ signal. As far as the novelty of **66** and **67**, both of these compounds represent the first examples of “clickable” glycoconjugates produced from sugar azido acids and amino acids.

Considering the ease in using the DCC/DMAP coupling protocol, this methodology was utilized in the synthesis of conjugates containing protected lysine amino acids. In comparison to the previous serine-based examples however, the synthesis of these conjugates proved less efficient using this protocol, with the coupling of *glc*- sugar azido acid **68** to Ac.Lys.OMe.HCl yielding only 31% after 48 hours (Table 2.1). It is likely that the poor solubility of the lysine donor in dichloromethane, in addition to the reduced nucleophilicity of the primary amine of the lysine sidechain with respect to the serine hydroxyl group, significantly impeded the progress of the reaction. These conclusions are further illustrated by the significant quantity of DCC-activated ester that was left unreacted as observed by TLC. Hence, in an attempt to improve the efficiency of this reaction, a modified procedure was employed utilizing hydroxybenzotriazole (HOBt) as an activator and DIPEA as a base in DMF.^{150,168} This procedure resulted in a significant improvement in reaction time and yield, producing

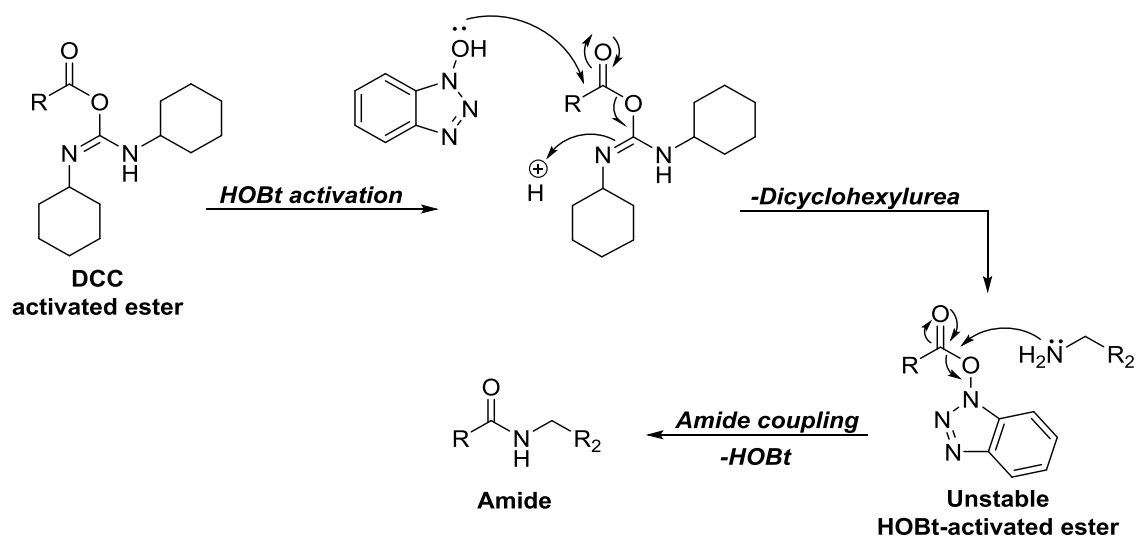
the novel *glc*- and *gal*- lysine-based conjugates **68** and **69** in 75% and 60% yield, respectively (Table 2.1).

Table 2.1: Reaction conditions for the synthesis of lysine-based “clickable” glycoconjugates **68 and **69****



SAA	Coupling Reagent	Activator	Base	Solvent	°C/Time	Product	R ₁ /R ₂	Yield
60	DCC	-	DMAP	CH ₂ Cl ₂	RT/48 h	68	OAc/H	31%
60	DCC	HOBt	DIPEA	DMF	RT/24 h	68	OAc/H	75%
65	DCC	HOBt	DIPEA	DMF	RT/24 h	69	H/OAc	60%

An important constituent of coupling reagents such as *N,N,N',N'*-Tetramethyl-*O*-(1*H*-benzotriazol-1-yl)uronium hexafluorophosphate (HBTU), *N,N,N',N'*-Tetramethyl-*O*-(1*H*-benzotriazol-1-yl)uranium tetrafluoroborate (TBTU) and (benzotriazol-1-yl)-tripyrrolidinophosphonium hexafluorophosphate (PyBOP); HOBt in the presence of a DCC-activated ester will displace *N,N'*-dicyclohexylurea and form an unstable HOBt-activated ester. The sidechain -NH₂ group of Ac.Lys.OMe.HCl is a suitable nucleophile, and in the presence of this activated ester will displace HOBt, undergoing coupling to form the amide-linked conjugates **68** or **69** (Scheme 2.16).¹⁵⁰



Scheme 2.16: Mechanism of the synthesis of amides using a DCC/HOBt coupling approach.

The identity of both **68** and **69** were confirmed by their HR-ESIMS with signals at m/z 552.1918 and 552.1935 (calculated for $\text{C}_{21}\text{H}_{31}\text{N}_5\text{O}_{11}\text{Na}$ $[\text{M} + \text{Na}]^+$: 552.1918) indicative of the desired products. Furthermore, the NMR spectra of *glc*-**68** and *gal*-**69** highlighted the contrasting stereochemistry at the C4 position between these conjugates, and the steric consequences that result from this variation. In the ^1H NMR spectrum of **68**, two matching signals present at 3.40 ppm and 3.15 ppm each displaying an integration of 1H are present (Figure 2.4). A gCOSY 2D NMR experiment of **68** suggested that both of these protons were those of the CH_2 group bound directly to the amide bond formed during the coupling reaction (H^e).

The different chemical environments of the two geminal protons are potentially indicative of hydrogen bond stabilization resulting from the neighbouring amide bond. It is possible that under the conditions of the ^1H NMR experiment performed (CDCl_3 , 25°C) the proton of the newly-formed amide nitrogen of **68** may be in close proximity to the C4-linked oxygen of the pyran ring. Though the amide itself is an sp^2 hybridized system, if this were the case the proton would be in close enough proximity to the ring-

bound oxygen at the 4-position to form a pseudo six-membered ring. Whilst the presence of this interaction is completely speculative, if present the ring would display a configuration close to that of a “chair,” with the stability of this interaction effectively limiting the rotation by the C-C bond at the C5 position (Figure 2.4).

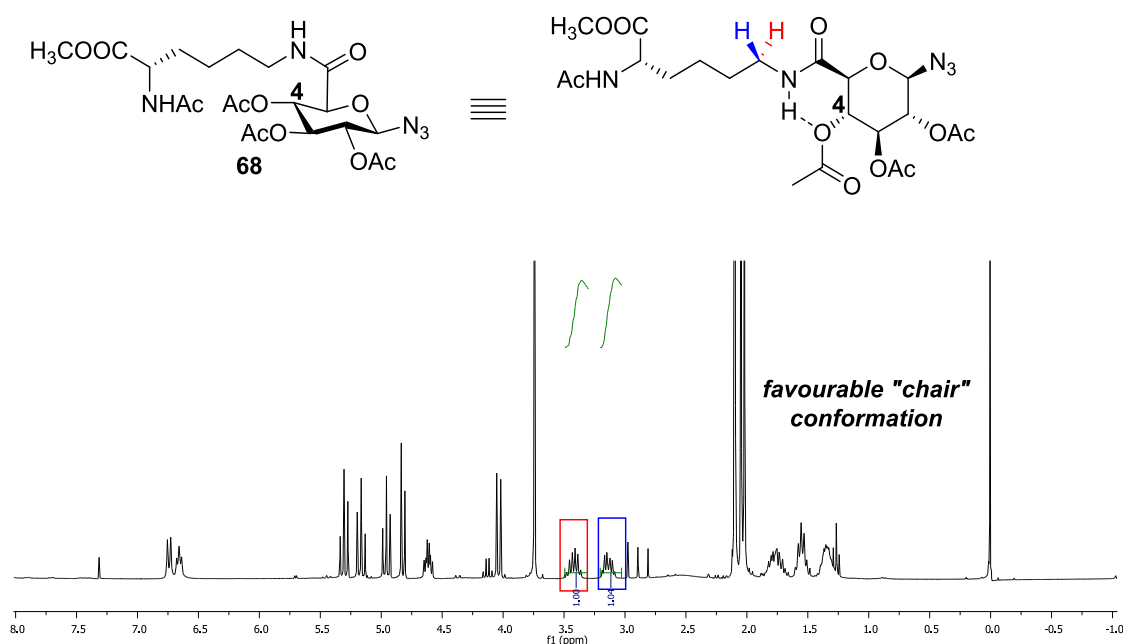


Figure 2.4: ^1H NMR spectrum of **68**, highlighting the pseudo 6-membered ring formed through hydrogen bonding, inducing rigidity at the C4 position.

In contrast, the ^1H NMR spectrum of **69** displays two asymmetrical signals – two multiplets at 3.25-3.49 ppm integrating for the two hydrogens bound to C⁶ (Figure 2.21). The axial C4 stereochemistry of **69** produces a “cis” configuration in the C-C bond linking the C4 and C5 of the pyran ring, resulting in a shorter relative distance between the C4-OAc group and the C5-amide linkage. When aligned in a manner akin to that described for the ^1H NMR of **68** (CDCl_3 , 25°C), it can be speculated

that the amide proton of **69** is facing in an opposing direction to the ring-bound oxygen at the 4-position. The greater distance between these groups would limit their interaction, and thus likelihood of forming a hydrogen bond. Hence, near-free rotation of the C-C bond present at the C5 would occur, resulting in a greater degree of chemical equivalence for the C $^{\epsilon}$ compared to the corresponding protons in **68** (Figure 2.5).

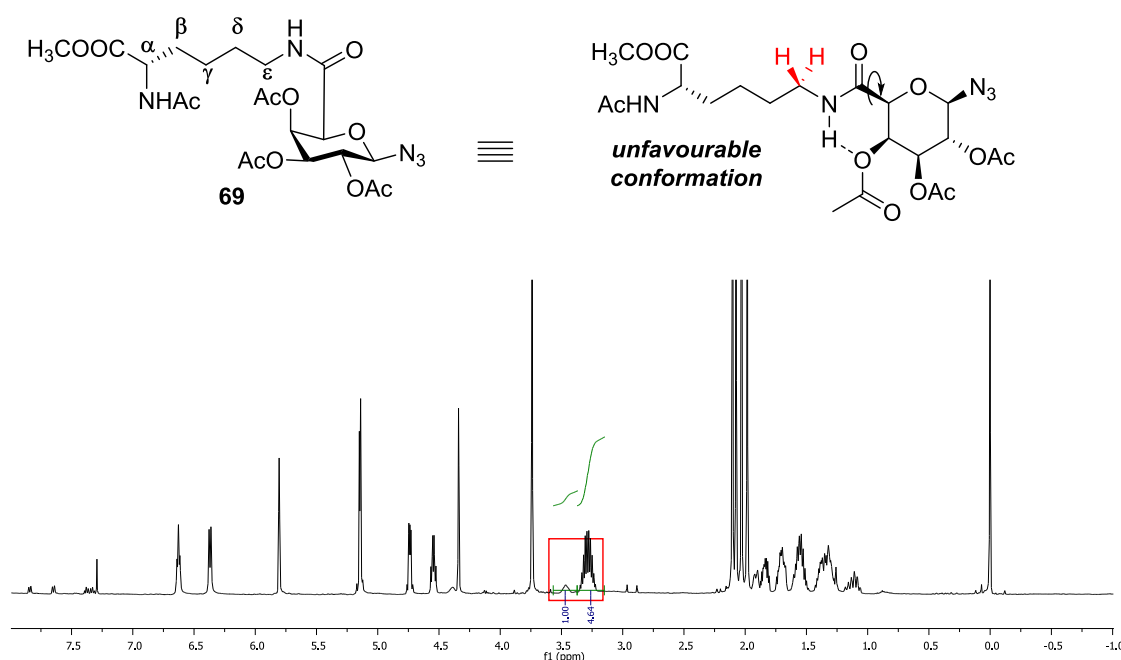


Figure 2.5: ^1H NMR spectrum of **69**, highlighting the chemical equivalence of the two protons bound to C $^{\epsilon}$, allowing for bond rotation at the C5 position.

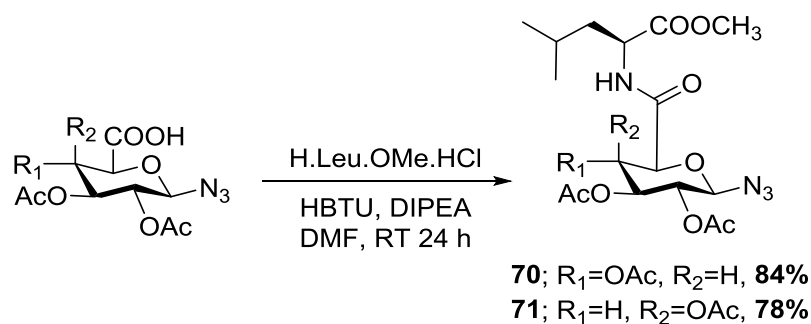
2.4.2 Synthesis of Leucine, Methionine and Glutamine α -Amino linked Derivatives (70-73)

Based on the success of coupling **60** and **65** to lysine and serine residues, this methodology was next applied to the coupling of amino acid residues via their α -amino group. Leucine (Leu), methionine (Met) and glutamine (Gln) were selected as ideal coupling amino acids, with these residues comprising a range of sidechain functional groups that are resistant to coupling conditions (aliphatic chain, thioether and amide). In addition to this trait, the synthesis of derivatives including glutamine, leucine and methionine would be highly advantageous, as previous studies have highlighted the utility of these amino acids in targeting of amino acid transport.^{169–172}

Glutamine has been targeted primarily for magnetic resonance imaging of tumour cells,^{173,174} with some studies utilizing fluorinated derivatives of glutamine in the metabolic imaging of tumour cells.¹⁷⁵ Leucine has been investigated for ultrasonic imaging of tumour angiogenesis as part of the cell binding tripeptide arginine-arginine-leucine.¹⁷⁶ Methionine (Met) is the most widely used [¹¹C]-labelled amino acid in clinical PET imaging,^{170,177} with derivatives also labelled with fluorine-18 under current investigation for use in the imaging of tumours.^{169,171,178} The linkage of these amino acids to either **60** or **65** would generate a novel class of *N*- α -linked “clickable” glycoconjugates that could be evaluated potentially in the development of radiolabelled glycoconjugates formed using the CuAAC “click” reaction.¹⁷⁹

Contrasting the previously used DCC and DCC/HOBt coupling protocols in the syntheses of **66-69**, HBTU was selected as the coupling reagent. Possessing milder reactivity than carbodiimide-based coupling reagents such as DCC and DIC, HBTU and

related coupling reagents (HATU, TBTU, HCTU) display a lower propensity to induce racemization in the coupling amino acid residue – an important attribute considering the position of the unhindered α -amino group adjacent to the stereocentre of the amino acid.¹⁵⁰ Hence, using HBTU in the presence of DIPEA in DMF, attempts were undertaken to couple *glc*-sugar azido acid **60** to H.Leu.OMe.HCl, producing the novel conjugate **70** in 84% yield (Figure 2.22). This method was extended to the synthesis of the novel *gal*- sugar azido acid leucine conjugate **71**, which was produced from **65** and H.Leu.OMe.HCl in 78% yield (Scheme 2.17).



Scheme 2.17: Synthesis of leucine-based “clickable” glycoconjugates **70 and **71****

The presence of doublets at 6.70 and 6.82 ppm in the ^1H NMR spectra of **70** and **71**, respectively is indicative of the amide-bond formed during the coupling procedure, with further signals at 4.57 and 4.70 ppm correlating to the proton at the α -carbon of the leucine each integrating for one proton (Figure 2.6).

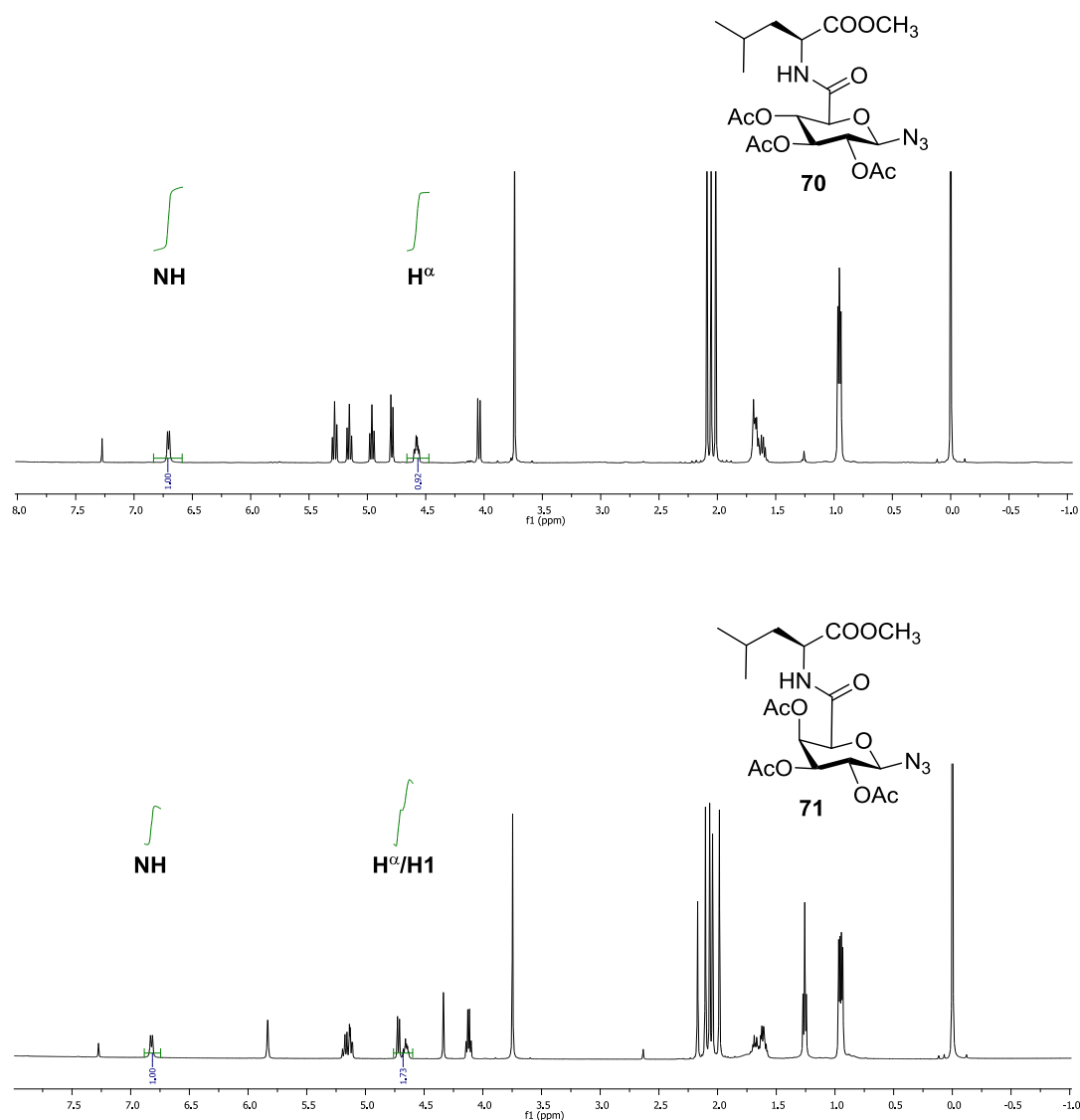
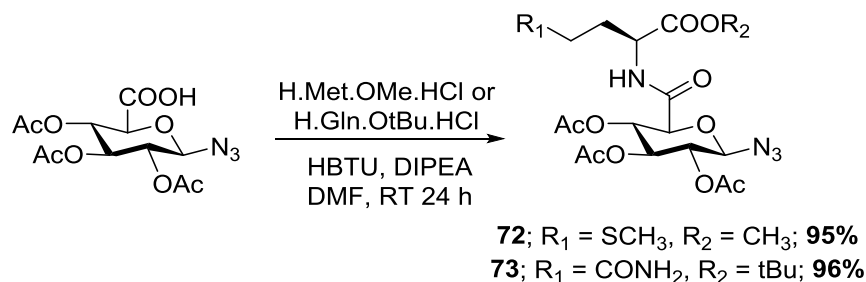


Figure 2.6: ^1H NMR spectra of leucine-based “clickable” glycoconjugates **70** and **71**, highlighting the deshielded amide nitrogen and proton of the α -carbon of leucine

Following on from the efficient coupling of H.Leu.OMe.HCl to **60** and **65**, this procedure was extended to the coupling of *glc*- sugar azido acid **60** with H.Met.OMe.HCl and H.Gln.OtBu.HCl, producing the glycosyl amino acids **72** and **73** in 95% and 96% yields, respectively (Scheme 2.18).



Scheme 2.18: Synthesis of “clickable” glycoconjugates **72** and **73**.

Containing thioether and amide functional groups, the coupling of both H.Met.OMe.HCl and H.Gln.OtBu.HCl were both well tolerated under the conditions used, with clean coupling occurring. This is verified by the ^{13}C NMR spectrum of **72**, where a signal at 165.7 ppm indicates coupling of the carboxylic acid to form an amide bond (Figure 2.7). In the ^{13}C NMR spectrum of **73**, coupling was verified by the presence of a signal at 167.5 ppm, with a downfield signal 174.9 ppm highlighting the shielding effect imposed on the carbonyl carbon by the α -amino group as opposed to the amide present on the sidechain (Figure 2.8).

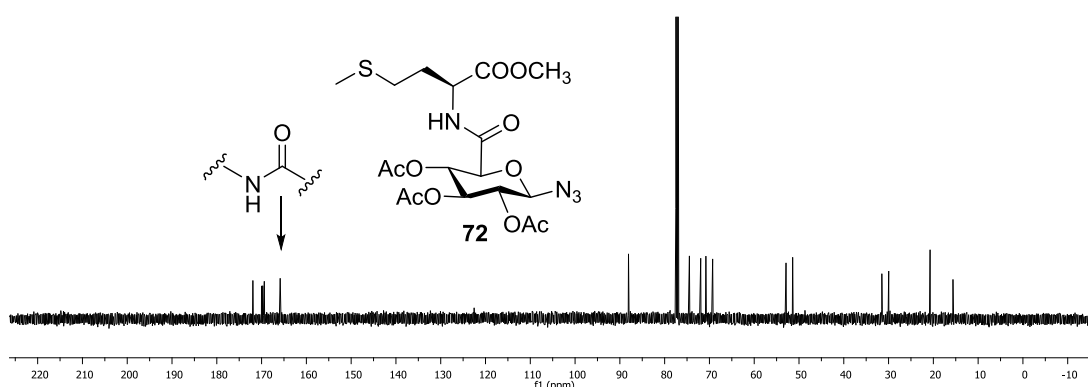


Figure 2.7: ^{13}C NMR spectrum of methionine-based “clickable” glycoconjugate **72**, highlighting the shielded carbonyl signal resulting from amide bond formation.

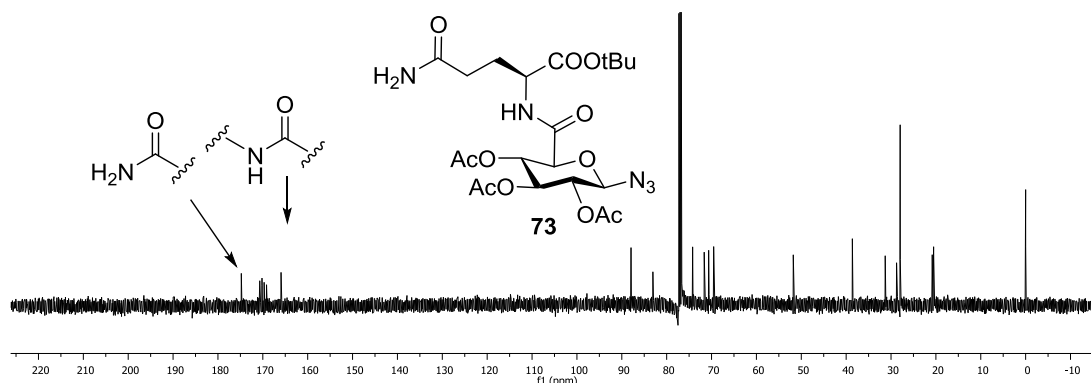


Figure 2.8: ^{13}C NMR spectrum of glutamine-based “clickable” glycoconjugate **73**, highlighting the shielded signal resulting from amide bond formation in comparison to the sidechain amide bond carbonyl.

2.5 Synthesis of Functionalized Glycoconjugates

2.5.1 Optimisation of CuAAC “Click” Reaction Conditions

With the production of “clickable” glycoconjugates **66-73** successfully achieved, efforts were subsequently made to demonstrate the versatility of the CuAAC “click” reaction towards this class of compounds. In order to optimize reaction conditions for all “click” reactions to be performed, the previously synthesized allyl ester intermediate **59** was utilized as an azide bearing glycoside, with the cheap and widely available 3-butyn-1-ol used as an alkyne donor. Using varying quantities of different copper salts (CuSO_4 , $\text{Cu}(\text{OAc})_2$) and sodium ascorbate,^{131,180} different solvent conditions, reaction times and the use of copper-stabilizing additives (e.g TBTA),¹⁸¹ the CuAAC “click” reaction between **59** and 3-butyn-1-ol was successfully optimized, producing the

triazole-containing glycoconjugate **74** in 88% yield after 24 hours of reaction time (Table 2.2, Entry F).

Table 2.2: Optimization of CuAAC “Click” reaction conditions, producing the triazole-bearing functionalized glycoconjugate **74.**

Entry	Cu(II)X ₂ .nH ₂ O	eq. Na Ascorbate	eq. Y	Solvent	Time	°C	Additives	Yield
A	CuSO ₄ .5H ₂ O	0.20	2.00	3:1 ACN:H ₂ O	8h	RT	-	37%
B	CuSO ₄ .5H ₂ O	0.20	2.00	1:1 nBuOH:H ₂ O	4h	40	-	49%
C	CuSO ₄ .5H ₂ O	0.20	4.00	1:1 nBuOH:H ₂ O	8h	RT	-	52%
D	CuOAc ₂ .2H ₂ O	0.20	4.00	1:1 nBuOH:H ₂ O	8h	RT	-	55%
E	CuOAc ₂ .2H ₂ O	0.20	4.00	1:1 nBuOH:H ₂ O	8h	RT	TBTA	60%
F	CuOAc₂.2H₂O	0.20	4.00	1:1 nBuOH:H₂O	24h	RT	-	88%

TLC monitoring of the reaction mixture highlighted the formation of a spot at significantly reduced R_f (0.18, 1:1 Hexane: EtOAc), which was indicative of the formation of a more polar product than the starting material, due to the presence of the terminal alcohol present on the alkyne. It is interesting to note that during our evaluation of different reaction conditions, the utilization of the known additive TBTA provided some increase in reaction yield, but was not ultimately used further (Table 2.2, Entry E). This is a result of the extra purification required to isolate **74** from the reaction mixture in the presence of TBTA, which during chromatographic isolation co-eluted with the product. In addition to visualization using TLC, the formation of **74** was highlighted in the ¹H NMR spectrum, where the presence of a singlet at 7.74 ppm was

indicative of the proton present at the 5'-position of the newly-formed triazole ring of **74**, with multiplets at 2.92 and 3.87 ppm each integrating for two protons indicative of the CH₂ groups linked to the triazole and hydroxyl groups, respectively (Figure 2.9).

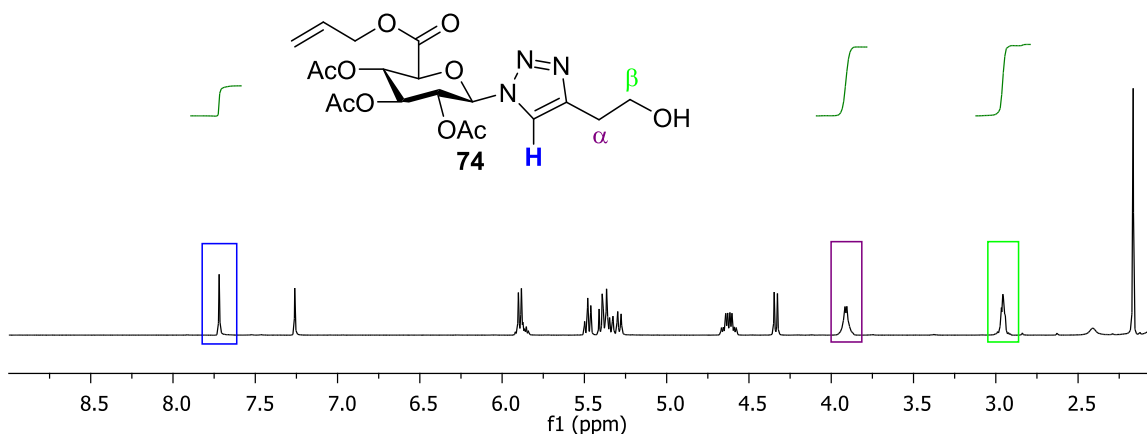
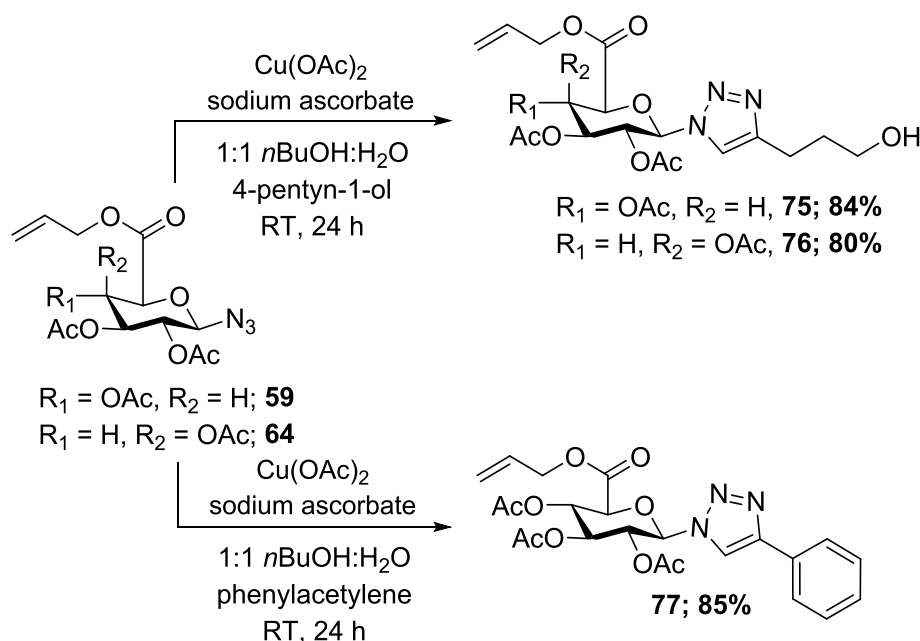


Figure 2.9: ¹H NMR spectrum of the functionalized triazole-bearing glycoconjugate **74**.

Following on from the formation of **74**, the CuAAC “click” reaction was further evaluated against a variety of alkyne donors. In the presence of 4-pentyn-1-ol, **59** and its respective *gal*-analogue **64** underwent successful “click” reaction, producing the triazole-bearing glycoconjugates **75** and **76** in 84% and 80% yields, respectively (Scheme 2.19). Compared to **74**, the ¹H NMR spectrum of **75** was quite similar except for the presence of a multiplet at 1.95 ppm, which was indicative of the central CH₂ group of the ligated alkyne. This too was represented in the ¹H NMR spectrum of **75** at 1.95 ppm. Following on from these examples, **59** was subjected to CuAAC “click” reaction with phenylacetylene, producing the glycoconjugate **77** in 85% yield (Scheme 2.19). A very different alkyne donor to those used in the production of **74-76**, the formation of the triazole was distinguished in the ¹H NMR by a signal at 8.08 ppm,

with the deshielding of the triazole proton compared to **74-76** likely due to the deshielding effect of the neighbouring phenyl ring.

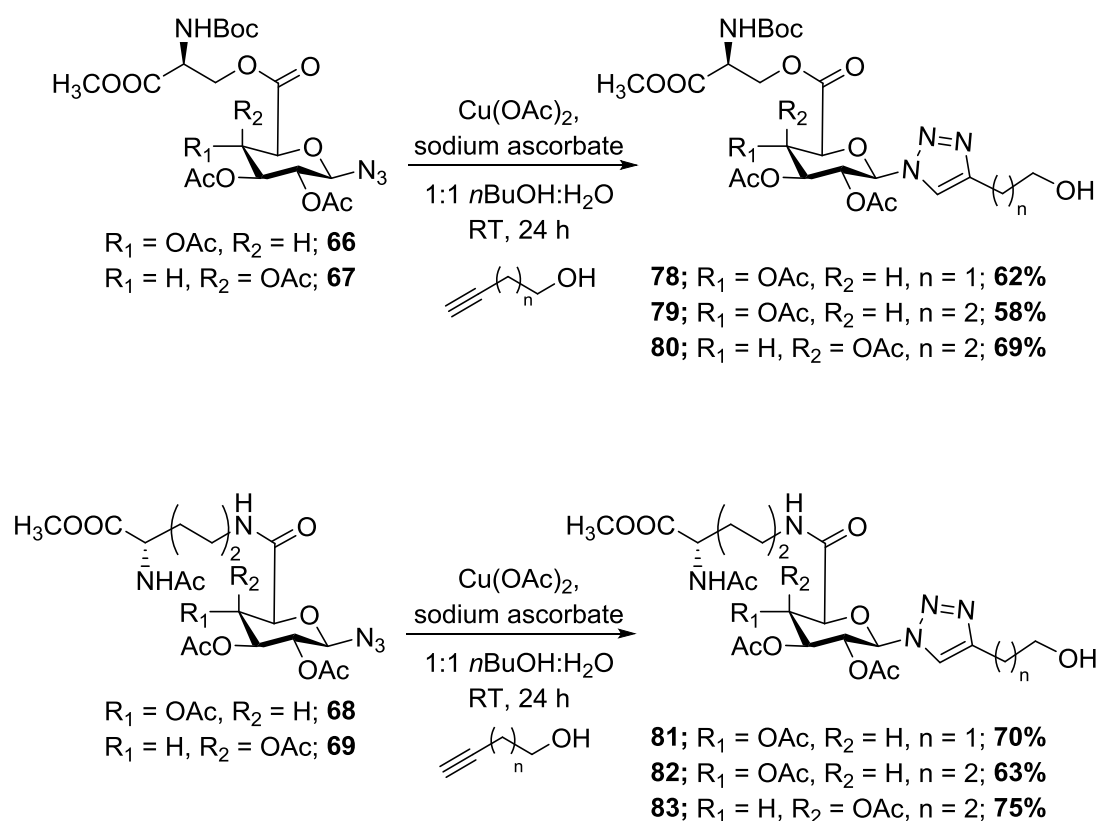


Scheme 2.19: Synthesis of triazole-bearing functionalized glycoconjugates **75-77**.

2.5.2 Synthesis of Functionalized Glycoconjugates (78-87)

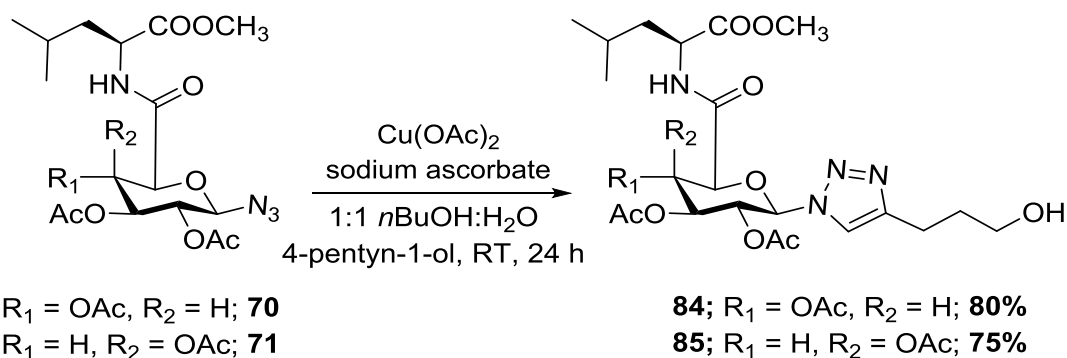
With reaction conditions for the CuAAC “click” reaction optimized, the functionalization of “clickable” glycoconjugates was undertaken. Initially evaluating sidechain-linked derivatives, the serine-based *glc* “clickable” glycoconjugate **66**, CuAAC “click” reaction with 3-butyne-1-ol resulted in the functionalized glycoconjugate **78** in 62% yield (Scheme 2.20). Similarly to **59** and **64**, this was extended to 4-pentyn-1-ol, where “click” reaction with **66** and the *gal* serine-based “clickable” glycoconjugate **67** resulted in the production of functionalized glycoconjugates **79** and **80** in 58% and

69% yield, respectively (Scheme 2.20), with LR-ESIMS of **79** and **80** (m/z 653, molecular formula $C_{26}H_{38}N_4O_{14} + Na$) confirming their production. Similarly, the *glc* and *gal* lysine-based “clickable” glycoconjugates **68** and **69** were subjected to the CuAAC “click” reaction. In the presence of 3-butyn-1-ol, “click” reaction with **68** resulted in the production of the functionalized glycoconjugate **81** in 70% yield (Scheme 2.20). The presence of a singlet in the 1H NMR spectrum of **81** at 7.87 ppm was indicative of triazole formation. Subsequently, **68** and **69** were subject to the CuAAC “click” reaction in the presence of 4-pentyn-1-ol, producing the functionalized glycoconjugates **82** and **83** in 63% and 75% yields, respectively (Scheme 2.20).



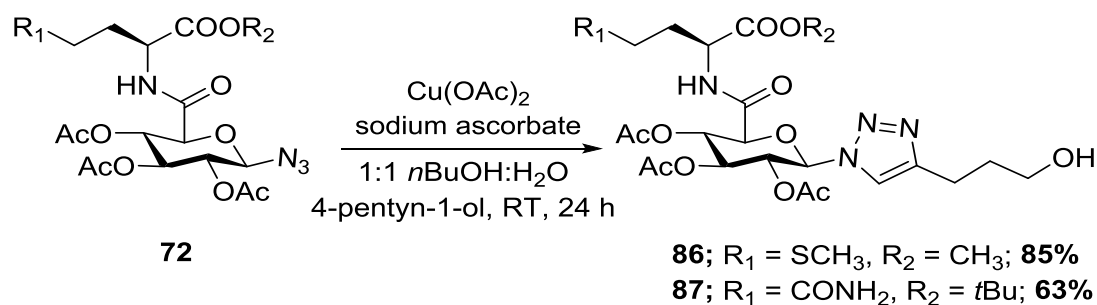
Scheme 2.20: Synthesis of triazole-bearing functionalized glycoconjugates **78-83**.

As a result of the successful production of functionalized glycoconjugates **78-83**, our focus turned to the synthesis of analogues derived from the previously synthesized α -amino derivatives **70-73**. Beginning with the *glc* and *gal*-linked leucine derivatives **70** and **71**, in the presence of 4-pentyn-1-ol both of these underwent CuAAC “click” reaction to produce the triazole-bearing functionalized glycoconjugates **84** and **85** in 80% and 75% yield, respectively (Scheme 2.21). HR-ESIMS of both **84** and **85** displayed molecular ions of m/z 579.2271 and 579.2273 respectively, which corresponded to a molecular formula of $C_{24}H_{36}N_4O_{11} + Na$ (579.2278) confirming the formation of the desired products.



Scheme 2.21: Synthesis of triazole-bearing functionalized glycoconjugates **84 and **85****

Subsequently, the CuAAC “click” reaction was extended to the methionine and glutamine-based derivatives **72** and **73**, whereby reaction with 4-pentyn-1-ol under the previously optimized conditons produced the triazole-bearing functionalized glycoconjugates **86** and **87** in 85% and 63% yields, respectively (Scheme 2.22).



Scheme 2.22: Synthesis of triazole-bearing functionalized glycoconjugates **86** and **87**

The ^1H NMR spectra of **86** and **87** displayed the presence of signals at 7.63 ppm and 8.15 ppm, both indicative of the triazole protons present in **86** and **87**. Furthermore, a deshielded signal at 2.86 ppm in the ^1H NMR spectrum of **86** is indicative of a CH_2 adjacent to an aromatic ring, indicative of the H^α protons introduced into **86** post “click” reaction (Figure 2.10). These protons are readily distinguished from the more shielded H^β , and the more deshielded H^γ protons of **86** (Figure 2.10).

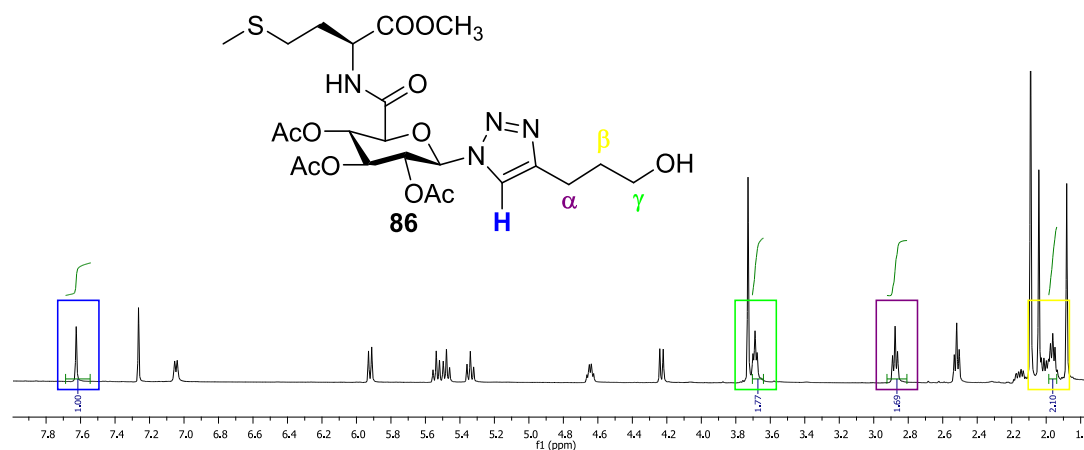


Figure 2.10: ^1H NMR spectrum of the functionalized glycoconjugate **86**, highlighting the formation of the triazole ring.

2.6 Towards the Synthesis and Functionalization of “Clickable” Glycopeptides

2.6.1 Synthesis of Sugar Azido Acid-Ac.Lys-Pro-Val.NH₂

Considering the success achieved in the synthesis and functionalization of “clickable” glycoconjugates **78-87**, the methodology was next investigated for expansion to the production and functionalization of “clickable” glycopeptides. Hence, in order to evaluate this possibility, our focus turned to the replication of this methodology on a small peptide system. In evaluating a peptide for coupling, it was recognized that a few key criteria would be important in selecting the peptide, including:

- Relevance to bioconjugation
- Contains a number of different functional groups that would be stable to the condition of the CuAAC “click” reaction

With these criteria in mind, an analysis of the literature was undertaken to discover a suitable candidate for this study. During this investigation, the protected tripeptide analogue Ac.Lys-Pro-Val.NH₂ (Ac.KPV.NH₂) (Figure 2.11) drew considerable attention. Forming the C-terminus of the naturally-occurring peptide α -melanocortin stimulating hormone (α -MSH) (Figure 2.11), Ac.KPV.NH₂ and its parent peptide have been found to display anti-inflammatory and antimicrobial activities, with Ac.KPV.NH₂ displaying activity comparable to the parent α -MSH.^{100,182,183} Furthermore, in respect to the compatibility of Ac.KPV.NH₂, the variety of functional groups it encompasses aligned well with those present in previously functionalized “clickable”

glycoconjugates, suggesting that the peptide would be stable to the CuAAC “click” reaction conditions previously optimized.

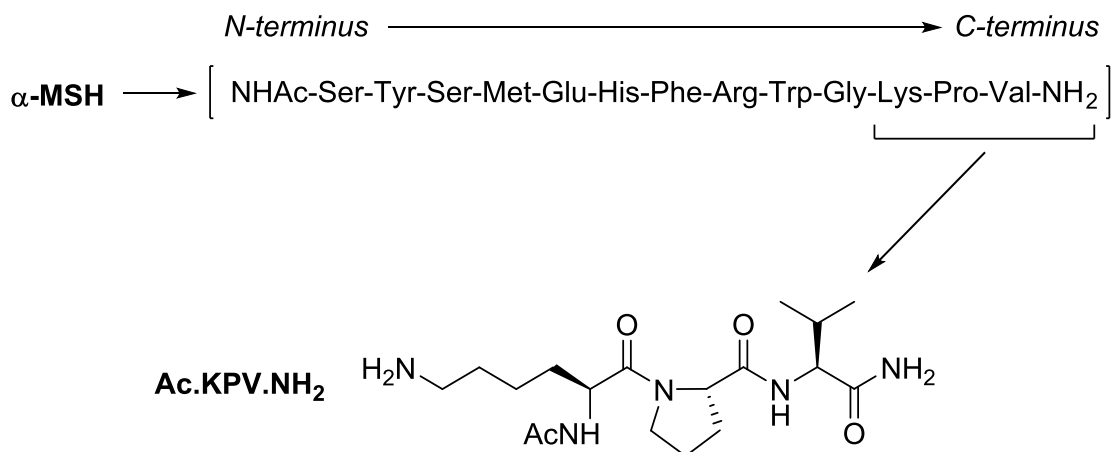
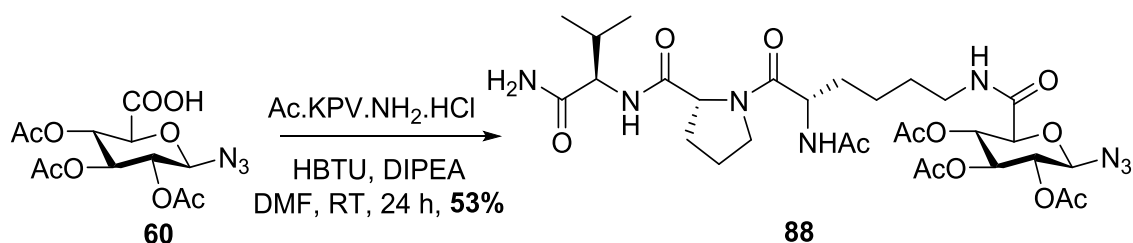


Figure 2.11: Primary structure of α -melanocortin stimulating hormone (α -MSH), and N^{α} -acetyl lysine-proline-valinamide (Ac.KPV.NH₂), a tripeptide analogue of the C-terminus of α -MSH

Therefore, in order to evaluate the CuAAC “click” reaction on a small glycopeptide, the *glc*- sugar azido acid **60** was coupled to the commercially available tripeptide Ac.Lys-Pro-Val-NH₂.HCl, which in the presence of HBTU and DIPEA in DMF produced the β -azide containing glycopeptide **88** in 53% yield (Scheme 2.23).



Scheme 2.23: Synthesis of Ac.KPV.NH₂-based “clickable” glycopeptide **88**

Evaluation of the ^1H NMR spectrum of **88** showed clear evidence of the desired coupled product, with a signal 6.83 ppm indicative of the sidechain NH_2 of the lysine of Ac.KPV. NH_2 .HCl (Figure 2.35). Furthermore, two multiplets integrating for one proton each at 3.38 and 3.05 ppm indicate splitting of the two geminal protons present on the C^ϵ of the lysine of the peptide – a result of their significantly different “environments” resulting from hydrogen bond stabilization (Figure 2.12). The correlations between these protons – similarly to the previously synthesized “clickable” glycoconjugate **68**, were exemplified in a gCOSY 2D NMR experiment of **88**, displaying a clear three-bond coupling between the geminal protons linked to the C^ϵ of the lysine of Ac.KPV. NH_2 .HCl and the neighbouring NH (Figure 2.13).

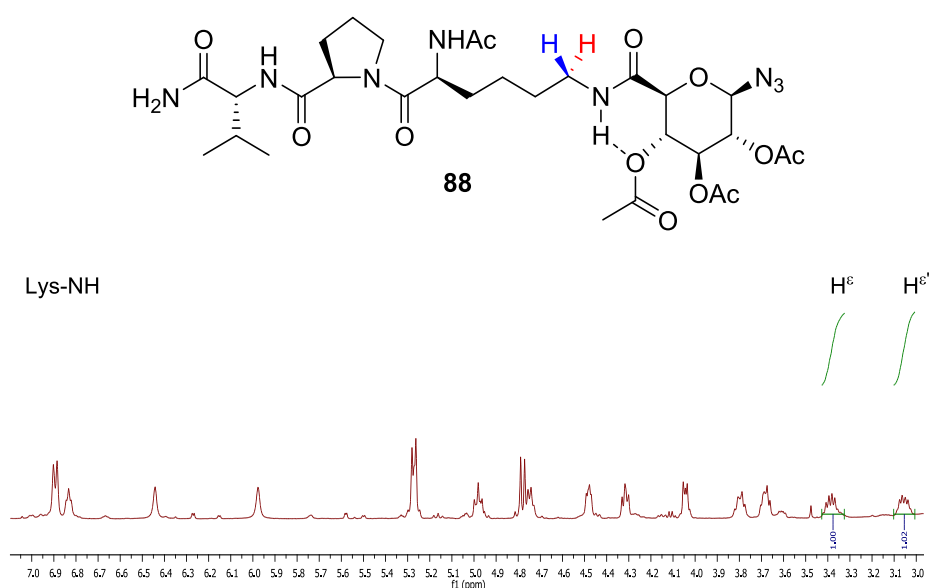


Figure 2.12: ^1H NMR spectrum of the *glc*-Ac.KPV. NH_2 -based “clickable” glycopeptide **88**, highlighting the pseudo 6-membered ring formed through hydrogen bonding, and three-bond coupling correlation.

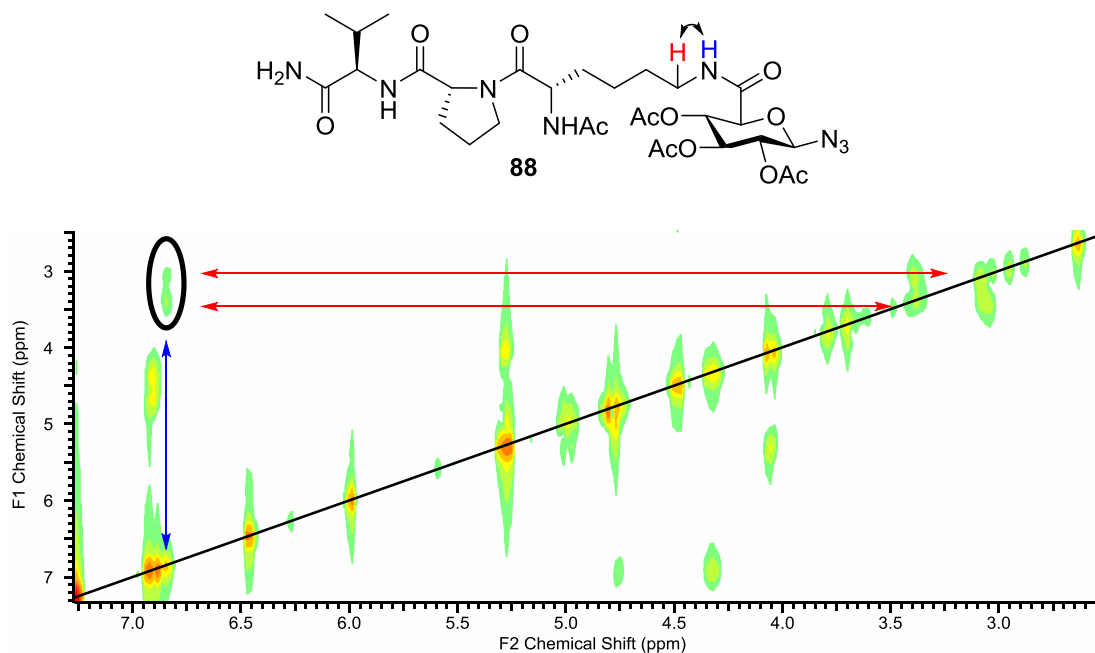
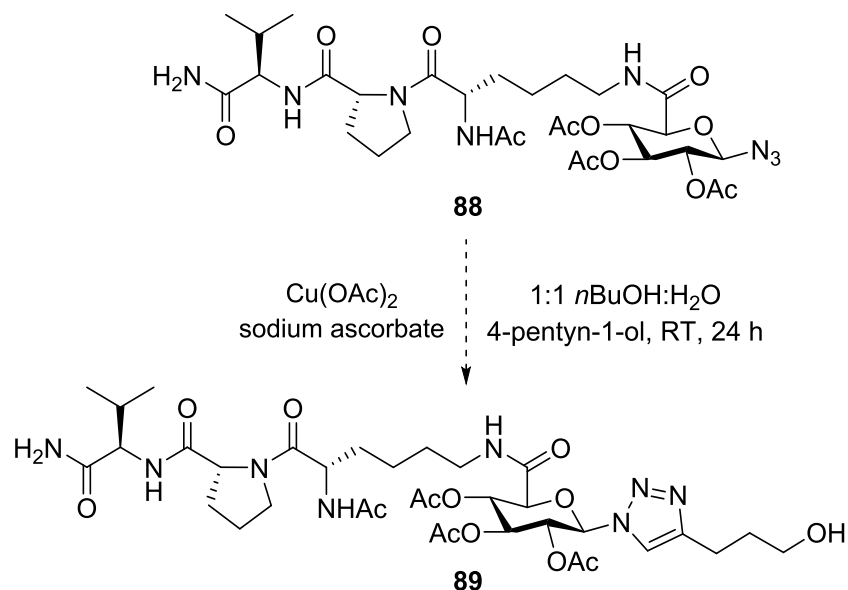


Figure 2.13: 2D ^1H NMR gCOSY experiment of the *glc*-Ac.KPV.NH₂-based “clickable” glycopeptide **88**, highlighting the pseudo 6-membered ring formed through hydrogen bonding, and three-bond coupling correlation.

With the synthesis and isolation of **88** achieved, the functionalization of the azide-bearing glycopeptide is expected to be straightforward. However, the production of **89** using the CuAAC “click” reaction was not performed due to time restraints. (Figure 2.24).



Scheme 2.24: Postulated synthesis of the *glc*-Ac.KPV.NH₂-based functionalized glycopeptide **89**

Herein, the synthesis and functionalization of a range of sidechain and α -amino linked glycoconjugates utilizing the CuAAC “click” reaction, has been described. Furthermore, the synthesis of the biologically-relevant glycopeptide **88** has provided an opportunity for the production of functionalized glycopeptides (such as **89**) via the CuAAC “click” reaction. In chapter 3, the synthesis and functionalization of “clickable” glycoconjugates will be further discussed, encompassing sidechain carboxyl-containing amino acids.

Chapter 3 : Synthesis and Functionalization of Sidechain-Linked “Clickable” Glycoconjugates

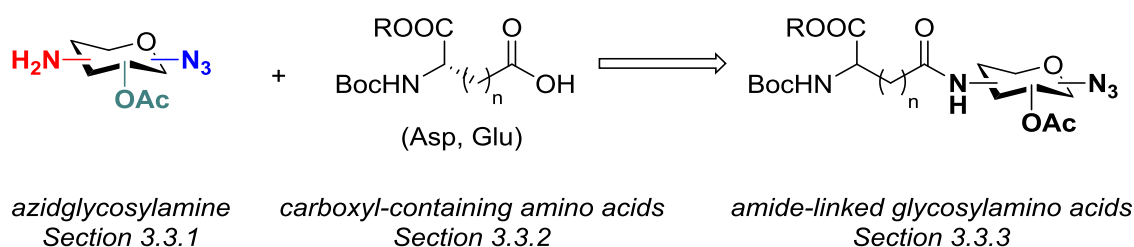
As illustrated in Chapter 2, “clickable” glycoconjugates represent a class of molecules that can be readily incorporated into biologically-active peptides, whilst retaining free handles for use in the CuAAC “click” reaction. In this chapter, the development of sidechain-linked “clickable” glycoconjugates will be examined.

3.1 Synthetic Rationale

In Chapter 2, the development of serine and lysine sidechain and leucine, methionine and glutamine α -amino linked “clickable” glycoconjugates, and their functionalization using the CuAAC “click” reaction, highlighted the potential of these species for utilization in the labelling of biologically-active peptides. Exploiting ester and amide-coupling chemistry in the preparation of these conjugates,¹⁵⁰ this platform methodology allows for the conjugation of sugar azido acids to a variety of different compatible amino acid residues used in bioconjugation, as highlighted by the synthesis of the “clickable” glycopeptide **88**. This strategy is highly advantageous in the synthesis of conjugates with free hydroxyl and amino groups, however it would also be useful to expand this methodology to other amino acid residues used in labeling and

bioconjugation. These include those bearing sidechain carboxyl groups, such as aspartic acid and glutamic acid.

Carboxyl-containing amino acid residues can be readily coupled to a glycosylamine to give rise to stable amide linkages formed using peptide-coupling chemistry. Hence, in consideration of the research detailed in Chapter 2, if a methodology utilizing amide coupling was developed to form conjugates between carboxylic acid-containing amino acids and azido glycosylamines, such analogues would be examples of amide-linked "clickable" glycoconjugates. Analogous to the glucuronic acid derivatives **66-73** described in Chapter 2, these conjugates would be amenable to the CuAAC "click" reaction, allowing for their use in the labelling and conjugation of biologically-active peptides (Scheme 3.1).



Scheme 3.1: Proposed synthesis of sidechain carboxyl-linked "clickable" glycoconjugates.

3.2 Synthetic Approach

It was recognized that the pronounced reactivity of the anomeric and 6-positions of a pyranoside would favour azidation or amination/conjugate formation, compared to other positions on the pyran ring. Using a simple glycosyl precursor containing a

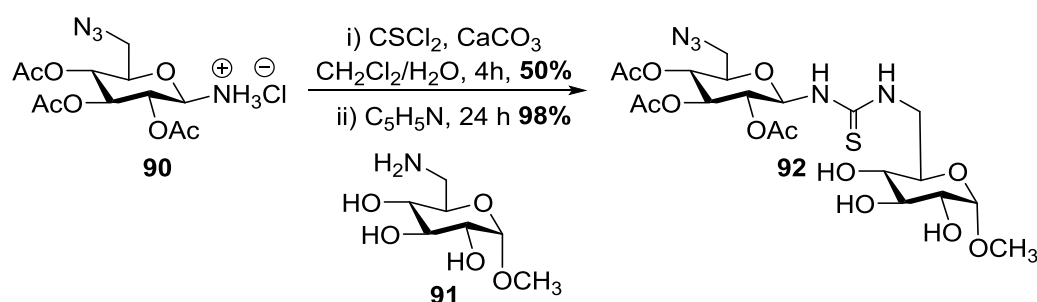
suitable leaving group (Ts, etc) at the 6-position, in stallation of an azide moiety via S_N^2 nucleophilic substitution would be highly favourable. Such 6-azidonated glycosides may then be subjected to reduction, producing an amine at the 6-position that could be coupled to carboxylic acid-containing derivatives to produce 6-amide linked sugar derivatives.^{146,184} Accordingly, a second azide group could be introduced at the anomeric centre, resulting in 6-linked azido sugar derivatives that may be amenable to the CuAAC click reaction (Scheme 3.1).

Conversely, an azide could be introduced at the 6-position of a relevant furanoside or pyranoside, and left available for utilization in the CuAAC reaction, with the introduction of an amine at the anomeric position, and subsequent protection and coupling of a sidechain carboxyl-containing amino acid would produce anomeric amide-linked conjugates (Scheme 3.1).^{185,186} The literature precedence for the synthesis of 6-azidoglycosylamines, endorses this strategy in the production of sidechain-linked “clickable” glycoconjugates (Scheme 3.1).

3.3 - Synthesis and Functionalization of Anomeric-linked “Clickable” Glycoconjugates

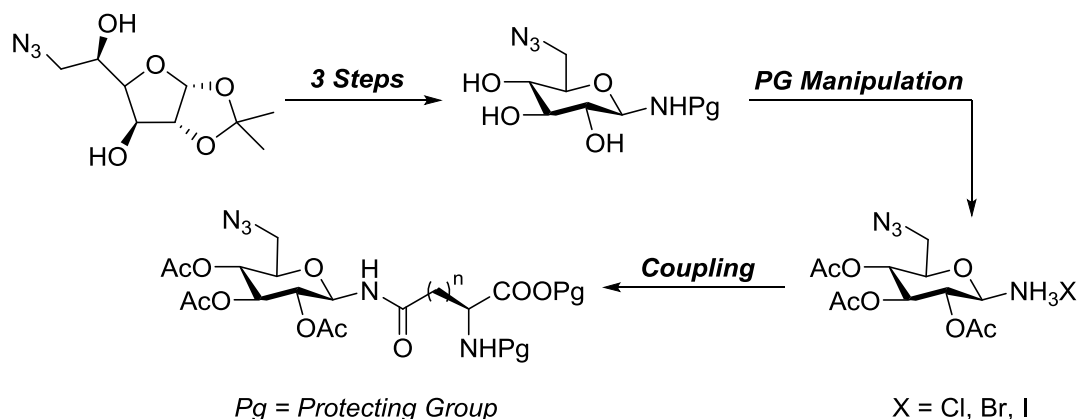
Thus, to further extend the library of “clickable” glycoconjugates to those linked via an acidic sidechain or α -carboxyl group, derivatives linked via the anomeric centre were investigated. As mentioned, an evaluation of the literature showed precedence for the preparation of glycoconjugates based upon glucopyranosylamines, including those bearing azide groups at a variety of different positions on the pyran ring.^{187,188}

Stereoselective amination of the anomeric centre of pyranoside has been thoroughly investigated, with the early work of Likhoshesterov and coworkers utilizing either ammonium carbonate, ammonium bicarbonate and ammonium carbamate in the production of β -glucopyranosylamines.¹⁸⁹ As a result, the tandem use of azidosugars encompassing an anomeric amine, such as the azidoglucopyranosylamines prepared by Garcia Fernandez and coworkers, have been used to great effect, providing synthons (such as **90**) that can readily undergo reaction at the anomeric centre, whilst maintaining an additional handle for derivatization (Scheme 3.2).¹⁸⁸



Scheme 3.2: Further derivatization of an azidoglucosylamine (90**) previously described by Garcia Fernandez and Co-workers.**¹⁸⁸

In the current context, azidoglucopyranosylamines can be accessed concisely from the known precursor 6-azido-1,2- α -D-glucofuranose (**96**), with protecting group manipulation providing synthons that can be coupled to both an acidic sidechain or α -carboxyl containing amino acid derivatives, and be available for use in the CuAAC “click” reaction (Scheme 3.3). Furthermore, the convergent nature of this approach allows for the utilization of a variety of different amino acid protecting group strategies, making such molecules amenable to further amino acid coupling (Scheme 3.3).

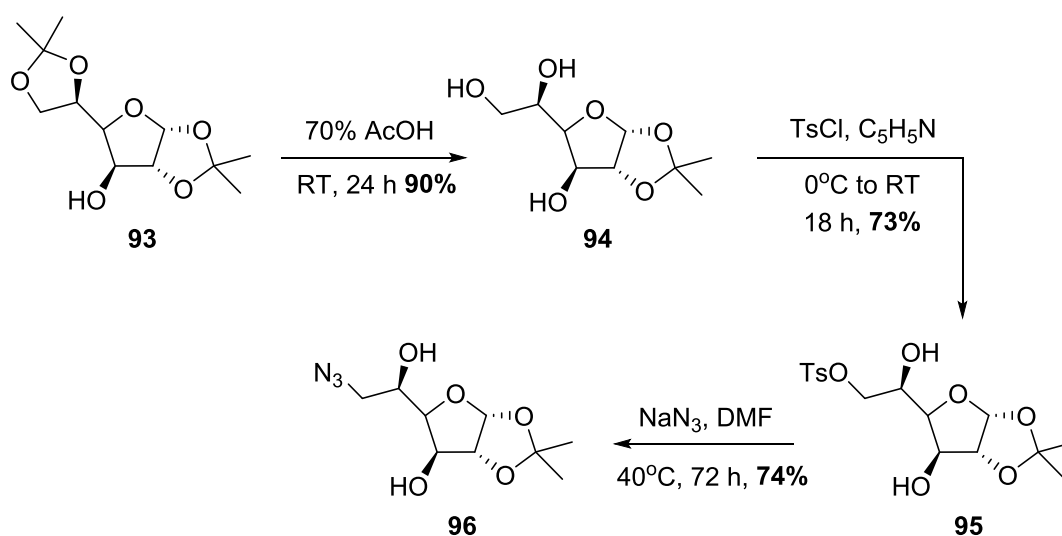


Scheme 3.3: Approach towards the synthesis of amide-linked “clickable” glycoconjugates linked at the anomeric position.

3.3.1 Synthesis of Key β -Azidoglycosylamine Intermediate 103

As a starting point for the production of amide-linked “clickable” glycoconjugates, the synthesis of the known 6-azido-1,2-isopropylidene- α -D-glucofuranose (**96**) was initiated. Starting from the commercially available, 1,2:5,6-di-isopropylidene- α -D-glucofuranose (**93**), cleavage of the primary acetonide under mild 70% acetic acid was effected, resulting in the production of 1,2-isopropylidene- α -D-glucofuranose (**94**) in 90% yield (Scheme 3.4), which was confirmed by ^1H and ^{13}C NMR spectroscopy.¹⁹⁰ Subsequently, **94** was subjected to standard tosylation conditions, with selective tosylation of the primary 6-OH resulting in the production of 6-*p*-toluenesulfonyl-1,2-isopropylidene- α -D-glucofuranose (**95**) in 73% yield (Scheme 3.4). The presence of two doublets at 7.79 and 7.33 ppm ($J = 7.9$ Hz) in the ^1H NMR spectrum, each integrating for two protons is indicative of the formation of the

mono-tosylated product, with the LR-ESIMS spectrum of **95** highlighting a signal at m/z 397, which was indicative of the product. The selectivity observed is a result of the steric hinderance encountered by the 3- and 5-OH groups, with the additional freedom of rotation experienced by the primary 6-OH providing a greater level of selectivity towards the 6-OH of **94**.



Scheme 3.4: Synthesis of 6-azido-1,2-isopropylidene- α -D-glucofuranose (**96**).

With **95** in hand, a modified procedure of Fleet *et al.* was trialed in the production of **96**.¹⁹¹ S_N² nucleophilic substitution of the 6-tosyl group by NaN₃ in DMF resulted in the requisite 6-azido-1,2-isopropylidene- α -D-glucofuranose (**96**) in 74% yield (Scheme 3.4). This was confirmed in the ¹H NMR spectrum of **96**, where disappearance of the aromatic protons of **95** indicated substitution with the azide group (Figure 3.1). Furthermore, the HR-ESIMS displayed a signal of m/z 280.0710 of chemical formula C₉H₁₅N₃O₅+ Cl (280.0700), which was indicative of the formed product.

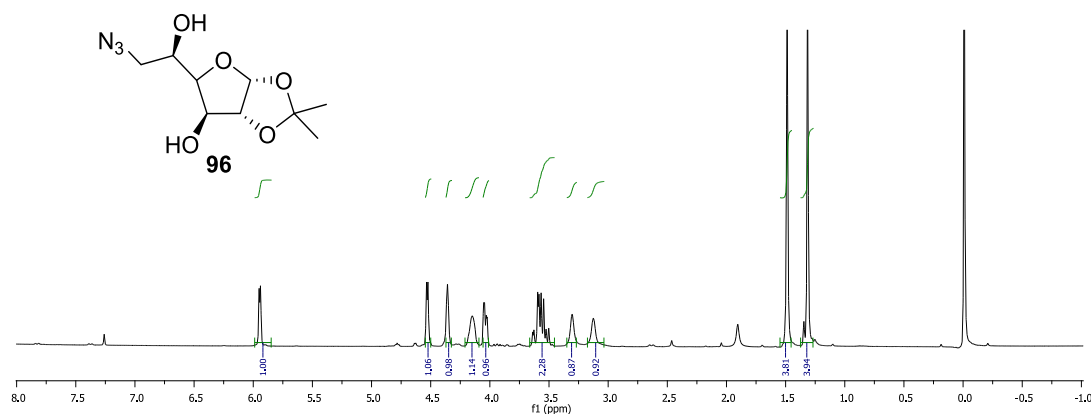
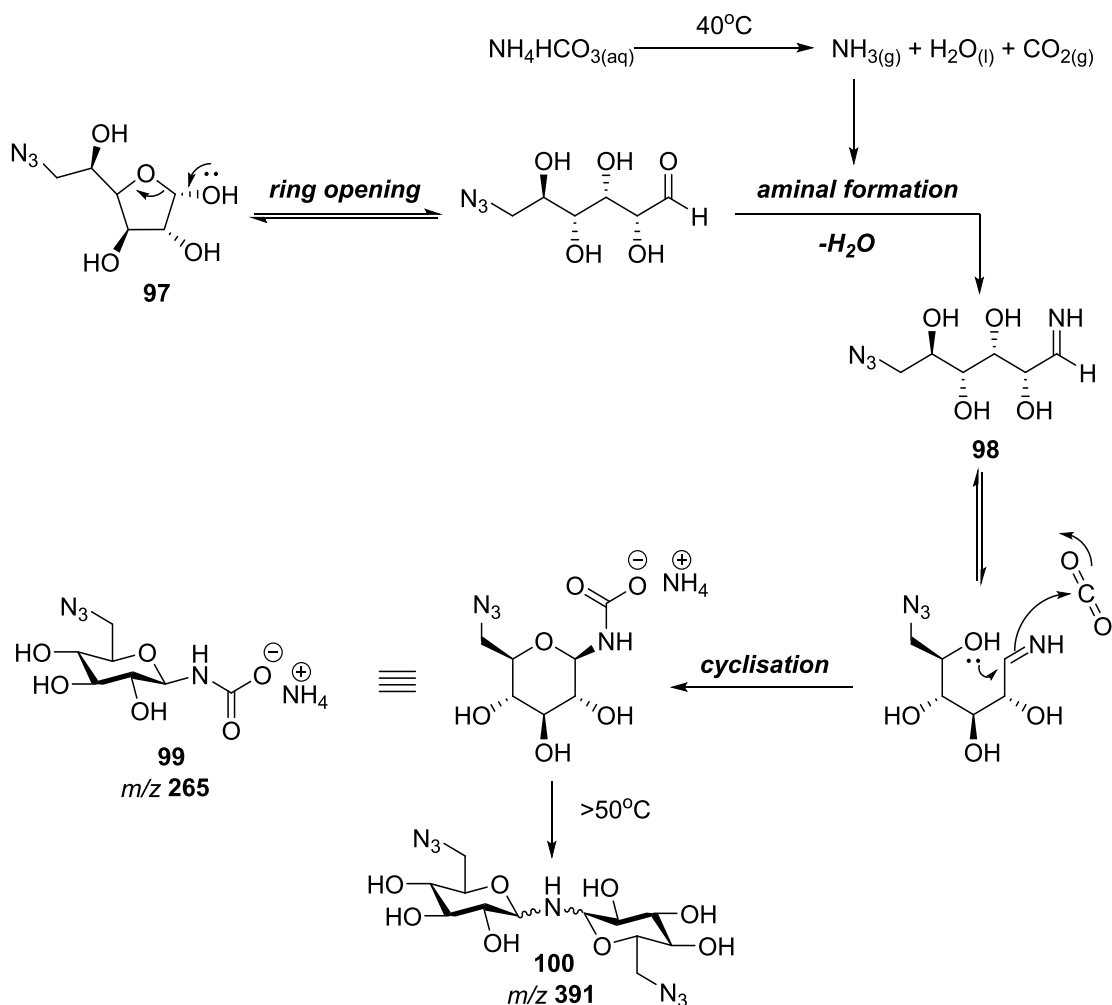


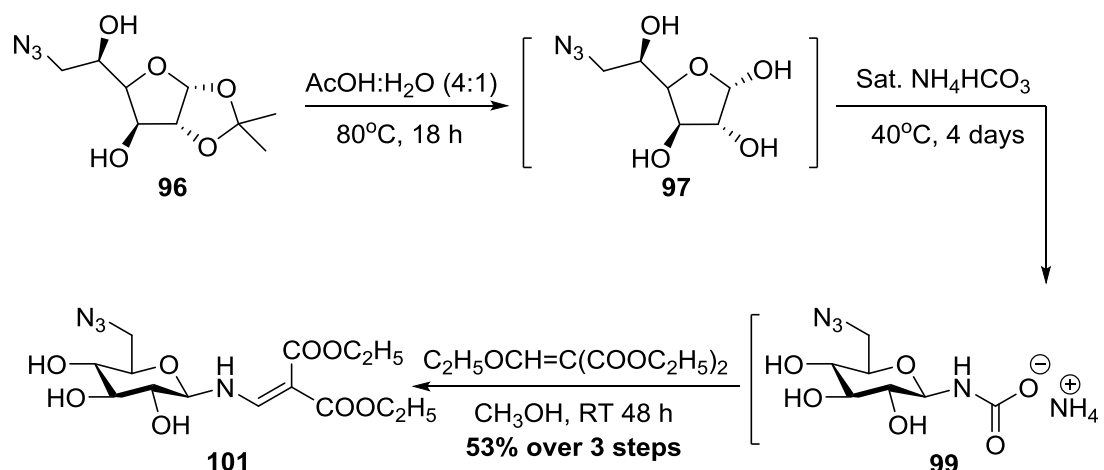
Figure 3.1: ^1H NMR spectrum of 6-azido-1,2-isopropylidene- α -D-glucofuranose (**96**).

Following the successful production of **96**, our focus next shifted to the synthesis of the key 6-azido- β -D-glucopyranosylamine intermediate **118**. Conversion of the furan ring to a pyran ring initially began with cleavage of the 1,2-isopropylidene group, using 80% acetic acid at 80°C, to yield the lactol intermediate **97** (Scheme 3.5). Subsequently, the glycoside was subject to prolonged heating in a saturated solution of NH_4HCO_3 at 40°C over four days. In this aqueous solution, it is proposed that the furanose intermediate underwent interconversion to its respective reducing sugar, which in the presence of NH_3 (formed from the decomposition of NH_4HCO_3) resulted in the formation of the aминаl intermediate **98**. Driven forward by the abstraction of dissolved CO_2 from the solution, **98** could then cyclize through the 5-OH of the reducing sugar, forming the pyranose carbamate ammonium salt **99** (Scheme 3.5). Indeed, the potential presence of this intermediate was suggested by the presence of a signal in the LR-ESIMS of the reaction mixture (m/z 265). Key to the formation of **99** was the maintenance of a saturated NH_4HCO_3 solution at precisely 40°C, with dissolved NH_3 and CO_2 gas essential for the reaction. Furthermore, if heated above 50°C, significant dimerization to form the bisglycosylamine compound **100** (m/z 409, $\text{M} + \text{NH}_4^+$) was observed (Scheme 3.5).



Scheme 3.5: Proposed mechanism for the production of **99** utilizing an NH_4HCO_3 -promoted anomeric amination.

Following lyophilisation, the ammonium salt **99** was subjected to protection of the anomeric amine using diethyl (ethoxymethylene)malonate, which as an excellent Michael acceptor that readily underwent nucleophilic substitution, liberating CO_2 , NH_3 and EtOH to produce the required enamine-protected 6-azido- β -D-glucopyranosylamine **101** in 53% yield from 6-azido-1,2-isopropylidene- α -D-glucopyranose (Scheme 3.6).



Scheme 3.6: Synthesis of enamine-protected 6-azido- β -D-glucopyranosylamine **101**.

Evaluation of the ^1H and ^{13}C NMR spectra of **101** (Figure 3.2, A and B) were inconclusive in their identification of the stereochemistry at the anomeric centre, with only the ^{13}C NMR spectrum displaying an upfield signal at 91.6 ppm suggesting that the stereochemistry around the anomeric centre of **101** may be beta (β -). The sole β -stereochemistry present at the anomeric carbon of **101** was however confirmed by a NOESY 2D ^1H NMR experiment, highlighting correlations between the H1 and H5 of **101**, suggesting they are both axially configured (Figure 3.3).

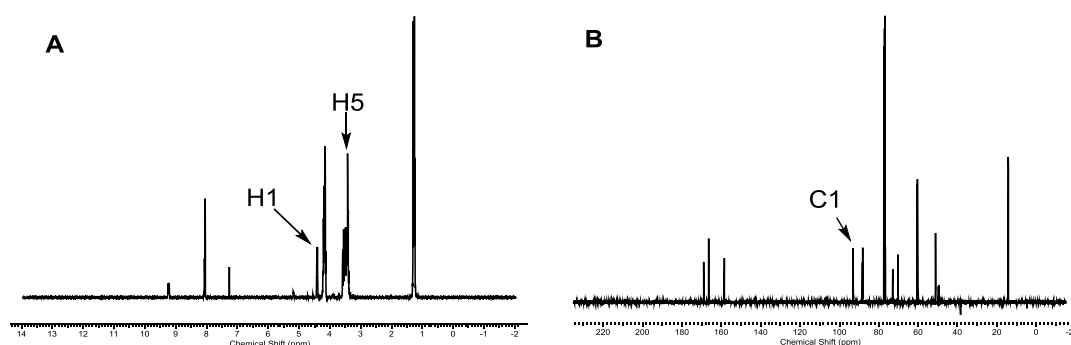


Figure 3.2: A: ^1H NMR spectrum of **101**, highlighting signals indicating H1 and H3, B: ^{13}C NMR spectrum of **101**, highlighting the downfield C1 carbon.

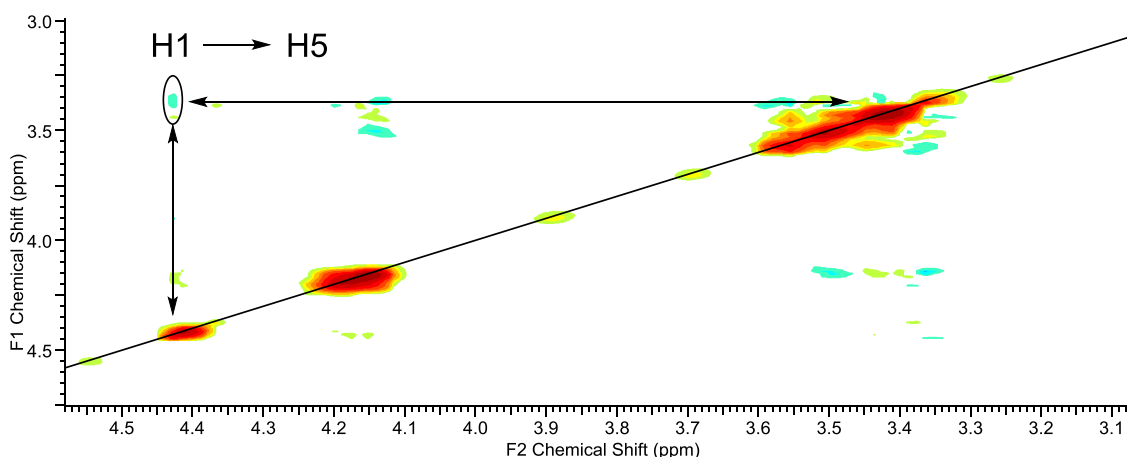
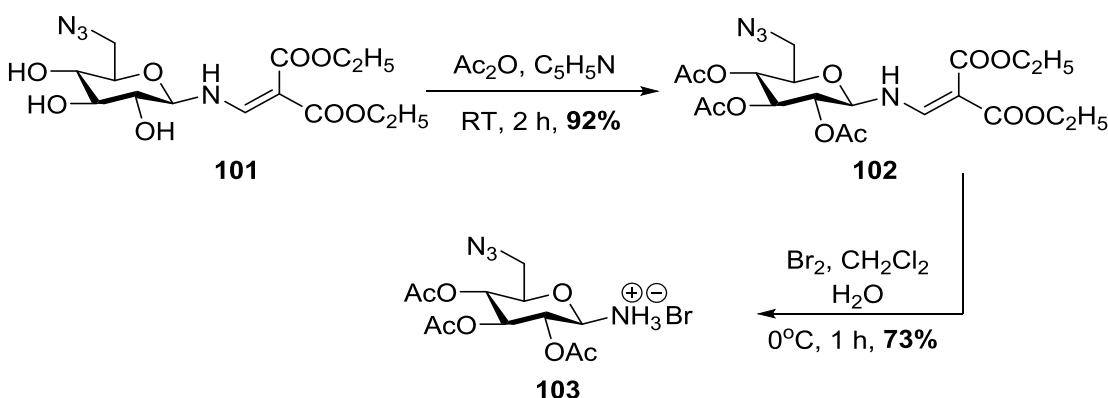


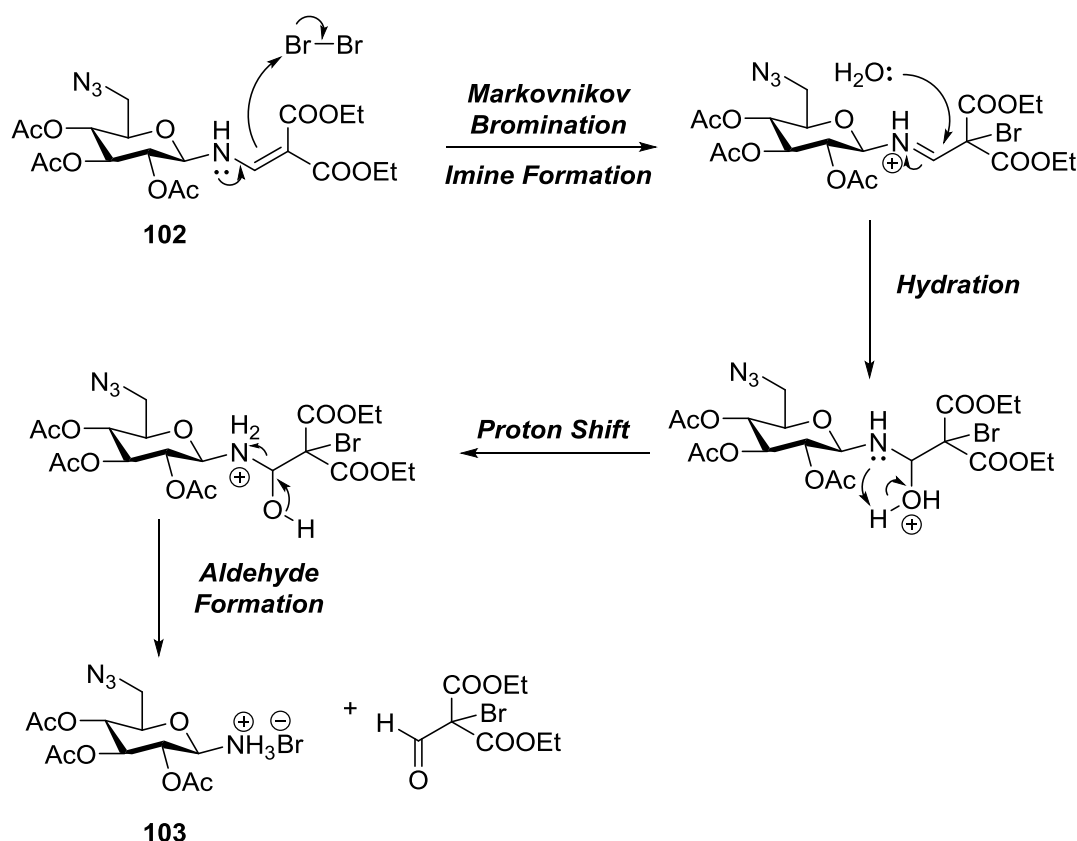
Figure 3.3: NOESY 2D ^1H NMR experiment of **101**, showing weak H1/H5 correlation.

Following the installation and protection of the required anomeric β -amine, **101** was then subject to peracetylation of the free 2-,3- and 4-OH groups under standard Ac_2O /pyridine conditions, yielding the fully protected glycoside **102** in 92% yield (Scheme 3.7). Subsequently, the anomeric enamine of **102** was cleaved under aqueous Br_2 , unmasking the anomeric amine, which was stabilized as a hydrobromide salt, producing **103** in 73% yield (Scheme 3.7).



Scheme 3.7: Synthesis of the 6-azido-2,3,4-tri-*O*- β -D-glucopyranosylamine hydrobromide salt **103**.

In the presence of Br_2 , the enamine **102** is subject to Markovnikov addition across the double bond, resulting in the formation of an iminium intermediate (Scheme 3.8). The presence of water in the reaction mixture drives nucleophilic substitution of the imine, which following proton transfer results in the formation of a α -hydroxy intermediate. Subsequently, the presence of bromide ions *in situ* from the initial use of Br_2 drive the formation of an aldehyde, resulting in the production of the desired ammonium hydrobromide salt **103** (Scheme 3.8). Whilst the synthesis of the corresponding hydrochloride salt (**90**) of **103** has previously been detailed,¹⁸⁸ the use of Br_2 represents a more readily accessible, safer option compared to the Cl_2 gas previously utilized.



Scheme 3.8: Proposed mechanism for the formation of **103** through enamine cleavage mediated by wet Br_2 .

The formation of **103** was indicated in the ^{13}C NMR spectrum, where the disappearance of the signal for the methylene carbon of **102**, and the shielding of the anomeric carbon from 95.2 ppm in **102** to 79.1 ppm in **103** due to the unmasking of the free amine, verified the cleavage of the anomeric protecting group (Figure 3.4).

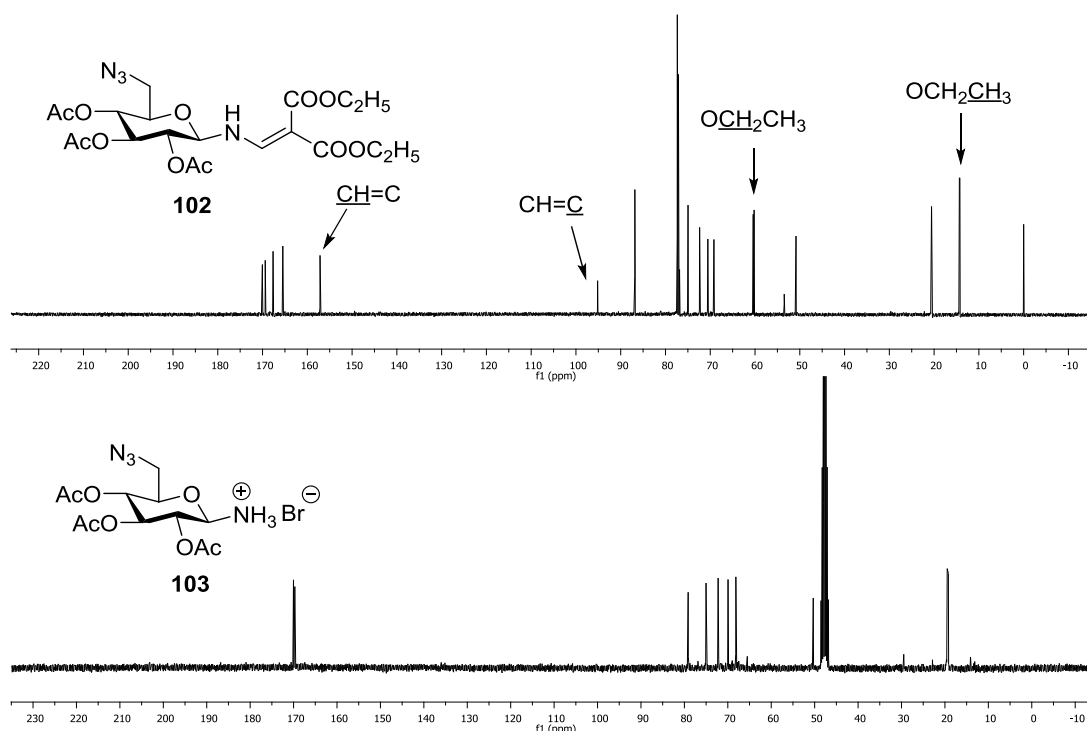


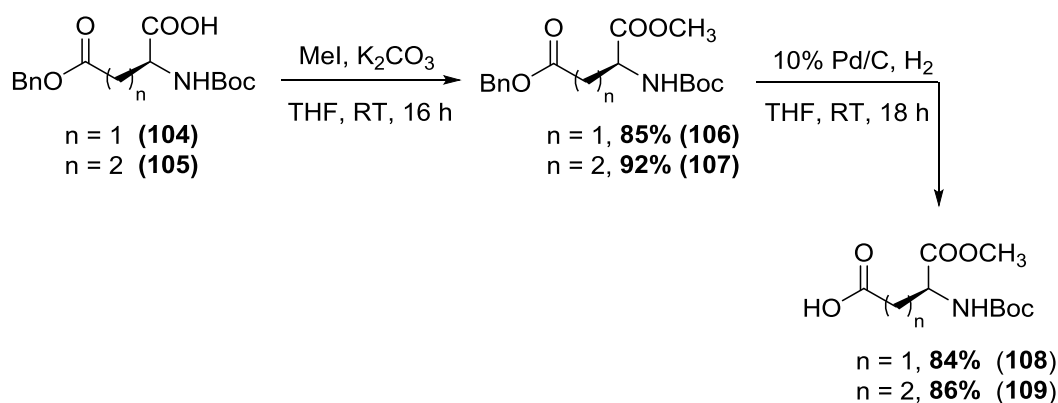
Figure 3.4: ^{13}C NMR spectra of **102** and **103**, highlighting the deprotection of the anomeric enamine.

3.3.2 Synthesis of Boc-protected Amino Acids **108** and **109**

With the required 6-azido- β -D-glucopyranosylamine **103** in hand, our focus now shifted to the synthesis of amino acids that could be coupled with **103**. Considering the widespread use of both aspartic and glutamic acid residues in the synthesis of

bioconjugates,¹⁹² it was decided that conjugates between **103** and protected aspartic and glutamic acid residues would be synthesised to broaden the scope of our current studies.

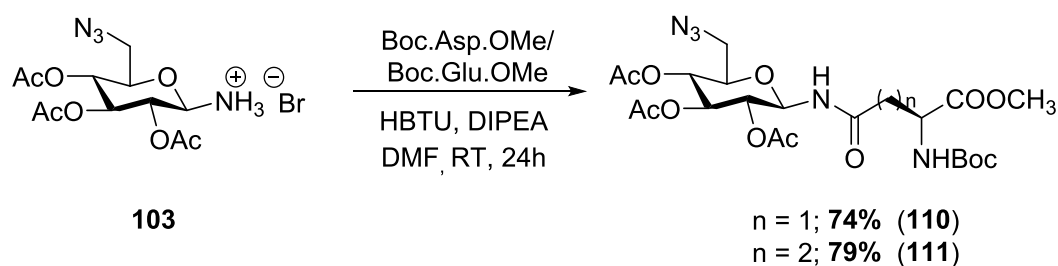
Hence, the synthesis of both protected aspartic acid and glutamic acid derivatives was performed, with the known Boc.Asp.OMe (**108**) and Boc.Glu.OMe (**109**) chosen. Starting from the Boc-*N*-protected benzyl ester derivatives **104** and **105**, using our own developed method methyl iodide and K₂CO₃ were employed to protect the α -carboxylic acid group of **104** and **105**, with successful esterification producing Boc.Asp(OBn).OMe (**106**) and Boc.Glu(OBn).OMe (**107**) in 85% and 92% yields, respectively (Scheme 3.9). Subsequently, reduction of the sidechain benzyl ester protecting groups of **106** and **107** produced the required Boc.Asp.OMe (**108**) and Boc.Glu.OMe (**109**) in 84% and 86% yields, respectively (Scheme 3.9).



Scheme 3.9: Synthesis of Boc.Asp.OMe (**108**) and Boc.Glu.OMe (**109**).

3.3.3 Synthesis of Sidechain Carboxyl-linked “Clickable” Glycoconjugates **110** & **111**

With our key building blocks synthesized, coupling between these protected amino acids **108** and **109** commenced. Utilizing HBTU as a coupling reagent in the presence of DIPEA, Boc.Asp.OMe (**108**) was successfully coupled to **103**, with reaction over 24 hours resulting in the “clickable” glycoconjugate **110** in 74% yield (Scheme 3.10).



Scheme 3.10: Synthesis of sidechain carboxyl-linked “clickable” glycoconjugates **110** and **111**.

In the ^1H NMR spectrum of **110**, the presence of a deshielded doublet at 6.55 ppm with coupling of 9.0 Hz was suggestive of a proton present on an amide nitrogen, indicative of the amide bond formed through the coupling (Figure 3.5, A). Furthermore, evaluation of a gCOSY experiment of **110** displays a correlation between this signal and a multiplet at 5.26 ppm, representing the three bond coupling present between H1 and the anomeric-linked NH (Figure 3.5, B). In addition to these, signals at 3.74 and 1.44 ppm integrating for three and nine protons respectively, and a signal in the HR-ESIMS of m/z 582.2029 representing a chemical formula $\text{C}_{22}\text{H}_{33}\text{N}_5\text{O}_{12}+\text{Na}$ (582.2023), definitively illustrated the production of **110**.

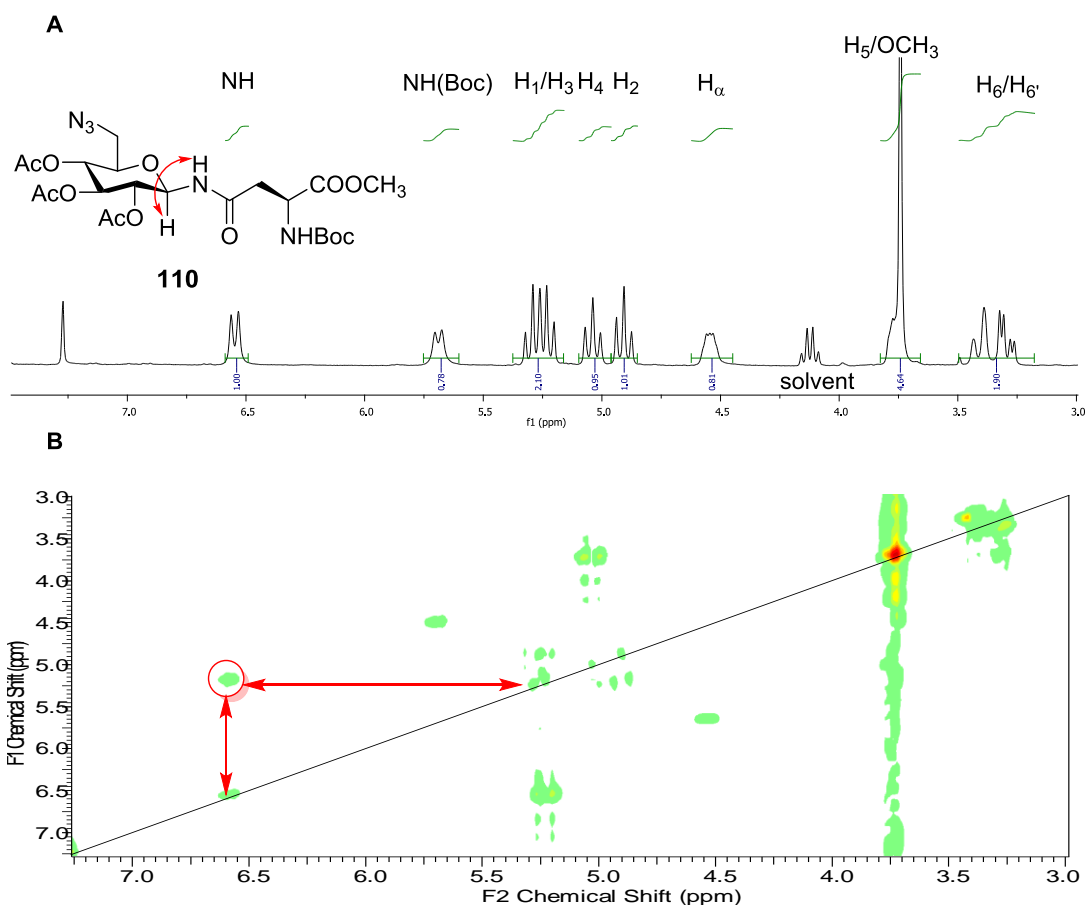


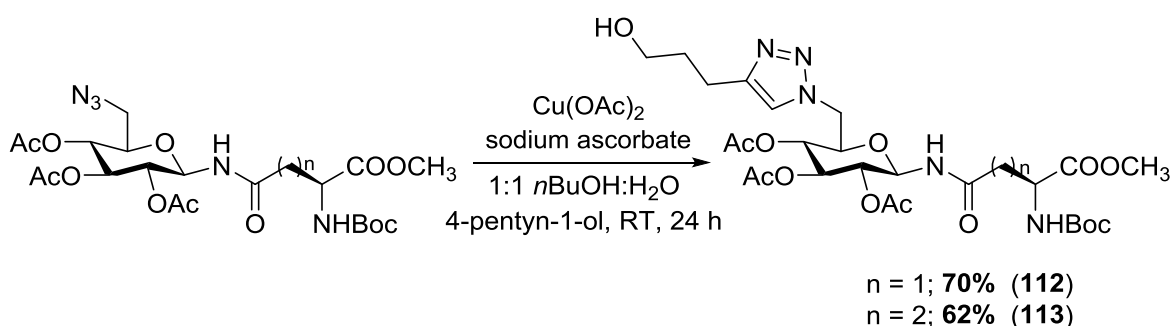
Figure 3.5: ^1H NMR spectrum (A) and gCOSY 2D ^1H NMR experiment (B) of the sidechain carboxyl-linked “clickable” glycoconjugate **110**, highlighting the correlation between the H1 and NH resulting from amide bond formation.

The success achieved in the formation of **110** was subsequently extended to the coupling of Boc.Glu.OMe. Reaction of **103** with under HBTU-mediated coupling conditions resulted in the production of the Glu-linked “clickable” glycoconjugate **111** in 79% yield (Scheme 3.10). Similarly to **110**, the presence of a deshielded doublet at 6.85 ppm in the ^1H NMR spectrum of **111** was indicative of the proton bound to the anomeric amide nitrogen, with a gCOSY experiment of **111** showing a correlation between the NH proton and a multiplet at 5.31 ppm representing the H1 proton. In the ^{13}C NMR spectrum of **111**, a signal at 172.7 ppm was indicative of the carbon of an

amide linkage, indicative of the coupling of **100** and **106**. Furthermore, the HR-ESIMS displayed a signal of m/z 596.2204 representing a chemical formula of $C_{23}H_{35}N_5O_{12}+Na$ (596.2180), indicative of the desired product. Examples of sidechain carboxyl-linked “clickable” glycoconjugates, **110** and **111** represent the first instances of sidechain carboxyl-linked “clickable” glycoconjugates described.

3.3.4 Synthesis of Functionalized Sidechain Carboxyl-linked Glycoconjugates **112** & **113**

With the production of carboxyl sidechain-linked “clickable” glycoconjugates **110** and **111** successfully achieved, our attention now turned to their functionalization via the CuAAC “click” reaction. Utilizing the conditions previously described in Chapter 2 for the functionalization of “clickable” glycoconjugates **66-73**, aspartic acid derivative **110** was subject to the CuAAC “click” reaction with 4-pentyn-1-ol. Subsequently, after work up and flash column chromatography the functionalized derivative **112** was isolated, in 70% yield (Scheme 3.11).



Scheme 3.11: Synthesis of functionalized sidechain carboxyl-linked “clickable” glycoconjugates **112** and **113** through the CuAAC “click” reaction.

An evaluation of the ^1H NMR spectrum of **112** illustrated the formation of the desired triazole-bearing product, with a singlet at 7.54 ppm ascribed to the triazole proton (Figure 3.6). Interestingly, two signals at 4.55 ppm and 4.61 ppm were suggestive of the H6/H6' protons adjacent to the triazole ring, with the electron-rich nature of the neighbouring triazole ring deshielding these protons by approximately 1.1 ppm compared to the parent glycoconjugate **110** (Figure 3.5). Furthermore, HR-ESIMS of **112** displayed a signal of m/z 666.2621, which was indicative of the product with a molecular formula of $\text{C}_{27}\text{H}_{41}\text{N}_5\text{O}_{13} + \text{Na}$ (666.2599).

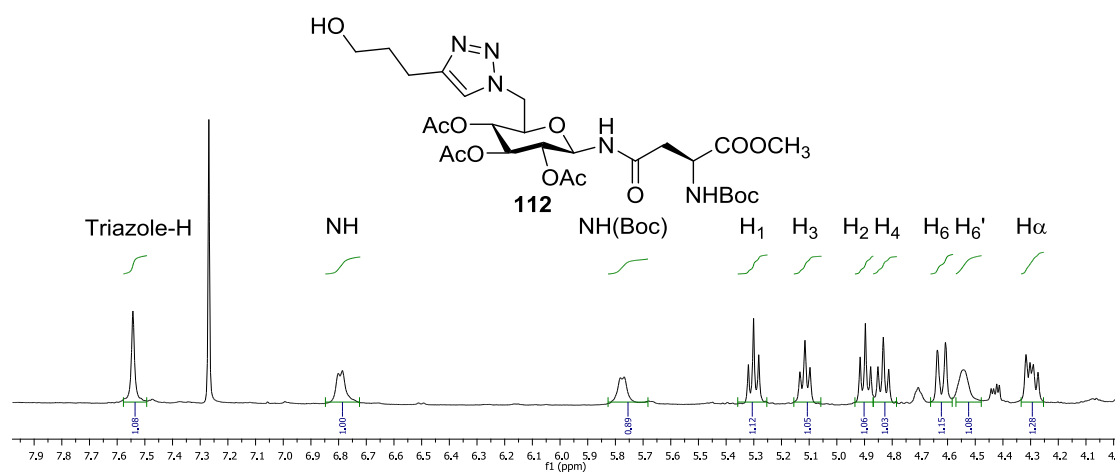


Figure 3.6: ^1H NMR spectrum (4.0 ppm – 8.0 ppm) of functionalized glycoconjugate **112**, highlighting the formation of a 1,4-substituted triazole.

Subsequently, following on from the successful production of **112**, the glutamic acid derivative **111** was also subjected to the CuAAC “click” reaction with 4-pentyn-1-ol, which up on work up and isolation yielded the functionalized derivative **113** in 62% yield (Scheme 3.11). Similarly to **112**, a downfield singlet in the ^1H NMR spectrum of **113** at 7.72 ppm was indicative of the desired product, representing the

triazole proton. Furthermore, a more deshielded doublet at 4.31 ppm was ascribed to the H6/6' protons of **113**, with the HR-ESIMS of **113** displaying a signal for the desired product of m/z 680.2793, corresponding to the formula $C_{28}H_{43}N_5O_{13} + Na$ (680.2755).

To summarize, the synthesis of the azidoglucosylamine **103** has provided access to the development of “clickable” glycoconjugates **110** and **111** through amino acids coupled to sidechain-carboxyl groups. Further derivatization of these glyconjugates utilizing the CuAAC “click” reaction has broadly extended the utility of this methodology beyond the ester and amide-linked conjugates produced in chapter 2. In chapter 4, the extension of this approach to the synthesis and functionalization of thioether-linked “clickable” glycoconjugates will be discussed.

Chapter 4 : Synthesis and Functionalization of Thioether-linked “Clickable” Glycoconjugates

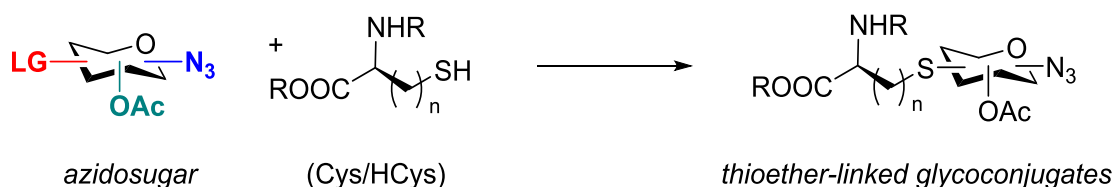
Chapters 2 and 3 detailed the development of ester and amide linked azido sugar amino acid derivatives attached through either sidechain groups such as NH₂, OH or COOH, or via the N-terminus. These “clickable” glycoconjugates could be readily incorporated into biologically-active peptides, whilst retaining free handles for use in the CuAAC “click” reaction. In this chapter, the development of thioether-linked “clickable” glycoconjugates will be presented.

4.1 Synthetic Rationale

In Chapters 2 and 3, the synthesis of “clickable” glycoconjugates exploiting amide-coupling chemistry was highlighted. Demonstrating the coupling of sugar azido acids to a variety of different amino acid residues (e.g. Ser, Lys, Asp and Glu), the following approach provides a highly advantageous method for the synthesis of bioconjugates. However, beyond the following amide and ester-linked examples, there are a number of different conjugate types that are incompatible with this approach. These include thioesters formed through the coupling of thiol-containing amino acids such as cysteine or homocysteine to carboxylic acids, which are less stable than their corresponding esters.¹⁹³ Thioesters are susceptible to degradation under acidic or basic

conditions and prone to substitution in the presence of stronger oxygen and nitrogen-based nucleophiles. Although their use has been widely applied in areas of peptide and ligation chemistry, such as native chemical ligation,^{193,194} the lability of these linkages has made their use in the development of stable bioconjugates unsuitable.

In contrast, thioethers represent linkages which provide excellent chemical stability under a range of different conditions. Widely accessible through alkylation, they have been commonly used in the developments of conjugates with thiol or alcohol-containing amino acids.¹⁹⁵ If a class of azidosugars were developed that had the capacity to form thioether linkages, these could produce glycoconjugates with amino acids such as cysteine and homocysteine. Comparable to the examples described in Chapter 2 and Chapter 3, these glycoconjugates would be “clickable,” and could therefore be utilized to functionalize biologically-active peptides via “click” chemistry (Scheme 4.1).

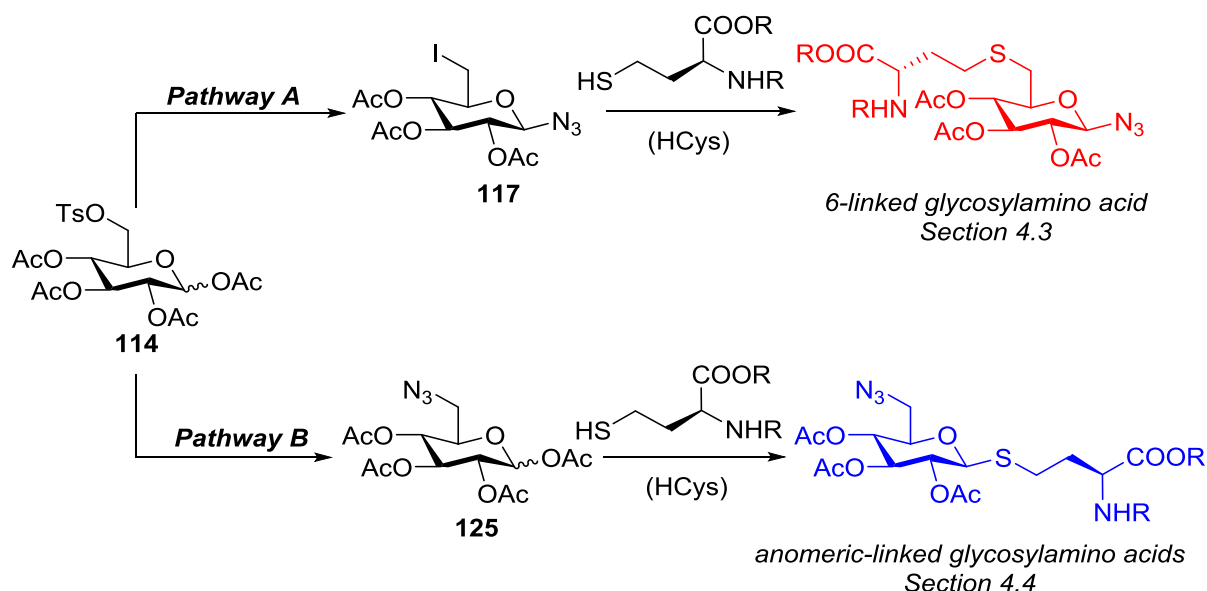


Scheme 4.1: Proposed synthesis of thioether-linked "clickable" glycoconjugates.

4.2 Initial Synthetic Approach

Building upon the earlier strategies that produced “clickable” glycoconjugates bearing azides at the anomeric (Chapter 2) and 6-position (Chapter 3) of the glycoside,

respectively, a divergent synthetic strategy that could produce both of these types of glycoconjugates was initially undertaken. Using a simple precursor such as D-glucose would allow for the introduction of the required azide moiety. Also, the presence of a suitable leaving group would allow for the installation of a thioether-linkage through alkylation. A *p*-toluenesulfonyl (tosyl; Ts) group, when utilized in a fully-protected glycoside (such as **114**, Figure 4.3), provides a strategy whereby an azide moiety can be introduced into the molecule by a number of different ways (Scheme 4.2, pathway A).



Scheme 4.2: Pathways towards the synthesis of thioether-linked “clickable” glycoconjugates.

Akin to examples described in chapter 2 (*cf* earlier synthesis of **58** and **63**, section 2.3), bromination of the anomeric acetate of **114** using HBr in acidic conditions could be utilized to produce an anomeric α -bromide intermediate (**115**). Based on Hard Acid Soft Base (HSAB) theory, both the anomeric α -bromide and OTs groups represent soft leaving groups. The bromide of **115** however is a better leaving group than the

6-OTs moiety, with this judgement based on the pK_a of the conjugate acid of each leaving group (pK_a : HBr = -9, TsOH = -2.8). As a result of this difference, in the presence of NaN_3 selective S_N^2 nucleophilic substitution of the anomeric centre of **115** would be favoured, resulting in the production of the β -azide **116**. Subsequently, the replacement of the stable 6-OTs of **116** with a more labile leaving group (e.g. halide - Br, I) would produce a glycoside that could be alkylated to yield thioether-linked glycoconjugates (Figure 4.2, pathway A). This judgement is based on the soft nature of a thiol nucleophile, with a softer leaving group (for example, pK_a HI = -10), more likely to undergo nucleophilic substitution in the presence of a relatively soft nucleophile. Alternatively to this approach, the tosyl group of **114** could be subjected to directly nucleophilic substitution in the presence of NaN_3 , resulting in the production of the 6-azidonated glycoside **125**. The subsequent introduction of an anomeric leaving group would allow for the formation of the desired glycoconjugates through glycosylation chemistry (Scheme 4.2, pathway B).

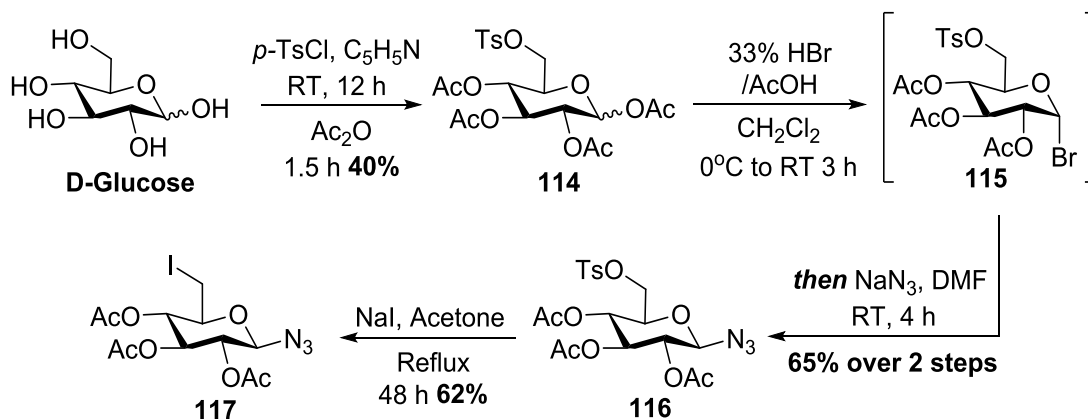
4.3 Attempted Synthesis of 6-Thioether-linked “Clickable” Glycoconjugates

4.3.1 Synthesis of 6-Iodo-2,3,4-tri-*O*-acetyl- β -D-glucosyl azide (**117**)

With the following options available, the synthesis of thioether-linked “clickable” glycoconjugates initially focused on the synthesis of derivatives incorporating amino acids linked to the glycoside at the 6-position. The lack of a stereocentre at the 6-position of these glycosides would remove problems regarding

stereoselectivity in these conjugates, and the potential formation of epimers during alkylation. Hence, D-glucose was initially subject to *p*-tosylation at the 6-position using *p*-toluenesulfonyl chloride and pyridine, with the subsequent addition of acetic anhydride resulting in the acetylation of the remaining alcohols, producing 6-*p*-toluenesulfonyl-1,2,3,4-tetra-*O*-acetyl-D-glucose (**114**, Scheme 4.3) in 40% yield.¹⁹⁶ The moderate yield of this reaction is a direct result of the lack of selectivity of the *p*-tosylation step, which in comparison to the previously synthesized furanose *p*-tosylate **95** is much less hindered. The inefficiency of this process however, was offset by the high scalability and simple purification of this process, in addition to the divergent nature of the synthesis to be performed from this key intermediate.

With **114** in hand, installation of the anomeric β -azide to produce the required 6-*p*-toluenesulfonyl- β -D-glucosyl azide **116** was undertaken. In comparison to the synthesis of β -azides previously described in chapter 2, SnCl₄-mediated azidation was not considered, due to the likely cleavage of the tosyl group in the presence of the tin catalyst. Hence, **114** was instead subjected to anomeric α -bromination conditions by reaction with 33% w/v HBr/AcOH in dichloromethane producing the anomeric bromide intermediate **115** (Scheme 4.3). Under subsequent S_N² nucleophilic azidation using sodium azide in DMF, 6-*p*-toluenesulfonyl-2,3,4-tri-*O*-acetyl- β -D-glucopyranosyl azide was isolated in 65% yield over the two steps (**116**, Scheme 4.3).



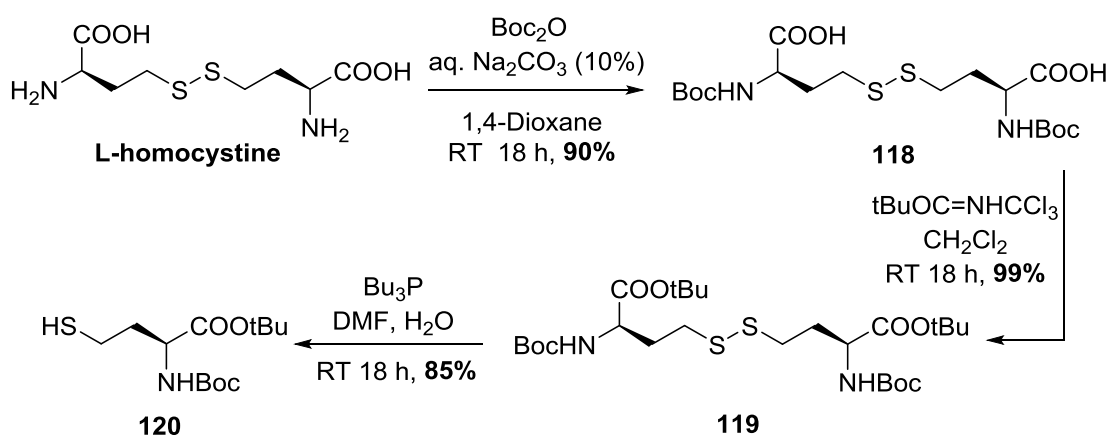
Scheme 4.3: Synthesis of 6-iodo-2,3,4-tri-*O*-acetyl- β -D-glucopyranosyl azide (**117**).¹⁹⁶

The production of **116** was confirmed by the ^1H NMR spectrum, where a shielded doublet at 4.56 ppm ($J = 9.8$ Hz) indicated the introduction of a β -azide into the molecule. Whilst in its own right the *p*-tosyl group represents a good leaving group, it was believed that the stability of this group (compared to more labile, soft leaving groups) would prevent the formation of **124** under mild alkylating conditions. Hence, the introduction of a more labile leaving group was investigated. A halide, such as an iodo group, would be more inclined to undergo elimination in the presence of a suitable nucleophile, negating the requirement for stronger basic conditions to drive alkylation. Furthermore, it is possible that nucleophilic substitution of the iodo group could be favoured over the dimerization of the alkylating thiol, a common side reaction in the presence of base. Hence, utilizing classical Finkelstein iodination conditions employing 4.0 equivalents of sodium iodide in acetone,¹⁹⁶ the *p*-tosyl containing azidosugar **116** was iodinated at the 6-position, to produce 6-iodo-2,3,4-tri-*O*-acetyl-D-glucosyl azide in 62% yield (**117**, Scheme 4.3). In the ^1H NMR spectrum of **117**, the disappearance of two doublets at 7.80 ppm and 7.36 ppm were indicative of substitution of the tosyl

group, with a more shielded signal at 3.60 ppm in the ^{13}C NMR spectrum of **117** indicative of the formation of a C-I bond at the 6-position.

4.3.2 Synthesis of Thiol-bearing Amino Acid Boc.HCys.OtBu (**120**)

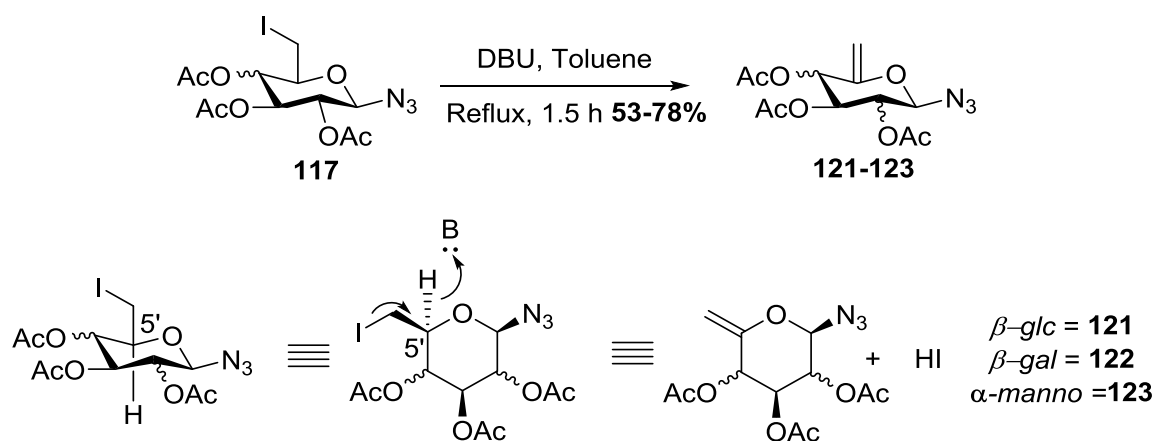
With the requisite carbohydrate building block in hand, the synthesis of the thiol-containing amino acid was attempted, with the homocysteine (HCys) derivative *N*-tert-butoxycarbonyl-L-cysteine-*t*-butyl ester (Boc.HCys.OtBu) chosen as the thiol-containing amino acid. Starting from L-homocystine, Boc-protection of the α -amino groups using aqueous Na_2CO_3 yielded **118** in 90% (Scheme 4.4), which in the presence of an excess of *t*-butyl-2,2,2-trichloroacetimidate yielded the *t*-butyl diester **119** in near-quantitative yield (Scheme 4.4).¹⁹⁷ Subsequently, the disulfide bond of **119** was reduced to the thiol using *n*-tributylphosphine, yielding Boc.HCys.OtBu in 85% yield (**120**, Scheme 4.4), with an analysis of the ^1H NMR spectrum of **120** highlighting a new triplet at 1.55 ppm ($J = 5.7$ Hz) that was indicative of the free thiol group present in **120**.



Scheme 4.4: Synthesis of Boc.HCys.OtBu (**120**) from L,L-homocystine.^{178,197}

4.3.3 Attempted Alkylation of 6-Iodo-2,3,4-tri-*O*-acetyl- β -D-glucosyl azide (**117**)

With the 6-iodosugar **117** and Boc.HCys.O*t*Bu in hand, efforts were made towards the alkylation of thioether-containing amino acids. In endowing **117** with a better leaving group in our attempts to form thioether-linked “clickable” glycoconjugates, it was recognized that the iodo group may be susceptible to cleavage under the alkylation conditions proposed. This premise was based on the previous work of Murphy and co-workers, who *en route* to the production of *glc*, *gal* and *manno* iminosugars **121-123** produced the hex-5-enopyranosides from 6-iodopyranosides, with DBU catalysis resulting in HI elimination (Scheme 4.5).¹⁹⁸

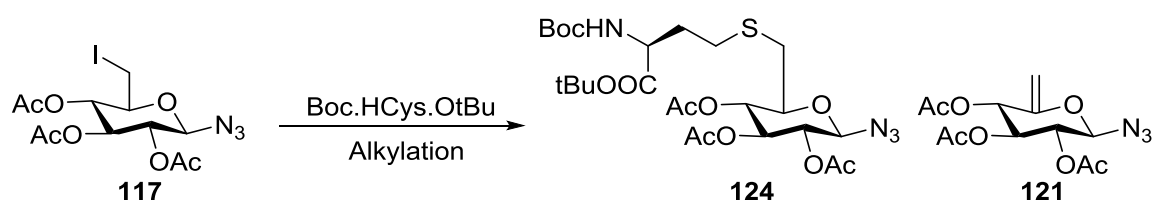


Scheme 4.5: Proposed mechanism for the elimination of hydrogen iodide from **121-123** in the presence of a non-nucleophilic base.

Considering that the reported conditions in the *glc* example (**121**) required much higher temperatures to induce elimination (reflux, >110°C)¹⁹⁸ than the conditions we

proposed, it was believed that the competing process of alkylation would occur favorably with an amino acid containing a good nucleophile. Hence, alkylation of Boc.HCys.OtBu by **117** was attempted, utilizing a range of different non-nucleophilic bases to catalyse alkylation. However, under these conditions the formation of the desired product (**124**) was not observed, with the azidosugar side product **121** instead procured in moderate quantities (Table 4.1, Entries 1-3).

Table 4.1: Attempted alkylation of 6-iodo-2,3,4-tri-*O*-acetyl- β -D-glucopyranosyl azide (**117**) by Boc.HCys.OtBu (**120**).



Entry	117 (eq.)	120 (eq.)	Base (eq.)	Solvent	T (°C)	Time	Yield (124)	Yield (121)
1	1	2.0	Et ₃ N (2.0)	THF	RT	48 h	0%	(39%*)
2	1	2.0	DBU (2.0)	THF	RT	48 h	0%	(48%*)
3	1	2.0	Cs ₂ CO ₃ (2.0)	DMF	RT	48 h	0%	(49%*)
4	1	2.0	Ag ₂ O (4.0)	DMF	RT	96 h	0%	(0%^)
5	1	2.0	Ag ₂ O (4.0)	THF	RT	192 h	0%	(3%^)

* Formation of (Boc.HCys.OtBu)₂ observed

^ Performed in the absence of light

Comparison of the ¹H NMR spectra of **117**, Boc.HCys.OtBu and the crude reaction mixture when Cs₂CO₃ was used as the alkylating base (Figure 4.1, A-D respectively), highlighted the degradation of **117** and the near-quantitative conversion of Boc.HCys.OtBu to the dimerized precursor (Boc.HCys.OtBu)₂ (Figure 4.1). This also was clearly illustrated by LR-ESIMS, with a signal of *m/z* 603 (M + Na) indicative of Boc.HCy.OtBu dimerization. The disappearance of signals from 3.0-4.0 ppm in A

ascribed to the H5 and H6/H6' protons of **117**, the downfield shift of a CH₂ signal (**120**) to ~2.75 ppm in B, and the appearance of methine protons between 4.5-5.0 ppm in C, are indicative of the elimination of HI from **117**, the reformation of (Boc.HCys.OtBu)₂ (**119**) and the formation and isolation of the unwanted *glc* hex-5-enepyranoside **121** (Figure 4.1, D).

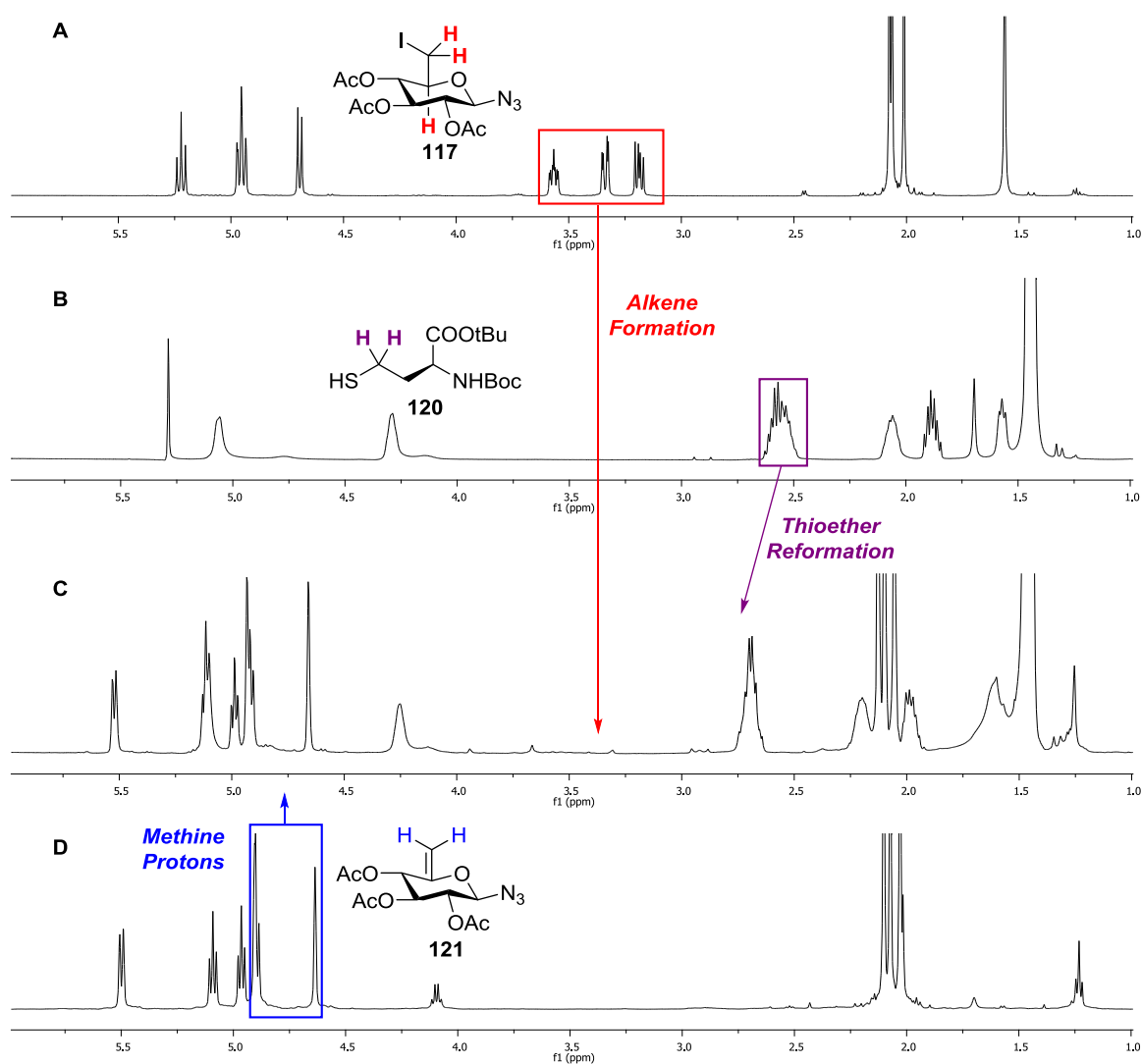


Figure 4.1: Comparison of the ¹H NMR spectrums of **117** (A), Boc.HCys.OtBu (**120**, B) and the crude alkylation reaction mixture (C), highlighting reformation of (Boc.HCys.OtBu)₂ (**119**) and the *glc* hex-5-enepyranoside **121** (D).

Based on the observed dimerization of **120**, it is plausible that the bases used in the attempted alkylations were too strong for the thiol-containing amino acid used. The pK_a values for NEt_3 (~10.45), DBU (~12) and Cs_2CO_3 (~10.3) are all much higher than that of the thiol of the amino acid used (~8.5), thus it is likely that in solution the thiol of **120** may have been more readily present as a thiolate. A good nucleophile, it is possible (but speculative) that the presence of this species may have encouraged nucleophilic attack of the thiol of another amino acid in solution, resulting in the observed dimerized amino acid.

Interestingly, TLC analysis of the reaction mixture highlighted the presence of significant quantities of the starting iodide (**117**), with 25-35% recovered across the three approaches used. Whilst the undesired hex-5-enopyranoside (**121**) was also isolated in significant quantities, its rate of formation was much slower compared to the dimerization of **120**, which was observed over 4-6 hours of reaction time compared to the 48 hours for the HI elimination. The lack of desired product formed, in addition to the slow rate of by-product formation and the presence of significant quantities of starting material, suggested that lower temperature would not inhibit elimination.

Thus, a base-free alternative approach using the halide scavenger Ag_2O was trialled to catalyze the alkylation of Boc.HCys.OtBu by **117**. Exhibiting a strong affinity for halides, it was believed that Ag_2O would act to promote the alkylation without promoting side product formation through proton scavenging.¹⁹⁹ However, whilst this methodology was effective in preventing the formation of the side product **121**, after stirring for 4 days in the presence of 4.0 equivalents Ag_2O in DMF no reaction was observed (Table 4.1, entry 4). To further evaluate this reaction, the reaction time was extended to 8 days, and THF was utilized as a reaction solvent. Similarly though, this

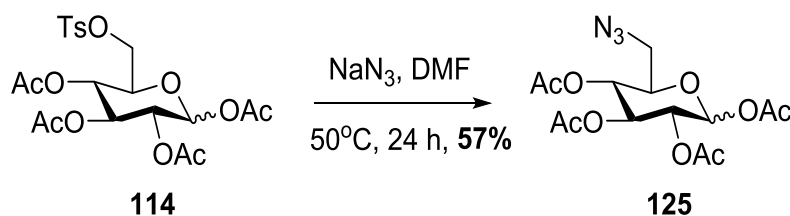
non-reaction proved unsuccessful, with only a trace amount of **121** detected (Table 4.1, Entry 5). Thus, after multiple attempts to produce 6-thioether-linked “clickable” glycoconjugates, the synthesis of these was discontinued, and focus shifted to the synthesis of conjugates linked to the anomeric position of a pyranoside.

4.4 Synthesis of Anomeric Thioether-linked “Clickable” Glycoconjugate 131

Akin to the carboxyl-linked glycoconjugates synthesized in Chapter 3, attempts to produce thioether-linked derivatives through linkages at the anomeric centre were investigated. Utilizing the previously synthesized acetyl protected 6-tosyl bearing glycoside **114**, S_N^2 nucleophilic substitution with an azide donor (such as NaN_3) would produce an azidosugar such as **125** that could be directly glycosylated (using SnCl_4 or $\text{BF}_3 \cdot \text{OEt}_2$). Alternatively, the introduction of a better leaving group (e.g bromide, trichloroacetimidate, etc.) at the anomeric centre, would provide a better glycosyl donor that could undergo stereoselective glycosylation.²⁰⁰ If a thiol-containing glycosyl acceptor such as cysteine or homocysteine were utilized, these molecules would represent anomeric thioether-linked “clickable” glycoconjugates, and thus would be amenable to further functionalization using the CuAAC “click” reaction.

4.4.1 Synthesis of 6-Azido-2,3,4-tri-*O*-acetyl- α -D-glucopyranosyl trichloroacetimidate (**127**)

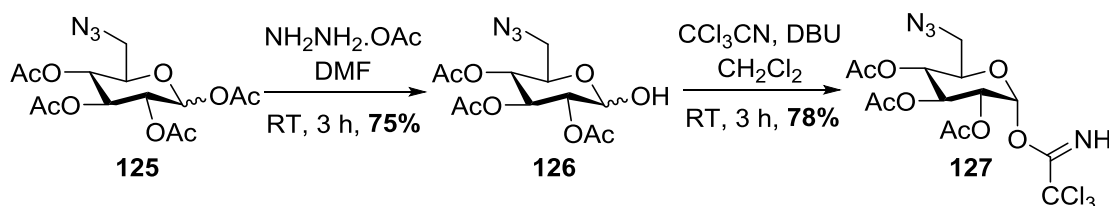
The synthesis of the target thioether-linked glycoconjugates commenced using 6-*p*-toluenesulfonyl-1,2,3,4-tetra-*O*-acetyl-D-glucopyranose (**114**) as a key synthon. In the presence of NaN₃ in DMF, and under mild heating over 24 hours, **114** was converted into the requisite 6-azido-6-deoxy-1,2,3,4-tetra-*O*-acetyl-D-glucopyranose (**125**) in 57% yield (Scheme 4.6), as a ~1:1 mixture of α - and β -anomers. Compared to previous azidations discussed in this work, the yield of **125** was somewhat reduced due to the competing azidation of the anomeric centre of **114**, as opposed to the *p*-tosyl group. The formation of this side product was initially indicated by TLC analysis, with LR-ESIMS of the reaction mixture displaying a signal of m/z 379 ($M + Na$) indicative of the side product. As a result, additional recrystallization from EtOAc/Hexane following chromatography was required to yield spectroscopically pure **125**, the structure of which was confirmed from the ¹H NMR spectra, where the loss of two doublets at 7.80 and 7.36 ppm ($J = 8.2$ Hz), indicated the loss of the *p*-tosyl group. This was further confirmed by the LR-ESIMS of **125**, where a value of m/z 396 was indicative of the desired product plus sodium (C₁₄H₁₉N₃O₉Na).



Scheme 4.6: Synthesis of 6-azido-6-deoxy-1,2,3,4-tetra-*O*-acetyl-D-glucose **125**.

In order to evaluate glycosylation at the anomeric centre, a suitable glycosyl donor was required. As mentioned previously (section 2.3), anomeric acetates have been known for their susceptibility to glycosylation under Lewis acid catalysis – utilizing SnCl_4 and $\text{BF}_3\cdot\text{OEt}_2$.²⁰⁰ However, the potential formation of epimers in using these methods limits their favourability in these reactions. Alternatively, glycosyl trichloroacetimidates represent a class of compounds that have historically been used as glycosyl donors. Developed by Schmidt and co-workers,²⁰¹ the versatility of these glycosyl donors to undergo stereoselective glycosylation using Lewis acids such as TMSOTf, in the presence of a range of *O*- and *S*-acceptors has validated their widespread use in chemical glycosylation.²⁰² Considering the breadth of literature into anomeric glycosylation via both of these methodologies, they were both evaluated in the production of the target anomeric-linked glycosyl azides.

Therefore, with peracetylated 6-azidoglycoside **125** in hand the synthesis of the desired azidosugar bearing an α -trichloroacetimidate at the anomeric position was initiated. Commencing from **125**, selective deacetylation at the anomeric position using hydrazine acetate resulted in the lactol intermediate **126** in 75% yield (Scheme 4.7). This isolated intermediate was then subjected to reaction with trichloroacetonitrile and DBU, producing the desired α -trichloroacetimidate bearing compound **127**, isolated solely as the α -anomer in 78% yield (Scheme 4.7).¹⁴⁶



Scheme 4.7: Synthesis of α -trichloroacetimidate bearing azidosugar **127**.¹⁴⁶

Confirmation of the formation of **127** was highlighted by the ^1H NMR spectrum, where a singlet at 8.76 ppm corresponded to the imide proton present on the trichloroacetimidate (Figure 4.2). Furthermore, a doublet at 6.63 ppm ($J = 3.7$ Hz) signified the equatorial H1 proton of **127**, suggesting a small dihedral angle between H1 and H2, indicative of the α -stereochemistry of the trichloroacetimidate present at the anomeric position, with no signal indicating the presence of the β -anomer observed (Figure 4.2).¹⁴⁶

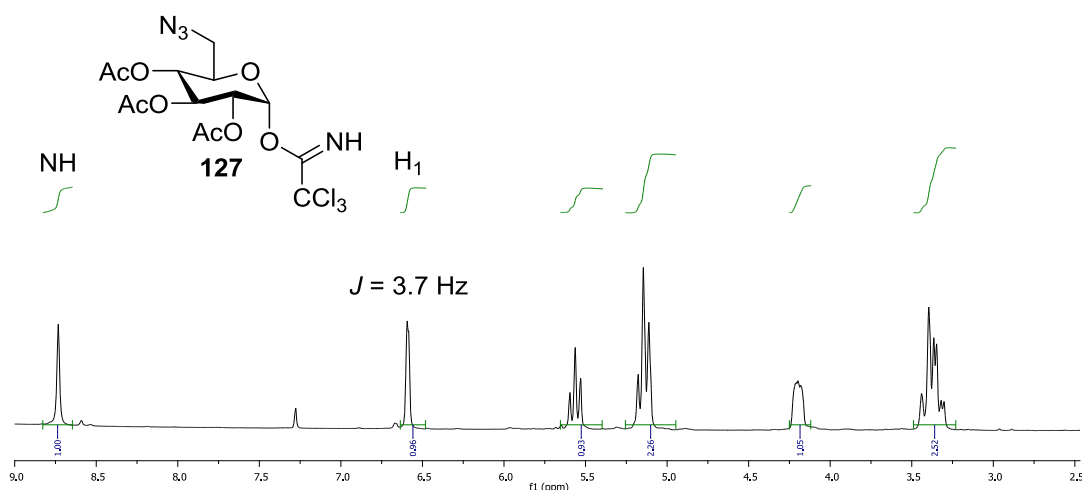
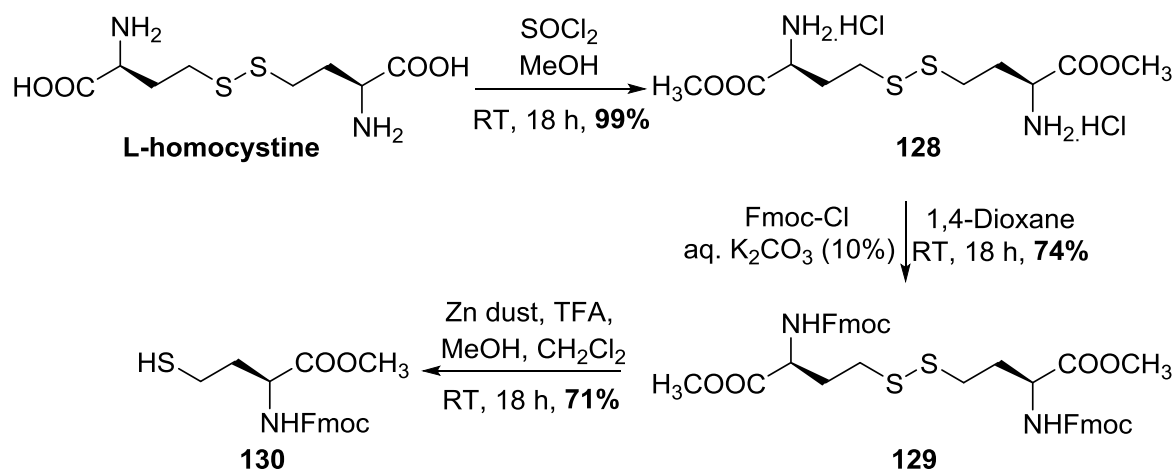


Figure 4.2: ^1H NMR spectrum of **127**, highlighting the small coupling constant ($J = 3.7$ Hz) between the H1 and H2 protons, indicative of the α -stereochemistry present in **127**.

4.4.2 Synthesis of Fmoc.HCys.OMe (130)

With the trichloroacetimidate **127** in hand, our attention turned to the required thiol-containing amino acid. Previously utilizing Boc.HCys.OtBu (**120**), it was recognized that the acid-sensitive Boc and tBu protecting groups would not be compatible with the current Lewis acid-catalysed strategy. Therefore as an alternative, a homocysteine derivative protected with groups compatible with Lewis acid-mediated glycosylation conditions (Fmoc, OMe groups) was chosen for use in this strategy. Thus, commencing from L,L-homocystine, esterification using thionyl chloride (SOCl₂) in dry methanol resulted in the formation of the dimethyl ester dihydrochloride derivative **128** in near quantitative yields (Scheme 4.8).²⁰³



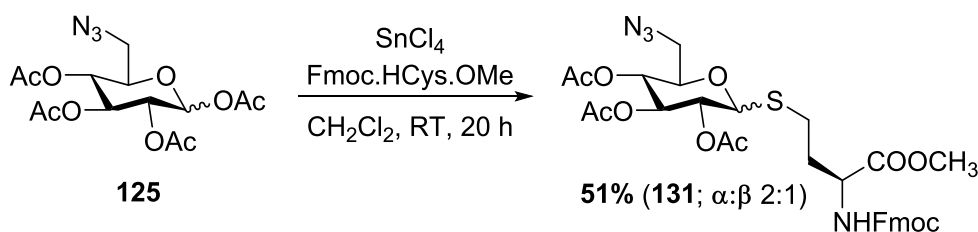
Scheme 4.8: Synthesis of Fmoc.HCys.OMe (**130**) from L,L-homocystine.²⁰³

The α -amino groups of **128** were subsequently protected using Fmoc-Cl in aqueous K₂CO₃, yielding the protected derivative (Fmoc.HCys.OMe)₂ (**129**) in 74% yield (Scheme 4.8). Finally, disulfide bond reduction of **129** utilizing Zinc

dust/TFA conditions, resulted in the isolation of the requisite thiol-containing amino acid Fmoc.HCys.OMe (**130**) in 71% yield respectively (Scheme 4.8), with ^1H and ^{13}C NMR spectra in accordance with those previously described elsewhere.²⁰³

4.4.3 Synthesis of Thioether-Linked “Clickable” Glycoconjugate **131**

With both the glycosyl donors **125** and **127**, and the amino acid acceptor **130** prepared, the synthesis of the desired thioether-linked glycoconjugate was attempted. As previously discussed in section 2.3, the utilization of contrasting non-stereoselective and stereoselective Lewis acid-mediated glycosylation strategies was trialled. In the first instance, the anomeric acetate-bearing azidosugar **125** was subjected to SnCl_4 -mediated glycosylation by Fmoc.HCys.OMe (**130**). As a result, the target compound **131** was synthesised, as ~2:1 α - to β -anomeric mixture in 51% yield (Scheme 4.9).



Scheme 4.9: Synthesis of thioether-linked “clickable” glycoconjugate **131** from anomeric acetate **125**.

Isolable individually by flash column chromatography, both α - and β -anomers of **131** displayed m/z values of 707 ($\text{C}_{32}\text{H}_{36}\text{N}_4\text{O}_{11}\text{S}+\text{Na}$), which were both indicative of the desired product plus sodium. The ^1H NMR spectra for both α - and β -anomers of **131** also highlighted their differing conformations (Figure 4.3). For the α -anomer, a

deshielded doublet at 6.35 ppm ($J = 3.6$ Hz) was indicative of the equatorial H1 proton, with the small coupling constant between the H1 proton and the neighbouring axial H2 proton highlighting their “cis” configuration (Figure 4.3, A). Comparably, in the ^1H NMR spectrum of the β -anomer of **131**, the presence of a doublet ($J = 9.9$ Hz) at 4.51 ppm was indicative of the H1 proton (Figure 4.3, B), with the larger coupling constant highlighting the “trans” relationship that exists between the axial H1 and H2 protons (Figure 4.3, B).

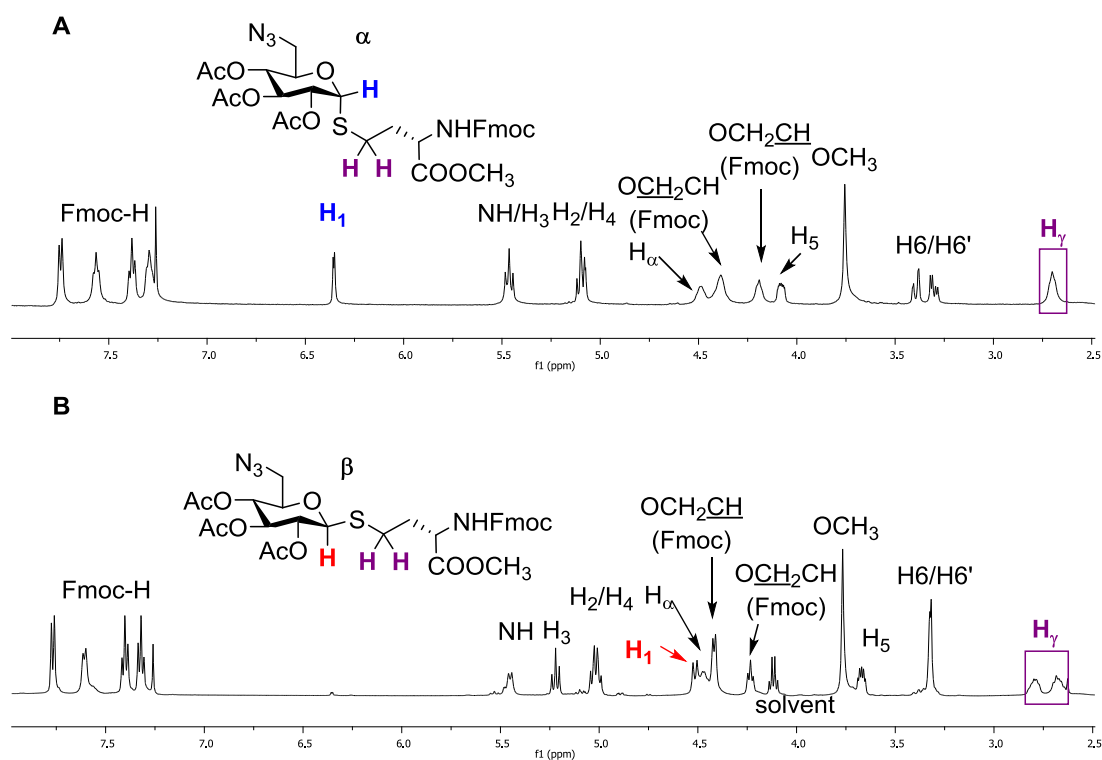


Figure 4.3: ^1H NMR spectra for both α - and β -anomers (A and B) of the thioether-linked “clickable” glycoconjugate **131**.

Additionally, variations between the signals for the H^γ of the amino acid portion, and H6/H6' protons of the pyran ring portion of **128** highlighted the different anomeric configurations. In the β -anomer, two multiplets each integrating for one proton at

2.69 ppm and 2.79 ppm represented the geminal H^{γ} protons (Figure 4.12, B). The different signals for each proton in the β -anomer of **131** indicated that in the 1H NMR conditions utilized ($CDCl_3$, $25^\circ C$) these geminal protons may be in different chemical environments. Considering the adjacent 2-OAc group, it is possible that one of these protons may be sterically hindered by this neighbouring group, with the β -configuration of the thioether at the anomeric centre placing one of these protons in close proximity to the neighbouring ring-bound oxygen. Such hinderance would limit free rotation of the C-S bond, resulting in the diastereotopic signals observed in the 1H NMR spectrum of **131** (Figure 4.4). This phenomenon is specific to the β -anomer of **131**, as the corresponding protons of the α -anomer do not display the same divergence (Figure 4.3, A). The non-stereoselective synthesis of **131** represents the second instance where a thiol-containing amino acid has been utilized in the glycosylation of an azidosugar, producing thioether-linked “clickable” glycoconjugates.²⁰⁴

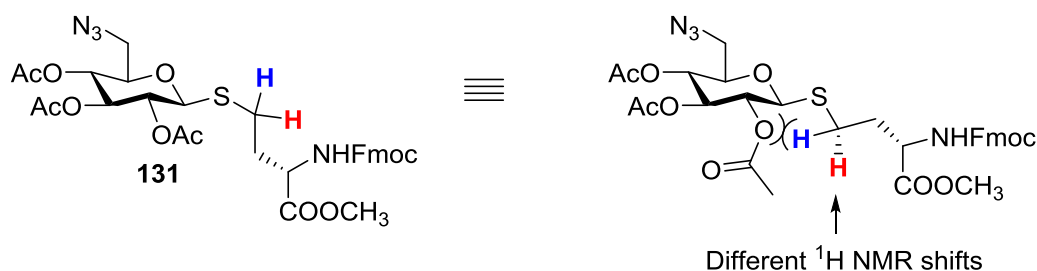
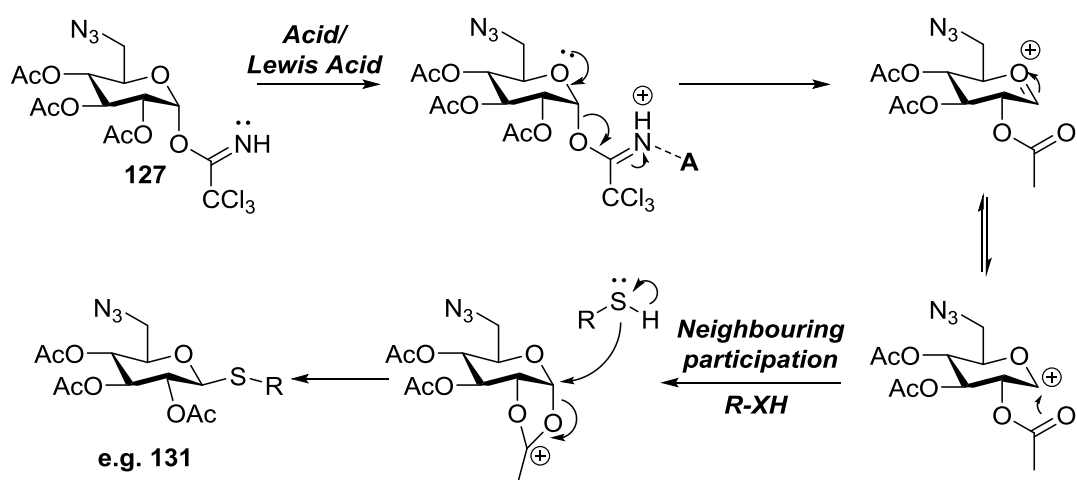


Figure 4.4: Proposed steric hinderance between the amino acid H^{γ} methylene protons and neighbouring acetate group of **131**, resulting in different chemical environments for the two H^{γ} protons in the 1H NMR spectrum ($CDCl_3$, $25^\circ C$) of **131**.

With the non-stereoselective production of **131** successfully achieved, efforts to replicate these results utilizing a stereoselective strategy were attempted. As with the

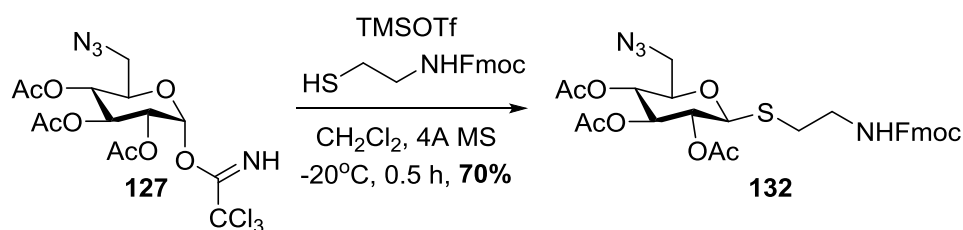
previously described glycosylation, Lewis acid catalysis provided the best opportunity to catalyse this glycosylation, with TMSOTf widely used for such a procedure.²⁰⁵ In the presence of a trichloroacetimidate (such as the synthesised **127**), coordination of the imidate by TMSOTf results in the elimination of trichloroacetamide (Scheme 4.10). Equilibration between the formed oxocarbenium ion, and the formation of a stable anomeric carbocation, results in neighbouring group participation by the 2-OAc group, forming a stable acetal intermediate (Scheme 4.10). Subsequently, in the presence of an *O*- or *S*-containing acceptor the anomeric centre is susceptible to nucleophilic substitution, with the α -stereochemistry of the acetal intermediate favouring the stereoselective formation of a β -substituted product (Scheme 4.10).



Scheme 4.10: Proposed mechanism for the stereoselective formation of β -glycosides from an α -trichloroacetimidate.

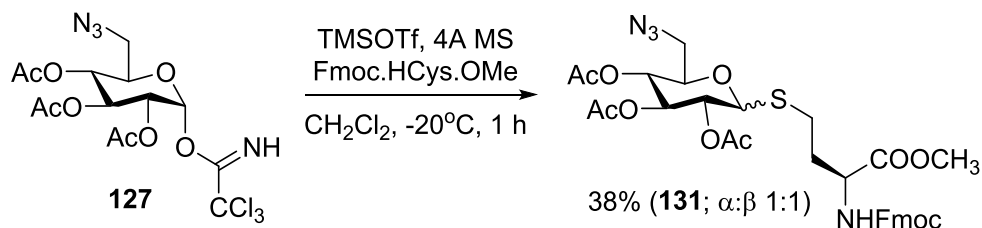
In respect to the proposed mechanism for glycosylation, the resonance stabilization of the oxocarbenium ion provides an opportunity for glycosylation to occur via either an S_N^1 -mediated mechanism (kinetic control - direct glycosylation) or an

S_N^2 -mediated mechanism (thermodynamic control - neighbouring group participation), potentially producing both α - and β -anomers of the desired glycoconjugates.^{200,206} Whilst the potential formation of both anomers was a concern, previous literature had highlighted that the selective formation of azido- β -thioglycosides via this methodology was feasible, with Gouin and co-workers successfully utilizing **127** and TMSOTf to produce the β -thioglycoside **132** *en route* to tethering fluorescein to heptyl α -D-mannosides.²⁰⁷ This work highlights the importance of reaction temperature in stereoselectively producing β -thioglycosides via this methodology, suggesting that a reaction temperature of less than -20°C would be sufficient to maintain kinetic control, and thus produce the desired β -glycoconjugate.



Scheme 4.11: Synthesis of azido- β -thioglycoside **132** performed by Gouin and co-workers.²⁰⁷

Thus, based on this literature precedence the stereoselective synthesis of thioether-linked **131** was attempted. After being thoroughly dried under vacuum, **127** and Fmoc.HCys.OMe (**130**) were subjected to TMSOTf catalysis in dichloromethane. After 1 hour at -20°C , subsequent work up resulted in the isolation of the desired glycoconjugate **131** in a moderate yield of 38% (Scheme 4.12). Monitored by TLC, unfortunately the appearance of two spots at R_f 0.23 and R_f 0.30 (2:1 Hexane:EtOAc) represented the presence of both α - and β -anomers, with the ^1H and ^{13}C spectra of these samples in agreement with those previously produced using SnCl_4 .



Scheme 4.12: Synthesis of thioether-linked “clickable” glycoconjugate **131** from α -trichloroacetimidate **127**.

The stringent requirement of moisture and oxygen-free conditions made the synthesis of **131** via this method precarious, with the TMSOTf used in each reaction highly susceptible to degradation. Forming triflic acid as a by-product, it is likely that this occurred in both these instances, with the presence of spots on the baseline of the TLC of each reaction suggesting the degradation of the trichloroacetimidate **127**, contributing to the moderate yields gained for **131**. In regards to the lack of stereoselectivity observed, it is likely that in our hands at -20°C , neighbouring group participation was not favoured, leading to ambivalent nucleophilic substitution of the anomeric centre. Additionally, whilst **127** was stable when stored under argon at less than 0°C , it was noticed over time the trichloroacetimidate was susceptible to degradation, particularly during reaction set up. Considering the issues with this synthetic strategy, and our shortcomings in the stereoselective production of **131**, the focus of our efforts shifted to the development of a broader methodology for the "formation of “clickable” glycoconjugates between azidosugars and thiol-containing amino acids and peptides, and thus the functionalization of **131** by the CuAAC “click” reaction was not attempted.

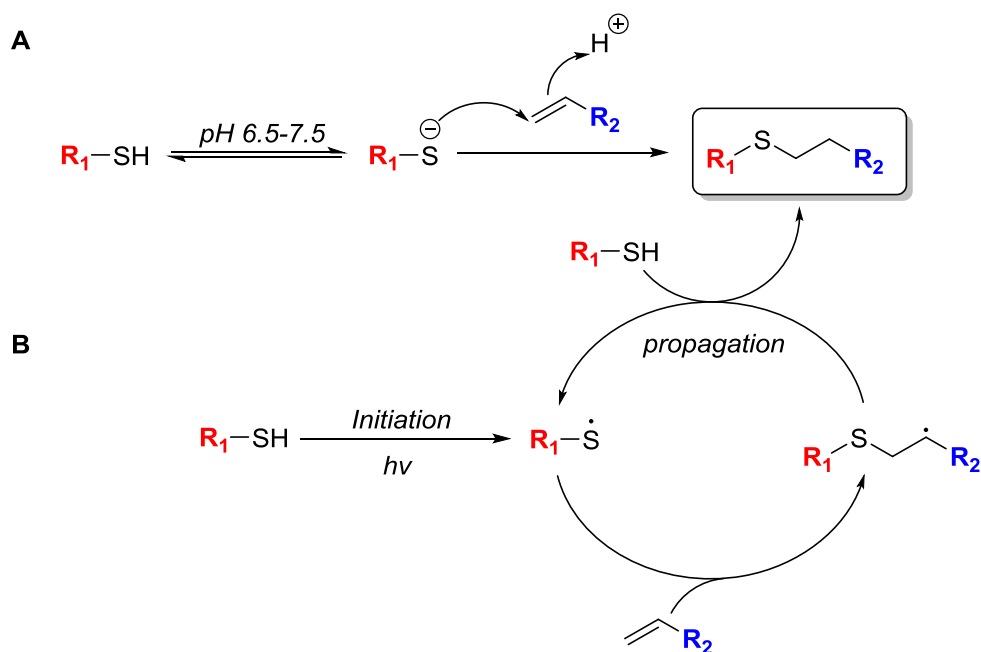
4.5 Synthesis of Thioether-linked “Clickable” Glycoconjugate

138 Using a “Click” Thiol-ene Approach

As described, problems were encountered in the attempted production of anomeric and 6-thioether linked derivatives (**124** and **131**), and it was also recognised that these strategies may not be so well suited for use in the formation of higher glycoconjugates. Challenges in producing **124** and **131** including reactivity, stereoselectivity and protecting group orthogonality could be overcome to yield thioether-linked glycoconjugates encompassing a single amino acid. It is unlikely however whether this would be true for the synthesis of thioether-linked peptides or proteins. This is particularly relevant in regards to protecting group orthogonality, as many glycosylating reagents (including $\text{SnCl}_4/\text{TMSOTf}$) are not compatible with acid-sensitive protecting groups. Additionally, reduction-labile protecting groups may compete with the 6-azido group during deprotection, thus further limiting the access of produced synthons to solid or solution phase peptide synthesis. Furthermore, as many proteins and peptides require specific aqueous pH environments to maintain structure (and function) it is likely that the acidity of reagents could interfere with the coupling peptide or protein. Considering these arguments, a methodology that allowed for the ligation of azidosugars to thiol-containing peptides or proteins in benign conditions would be highly advantageous.

Thus, an evaluation of the literature was undertaken to identify methods that could be utilized to readily produce “clickable” glycoconjugates between azidosugars and thiol-containing peptides or proteins. One such method that has grown in use for the labelling and tagging of peptides containing thiol groups is the thiol-ene reaction.

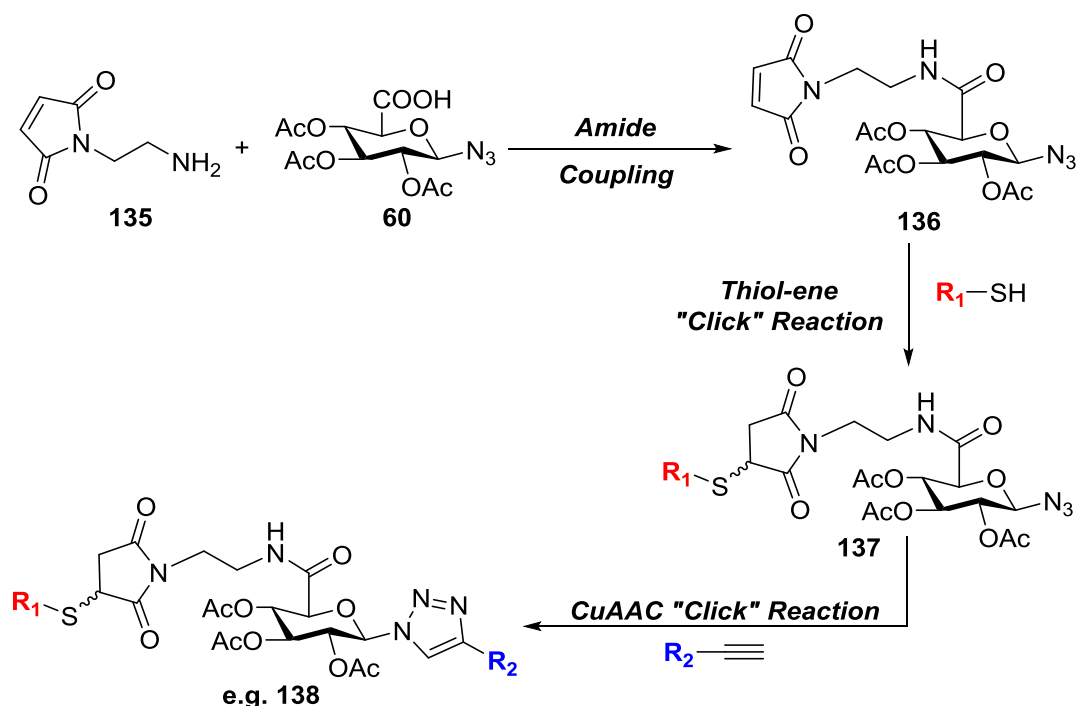
Encompassing the anti-Markovnikov addition of a free thiol group to an alkene, the result of this reaction is a saturated thioether.^{208,209} Mechanistically, the thiol-ene reaction can proceed via either an ionic or radical reaction mechanism. Under the ionic reaction conditions, the reaction is often performed in a buffered solvent at pH 6.5-7.5. At this pH, the thiol group may disproportionate to form the respective thiolate anion, which in the presence of an alkene will undergo addition, forming the desired thioether (Scheme 4.13, A).²⁰⁸ Alternatively to this, in the presence of a suitable radical initiator a thiyl radical may instead be produced from a thiol. In the presence of an alkene, anti-Markovnikov addition across the double bond ensues, resulting in the formation of a thioether containing a stabilized secondary radical. In the propagation phase of the reaction, this radical can go on to form an additional sulfanyl radical, producing the desired thioether (Scheme 4.13, B).²⁰⁸



Scheme 4.13: Ionic (A) and radical (B) mechanisms for the synthesis of thioethers via the thiol-ene reaction.²⁰⁸

The use of relatively pH-neutral, environmentally benign conditions in the ionic thiol-ene reaction have promoted its widespread use in synthetic biology.²¹⁰ The utilization of maleimides as alkene donors drastically increases the reaction rate for the formation of thiol-enes, with these reactions finding widespread usage in the labelling of thiol-containing bioconjugates. As a result of its speed and efficiency in the formation of thioethers, the thiol-ene reaction is often referred to as a “click” reaction, and is often discussed alongside the CuAAC “click” reaction utilised in this work.²⁰⁸ Examples such as the previously discussed development of [¹⁸F]-FDR by O’Hagan and co-workers (Chapter 1, Scheme 1.5), have illustrated the utility of this method in the formation of bioconjugates. Utilizing a maleimide-containing hydroxylamine to attach to the thiol-containing tripeptide glutathione (γ -Glu-Cys-Gly), subsequent oxime formation resulted in the labelling of the bioconjugate with [¹⁸F]-FDR.¹¹⁴

Beyond the usage of an oxime in this example, an abundance of literature for the introduction of maleimides into macromolecules using amide-coupling chemistry exists, linking maleimides through linkers bearing an amine or carboxylic acid.²¹⁰ As described in chapter 2, the *glc*- and *gal*-sugar azido acids **60** and **65** were extensively derivatized using amide-coupling chemistry (Chapter 2, Pg 66-76), displaying broad scope for their usage in the synthesis of “clickable” glycoconjugates. Bearing these considerations in mind, if a maleimide bearing a free amine was produced and linked to a SAA using amide-coupling chemistry, this molecule could be subjected to the “click” thiol-ene reaction. The resulting thioether-linked “clickable” glycoconjugates could then be further derivatized at the free azide by the CuAAC “click” reaction (Scheme 4.14).

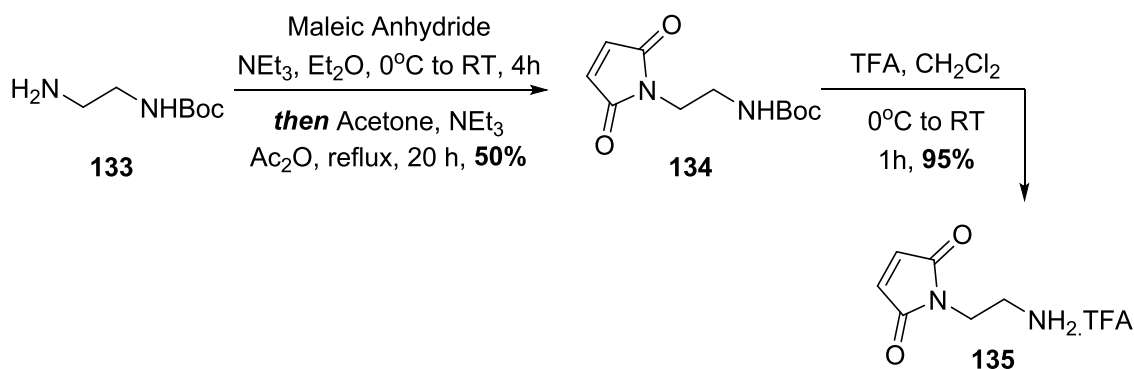


Scheme 4.14: Approach towards the synthesis and functionalization of thioether-linked “clickable” glycoconjugates utilizing the thiol-ene “click” reaction.

4.5.1 Synthesis of Maleimide-Sugar Azido Acid-linked Derivative 136

Thus, in order to synthesise glycoconjugates of this form, the synthesis of a maleimide bearing an amine-containing linker was required. An ethylenediamine-based linker was chosen for conjugation between the maleimide and sugar azido acid, with the short distance between the two limiting the likelihood of any issues due to linker folding. Additionally, the lack of cleavable functional groups on the linker would allow for the use of the glycoconjugate in a broad range of acidic or basic conditions. To form

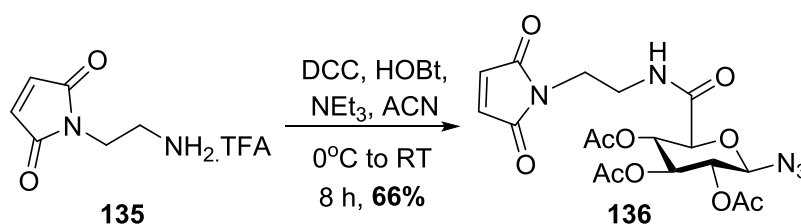
the maleimide, *N*-Boc-ethylenediamine (**133**) was subject to reaction with maleic anhydride in diethyl ether in the presence of triethylamine. Subsequent refluxing in acetone with Ac₂O followed by workup, resulted in the isolation of the desired *N*-Boc-ethylenediamine maleimide **134** in 50% yield (Scheme 4.15).²¹¹ With the desired maleimide core isolated, the Boc protecting group of **134** was subject to deprotection under standard TFA/dichloromethane conditions. Stirring for 1 hour, solvent evaporation followed by trituration with diethyl ether resulted in the isolation of **135** as a TFA salt in 95% yield (Scheme 4.15).²¹¹ The isolation of **135** was confirmed by the ¹H NMR spectrum, where the disappearance of a signal from 1.42 ppm integrating for nine protons was indicative of the cleavage of the Boc protecting group, with both ¹H and ¹³C NMR spectra for **135** consistent with those previously described in the literature.²¹¹



Scheme 4.15: Synthesis of ethylenediamine maleimide **135**.

With **135** in hand, our focus now shifted to the formation of the maleimide-sugar azido acid glycoconjugate **136**. Considering that the previously synthesised **131** was a *glc*-based derivative, it seemed fitting that the *glc*-sugar azido acid **60** should be used in

the formation of the required conjugate. Thus, under standard DCC/HOBt coupling conditions in acetonitrile, **60** was subjected to reaction with maleimide linker **135**, with work up and flash column chromatography resulting in the isolation of the maleimide-linked azido sugar **136** in a respectable 66% yield (Scheme 4.16).

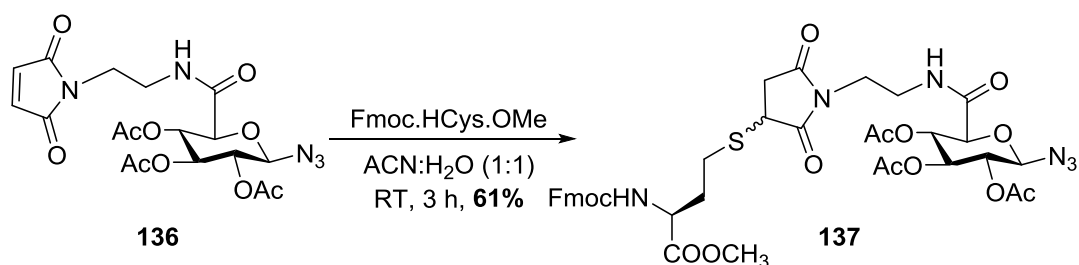


Scheme 4.16: Synthesis of maleimide-SAA linked derivative 136.

In the ^1H NMR spectrum of **136**, the presence of a broad signal at 6.86 ppm accounting for one proton was indicative of the amide proton formed during the reaction, with a signal in the HR-ESIMS at m/z 490.1204 representing the desired product plus sodium ($\text{C}_{18}\text{H}_{21}\text{N}_5\text{O}_{10} + \text{Na}$; 490.1186). Interestingly, the signals representing the hydrogens on the carbon adjacent to the amide bond in **136** are not split as they are in previous conjugates bearing CH_2 groups adjacent to the amide (**68** and **88**), with these protons forming a multiplet at 3.43 ppm. It is possible (but speculative) that in the conditions of the ^1H NMR (CDCl_3 , 25°C) the amide NH moiety present in **136** may hydrogen bond with either of the ketones of the maleimide, forming a seven-membered interaction that places both of these protons into identical chemical environments. The plausibility of this argument is justified by both the planarity and the α,β -unsaturated nature of the maleimide present in **136**.

4.5.2 Thiol-ene “Click” Reaction of Maleimide-linked Derivative **136** and Fmoc.HCys.OMe (**130**).

With the maleimide-linked derivative **136** synthesised, its derivatization using the “click” thiol-ene reaction was subsequently evaluated. Instead of using a protected peptide (such as reduced L-glutathione), Fmoc.HCys.OMe (**130**) would instead be used to develop a methodology that could be used on protected thiol-bearing peptides. In addition to the ready availability of the homocysteine derivative **130**, it was believed that the pKa of the thiol group of L-homocysteine (pKa 8.57) would provide a good comparison to the thiol groups present in other thiol-containing amino acids and peptides, such as L-cysteine (pKa 8.14) and reduced L-glutathione (pKa 9.2).^{212–214} Thus, reaction between **136** and Fmoc.HCys.OMe (**130**) was trialled in a 1:1 acetonitrile:water solution. Monitored by LR-ESIMS, after complete consumption of **136** (3 hours) the solvents were evaporated, with purification by flash column chromatography yielding thioether-linked glycoconjugate **137** as a mixture of diastereomers in 61% yield (Scheme 4.17).



Scheme 4.17: Synthesis of thioether-linked “clickable” glycoconjugate **137** by “click” thiol-ene reaction of **136** and Fmoc.HCys.OMe (**130**).

Whilst compound **137** was similar to the previously synthesized **131** in being a mixture of diastereomers, their presence in **137** was tolerated. This was because this strategy was targeted at the functionalization of thiol-containing peptides and proteins, with the relative chemistry of the linkage to the maleimide unlikely to affect the higher function and structure of peptides or proteins conjugated. The formation of **137** was supported by signals in the positive and negative ion modes of the LR-ESIMS of m/z 861 and 873, with these masses represented the product ($C_{38}H_{42}N_6O_{14}S$) plus sodium and chloride, respectively. Furthermore, in the 1H NMR spectrum of **137**, the disappearance of a signal from ~6.7 ppm ascribed to the maleimide methine protons highlights the formation of the glycoconjugate, illustrating the change in hybridization of the alkene carbons from Sp^2 in **136** to Sp^3 in **137**.

Interestingly in the 1H NMR spectrum, the signals representing the CH_2 protons adjacent to the amide linking the succinimide in **137** have different chemical shifts of ~3.35 ppm (H^b) and ~3.71 ppm (H^a). This directly compares to the starting maleimide-sugar azido acid **136**, where these protons are represented by a single two-proton multiplet (3.44 ppm). It is likely that the difference in the signals for these protons in the 1H NMR spectra of **136** and **137** may be due to the planarity of the maleimide in **136** versus the less planar succinimide in **137**. Lacking symmetry in the succinimide of **137**, the less planar succinimide ketones provide different chemical environments for the two geminal protons, resulting in two different signals in the 1H NMR spectrum of **137**. (Figure 4.5).

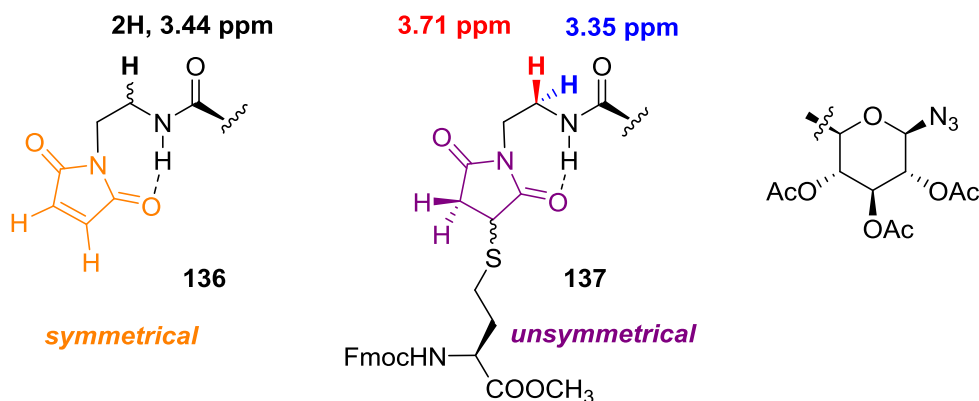
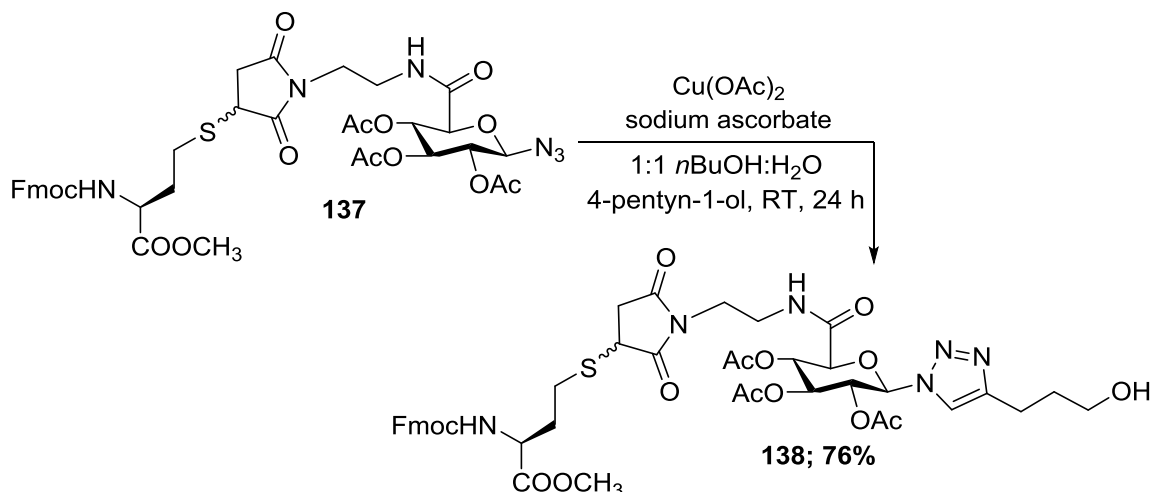


Figure 4.5: Comparison between the chemical shift for H^b protons in the ^1H NMR spectra of **136** and **137**, highlighting the effect of planarity and symmetry in the maleimide of **136** versus the succinimide of **137**.

4.6 Functionalization of Thioether-linked “Clickable” Glycoconjugate **137**

With the production of the “clickable” glycoconjugate **137** through the ‘click’ thiol-ene reaction successfully achieved, our attention now turned to its functionalization via the CuAAC “click” reaction. Utilizing the reaction conditions previously optimized for **74** in Chapter 2, reaction of **137** with 4-pentyn-1-ol resulted in the production of the functionalized thioether-linked glycoconjugate **138** in 76% yield, as a mixture of diastereomers (Scheme 4.17). The production of **138** was supported by LR-ESIMS of the isolated product, where a signal of m/z 946 calculated for a chemical formula $\text{C}_{43}\text{H}_{50}\text{N}_6\text{O}_{15}\text{S} + \text{Na}$ was indicative of the desired compound. Additionally,

signals at 7.87 ppm in the ^1H NMR spectrum and 120.2 ppm and 148.4 ppm in the ^{13}C NMR spectrum of **138** were characteristic of the formed triazole ring.



Scheme 4.18: Synthesis of the functionalized maleimide-linked glycoconjugate 136.

Alongside the previously synthesised “clickable” glycoconjugate **131**, **137** represents one of the first examples of a thioether-linked glycoconjugate that may be functionalized via the CuAAC “click” reaction. Thus in this chapter the synthesis of thioether-linked glycoconjugates formed by azidosugars and thiol-containing amino acids (HCys) was performed. Furthermore, the development of a methodology for the synthesis and functionalization of thioether-linked glycoconjugates using the “click” thiol-ene reaction has also been described, allowing for its further use in the formation of glycoconjugates with thiol-containing peptides. In Chapter 5, the development of strategies towards the synthesis and functionalization of neoglycopeptides by the CuAAC “click” reaction will be discussed.

Chapter 5 : Strategies Towards the Synthesis and Functionalization of “Clickable” Neoglycopeptides

As illustrated in chapters 2, 3 and 4, the development of new carbohydrate molecules that can be readily incorporated into biologically-active peptides, and comprise functional groups that allow for further conjugation are greatly warranted. This chapter will focus on the development of sugar azido acid-containing neoglycopeptides; key intermediates in the production of “clickable” neoglycopeptides.

5.1 Synthetic Rationale

In earlier chapters, a broad range of azidosugars were conjugated to a range of different proteinogenic amino acids, to produce a library of different “clickable” glycoconjugates that were amenable to further functionalization via the CuAAC “click” reaction. To this end, the examples described thus far have been of azidosugars linked to the sidechain, α -amino group or carboxyl group of an amino acid. Hence, if these “clickable” glycoconjugates were to be incorporated into a peptide (such as in the KPV-glycopeptide derivative **88**), the azidosugar would be external to the amino acid sequence of the synthesized peptide.

In the development of new peptidomimetics and glycoconjugates, keen interest has been shown in the imbedding of glycosides, including azidosugars, into the primary structure of both linear and cyclic peptides. Kessler and co-workers have illustrated this, producing a number of different neoglycopeptides – glycopeptides whereby the glycoside has been integrated into the peptide's primary structure in an 'unnatural' fashion.^{156,215–217} Examples of linear neoglycopeptides include the sugar amino acid (SAA)-containing Leu-Enkephalin analogues **139** and **140**, where a native Gly-Gly dipeptide motif was replaced with a sugar amino acid (Figure 5.1), with both of these analogues evaluated for their biological activity in a guinea pig ileum assay.¹⁵⁶

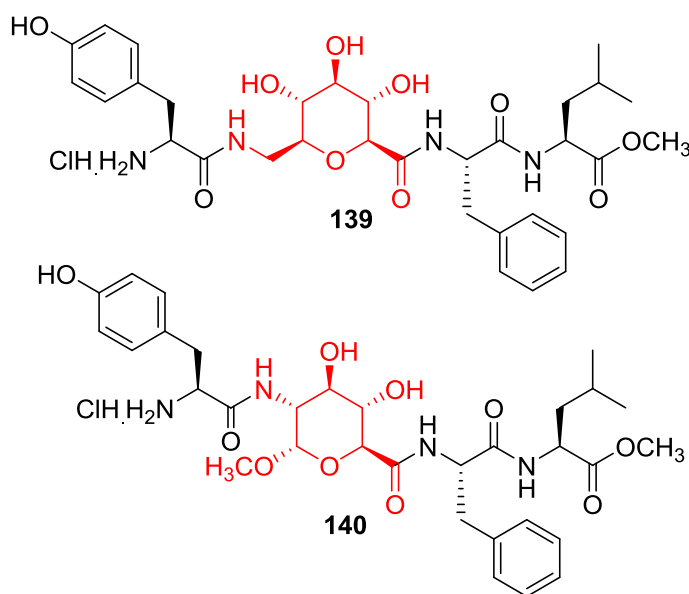


Figure 5.1: Leu-Enkephalin neoglycopeptide analogues **139** and **140**, containing sugar amino acids (in red) -mimicking a Gly-Gly dipeptide motif.¹⁵⁶

In addition, a number of SAAs have been incorporated into cyclic peptides, giving rise to different peptide secondary structures based on the differing substitution patterns of NH_2 and COOH groups present in the glycosides used. These include SAA's that impart linear (2,5-substituted, Figure 5.2, A) and flexible β -turn (1,6-substituted,

Figure 5.2, B) conformations to cyclic peptides, and more restricted β -turn (1,5-substituted, Figure 5.2, C), γ -turn (2,3 substituted, Figure 5.2, D) and homoproline peptide conformations (Figure 5.2, E).¹⁵⁶

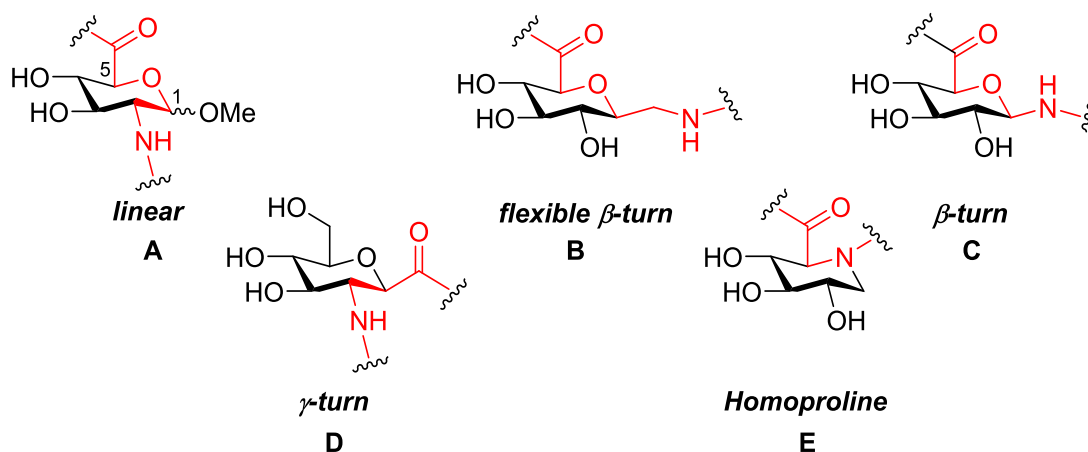


Figure 5.2: Conformations induced by differing substitution patterns of various sugar amino acids embedded into cyclic peptides.¹⁵⁶

Based on these structural differences, a number of neoglycopeptides exploring these different motifs have been synthesised. In particular, much focus of their potential has been centred on biologically-derived scaffolds, with those such as the cyclic tetradecapeptide hormone somatostatin widely targeted.^{156,215,217,218} Subsequently, the synthesis of a number of cyclic peptide SAA derivatives displaying desirable biological activities has been achieved, including the furanosyl SAA-containing derivative **141** (present in a homoproline conformation), which displayed IC_{50} values of 31 μ M and 25 μ M against the drug-sensitive rat hepatoma carcinoma cell line Clone 2, and the multidrug resistant subclone Clone 2(10 x 80)T1, respectively (Figure 5.3).²¹⁵ Furthermore, the flexible β -turn containing cyclic neoglycopeptide **142** has also displayed great potential, (Figure 5.3), exhibiting inhibitory activity at an IC_{50} of

150 nM when displacing the receptor bound radioligand [125 I]-Tyr¹¹-somatostatin-14 in AtT20 epithelial-like tumour cell membranes.¹⁵⁶

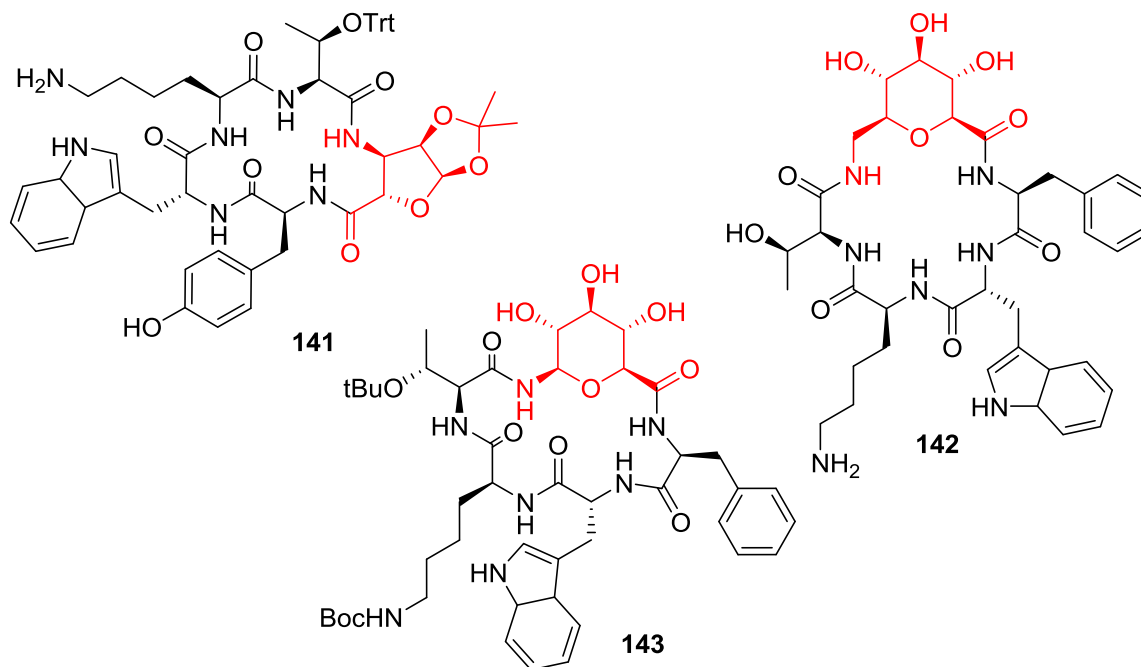


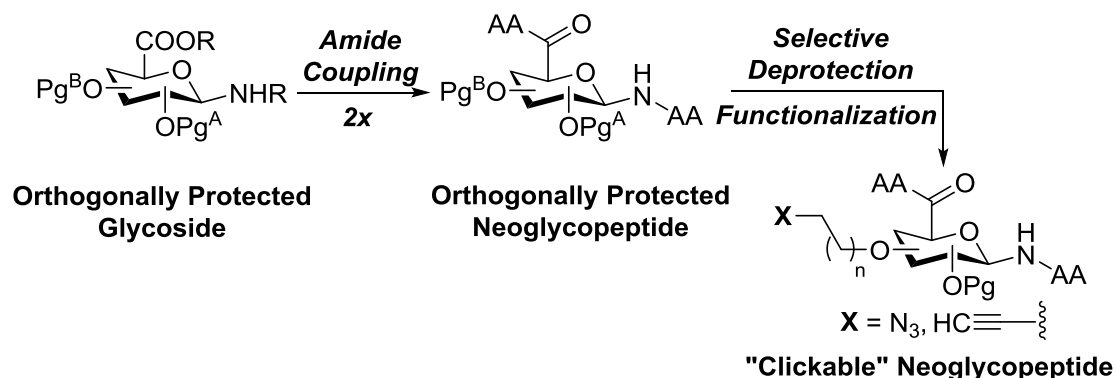
Figure 5.3: Cyclic neoglycopeptide derivatives **141**, **142** and **143**, as sugar amino acid (red) containing analogues of somatostatin.^{156,215,217}

In addition to these examples, the synthesis of glycoside-containing analogues of somatostatin has been extended to neoglycopeptides bearing other β -turn inducing glycosides, including the *glu*-sugar azido acid **60** previously synthesised in Chapter 2 (Figure 5.3, **141**).¹⁵⁶ From a synthetic perspective, sugar azido acids such as **60** and **65** are more readily accessible than the SAAs utilized in the cyclic somatostatin derivatives **141** and **142**, and hence show great promise as synthons in the production of substituted neoglycopeptides.¹⁵⁶

However, as seen in both the synthesis of sugar azido acids **60** and **65** in chapter 2, and in the synthesis of azidosugars in Chapters 3 and 4, selective substitution

of a secondary alcohol in a pyran based glycoside represents a significant challenge. Current protecting group strategies limit the selective substitution of secondary alcohols in *glc*-pyran ring systems, with the 2-, 3- and 4-positions of the pyran ring possessing comparable reactivity. In order to selectively substitute these different positions, lengthy, atom uneconomical chemical manipulations are required.²¹⁸ Hence, the development of an orthogonal protecting group strategy that could be used to selectively derivatize the secondary alcohols at either the 2-, 3- or 4-positions of a pyran ring would be highly advantageous.

If these pyranosides are also incorporated an accessible amine and carboxylic acid (Scheme 5.1), they would additionally be compatible with amino acid coupling. This would produce neoglycopeptides that could be functionalized such that they can participate in the CuAAC “click” reaction (Scheme 5.1). Bearing such a handle for derivatization, these so-called “clickable” neoglycopeptides could be utilized to introduce a variety of different functional groups. These would provide an evaluation of the use of functionalized neoglycopeptides as molecular scaffolds, in addition to expanding the utility and chemical space surrounding the structure and function of linear and cyclic peptides (Scheme 5.1).



Scheme 5.1: Proposed approach towards the synthesis of "clickable" neoglycopeptides.

5.2 Initial Synthetic Strategy

5.2.1 Synthetic Criteria

A number of different synthetic pathways could be employed to yield glycosides bearing handles capable of further ligation. One purported strategy is to synthesize and incorporate sugar diamino acids (SDAs), as previously described by Wittmann *et al.* (Figure 5.4, **144** & **145**) and Gervay-Hague *et al.* (Figure 5.4, **146**).^{219–221}

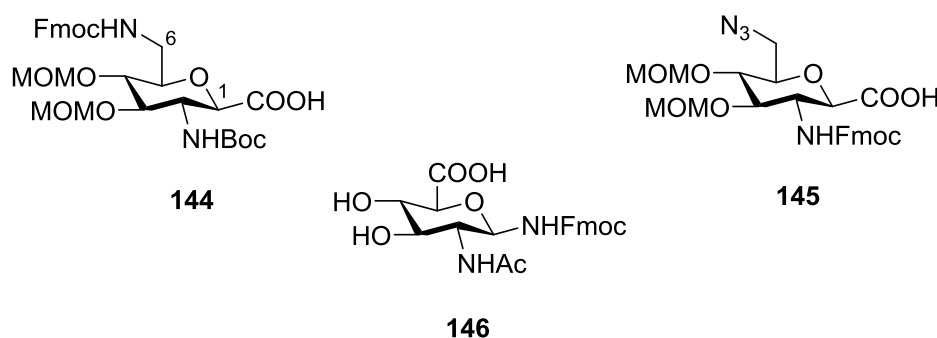


Figure 5.4: Sugar diamino acids (SDAs) reported by Wittmann *et al.* and Gervay-Hague *et al.*^{219–221}

Containing an accessible amine and carboxylic acid substituted primarily at the 1-,2- and 6-positions of the glycoside, these sugar amino acids also possess an additional amine or azide handles that can be further functionalized (Figure 5.4). Hence, these synthons represent an expansion of sugar amino acids that are amenable to amide coupling, and hence may be utilized to form either linear or cyclic neoglycopeptides. They may also participate in the CuAAC “click” reaction either directly, or through further chemical manipulation.

Synthetically though, SDA analogues such as **144** and **145** are far from trivial to prepare, requiring 10 and 8 steps, respectively from an advanced intermediate.²¹⁹ Furthermore, the additional steps required to convert **144** and **145** to synthons that

contain a group available for use in the CuAAC “click” reaction, further decreases the feasibility of this approach. However, the greatest barrier to the successful use of these molecules is the limitation of the use of an azide as a “handle” for functionalization, which requires a rigorous orthogonal protecting group strategy in order to be introduced in the presence of another protected amine. Alternatively, an approach that allows for the late-stage introduction of a handle - potentially by a linker, would provide efficient access to a glycoside that can be introduced into linear or cyclic peptides and functionalized. Furthermore, this approach allows for the interchangeable usage of different handles (in this case, azide vs. alkyne), providing wider flexibility to the synthesis. Thus, an approach employing the late-stage derivatization was developed (Scheme 5.2).

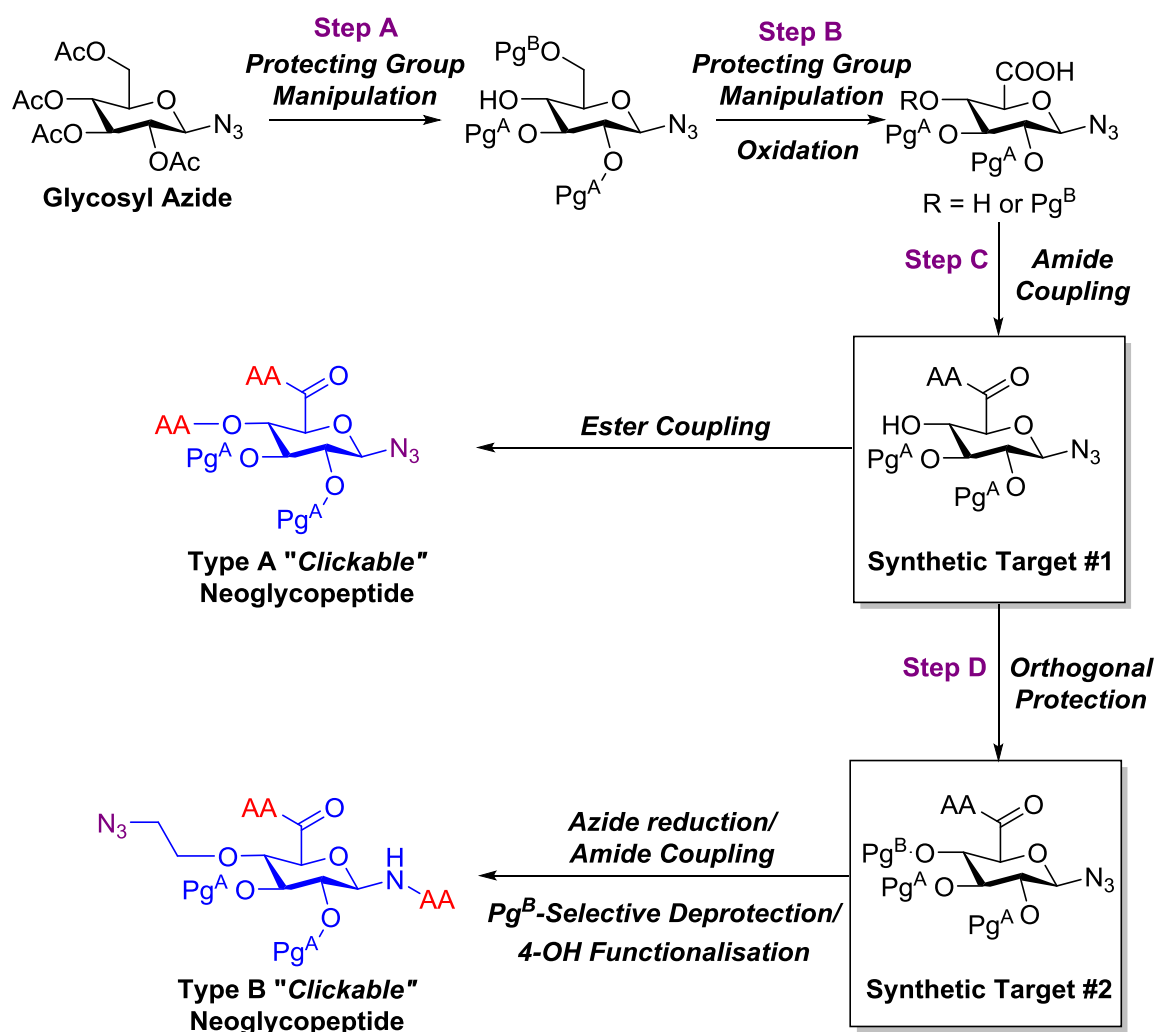
Based on the previous employment of a pyran-based sugar azido acid core (**60** and **65**), and its use in the somatostatin analogue **145**,¹⁵⁶ it was believed that the same core bearing an anomeric β -azide and 6-COOH would provide the easiest access to the targeted *glc*-sugar azido acid. Allowing for the introduction of the required handle at either the 2, 3- or 4-OH group of the *glc*-sugar azido acid, it was apparent that the 4-position of the glycoside would provide the most easily accessible site for substitution through an orthogonal protecting group strategy, and hence was initially targeted. Adjacent to the primary 6-OH group on the pyran ring, both the 4-OH and 6-OH may be protected together as an acetal from a simple glycosyl azide (Scheme 5.2), with subsequent protection of the remaining 2,3-OH groups and deprotection of the acetal producing a 4,6-diol. This intermediate can be selectively protected using a sterically bulky protecting group (e.g. TBDPS, trityl, etc.) at the primary 6-OH, producing a free 4-OH group (Scheme 5.2, Step A). Further protecting group manipulation would allow

for the protection of the 4-OH group, with deprotection, oxidation of the primary 6-OH and orthogonal deprotection of the 4-OH yielding a mono-hydroxylated *glc*-sugar azido acid (Scheme 5.2, Step B).

Considering the potential length of this synthetic strategy, it was recognized that the coupling of this intermediate to an amino acid, producing a glycoconjugate that could be further derivatized using standard ester coupling conditions, also represented a key synthetic target (Scheme 5.2, Step C). Producing “clickable” neoglycopeptides that are structurally different to those previously studied (e.g. Type A, Scheme 5.2), the free β -azide of this target molecule would be available for functionalization via the CuAAC “click” reaction. As well as being a synthon in the production of Type A “clickable” neoglycopeptides, the orthogonal protection of the 4-OH group would provide an approach towards the synthesis of neoglycopeptides linked at the anomeric and 6-positions, similar to those previously described (Scheme 5.2, Step D).¹⁵⁶ Tandem reduction/amide coupling of the β -azide would yield a neoglycopeptide which following selective deprotection and functionalization of the 4-position would yield a “clickable” neoglycopeptide (Type B, Scheme 5.2).

Synthetic approaches towards the development of both Type A and B neoglycoconjugates would have different biological purposes. If Type A derivatives of biologically-active neoglycopeptides were developed bearing different substitution patterns (i.e. 2,6-, 3,6- or 4,6-), the effect of peptide conformation on biological activity could be evaluated. These studies could serve as a guide, providing a platform for the replacement of the ester linkage with a more stable linkage (i.e. amide). Also, if the neoglycoconjugate synthesised bears relevance to nuclear imaging, the anomeric β -azide could be utilized for radiolabelling via the CuAAC “click” reaction. In regards

to Type B neoglycoconjugates, a synthetic approach for derivatives of this form will allow for the evaluation of cyclic peptides as nuclear imaging agents, again via labelling using the CuAAC “click” reaction. Examples of cyclic peptide derivatives that could be produced include labelled derivatives of the somatostatin mimics **141-143**. Hence, in the current study our focus was on developing a synthetic strategy to both of these key synthetic targets, that would allow for the future synthesis of Type A and Type B “clickable” neoglycopeptides (Scheme 5.2).

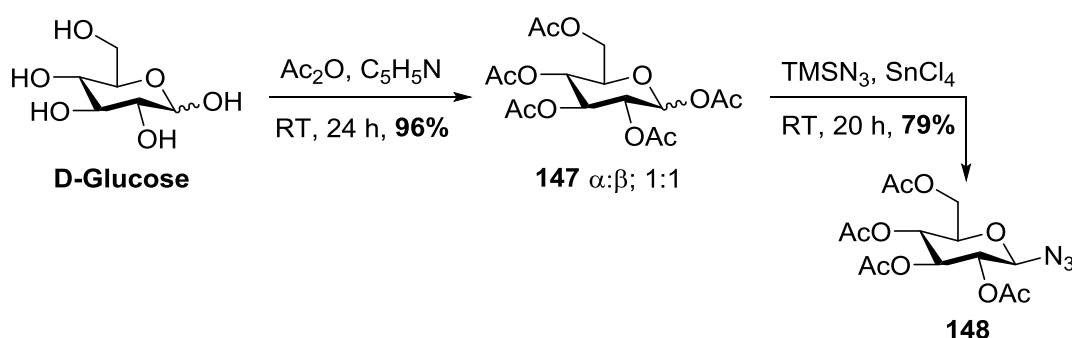


Scheme 5.2: Key strategy towards the development of "clickable" neoglycopeptides.

5.3 Synthesis of Orthogonally-protected Glycoconjugates

5.3.1 Initial Pathway Towards 4-Protected Sugar Azido Acids

En route to the synthesis of our key intermediate *glc*-sugar azido acid, the preparation of a glycoside with a selectively unmasked 4-OH group in the presence of 2,3-OH protection was required. Hence, our synthesis of this target glycoside was initiated from D-glucose, where peracetylation yielded the known penta-acetylated glycoside **147** in 96% yield (Scheme 5.3).²²²

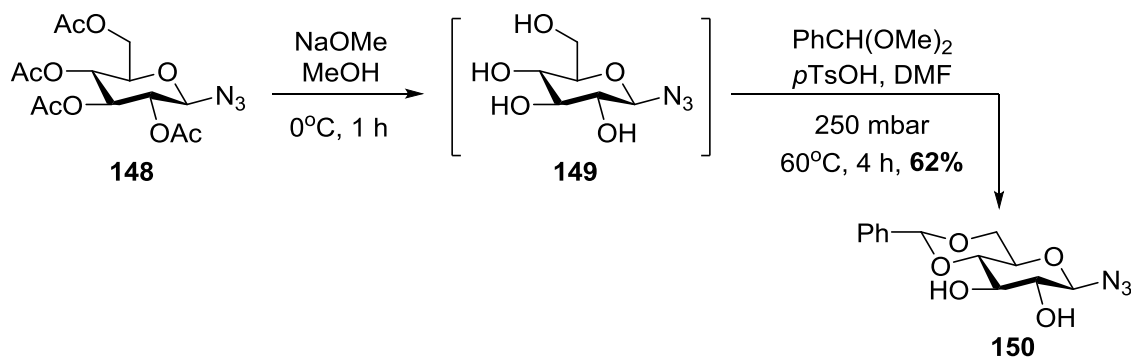


Scheme 5.3: Synthesis of 2,3,4,6-tetra-*O*- β -D-glucopyranosyl azide (**148**) from D-glucose.

Obtained as a white solid, evaluation of the ^1H NMR spectrum of **147** highlighted two doublets at 6.31 ppm ($J = 3.9$ Hz) and 5.72 ppm ($J = 8.2$ Hz) indicative of the α - and β -anomers, respectively. Equally integrating for 0.5 protons, this suggests an equal abundance of both anomers present. Subsequently, the penta-acetate **147** was then subject to anomeric azidation, under previously utilized $\text{SnCl}_4/\text{TMSN}_3$ conditions. After 20 hours, subsequent work up yielded the known 2,3,4,6-tetra-*O*-acetyl- β -D-glycopyranosyl azide (**148**) in 79% yield (Scheme 5.3).¹⁵³ Compared to the SnCl_4 -mediated azidation discussed in Chapter 2 (for compound **59**), the longer time

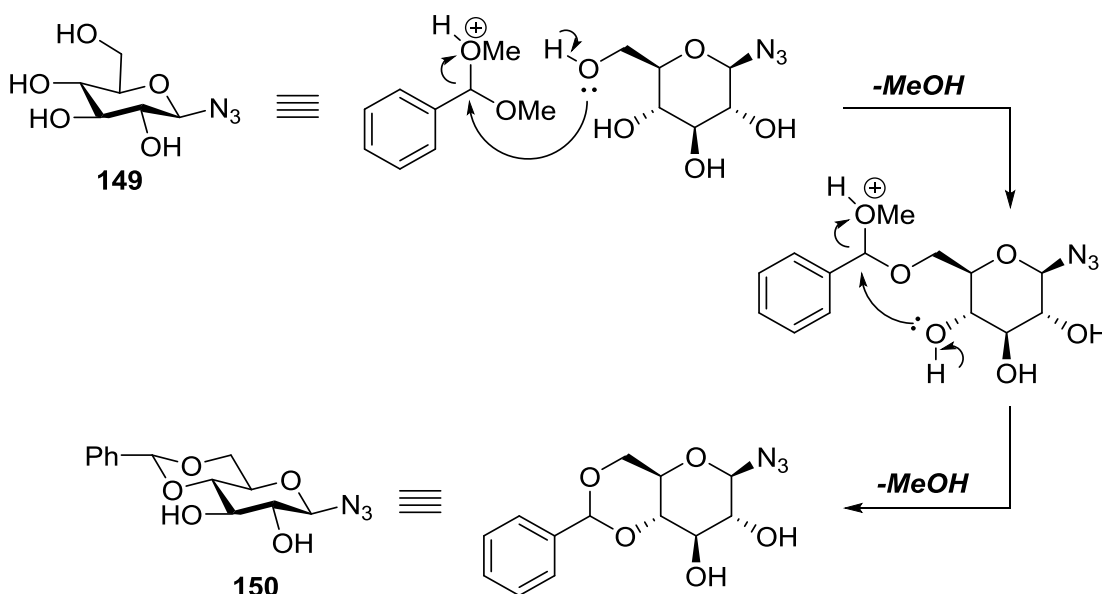
period utilized here allows for epimerization of the anomeric α -acetate, with the presence of the 6-OAc providing a coordination site for SnCl_4 with a much closer proximity than that described previously for the β -azido glucuronic acid allyl ester **59**. The presence of a signal in the ^1H NMR at 4.66 ppm was indicative of the anomeric H1, with the downfield position of the signal indicative of shielding effects of the azide group, and a coupling constant of $J = 8.8$ Hz indicative of the *trans* stereochemistry that exists between the H3 and the β -H1 protons. This was consistent with data for **148** previously reported.²²³

With **148** in hand, our focus shifted to the regioselective formation of the 4,6-benzylidene acetal, which is a key requirement of our orthogonal faprotection strategy. In order to install our acetal, **148** was subjected to classical Zemplen deacetylation conditions,²²⁴ with stirring in the presence of NaOMe dissolved in methanol yielding the β -D-glucopyranosyl azide intermediate **149** (Scheme 5.4). Subsequent heating of **149** under vacuum (~250 mbar) at 60°C for 4 hours in the presence of benzylidene dimethyl acetal and *p*-toluenesulfonic acid resulted in the formation of the requisite 4,6-benzylidene acetal, which upon isolation following flash column chromatography yielded **150** in 62% as a white solid (Scheme 5.4).^{158,225}



Scheme 5.4: Synthesis of 4,6-benzylidene- β -D-glucopyranosyl azide (**150**).^{158,225}

Mechanistically, in the presence of a catalytic quantity of *p*-TsOH a methoxy group of benzylidene dimethyl acetal is protonated. Subsequently, the primary 6-OH of **149** may undergo nucleophilic attack of the α -carbon of benzylidene dimethyl acetal, resulting in the elimination of methanol and the proton of the primary alcohol. The remaining methoxy group can then be protonated, with nucleophilic substitution by the neighbouring 4-OH resulting in the elimination of a second molecule of MeOH, proton and the desired benzylidene acetal **150** (Scheme 5.5).



Scheme 5.5: Mechanism for the acid catalysed formation of the 4,6-benzylidene acetal **150**.

Producing an acetal only between the 4- and 6- positions, the regioselectivity of this reaction is a result of their direct proximity, with the acetal forming a 6-membered ring displaying a geometric chair arrangement. This is exemplified by a 2D NOESY NMR experiment of **150**, where the proton situated on the α -carbon (5.55 ppm) present in the acetal shows a clear correlation with the H4 proton (3.56 ppm) present on the pyran ring, in addition to a H6 proton (Figure 5.5).

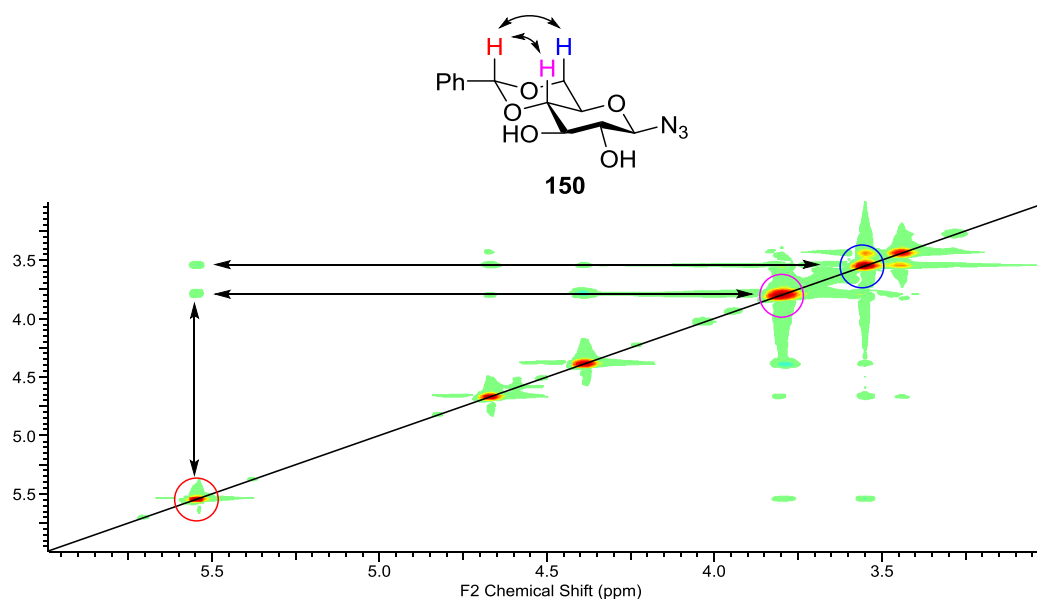
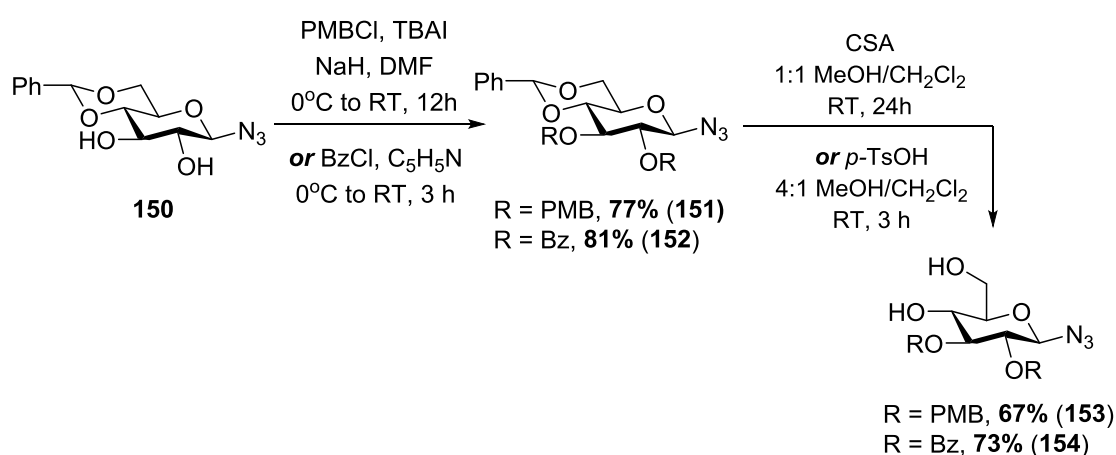


Figure 5.5: 2D NOESY experiment highlighting correlations between the acetal CH, and H4 and H6 in 150.

With the required acetal installed, the remaining 2-OH and 3-OH were subjected to protection. Considering the later introduction of our handle, multiple protecting group conditions were trialled to achieve the requisite 4,6-diol, with *p*-methoxybenzyl ethers (PMB) and benzoyl ester (Bz) protecting groups both utilized. Removed under concentrated acid, hydrogenolysis or oxidative conditions, the PMB ether allows for the introduction of our requisite handle through standard alkylation conditions, permitting the use of stronger hydride bases (NaH, KH).¹⁵⁹ Conversely, the benzoyl ester is highly susceptible to base hydrolysis, a distinct disadvantage compared to the PMB ether, requiring the use of trichloroacetimidate chemistry to install the required handle at the 4-OH. However, benzoyl esters display high compatibility to the reduction of anomeric β -azides to produce an amine, maintaining β -stereochemistry through neighbouring group participation, whilst PMB may be cleaved under such conditions.¹⁵⁹

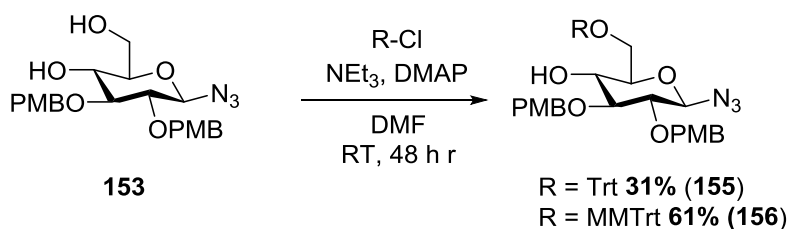
Thus to evaluate both of these protecting group strategies, the 2,3-OH groups of **150** were protected. Using *p*-methoxybenzyl chloride (PMB-Cl) in the presence of tetrabutylammonium iodide (TBAI) as an activator, and NaH as base, the novel 2,3-OPMB protected derivative **151** was synthesized in 77% yield (Scheme 5.6). This was confirmed by the LR-ESIMS spectrum of **151**, where a signal at m/z 556 ($C_{29}H_{31}N_3O_7 + Na$) represented the desired product plus sodium. Similarly, **150** was protected with benzoyl chloride (BzCl) in the presence of pyridine, with subsequent recrystallization yielding the novel 2,3-OBz protected derivative **152** in 81% yield (Scheme 5.6). The benzoyl protection of the 2,3-OH's of **150** was highlighted in the 1H NMR spectrum, where signals at 5.81 ppm and 3.88 ppm were indicative of the H3 and H2 protons of **152**. These signals are in direct contrast to the corresponding protons in **150** (3.46 ppm, H3; 3.25 ppm, H2) with the benzoyl protecting group delocalizing the electrons of the oxygen at the 2- and 3-position significantly, reducing the shielding effect imparted on the neighbouring protons.



Scheme 5.6: Synthesis of 2,3-protected-4,6-diol derivatives **153** and **154**.

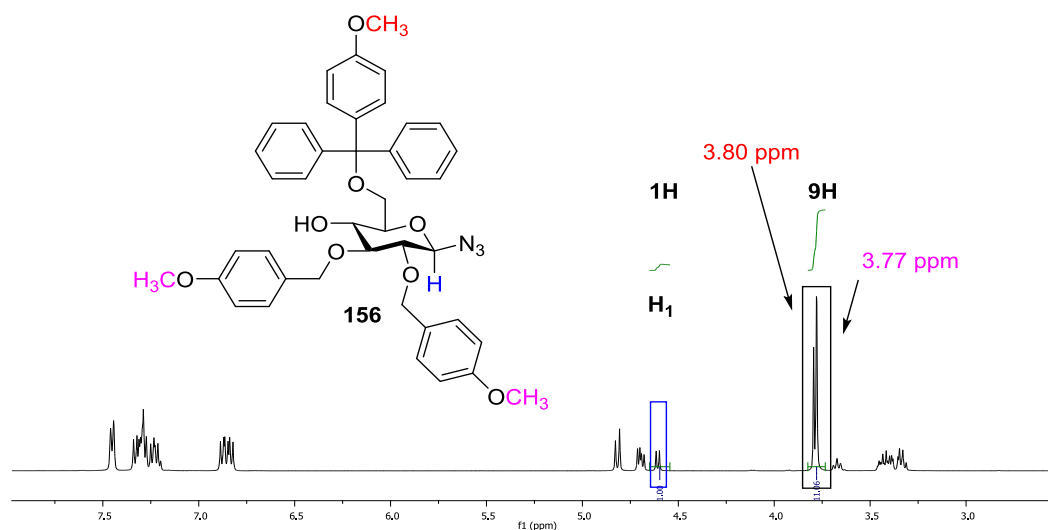
With **151** and **152** in hand, the acetals of both were exposed to acidic deprotection conditions to unmask the 4-OH group. Initially, (-)-camphorsulphonic acid (CSA) was utilized in the deprotection of **151**, with stirring in MeOH/CH₂Cl₂ (1:1) over 24 hours resulting in cleavage of the acetal, to produce the 2,3-OPMB-4,6-diol **153** in 67% yield (Scheme 5.6). Deprotection of the acetal was signified by the disappearance of a signal in the ¹H NMR spectrum of the product **153** at 5.56 ppm, indicative of the axial proton present on the carbon linking the 4-OH and 6-OH. Subsequently, cleavage of the acetal of **152** was also performed under acidic conditions, with catalytic *p*-toluenesulfonic acid in MeOH/CH₂Cl₂ (4:1) producing the requisite diol **153** in 73% yield after 3 hours. (Scheme 5.6) Though benzoyl esters are more prone to cleavage in acidic pH than PMB ethers,¹⁵⁹ it was recognized that the catalytic use of a stronger acid such as *p*-TsOH, compared to CSA (*p*K_A -2.5 vs. 0.9),²¹² would reduce the reaction time required for diol cleavage, limiting the formation of cleaved-ester by products. It must be noted though that TLC analysis of the formation of **154** also showed the slow cleavage of the benzoyl esters after 3 hours of reaction time.

With both diols **153** and **154** synthesized, efforts were next made to selectively install the required 6-OH protecting group. For this purpose, protecting groups based on the triphenylmethyl (trityl -Trt) group were chosen, due to their steric bulk, ease of introduction and wide availability. Hence, using the PMB-protected diol **153** trials were initiated, with the use of Trt-Cl, NEt₃ and DMAP over 48 hours resulting in the formation of the 6-OTrt derivative **155** in 31% yield (Scheme 5.7).



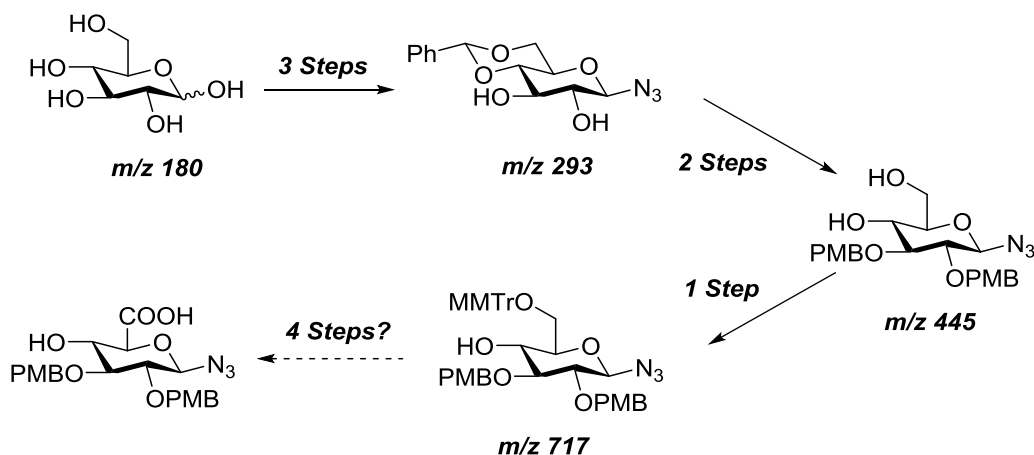
Scheme 5.7: Synthesis of 6-protected glycosides **155** and **156**.

Utilizing a catalytic quantity of DMAP as an activator, the formation of a trityl-DMAP intermediate ensued. In the presence of NEt_3 as a proton scavenger, nucleophilic substitution of this intermediate by the 6-OH group of **153** resulted in the formation of the desired 6-OTrt protected **155**, albeit in low yield. Thus, considering that this protection strategy may later be utilized in the 6-OH protection of the 2,3-OBz diol **154**, efforts were made to improve this selective protection without requiring stronger basic conditions. Subsequently, the more-activated trityl donor 4-methoxytriphenyl chloride (MMTrt-Cl) was used in place of Trt-Cl, which under the previously used NEt_3/DMAP conditions yielded the 6-OMMTTr-protected derivative **156** in 61% yield (Scheme 5.7). The isolation of **156** was evidenced by the ^1H NMR spectrum, whereby overlapping signals at 3.77 and 3.80 ppm accounted for the protons of the trityl-bound methoxy group and the *p*-methoxy groups of the PMB protecting groups present at the 2- and 3-OH's respectively (Figure 5.8).



Scheme 5.8: ^1H NMR spectrum of **156**, highlighting overlapping signals at 3.77 and 3.80 ppm that indicates the PMB and MMTr-methoxy groups, respectively.

Interestingly, LR-ESIMS of **156** highlighted a signal at m/z 740 ($\text{C}_{42}\text{H}_{43}\text{N}_3\text{O}_8\text{Na}$; $[\text{M} + \text{Na}^+]$) in a spectroscopically-pure sample of **156**. Representing the molecular ion for this compound, this signal shows only ~25% intensity compared to the highest intensity signal present, highlighting the weak ionizability of the compound in the mass spectrometer. The MMTr-protecting group added significant mass to the overall compound, which when taken into account alongside the PMB groups introduced at the 2- and 3- positions, accounted for a 245% increase in the molar mass of **156** from the 4,6-acetal intermediate **150** (Scheme 5.9). Furthermore, in order to produce our requisite sugar azido acid bearing handles capable of further derivatization, it would require at least four additional synthetic steps, which alongside the six steps to produce **156** from D-glucose, signified a lengthy, atom-uneconomical synthesis (Scheme 5.9). Thus, based on these findings, alternate pathways towards our target glycoside were sought.

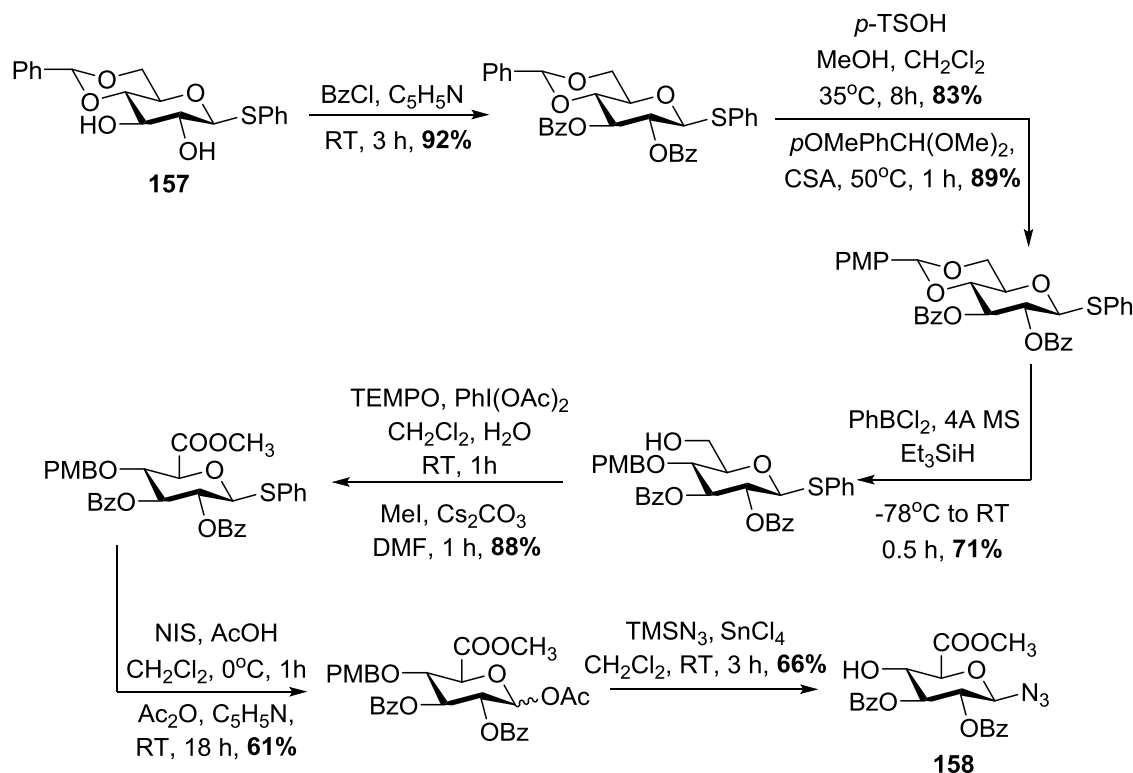


Scheme 5.9: Original synthetic pathway highlighting additional synthetic steps from 156 required to produce the desired sugar azido acid target.

5.3.2. Improved Pathway Towards 4-Protected Sugar Azido Acids

In the development of a new strategy for the synthesis of orthogonally-protected sugar azido acids, a number of approaches were evaluated. One approach included the selective reduction of the benzylidene acetal of either **151** or **152**, unmasking the 6-OH. This approach is effectively highlighted in the recently published work of Bera and Linhardt, whereby the 4-OH derivative **158** was produced *en route* to the synthesis of unnatural heparosan and chondroitin building blocks (Scheme 5.10).²²⁶ Synthesised in 7 steps from phenyl-4,6-benzylidene-1-thio- β -D-glucopyranoside (**157**), this work demonstrates the usage of a 2,3-OBz protecting group strategy in addition to the selective reductive opening of a benzylidene acetal. Oxidation of the 6-OH group to the carboxylic acid, and one-pot azidation/4-deprotection result in the desired sugar azido acid bearing a free 4-OH group. This work represents a concise route to sugar azido

acids that can be derivatized with a handle and coupled to produce numerous glycoconjugates (Scheme 5.10).

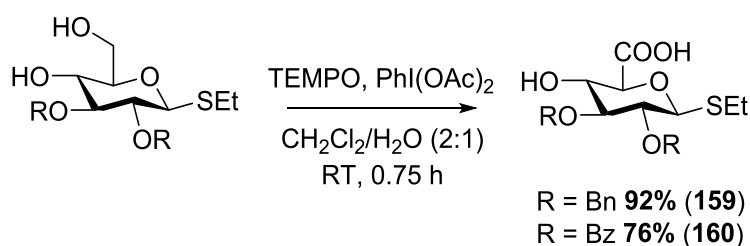


Scheme 5.10: Synthesis of 1-azido-2,3-O-benzoyl-β-D-glucuronic acid methyl ester (158) from phenyl-4,6-benzylidene-1-thio-β-D-glucopyranoside (157) published by Bera and Linhardt.²²⁶

Reflecting on our previous endeavours, there are clear distinctions between these two approaches – namely, the selective reduction of the benzylidene acetal and the timing of the introduction of the requisite anomeric β-azide. Whilst an attractive and noteworthy concept, the selective benzylidene reduction could potentially complicate the synthesis, with Bera and Linhardt highlighting that the removal of a 4-PMB group would require orthogonal protection of the carboxylic acid.²²⁶ Whilst more than adequate in this example, our requirement for coupling to the carboxylic acid would result in additional protection and deprotection steps. Instead, an approach that could

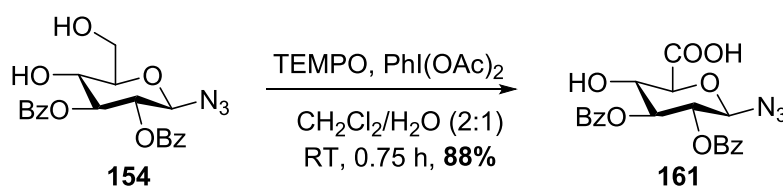
adapt the previously attempted synthesis of 4-OH bearing sugar azido acids would be highly advantageous.

Considering the synthesis of the 2,3-OBz diol **154**, it was recognized that a strategy where the required carboxylic acid could be produced selectively in the presence of a 4-OH would be optimal. Requiring minimal protecting group manipulation, the carboxylic acid could then be coupled to an amino acid with a free amine. Subsequently, the 4-OH could then be coupled to another amino acid bearing a free carboxylic acid, to produce a Type A “clickable” neoglycopeptide. Alternatively, the 4-OH group could be orthogonally protected, allowing for the coupling of another amino acid at the anomeric position following reduction of the azide to an amine (See Scheme 5.2). Indeed, previous studies by Van Den Bos and co-workers have highlighted the efficiency of oxidants such as TEMPO and bisacetoxyiodobenzene ($\text{PhI}(\text{OAc})_2$) in the selective oxidation of the primary alcohol of pyranosides carboxylic acids.²²⁷ Encompassing a broad range of differently pyranosides bearing different mono- and dihydroxylated substitution patterns, these include a number of 4,6-OH bearing derivatives, such as **159** and **160** (Scheme 5.11).



Scheme 5.11: Examples of selective oxidation of a primary alcohol present on a pyran-based glycoside previously described by Van Den Bos and coworkers.²²⁷

Affording selective oxidation in the presence of a 4-OH in glucosyl-based examples, **159** and **160** show that the TEMPO/PhI(OAc)₂ oxidation system can tolerate a variety of different protecting groups at the 2- and 3-positions, including benzyl and benzoyl groups.²²⁷ In relation to the previously synthesised **154**, it was believed that this methodology could be utilized to produce a sugar azido acid that would also possess a 4-OH free for further protection or derivatization, *en route* to the production of “clickable” neoglycopeptides. Therefore, **154** was subjected to TEMPO/PhI(OAc)₂ oxidation condition, with stirring in CH₂Cl₂/H₂O (2:1).²²⁷ After 45 minutes, workup and purification by flash column chromatography resulted in the isolation of the partially-deprotected sugar azido acid **161** in 88% yield (Scheme 5.12).



Scheme 5.12: TEMPO/BAIB-mediated oxidation of diol **154** to form the sugar azido acid **161**.

The oxidation of **154** to form the sugar azido acid **161** was monitored by TLC, with the formation of a spot (solvent, 1:1 EtOAc/Hexane + 5% AcOH) much lower on the TLC plate (R_f 0.28) highlighting the transformation of **154** to the more polar carboxylic acid. Furthermore, the ¹H NMR spectrum of **161** highlights the presence of five protons between 3.0 – 6.0 ppm as opposed to the seven protons observed in **154**, indicative of the oxidation of the primary 6-OH to form a carboxylic acid (Figure 5.6).

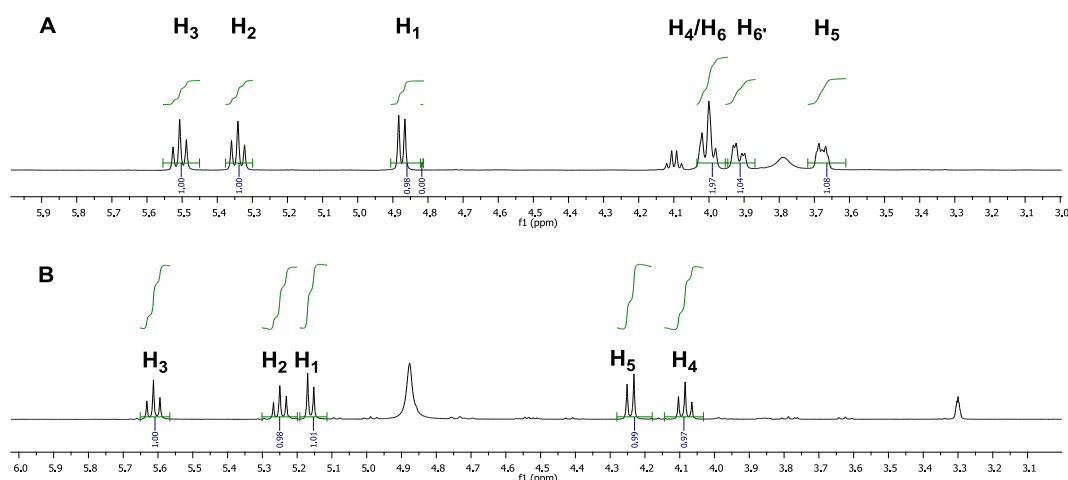
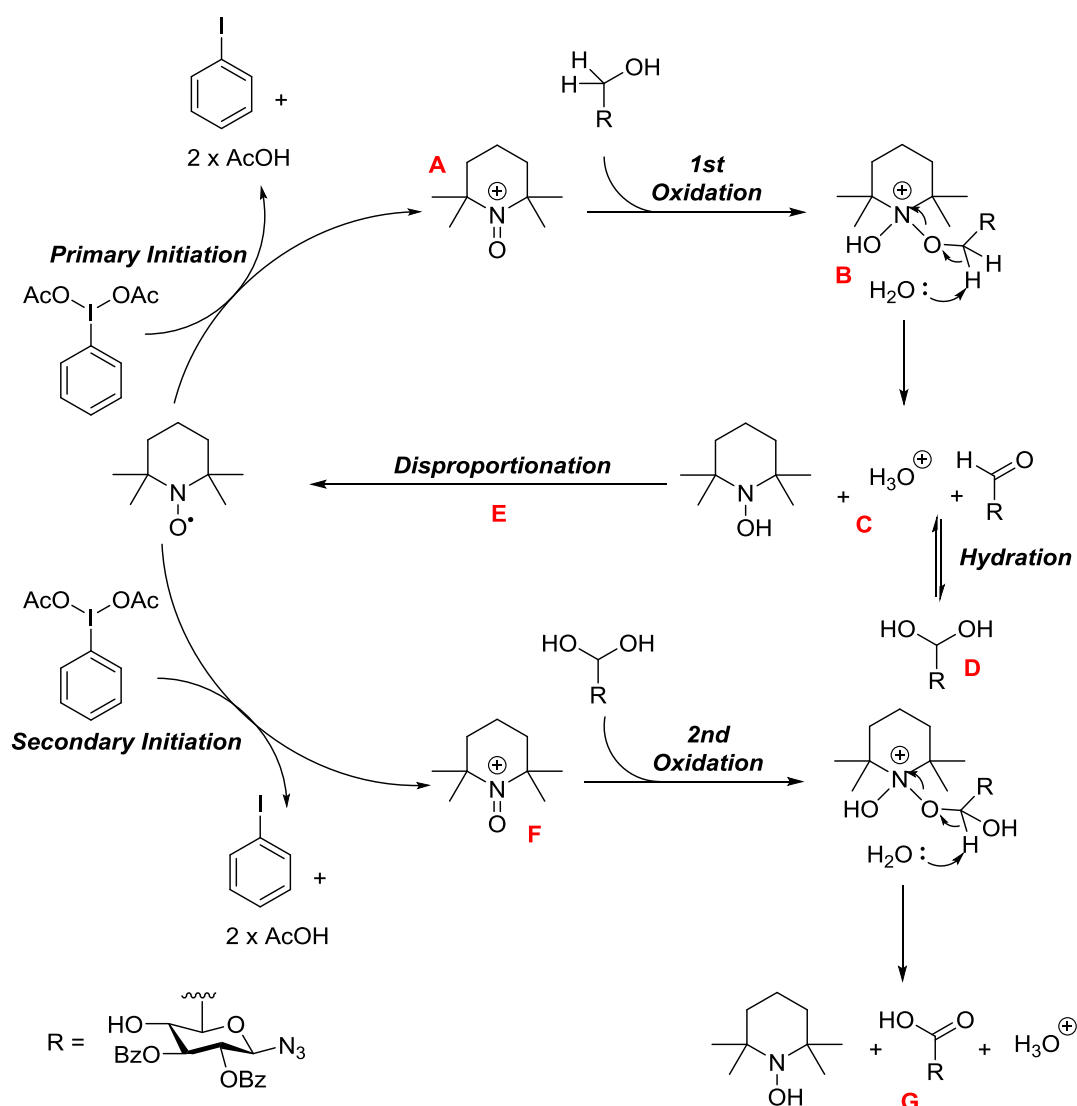


Figure 5.6: Comparison of the ^1H NMR spectra of **154** (A) and **161** (B), highlighting the loss of two protons (A – H6/H6') through oxidation, resulting in the sugar azido acid (B).

Utilizing a catalytic quantity of TEMPO, the reaction is initiated by an excess of $\text{PhI}(\text{OAc})_2$, resulting in the production of a piperidinium *N*-oxide intermediate (Scheme 5.13, A). In the presence of **154**, the piperidinium *N*-oxide is subject to nucleophilic substitution by the alcohol, resulting in the formation of a dihydroxylamine intermediate (Scheme 5.13, B). Deprotonation at the C6 position of **154** drives the oxidation of the primary alcohol, resulting in the production of an intermediate aldehyde, in addition to a hydroxylamine derivative (Scheme 5.13, C).

The biphasic solvent conditions present in the reaction are ideal for aldehyde hydration, resulting in the formation of a geminal diol intermediate (Scheme 5.13 D). Concurrently, the disproportionation of the hydroxylamine derivative back to TEMPO allows for its further usage in the catalytic cycle (Scheme 5.13, E). Secondary initiation of TEMPO by $\text{PhI}(\text{OAc})_2$ resulted in the reformation of the piperidinium *N*-oxide intermediate (Scheme 5.13, F). Finally, nucleophilic substitution by one of the geminal diols resulted in the production of a second dihydroxylamine intermediate, which

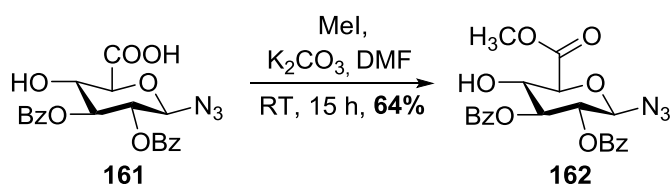
following oxidation yielded the desired carboxylic acid **161** (Scheme 5.13, **G**). It is likely that the tight transition state at the 6-OH, the steric bulk provided by the neighbouring 3-OBz group present on **154** and the mild/short reaction conditions utilized, significantly reduced the susceptibility of the 4-OH group of **154** to oxidation.^{228–234}



Scheme 5.13: Proposed mechanism for the oxidation of primary alcohols to carboxylic acids utilizing the TEMPO/PhI(OAc)₂ oxidation protocol.

5.3.3 Synthesis of 4-Orthogonally Protected Intermediate **165**

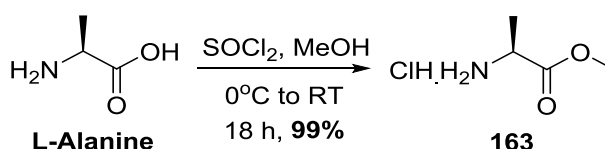
With access to the key intermediate sugar azido acid **161** achieved, our focus turned to the formation of a hydroxyl-bearing glycoconjugate, the first key synthetic target of this project. Orthogonal protection of the 4-OH of **161** prior to amino acid coupling would likely deliver the highest yielding approach to this target, providing future access to Type A and B neoglycopeptides. The presence of both an alcohol and carboxylic acid group in **161** though raises questions regarding protecting group selectivity, with the greater acidity of the carboxylic acid in comparison to the 4-OH of **161** likely to favour carboxyl protection rather than alkylation. This is exemplified by the selective methylation of **161** by MeI and K₂CO₃ in DMF, which produced the ester **162** in 64% yield, with this molecule displaying ¹H and ¹³C NMR spectral data corresponding with those previously reported (Scheme 5.14).²²⁶



Scheme 5.14: Synthesis of previously reported glucuronic acid methyl ester **162**.²²⁶

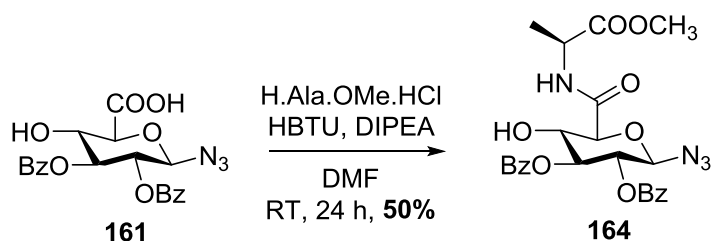
Hence, as the presence of a 4-OH would be highly advantageous in the future production of Type A neoglycopeptides, direct coupling of **161** to a respective amino acid was performed prior to the protection of the 4-OH group. As a requirement of this strategy, suitably carboxyl-protected amino acids were required for coupling to the carboxylic acid group of **161**. As a result, L-alanine (Ala) was chosen as our model-

coupling amino acid, with its simplicity in being *N*- or *C*-protected, and its minimal sidechain steric bulk making it ideal for the development of a broader strategy. Utilizing thionyl chloride in dry MeOH, the carboxylic acid of L-alanine was methylated, producing the carboxyl-protected derivative L-alanine methyl ester hydrochloride (H.Ala.OMe.HCl; **163**) in near quantitative yield (Scheme 5.15). The ^1H and ^{13}C NMR spectral data for **163** were consistent with those previously reported.^{235,236}



Scheme 5.15: Synthesis of L-alanine methyl ester hydrochloride (**163**).^{235,236}

With both **161** and our requisite amino acid in hand, coupling and protection was initiated. Utilizing the coupling reagent HBTU and 2.1 equivalents of DIPEA, H.Ala.OMe.HCl (**163**) was coupled to **161**, selectively producing the novel glycopeptide **164** in 50% yield (Scheme 5.16).



Scheme 5.16: Synthesis of alanine-sugar azido acid glycoconjugate **164** via amide coupling.

An evaluation of the ^1H NMR spectrum of **164**, highlighted the presence of a doublet at 7.13 ppm ($J = 6.9$ Hz) integrating for one proton, which was indicative of the

amide nitrogen formed during coupling (Figure 5.7, A). Furthermore, when analysed with respect to a 2D gCOSY ^1H NMR experiment of **164**, correlations were observed between this signal and a triplet at 4.62 ppm ($J = 7.5$ Hz) integrating for one proton. Further correlations with a signal at 1.55 ppm highlighted sequential 3-bond couplings between the amide NH, H^α and H^β of the coupled amino acid in **164** (Figure 5.7, B). The first key objective of this project, to our knowledge the synthesis of **164** represents the first example of a glycoconjugate formed by the selective coupling of a sugar azido acid bearing a hindered alcohol.

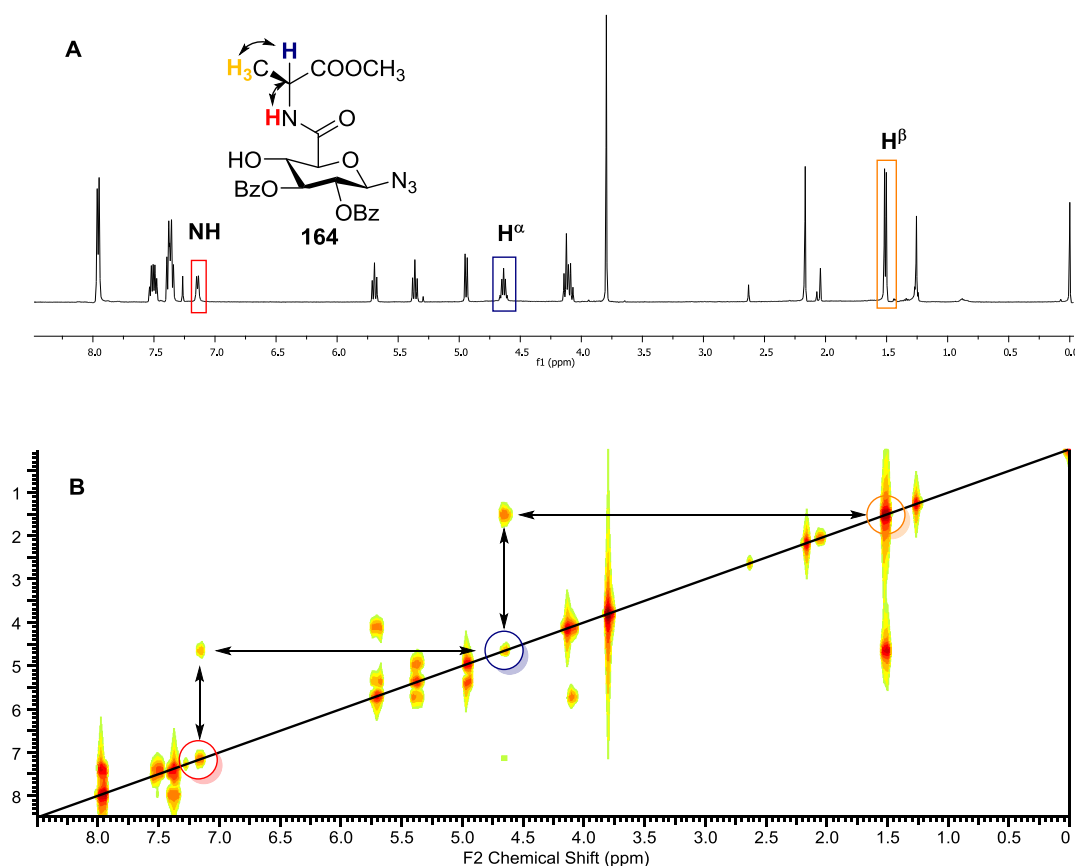
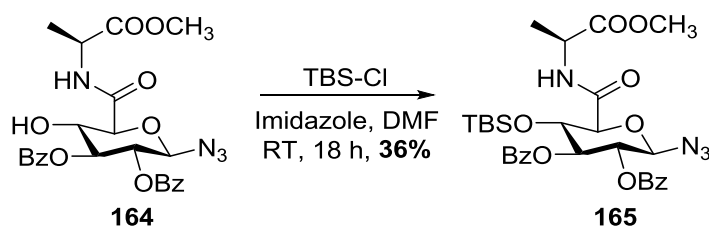


Figure 5.7: ^1H NMR experiment (A) and 2D gCOSY experiment (B) of glycoconjugate **164**.

Following the success encountered in producing the coupled product, efforts were undertaken to protect the 4-OH group of **164**, and thus complete the second key objective of this project. Mindful of the need for an orthogonal protecting group, the *tert*-butyldimethylsilyl (TBS) group was chosen. Displaying favourable stability to reduction, and removed using mildly acidic conditions or through the use of fluoride donors such as tetrabutylammonium fluoride (TBAF),¹⁵⁹ TBS-protection of **164** would provide access to the required neoglycopeptide, with selective deprotection unmasking the 4-OH group in order to introduce our handle for derivatization. Hence, **164** was subjected to TBS protection, with stirring in the presence of TBS-Cl and imidazole in DMF overnight resulting in the isolation of the 4-OTBS derivative **165** in 36% yield (Scheme 5.17).



Scheme 5.17: Synthesis of the orthogonally-protected glyconjugate 165.

The low yield gained for **165**, was likely a result of the bulky nature of the TBS protecting group, with the surrounding benzoyl esters and linked amino acid hindering the approach of the active TBS-imidazole intermediate. Furthermore, the relative distance between the amide carbonyl of **164** and its corresponding 4-OH allows for hydrogen bonding, stabilizing the hydroxyl group and thus decreasing its nucleophilicity. As a result, even with an excess of TBS-Cl (2 eq.) and imidazole (4 eq.) present, protection of the 4-OH group of **164** would still have been highly unfavourable.

The formation of **165** was highlighted in the TLC by a dramatic increase in R_f (0.85, 1:1 Hexane:EtOAc) from **164**, with TBS protection greatly decreasing the polarity of the molecule. The effect of protecting the 4-OH group of **164** was also highlighted in the ^1H NMR spectrum, where the signal representing the H4 proton of **165** shifted downfield (~ 0.3 ppm) compared to the corresponding proton in **164** (Figure 5.8). Attachment of the TBS group in **165** delocalizes electron density present on the 4-bound oxygen to the electropositive silicon atom of the TBS group, which as a result deshields the neighbouring H4, increasing the chemical shift (Figure 5.8). The second key objective of this project, the synthesis of **165** represents an important milestone in the development of Type B “clickable” neoglycopeptides.

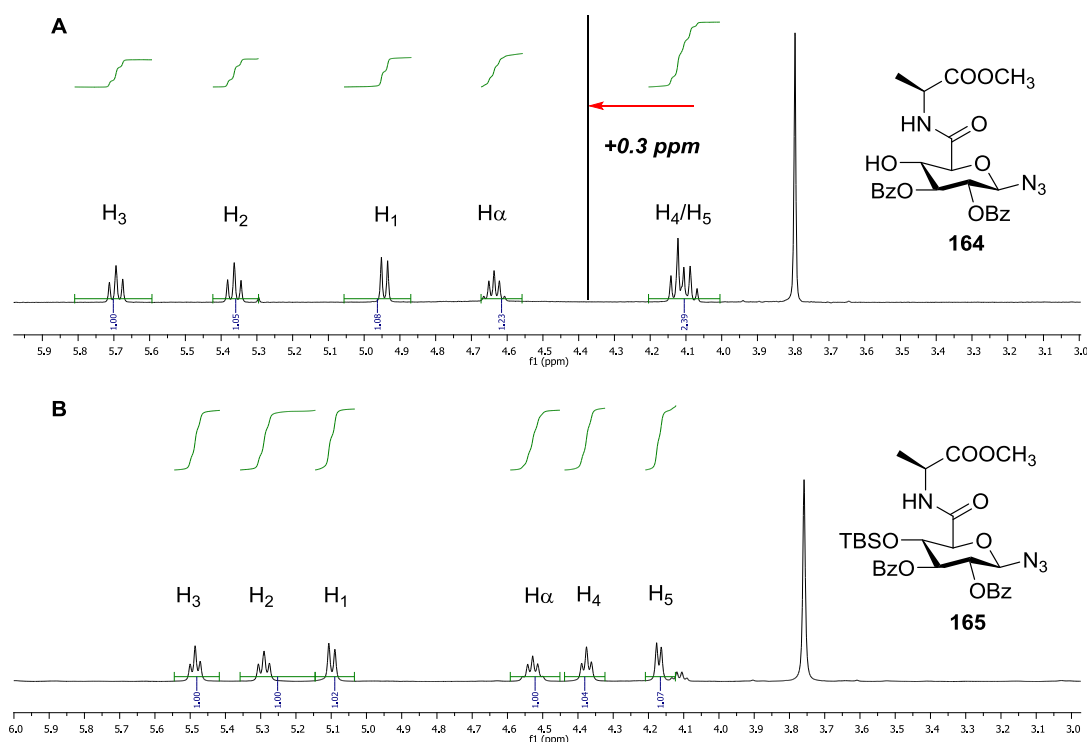


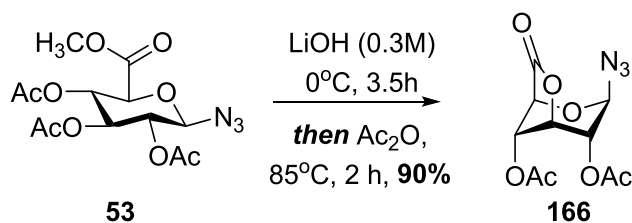
Figure 5.8: Comparison of the ^1H NMR spectra of **164** (A) and **165** (B), highlighting the deshielding effect on the H4 of **165** through TBS-protection.

5.3.4 Synthesis of the 3-Orthogonally Protected Intermediate 170

Building on the production **164** and **165** towards the development of “clickable” neoglycopeptides, it was recognised that the development of derivatives that could be functionalised at alternate positions of the glycoside would also be highly advantageous. Increasing the structural diversity of analogues, the development of differently-substituted derivatives may also deliver a more concise route in the development of neoglycopeptides that may be functionalized by the CuAAC “click” reaction.

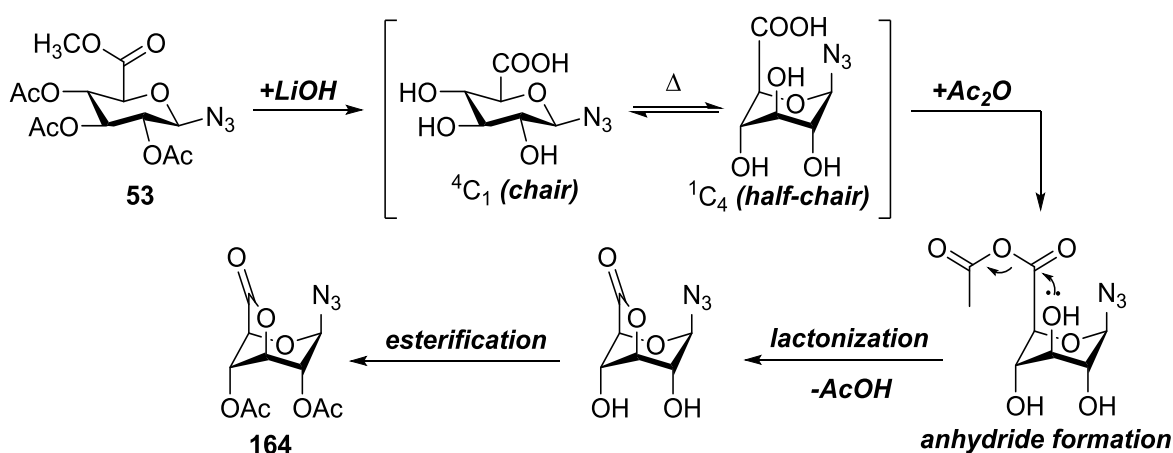
The development of a more efficient approach was of particular importance, considering that the production of **165** from D-glucose required seven synthetic steps. Of these steps, the synthesis of the benzylidene acetal **150** and the low yielding production of the 4-OTBS glycoconjugate **165**, stood out as those that would limit the scalability of this methodology. The use of *p*-toluenesulfonic acid, the same acid used to catalyze the acetals’ deprotection, made scaling up the production of **150** quite problematic, with the steric hinderance imposed by surrounding groups in **164** making the production of **165** highly unfavourable.

Hence, in continuing on with the use of a sugar azido acid scaffold, an evaluation of the relevant literature was undertaken in order to develop an alternate route to development of orthogonally-protected neoglycopeptides that could be further functionalized by the CuAAC “click” reaction. During this process, a re-evaluation of the work of Tosin *et al.* highlighted that un-protected sugar azido acids (such as **53**) can undergo intramolecular cyclisation to efficiently produce 6,3-lactones (Scheme 5.18, **166**).^{157,237}



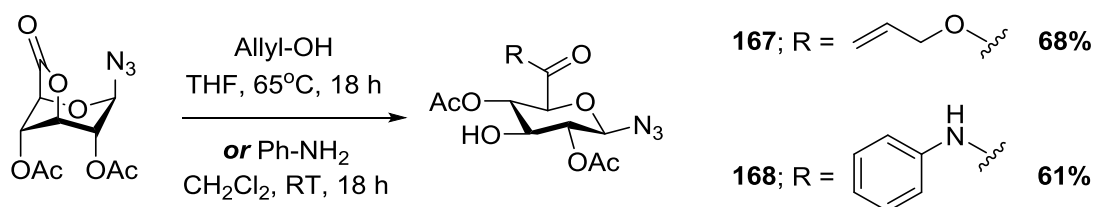
Scheme 5.18: Conversion of 1-azido-2,3,4-tri-O-acetyl-β-D-glucuronic acid methyl ester (**53**) to the 6,3-lactone **166** reported by Tosin *et al.*^{157,237}

In the presence of a strong nucleophilic base such as LiOH, global deprotection of the protected sugar azido acid **53** takes place, resulting in a glucuronic acid intermediate (Scheme 5.19). Present in an equatorial “chair” conformation, heating (85°C) results in conversion to a “half-chair” conformation, where the 3-OH and 6-COOH are more confined “axial” geometry relative to one another. In the presence of Ac₂O, the formation of a mixed anhydride with the carboxyl group occurs. Prone to nucleophilic substitution from the 3-OH group, lactonization occurs, with the remaining 2- and 4-OH acetylated to yield the requisite protected 6,3-lactone product (Scheme 5.19).



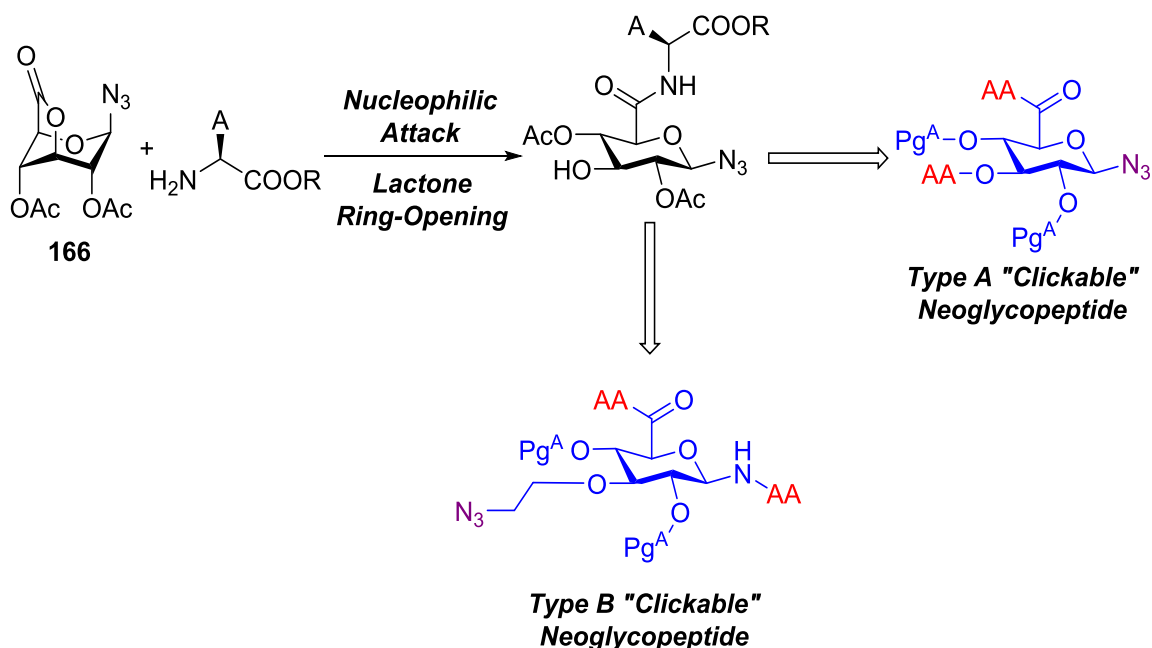
Scheme 5.19: Mechanism for the formation of 6,3-lactone **53** from **166**, utilizing saponification and chair conformation interconversion.

Whilst not initially obvious, the importance of this conversion lies in the susceptibility of 6,3-lactones to nucleophilic attack, with Tosin *et al.* subjecting **166** to attack by weak nucleophiles such as allyl alcohol and aniline, producing the ester and amide derivatives **167** and **168** (Scheme 5.20).^{157,237} As a result of ring opening of the lactone, the 3-positions of both products **167** and **168** bear free-hydroxyl groups that may be further protected, alkylated or glycosylated (Scheme 5.20).^{157,237}



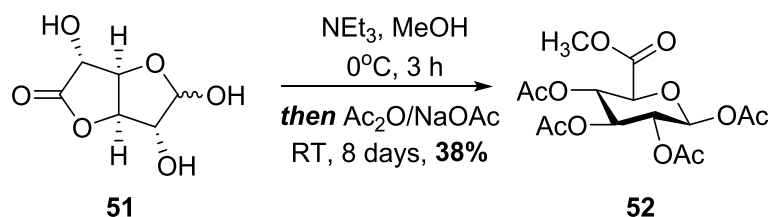
Scheme 5.20: Nucleophilic substitution of the 6,3-lactone **164**, resulting in the ester and amide derivatives **167** and **168** that bear unprotected 3-OH groups.^{157,238}

In relation to the previously synthesised 4-OH-bearing intermediate **164**, it could be envisaged that if an amino acid bearing an unprotected α -amino group, such as the previously used H.Ala.OMe.HCl (**163**), was reacted with **166**, it may generate a respective glycoconjugate bearing a free 3-OH group (Scheme 5.21). Such a glycoconjugate would provide a mechanism for the production of Type A “clickable” neoglycopeptides linked to amino acids by the 3- and 6-positions. Additionally, protection of the 3-OH with a TBS-group akin to **165** would provide an orthogonally protected glycoconjugate that could be utilized as a key synthon in the development of Type B “clickable” neoglycoconjugates (Scheme 5.21).



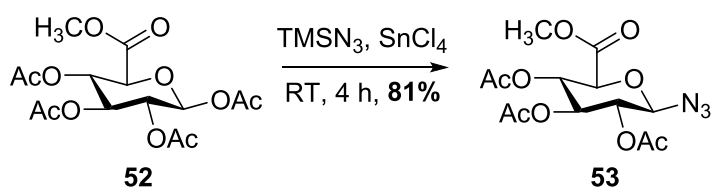
Scheme 5.21: Proposed synthesis of glycoconjugates bearing a free 3-OH group from the 6,3-lactone **166**, towards the synthesis of “clickable” neoglycopeptides.

With this in mind, efforts were undertaken to produce the requisite 3-OH and 3-OTBS protected glycoconjugates, with the synthesis of the peracetylated azido glucuronic acid methyl ester **53**, the precursor molecule to the 6,3-lactone **166**, first targeted. Glucuronolactone (**51**) was utilized as starting material, with initial stirring in the presence of triethylamine in MeOH for 3 hours resulting in esterification and expansion of the furan ring of glucuronolactone to a pyran ring. Subsequently, workup followed by the addition of Ac₂O and NaOAc, and stirring at room temperature for 8 days resulted in the formation of the peracetylated methyl ester derivative **52**, which was isolated by recrystallization in 38% yield (Scheme 5.22).



Scheme 5.22: Synthesis of 1,2,3,4-tetra-*O*-acetyl- β -D-glucuronic acid methyl ester (**52**) from glucuronolactone.

^1H and ^{13}C NMR spectra for **52** synthesised were identical to those previously reported.¹⁵⁶ Though produced in low yield due to the concurrent formation of the α -anomer of **52**, the scalability of this reaction (>10 g product) and easy work up made it ideal for producing our requisite azidosugar. Hence, with **52** in hand, the β -azido group was introduced at the anomeric position. Using the $\text{TMSN}_3/\text{SnCl}_4$ conditions, the required 1-azido-2,3,4-tri-*O*-acetyl- β -D-glucuronic acid methyl ester (**53**) was synthesised, isolated in 81% yield (Scheme 5.23), with ^1H and ^{13}C NMR spectra, and LR-ESIMS data consistent with those previously described.¹⁵⁶



Scheme 5.23: Synthesis of 1-azido-2,3,4-tri-*O*-acetyl- β -D-glucuronic acid methyl ester (**53**).¹⁵⁶

With the production of the required peracetylated precursor **53** achieved, efforts were made to produce the desired 3-OH glycoconjugate **169**. Initially, saponification of the acetyl groups and methyl ester were performed under base hydrolysis, with

neutralization and lyophilisation, followed by heating in Ac_2O at 85°C producing the desired 6,3-lactone intermediate **166**. The formation of this intermediate was confirmed by TLC (R_f 0.45, 1:1 Hexane:EtOAc), with further evaluation of the crude ^1H NMR spectrum of **166** (Figure 5.9, A) highlighting the presence of two signals at 2.18 and 2.10 ppm each integrating for 3 protons. Furthermore, signals in the ^{13}C NMR spectrum (Figure 5.9, B) at 169.0 and 168.9 ppm corresponding to the carbonyl carbons of the acetyl esters highlighted the presence of only two ester groups in **166**.

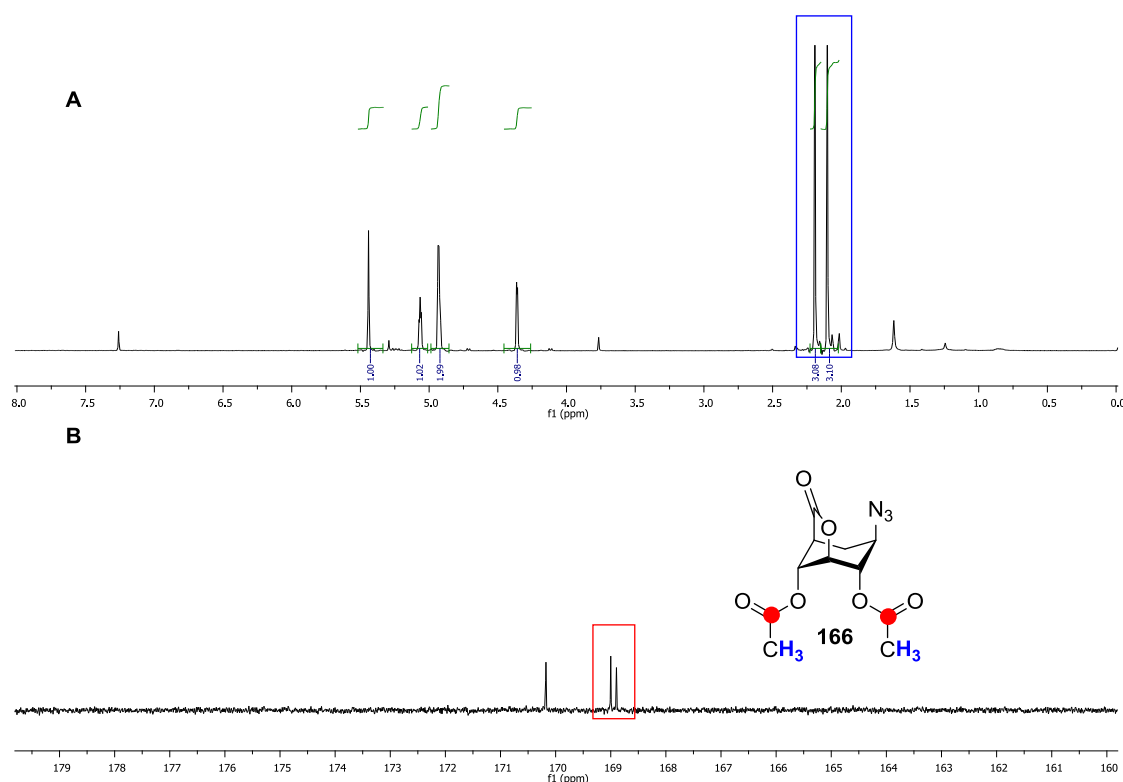
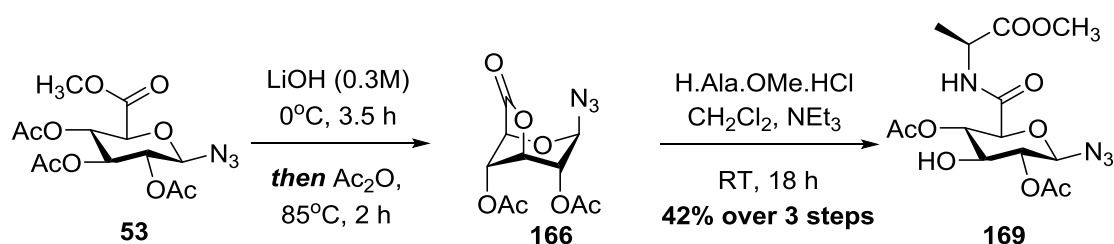


Figure 5.9: ^1H (A) and ^{13}C (B) NMR spectra of the crude 6,3-lactone **166**, highlighting the presence of 2 acetyl protecting groups at the 2- and 4- positions.

Consequently, the 6,3-lactone **166** was subjected to nucleophilic substitution, utilizing H.Ala.OMe.HCl (**163**). Under stirring in dichloromethane, the addition of a

slight excess of triethylamine (1.2 equivalents) neutralised the hydrochloride salt of **163**, liberating the α -amino group as a nucleophile. The subsequent nucleophilic attack of the lactone resulted in ring-opening, producing the desired 3-OH-bearing glycoconjugate **169** in 42% yield from **53** (Scheme 5.24).



Scheme 5.24: Synthesis of 3-OH bearing glycoconjugate **169** via ring-opening of the 6,3-lactone **166**.

The ^1H NMR spectrum of **167** highlighted the formation of the amide linkage from ring-opening of the lactone, with a doublet at 6.93 ppm ($J = 7.5$ Hz) integrating for one proton indicative of the amide hydrogen (Figure 5.34). The formation of the amide bond was further established in the ^{13}C NMR spectrum, where a signal at 165.9 ppm represented the carbonyl formerly constituting the lactone, bound to the α -amino group of the protected alanine (Figure 5.10). This signal appeared slightly shielded compared to that representing the same carbon in **166**, the result of this carbon being bound to the comparatively less electronegative nitrogen atom, rather than the oxygen atom present in the lactone. The synthesis of **169** represents the first reported use of a 6,3-lactone, and only the second reported usage of lactone ring-opening in the preparation of glycoconjugates between a glycoside and a proteinogenic amino acid.²³⁹ Furthermore, **169** represents a key intermediate in the production of Type A “clickable” glycoconjugates.

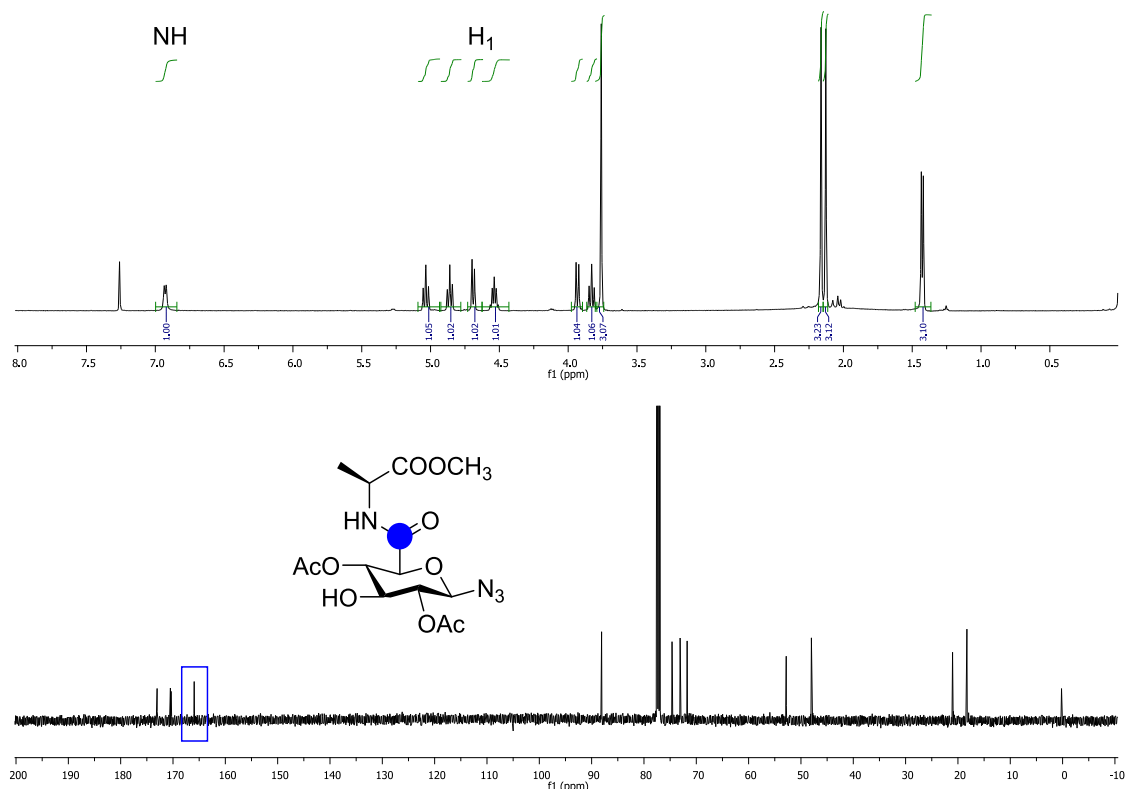
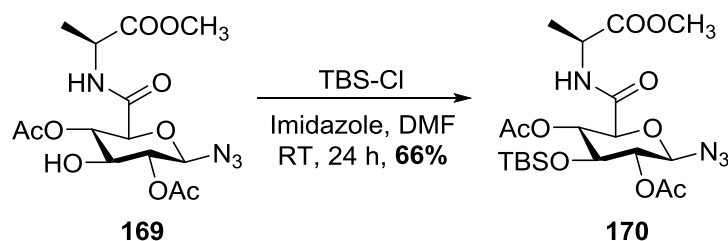


Figure 5.10: ^1H and ^{13}C NMR spectra of the 3-OH glycoconjugate **169**, highlighting the formation of an bond resulting from the nucleophilic ring-opening of **164** by H.Ala.OMe.HCl.

With the synthesis of **169** successfully completed, the 3-OH of **169** was subjected to TBS-protection. Utilizing TBS-Cl (2.0 equivalents) and imidazole (4.0 equivalents), the 3-OTBS glycoconjugate **170** was isolated in 66% yield (Scheme 5.25). Comparably to the previously synthesised 4-OH glycoconjugate **165**, it is likely that the higher yield gained in the production of **170** is a result of the reduced steric hindrance present on the adjacent 2- and 4-positions, with the less-bulky acetyl groups allowing sufficient access to the 3-OH group by the TBS-imidazole reactive intermediate.



Scheme 5.25: Synthesis of the orthogonally-protected glycoconjugate **170**.

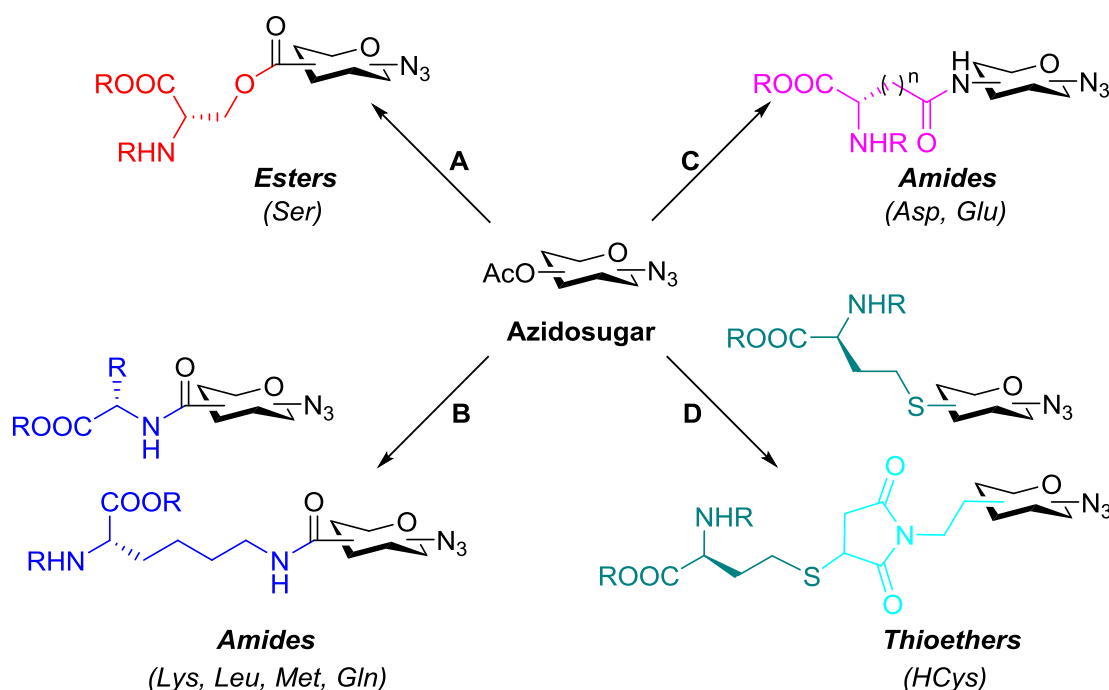
The production of **170** was confirmed by the ^1H NMR spectrum, where the presence of singlets at 0.81 and 0.05 ppm integrating for nine and six protons respectively, were indicative of the *tert*-butyl and methyl protons of the TBS group. Furthermore, these signals correlated to two signals in the ^{13}C NMR spectrum of **170** at -4.6 and -4.9 ppm, both indicative of carbons linked to a silicon atom. A key intermediate in the production of Type B “clickable” glycoconjugates, the synthesis of **170** from glucuronolactone represents a more concise and higher yielding approach to their production (8.5% over 6 steps), compared to the synthesis of **165** from D-glucose (4.4% over 9 steps). Nonetheless, the synthesis of **165** and **170** from D-glucose and glucuronolactone described in this chapter, have laid the foundation for the synthesis and development of Type A and Type B “clickable” neoglycopeptides.

Chapter 6 : Conclusions and Future Directions

6.1 Conclusions

6.1.1 “Clickable” Glycoconjugates

The CuAAC “click” reaction has greatly impacted on the synthesis and development of new bioconjugates.²⁴⁰ Allowing for the rapid and stereoselective production of conjugates based on the 1,4-substituted triazole motif, until recently apart from metabolically incorporated azido sugars, the utilization of this ligation method in the synthesis and functionalization of bioconjugates incorporating carbohydrates has been limited.^{133,136} In the study discussed herein, the scope and variety of glycoconjugates that can be formed between azidosugars and proteinogenic amino acids - and thus can participate in the CuAAC “click” reaction, has been significantly broadened. As a result, a number of glycoconjugates linked via ester (A, Scheme 6.1), amide (B and C, Scheme 6.1) and thioether linkages (D, Scheme 6.1) have been developed and further functionalized using the CuAAC “click” reaction.



Scheme 6.1: The diversity of “clickable” glycoconjugates synthesised from azidosugars, and functionalized using the CuAAC “click” reaction that have been described in the current study.

Building on the successful production of *glc*- and *gal*-sugar azido acids **60** and **65** from uronic acid precursors in Chapter 2, the variety of ester (**66** and **67**), sidechain (**68** and **69**) and α -amide (**70-73**) linked glycosyl azides produced highlighted the versatility of these molecules as scaffolds in the formation of glycoconjugates that can be functionalized using the CuAAC “click” reaction. This point was further demonstrated by the synthesis of the azide-bearing glycopeptide **88** as a key “click” precursor, promoting the use of this strategy in the synthesis and labelling of biologically-relevant peptides.

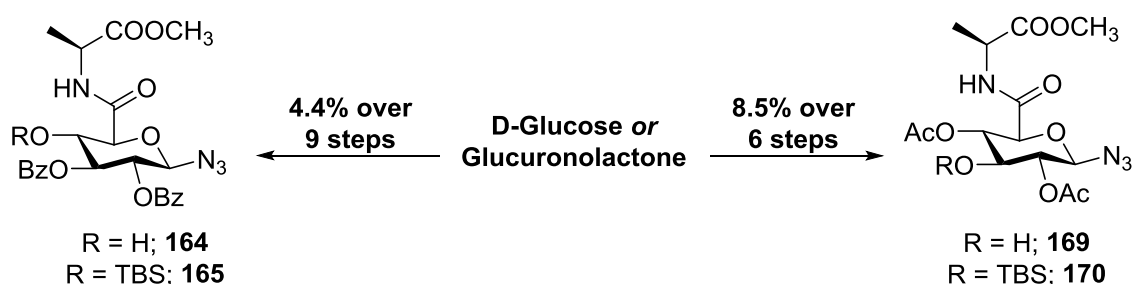
In Chapter 3, the synthesis of “clickable” glycoconjugates linked via the sidechain or α -carboxyl group of an amino acid was investigated, with the conversion of

the azidoglucofuranose derivative **96** to the key intermediate azidoglucosylamine (**102**) achieved. Subsequently, the synthesis of amide-linked glycoconjugates **110** and **111** through the coupling of **102** to the sidechain (Asp, Glu) groups of protected amino acids was also performed, along with their functionalization via the CuAAC “click” reaction. The synthesis and functionalization of **110** and **111** further demonstrated the versatility of azidosugars in forming amide-linked glycoconjugates with amino acids. In doing so, the development of glycoconjugates of this design has broadly extended the scope of this methodology to the formation of glycoconjugates between azidosugars and amino acids or peptides that bear a free sidechain-carboxyl group.

Moving on from amide-linked examples, in chapter 4 the synthesis of thioether-linked “clickable” glycoconjugates was also explored. In doing so, the challenges that exist in the production of thioether-linked conjugates with glycosides were highlighted. The individual reactivity of positions on a pyran-based glycoside (as illustrated in the attempted synthesis of **124**), in addition to issues with stereoselectivity and scalability (**131**), significantly hindered the feasibility of producing glycoconjugates with individual thiol-containing amino acids. To address this issue, the development of the maleimide derivative **135** and the formation of glycoconjugate **136** by the “click” thiol-ene reaction provided a concise method for the synthesis of thioether-linked “clickable” glycoconjugates. Utilizing the *glc*-sugar azido acid **60**, the divergent nature of this synthesis added to the advantages that sugar azido acids possess in the formation of glycoconjugates that can be further derivatized by the CuAAC “click” reaction, endorsing their use in the development of glycoconjugates through the “click” thiol-ene reaction.

6.1.2 Functionalized Neoglycopeptides

In chapter 5, the development of a strategy towards the production of “clickable” neoglycopeptides based on sugar azido acids was also described. The development of an orthogonal protecting group strategy leading to the synthesis of the glycoconjugate **165** was achieved (Scheme 6.2). Starting from D-glucose, an initial methodology utilizing acetal, *p*-methoxybenzyl, trityl and 4-methoxytrityl-protecting groups proved highly atom uneconomical. Revision of this methodology to utilize benzoyl protecting groups and selective TEMPO/BAIB oxidation conditions resulted in the partially protected *glc*-sugar azido acid derivative **164**. Amide coupling followed by TBS protection subsequently yielded the desired orthogonally-protected **165**.



Scheme 6.2: The synthesis of orthogonally-protected glycoconjugates **165** and **170** from simple precursors (D-glucose; **165**, and glucuronolactone; **170**).

Bearing a TBS protecting group at the 4-position, the potential formation of differently-substituted derivatives, in addition to the efficiency of the synthesis of **163** (4.4% over 9 steps) validated the investigation of an alternate method that may lead to the production of Type A and B “clickable” neoglycopeptides. Subsequently, the design and synthesis of the orthogonally-protected glycoconjugate **170** was achieved,

with **170** instead bearing a TBS group at the 3-position of the glycoconjugate (Scheme 6.2, 8.5% over 6 steps). Utilizing glucuronolactone (**51**), the formation of the key glycoconjugate **169** through nucleophilic substitution of a 6,3-lactone (**166**) represents a unique approach to the formation of glycoconjugates, providing a concise, atom economical route to a key intermediate in the production of Type A and B “clickable” neoglycopeptides. The orthogonal protecting group strategies developed for the creation of **165** and **170** provides a mechanism for their further derivatization, which following protecting group manipulation would allow for their functionalization with a plethora of different functional groups.

6.2 Future Directions

6.2.1 Improved Access to Sugar Azido Acids From Protected Derivatives

Key to the synthesis of “clickable” glycoconjugates performed in this study was the use of azidosugars, with sugar azido acids (such as the *glc*-sugar azido acid **60**) shown to be exceedingly versatile in forming a variety of different linkages - directly or indirectly, with proteinogenic amino acids. One obvious drawback though in the production of sugar azido acids of this form is their scalability. This is predominantly a result of the utilization of allyl ester protection, as illustrated by the SAA precursors **59** and **64**. Both requiring Pd(0)-catalyzed de-allylation to produce the *glc* and *gal*-SAA's **60** and **65**, the large quantities of catalyst (10 mol% loading) used in these processes is enough to limit their large scale production purely on economic grounds. However, the

competing reduction of the β -azide present in **60** and **65** by PPh_3 that has leached from the catalyst is a much greater limitation, with the high variability in the quality of $\text{Pd}(\text{PPh}_3)_4$ that may be procured commercially reducing the consistency of yields obtained in the production of sugar azido acids.

Thus, in order to scale up the synthesis of sugar azido acids and make their utility in the development of radiolabelled glycoconjugates more viable, an alternative strategy that doesn't require the use of allyl esters or $\text{Pd}(0)$ catalysis in their production would be required. Considering the ease and scale in which the methyl ester derivative **53** was produced, an approach that used molecules of this form to produce sugar azido acids would be ideal. Generally cleaved under basic conditions akin to acetyl groups, reagents such as trimethyltin(IV) hydroxide have emerged as a mild alternative in the cleavage of methyl esters. This work has been pioneered by Nicolaou and co-workers, proving highly efficient and selective in the cleavage of methyl esters in the presence of acetyl groups.²⁴¹ The development of such a strategy would have far reaching implications beyond the scope of our studies, generally improving accessibility to uronic acids for use in the development of biologically active molecules.

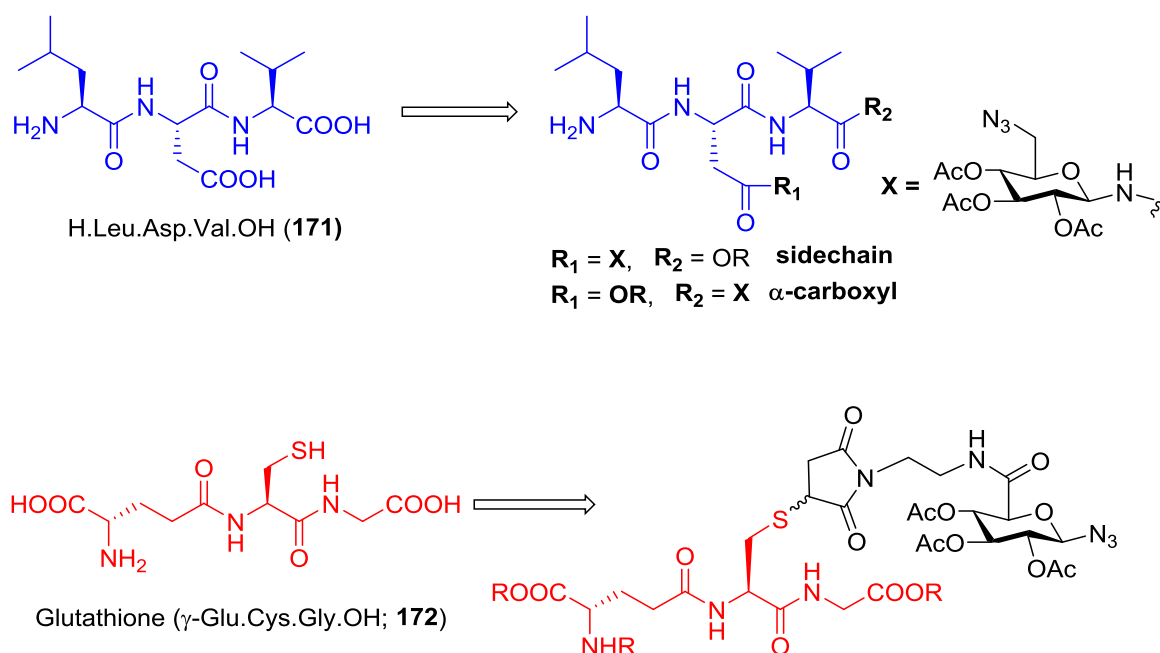
6.2.2 Extension of the Synthesis of “Clickable” Glycoconjugates to Carboxyl and Thiol-containing Peptides

In chapter 2, the synthesis of the neoglycopeptide **88** represented a key milestone in the development of glycoconjugates that may be derivatized by the CuAAC “click” reaction for the development of radiolabelled glycoconjugates.

Following on from the synthesis and functionalization of “clickable” glycoconjugates **66-73**, the production of **88** provided a substrate for the porting of this method to small, biologically-active peptides. The further functionalization of **88** to form **89** would illustrate the power of the CuAAC “click” reaction in the further derivatization of glycopeptides. In chapters 3 and 4, the formation of “clickable” glycoconjugates bearing thiol or carboxyl-containing amino acids was also achieved. In comparison though, the formation of glycoconjugates through these linkages was not extended to thiol or carboxyl-containing peptides. In order to validate the use of the CuAAC “click” reaction in the synthesis and labelling of glycoconjugates formed through these linkages, the methods developed in this project should be extended to peptides bearing these functional groups. Comparable to Ac.KPV.NH₂ utilized in chapter 2, the synthesis of “clickable” glycoconjugates linked to small biologically-active tripeptides via an amide or thioether linkages would provide a good platform for the further utilization of conjugates linked in this manner.

For amide-linked glycopeptides, the tripeptide motif LDV (H-Leu-Asp-Val-OH, **171**) represents a great example of a small peptide that could be utilized for this function. Commonly known as the Fibronectin Adhesion Motif, LDV motifs form key interactions with the $\alpha_4\beta_1$ integrin, which has clinical implications in the promotion of tumour cell migration, invasion and metastasis.^{100,242,243} In addition to its biological relevance, the LDV motif bears both sidechain and terminal carboxyl groups, which through protecting group manipulation could be used to highlight the formation of “clickable” glycopeptides linked via either carboxyl group (Scheme 6.3). Additionally, the previously discussed thiol-containing peptide reduced-glutathione (**172**) would be ideally suited in validating the synthesis of “clickable” thioether-linked glycopeptides.

This is a result of its widespread use as model thiol-containing peptide in bioconjugate chemistry – particular when used in tandem with the “click” thiol-ene reaction, in addition to its important roles as an antioxidant in biological systems.²⁴⁴



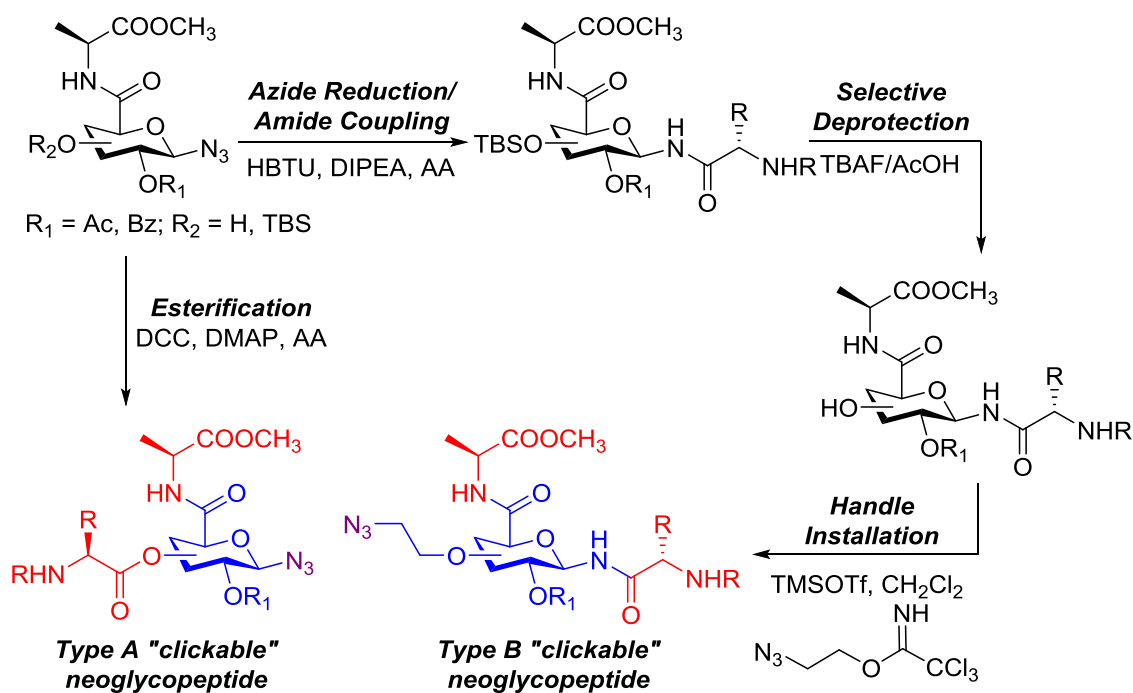
Scheme 6.3: The tripeptides Fibronectin Binding Motif (LDV; 171) and reduced-Glutathione (172), potential model peptides in the synthesis of amide and thioether-linked “clickable” glycopeptides.

6.2.3 Synthesis of “Clickable” Neoglycopeptides

In chapter 5, the successful development of orthogonally-protected glycoconjugates **165** and **170** was described. Bearing TBS protecting groups at the 3- and 4-positions, the basis for their production was to broaden the utility of sugar azido acids as molecular scaffolds in the synthesis of neoglycoconjugates. Considering that the general theme of this project was to develop glycoconjugates that were

amenable to the CuAAC “click” reaction, it seems appropriate that this ligation method could be applied to the functionalization of these neoglycopeptides formed from these precursors.

If the 4- and 3-OH bearing derivatives **164** and **169** were subject to standard DCC/DMAP-mediated esterification, this would produce derivatives joined via an ester linkage (Scheme 6.4). As Type A “clickable” neoglycopeptides, these derivatives could then be further derivatized using the CuAAC “click” reaction. Alternatively, the 4- and 3-OTBS derivatives **165** and **170** could be subjected to tandem azide reduction/amide coupling, to produce neoglycopeptides linked at the position (Scheme 6.4). The TBS groups of these derivatives are susceptible to selective cleavage by nucleophilic fluoride donors such as tetrabutylammonium fluoride (TBAF), which would unmask a free alcohol that could be derivatized (Scheme 6.4). Employing trichloroacetimidate chemistry akin to that used in the production of **128**, azide-containing handles could be readily introduced, producing Type B “clickable” neoglycopeptides (Scheme 6.4). The utilization of this methodology would also allow for the functionalization of neoglycopeptides with a variety of different groups bearing a trichloroacetimidate, additional glycosides (such as **127**). This could subsequently be ported to the development of a wider range of functionalized neoglycopeptides.



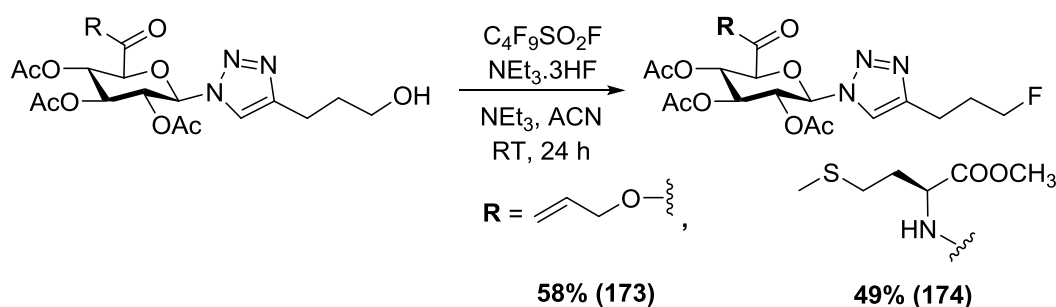
Scheme 6.4: Proposed synthetic strategy for the synthesis of Type A and B "clickable" neoglycopeptides from 164 and 169.

6.2.4 Development and Synthesis of Radiolabelled Glycoconjugates Using the CuAAC "Click" Reaction

With the development of "clickable" glycoconjugates achieved, the next step would be to examine this approach in the synthesis of radiolabelled glycoconjugate-based molecular probes. In line with previous studies,¹³⁷ a strategy utilizing fluorine-18 as a radiolabel would represent the most viable approach to producing radiolabelled glycoconjugates. Such probes would be generated by the CuAAC "click" reaction of glycoconjugates to fluorine-18 containing species, with the subsequent purification of

these probes occurring prior to injection. This would limit the possibility of copper toxicity, a problem encountered in *in vivo* CuAAC “click” imaging approaches such as live or whole cell imaging.

Such derivatives would require cold standards, analogues of the radiolabelled compound containing fluorine-19, that provide a comparison for the radiolabelled derivative during purification.⁸⁴ During our investigation into the production of “clickable” glycoconjugates based on the *glc*-sugar azido acid **60**, the synthesis of fluorinated derivatives for the purpose of producing cold standards was explored. Using the methodology of Yin and co-workers,²⁴⁵ the fluorinated glycoconjugates **173** and **174** were produced from the allyl ester **59**, and the methionine derivative **72** in 58% and 49% yields, respectively (Scheme 6.5). These examples confirm the viability of fluorinated glycoconjugates of this form, validating the development of different [¹⁸F]-radiolabelled glycoconjugates using the CuAAC “click” reaction.



Scheme 6.5: Synthesis of fluorinated glycoconjugates **173** and **174**.

In order to utilize this strategy in the development of radiolabelled glycoconjugates, the synthesized analogues must target biological function up-regulated in malignancies. Targets that may be suitable for this strategy include amino acid

transporters such as the neutral large amino acid transporter LAT-1 and the neutral small amino acid transporter ASCT-2.^{246,247} Key mediators of kinase signalling pathways such as PI3K, PKB and mTOR, these amino acid transporters coordinate cellular growth, metabolism and proliferation, and have been found to be up-regulated in metastases such as glioblastoma and non-small cell lung cancer (LAT-1).²⁴⁸ Previously evaluated using radiolabelled derivatives of methionine^{171,178} and glutamine,¹⁷⁵ the development of carbohydrate-containing derivatives of these analogues (such as **72**, **73**, **111** & **131**) would probe both the effect of glycosylation on uptake of these amino acids, in addition to the pharmacokinetics of their excretion.

In addition, the small scale nature of these conjugates would allow for the fine-tuning of radiofluorination conditions. This would subsequently allow for the extension of this methodology to more complex systems, including the formation of [¹⁸F]-radiolabelled glycoconjugates with peptides currently used in the evaluation of metastasis. These include those containing the RGD tripeptide motif targeting angiogenesis, those linked to the somatostatin analogue octreotide targeting neuroendocrine tumours, and full derivatives of α -MSH targeting melanoma. Herein, the foundation for the incorporation and utilization of azidosugars into a variety of peptides and other biomolecules has been laid. There is great scope for future work in this area, as azidosugars can be incorporated into a wide range of molecules (e.g. amino acids, peptides, proteins and lipids), and functionalised with a variety of different groups (e.g. with fluorophores, radiolabels).

Chapter 7 : Experimental

7.1 Chemical Procedures

7.1.1 General Experimental

All reactions were performed in standard glassware, acetone washed and oven dried prior to use. Solvents and reagents used were purchased from Sigma Aldrich Chemical Company (St Louis, MO, USA), Ajax Fine Chemicals (Taren Point, NSW), Thermofisher Scientific (Waltham, MA, USA), Acros (Geel, Belgium), Alfa Aesar (Ward Hill, MA, USA), Carbosynth (Berkshire, UK) or Bachem (Bubendorf, Switzerland), and used as supplied. All solvents used were of analytical reagent (AR) grade or higher except for Hexane which was of LR grade, and was distilled for purity prior to use. The term petroleum spirit specifically refers to the solvent of the same name with a boiling point range of 40-60°C. The removal of large quantities of solvent *in vacuo* was carried out using Buchi and Heidolph rotary evaporators, at temperatures ranging from 35-65°C. When required, removal of trace quantities of solvent and drying *in vacuo* were performed using a CustomBlown Glassware high-vacuum manifold (Sydney, Australia), equipped with a JAVAC high vacuum pump.

Sonication of reaction mixtures and solutions was performed using a Soniclean 250HT ultrasonic bath (Thebarton, Victoria). Celite (Celite 545, particle size 0.02-0.1 mm, Merck, Germany) was used to filter out metal catalysts from reaction mixtures.

4Å molecular sieves (Sigma Aldrich) were used to dry reaction solvents, and Amberlite IR-120 or Dowex 50W cationic exchange resins (Sigma Aldrich) were utilized to neutralize basic aqueous solutions. All reactions were performed under an atmosphere of N₂ or argon where possible. In particularly sensitive dry/inert reaction conditions, acetonitrile, CH₂Cl₂ and DMF used were supplied as pre-dried reagents. All melting points were acquired using a Reichert and Buchi melting point apparatus, standardised with (3,4-dimethoxyphenyl)acetic acid. All temperatures are recorded in °C, and are reported uncorrected.

7.1.2 Chromatography

All thin layer chromatography (TLC) was performed using Merck Silica Gel 60 F₂₅₄ aluminium backed plates. In general, all TLC plates used were stained to enhance visualization using either vanillin, potassium permanganate, cerium molybdate or ninhydrin dips. For those bearing aromatic substituents, fluorescence was detected by exposure to ultraviolet (UV) light at a wavelength of (λ) 254 nm. Flash column chromatography was performed using Davisil™ Silica Gel 60 (40-63 µm mesh) under air pressure. All eluents used for chromatographic purposes are indicated, with solvent proportions used given in volume: volume (v: v) ratios.

7.1.3 Nuclear Magnetic Resonance (NMR) Spectroscopy

Nuclear magnetic resonance (NMR) spectra for all samples were acquired on a Varian VNMRs PS54 500 MHz spectrometer, with proton (¹H) for all samples, and

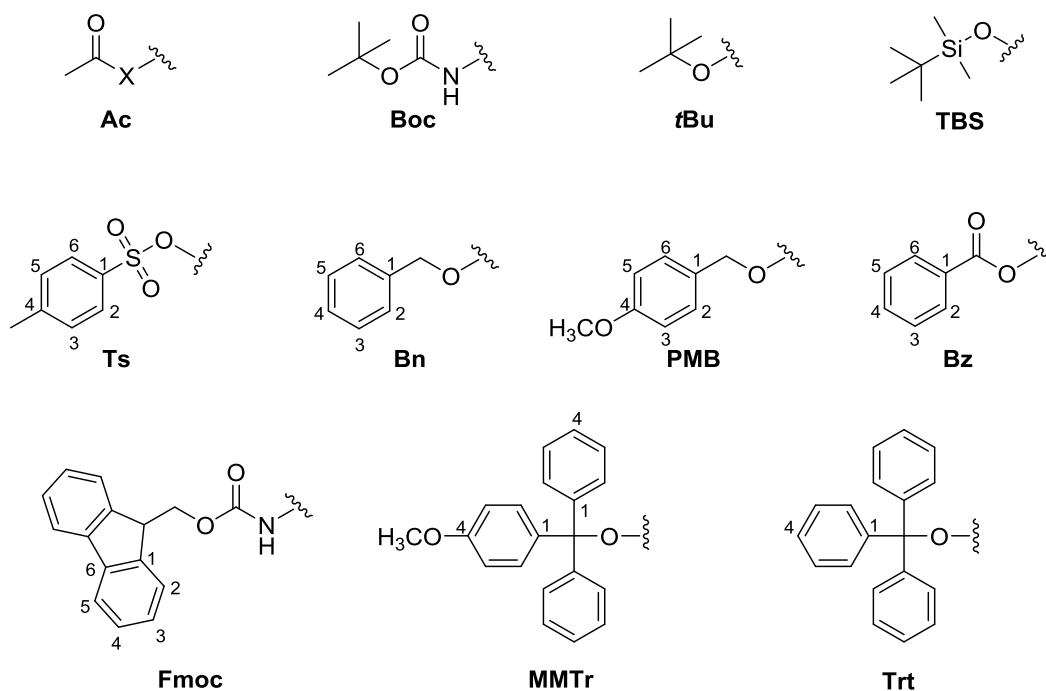
carbon (^{13}C) spectra for novel samples obtained at 500 MHz and 125 MHz, respectively. All spectra were obtained using a 5 mm PFG AutoX DB probe, at an operating temperature of 25.0 °C. Unless specifically stated, all samples subjected to NMR spectroscopy were dissolved in deuterated solvents, including chloroform (CDCl_3), methanol (CD_3OD), dimethylsulfoxide (d_6 -DMSO), acetonitrile (CD_3CN) or water (D_2O). Each provided internal references in ^1H and ^{13}C NMR spectra at δ 7.26 ppm and 77.0 ppm (CDCl_3), 3.31 ppm and 49.00 ppm (CD_3OD), 3.50 ppm and 39.52 ppm (d_6 -DMSO) 1.94 and 1.32 ppm (CD_3CN) and 4.79 ppm (D_2O , ^1H only), respectively. Chemical shifts of peaks in NMR spectra are expressed in ppm with peak multiplicities reported as either singlets (s), doublets (d), triplets (t) or multiplets (m). Spectral data are assigned in the following format; ($^1\text{H}/^{13}\text{C}$ NMR) (δ ppm) (m, iH, cc Hz, a) where m = multiplicity, i = integration, cc = coupling constant and a = assignment. All ^1H and ^{13}C NMR spectral assignments were assigned based on a combination of comparisons with literature data, 2D NMR spectral data, and using computer-aided identification methods.

7.1.4 Mass Spectrometry

Electrospray ionisation (ESI) mass spectra were obtained using both a Micromass Platform LCZ spectrometer and a Shimadzu Tandem LCMS-2010 liquid chromatograph mass spectrometer. For the majority of samples, High Resolution Electrospray Ionisation Mass Spectra (HRESI-MS) were performed on a Waters XEVO G2 Quadrupole Time-Of-Flight (Q-TOF) mass spectrometer, with leucine enkephalin (LeuEnk) used as an internal standard.

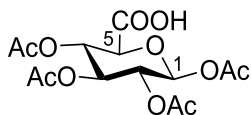
7.1.5 Chemical and Spectral Illustrations/Calculations

All figures, schemes and tables were drawn using ChemBioDraw Ultra versions 10.0-13.0 (CambridgeSoft/PerkinElmer, Waltham, MA, USA). All representations of 1D ^1H and ^{13}C NMR spectra, and 2D gCOSY/NOESY experiments were analysed and displayed using either MestReNova NMR Lite (Santiago, Chile) or ACD NMR Labs 12.00 (Toronto, Canada). All heat of formation ΔH_f calculations were performed using ChemBio3D Ultra 11.00 (PerkinElmer) using the AM1 (semi-empirical) level of theory. The following non-IUPAC structural abbreviations were used in the illustration of synthesised compounds:

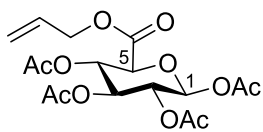


7.2 Chapter 2 Experimental Data:

1,2,3,4-tetra-*O*-acetyl- β -D-glucuronic acid (**56**)



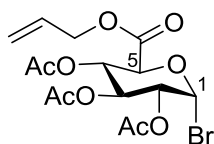
According to the method of Bergeon *et al.*,¹⁶⁰ a round bottom flask containing D-glucuronic acid (**55**, 3.01 g, 15.50 mmol) was added acetic anhydride (50 mL), and the resulting suspension was chilled to 0°C. Solid I₂ (0.215 g, 0.847 mmol) was added portionwise to the mixture, which was then allowed to stir at 0°C for 2 hours before being allowed to gradually warm to room temperature. After 5 hours, the reaction mixture was cooled back to 0°C, and dry MeOH (20 mL) was added dropwise to the solution, and allowed to stir overnight. The crude reaction mixture was then evaporated to dryness, resuspended in CH₂Cl₂ (50 mL) and washed sequentially with 0.1 M Na₂S₃O₃ solution (2 x 20 mL) and brine (20 mL). The organic phases were combined, dried and evaporated, before recrystallization from Hexane/EtOAc yielded **56** as a white solid. (3.70 g, 58%), M.p. 153-155°C (lit. 154-155°C)²⁴⁹ **¹H NMR** (500 MHz, CDCl₃) δ 5.79 (d, 1H, *J* = 7.6 Hz, H1), 5.29 (m, 2H, H3/H4), 5.13 (m, 1H, H2), 4.24 (m, 1H, H5), 2.11-2.02 (4s, 12H, CH₃, 4 x OAc). **¹³C NMR** (CDCl₃, 125 MHz): 170.2 (C=O, OAc), 169.9 (C=O, OAc), 169.5 (C=O, OAc), 169.1 (C=O, OAc), 91.5 (C1), 72.7 (C5), 72.1 (C4), 70.4 (C3), 68.9 (C2), 20.9 (CH₃, OAc), 20.7 (CH₃, OAc), 20.6 (CH₃, OAc), 20.6 (CH₃, OAc). **LRMS (ESI):** *m/z* 361 [M - H]⁻, **HRMS (ESI):** *m/z* calculated for C₁₄H₁₇O₁₁ [M - H]⁻: 361.0771; Found 361.0774.

1,2,3,4-Tetra-*O*-acetyl- β -D-glucuronic acid allyl ester (57)

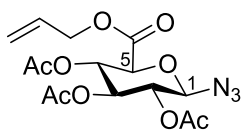
According to the method of Tosin *et al.*,¹⁵⁷ a solution of **56** (4.65 g, 12.84 mmol) dissolved in dry CH₂Cl₂ (120 mL) was chilled to 0°C. Under an argon atmosphere, oxalyl chloride (1.2 mL, 1.68 g, 13.23 mmol) and DMF (0.60 mL) were added, and the reaction mixture was allowed to stir at 0°C for 30 minutes, before being allowed to warm to room temperature. After 2 hours, the reaction mixture was cooled back down to 0°C, and in a separate dry round bottom flask, a solution of allyl alcohol (1.00 mL, 0.854 g, 14.70 mmol), pyridine (3 mL) and CH₂Cl₂ (20 mL) stirring in the presence of 4Å molecular sieves was prepared. The solution containing the alcohol and pyridine was added dropwise to the reaction mixture, and allowed to stir at 0°C for 30 minutes before being warmed to room temperature. After a further 3 hours, the reaction mixture was diluted with CH₂Cl₂, before being quenched with sat. NaHCO₃ solution (100 mL). The organic phases were washed with cold 0.1 M HCl (100 mL) and brine (50 mL), before being dried and evaporated. The resultant milky residue was triturated with petroleum spirit and left in the freezer overnight, to produce **57** as a waxy white solid. (4.81 g, 93%), M.p. 97-99°C (lit. 95-97°C)¹⁵⁷ R_f 0.77 (1:1 Hexane:EtOAc.). ¹H NMR (500 MHz, CDCl₃) δ 5.89 (m, 1H, CH₂-CH=CH₂), 5.79 (d, 1H, *J* = 7.7 Hz, H1), 5.37 - 5.26 (m, 4H, CH₂-CH=CH₂, H3 and H4), 5.15 (dd, 1H, *J* = 8.7 Hz, H2), 4.61 (m, 2H, CH₂-CH=CH₂), 4.20 (d, 1H, *J* = 9.4 Hz, H5), 2.12-2.02 (4s, 12H, CH₃, 4 x OAc). ¹³C NMR (125 MHz, CDCl₃) δ 170.1 (C=O, OAc), 170.0 (C=O, OAc), 169.5 (C=O, OAc), 169.1 (C=O, OAc), 166.3 (C=O), 131.2 (CH₂-CH=CH₂), 119.8 (CH₂-CH=CH₂), 91.6 (C1), 73.2 (C5), 72.1 (C4), 70.4 (C2), 69.1 (C3), 67.0 (CH₂-CH=CH₂), 21.0 (CH₃, OAc), 20.7 (CH₃, OAc), 20.7 (CH₃, OAc), 20.6 (CH₃, OAc). LRMS (ESI): *m/z* 425

$[M + Na]^+$ **HRMS (ESI):** m/z calculated for $C_{17}H_{22}O_{11}Na$ $[M + Na]^+$: 425.1060;
Found 425.1050.

1-Bromo-2,3,4-tri-*O*-acetyl- α -D-glucuronic acid, allyl ester (**58**)



A solution of **57** (0.531 g, 1.33 mmol) dissolved in dry CH_2Cl_2 (2 mL) was chilled to $0^\circ C$. 33% w/v HBr in AcOH (4 mL) was added dropwise to the solution, and upon addition the reaction mixture was allowed to gradually warm to room temperature under constant stirring. After 3 hours, the reaction mixture was diluted with CH_2Cl_2 (10 mL), and washed with H_2O (5 mL), ice cold sat. $NaHCO_3$ solution (5 mL) and brine (5 mL). The organic phases were then dried and evaporated, producing **58** as an orange oil that was used without further purification. (0.355 g, 67%), R_f 0.24 (3:1 Hexane:EtOAc). **1H NMR** (500 MHz, $CDCl_3$) δ 6.65 (d, 1H, $J = 4.1$ Hz, H1), 5.91 (m, 1H, $CH_2-\underline{CH}=\underline{CH}_2$), 5.61 (1H, t, $J = 9.9$ Hz, H3), 5.35 (m, 2H, $CH_2-\underline{CH}=\underline{CH}_2$), 5.24 (t, 1H $J = 10.1$ Hz, H4), 4.86 (dd, 1H, $J = 10.0$ Hz, 4.1 Hz, H2), 4.62 (m, 3H, $\underline{CH}_2-\underline{CH}=\underline{CH}_2/H5$), 2.12-2.01 (3s, 9H, CH_3 , 3 x OAc). **^{13}C NMR** ($CDCl_3$, 125 MHz): δ 169.7 (C=O, OAc), 169.6 (C=O, OAc), 169.2 (C=O, OAc), 166.0 (C=O), 130.8 ($CH_2-\underline{CH}=\underline{CH}_2$), 119.9 ($CH_2-\underline{CH}=\underline{CH}_2$), 85.4 (C1), 72.1 (C5), 70.3 (C4), 69.3 (C3), 68.5 (C2), 67.0 ($\underline{CH}_2-\underline{CH}=\underline{CH}_2$), 20.6 (CH_3 , OAc), 20.6 (CH_3 , OAc), 20.5 (CH_3 , OAc). **LRMS (ESI):** m/z 423; 425 $[M + H]^+ Br^{79}; Br^{81}$

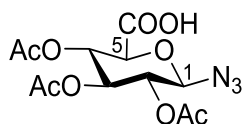
1-Azido-2,3,4-tri-*O*-acetyl- β -D-glucuronic acid, allyl ester (59)

Method A: **58** (0.355 g, 0.85 mmol) was dissolved in dry DMF (3 mL), and the solution was cooled to 0°C. NaN₃ (0.250 g, 3.84 mmol) was added portion wise to the mixture, and allowed to stir at 0°C for 30 minutes, after which it was allowed to warm to room temperature. After 3 hours, the reaction mixture was diluted with H₂O (5 mL), with the aqueous phase extracted with EtOAc (3 x 25 mL). The organic phases were dried and evaporated, with recrystallization from EtOAc/Hexanes producing **59** as a fluffy white solid. (0.223 g, 68%)

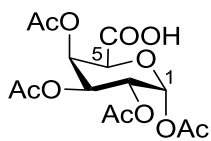
Method B: According to the method of Tosin *et al*¹⁵⁷ **57** (4.00 g, 9.95 mmol) was dissolved in dry CH₂Cl₂ (100 mL) under an atmosphere of argon. TMS-N₃ (3.30 mL, 2.89 g, 25.09 mmol) was added, and the resultant mixture was cooled to 0°C. SnCl₄ (0.60 mL, 1.34 g, 5.14 mmol) was added slowly to the cooled mixture and allowed to stir at 0°C for 15 minutes, after which the mixture was warmed to room temperature. After 4 hours, the mixture reaction mixture was diluted with CH₂Cl₂ (50 mL), and extracted with sat. NaHCO₃ solution (2 x 50 mL) and brine (50 mL). The organic phase was dried and evaporated, with recrystallization from EtOAc/Hexanes yielding **59** as a fluffy white solid. (2.43 g, 63%), M.p. 132-133°C, R_f 0.81 (1:1 Hexane:EtOAc). ¹H NMR (500 MHz, CDCl₃) δ 5.91 (m, 1H, CH₂-CH=CH₂), 5.36-5.26 (m, 4H, CH₂-CH=CH₂/ H3/H4), 4.97 (m, 1H, *J* = 9.5 Hz, 8.6 Hz, H2), 4.71 (d, 1H, H1), 4.63 (m, 2H, CH₂-CH=CH₂), 4.14 (d, 1H, *J* = 9.8 Hz, H5), 2.08-2.01 (3s, 9H, CH₃, 3 x OAc). ¹³C NMR (CDCl₃, 125 MHz): 170.2 (C=O, OAc), 169.4 (C=O, OAc), 169.3 (C=O, OAc), 166.1 (C=O), 131.2 (CH₂-CH=CH₂), 119.9 (CH₂-CH=CH₂), 88.3 (C1), 74.6 (C5), 72.2 (C4), 70.7 (C2), 69.3 (C3), 67.0 (CH₂-CH=CH₂), 20.7 (CH₃, OAc), 20.7

(CH₃, OAc), 20.6 (CH₃, OAc). **LRMS (ESI):** m/z 408 [M + Na]⁺ **HRMS (ESI):** m/z calculated for C₁₅H₁₉N₃O₉Na [M + Na]⁺: 408.1019; Found 408.1039.

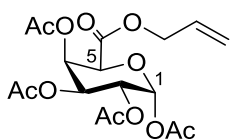
1-Azido-2,3,4-tri-*O*-acetyl-β-D-glucuronic acid (**60**)



According to the method of Tosin *et al.*¹⁵⁷ **59** (0.510 g, 1.33 mmol) was dissolved in dry ACN (7 mL), and the reaction mixture was cooled to 0°C. To this solution, Pd(PPh₃)₄ (0.155 g, 0.132 mmol) was added, and the mixture was immersed in an atmosphere of argon. Pyrrolidine (0.12 mL, 1.34 mmol) was then added dropwise, and the reaction mixture was allowed to warm gradually to room temperature. After 1 hour, the reaction mixture was filtered through Celite, with the filtrate evaporated to dryness. The residue was re-dissolved in EtOAc (20 mL), before extraction with H₂O (2 x 20 mL). The aqueous phase was collected and acidified to pH 2 using Amberlite IR-120 resin, and subsequently extracted with EtOAc (3 x 40 mL). The organic phase was dried and evaporated, with the residue allowed to sit under high vacuum overnight, producing **60** as a yellow foam. (0.303 g, 66%), **¹H NMR** 500 MHz, CD₃OD) δ 5.36 (t, 1H, J = 9.4 Hz, H3), 5.19 (t, 1H, H4), 5.02 (d, 1H, J = 8.8 Hz, H1), 4.91 (t, 1H, J = 9.3 Hz, H2), 4.33 (d, 1H, J = 10.0 Hz, H5), 2.07-2.01 (3s, 9H, CH₃, 3 x OAc). **¹³C NMR** (CDCl₃, 125 MHz): 173.2 (C=O, COOH), 172.5 (C=O, OAc), 172.4 (C=O, OAc), 172.4 (C=O, OAc), 87.5 (C1), 74.7 (C5), 72.9 (C4), 71.2 (C2), 69.9 (C3), 20.3 (CH₃, OAc), 20.3 (CH₃, OAc), 20.2 (CH₃, OAc). **LRMS (ESI):** m/z 344 [M - H]⁻ **HRMS (ESI):** m/z calculated for C₁₂H₁₄N₃O₉ [M - H]⁻: 344.0730; Found 344.0746.

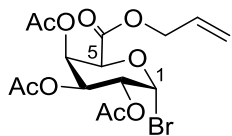
1,2,3,4-Tetra-*O*-acetyl- α -D-galacturonic acid (61)

According to the method of Vogel *et al.*,¹⁶³ a round bottom flask containing D-galactouronic acid (4.032 g, 19 mmol) was added acetic anhydride (25 mL), and the resulting suspension was chilled to 0°C. 70% perchloric acid (0.20 mL) was added dropwise over a 5 minute period, with the mixture allowed to gradually come to room temperature over a 30 minute period. After stirring at room temperature for 3 hours, the reaction mixture was cooled back to 0°C, and dry MeOH (6 mL) was added dropwise to the solution. The reaction mixture was the diluted with H₂O (20 mL), and subsequently extracted with CHCl₃ (3 x 50 mL). The organic phases were dried (MgSO₄), filtered and evaporated to dryness, producing a white residue which following recrystallization with EtOAc/Heptane produced **61** as a white solid. (2.46 g, 35%), M.p (103-105 °C) ¹H NMR (500 MHz, CDCl₃) δ 6.47 (d, 1H, *J* = 2.9 Hz, H1), 5.84 (t, 1H, H4), 5.38 (t, 1H, *J* = 2.8 Hz, H3), 5.33 (dd, 1H, *J* = 9.5 Hz, 11.0 Hz, H2), 4.76 (d, 1H, *J* = 1.5 Hz, H5), 2.15-1.99 (4s, 12H, CH₃, 4 x OAc). ¹³C NMR (CDCl₃, 125 MHz): 170.4 (C=O, OAc), 170.2 (C=O, OAc), 170.1 (C=O, OAc), 169.1 (C=O, OAc), 168.6 (C=O), 89.5 (C1), 70.5 (C5), 68.7 (C4), 67.3 (C3), 66.2 (C2), 20.8 (CH₃, OAc), 20.8 (CH₃, OAc), 20.7 (CH₃, OAc), 20.6 (CH₃, OAc). LRMS (ESI): *m/z* 361 [M – H][–] HRMS (ESI): *m/z* calculated for C₁₄H₁₇O₁₁ [M – H][–]: 361.0771; Found 361.0778.

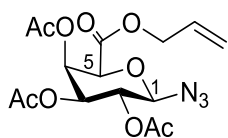
1,2,3,4-Tetra-*O*-acetyl- α -D-galacturonic acid, allyl ester (62)

A solution of **61** (4.65 g, 12.84 mmol) dissolved in dry CH₂Cl₂ (120 mL) was chilled to 0°C. Under an argon atmosphere, oxalyl

chloride (1.2 mL, 1.68 g, 13.23 mmol) and DMF (0.60 mL) were added, and the reaction mixture was allowed to stir at 0°C for 30 minutes, before being allowed to warm to room temperature. After 2 hours, the reaction mixture was cooled back down to 0°C, and in a separate dry round bottom flask, a solution of allyl alcohol (1.00 mL, 0.854 g, 14.70 mmol), pyridine (3 mL) and CH₂Cl₂ (20 mL) stirring in the presence of 4Å molecular sieves was prepared. The solution containing the alcohol and pyridine was added dropwise to the reaction mixture, and allowed to stir at 0°C for 30 minutes before being warmed to room temperature. After a further 3 hours, the reaction mixture was diluted with CH₂Cl₂, before being quenched with sat. NaHCO₃ solution (100 mL). The organic phases were washed with cold 0.1 M HCl (100 mL) and brine (50 mL), before being dried and evaporated. The resultant milky residue was triturated with petroleum spirit and left in the freezer overnight, to produce the novel **62** as an off-white solid. (4.38 g, 85%), M.p. 82-85°C R_f 0.80 (1:1 Hexane:EtOAc). ¹H NMR (500 MHz, CDCl₃) δ 6.41 (d, 1H, *J* = 2.4 Hz, H1), 5.75 (m, 2H, CH₂-CH=CH₂/H4), 5.28 (m, 2H, H2/H3), 5.19 (dd, 2H, *J* = 10.3 Hz, 17.1 Hz, CH₂-CH=CH₂), 4.70 (m, 1H, H5), 4.56 (m, 2H, CH₂-CH=CH₂), 2.07-1.91 (4s, 12H, CH₃, 4 x OAc). ¹³C NMR (125 MHz, CDCl₃) δ 170.1 (C=O, OAc), 169.8 (C=O, OAc), 169.8 (C=O, OAc), 168.8 (C=O, OAc), 165.9 (C=O), 132.1 (CH₂-CH=CH₂), 120.0 (CH₂-CH=CH₂), 89.8 (C-1), 70.9 (C-5), 68.8 (C4), 67.2 (C3), 66.7 (C2), 66.0 (CH₂-CH=CH₂), 20.4 (CH₃, OAc), 20.2 (CH₃, OAc), 20.1 (CH₃, OAc), 20.1 (CH₃, OAc). LRMS (ESI): *m/z* 425 [M + Na]⁺ HRMS (ESI): *m/z* calculated for C₁₇H₂₂O₁₁Na [M + Na]⁺: 425.1060; Found 425.1063.

1-Bromo-2,3,4-tri-*O*-acetyl- α -D-galacturonic acid, allyl ester (63)

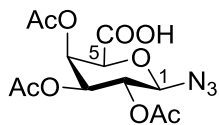
A solution of **62** (2.113 g, 5.24 mmol) dissolved in dry CH₂Cl₂ (6 mL) was chilled to 0°C. 33% w/v HBr in AcOH (14 mL) was added dropwise to the solution, and upon addition the reaction mixture was allowed to gradually warm to room temperature under constant stirring. After 3 hours, the reaction mixture was diluted with CH₂Cl₂ (50 mL), and washed with H₂O (50 mL), ice cold sat. NaHCO₃ solution (50 mL) and brine (50 mL). The organic phases were then dried and evaporated, producing **63** as an orange oil that was used without further purification (1.494 g, 66%), R_f 0.21 (3:1 Hexane:EtOAc). ¹H NMR (500 MHz, CDCl₃) δ 6.78 (d, 1H, *J* = 3.3 Hz, H1), 5.86 (m, 2H, CH₂-CH=CH₂/H4), 5.46 (dd, 1H, *J* = 3.0 Hz, 9.5 Hz, H3), 5.32 (dd, 2H, *J* = 10.2 Hz, 17.3 Hz, CH₂-CH=CH₂), 5.11 (dd, 1H, *J* = 2.9 Hz, 9.5 Hz, H2), 4.90 (m, 1H, H5), 4.65 (m, 2H, CH₂-CH=CH₂), 2.14-2.01 (3s, 9H, CH₃, 3 x OAc). ¹³C NMR (125 MHz, CDCl₃) δ 170.1 (C=O, OAc), 169.9 (C=O, OAc), 169.6 (C=O, OAc), 165.2 (C=O), 130.9 (CH₂-CH=CH₂), 120.3 (CH₂-CH=CH₂), 87.4 (C1), 72.6 (C5), 68.1 (C4), 67.8 (C3), 67.3 (C2), 66.8 (CH₂-CH=CH₂), 20.8 (CH₃, OAc), 20.7 (CH₃, OAc), 20.6 (CH₃, OAc). LRMS (ESI): *m/z* 423; 425 [M + H]⁺Br⁷⁹; Br⁸¹

1-Azido-2,3,4-tri-*O*-acetyl-β-D-galacturonic acid, allyl ester (64)

Method A: **62** (1.00 g, 2.48 mmol) was dissolved in dry CH₂Cl₂ (30 mL) under an atmosphere of argon. TMS-N₃ (0.83 mL, 0.727 g, 6.31 mmol) was added, and the resultant mixture was cooled to 0°C. SnCl₄ (0.15 mL, 0.335 g, 1.29 mmol) was added slowly to the cooled

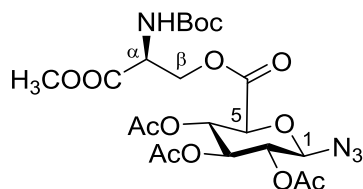
mixture and allowed to stir at 0°C for 15 minutes, after which the mixture was warmed to room temperature. After 20 hours, the mixture reaction mixture was diluted with CH₂Cl₂ (20 mL), and extracted with sat. NaHCO₃ solution (2 x 20 mL) and brine (20 mL). The organic phases were combined, dried and evaporated, with recrystallization from EtOAc/Hexanes yielding **64** as an off-white solid. (0.274 g, 29%)

Method B: **63** (1.494 g, 3.54 mmol) was dissolved in dry DMF (10 mL), and the solution was cooled to 0°C. NaN₃ (1.036 g, 15.98 mmol) was added portion wise to the mixture, and allowed to stir at 0°C for 30 minutes, after which it was allowed to warm to room temperature. After 3 hours, the reaction mixture was diluted with H₂O (10 mL), with the aqueous phase extracted with EtOAc (3 x 50 mL). The organic phases were dried and evaporated, with recrystallization from EtOAc/Hexanes producing **64** as an off-white solid. (1.006 g, 70%), M.p. 113-114°C R_f 0.84 (1:1 Hexane:EtOAc). ¹H NMR (500 MHz, CDCl₃) δ 5.87 (m, 1H, CH₂-CH=CH₂), 5.76 (m, 1H, H₄), 5.32 (dd, 2H, *J* = 10.4 Hz, 17.1 Hz, CH₂-CH=CH₂), 5.18 (t, 1H, *J* = 9.0 Hz, H₂), 5.10 (m, 1H, H₃), 4.68-4.64 (m, 3H, CH₂-CH=CH₂/H₁), 4.43 (m 1H, H₅), 2.11-1.99 (3s, 9H, CH₃, 3 x OAc). ¹³C NMR (125 MHz, CDCl₃) δ 170.1 (C=O, OAc), 169.9 (C=O, OAc), 169.4 (C=O, OAc), 165.2 (C=O), 131.2 (CH₂-CH=CH₂), 120.1 (CH₂-CH=CH₂), 88.6 (C₁), 74.3 (C₅), 70.6 (C₄), 68.2 (C₃), 67.8 (C₂), 66.8 (CH₂-CH=CH₂), 20.9 (CH₃, OAc), 20.7 (CH₃, OAc), 20.6 (CH₃, OAc). **LRMS (ESI):** *m/z* 408 [M + Na]⁺ **HRMS (ESI):** *m/z* calculated for C₁₅H₁₉N₃O₉Na [M + Na]⁺: 408.1019; Found 408.1024

1-Azido-2,3,4-tri-*O*-acetyl- β -D-galacturonic acid (65)

64 (0.511 g, 1.33 mmol) was dissolved in dry ACN (7 mL), and the reaction mixture was cooled to 0°C. To this solution, Pd(PPh₃)₄ (0.155 g, 0.132 mmol) was added, and the mixture was placed under an atmosphere of argon. Pyrrolidine (0.12 mL, 1.34 mmol) was then added dropwise, and the reaction mixture was allowed to warm gradually to room temperature. After 1 hour, the reaction mixture was filtered through Celite, with the filtrate evaporated to dryness. The residue was re-dissolved in EtOAc (20 mL), before extraction with H₂O (2 x 20 mL). The aqueous phase was collected and acidified to pH 2 using Amberlite IR-120 resin, and subsequently extracted with EtOAc (3 x 40 mL). The organic phase was dried and evaporated, with the residue placed under high vacuum overnight, producing **65** as a yellow foam. (0.308 g, 67%). **¹H NMR** (500 MHz, CDCl₃) δ 5.78 (m, 1H, H4), 5.16 (t, 1H, *J* = 8.5 Hz, H2), 5.12 (t, 1H, *J* = 8.5 Hz, H3), 4.71 (d, 1H, *J* = 8.8 Hz, H1), 4.44 (m, 1H, H5), 2.10, 2.09, 1.99 (3s, 9H, CH₃, 3 x OAc). **¹³C NMR** (125 MHz, CDCl₃) δ 170.1 (C=O, OAc), 170.0 (C=O, OAc), 169.4 (C=O, OAc), 167.8 (C=O), 88.4 (C1), 74.0 (C5), 70.5 (C4), 68.0 (C3), 67.7 (C2), 20.7 (CH₃, OAc), 20.6 (CH₃, OAc), 20.5 (CH₃, OAc). **LRMS (ESI):** *m/z* 344 [M - H]⁻ **HRMS (ESI):** *m/z* calculated for C₁₂H₁₄N₃O₉ [M - H]⁻:344.0730; Found 344.0736.

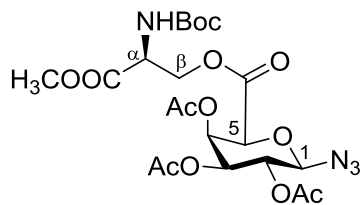
***N*^α-(*tert*-Butoxycarbonyl)-*O*-(1-azido-2,3,4-tri-*O*-acetyl-β-*D*-glucuronoyl)-*L*-serine methyl ester (**66**)**



A solution of **60** (0.141 g, 0.41 mmol) and Boc.Ser.OMe (0.092 g, 0.41 mmol) in dry CH₂Cl₂ (10 mL) was cooled to 0°C. DCC (0.170 g, 0.81 mmol) and DMAP (0.010 g, 0.08 mmol) were added, and the solution stirred at room

temperature for 24 hours. Upon completion, the reaction mixture was filtered, and the filtrate was diluted with CH₂Cl₂ (10 mL). The organic phase was washed with sat. NaHCO₃ solution (10 mL) and brine (10 mL), and dried and evaporated. The resulting residue was purified using flash column chromatography (2:1 Hexane: EtOAc) to produce **66** as a white solid. (0.172 g, 80%), M.p. 112-114°C R_f 0.18 (2:1 Hexane:EtOAc.). ¹H NMR (500 MHz, CDCl₃) δ 5.40 (bs, 1H, NH), 5.26 (m, 2H, H₃/H₄), 4.96 (t, 1H, *J* = 8.7 Hz, H₂), 4.73 (d, 1H, *J* = 8.1 Hz, H₁), 4.58 (m, 2H, H^β), 4.41 (m, 1H, H^α), 4.16 (d, 1H, *J* = 8.7 Hz, H₅), 3.78 (s, 3H, OCH₃), 2.08-2.02 (3s, 9H, CH₃, 3 x OAc), 1.45 (s, 9H, Boc-H). ¹³C NMR (125 MHz, CDCl₃) δ 170.1, (C=O, OAc), 169.9, (C=O, OAc), 169.6, (C=O, OAc), 169.3 (C=O, COOCH₃), 165.9 (C=O), 155.3 (C=O, Boc), 88.1 (C₁), 80.6, (C(CH₃)₃), 74.3 (C₅), 72.0 (C₄), 70.5 (C₃), 69.1 (C₂), 66.0 (C^β), 53.1 (OCH₃), 52.8 (C^α), 28.4 (C(CH₃)₃), 20.7 (CH₃, OAc), 20.7 (CH₃, OAc), 20.6 (CH₃, OAc). LRMS (ESI): *m/z* 569 [M + Na]⁺

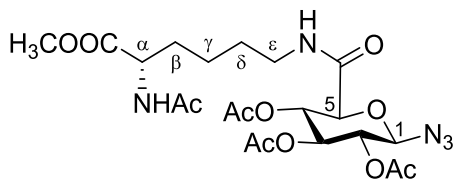
***N*^α-(*tert*-Butoxycarbonyl)-*O*-(1-azido-2,3,4-tri-*O*-acetyl-β-*D*-galacturonoyl)-*L*-serine methyl ester (67)**



A solution of **60** (0.142 g, 0.410 mmol) and Boc.Ser.OMe (0.095 g, 0.430 mmol) in dry CH₂Cl₂ (10 mL) was cooled to 0°C. DCC (0.170 g, 0.810 mmol) and DMAP (0.011 g, 0.080 mmol) were added, and the

solution stirred at room temperature for 24 hours. Upon completion, the reaction mixture was filtered, and the filtrate was diluted with CH₂Cl₂ (10 mL). The organic phase was washed with sat. NaHCO₃ solution (10 mL) and brine (10 mL), and dried and evaporated. The resulting residue was purified using flash column chromatography (2:1 Hexane: EtOAc) to produce **66** as a colourless oil. (0.138 g, 64%), *R*_f 0.22 (2:1 Hexane:EtOAc). ¹H NMR (500 MHz, CDCl₃) δ 5.69 (s, 1H, H₄), 5.38 (d, 1H, *J* = 7.3 Hz, NH), 5.16 (t, 1H, *J* = 8.7 Hz, H₂), 5.08 (dd, 1H, *J* = 3.0 Hz, 10.3 Hz, H₃), 4.64 (d, 1H, *J* = 8.7 Hz, H₁), 4.55 (m, 1H, H^α), 4.47 (m, 2H, H^β), 4.38 (m, 1H, H₅), 3.76 (s, 3H, OCH₃), 2.07-1.98 (3s, 9H, CH₃, 3 x OAc), 1.43 (s, 9H, CH₃, Boc). ¹³C NMR (125 MHz, CDCl₃) δ 170.2 (C=O, OAc), 170.0 (C=O, OAc), 169.8 (C=O, OAc), 169.4 (C=O, COOCH₃), 165.0 (C=O), 155.4 (C=O, Boc), 88.5 (C₁), 80.6 (C(CH₃)₃), 74.0 (C₅), 70.4 (C₃), 68.0 (C₄), 67.9 (C₂), 66.1 (C^β), 53.1 (OCH₃), 52.9 (C^α), 28.5 (C(CH₃)₃), 20.8 (CH₃, OAc), 20.8 (CH₃, OAc), 20.7 (CH₃, OAc). **LRMS (ESI):** *m/z* 569 [M + Na]⁺

***N*^α-(Acetyl)-*N*^ε-(1-azido-2,3,4-tri-*O*-acetyl-β-*D*-glucuronoyl)-*L*-lysine methyl ester
(68)**



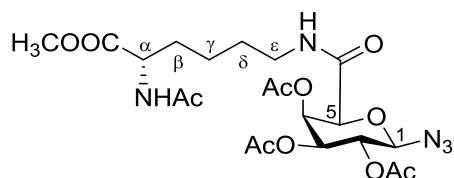
Method A: A solution of **60** (0.140 g, 0.40 mmol) and Ac.Lys.OMe.HCl (0.100 g, 0.41 mmol) in dry CH₂Cl₂ (10 mL) was cooled to 0°C. DCC (0.171 g, 0.81 mmol) and DMAP (0.16 g,

0.13 mmol) were added, and the solution was allowed to stir at room temperature for 24 hours. Upon completion, the reaction mixture was filtered, and the filtrate was diluted with CH₂Cl₂ (10 mL). The organic phase was washed with sat. NaHCO₃ solution (10 mL) and brine (10 mL), and dried and evaporated. The resulting residue was purified using flash column chromatography (1:2 Hexane: EtOAc) to produce **68** as a light yellow oil. (0.67 g, 31%).

Method B: **60**, (0.141 g, 0.41 mmol) Ac.Lys.OMe.HCl (0.100 g, 0.41 mmol), DCC (0.175 g, 0.815 mmol) and HOBt (0.077 g, 0.528 mmol) were dissolved in DMF (5 mL), and the solution was cooled to 0°C. DIPEA (0.075 mL, 0.056 g, 0.446 mmol) was added dropwise to the solution, and the reaction mixture was allowed to warm to room temperature and stir for 24 hours. Upon completion, the reaction mixture was filtered, and the filtrate was diluted with EtOAc (20 mL), and extracted with H₂O (5 mL). The organic phase was dried and evaporated, with the following residue purified by flash column chromatography (1:2 Hexane: EtOAc) to produce **68** as a light yellow solid. (0.163 g, 75%), M.p 145-148°C, R_f 0.16 (1:2 Hexane:EtOAc). ¹H NMR (500 MHz, CDCl₃) δ 6.76 (bs, 1H, NH), 6.70 (bs, 1H, NH), 5.31 (t, 1H, *J* = 9.5 Hz, 10.0 Hz, H4), 5.17 (t, 1H, *J* = 9.5 Hz, 10.0 Hz, H3), 4.95 (t, 1H, *J* = 9.2 Hz, H2), 4.83 (d, 1H, *J* = 8.9 Hz, H1), 4.61 (m, 1H, CH^α), 4.05 (d, 1H, *J* = 10.1 Hz, H5), 3.73 (s, 3H,

OCH₃), 3.40 (m, 1H, CH^ε), 3.15 (m, 1H, CH^ε), 2.09-2.01 (4s, 12H, CH₃, NHAc/3 x OAc), 1.79 (m, 1H, CH^β), 1.72 (m, 1H, CH^β), 1.55 (m, 2H, CH^δ), 1.35 (m, 2H, CH^γ). ¹³C NMR (125 MHz, CDCl₃) δ 173.1 (C=O, NHAc), 170.5 (C=O, OAc), 170.3 (C=O, OAc), 169.9 (C=O, OAc), 169.4 (C=O, COOCH₃), 166.2 (C=O), 88.1 (C1), 74.6 (C5), 72.1 (C4), 70.8 (C3), 69.5 (C2), 52.5 (OCH₃), 52.2 (CH^ε), 38.7 (CH^α), 31.9 (CH^δ), 29.1 (CH^β), 23.1 (CH₃, NHAc), 22.4 (CH^γ), 20.8 (CH₃, OAc), 20.7 (CH₃, OAc), 20.7 (CH₃, OAc). LRMS (ESI): *m/z* 552 [M + Na]⁺ HRMS (ESI): *m/z* calculated for C₂₁H₃₁N₅O₁₁Na [M + Na]⁺: 552.1918; Found 552.1918.

***N*^α-(Acetyl)-*N*^ε-(1-azido-2,3,4-tri-*O*-acetyl-β-D-galacturonoyl)-L-lysine methyl ester (69)**

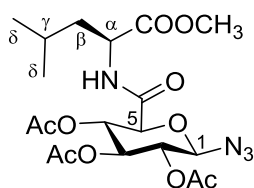


65 (0.141 g, 0.41 mmol) Ac.Lys.OMe.HCl (0.100 g, 0.42 mmol), DCC (0.176 g, 0.817 mmol) and HOBt (0.079 g, 0.530 mmol) were dissolved in DMF (5 mL), and the solution was cooled to

0°C. DIPEA (0.075 mL, 0.056 g, 0.446 mmol) was added dropwise to the solution, and the reaction mixture was allowed to warm to room temperature and stir for 24 hours. Upon completion, the reaction mixture was filtered, and the filtrate was diluted with EtOAc (20 mL), and extracted with H₂O (5 mL). The organic phases were combined, dried and evaporated, and the residue purified by flash column chromatography (1:2 Hexane: EtOAc) to produce **69** as a light yellow oil. (0.130 g, 60%), M.p. 154-156°C (decomp.), R_f 0.18 (1:2 Hexane:EtOAc.). ¹H NMR (500 MHz, CDCl₃) δ 6.63 (t, 1H, *J* = 6.2 Hz NH), 6.37 (d, 1H, *J* = 7.7 Hz, NH), 5.81 (m, 1H, H4), 5.14 (m 2H, H3/H2), 4.74 (m, 1H, H1), 4.54 (m, 1H, H^α), 4.34 (m, 1H, H5), 3.74 (s, 3H, OCH₃),

3.32-3.25 (m, 2H, CH^ε), 2.10 -1.98 (4s, 12H, CH₃, NHAc/3 x OAc), 1.83 (m, 1H, CH^β), 1.70 (m, 1H, CH^β), 1.58 (m, 2H, CH^δ), 1.37 (m, 2H, CH^γ). ¹³C NMR (125 MHz, CDCl₃) δ 173.0 (C=O, NHAc), 170.3 (C=O, OAc), 169.9 (C=O, OAc), 169.8 (C=O, OAc), 169.4 (C=O, COOCH₃), 165.4 (C=O), 88.4 (C1), 76.8 (C4), 75.4 (C5), 70.4 (C3), 67.8 (C2), 52.4 (OCH₃), 52.0 (CH^ε), 38.7 (CH^α), 31.7 (CH^δ), 29.2 (CH^β), 23.1 (CH₃ NHAc), 22.4 (CH^γ), 20.7 (CH₃, OAc), 20.7 (CH₃, OAc), 20.5 (CH₃, OAc). **LRMS (ESI):** *m/z* 552 [M + Na]⁺ **HRMS (ESI):** *m/z* calculated for C₂₁H₃₁N₅O₁₁Na [M + Na]⁺: 552.1918; Found 552.1935

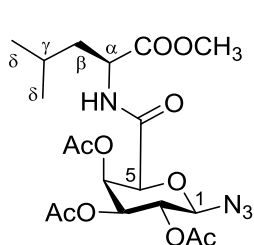
N-(1-Azido-2,3,4-tri-*O*-acetyl-β-*D*-glucuronoyl)-*L*-leucine methyl ester (**70**)



60 (0.173 g, 0.50 mmol), H.Leu.OMe.HCl (0.136 g, 0.74 mmol) and HBTU (0.379 g, 1.00 mmol) were dissolved in DMF (5 mL), and the solution was cooled to 0°C. DIPEA (0.10 mL, 0.074 g, 0.55 mmol) was added dropwise to the solution, and the reaction mixture was allowed to warm to room temperature and stirred for 24 hours. Upon completion, the reaction mixture was filtered, and the filtrate was diluted with EtOAc (20 mL), and extracted with H₂O (5 mL). The organic phase was dried and evaporated, and the residue purified by flash column chromatography (3:1 Hexane: EtOAc) to produce **71** as a white solid. (0.199 g, 84%), M.p. 122-124°C, R_f 0.72 (1:1 Hexane:EtOAc.). ¹H NMR (500 MHz, CDCl₃) δ 6.70 (d, 1H, *J* = 8.4 Hz, NH), 5.28 (t, 1H, *J* = 9.4 Hz, H4), 5.15 (t, 1H, *J* = 9.8 Hz, H3), 4.96 (t, 1H, *J* = 9.1 Hz, H2), 4.79 (d, 1H, *J* = 8.9 Hz, H1), 4.57 (m, 1H, H^α), 4.04 (d, 1H, *J* = 10.1 Hz, H5), 3.74 (s, 3H, OCH₃), 2.08 – 2.01 (3s, 9H, CH₃, 3 x OAc), 1.69 - 1.64 (m, 3H, H^β/H^γ), 0.95 (m, 6H, CH₃, 2 x H^δ). ¹³C NMR (125 MHz, CDCl₃) δ 172.8 C=O (COOCH₃), 169.8 (C=O,

OAc), 169.4 (C=O, OAc), 169.2 (C=O, OAc), 165.5 (C=O), 87.9 (C1), 74.2 (C5), 71.9 (C4), 70.6 (C3), 69.1 (C2), 52.4 (C^α), 50.4 (OCH₃), 41.2 (C^β), 24.8 (C^γ), 22.8 (C^δ), 21.8 (C^δ), 20.6 (CH₃, OAc), 20.5 (CH₃, OAc), 20.5 (CH₃, OAc). **LRMS (ESI):** m/z 495 [M + Na]⁺ **HRMS (ESI):** m/z calculated for C₁₉H₂₄N₄O₁₀Na [M + Na]⁺: 495.1703; Found 495.1697.

N-(1-Azido-2,3,4-tri-*O*-acetyl-β-*D*-galacturonoyl)-*L*-leucine methyl ester (**71**)

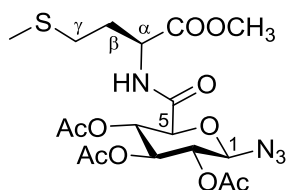


65 (0.173 g, 0.50 mmol), H.Leu.OMe.HCl (0.137 g, 0.75 mmol) and HBTU (0.380 g, 1.00 mmol) were dissolved in DMF (5 mL), and the solution was cooled to 0°C. DIPEA (0.10 mL, 0.074 g, 0.55 mmol) was added dropwise to the solution, and the reaction mixture was allowed to warm to room temperature and stir for 24 hours. Upon completion, the reaction mixture was filtered, and the filtrate was diluted with EtOAc (20 mL), and extracted with H₂O (5 mL). The organic phase was dried and evaporated, with the following residue purified by flash column chromatography (2:1 Hexane: EtOAc) to produce **71** as a clear oil. (0.184 g, 78%), R_f 0.65 (1:1 Hexane:EtOAc). **¹H NMR** (500 MHz, CDCl₃) δ 6.82 (d, 1H, J = 7.6 Hz, NH), 5.83 (m, 1H, H4), 5.17 (m, 2H, H2/H3), 4.70 (m, 2H, H1/H^α), 4.33 (m, 1H, H5), 3.75 (s, 3H, OCH₃), 2.11 – 1.99 (3s, 9H, CH₃, 3 x OAc), 1.69 – 1.60 (m, 3H, H^β/H^γ), 0.95 (m, 6H, CH₃, 2 x H^δ). **¹³C NMR** (125 MHz, CDCl₃) δ 172.9 (C=O, COOCH₃), 170.0 (C=O, OAc), 169.6 (C=O, OAc), 169.3 (C=O, OAc), 164.9 (C=O), 88.4 (C1), 75.4 (C5), 70.4 (C3), 67.7 (C2), 67.6 (C4), 52.5 (OCH₃), 50.4 (C^α), 41.4 (C^β), 24.8 (C^γ), 22.9 (C^δ), 20.7 (CH₃, OAc), 20.5 (CH₃, OAc), 20.4 (CH₃, OAc). **LRMS (ESI):** m/z

495 $[M + Na]^+$ **HRMS (ESI)**: m/z calculated for $C_{19}H_{24}N_4O_{10}Na$ $[M + Na]^+$: 495.1703;

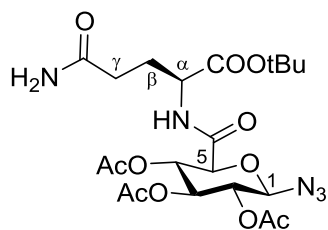
Found 495.1696

***N*-(1-Azido-2,3,4-tri-*O*-acetyl- β -D-glucuronoyl)-L-methionine methyl ester (**72**)**



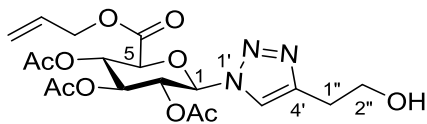
60 (0.342 g, 1.01 mmol), H.Met.OMe.HCl (0.302 g, 1.51 mmol) and HBTU (0.764 g, 2.00 mmol) were dissolved in DMF (15 mL), and the solution was cooled to 0°C. DIPEA (0.20 mL, 0.148 g, 1.1 mmol) was added

dropwise to the solution, and the reaction mixture was allowed to warm to room temperature and stirred for 24 hours. Upon completion, the reaction mixture was filtered, and the filtrate was diluted with EtOAc (50 mL), and extracted with H_2O (5 mL). The organic phase was dried and evaporated, with the following residue purified by flash column chromatography (2:1 Hexane: EtOAc) to produce **72** as a fluffy white solid. (0.461 g, 95%), M.p. 106-107°C, R_f 0.71 (1:1 Hexane:EtOAc). 1H NMR (500 MHz, $CDCl_3$) δ 7.14 (bs, 1H, NH), 5.27 (t, 1H, $J = 9.5$ Hz, H3), 5.16 (t, 1H, $J = 9.8$ Hz, H4), 4.97 (t, 1H, $J = 9.6$ Hz, H2), 4.78 (d, 1H, $J = 9.8$ Hz, H1), 4.68 (m, 1H, H α), 4.02 (d, 1H, $J = 9.8$ Hz, H5), 3.78 (s, 3H, OCH_3), 2.54 (t, 2H, $J = 7.3$ Hz, H γ), 2.19 (m, 2H, H β), 2.13 (s, 3H, S- CH_3), 2.09-2.02 (3s, 9H, CH_3 , 3 x OAc). ^{13}C NMR (125 MHz, $CDCl_3$) δ 171.8 ($\underline{C}OOCH_3$), 169.9 (C=O, OAc), 169.6 (C=O, OAc), 169.3 (C=O, OAc), 165.7 (C=O), 87.9 (C1), 74.2 (C5), 71.7 (C4), 70.5 (C3), 69.1 (C2), 52.7 (C α), 51.2 ($-OCH_3$), 31.2 (C β), 29.7 (C γ), 20.7 (CH_3 , OAc), 20.6 (CH_3 , OAc), 20.6 (CH_3 , OAc), 15.4 (S CH_3). **LRMS (ESI)**: m/z 513 $[M + Na]^+$ **HRMS (ESI)**: m/z calculated for $C_{18}H_{26}N_4O_{10}SNa$ $[M + Na]^+$: 513.1267; Found 513.1273.

***N*-(1-Azido-2,3,4-tri-*O*-acetyl- β -D-glucuronoyl)-L-glutamine *tert*-butyl ester (**73**)**

60 (0.173 g, 0.50 mmol), H.Glu.OtBu.HCl (0.179 g, 0.75 mmol) and HBTU (0.376 g, 0.99 mmol) were dissolved in DMF (5 mL), and the solution was cooled to 0°C. DIPEA (0.10 mL, 0.074 g, 0.55 mmol) was added dropwise to the solution, and the reaction mixture was allowed to warm to room temperature and stir for 24 hours. Upon completion, the reaction mixture was filtered, and the filtrate was diluted with EtOAc (20 mL), and extracted with H₂O (5 mL). The organic phase was dried and evaporated, with the following residue purified by flash column chromatography (1:3 Hexane: EtOAc) to produce **73** as an off-white solid. (0.254 g, 96%), M.p. 129-130°C, R_f 0.24 (1:3 Hexane:EtOAc.). ¹H NMR (500 MHz, CDCl₃) δ 7.24 (d, 1H, *J* = 7.7 Hz, NH), 5.31 (t, 1H, *J* = 9.5 Hz, H₃), 5.18 (t, 1H, *J* = 9.6 Hz, H₄), 4.98 (t, 1H, *J* = 9.4 Hz, H₂), 4.82 (d, 1H, *J* = 9.0 Hz, H₁), 4.45 (m, 1H, H^a), 4.02 (d, 1H, *J* = 9.9 Hz, H₅), 2.35 - 2.28 (m, 2H, H^γ), 2.20-1.90 (m, 2H, H^β), 2.09 - 2.02 (3s, 9H, CH₃, 3 x OAc), 1.48 (s, 9H, OtBu). ¹³C NMR (125 MHz, CDCl₃) δ 174.9 (CONH₂), 170.6 (COOtBu), 170.2 (C=O, OAc), 169.7 (C=O, OAc), 169.2 (C=O, OAc) 167.5 (C=O), 87.9 (C₁), 83.0 (C(CH₃)₃), 74.2 (C₅), 71.6 (C₄), 70.6 (C₃), 69.5 (C₂), 51.8 (C^a), 38.6 (C^γ), 31.3 (C^β), 27.9 (C(CH₃)₃), 20.8 (CH₃, OAc), 20.5 (CH₃, OAc), 20.5 (CH₃, OAc). LRMS (ESI): *m/z* 552 [M + Na]⁺ HRMS (ESI): *m/z* calculated for C₂₁H₃₁N₅O₁₁Na [M + Na]⁺: 552.1918; Found 552.1922.

1-(4'-(2''-Hydroxyethyl)-1',2',3'-triazol-1'-yl)-2,3,4-tri-*O*-acetyl- β -D-glucuronic acid allyl ester (74**)**



Method A: To a round bottom flask containing **59**

(0.100 g, 0.260 mmol), 3-butyn-1-ol (0.034 mL, 0.037 g, 0.52 mmol), CuSO₄·5H₂O (0.013 g,

0.052 mmol) and sodium ascorbate (0.010 g, 0.052 mmol) was added a 3:1 solution of ACN:H₂O, (0.500 mL), with the solution stirred vigorously under an atmosphere of nitrogen at room temperature for 8 hours. Upon completion, the reaction mixture was diluted with CH₂Cl₂ (5 mL), and extracted with H₂O (1 mL), then brine (1 mL). Subsequent drying (MgSO₄) of the organic phase, and evaporation *in vacuo* resulted in a residue which was purified by flash column chromatography (1:3 Hexane: EtOAc) to yield **74** as a light yellow oil. (0.044 g, 37%).

Method B: As for Method A, except that a solution of 1:1 *n*BuOH: H₂O was instead used, and the reaction mixture was stirred at 40°C for 4 hours. Work up and purification by flash column chromatography yielded **74** as a light yellow oil. (0.058 g, 49%).

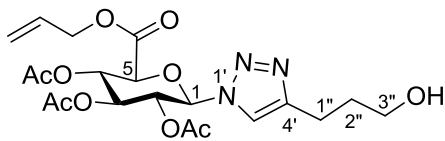
Method C: To a round bottom flask containing **59** (0.100 g, 0.260 mmol), 3-butyn-1-ol (0.067 mL, 0.073 g, 1.04 mmol), CuSO₄·5H₂O (0.013 g, 0.052 mmol) and sodium ascorbate (0.021 g, 0.104 mmol) was added a 1:1 solution of *n*BuOH:H₂O, (0.500 mL), with the solution stirred vigorously under an atmosphere of nitrogen at room temperature for 8 hours. Upon completion, the reaction mixture was diluted with CH₂Cl₂ (5 mL), and extracted with H₂O (1 mL), then brine (1 mL). Subsequent drying (MgSO₄) of the organic phase, and evaporation *in vacuo* resulted in a residue which was purified by flash column chromatography to yield **74** as a light yellow oil. (0.061 g, 52%)

Method D: As for Method C, except that CuOAc₂·H₂O (0.010 g, 0.052 mmol) was used instead of CuSO₄·5H₂O. Work up and purification by flash column chromatography yielded **74** as a light yellow oil. (0.065 g, 55%)

Method E: As for Method D, except that the additive TBTA (0.028 g, 0.052 mmol) was added to the reaction mixture. Work up and purification by flash column chromatography yielded **74** as a light yellow oil. (0.071 g, 60%)

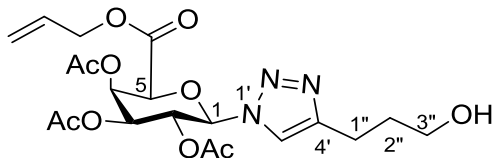
Method F: To a round bottom flask containing **59** (0.100 g, 0.260 mmol), 3-butyn-1-ol (0.070 mL, 0.075 g, 1.06 mmol), CuOAc₂·H₂O (0.011 g, 0.056 mmol) and sodium ascorbate (0.022 g, 0.110 mmol) was added a 1:1 solution of *n*BuOH:H₂O, (0.500 mL), with the solution stirred vigorously under an atmosphere of nitrogen at room temperature for 24 hours. Upon completion, the reaction mixture was diluted with CH₂Cl₂ (5 mL), and extracted with H₂O (1 mL), then brine (1 mL). Subsequent drying (MgSO₄) of the organic phase, and evaporation *in vacuo* resulted in a residue which was purified by flash column chromatography to yield **74** as a light yellow solid (0.104 g, 88%), M.p. 116-118°C, R_f 0.29 (1:3 Hexane:EtOAc.). ¹H NMR (500 MHz, CDCl₃) δ 7.74 (s, 1H, Triazole-H), 5.93-5.86 (m, 2H, H1/CH₂=CH-CH₂), 5.48-5.25 (m, 5H, H4/H3/H2/CH₂=CH-CH₂), 4.61 (m, 2H, CH₂=CH-CH₂), 4.35 (d, 1H, *J* = 9.8 Hz, H5), 3.87 (m, 2H, CH₂-CH₂-OH), 2.92 (m, 2H, CH₂-CH₂-OH), 2.04-1.98 (3, 9H, CH₃, 3 x OAc). Exchangeable OH not detected. ¹³C NMR (125 MHz, CDCl₃) δ 169.9 (C=O, OAc), 169.5 (C=O, OAc), 169.2 (C=O, OAc), 165.7 (C=O), 147.9 (Triazole), 130.9 (CH₂-CH=CH₂), 120.6 (Triazole), 120.0 (CH₂-CH=CH₂), 88.1 (C1), 74.9 (C5), 71.8 (C4), 70.3 (C3), 69.1 (C2), 67.1 (CH₂-CH=CH₂), 61.5 (CH₂-CH₂-OH), 29.1 (CH₂-CH₂-OH), 20.6 (CH₃, OAc), 20.6 (CH₃, OAc), 20.3 (CH₃, OAc). **LRMS (ESI):** *m/z* 478 [M + Na]⁺

1-(4'-(3''-Hydroxypropyl)-1',2',3'-triazol-1'-yl)-2,3,4-tri-*O*-acetyl- β -D-glucuronic acid allyl ester (75)



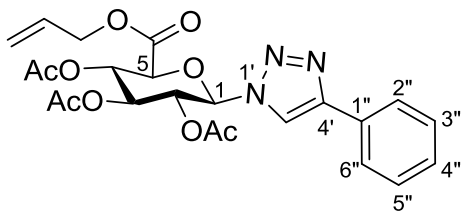
To a round bottom flask containing **59** (0.101 g, 0.261 mmol), 4-pentyn-1-ol (0.097 mL, 0.087 g, 1.04 mmol), $\text{CuOAc}_2 \cdot \text{H}_2\text{O}$ (0.010 g, 0.052 mmol) and sodium ascorbate (0.021 g, 0.104 mmol) was added a 1:1 solution of *n*BuOH:H₂O, (0.500 mL), with the solution stirred vigorously under an atmosphere of nitrogen at room temperature for 24 hours. Upon completion, the reaction mixture was diluted with CH_2Cl_2 (5 mL), and extracted with H₂O (1 mL), then brine (1 mL). Subsequent drying (MgSO_4) of the organic phase, and evaporation *in vacuo* resulted in a residue which was purified by flash column chromatography to yield **75** as a white solid. (0.114 g, 84%), M.p. 114-116°C, R_f 0.27 (1:3 Hexane:EtOAc). ¹H NMR (500 MHz, CDCl_3) δ 7.69 (s, 1H, Triazole-H), 5.95-5.84 (m, 2H, H1/CH₂=CH-CH₂), 5.48-5.27 (m, 5H, H4/H3/H2/CH₂=CH-CH₂), 4.63 (m, 2H, CH₂=CH-CH₂), 4.37 (d, 1H, J = 9.8 Hz, H5), 3.67 (m, 2H, CH₂-CH₂-CH₂-OH), 2.85 (m, 2H, CH₂-CH₂-CH₂-OH), 2.05 (s, 6H, CH₃, 2 x OAc), 1.93 (m, 2H, CH₂-CH₂-CH₂-OH), 1.88 (s, 3H, CH₃, OAc). Exchangeable OH not detected. ¹³C NMR (125 MHz, CDCl_3) δ 169.9 (C=O, OAc), 169.5 (C=O, OAc), 169.1 (C=O, OAc), 165.7 (C=O), 130.9 (Triazole C), 147.9 (CH₂-CH=CH₂), 120.0 (Triazole C), 119.9 (CH₂-CH=CH₂), 85.5 (C1), 74.9 (C5), 72.0 (C4), 70.1 (C3), 69.1 (C2), 67.1 (CH₂-CH=CH₂), 61.6 (CH₂-CH₂-CH₂-OH), 31.7 (CH₂-CH₂-CH₂-OH), 22.0 (CH₂-CH₂-CH₂-OH), 20.6 (CH₃, OAc), 20.6 (CH₃, OAc), 20.2 (CH₃, OAc). **LRMS (ESI):** m/z 492 $[\text{M} + \text{Na}]^+$ **HRMS (ESI):** m/z calculated for $\text{C}_{20}\text{H}_{27}\text{N}_3\text{O}_{10}\text{Na}$ $[\text{M} + \text{Na}]^+$: 492.1594; Found 492.1580.

1-(4'-(3''-Hydroxypropyl)-1',2',3'-triazol-1'-yl)-2,3,4-tri-*O*-acetyl- β -D-galacturonic acid allyl ester (76)



To a round bottom flask containing **64** (0.101 g, 0.261 mmol), 4-pentyn-1-ol (0.097 mL, 0.087 g, 1.04 mmol), CuOAc₂·H₂O (0.010 g, 0.052 mmol) and sodium ascorbate (0.020 g, 0.099 mmol) was added a 1:1 solution of *n*BuOH:H₂O, (0.500 mL), with the solution stirred vigorously under an atmosphere of nitrogen at room temperature for 24 hours. Upon completion, the reaction mixture was diluted with CH₂Cl₂ (5 mL), and extracted with H₂O (1 mL), then brine (1 mL). Subsequent drying (MgSO₄) of the organic phase, and evaporation *in vacuo* resulted in a residue which was purified by flash column chromatography to yield **76** as a light yellow oil. (0.109 g, 80%), R_f 0.30 (1:3 Hexane:EtOAc). ¹H NMR (500 MHz, CDCl₃) δ 7.73 (s, 1H, Triazole-H), 5.89-5.83 (m, 3H, CH₂-CH=CH₂/H1/H3), 5.56 (t, 1H, *J* = 10.0 Hz, H2), 5.30 (m, 3H, CH₂-CH=CH₂/H4), 4.68-4.61 (m, 3H, CH₂-CH=CH₂/H5), 3.68 (m, 2H, CH₂-CH₂-CH₂-OH), 2.85 (m, 2H, CH₂-CH₂-CH₂-OH), 2.02 (s, 6H, CH₃, 2 x OAc), 1.95 (m, 2H, CH₂-CH₂-CH₂-OH), 1.89 (s, 3H, CH₃, OAc). Exchangeable OH not detected. ¹³C NMR (125 MHz, CDCl₃) δ 169.8 (OAc), 169.6 (OAc), 169.2 (OAc), 164.7 (OAc), 147.8 (Triazole C), 130.8 (CH₂-CH=CH₂), 120.2 (Triazole C), 119.7 (CH₂-CH=CH₂), 85.9 (C1), 74.8 (C5), 70.4 (C4), 68.1 (C3), 67.6 (C2), 66.7 (CH₂-CH=CH₂), 61.5 (CH₂-CH₂-CH₂-OH), 31.7 (CH₂-CH₂-CH₂-OH), 21.9 (CH₂-CH₂-CH₂-OH), 20.6 (CH₃, OAc), 20.5 (CH₃, OAc), 20.2 (CH₃, OAc). LRMS (ESI): *m/z* 492 [M + Na]⁺ HRMS (ESI): *m/z* calculated for C₂₀H₂₇N₃O₁₀Na [M + Na]⁺: 492.1594; Found 492.1597.

1-(4'-Phenyl-1',2',3'-triazol-1'-yl)-2,3,4-tri-*O*-acetyl- β -D-glucuronic acid allyl ester
(77)



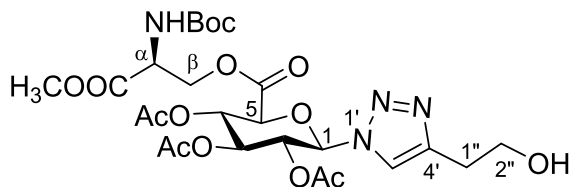
To a round bottom flask containing **59**
(0.101 g, 0.261 mmol), phenylacetylene
(0.115 mL, 0.107 g, 1.04 mmol),
CuOAc₂·H₂O (0.010 g, 0.052 mmol) and

sodium ascorbate (0.021 g, 0.104 mmol) was added a 1:1 solution of *n*BuOH:H₂O, (0.500 mL), with the solution stirred vigorously under an atmosphere of nitrogen at room temperature for 24 hours. Upon completion, the reaction mixture was diluted with CH₂Cl₂ (5 mL), and extracted with H₂O (1 mL), then brine (1 mL). Subsequent drying (MgSO₄) of the organic phase, and evaporation *in vacuo* resulted in a residue which was purified by flash column chromatography (2:1 Hexane: EtOAc) to yield **75** as a light yellow solid (0.108 g, 85%), M.p 207-210 °C (decomp.) R_f 0.25 (2:1 Hexane:EtOAc).

¹H NMR (500 MHz, CDCl₃) δ 8.08 (s, 1H, Triazole-H), 7.82 (d, 2H, *J* = 7.3 Hz, Ar-H2/H6), 7.34-7.44 (m, 3H, Ar-H3/H4/H5), 6.00 (d, 1H, *J* = 8.2 Hz, H1), 5.90 (m, 1H, CH₂=CH-CH₂), 5.52 (m, 2H, CH₂=CH-CH₂), 5.43-5.25 (3t (overlapping), 3H, *J* = 9.0 Hz, 9.9 Hz, H4/H3/H2), 4.63 (m, 2H, CH₂=CH-CH₂), 4.37 (d, 1H, *J* = 9.7 Hz, H5), 2.04 (2s, 6H, CH₃, 2 x OAc), 1.87 (s, 3H, CH₃, OAc). **¹³C NMR** (125 MHz, CDCl₃) δ 170.4 (C=O, OAc), 169.9 (C=O, OAc), 169.5 (C=O, OAc), 166.1 (C=O), 131.4 (CH₂-CH=CH₂), 130.4 (Triazole C), 129.5 (Ar-C), 129.2 (Ar-C), 126.5 (Ar-C), 120.6 (Triazole C), 118.6 (CH₂-CH=CH₂), 86.1 (C1), 75.6 (C5), 72.6 (C4), 70.5 (C3), 69.6 (C2), 67.6 (CH₂-CH=CH₂), 21.2 (CH₃, OAc), 21.2 (CH₃, OAc), 20.8 (CH₃, OAc).

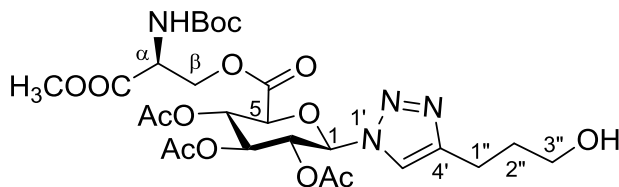
LRMS (ESI): *m/z* 486 [M - H]⁻ **HRMS (ESI):** *m/z* calculated for C₂₃H₂₄N₃O₉ [M - H]⁻: 486.1514; Found 486.1512.

***N*^α-(*tert*-Butoxycarbonyl)-*O*-(1-(4'-(2''-hydroxyethyl)-1',2',3'-triazol-1'-yl)-2,3,4-tri-*O*-acetyl-β-D-glucuronyl)-L-serine methyl ester (**78**)**



To a round bottom flask containing **66** (0.143 g, 0.261 mmol), 3-buten-1-ol (0.067 mL, 0.073 g, 1.04 mmol), CuOAc₂·H₂O (0.010 g, 0.052 mmol) and sodium ascorbate (0.022 g, 0.110 mmol) was added a 1:1 solution of *n*BuOH:H₂O, (0.500 mL), with the solution stirred vigorously under an atmosphere of nitrogen at room temperature for 24 hours. Upon completion, the reaction mixture was diluted with CH₂Cl₂ (5 mL), and extracted with H₂O (1 mL), then brine (1 mL). Subsequent drying (MgSO₄) of the organic phase, and evaporation *in vacuo* resulted in a residue which was purified by flash column chromatography (1:3 Hexane: EtOAc) to yield **78** as a light yellow solid. (0.100 g, 62%), M.p. 146-148°C R_f 0.20 (1:3 Hexane:EtOAc). ¹H NMR (500 MHz, CDCl₃) δ 7.74 (s, 1H, Triazole-H), 5.88 (d, 1H, *J* = 8.9 Hz, (H1), 5.47-5.33 (m, 4H, H4/H3/H2/NH), 4.55 (m, 2H, H^β), 4.37 (m, 2H, H^α/H5), 3.92 (m, 2H, CH₂-CH₂-OH), 3.75 (s, 3H, OCH₃), 2.96 (t, 2H, *J* = 6.9 Hz, CH₂-CH₂-OH), 2.10-1.89 (3s, 9H, CH₃, 3 x OAc), 1.44 (s, 9H, Boc-H). Exchangeable OH not detected. ¹³C NMR (125 MHz, CDCl₃) δ 169.7, 169.7, 169.5 (C=O, OAc), 169.1 (C=O, COOCH₃), 165.4 (C=O), 155.6 (C=O, Boc), 149.4 (Triazole C), 118.6 (Triazole C), 88.6 (C1), 80.6(C-CH₃), 74.9 (C5), 71.7 (C4), 70.2 (C3), 69.0 (C2), 66.0 (C^β), 62.7 (CH₂-CH₂-OH), 53.0 (OCH₃), 52.7 (C^α), 34.0 (CH₂-CH₂-OH), 28.3 (C-CH₃), 20.5 (CH₃, OAc), 20.5 (CH₃, OAc), 20.2 (CH₃, OAc). LRMS (ESI): *m/z* 639 [M + Na]⁺

***N*^α-(*tert*-Butoxycarbonyl)-*O*-(1-(4'-(3''-hydroxypropyl)-1',2',3'-triazol-1'-yl)-2,3,4-tri-*O*-acetyl-β-D-glucuronyl)-L-serine methyl ester (**79**)**



To a round bottom flask containing

66 (0.144 g, 0.262 mmol),

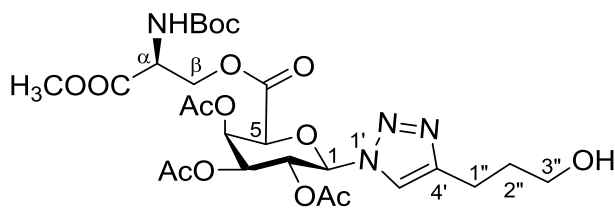
4-pentyn-1-ol (0.097 mL, 0.087 g,

1.04 mmol), CuOAc₂·H₂O (0.010 g,

0.052 mmol) and sodium ascorbate (0.020 g, 0.099 mmol) was added a 1:1 solution of *n*BuOH:H₂O, (0.500 mL), with the solution stirred vigorously under an atmosphere of nitrogen at room temperature for 24 hours. Upon completion, the reaction mixture was diluted with CH₂Cl₂ (5 mL), and extracted with H₂O (1 mL), then brine (1 mL). Subsequent drying (MgSO₄) of the organic phase, and evaporation *in vacuo* resulted in a residue which was purified by flash column chromatography (1:3 Hexane: EtOAc) to yield **79** as a light yellow solid. (0.096 g, 58%), M.p 174-176°C, R_f 0.16 (1:3 Hexane:EtOAc.). ¹H NMR (500 MHz, CDCl₃) δ 7.64 (s, 1H, Triazole-H), 5.88 (d, 1H, *J* = 8.7 Hz, H1), 5.44 (m, 2H, H4/H3), 5.33 (m, 2H, H2/NH), 4.59 (m, 1H, H^α), 4.52 (dd, 1H, *J* = 3.7 Hz, 11.4 Hz, H^β), 4.40 (dd, 1H, *J* = 2.6 Hz, 11.2 Hz, H^β), 4.31, (d, 1H, *J* = 9.9 Hz, H5), 3.76 (s, 3H, OCH₃), 3.68 (m, 2H, CH₂-CH₂-CH₂-OH), 2.85 (t, 2H, *J* = 7.2 Hz, CH₂-CH₂-CH₂-OH), 2.10, 2.05 (2s, 6H, CH₃, 2 x OAc), 1.95 (t, 2H, *J* = 6.7 Hz, CH₂-CH₂-CH₂-OH), 1.88 (s, 3H, CH₃, OAc), 1.44 (s, 9H, Boc). Exchangeable OH not detected. ¹³C NMR (125 MHz, CDCl₃) δ 169.9 (C=O, OAc), 169.9 (C=O, OAc), 169.7 (C=O, OAc), 169.1 (C=O, COOCH₃), 165.6 (C=O), 155.5 (C=O, Boc), 148.6 (Triazole C), 119.6 (Triazole C), 85.6 (C1), 81.1(C-CH₃), 75.1 (C5), 72.1 (C4), 70.2 (C3), 69.2 (C2), 66.0 (C^β), 61.8 (CH₂-CH₂-CH₂-OH), 53.1 (OCH₃), 52.9 (C^α), 31.8

(CH₂-CH₂-CH₂-OH), 28.5 (C-CH₃), 22.2 (CH₂-CH₂-CH₂-OH), 20.7 (CH₃, OAc), 20.7 (CH₃, OAc), 20.3 (CH₃, OAc). **LRMS (ESI):** m/z 653 [M + Na]⁺

***N*^α-(*tert*-Butoxycarbonyl)-*O*-(1-(4'-(3''-hydroxypropyl)-1',2',3'-triazol-1'-yl)-2,3,4-tri-*O*-acetyl-β-D-galacturonyl)-L-serine methyl ester (**80**)**

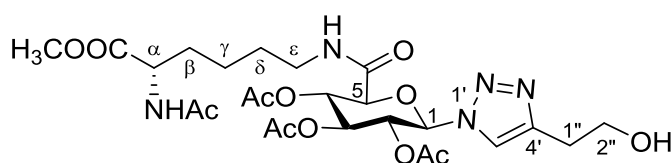


To a round bottom flask containing **67** (0.143 g, 0.261 mmol), 4-pentyn-1-ol (0.097 mL, 0.087 g, 1.04 mmol), CuOAc₂·H₂O (0.010 g,

0.052 mmol) and sodium ascorbate (0.020 g, 0.099 mmol) was added a 1:1 solution of *n*BuOH:H₂O, (0.500 mL), with the solution stirred vigorously under an atmosphere of nitrogen at room temperature for 24 hours. Upon completion, the reaction mixture was diluted with CH₂Cl₂ (5 mL), and extracted with H₂O (1 mL), then brine (1 mL). Subsequent drying (MgSO₄) of the organic phase, and evaporation *in vacuo* resulted in a residue which was purified by flash column chromatography (1:3 Hexane: EtOAc) to yield **76** as a light yellow oil. (0.114 g, 69%), *R*_f 0.22 (1:3 Hexane:EtOAc). **¹H NMR** (500 MHz, CDCl₃) δ 7.78 (bs, 1H, Triazole-H) 5.87 (m, 2H, H₃/H₄), 5.58 (t, 1H, *J* = 9.9 Hz, H₂), 5.47 (d, 1H, *J* = 7.0 Hz, NH), 5.35 (d, 1H, *J* = 10.3 Hz, H₁), 4.67 (m, 1H, H₅), 4.59 (m, 1H, H^a), 4.48 (d, 1H, *J* = 9.7 Hz, H^b), 3.78-3.73 (m, 5H, OCH₃/CH₂-CH₂-CH₂-OH), 2.86 (m, 2H, CH₂-CH₂-CH₂-OH), 2.21 (s, 3H, CH₃, OAc), 2.04 (s, 3H, CH₃, OAc), 1.97 (m, 2H, CH₂-CH₂-CH₂-OH), 1.90 (s, 3H, CH₃, OAc), 1.46 (s, 9H, Boc-H). Exchangeable OH not detected. **¹³C NMR** (125 MHz, CDCl₃) δ 169.9 (C=O, OAc), 169.7 (C=O, OAc), 169.6 (C=O, OAc), 169.1 (C=O, COOCH₃), 164.6 (C=O), 155.2 (C=O, Boc), 148.3 (Triazole C), 120.0 (Triazole C), 85.9 (C₁), 80.5 (C(CH₃)₃), 74.6 (C₄), 70.2 (C₅), 67.8 (C₃), 67.6 (C₂), 66.1 (C^β), 61.5

(CH₂-CH₂-CH₂-OH), 52.9 (OCH₃), 52.7 (C^α), 31.6 (CH₂-CH₂-CH₂-OH), 28.2 (C(CH₃)₃), 22.0 (CH₂-CH₂-CH₂-OH), 20.6 (CH₃, OAc), 20.5 (CH₃, OAc), 20.2 (CH₃, OAc). **LRMS (ESI):** m/z 653 [M + Na]⁺

***N*^α-(Acetyl)-*N*^ε-(1-(4'-(2''-hydroxyethyl)-1',2',3'-triazol-1'-yl)-2,3,4-tri-*O*-acetyl-β-D-glucuronyl)-L-lysine methyl ester (81)**

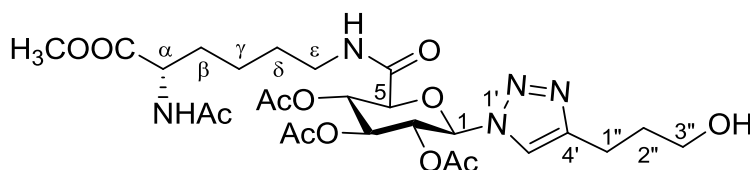


To a round bottom flask containing **68** (0.138 g, 0.261 mmol), 3-butyn-1-ol (0.067 mL, 0.073 g, 1.04 mmol), CuOAc₂·H₂O

(0.010 g, 0.052 mmol) and sodium ascorbate (0.022 g, 0.110 mmol) was added a 1:1 solution of *n*BuOH:H₂O, (0.500 mL), with the solution stirred vigorously under an atmosphere of nitrogen at room temperature for 24 hours. Upon completion, the reaction mixture was diluted with CH₂Cl₂ (5 mL), and extracted with H₂O (1 mL), then brine (1 mL). Subsequent drying (MgSO₄) of the organic phase, and evaporation *in vacuo* resulted in a residue which was purified by flash column chromatography (EtOAc) to yield **81** as a light yellow oil (0.110 g, 70%). *R*_f 0.05 (1:3 Hexane:EtOAc). **¹H NMR** (500 MHz, CDCl₃) δ 7.87 (s, 1H, Triazole-H) 6.71 (bs, 1H, NH), 6.55 (d, 1H, *J* = 7.5 Hz, NH), 5.94 (d, 1H, *J* = 9.5 Hz, H1), 5.58 (t, 1H, *J* = 9.5 Hz, H4), 5.49 (t, 1H, *J* = 9.5 Hz, H3), 5.37 (t, 1H, *J* = 9.4 Hz, H2), 4.59 (m, 1H, CH^α), 4.23 (d, 1H, *J* = 10.0 Hz, H5), 3.93 (m, 2H, CH₂-CH₂-OH), 3.74 (s, 3H, OCH₃), 3.34 (m, 1H, CH^ε), 3.11 (m, 1H, CH^ε), 2.98 (m, 2H, CH₂-CH₂-OH), 2.11-2.03 (3s, 9H, CH₃, 2 x OAc, NHAc), 1.88 (s, 3H, CH₃, OAc), 1.77 (m, 1H, CH^β), 1.68 (m, 1H, CH^β), 1.53 (m, 2H, CH^δ), 1.34 (m, 2H, CH^γ). Exchangeable OH not detected. **¹³C NMR** (125 MHz, CDCl₃)

δ 173.0 (C=O, NHAc), 170.6 (C=O, OAc), 170.0 (C=O, OAc), 169.7 (C=O, OAc),
 169.2 (C=O, COOCH₃), 165.6 (C=O), 148.3 (Triazole C), 120.6 (Triazole C), 85.1
 (C1), 75.3 (C5), 72.0 (C4), 70.2 (C3), 69.1 (C2), 61.2 (CH₂-CH₂-OH), 52.5 (OCH₃),
 51.7 (CH^ε), 38.6 (CH^α), 32.2 (CH^δ), 28.8 (CH^β), 28.3 (CH₂-CH₂-OH), 23.1(NHAc),
 22.1 (CH^γ), 20.7 (CH₃, OAc), 20.5 (CH₃, OAc), 20.2 (CH₃, OAc). **LRMS (ESI):** m/z
 622 [M + Na]⁺ **HRMS (ESI):** m/z calculated for C₂₅H₃₇N₅O₁₂Na [M + Na]⁺: 622.2336;
 Found 622.2360.

***N*^α-(Acetyl)-*N*^ε-(1-(4'-(3''-hydroxypropyl)-1',2',3'-triazol-1'-yl)-2,3,4-tri-*O*-acetyl-β-D-glucuronyl)-L-lysine methyl ester (82)**

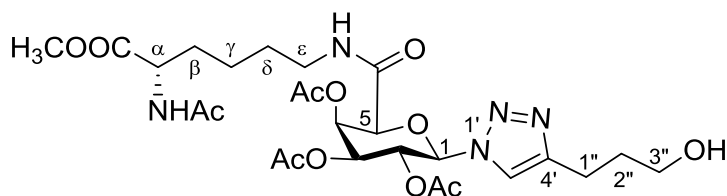


To a round bottom flask containing **68** (0.137 g, 0.261 mmol), 4-pentyn-1-ol (0.097 mL, 0.087 g,

1.04 mmol), CuOAc₂·H₂O (0.010 g, 0.052 mmol) and sodium ascorbate (0.020 g, 0.099 mmol) was added a 1:1 solution of *n*BuOH:H₂O, (0.500 mL), with the solution stirred vigorously under an atmosphere of nitrogen at room temperature for 24 hours. Upon completion, the reaction mixture was diluted with CH₂Cl₂ (5 mL), and extracted with H₂O (1 mL), then brine (1 mL). Subsequent drying (MgSO₄) of the organic phase, and evaporation *in vacuo* resulted in a residue which was purified by flash column chromatography (EtOAc) to yield **82** as a light yellow oil. (0.101 g, 63%), R_f 0.07 (1:3 Hexane:EtOAc.). ¹H NMR (500 MHz, CDCl₃) δ 7.79 (s, 1H, Triazole-H) 6.77 (bs, 1H, NH), 6.47 (bs, 1H, NH), 5.99 (d, 1H, *J* = 9.5 Hz, H1), 5.62 (t, 1H, *J* = 9.5 Hz, H4), 5.50 (t, 1H, *J* = 9.5 Hz, H3), 5.39 (t, 1H, *J* = 9.4 Hz, H2), 4.58 (m, 1H, CH^α), 4.27 (d,

1H, $J = 10.0$ Hz, H5), 3.73 (s, 3H, OCH₃), 3.67 (m, 2H, CH₂-CH₂-CH₂-OH), 3.34 (m, 1H, CH^ε), 3.11 (m, 1H, CH^ε), 2.86 (m, 2H, CH₂-CH₂-CH₂-OH), 2.11-2.02 (3s, 9H, CH₃, 2 x OAc, NHAc), 1.94 (m, 2H, CH₂-CH₂-CH₂-OH), 1.88 (s, 3H, CH₃, OAc), 1.77 (m, 1H, CH^β), 1.68 (m, 1H, CH^β), 1.53 (m, 2H, CH^δ), 1.34 (m, 2H, CH^γ). Exchangeable OH not detected. ¹³C NMR (125 MHz, CDCl₃) δ 173.0 (C=O, NHAc), 170.7 (C=O, OAc), 170.0 (C=O, OAc), 169.9 (C=O, OAc), 169.0 (C=O, COOCH₃), 165.8 (C=O), 149.8 (Triazole C), 120.1 (Triazole C), 85.1 (C1), 75.4 (C5), 72.2 (C4), 70.1 (C3), 69.2 (C2), 61.4 (CH₂-CH₂-CH₂-OH), 52.4 (OCH₃), 51.8 (CH^ε), 38.6 (CH^α), 32.1 (CH^δ), 31.6 (CH₂-CH₂-CH₂-OH), 28.5 (CH^β), 28.4 (CH₂-CH₂-CH₂-OH), 23.0 (NHAc), 22.2 (CH^γ), 20.7 (CH₃, OAc), 20.5 (CH₃, OAc), 20.2 (CH₃, OAc). **LRMS (ESI):** m/z 636 [M + Na]⁺ **HRMS (ESI):** m/z calculated for C₂₆H₃₉N₅O₁₂Na [M + Na]⁺: 636.2493; Found 636.2520.

***N*^α-(Acetyl)-*N*^ε-(1-(4'-(3''-hydroxypropyl)-1',2',3'-triazol-1'-yl)-2,3,4-tri-*O*-acetyl-β-D-galacturonyl)-L-lysine methyl ester (83)**

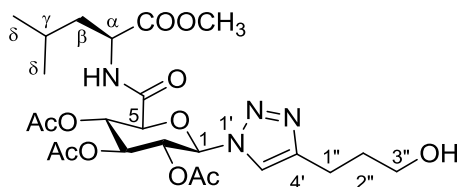


To a round bottom flask containing **69** (0.137 g, 0.261 mmol), 4-pentyn-1-ol (0.097 mL, 0.087 g, 1.04

mmol), CuOAc₂·H₂O (0.010 g, 0.052 mmol) and sodium ascorbate (0.020 g, 0.099 mmol) was added a 1:1 solution of *n*BuOH:H₂O, (0.500 mL), with the solution stirred vigorously under an atmosphere of nitrogen at room temperature for 24 hours. Upon completion, the reaction mixture was diluted with CH₂Cl₂ (5 mL), and extracted with H₂O (1 mL), then brine (1 mL). Subsequent drying (MgSO₄) of the organic phase, and evaporation *in vacuo* resulted in a residue which was purified by flash column

chromatography (EtOAc) to yield **83** as a light yellow oil. (0.121 g, 75%), R_f 0.05 (1:3 Hexane:EtOAc). $^1\text{H NMR}$ (500 MHz, CDCl_3) δ 7.73 (s, 1H, Triazole-H), 6.47 (t, 1H, $J = 6.2$ Hz NH), 6.23 (d, 1H, $J = 7.7$ Hz, NH), 5.94 (m, 2H, H4/H3), 5.65 (m 1H, H2), 5.33 (d, 1H, $J = 9.9$ Hz, H1), 4.57-4.51, (m, 2H, H5/H a), 3.72 (s, 3H, OCH_3), 3.68 (m, 2H, $\text{CH}_2\text{-CH}_2\text{-CH}_2\text{-OH}$), 3.23 (m, 2H, H e), 2.87 (m, 2H, $\text{CH}_2\text{-CH}_2\text{-CH}_2\text{-OH}$), 2.10 (s, 3H, CH_3 , NHAc), 2.01 (s, 6H, CH_3 , 2 x OAc), 1.95 (m, 2H, $\text{CH}_2\text{-CH}_2\text{-CH}_2\text{-OH}$) 1.88 (s, 3H, CH_3 , OAc), 1.81 (m, 1H, CH b), 1.68 (m, 1H, CH b), 1.50 (m, 2H, CH d), 1.32 (m, 2H, CH c). Exchangeable OH not detected. $^{13}\text{C NMR}$ (125 MHz, CDCl_3) δ 172.9 (C=O, NHAc), 170.3 (C=O, OAc), 169.7 (C=O, OAc), 169.2 (C=O, OAc), 169.1 (C=O, COOCH_3), 164.9 (C=O), 148.4 (Triazole-C), 119.9 (Triazole-C), 85.7 (C1), 76.1 (C4), 70.8 (C5), 67.7 (C2), 67.5 (C3), 61.5 ($\text{CH}_2\text{-CH}_2\text{-CH}_2\text{-OH}$), 52.4 (OCH_3), 51.9 (CH e), 38.7 (CH a), 31.9 ($\text{CH}_2\text{-CH}_2\text{-CH}_2\text{-OH}$), 31.7 (CH d), 29.0 (CH b), 23.0 (CH_3 NHAc), 22.5 (CH c), 22.0 ($\text{CH}_2\text{-CH}_2\text{-CH}_2\text{-OH}$), 20.6 (CH_3 , OAc), 20.5 (CH_3 , OAc), 20.2 (CH_3 , OAc). **LRMS (ESI):** m/z 636 $[\text{M} + \text{Na}]^+$ **HRMS (ESI):** m/z calculated for $\text{C}_{26}\text{H}_{39}\text{N}_5\text{O}_{12}\text{Na} [\text{M} + \text{Na}]^+$: 636.2493; Found 636.2493.

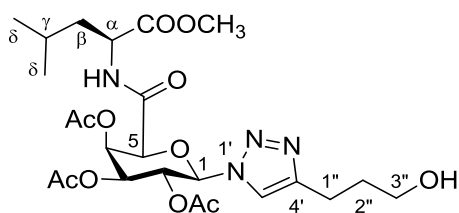
***N*-(1-(4'-(3''-Hydroxypropyl)-1',2',3'-triazol-1'-yl)-2,3,4-tri-*O*-acetyl- β -D-glucuronoyl)-L-leucine methyl ester (**84**)**



To a round bottom flask containing **70** (0.123 g, 0.261 mmol), 4-pentyn-1-ol (0.097 mL, 0.087 g, 1.04 mmol), $\text{CuOAc}_2 \cdot \text{H}_2\text{O}$ (0.010 g, 0.052 mmol) and sodium ascorbate (0.020 g, 0.099 mmol) was added a 1:1 solution of $n\text{BuOH}:\text{H}_2\text{O}$, (0.500 mL), with the solution stirred vigorously under an atmosphere of nitrogen at room temperature for 24 hours.

Upon completion, the reaction mixture was diluted with CH_2Cl_2 (5 mL), and extracted with H_2O (1 mL), then brine (1 mL). Subsequent drying (MgSO_4) of the organic phase, and evaporation *in vacuo* resulted in a residue which was purified by flash column chromatography (1:2 Hexane: EtOAc) to yield **84** as a light yellow solid. (0.116 g, 80%), M.p. 132-133°C, R_f 0.10 (1:2 Hexane:EtOAc.). $^1\text{H NMR}$ (500 MHz, CD_3OD) δ 8.10 (s, 1H, triazole-H), 6.16 (d, 1H, $J = 8.9$ Hz, H1), 5.62-5.44 (2t (overlapping), 2H, $J = 9.2$ Hz, H4/H3), 5.39 (t, 1H, $J = 9.7$ Hz, H2), 4.46 (m, 2H, H5/H a), 3.67 (s, 3H, OCH_3), 3.57 (m, 2H, $\text{CH}_2\text{-CH}_2\text{-CH}_2\text{-OH}$), 2.79 (m, 2H, $\text{CH}_2\text{-CH}_2\text{-CH}_2\text{-OH}$), 2.05 (s, 3H, CH_3 , OAc), 2.00 (2s, 6H, CH_3 , 2 x OAc), 1.87 (m, 2H, $\text{CH}_2\text{-CH}_2\text{-CH}_2\text{-OH}$), 1.65-1.59 (m, 3H, H $^\beta$ /H $^\gamma$), 0.90 (m, 6H, 2 x CH_3 , H $^\delta$). Exchangeable OH not detected. $^{13}\text{C NMR}$ (125 MHz, CD_3OD) δ 172.7 (C=O, COOCH_3), 170.3 (C=O, OAc), 169.8 (C=O, OAc), 169.1 (C=O, OAc), 167.0 (C=O), 148.4 (Triazole C), 121.3 (Triazole C), 5.3 (C1), 75.4 (C5), 72.6 (C4), 70.5 (C3), 69.4 (C2), 60.7 ($\text{CH}_2\text{-CH}_2\text{-CH}_2\text{-OH}$), 51.6 (C a), 50.9 (OCH_3), 40.1 (C $^\beta$), 31.9 ($\text{CH}_2\text{-CH}_2\text{-CH}_2\text{-OH}$), 24.7 (C $^\gamma$), 22.1 (C $^\delta$), 21.5 ($\text{CH}_2\text{-CH}_2\text{-CH}_2\text{-OH}$), 20.7 (C $^\delta$), 19.5 (CH_3 , OAc), 19.3 (CH_3 , OAc), 18.9 (CH_3 , OAc). **LRMS (ESI):** m/z 579 $[\text{M} + \text{Na}]^+$, **HRMS (ESI):** m/z calculated for $\text{C}_{24}\text{H}_{36}\text{N}_4\text{O}_{11}\text{Na}$ $[\text{M} + \text{Na}]^+$: 579.2278; Found 579.2271.

***N*-(1-(4'-(3''-Hydroxypropyl)-1',2',3'-triazol-1'-yl)-2,3,4-tri-*O*-acetyl- β -D-galacturonoyl)-L-leucine methyl ester (**85**)**

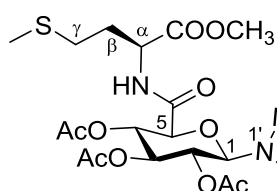


To a round bottom flask containing **71** (0.122 g, 0.261 mmol), 4-pentyn-1-ol (0.097 mL, 0.087 g, 1.04 mmol), $\text{CuOAc}_2 \cdot \text{H}_2\text{O}$ (0.010 g, 0.052 mmol) and sodium ascorbate

(0.020 g, 0.099 mmol) was added a 1:1 solution of *n*BuOH: H_2O , (0.500 mL), with the

solution stirred vigorously under an atmosphere of nitrogen at room temperature for 24 hours. Upon completion, the reaction mixture was diluted with CH₂Cl₂ (5 mL), and extracted with H₂O (1 mL), then brine (1 mL). Subsequent drying (MgSO₄) of the organic phase, and evaporation *in vacuo* resulted in a residue which was purified by flash column chromatography (1:2 Hexane: EtOAc) to yield **85** as a light yellow oil. (0.109 g, 75%), R_f 0.12 (1:2 Hexane:EtOAc.). ¹H NMR (500 MHz, CDCl₃) δ 7.68 (s, 1H, Triazole-H), 6.72 (d, 1H, *J* = 8.4 Hz, NH), 5.95 (m, 2H, H₄/H₃), 5.65 (t, 1H, *J* = 9.7 Hz, H₂), 5.36 (d, 1H, *J* = 10.1 Hz, H₁), 4.62 (m, 1H, H^α), 4.59 (m, 1H, H₅), 3.76 (t, 2H, *J* = 6.0 Hz, CH₂-CH₂-CH₂-OH), 3.69 (s, 3H, OCH₃), 2.88 (t, 2H, *J* = 7.1 Hz, CH₂-CH₂-CH₂-OH), 2.32 (t, 2H, *J* = 2.1 Hz, 7.3 Hz, CH₂-CH₂-CH₂-OH) 2.13 – 1.88 (3s, 9H, CH₃, 3 x OAc), 1.65 – 1.55 (m, 3H, H^β/ H^γ), 0.94 (m, 6H, 2CH₃, H^δ). Exchangeable OH not detected. ¹³C NMR (125 MHz, CDCl₃) δ 172.7 (C=O, COOCH₃), 169.6 (C=O, OAc), 169.1(C=O, OAc), 169.1(C=O, OAc), 164.5 (C=O), 148.4 (Triazole-C), 119.9 (Triazole-C) 85.7 (C₁), 76.2 (C₄), 70.7 (C₅), 67.7 (C₂), 67.5 (C₃), 61.5 (CH₂-CH₂-CH₂-OH), 52.5 (OCH₃), 50.5 (C^α), 41.1 (C^β), 31.7 (CH₂-CH₂-CH₂-OH), 24.9 (C^γ), 22.8 (C^δ), 22.0 (C^{δ'}) 21.7 (CH₂-CH₂-CH₂-OH), 20.5 (CH₃, OAc), 20.5 (CH₃, OAc), 20.2 (CH₃, OAc). LRMS (ESI): *m/z* 579 [M + Na]⁺ HRMS (ESI): *m/z* calculated for C₂₄H₃₆N₄O₁₁Na [M + Na]⁺: 579.2278; Found 579.2274.

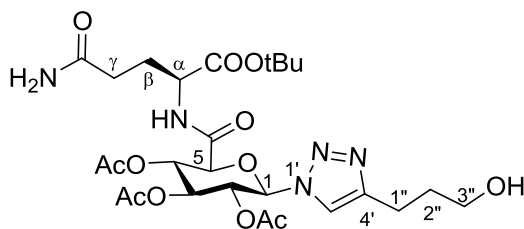
***N*-(1-(4'-(3''-Hydroxypropyl)-1',2',3'-triazol-1'-yl)-2,3,4-tri-*O*-acetyl-β-D-glucuronoyl)-L-methionine methyl ester (**86**)**



To a round bottom flask containing **72** (0.129 g, 0.261 mmol), 4-pentyn-1-ol (0.097 mL, 0.087 g, 1.04 mmol),

CuOAc₂·H₂O (0.010 g, 0.052 mmol) and sodium ascorbate (0.020 g, 0.099 mmol) was added a 1:1 solution of *n*BuOH:H₂O, (0.500 mL), with the solution stirred vigorously under an atmosphere of nitrogen at room temperature for 24 hours. Upon completion, the reaction mixture was diluted with CH₂Cl₂ (5 mL), and extracted with H₂O (1 mL), then brine (1 mL). Subsequent drying (MgSO₄) of the organic phase, and evaporation *in vacuo* resulted in a residue which was purified by flash column chromatography (1:3 Hexane:EtOAc.) to yield **86** as a white solid. (0.128 g, 85%), M.p. 132-133°C R_f 0.10 (1:3 Hexane:EtOAc.). **¹H NMR** (500 MHz, CDCl₃) δ 7.63 (s, 1H, Triazole-H), 7.06 (d, 1H, *J* = 7.6 Hz, NH), 5.94 (d, 1H, *J* = 9.5 Hz, H¹), 5.55 (t, 1H, *J* = 9.7 Hz, H³), 5.48 (t, 1H, *J* = 9.7 Hz, H⁴), 5.35 (t, 1H, *J* = 9.7 Hz, H²), 4.64 (m, 1H, H^α), 4.23 (d, 1H, *J* = 10.0 Hz, H⁵), 3.73 (s, 3H, OCH₃), 3.68 (t, 2H, *J* = 7.2 Hz, CH₂CH₂CH₂OH), 2.86 (t, 2H, *J* = 7.3 Hz, CH₂CH₂CH₂OH), 2.51 (t, 1H, *J* = 7.2 Hz, H^γ), 2.19-2.15 (m, 2H, H^β), 2.09-2.04 (2s, 9H, CH₃, 3 x OAc), 2.04-1.99, (m, 2H, CH₂CH₂CH₂OH), 1.89 (s, 3H, SCH₃). Exchangeable OH not detected. **¹³C NMR** (125 MHz, CD₃OD) δ 173.1 (COOCH₃), 171.4 (C=O, OAc), 171.0 (C=O, OAc), 170.2 (C=O, OAc), 168.2 (C=O), 149.9 (Triazole-C), 122.6 (Triazole-C), 86.3 (C¹), 76.4 (C⁵), 73.6 (C²), 71.6 (C⁴), 70.5 (C³), 61.8 (CH₂-CH₂-CH₂-OH), 53.0 (C^α), 52.6 (-OCH₃), 33.0 (C^β), (CH₂-CH₂-CH₂-OH) 31.0 (C^γ), 22.7 (CH₂-CH₂-CH₂-OH), 20.7 (CH₃, OAc), 20.5 (CH₃, OAc), 20.1 (CH₃, OAc), 15.2 (SCH₃). **LRMS (ESI):** *m/z* 597 [M + Na]⁺ **HRMS (ESI):** *m/z* calculated for C₂₃H₃₄N₄O₁₁SNa [M + Na]⁺: 597.1842; Found 597.1857.

***N*-(1-(4'-(3''-Hydroxypropyl)-1',2',3'-triazol-1'-yl)-2,3,4-tri-*O*-acetyl- β -D-glucuronoyl)-L-glutamine *tert*-butyl ester (87)**

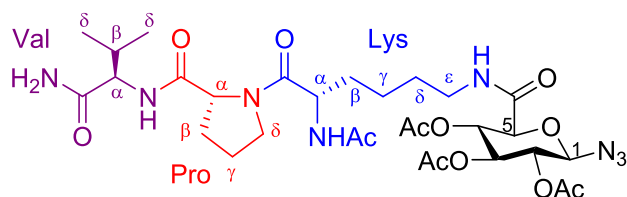


To a round bottom flask containing **73** (0.137 g, 0.260 mmol), 4-pentyn-1-ol (0.097 mL, 0.087 g, 1.04 mmol), CuOAc₂·H₂O (0.010 g, 0.052 mmol) and

sodium ascorbate (0.020 g, 0.099 mmol) was added a 1:1 solution of *n*BuOH:H₂O, (0.500 mL), with the solution stirred vigorously under an atmosphere of nitrogen at room temperature for 24 hours. Upon completion, the reaction mixture was diluted with CH₂Cl₂ (5 mL), and extracted with H₂O (1 mL), then brine (1 mL). Subsequent drying (MgSO₄) of the organic phase, and evaporation *in vacuo* resulted in a residue which was purified by flash column chromatography (EtOAc) to yield **76** as a light yellow foam. (0.101 g, 63%), R_f 0.05 (1:3 Hexane:EtOAc). ¹H NMR (500 MHz, CD₃OD) δ 8.4 (d, 1H, *J* = 7.8 Hz, NH), 8.15 (s, 1H, Triazole-H), 6.16 (d, 1H, *J* = 8.4 Hz, H1), 5.58 (m, 2H, H3/H4), 5.37 (t, 1H, *J* = 8.9 Hz, H2), 4.45 (d, 1H, *J* = 10.0 Hz, H5), 4.27 (m, 1H, H^a), 3.58 (m, 2H, CH₂-CH₂-CH₂-OH), 2.79 (m, 2H, CH₂-CH₂-CH₂-OH), 2.34-2.26 (m, 2H, H^γ), 2.16-1.93 (m, 2H, H^β), 2.05, 2.00 (s, 6H, 2x OAc), 1.89-1.86 (m, 2H, CH₂-CH₂-OH), 1.83 (s, 3H, OAc), 1.43 (s, 9H, OtBu). Exchangeable OH not detected. ¹³C NMR (125 MHz, CDCl₃) δ 177.6 (CONH₂), 171.7 (C=O, OAc), 171.4 (C=O, OAc), 171.4 (C=O, OAc), 170.4 (COOtBu), 168.3 (C=O), 149.6 (Triazole-C), 122.6 (Triazole C), 86.2 (C1), 83.3 (C(CH₃)₃), 76.3 (C5), 73.4 (C2), 71.7 (C4), 70.6 (C3), 61.8 (CH₂-CH₂-CH₂-OH), 54.0 (C^a), 33.0 (CH₂-CH₂-CH₂-OH), 33.0 (C^γ), 31.3 (C^β), 28.2 (C(CH₃)₃), 22.6 (CH₂-CH₂-CH₂-OH), 20.8 (CH₃, OAc), 20.5 (CH₃, OAc),

20.1 (CH₃, OAc). **LRMS (ESI):** m/z 636 [M + Na]⁺ **HRMS (ESI):** m/z calculated for C₂₆H₃₉N₅O₁₂Na [M + Na]⁺: 636.2493; Found 636.2501

***N*^α-Acetyl-*N*^ε-(1-azido-2,3,4-tri-*O*-acetyl-β-*D*-glucuronoyl)-*L*-lysine-*L*-proline-*L*-valinamide (**88**)**



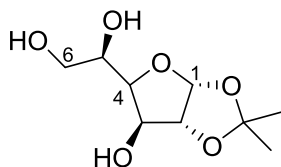
60 (0.041 g, 0.119 mmol), Ac.Lys.Pro.Val.NH₂.HCl (0.050 g, 0.119 mmol) and HBTU (0.068 g, 0.178 mmol) were

dissolved in DMF (1 mL), and the solution was cooled to 0°C. DIPEA (0.228 mL, 0.017 g, 0.131 mmol) was added dropwise to the solution, and the reaction mixture was allowed to warm to room temperature and stir for 24 hours. Upon completion, the reaction mixture was diluted with EtOAc (5 mL), and extracted with H₂O (2 x 1 mL). The organic phase was dried and evaporated, with the following residue purified by flash column chromatography (EtOAc) to produce **88** as a light yellow foam (0.049 g, 53%), R_f 0.29 (EtOAc.). **¹H NMR** (500 MHz, CDCl₃) δ 6.89 (m, 2H, NH₂), 6.83 (m, 1H, NH), 6.44 (m, 1H, NH), 5.98 (m, 1H, NH), 5.27 (m, 2H, H₃/H₄), 4.97 (m, 1H, H₂), 4.78 (d, 1H, *J* = 8.8 Hz, H₁), 4.75 (m, 1H, C^αPro), 4.47 (m, 1H, C^αLys), 4.31 (t, 1H, *J* = 6.1 Hz, C^αVal), 4.04 (m, 1H, H₅), 3.80 (m, 1H, C^δPro), 3.67 (m, 1H, C^δPro), 3.38 (m, 1H, C^εLys), 3.05 (m, 1H, C^εLys), 2.16 (m, 1H, H^βVal), 2.11 (m, 2H, H^βLys), 2.07-1.99 (4s, 12H, CH₃, 3 x Ac/NHAc), 1.72 (m, 2H, H^βPro), 1.50 (m, 2H, H^δLys), 1.38 (m, 2H, H^γPro), 1.25 (m, 2H, H^γLys), 0.95 (2q, 6H, *J* = 6.5 Hz, 2 x CH₃). **¹³C NMR** (125 MHz, CDCl₃) δ 173.9 (C=O, CONH₂), 172.5 (C=O, NHAc), 171.8 (C=O, CONH), 170.6 (C=O, CONH), 170.1 (C=O, OAc), 170.1 (C=O, OAc), 169.6 (C=O, OAc), 166.4

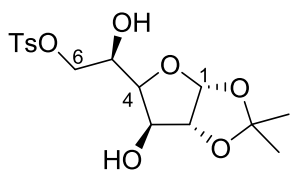
(C=O), 88.3 (C1), 75.2 (C5), 72.2 (C4), 70.7 (C2), 69.6 (C3), 61.0 (C^αLys), 58.4 (C^αVal), 50.9 (C^αPro), 47.9 (C^εLys), 38.9 (C^δPro), 32.2 (C^βPro), 31.2 (C^βVal), 29.5 (C^γLys), 28.7 (C^δLys), 25.5 (C^βLys), 23.3 (CH₃, NHAc), 22.1 (C^γPro), 20.9 (CH₃, OAc), 20.8 (CH₃, OAc), 20.7 (CH₃, OAc), 19.5 (C^γVal), 18.0 (C^γVal). **LRMS (ESI):** m/z 733 [M + Na]⁺

7.3 Chapter 3 Experimental Data:

1,2-Isopropylidene- α -D-glucofuranose (**94**)

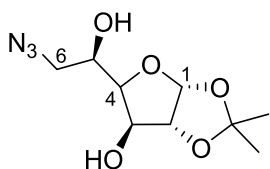


According to the method of Monrad and Madsen,¹⁹⁰ a round bottom flask containing 1,2:5,6-di-isopropylidene- α -D-glucofuranose (**93**, 5.00 g, 19.2 mmol) was added a solution of 70% acetic acid (80 mL), and the reaction was stirred at room temperature for 24 hours. Upon completion, the solvent was evaporated *in vacuo*, with addition of water (50 mL) and azeotropic distillation resulting in **94** as a flaky white solid. (3.82 g, 90%), M.p. 157-160°C (Lit. 157-160°C)¹⁹⁰ **¹H NMR** (500 MHz, D₂O) δ 5.90 (d, 1H, J = 3.7 Hz, H1), 4.58 (d, 1H, J = 3.7 Hz, H3), 4.20 (d, 1H, J = 2.0 Hz, H2), 3.98 (dd, 1H, J = 2.5, 9.0 Hz, H4), 3.80 (m, 1H, H5), 3.70 (ddd, 1H J = 1.3 Hz, 2.7 Hz, 12.0 Hz, H6), 3.53 (ddd, 1H, J = 1.3 Hz, 6.0 Hz, 12.1 Hz, H6'), 1.41 (s, 3H, CH₃), 1.26 (s, 3H, CH₃). **¹³C NMR** (125 MHz, D₂O) δ 113.5 (CH(CH₃)₂), 105.6 (C1), 85.3 (C4), 80.6 (C2), 74.5 (C3), 69.3 (C5), 64.4 (C6), 26.4 (CH₃), 26.0 (CH₃). **LRMS (ESI):** m/z 255 [M + Cl]⁻ **HRMS (ESI):** m/z calculated for C₉H₁₆O₆Cl [M + Cl]⁻: 255.0635; Found 255.0625.

6-*p*-Toluenesulfonyl-1,2-isopropylidene- α -D-glucofuranose (95)

To a round bottom flask containing **94** (3.00 g, 13.62 mmol) was added pyridine (30 mL), and the mixture was cooled to 0°C. Under stirring, *p*-toluenesulfonyl chloride (3.12 g, 16.34 mmol) was added to the solution portionwise, with the

reaction mixture allowed to warm to room temperature and stir for an additional 18 hours. Upon completion, the reaction mixture was evaporated *in vacuo*. The resulting slurry was subject to recrystallization from ethanol, to produce **95** as an amorphous white solid. (3.77 g, 73%), R_f 0.29 (1:1 Hexane:EtOAc). **^1H NMR** (500 MHz, CDCl_3) δ 7.79 (d, 2H, J = 7.9 Hz, Ar-H), 7.33 (d, 2H, J = 7.9 Hz, Ar-H), 5.88 (m, 1H, H1), 4.50 (m, 1H, H2), 4.34 (m, 1H, H3), 4.28 (d, 1H, J = 9.5 Hz, H4), 4.19 (m, 1H, H5), 4.11 (m, 1H, H6), 4.01 (m, 1H, H6'), 2.43 (s, 3H, Ar-CH₃), 1.45 (s, 3H, CH₃), 1.29 (s, 3H, CH₃). **^{13}C NMR** (125 MHz, CDCl_3) δ 148.9 (Ar-C1), 145.1 (Ar-C4), 130.0 (Ar-C3/C5), 128.0 (Ar-C2/C6), 111.9 (CH(CH₃)₂), 105.1 (C1), 85.1 (C4), 79.3 (C2), 74.7 (C3), 72.4 (C5), 67.6 (C6), 26.8 (CH₃), 26.2 (CH₃), 21.6 (Ar-CH₃). **LRMS (ESI):** m/z 409 [M + Cl]⁻

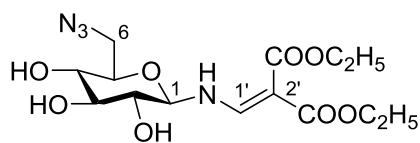
6-Azido-6-deoxy-1,2-isopropylidene- α -D-glucofuranose (96)

To a round bottom flask containing **95** (3.00 g, 8.01 mmol), was added NaN₃ (2.08 g, 32.04 mmol). The solids suspended in DMF (30 mL), and stirred under an argon atmosphere at 40°C for 72 hours. Upon completion, the reaction mixture was diluted

with ethyl acetate (50 mL), and washed with water (2 x 25 mL). Subsequently, the

aqueous phases was washed with ethyl acetate (3 x 50 mL), and the combined organic fractions were dried (MgSO₄) and evaporated *in vacuo*. Flash column chromatography (2:1 Hexane: EtOAc) of the mixture yielded the product **96** as a fine white solid, (1.46 g, 74%), M.p. 98-99°C (Lit. 104°C)²⁵⁰ R_f 0.45 (1:1 Hexane:EtOAc.). **¹H NMR** (500 MHz, CDCl₃) δ 5.94 (d, 1H, *J* = 7.6 Hz, H1), 4.53 (d, 1H, *J* = 3.7 Hz, H3), 4.36 (m, 1H, H2), 4.15 (m, 1H, H5), 3.80 (dd, 1H, *J* = 2.3 Hz, 6.6 Hz, H4), 3.59-3.54 (m, 2H, H6/H6'), 3.30 (bs, 1H, OH), 3.13 (bs, 1H, OH), 1.49 (s, 3H, CH₃), 1.32 (s, 3H, CH₃). **¹³C NMR** (125 MHz, CDCl₃) δ 112.0 (CH(CH₃)₂), 104.9 (C1), 85.2 (C4), 79.7 (C2), 75.3 (C3), 69.43 (C5), 54.0 (C6), 26.8 (CH₃), 26.2 (CH₃). **LRMS (ESI):** *m/z* 280 [M + Cl]⁻ **HRMS (ESI):** *m/z* calculated for C₉H₁₅N₃O₅Cl [M + Cl]⁻: 280.0700; Found 280.0710.

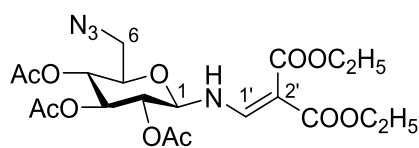
6-Azido-6-deoxy-1-amino-*N*-(2',2'-diethoxycarbonylvinyl)-β-D-glucose (101)



In a round bottom flask, **96** (1.00 g, 4.08 mmol) was dissolved in 80% acetic acid (20 mL). The mixture was heated to 80°C, and stirred for 18 hours. After this period, the reaction mixture was cooled to room temperature, and the solvent removed *in vacuo* using water as an azeotrope. The resulting oil was then re-dissolved in a saturated solution of NH₄HCO₃ (50 mL), and stirred at 40°C for a further 4 days. Additional solid NH₄HCO₃ (2 g) was added to the reaction mixture every 24 hours to maintain saturation. Upon completion monitored using LR-ESIMS, the reaction mixture was evaporated to half volume at 20°C and then subject to lyophilisation overnight. The resultant foam was resuspended in MeOH (10 mL), and diethyl ethoxymethylenemalonate (1.24 mL, 1.32 g, 6.12 mmol) was added and allowed to stir

at room temperature for 48 hours. Upon completion, the reaction mixture was evaporated to dryness, and the residue subject to column chromatography (45:5:3 EtOAc/EtOH/H₂O), producing **101** as a colourless oil. (0.809 g, 53%), *R_f* 0.54 (45:5:3 EtOAc/EtOH/H₂O). ¹H NMR (500 MHz, CD₃OD) δ 9.40 (m, 1H, NH), 8.22 (d, 1H, *J* = 13.7 Hz, CH=C), 4.57 (t, 1H, *J* = 8.3 Hz, H1), 4.28-4.10 (2q, 4H, *J* = 7.0 Hz, 2 x CH₂CH₃), 3.62 (m, 1H, H3), 3.57 (m, 1H, H4), 3.49-3.31 (m, 4H, H6/H6'/H2/H5), 1.28 (t, 6H, *J* = 7.1 Hz, CH₂CH₃). ¹³C NMR (125 MHz, CDCl₃) δ 168.1 (C=O), 166.3 (C=O), 158.5 (CH=C), 91.6 (CH=C), 88.2 (C1), 77.3 (C4), 76.7 (C5), 73.2 (C2), 70.4 (C3), 59.7 (C6), 51.1 (CH₂CH₃), 13.3 (CH₂CH₃). LRMS (ESI): *m/z* 409 [M + Cl]⁻. HRMS (ESI): *m/z* calculated for C₁₄H₂₂N₄O₈Cl [M + Cl]⁻: 409.1126; Found 409.1120. Data gained in the production of this compound was not consistent with that published elsewhere.¹⁸⁷

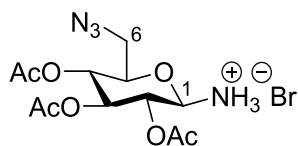
6-Azido-6-deoxy-1-amino-*N*-(2',2'-diethoxycarbonylvinyl)-2,3,4-tri-*O*-acetyl-β-D-glucose (**102**)



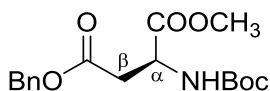
To a round bottom flask containing **101** (0.400 g, 1.07 mmol), was added acetic anhydride (10 mL) and pyridine (10 mL), and the reaction mixture was stirred at room temperature for 2 hours. Upon completion, the reaction mixture was evaporated to dryness, with flash column chromatography (2:1 Hexane: EtOAc) of the crude mixture producing **102** as a white solid. (0.491 g, 92%), M.p. 88-91°C, *R_f* 0.75 (1:1 Hexane:EtOAc). ¹H NMR (500 MHz, CDCl₃) δ 9.22 (m, 1H, NH), 7.94 (d, 1H, *J* = 13.7 Hz, CH=C), 5.29 (t, 1H, *J* = 9.3 Hz, H3), 5.06 (t, 1H, *J* = 9.5 Hz, H2), 5.04 (t, 1H, *J* = 9.5 Hz, H4), 4.59 (t, 1H, *J* = 8.5 Hz, H1) 4.26-4.18 (2q, 4H, *J* = 7.1 Hz, 2 x

CH₂CH₃), 3.77 (m, 1H, H5), 3.38 (m, 2H, H6/H6'), 2.08-2.03 (3s, 9H, CH₃, 3 x OAc), 1.30 (t, 6H, $J = 7.1$ Hz, CH₂CH₃). ¹³C NMR (125 MHz, CDCl₃) δ 170.1 (C=O, OAc), 169.6 (C=O, OAc), 169.4 (C=O, OAc), 167.6 (C=O), 165.5 (C=O), 157.2 (CH=C), 95.2 (CH=C), 86.9 (C1), 75.0 (C5), 72.4 (C3), 70.5 (C2), 69.2 (C4), 60.4 (CH₂CH₃), 60.2 (CH₂CH₃), 50.8 (C6), 20.6 (CH₃, OAc), 20.6 (CH₃, OAc), 20.5 (CH₃, OAc), 14.4 (CH₂CH₃), 14.2 (CH₂CH₃). **LRMS (ESI):** m/z 523 [M + Na]⁺ **HRMS (ESI):** m/z calculated for C₂₀H₂₈N₄O₁₁Na [M + Na]⁺: 523.1652; Found 523.1663.

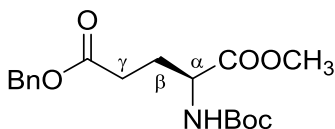
6-Azido-6-deoxy-1-amino-2,3,4-tri-*O*-acetyl-β-D-glucose hydrobromide (**103**)



In a round bottom flask, **100** (0.300 g 0.60 mmol) was dissolved in CH₂Cl₂ (5 mL) and cooled to 0°C. Br₂ (0.060 mL, 0.186 g, 1.16 mmol) was then added dropwise, followed by the addition of H₂O (0.20 mL) and the reaction mixture was stirred at 0°C for 1 hour. Upon completion, the reaction mixture was evaporated *in vacuo*, resulting in an orange residue. Subsequent trituration and storage of the residue at -20°C overnight in diethyl ether (5 mL) resulted in the isolation of **103** as an orange solid. (0.181 g, 73%), ¹H NMR (500 MHz, CD₃OD) δ 5.36 (t, 1H, $J = 9.5$ Hz, H3), 5.12 (m, 2H, H2/H4) 5.02 (m, 1H, H1), 4.09 (m, 1H, H5), 3.60 (m, 1H, H6), 3.42 (m, 1H, H6'), 2.09-1.98 (3s, 9H, 3 x OAc). ¹³C NMR (125 MHz, CD₃OD) δ 171.4 (C=O, OAc), 171.3 (C=O, OAc), 171.1 (C=O, OAc), 80.5 (C1), 76.3 (C5), 73.6 (C3), 71.3 (C2), 69.5 (C4), 51.6 (C6), 20.6 (CH₃, OAc), 20.5 (CH₃, OAc), 20.4 (CH₃, OAc). **LRMS (ESI):** m/z 331 [M + H-Br]⁺

***N*-(*tert*-Butoxycarbonyl)-4-benzyl-L-aspartic acid, methyl ester (106)**

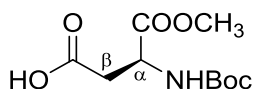
To a round bottom flask containing BocAsp.(OBn).OH (**104**, 0.648 g, 2.00 mmol) and THF (10 mL) was added K₂CO₃ (1.106 g, 8.00 mmol), and the solution was allowed to cool to 0°C under stirring. MeI (0.182 mL, 0.415 g, 3.00 mmol) was added dropwise to the solution, and stirred for 30 minutes at 0°C, before warming to room temperature. After 18 hours, the reaction was diluted with THF (10 mL), and washed with sat. NaHCO₃ solution (10 mL) and brine (10 mL). The organic phases were dried (MgSO₄) and evaporated *in vacuo*, with recrystallization from EtOH/Hexanes producing **106** as a white solid. (0.576 g, 85%), M.p 64-66°C. (Lit. 61-62°C)²⁵¹ R_f 0.90 (1:1 Hexane:EtOAc.). ¹H NMR (500 MHz, CDCl₃) δ 7.35 (m, 5H, Ar-H), 5.49 (d, 1H, *J* = 7.6 Hz, NH), 5.13 (s, 2H, CH₂Ph), 4.59 (m, 1H, H^α), 3.70 (s, 3H, OCH₃), 3.03 (dd, 1H, *J* = 3.6 Hz, 16.7 Hz, H^β), 2.86 (dd, 1H, *J* = 3.6 Hz, 16.7 Hz, H^{β'}), 1.44 (s, 9 H, Boc-H). ¹³C NMR (125 MHz, CDCl₃) δ 171.7 (C=O, OBn), 171.1 (C=O, OBn), 155.8 (C=O, Boc), 135.6 (Ar-C1), 128.8 (Ar-C), 128.6 (Ar-C), 128.5 (Ar-C), 80.4 (CCH₃), 67.0 (CH₂Ph), 52.9 (C^α), 50.2 (OCH₃), 37.1 (C^β), 28.5 (CCH₃). LRMS (ESI): *m/z* 360 [M + Na]⁺ HRMS (ESI): *m/z* calculated for C₁₇H₂₃NO₆Na [M + Na]⁺: 360.1423; Found 360.1430.

***N*-(*tert*-Butoxycarbonyl)-5-benzyl-L-glutamic acid, methyl ester (107)**

To a round bottom flask containing BocGlu.(OBn).OH (**105**, 0.671 g, 1.99 mmol) and THF (10 mL) was added K₂CO₃ (1.106 g, 8.00 mmol), and the solution was

allowed to cool to 0°C under stirring. MeI (0.182 mL, 0.415 g, 3.00 mmol) was added dropwise to the solution, and stirred for 30 minutes at 0°C, before warming to room temperature. After 18 hours, the reaction was diluted with THF (10 mL), and washed with sat. NaHCO₃ solution (10 mL) and brine (10 mL). The organic phases were dried (MgSO₄) and evaporated *in vacuo*, with recrystallization from EtOH/Hexanes producing **107** as a white solid. (0.644 g, 92%), M.p. 42-45°C (Lit 38-41°C),²⁵² R_f 0.85 (1:1 Hexane:EtOAc.). ¹H NMR (500 MHz, DMSO-*d*₆) δ 7.39 - 7.28 (m, 5H, Ar-H), 5.09 (s, 2H, CH₂Ph), 4.02 - 3.90 (m, 1H, H_α), 3.62 (s, 3H, OCH₃), 2.47 - 2.42 (m, 2H, H_γ), 2.02 - 1.94 (m, 1H, H_β), 1.86 - 1.76 (m, 1H, H_β), 1.37 (s, 9 H, Boc-H). ¹³C NMR (125 MHz, DMSO-*d*₆) δ 172.6 (C=O), 172.1 (C=O), 155.5 (C=O, Boc), 136.2 (Ar-C1), 128.4 (Ar-C), 128.0 (Ar-C), 127.9 (Ar-C), 78.3 (CCH₃), 65.5 (CH₂Ph), 52.6 (C_α), 51.8 (OCH₃), 29.9 (C_γ), 28.1 (C_β), 25.9 (CCH₃). LRMS (ESI): *m/z* 374 [M + Na]⁺ HRMS (ESI): *m/z* calculated for C₁₈H₂₅NO₆Na [M + Na]⁺: 374.1580; Found 374.1572.

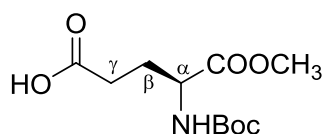
N-(*tert*-Butoxycarbonyl)- L-aspartic acid, methyl ester (**108**)



To a round bottom flask containing **106** (0.400 g, 1.19 mmol) dissolved in THF (10 mL), 10% palladium on carbon (0.100 g) was added. The reaction mixture was placed under an atmosphere of H₂ gas, and stirred for 18 hours. Upon completion, the H₂ atmosphere was removed, and the reaction mixture was filtered through a pad of Celite, with the pad washed with EtOAc (4 x 20 mL). Subsequent evaporation to dryness of the filtrate resulted in the isolation of **108** as an off-white solid. (0.248 g, 84%), M.p. 80-82°C (Lit. 79-81°C).²⁵³ ¹H NMR (500 MHz, CD₃OD) δ 4.48 (m, 1H, H^α), 3.71 (s, 3H, OCH₃), 2.80-2.72 (m, 1H, H^β), 1.43 (s, 9H, Boc-H). ¹³C NMR (125 MHz, CD₃OD) δ

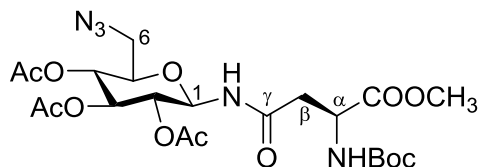
172.7 (C=O, COOH), 172.1 (C=O, COOCH₃), 156.3 (C=O, NHBoc), 79.4 (C(CH₃)₃), 51.5 (C^α), 50.1 (OCH₃), 30.1 (C^γ), 35.8 (C^β), 27.2 (C(CH₃)₃). **LRMS (ESI):** m/z 270 [M + Na]⁺ **HRMS (ESI):** m/z calculated for C₁₀H₁₇NO₆Na [M + Na]⁺: 270.0954; Found 270.0962.

N-(*tert*-Butoxycarbonyl)- L-glutamic acid, methyl ester (**109**)



To a round bottom flask containing **107** (0.450 g, 1.28 mmol) dissolved in THF (10 mL), 10% Palladium on carbon (0.120 g) was added. The reaction mixture was then subject to an atmosphere of H₂ gas, and stirred for 18 hours. Upon completion, the H₂ atmosphere was removed, and the reaction mixture was filtered through a pad of Celite, with the pad washed with EtOAc (4 x 20 mL). Subsequent evaporation to dryness of the filtrate resulted in the isolation of **109** as an off-white solid. (0.288 g, 86%), M.p. 41-42°C (Lit. 42-45°C).²⁵² **¹H NMR** (500 MHz, CDCl₃) δ 5.17 (d, 1H, J = 7.1 Hz, NH), 4.36 (m, 1H, H^α), 3.74 (s, 3H, OCH₃), 2.52-2.35 (m, 1H, H^γ), 2.21-2.15 (m, 1H, H^β), 2.01-1.90 (m, 1H, H^{β'}), 1.43 (s, 9H, Boc-H). **¹³C NMR** (125 MHz, CDCl₃) δ 177.7 (C=O, COOH), 173.8 (C=O, COOCH₃), 155.8 (C=O, NHBoc), 80.3 (C(CH₃)₃), 52.8 (C^α), 52.5 (OCH₃), 30.1 (C^γ), 28.3 (C(CH₃)₃), 27.7 (C^β). **LRMS (ESI):** m/z 284 [M + Na]⁺ **HRMS (ESI):** m/z calculated for C₁₁H₁₉NO₆Na [M + Na]⁺: 284.1110; Found 284.1124.

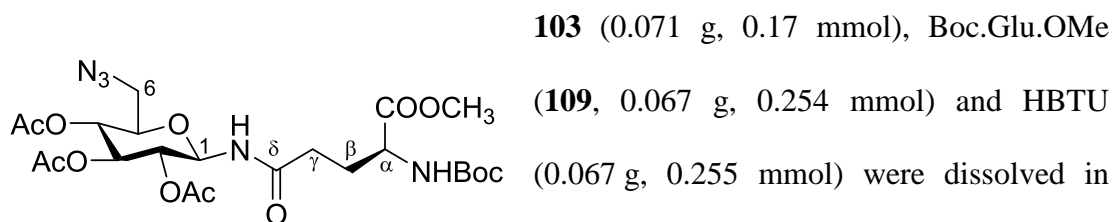
***N*^α-(*tert*-Butoxycarbonyl)-*N*^γ-(6-azido-6-deoxy-1-amino-2,3,4-tri-*O*-acetyl-β-D-glucosyl)-L-aspartic acid, methyl ester (**110**)**



103 (0.070 g, 0.17 mmol), Boc.Asp.OMe (**108**, 0.063 g, 0.254 mmol) and HBTU (0.0965 g, 0.254 mmol) were dissolved in DMF (1 mL), and the solution was cooled to 0°C. DIPEA

(0.060 mL, 0.080 g, 0.625 mmol) was added dropwise to the solution, and the reaction mixture was allowed to warm to room temperature and stirred for 24 hours. Upon completion, the reaction mixture was filtered, and the filtrate was diluted with EtOAc (10 mL), and extracted with H₂O (2 x 1 mL). The organic phase was dried and evaporated, and the resulting residue purified by flash column chromatography (2:1 Hexane:EtOAc) to produce **110** as a clear oil. (0.066 g, 70%), *R*_f 0.30 (1:1 Hexane:EtOAc). ¹H NMR (500 MHz, CDCl₃) δ 6.54 (d, 1H, *J* = 9.0 Hz, NH), 5.68 (d, 1H, *J* = 9.0 Hz, NH_{Boc}), 5.25 (d/t, 2H, *J* = 9.9 Hz, 9.0 Hz, H1/H3), 5.05 (t, 1H, *J* = 9.6 Hz, H4), 4.93 (t, 1H, *J* = 9.0 Hz, H2), 4.56 (m, 1H, H^α), 3.78 (m, 1H, H5), 3.74 (s, 3H, OCH₃), 3.40 (dd, 1H, *J* = 5.4 Hz, 12.4 Hz, H6), 3.31 (dd, 1H, *J* = 2.1 Hz, 12.4 Hz, H6'), 2.87 (dd, 1H, *J* = 4.2 Hz, 16.5 Hz, H^β), 2.72 (dd, 1H, *J* = 4.2 Hz, 16.5 Hz, H^{β'}), 2.09-2.02 (3s, 9H, CH₃, 3 x OAc), 1.44 (s, 9H, Boc-H). ¹³C NMR (125 MHz, CDCl₃) δ 171.7 (C=O, CONH₂), 171.2 (C=O, COOCH₃), 170.9 (C=O, OAc), 169.9 (C=O, OAc), 169.6 (C=O, OAc), 155.6 (C=O, Boc), 80.2 (C1), 77.9 (C(CH₃)₃), 74.6 (C5), 72.5 (C3), 70.4 (C2), 69.2 (C4), 52.7 (C^α), 50.6 (C6), 50.0 (OCH₃), 38.0 (C^β), 28.3 (C(CH₃)₃), 20.6 (CH₃, OAc), 20.6 (CH₃, OAc), 20.6 (CH₃, OAc). **LRMS (ESI):** *m/z* 582 [M + Na]⁺ **HRMS (ESI):** *m/z* calculated for C₂₂H₃₃N₅O₁₂Na [M + Na]⁺: 582.2023; Found 582.2029.

***N*^α-(*tert*-Butoxycarbonyl)-*N*^δ-(6-azido-6-deoxy-1-amino-2,3,4-tri-*O*-acetyl-β-*D*-glucosyl)-*L*-glutamic acid, methyl ester (**111**)**



DMF (1 mL), and the solution was cooled to

0°C. DIPEA (0.060 mL, 0.080 g, 0.625 mmol) was added dropwise to the solution, and the reaction mixture was allowed to warm to room temperature and stirred for 24 hours.

Upon completion, the reaction mixture was filtered, and the filtrate was diluted with EtOAc (10 mL), and extracted with H₂O (2 x 1 mL). The organic phase was dried and evaporated, with the following residue purified by flash column chromatography

(2:1 Hexane: EtOAc) to produce **111** as a clear oil. (0.061 g, 62%), *R*_f 0.35

(1:1 Hexane:EtOAc). ¹H NMR (500 MHz, CDCl₃) δ 6.85 (d, 1H, *J* = 9.0 Hz, NH), 5.28

(m, 3H, NH-Boc, H1/H3), 5.06 (t, 1H, *J* = 9.6 Hz, H4), 4.94 (t, 1H, *J* = 9.0 Hz, H2), 4.26

(m, 1H, H^α), 3.81 (m, 1H, H5), 3.75 (s, 3H, OCH₃), 3.43 (dd, 1H, *J* = 2.0 Hz, 13.0 Hz,

H6), 3.29 (dd, 1H, *J* = 4.5 Hz, 13.0 Hz, H6'), 2.31 (m, 2H, H^γ), 2.17 (m, 1H, H^β), 2.04-

2.01 (3s, 9H, CH₃, 3 x OAc), 1.88 (m, 1H, H^β), 1.44 (s, 9H, Boc-H). ¹³C NMR

(125 MHz, CDCl₃) δ 172.7 (C=O, CONH₂), 172.5 (C=O, COOCH₃), 170.7 (C=O,

OAc), 170.0 (C=O, OAc), 169.5 (C=O, OAc), 155.7 (C=O, Boc), 80.3 (C1), 78.0

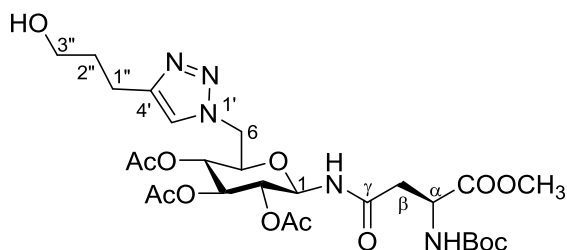
(C(CH₃)₃), 74.5 (C5), 72.9 (C3), 70.4 (C2), 69.3 (C4), 52.7 (C^α), 52.4 (C6), 50.6 (C6),

32.3 (C^γ), 28.6 (C^β), 28.3 (C(CH₃)₃), 20.6 (CH₃, OAc), 20.6 (CH₃, OAc), 20.6 (CH₃,

OAc). **LRMS (ESI):** *m/z* 596 [M + Na]⁺ **HRMS (ESI):** *m/z* calculated for

C₂₅H₃₅N₅O₁₂Na [M + Na]⁺: 596.2180; Found 596.2204.

***N*^α-(*tert*-Butoxycarbonyl)-*N*^ε-(6-(4'-(3''-hydroxypropyl)-1',2',3'-triazol-1'-yl)-6-deoxy-1-amino-2,3,4-tri-*O*-acetyl-β-D-glucosyl)-L-aspartic acid, methyl ester (**112**)**

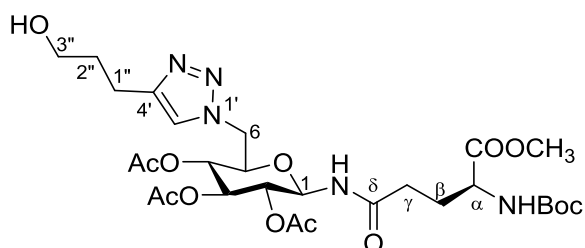


To a round bottom flask containing **110** (0.061 g, 0.131 mmol), 4-pentyn-1-ol (0.050 mL, 0.045 g, 0.54 mmol), CuOAc₂·H₂O (0.005 g, 0.026 mmol) and sodium ascorbate (0.010 g, 0.049

mmol) was added a 1:1 solution of *n*BuOH:H₂O, (0.500 mL), with the solution stirred vigorously under an atmosphere of nitrogen at room temperature for 24 hours. Upon completion, the reaction mixture was diluted with CH₂Cl₂ (10 mL), and extracted with H₂O (1 mL), then brine (1 mL). Subsequent drying (MgSO₄) of the organic phase, and evaporation *in vacuo* resulted in a residue which was purified by flash column chromatography (EtOAc.) to yield **112** as a clear oil (0.057 g, 70%), R_f 0.15 (1:3 Hexane:EtOAc.). ¹H NMR (500 MHz, CDCl₃) δ 7.54 (s, 1H, Triazole-H), 6.79 (d, 1H, *J* = 8.9 Hz, NH), 5.77 (d, 1H, *J* = 9.0 Hz, NHBoc), 5.30 (t, 1H, *J* = 9.0 Hz, H1), 5.12 (t, 1H, *J* = 9.5 Hz, H3), 4.90 (t, 1H, *J* = 9.0 Hz, H2), 4.83 (t, 1H, *J* = 9.6 Hz, H4), 4.51-4.64 (dd, 2H, *J* = 5.2 Hz, 11.5 Hz, H6/H6'), 4.30 (m, 1H, H^α), 3.88 (m, 1H, H5), 3.75 (s, 3H, OCH₃), 3.68 (m, 2H, CH₂-CH₂-CH₂-OH), 3.31 (dd, 1H, *J* = 2.1 Hz, 12.4 Hz, H6'), 2.87 (m, 2H, CH₂-CH₂-CH₂-OH), 2.78 (dd, 2H, *J* = 4.0 Hz, 16.4 Hz, H^β), 2.10-2.00 (3s, 9H, CH₃, 3 x OAc), 1.96 (m, 2H, CH₂-CH₂-CH₂-OH), 1.46 (s, 9H, Boc-H). Exchangeable OH not detected. ¹³C NMR (125 MHz, CDCl₃) δ 171.7 (C=O, CONH₂), 171.3 (C=O, COOCH₃), 171.0 (C=O, OAc), 169.7 (C=O, OAc), 169.7 (C=O, OAc), 155.6 (C=O, Boc), 147.9 (Triazole-C), 122.0 (Triazole-C), 80.5 (C1), 78.4 (C(CH₃)₃), 74.2 (C5), 72.3 (C3), 70.3 (C2), 69.4 (C4), 61.4 (CH₂-CH₂-CH₂-OH), 52.8 (C^α), 50.5 (C6), 50.2 (OCH₃), 38.2 (C^β), 31.6 (CH₂-CH₂-CH₂-OH), 28.3 (C(CH₃)₃), 21.9 (CH₂-CH₂-CH₂-

OH), 20.7 (CH₃, OAc), 20.6 (CH₃, OAc), 20.5 (CH₃, OAc). **LRMS (ESI):** m/z 666 [M + Na]⁺ **HRMS (ESI):** m/z calculated for C₂₇H₄₁N₅O₁₃Na [M + Na]⁺: 666.2599; Found 666.2621

***N*^α-(*tert*-Butoxycarbonyl)-*N*^ε-(6-(4'-(3''-hydroxypropyl)-1',2',3'-triazol-1'-yl)-6-deoxy-1-amino-2,3,4-tri-*O*-acetyl-β-D-glucosyl)-L-glutamic acid, methyl ester (113)**



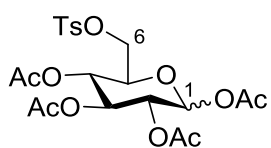
To a round bottom flask containing **111** (0.075 g, 0.131 mmol), 4-pentyn-1-ol (0.050 mL, 0.045 g, 0.54 mmol), CuOAc₂·H₂O (0.005 g, 0.026 mmol) and sodium ascorbate (0.010 g, 0.049 mmol)

was added a 1:1 solution of *n*BuOH:H₂O, (0.500 mL), with the solution stirred vigorously under an atmosphere of nitrogen at room temperature for 24 hours. Upon completion, the reaction mixture was diluted with CH₂Cl₂ (10 mL), and extracted with H₂O (1 mL), then brine (1 mL). Subsequent drying (MgSO₄) of the organic phase, and evaporation *in vacuo* resulted in a residue which was purified by flash column chromatography (EtOAc.) to yield **113** as a clear oil (0.053 g, 62%), R_f 0.26 (1:3 Hexane:EtOAc.). **¹H NMR** (500 MHz, CDCl₃) δ 7.71 (bs, 1H, Triazole-H), 7.16 (d, 1H, *J* = 8.7 Hz, NH), 5.35 (m, 2H, NH_{Boc}/H1), 5.19 (t, 1H, *J* = 9.4 Hz, H3), 4.96 (t, 1H, *J* = 9.5 Hz, H4), 4.89 (t, 1H, *J* = 9.3 Hz, H2), 4.68 (m, 1H, H6), 4.37 (m, 2H, H^α/H6'), 3.95 (m, 1H, H5), 3.79 (s, 3H, OCH₃), 3.70 (m, 2H, CH₂-CH₂-CH₂-OH), 2.86 (m, 2H, CH₂-CH₂-CH₂-OH), 2.34 (m, 4H, H^γ/CH₂-CH₂-CH₂-OH), (dd, 1H, *J* = 2.0 Hz, 13.0 Hz, H6), 3.29 (dd, 1H, *J* = 4.5 Hz, 13.0 Hz, H6'), 2.20 (m, 1H, H^β), 2.12-2.04 (3s, 9H, CH₃, 3 x OAc), 1.95 (m, 1H, H^β), 1.44 (s, 9H, Boc-H). Exchangeable OH not detected. **¹³C NMR** (125 MHz, CDCl₃) δ 173.3 (C=O, CONH₂), 172.7 (C=O,

COOCH₃), 171.0 (C=O, OAc), 170.0 (C=O, OAc), 169.9 (C=O, OAc), 156.0 (C=O, Boc), 147.4 (Triazole-C), 119.9 (Triazole-C), 80.7 (C1), 78.7 (C(CH₃)₃), 74.5 (C5), 72.9 (C3), 70.4 (C2), 69.3 (C4), 61.3 (CH₂-CH₂-CH₂-OH), 52.8 (C^α), 50.7 (OCH₃), 32.6 (C^γ), 31.1 (CH₂-CH₂-CH₂-OH), 28.9 (C^β), 28.5 (C(CH₃)₃), 22.9 (CH₂-CH₂-CH₂-OH), 20.9 (CH₃, OAc), 20.8 (CH₃, OAc), 20.7 (CH₃, OAc). **LRMS (ESI):** *m/z* 680 [M + Na]⁺
HRMS (ESI): *m/z* calculated for C₂₈H₄₃N₅O₁₃Na [M + Na]⁺: 680.2755; Found 680.2793.

7.4 Chapter 4 Experimental Data:

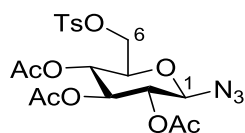
6-*p*-Toluenesulfonyl-1,2,3,4-tetra-*O*-acetyl-D-glucose (114)



According to the method of Nishimura *et al.*,¹⁹⁶ a round bottom flask containing D-glucose (10.0 g, 55 mmol), pyridine (150 mL) was added. The reaction mixture was cooled to 0°C, and *p*-toluenesulfonyl chloride (11.00 g, 58 mmol) was added portionwise to the reaction mixture, forming a yellow/green solution. The reaction mixture was slowly brought to room temperature, and allowed to stir for 16 hours. Following this time, acetic anhydride (40 mL) was added and the reaction mixture was stirred for an additional 1 hour. Upon completion, the reaction mixture was evaporated, with the resulting residue subject to recrystallization from ethanol, producing the desired product **114** as a white solid. (11.08 g, 40%), M.p. 192-196°C (decomp.), R_f 0.71 (1:1 Hexane:EtOAc.). ¹H NMR (500 MHz, CDCl₃) δ 7.75 (d, 4H, *J* = 8.3 Hz, Ar-H), 7.33 (d, 4H, *J* = 8.3 Hz, Ar-H), 5.71-5.63 (d, 2H, *J* = 8.2 Hz, H1α/β), 5.20-5.16 (m, 1H, H3α/β), 5.04-5.01 (m, 8H, H2α/β, H4α/β), 4.12-4.09 (m, 4H, H6α/β/H6'α/β),

3.83 (d, 2H, $J = 8.3$ Hz, H5 α/β), 2.44 (s, 6H, CH₃-Ar), 2.09-1.97 (4s, 24H, CH₃, 4 x OAc). ¹³C NMR (125 MHz, CDCl₃) δ 170.1 (C=O, OAc), 169.3 (C=O, OAc), 169.1 (C=O, OAc), 168.8 (C=O, OAc), 145.2 (Ar-C1), 132.4 (Ar-C4), 129.9 (Ar-C2/C6), 128.2 (Ar-C3/C5), 91.7 (C1 α), 91.5 (C1 β), 72.6 (C5), 72.2 (C3), 70.0 (C2), 67.9 (C4), 66.8 (C6), 21.7 (ArCH₃), 20.7 (Ar-CH₃), 20.5 (OAc), 20.5 (OAc), 20.5 (OAc). LRMS (ESI): m/z 525 [M + Na]⁺ HRMS (ESI): m/z calculated for C₂₁H₂₆O₁₂SNa [M + Na]⁺: 525.1043; Found 525.1062.

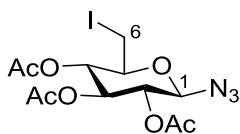
6-*p*-Toluenesulfonyl-1,2,3-tri-*O*-acetyl- β -D-glucosyl azide (**116**)



A solution of **114** (2.25 g, 4.48 mmol) dissolved in dry CH₂Cl₂ (5 mL) was chilled to 0°C. 33% w/v HBr in AcOH (12 mL) was added dropwise to the solution, and upon addition the reaction mixture was allowed to gradually warm to room temperature under constant stirring. After 3 hours, the reaction mixture was diluted with CH₂Cl₂ (50 mL), and washed with H₂O (10 mL), ice cold sat. NaHCO₃ solution (2 x 10 mL) and brine (10 mL). The organic phases were then dried and evaporated, producing the bromo intermediate **115** as a orange oil that was used without further purification. **115** was subsequently dissolved in dry DMF (20 mL), and the solution was cooled to 0°C. NaN₃ (1.166 g, 17.92 mmol) was added portion wise to the mixture, and allowed to stir at 0°C for 30 minutes, after which it was allowed to warm to room temperature. After 3 hours, the reaction mixture was diluted with H₂O (20 mL), with the aqueous phase extracted with EtOAc (3 x 50 mL). The organic phase was dried and evaporated, with recrystallization from EtOAc/Hexanes producing **116** as an off-white solid. (1.42 g, 65%), M.p. 137-138°C, R_f 0.76 (1:1 Hexane:EtOAc.). ¹H NMR (500 MHz, CDCl₃) δ 7.80 (d, 2H,

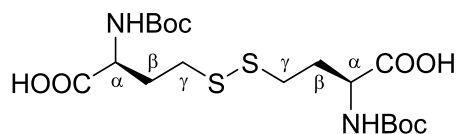
$J = 8.2$ Hz, Ar-H), 7.36 (d, 2H, $J = 8.2$ Hz, Ar-H), 5.18 (t, 1H, $J = 9.4$ Hz, H3), 4.96 (t, 1H, $J = 9.9$ Hz, H2), 4.85 (t, 1H, $J = 8.8$ Hz, 9.4 Hz, H4), 4.56 (d, 1H, $J = 9.8$ Hz, H1), 4.15 (dd, 1H, $J = 2.2$ Hz, 11.0 Hz, H6), 4.09 (dd, 1H, $J = 5.2$ Hz, 11.0 Hz, H6'), 3.83 (m, 1H, H5), 2.46 (s, 3H, ArCH₃), 2.06-1.99 (3s, 9H, CH₃, 3 x OAc). **¹³C NMR** (125 MHz, CDCl₃) δ 170.0 (C=O, OAc), 169.3 (C=O, OAc), 169.1 (C=O, OAc), 145.3 (Ar-C1), 132.2 (Ar-C4), 129.9 (Ar-C2/C6), 128.1 (Ar-C3/C5), 87.7 (C1), 73.6 (C3), 72.3 (C2), 70.4 (C4), 68.1 (C5), 67.2 (C6), 21.7 (ArCH₃), 20.5 (OAc), 20.5 (OAc), 20.5 (OAc). **LRMS (ESI):** m/z 508 [M + Na]⁺ **HRMS (ESI):** m/z calculated for C₁₉H₂₃N₃O₁₀SNa [M + Na]⁺: 508.1002; Found 508.0997.

6-Iodo-6-deoxy-1,2,3-tri-*O*-acetyl- β ,D-glucosyl azide (**117**)

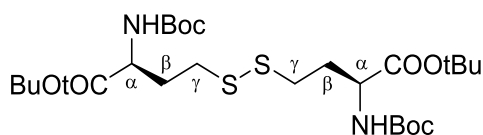


To a round bottom flask containing **116** (1.01 g, 2.08 mmol) and sodium iodide (1.25 g, 8.32 mmol), acetone (25 mL) was added.

The resulting suspension was heated under at reflux and stirred for 48 hours. After completion, the reaction mixture was evaporated to dryness, with the resulting residue suspended in ice cold H₂O (100 mL). Filtration of the precipitate, followed by recrystallization from ethanol resulted in the isolation of **117** as a white solid. (0.572 g, 62%), M.p. 127-128°C R_f 0.81 (1:1 Hexane:EtOAc.). **¹H NMR** (500 MHz, CDCl₃) δ 5.22 (t, 1H, $J = 9.5$ Hz, H3), 4.97 (t overlapping, 2H, $J = 9.5$ Hz, H2/4), 4.70 (d, 1H, $J = 9.6$ Hz, H1), 3.56 (dt, 1H, $J = 2.5$ Hz, 8.0 Hz, H5), 3.36-3.32 (dd, 1H, $J = 7.1$ Hz, 11.1 Hz, H6), 3.21-3.18 (dd, 1H, $J = 7.2$ Hz, 11.0 Hz, H6'), 2.07-2.01 (3s, 9H, CH₃, 3 x OAc). **¹³C NMR** (125 MHz, CDCl₃) δ 170.0 (C=O, OAc), 169.9 (C=O, OAc), 169.8, (C=O, OAc), 87.6 (C1), 72.2 (C3), 69.7 (C2), 69.6 (C4), 68.3 (C5), 20.1 (OAc), 19.0 (OAc), 18.9 (OAc), 3.6 (C6). **LRMS (ESI):** m/z 464 [M + Na]⁺

***N,N*-(*tert*-Butoxycarbonyl)-L-homocystine (118)**

According to the method of Zhu *et al.*,¹⁹⁷ a round bottom flask containing L,L-homocystine (2.68 g, 10.0 mmol) was added a 10% sodium carbonate solution (90 mL) and 1,4-dioxane (80 mL). The resultant suspension was cooled to 0°C and di-*t*-butyl dicarbonate (4.80 g, 22.2 mmol) was added. The reaction mixture was allowed to warm to room temperature and stirred for 18 hours. Following this time, 10% ascorbic acid was added to adjust the solution to pH 4, and the reaction mixture was extracted with ethyl acetate (3 x 50 mL). The organic layers were then combined, washed with brine (25 mL), dried (MgSO₄) and evaporated *in vacuo*, producing **118** as a white solid, (4.20 g, 90%), M.p. 162-164°C (decomp.)(Lit. 158-159°C).¹⁷⁸ ¹H NMR (500 MHz, CD₃OD) δ 4.20 (m, 2H, H^α), 2.74 (m, 4H, H^γ), 2.20 (m, 2H, H^β), 1.96 (m, 2H, H^{β'}), 1.42 (s, 18H, Boc-H). ¹³C NMR (125 MHz, CD₃OD) δ 175.7 (COOH), 158.2 (C=O, Boc), 80.7 (C(CH₃)₃), 53.7 (C^α), 35.8 (C^γ), 32.5 (C^β), 28.8 (C(CH₃)₃). **LRMS (ESI):** *m/z* 491 [M + Na]⁺, **HRMS (ESI):** *m/z* calculated for C₁₈H₃₂N₂O₈S₂Na [M + Na]⁺: 491.1498; Found 491.1470.

***N,N*-(*tert*-Butoxycarbonyl)-L-homocystine di-*tert*-butyl ester (119)**

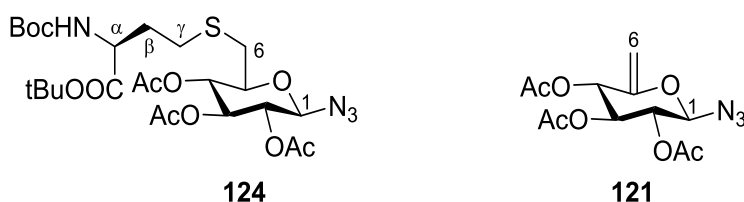
According to the method of Bourdier *et al.*,¹⁷⁸ a solution of **118** (0.895 g, 1.92 mmol) dissolved in CH₂Cl₂ (10 mL) under argon was added *tert*-butyl-2,2,2-trichloroacetimidate (2.20 g, 9.55 mmol). The reaction mixture was allowed to stir at room temperature for 18 hours, after which evaporation *in vacuo*, followed by flash column chromatography (6:1 Hexane: EtOAc) yielded the product **119** as a white solid. (1.108 g, 99%), M.p. 66-69°C (Lit.

66-68°C), ¹⁷⁸ R_f 0.60 (4:1 Hexane:EtOAc.). **¹H NMR** (500 MHz, CDCl₃) δ 5.22 (m, 2H, NH), 4.24 (m, 2H, H_α), 2.70 (m, 4H, H_γ), 2.19 (m, 2H, H_β), 1.97 (m, 2H, H_{β'}), 1.48 (s, 18H, *t*Bu), 1.45 (s, 18H, Boc-H). **¹³C NMR** (125 MHz, CDCl₃) δ 171.5 (C=O), 155.7 (C=O, Boc), 82.5 (C(CH₃)₃), 80.1 (Boc C-CH₃), 53.6 (C_α), 34.9 (C_γ), 33.1 (C_β), 28.7 (C(CH₃)₃), 28.3(Boc C-CH₃). **LRMS (ESI):** *m/z* 603 [M + Na]⁺ **HRMS (ESI):** *m/z* calculated for C₂₆H₄₈N₂O₈S₂Na [M + Na]⁺: 603.2750; Found 603.2771.

N-(*Tert*-butoxycarbonyl)-L-homocysetine *tert*-butyl ester (**120**)

According to the method of Bourdier *et al.*,¹⁷⁸ a solution of **119** (0.321 g, 0.551 mmol) in DMF (5 mL) under argon, was added H₂O (0.500 mL) and tributylphosphine (0.160 mL, 0.131 g, 0.631 mmol). The reaction mixture was allowed to stir at room temperature for 18 hours, after which the reaction was quenched with H₂O (50 mL). The aqueous phase was washed with EtOAc (3 x 25 mL), which was subsequently washed with brine (25 mL), dried (MgSO₄) and evaporated *in vacuo*. Purification by flash column chromatography (6:1 Hexane: EtOAc) resulted in the isolation of **120** as a clear solid. (0.274 g, 85%). M.p. 38-40°C, R_f 0.75 (4:1 Hexane:EtOAc.). **¹H NMR** (500 MHz, CDCl₃) δ 5.17 (d, 1H, *J* = 6.9 Hz, NH), 4.29 (m, 1H, H_α), 2.56 (m, 2H, H_γ), 2.06 (m, 1H, H_β), 1.95 (m, 1H, H_{β'}), 1.55 (t, 1H, *J* = 5.2 Hz, SH), 1.48 (s, 9H, *t*Bu), 1.45 (s, 9H, Boc-H) **¹³C NMR** (125 MHz, CDCl₃) δ 171.7 (C=O), 155.7 (C=O, Boc), 82.5 (C(CH₃)₃), 80.1 (Boc C-CH₃), 53.3 (C_α), 38.0 (C_β), 28.7 (C(CH₃)₃), 28.3(Boc C-CH₃) 21.1 (C_γ). **LRMS (ESI):** *m/z* 314 [M + Na]⁺ **HRMS (ESI):** *m/z* calculated for C₁₃H₂₅NO₄SNa [M + Na]⁺: 314.1402; Found 314.1390

Attempted synthesis of *N*^α-(*tert*-Butoxycarbonyl)-*S*-(1-azido-1-deoxy-2,3,4-tri-*O*-acetyl-6-thio-β-*D*-glucosyl)-*L*-homocysteine *tert*-butyl ester (124**)**



Method A: In a round bottom flask, **117** (0.100 g, 0.227 mmol) and Boc.HCys.OtBu (**120**; 0.132 g, 0.454 mmol) was dissolved in THF (5 mL). NEt₃ (0.065 mL, 0.047 g, 0.454 mmol) was added to the reaction mixture and allowed to stir at room temperature. Periodic monitoring by TLC highlighted the formation of the side product **121**, with the desired product **124** not detected. After 48 hours, the reaction mixture was evaporated *in vacuo* and dissolved in EtOAc (10 mL). After washing with H₂O (5 mL) and brine (5 mL), the organic phases were then dried and evaporated *in vacuo* with the resulting residue purified by flash column chromatography (3:1 Hexane: EtOAc), resulting in the isolation of the side product **121** as a white solid. (0.054g, 39%)

Method B: In a round bottom flask, **117** (0.100 g, 0.227 mmol) and Boc.HCys.OtBu (**120**; 0.132 g, 0.454 mmol) was dissolved in THF (5 mL). DBU (0.070 mL, 0.069 g, 0.454 mmol) was added to the reaction mixture and allowed to stir at room temperature. Periodic monitoring by TLC highlighted the formation of the side product **121**, with the desired product **124** not detected. After 48 hours, the reaction mixture was evaporated *in vacuo* and dissolved in EtOAc (5 mL). After washing with H₂O (5 mL) and brine (5 mL), the organic phases were then dried and evaporated *in vacuo* with the resulting residue purified by flash column chromatography (3:1 Hexane: EtOAc), resulting in the isolation of the side product **121** as a white solid. (0.066 g, 48%)

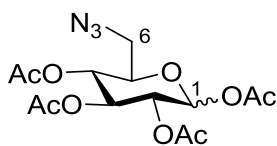
Method C: In a round bottom flask, **117** (0.102 g, 0.228 mmol) and Boc.HCys.OtBu (**120**; 0.130 g, 0.453 mmol) was dissolved in DMF (5 mL). Cs₂CO₃ (0.148 g, 0.454 mmol) was added to the reaction mixture and allowed to stir at room temperature. Periodic monitoring by TLC highlighted the formation of the side product **121**, with the desired product **124** not detected. After 48 hours, the reaction mixture was diluted with EtOAc (5 mL). After washing with H₂O (5 mL) and brine (5 mL), the organic phases were then dried and evaporated *in vacuo* with the resulting residue purified by flash column chromatography (3:1 Hexane: EtOAc), resulting in the isolation of the side product **121** as a white solid. (0.068 g, 49%)

Method D: In a round bottom flask, **117** (0.101 g, 0.227 mmol) and Boc.HCys.OtBu (**120**; 0.131 g, 0.454 mmol) was dissolved in DMF (5 mL). Ag₂O (0.210 g, 0.906 mmol) was added to the reaction mixture the reaction glassware was covered in foil and allowed to stir at room temperature in the dark for 4 days. Periodically monitored by TLC, neither the formation of side product **121**, or the desired product **124** were detected. As a result, the reaction was terminated, and a work up was not performed.

Method E: In a round bottom flask, **117** (0.100 g, 0.227 mmol) and Boc.HCys.OtBu (**120**; 0.130 g, 0.453 mmol) was dissolved in THF (5 mL). Ag₂O (0.213 g, 0.908 mmol) was added to the reaction mixture and allowed to stir at room temperature in the dark. Periodical monitoring by TLC highlighted the formation of the side product **121**, with the desired product **124** not detected. After 8 days, the reaction mixture was evaporated *in vacuo* and dissolved in EtOAc (5 mL). After washing with H₂O (5 mL) and brine (5 mL), the organic phases were then dried and evaporated. ¹H NMR of the reaction worked up displayed trace quantities of the side product **121**. As a result, the reaction mixture was discarded and no isolation of **121** was performed.

Analytical data for (121): R_f 0.41 (1:1 Hexane EtOAc), M.p. 84-86°C. ^1H NMR (500 MHz, CDCl_3) δ 5.50 (d, 1H, $J = 7.6$ Hz, H4), 5.08 (t, 1H, $J = 7.8$ Hz, H3), 4.96 (t, 1H, $J = 7.9$ Hz, H2), 4.90 (overlapping d, 2H, $J = 7.5$ Hz, H1/CH), 4.64 (m, 1H, CH), 2.10-2.02 (3s, 9H, CH_3 , 3 x OAc). ^{13}C NMR (125 MHz, CDCl_3) δ 169.9 (C=O, OAc), 169.4 (C=O, OAc), 169.3 (C=O, OAc), 150.8 (C5), 98.4, (C6) 88.3 (C1), 71.6 (C4), 70.9 (C3), 68.7 (C2), 20.9 (CH_3 , OAc), 20.8 (CH_3 , OAc), 20.8 (CH_3 , OAc). **LRMS (ESI):** m/z 336 $[\text{M} + \text{Na}]^+$ **HRMS (ESI):** m/z calculated for $\text{C}_{12}\text{H}_{15}\text{N}_3\text{O}_7$ $[\text{M} + \text{Na}]^+$: 336.0808, Found 336.0820.

6-Azido-6-deoxy-1,2,3,4-tetra-*O*-acetyl--D-glucose (125)

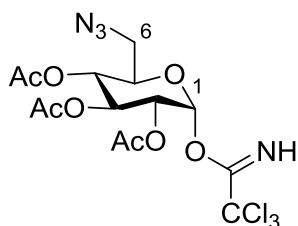


To a round bottom flask containing **114** (4.00 g, 7.96 mmol) was added NaN_3 (1.55 g, 23.88 mmol) and DMF (20 mL).

The resulting suspension was heated to 50°C and stirred under nitrogen for 24 hours, after which the solution was concentrated. The resulting residue was suspended in H_2O (10 mL), and subsequently washed with EtOAc (3 x 50 mL). The organic phases were collected, dried and evaporated, with the resulting residue subjected to flash column chromatography (3:1 Hexane: EtOAc). Further recrystallization by EtOAc/Hexanes yielded **125** as a white solid present as a 1:1 mixture of α and β anomers. (1.71 g, 57%), M.p. 130-133°C, R_f 0.79 (1:1 Hexane:EtOAc.). ^1H NMR (500 MHz, CDCl_3) δ α -anomer: 6.36 (d, 1H, $J = 8.2$ Hz, H1 α), 5.43 (t, 1H, $J = 9.2$ Hz, H3 α), 5.17-5.05 (m, 2H, H2/H4), 4.05 (dt, 1H, $J = 9.1$ Hz, H5 α), 3.36-3.32 (m, 2H, H6 α /H6 α'), 2.24-1.99 (4s, 12H, CH_3 , 4 x OAc). β -anomer: 5.70 (d, 1H, $J = 8.0$ Hz, H1 β), 5.22 (t, 1H, $J = 8.4$ Hz, H3 β), 5.10 (m, 2H, H2/H4), 3.80 (dt, 1H, $J = 9.3$ Hz, H5 β), 3.36-3.32 (m, 2H, H6 β /H6 β'), 2.24-2.04 (4s,

12H, CH₃, 4 x OAc). ¹³C NMR (125 MHz, CDCl₃) δ 170.1 (C=O, CH₃), 169.6 (C=O, CH₃), 169.4 (C=O, CH₃), 168.7 (C=O, CH₃), 91.4 (C1^β), 88.8 (C1^α), 73.8 (C5), 72.5 (C3^β), 70.8 (C3^β), 70.1 (C2^β), 69.7 (C5^β), 69.1 (C4^β), 68.9 (C4), 50.6 (C6), 20.8 (CH₃, OAc), 20.7 (CH₃, OAc), 20.6 (CH₃, OAc), 20.4 (CH₃, OAc). LRMS (ESI): *m/z* 396 [M + Na]⁺ HRMS (ESI): *m/z* calculated for C₁₄H₁₉N₃O₉Na [M + Na]⁺: 396.1019; Found 396.1019.

6-Azido-6-deoxy-1,2,3-tri-*O*-acetyl- α ,D-glucosyl trichloroacetimidate (**127**)

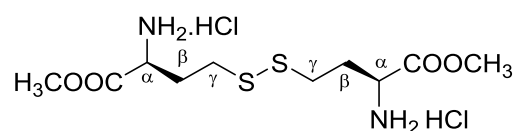


To a round bottom flask containing **125** (1.80 g, 4.80 mmol) DMF (40 mL) was added. The resultant was cooled to 0°C. Hydrazine acetate (0.60 g, 7.20 mmol) was then added portion wise to the reaction mixture, which was allowed to gradually warm to room temperature and stir for 3 hours.

Upon completion, the reaction mixture was evaporated to dryness and subject to flash column chromatography (1:1 Hexane: EtOAc), producing the lactol intermediate **126** (1.270 g, 80%). Subsequently, **126** was re-dissolved in dry CH₂Cl₂ (15 mL) under argon with trichloroacetonitrile (3.00 mL, 4.32 g, 29.92 mmol). The mixture was cooled to 0°C, and DBU (1.08 mL, 1.10 g, 7.23 mmol) was added to the mixture dropwise, with the reaction warmed to room temperature and allowed to stir for a further 3 hours. Upon completion, the reaction mixture was diluted with CH₂Cl₂, (15 mL) washed with sat. NaHCO₃ solution (25 mL) and brine (25 mL), dried (MgSO₄) and evaporated *in vacuo*. The resulting residue was subjected to flash column chromatography (2:1 Hexane: EtOAc), yielding **127** as an off-white solid. (1.37 g, 75%), M.p. 76-78°C,

R_f 0.55 (1:1 Hexane:EtOAc.). **^1H NMR** (500 MHz, CDCl_3) δ 8.76 (s, 1H, NHCCl_3), 6.63 (d, 1H, $J = 3.7$ Hz, H1), 5.51 (t, 1H, $J = 9.5$ Hz, H3), 5.19-5.16 (m, 2H, H2/H4), 4.22 (ddd, 1H, $J = 10.2$ Hz, H5), 3.46 (dd, 1H, $J = 3.0$ Hz, H6'), 3.36 (dd, 1H, $J = 5.5$ Hz, 13.5 Hz, H6), 2.10-2.05 (3s, 9H, CH_3 , 3 x OAc). **^{13}C NMR** (125 MHz, CDCl_3) δ 170.0, 169.8, 169.5 (C=O, OAc), 92.8 (C1), 71.1 (C5), 69.7 (C2), 69.6 (C3), 68.9 (C4), 50.6 (C6), 20.7 (CH_3 , OAc), 20.6 (CH_3 , OAc), 20.4 (CH_3 , OAc). **LRMS (ESI):** m/z 498 $[\text{M} + \text{Na}]^+$.

L-Homocystine dimethyl ester dihydrochloride (128)



To a round bottom flask containing

homocystine (0.786 g, 2.93 mmol) was added

methanol (10 mL). The resulting suspension

was cooled to 0°C , and thionyl chloride (0.240 mL, 0.383 g, 3.223 mmol) was added

dropwise. Upon addition, the reaction mixture was allowed to gradually warm to room

temperature, and was left to stir for 18 hours. Upon completion, the reaction solvents

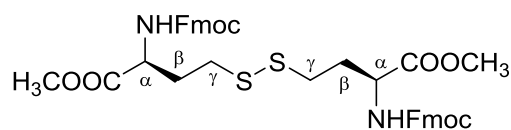
were removed *in vacuo*, producing the dimethyl ester dihydrochloride salt **128** as a light

yellow oil. (1.076 g, 99%). **^1H NMR** (500 MHz, CDCl_3) δ 4.17 (t, 2H, $J = 6.6$ Hz, H_α)

3.82 (s, 6H, NH_3), 3.69 (s, 6H, OCH_3), 2.81 (t, 4H, $J = 7.3$ Hz, H_γ), 2.37 (m, 4H, H_β).

^{13}C NMR (125 MHz, D_2O) δ 170.2 (C=O, COOCH_3), 53.7 (C^α), 51.44 (OCH_3),

32.0 (C^β), 28.9 (C^γ). **LRMS (ESI):** m/z 297 $[\text{M} + \text{H}]^+$

***N,N*-(Fluorenylmethylcarbonyl)-L-homocystine dimethyl ester (**129**)**

According to the method of Kelleman

et al.,²⁰³ a round bottom flask containing **128**

(0.594 g, 1.61 mmol), was added solid

K₂CO₃ (1.02 g, 7.25 mmol). H₂O (10 mL) and 1,4-dioxane (5 mL) were also added, and

the mixture was gently stirred at room temperature. Solid Fmoc-Cl (1.039 g, 4.03

mmol) was added to the reaction mixture portion wise, and the reaction mixture was

allowed to stir vigorously at room temperature for 18 hours. After this time, the reaction

mixture was subjected to sonication then filtered. The isolated solid was subjected to

flash column chromatography (4:1 Hexane: EtOAc), resulting in the isolation of **129** as

a light yellow solid. (0.884 g, 74%), M.p. 89-91°C, R_f 0.15 (4:1 Hexane:EtOAc). ¹H

NMR (500 MHz, CDCl₃) δ 7.74 (d, 4H, *J* = 7.3 Hz, Fmoc-H) 7.57 (d, 4H, *J* = 7.3 Hz,

Fmoc-H), 7.39 (t, 4H, *J* = 7.3 Hz, Fmoc-H), 7.24 (t, 4H, *J* = 7.3 Hz, Fmoc-H), 5.51 (d,

2H, *J* = 8.0 Hz, NH), 4.48 (m, 2H, H_α), 4.40 (m, 4H, OCH₂), 4.19 (t, 2H, *J* = 6.7 Hz),

3.75 (s, 6H, OCH₃), 2.70 (t, 4H, *J* = 7.3 Hz, H_γ), 2.17 (m, 4H, H_β). ¹³C NMR (125

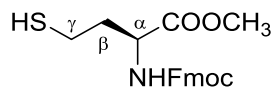
MHz, CDCl₃) δ 172.4 (C=O, COOCH₃), 155.9 (C=O, Fmoc), 143.8 (Fmoc Ar-C1),

143.4 (Fmoc Ar-C1), 141.3 (Fmoc Ar-C6), 127.7 (Fmoc Ar-C4), 127.1 (Fmoc Ar-C5),

125.0 (Fmoc Ar-C3), 120.0 (Fmoc Ar-C2), 67.0 (OCH₂CH), 52.7, 52.6 (OCH₃/C^α), 47.2

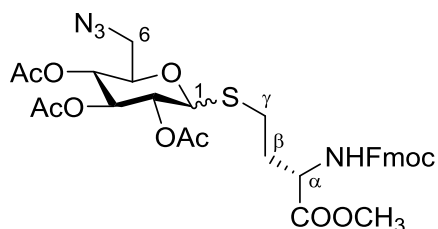
(OCH₂CH), 34.5 (C^β), 32.4 (C^γ). LRMS (ESI): *m/z* 763 [M + Na]⁺ HRMS (ESI): *m/z*

calculated for C₄₀H₄₀N₂O₈S₂Na [M + Na]⁺: 763.2124; Found 763.2151.

N-(Fluorenylmethylcarbonyl)-L-homocysteine methyl ester (130)

According to the method of Kelleman *et al.*,²⁰³ a round bottom flask containing **129** (0.519 g, 0.700 mmol) under argon, was added CH₂Cl₂ (20 mL) and MeOH (60 mL). To the flask, zinc dust (0.250 g, 3.50 mmol) was added followed by TFA (2.20 mL, 3.278 g, 28.75 mmol) dropwise. Subsequently, the flask was again flushed with argon, and the reaction mixture was allowed to stir at room temperature for 18 hours. Following this, the reaction mixture was filtered and evaporated *in vacuo*, with the resulting residues dissolved in EtOAc (50 mL). Subsequent washes with H₂O (10 mL) and brine (10 mL), followed by drying (MgSO₄) and concentration, resulted in the isolation of **130** as a light yellow solid. (0.370 g, 71%), M.p. 87-90°C, R_f 0.42 (4:1 Hexane:EtOAc.). ¹H NMR (500 MHz, CDCl₃) δ 7.74 (d, 2H, *J* = 7.3 Hz, Fmoc-H) 7.59 (d, 2H, *J* = 7.3 Hz, Fmoc-H), 7.39 (t, 2H, *J* = 7.3 Hz, Fmoc-H), 7.23 (t, 2H, *J* = 7.3 Hz, Fmoc-H), 5.34 (d, 1H, *J* = 8.0 Hz, NH), 4.54 (m, 1H, H_α), 4.44 (m, 2H, OCH₂), 4.22 (t, 1H, *J* = 6.7 Hz), 3.76 (s, 3H, OCH₃), 2.55 (t, 2H, *J* = 7.3 Hz, H^γ), 2.13 (m, 1H, H^β), 1.97 (m, 1H, H^β), 1.55 (t, 1H, *J* = 8.1 Hz, SH). ¹³C NMR (125 MHz, CDCl₃) δ 172.5 (COOCH₃), 156.0 (C=O, Fmoc), 143.9 (Fmoc Ar-C1), 143.6 (Fmoc Ar-C1), 141.4 (Fmoc Ar-C6), 127.8 (Fmoc Ar-C4), 127.1 (Fmoc Ar-C5), 125.0 (Fmoc Ar-C3), 120.0 (Fmoc Ar-C2), 67.0 (OCH₂CH), 52.7, 52.6 (OCH₃/C^α), 47.2 (OCH₂CH), 37.0 (C^β), 20.6 (C^γ). LRMS (ESI): *m/z* 394 [M + Na]⁺ HRMS (ESI): *m/z* calculated for C₂₀H₂₁NO₄SNa [M + Na]⁺: 394.1089; Found 394.1082.

***N*^α-(Fluorenylmethylcarbonyl)-S-(6-azido-6-deoxy-1-thio-2,3,4-tri-*O*-acetyl-D-glucosyl)-L-homocysteine methyl ester (**131**)**



Method A: To a round bottom flask containing **125** (0.100 g, 0.268 mmol) and Fmoc.HCys.OMe (**130**, 0.250 g, 0.670 mmol) under argon, was added dry CH₂Cl₂ (5 mL). The mixture was cooled to 0°C, and SnCl₄ (0.020 mL, 0.045 g, 0.0171 mmol) was added to the solution. The reaction mixture was subsequently allowed to warm to room temperature, and stirred overnight. Upon completion, the reaction mixture was diluted with CH₂Cl₂ (10 mL) and quenched with sat. NaHCO₃ solution (5 mL). The organic phases were then washed with H₂O (5 mL) and brine (10 mL), dried (Na₂SO₄) and evaporated *in vacuo* with the resulting residues purified by flash column chromatography (3.5:1 Hexane: EtOAc), producing **131** as an amorphous solid present in a ~2:1 ratio of α and β-anomers. (0.094 g, 51%).

Method B: A round bottom flask containing **127** (0.127 g, 0.268 mmol), Fmoc.HCys.OMe (**128**, 0.248 g, 0.669 mmol) and 4Å molecular sieves (0.100 g) was dried under high vacuum overnight. Upon drying, the flask was immersed in an atmosphere of argon and dry CH₂Cl₂ (2 mL) was added. The reaction mixture was cooled to -20°C, and stirred at this temperature for 30 minutes. After this time, TMSOTf (0.005 mL, 0.006 g, 0.027 mmol) was added to the reaction mixture dropwise, and the flask was stirred vigorously for an additional 1 hour. Upon reaction completion, the reaction mixture was diluted with CH₂Cl₂ (10 mL) and quenched with sat. NaHCO₃ solution (1 mL). The organic phases were then washed with H₂O (5 mL) and brine (5 mL), dried (Na₂SO₄) and evaporated *in vacuo* with the resulting residues purified by

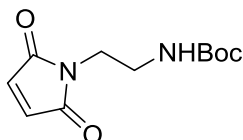
flash column chromatography (3.5:1 Hexane: EtOAc), producing **131** as a white foam present as a 1:1 mixture of α and β -anomers. (0.071 g, 38%).

α -anomer; R_f 0.30 (2:1 Hexane:EtOAc.). $^1\text{H NMR}$ (500 MHz, CDCl_3) δ 7.75 (m, 2H, Fmoc-H), 7.57 (m, 2H, Fmoc-H), 7.37 (m, 2H, Fmoc-H), 7.29 (m, 2H, Fmoc-H), 6.36 (d, 2H, $J = 4.0$ Hz, H1), 5.47 (overlapping t, 2H, $J = 9.9$ Hz, NH/H3), 5.10 (m, 2H, H2/H4), 4.48 (m, 1H, H^a), 4.39 (m, 2H, $\text{OCH}_2\text{-CH}$), 4.19 (m, 1H, $\text{OCH}_2\text{-CH}$), 4.08 (m, 1H, H5), 3.76 (s, 3H, OCH_3), 3.39 (dd, 1H, $J = 2.6, 13.6$ Hz, H6), 3.30 (dd, 1H, $J = 5.5; 13.4$ Hz, H6'), 2.70 (m, 2H, H^y), 2.24 (m, 1H, H^β), 2.10 (m, 1H, H^β), 2.02-2.06 (3s, 9H, CH_3 , 3 x OAc). $^{13}\text{C NMR}$ (125 MHz, CDCl_3) δ 172.5 (C=O, COOCH_3), 170.4 (C=O, OAc), 169.8 (C=O, OAc), 168.9 (C=O, OAc), 156.2 (C=O, Fmoc), 143.9 (Fmoc Ar-C1), 141.6 (Fmoc Ar-C6), 128.1 (Fmoc Ar-C4), 127.2 (Fmoc Ar-C5), 125.4 (Fmoc Ar-C3), 120.3 (Fmoc Ar-C2), 89.2 (C1), 71.2 (C5) 71.0 (C3), 69.9 (C2), 69.5 (C4), 67.3 (OCH_2CH), 53.1 (C^a), 52.7 (OCH_3), 51.0 (C6), 47.4 (OCH_2CH), 34.7 (C^β), 21.1 (C^y), 20.8 (CH_3 , OAc), 20.7 (CH_3 , OAc), 20.6 (CH_3 , OAc).

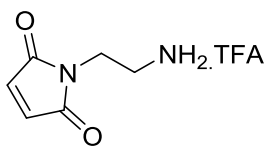
β -anomer, R_f 0.23 (2:1 Hexane:EtOAc.). $^1\text{H NMR}$ (500 MHz, CDCl_3) δ 7.76 (m, 2H, Fmoc-H), 7.61 (m, 2H, Fmoc-H), 7.40 (m, 2H, Fmoc-H), 7.32 (m, 2H, Fmoc-H), 5.45 (m, 1H, NH), 5.22 (t, 1H, $J = 9.9$ Hz, H3), 5.02 (m, 2H, H2/H4), 4.51 (d, 1H, $J = 9.8$ Hz, H1), 4.48 (m, 1H, H^a), 4.42 (d, 2H, $J = 8.1$ Hz, OCH_2CH), 4.23 (t, 1H, $J = 8.2$ Hz, OCH_2CH), 3.77 (s, 2H, OCH_3), 3.67 (m, 1H, H5), 3.32 (m, 2H, H6/H6'), 2.80 (m, 1H, H^y), 2.67 (m, 1H, $\text{H}^{y'}$), 2.18 (m, 1H, H^β), 2.07 (m, 1H, H^β), 2.01-2.05 (3s, 9H, CH_3 , 3 x OAc). $^{13}\text{C NMR}$ (125 MHz, CDCl_3) δ 172.3 (C=O, COOCH_3), 170.1 (C=O, OAc), 169.4 (C=O, OAc), 169.4 (C=O, OAc), 155.9 (C=O, Fmoc), 143.8 (Fmoc Ar-C1), 141.3 (Fmoc Ar-C6), 127.7 (Fmoc Ar-C4), 127.1 (Fmoc Ar-C5), 125.1 (Fmoc Ar-C3), 120.0 (Fmoc Ar-C2), 83.4 (C1), 77.0 (C5), 73.6 (C3) 69.6 (C2), 69.4 (C4), 67.0 (OCH_2CH), 53.0 (C^a), 52.6 (OCH_3), 51.1 (C6), 47.2 (OCH_2CH), 32.8 (C^β), 21.0 (C^y), 20.7 (CH_3 ,

OAc), 20.6 (CH₃, OAc), 20.6 (CH₃, OAc). **LRMS (ESI):** m/z 707 [M + Na]⁺ **HRMS (ESI):** m/z calculated for C₃₂H₃₆N₄O₁₁SNa [M + Na]⁺: 707.1999; Found 707.2008

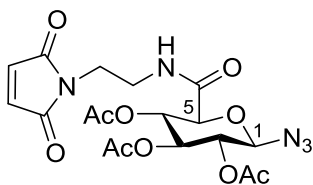
***N*-(*tert*-Butoxycarbonyl)ethylenediamine maleimide (134)**



According to the method of Richter *et al.*,²¹¹ round bottom flask containing *N*-Boc-ethylenediamine (**133**, 0.50 mL, 0.510 g, 3.20 mmol) and NEt₃ (0.66 mL) was suspended in Et₂O (5 mL) and cooled to 0°C. Maleic anhydride (0.311 g, 3.20 mmol) dissolved in Et₂O (5 mL) was added dropwise to the reaction mixture, after which it was allowed to stir for 4 hours gradually warming to room temperature. After this time, the reaction mixture was concentrated, and the resulting residue was dissolved in acetone (15 mL). NEt₃ (1.0 mL) and Ac₂O (0.500 mL) was added, and the mixture was heated to reflux for a further 20 hours. Upon completion, solvent evaporation resulted in a brown residue, which following flash column chromatography resulted in the isolation of the desired product **134** as a white solid. (0.388 g, 50%). M.p. 126-128°C, R_f 0.80 (1:1 Hexane: EtOAc). **¹H NMR** (500 MHz, CDCl₃) δ 6.70 (m, 2H, CH=CH), 4.78 (bs, 1H, NH), 3.64 (m, 2H, CH₂-CH₃-NHBoc), 3.31 (m, 2H, CH₂-CH₃-NHBoc), 1.39 (s, 9H, Boc-H) **¹³C NMR** (125 MHz, CDCl₃) δ 170.8 (C=O, maleimide), 155.9 (C=O, Boc), 134.2 (CH=CH), 79.5 (C(CH₃)₃), 39.4 (CH₂-CH₂-NHBoc), 38.0 (CH₂-CH₂-NHBoc), 28.3 (C(CH₃)₃). **LRMS (ESI):** m/z 263 [M + Na]⁺ **HRMS (ESI):** m/z calculated for C₁₁H₁₆N₂O₄Na [M + Na]⁺: 263.1008; Found 263.1061.

N-Ethylenediamine maleimide trifluoroacetate (135)

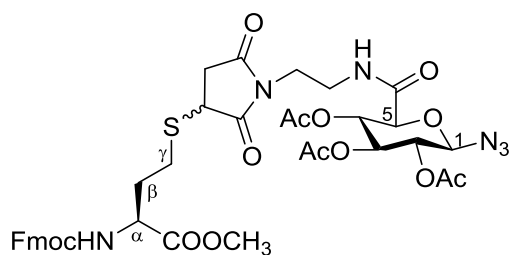
According to the method of Richter *et al.*,²¹¹ a round bottom flask containing **134** (0.150 g, 0.624 mmol) was added dry CH_2Cl_2 (5 mL). The flask was cooled to 0°C , and TFA (2.50 mL, 3.725 g, 32.67 mmol) was added to the solution dropwise. Upon addition, the reaction mixture was stirred for 1 hour, during which it was allowed to warm to room temperature. Upon completion, the reaction mixture was evaporated to dryness, with flushing of the mixture with ice-cold Et_2O (5 mL) resulting in precipitation of the desired product. Trituration with additional Et_2O (4 x 5 mL) followed by filtration resulting in the isolation of **135** as a white solid. (0.141 g, 95%). M.p. $133\text{--}134^\circ\text{C}$. $^1\text{H NMR}$ (500 MHz, D_2O) δ 6.95 (s, 2H, $\text{CH}=\text{CH}$), 3.88 (t, 2H, $J = 5.7$ Hz, $\text{CH}_2\text{--CH}_2\text{--NHBoc}$), 3.28 (t, 2H, $J = 5.7$ Hz, $\text{CH}_2\text{--CH}_2\text{--NHBoc}$). $^{13}\text{C NMR}$ (125 MHz, D_2O) δ 172.7 (C=O), 134.7 ($\text{CH}=\text{CH}$), 38.4 ($\text{CH}_2\text{--CH}_2\text{--NHBoc}$), 35.0 ($\text{CH}_2\text{--CH}_2\text{--NHBoc}$). **LRMS (ESI):** m/z 141 [$\text{M} - \text{TFA} + \text{H}$] $^+$

N-(1-Azido-2,3,4-tri-O-acetyl- β -D-glucuronoyl)-ethylenediamine maleimide (136)

135 (0.076 g, 0.322 mmol), **60** (0.075 g, 0.215 mmol), and DCC (0.066 g, 0.321 mmol) were dissolved in ACN (2 mL), and the solution was cooled to 0°C . HOBt (0.043 g, 3.21 mmol) was added portionwise to the reaction mixture, and allowed to warm to room temperature and stir for 8 hours. Upon completion, the reaction mixture was filtered, and the filtrate was evaporated to dryness. The resulting residue was subject to purification by flash column chromatography

(1:1 Hexane: EtOAc), producing the desired compound **136** as a white solid (0.066 g, 66%). M.p. 196-198°C (Decomp.), R_f 0.20 (1:1 Hexane:EtOAc). $^1\text{H NMR}$ (500 MHz, CDCl_3) δ 6.84 (m, 1H, NH), 6.74 (s, 2H, CH=CH), 5.27 (t, 1H, $J = 9.5$ Hz, H3), 5.12 (t, 1H, $J = 9.6$ Hz, H4), 4.95 (t, 1H, $J = 9.0$ Hz, H2), 4.73 (d, 1H, $J = 8.8$ Hz, H1), 3.71 (m, 2H, $\text{CH}_2\text{-CH}_2\text{-NH}$), 3.43 (m, 2H, $\text{CH}_2\text{-CH}_2\text{-NH}$), 2.08-2.01 (3s, 9H, CH_3 , 3 x OAc). $^{13}\text{C NMR}$ (125 MHz, CDCl_3) δ 170.9 (C=O, maleimide), 169.9 (C=O, OAc), 169.6 (C=O, OAc), 169.2 (C=O, OAc), 166.4 (C=O, CONH), 134.3 (CH=CH), 87.8 (C1), 74.1 (C5), 71.9 (C2), 70.5 (C3), 69.0 (C4), 38.9 ($\text{CH}_2\text{-CH}_2\text{-NH}$), 37.0 ($\text{CH}_2\text{-CH}_2\text{-NH}$), 20.6 (CH_3 , OAc), 20.6 (CH_3 , OAc), 20.5 (CH_3 , OAc). **LRMS (ESI):** m/z 490 $[\text{M} + \text{Na}]^+$ **HRMS (ESI):** m/z calculated for $\text{C}_{18}\text{H}_{21}\text{N}_5\text{O}_{10}\text{Na}$ $[\text{M} + \text{Na}]^+$: 490.1186; Found 490.1204.

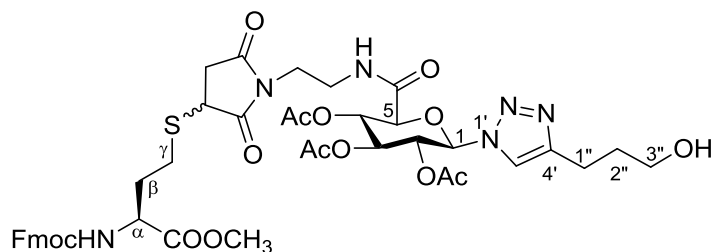
***N*^α-(Fluorenylmethylcarbonyl)-*S*-(*N*-(1-azido-2,3,4-tri-*O*-acetyl- β -D-glucuronoyl)-ethylenediamine succinimido)-*L*-Homocysteine methyl ester (**137**)**



To a round bottom flask containing **137** (0.020 g, 0.0428 mmol) and Fmoc.HCys.OMe (**130**, 0.016 g, 0.0428 mmol) was added a 1:1 solution of ACN:H₂O (0.5 mL). The reaction mixture was left to stir at room temperature for 3 hours, with periodic monitoring of product formation by LR-ESIMS. Upon completion the reaction mixture was evaporated to dryness, with the resulting residue purified by flash column chromatography (1:1 Hexane EtOAc) to yield the desired product **137** as a light yellow oil, present as a mixture of diastereomers

(0.022g, 62%). R_f 0.25 (1:1 Hexane: EtOAc) **1H NMR** (500 MHz, $CDCl_3$) δ 7.76 (d, 2H, $J = 7.3$ Hz, Fmoc-H), 7.62 (d, 2H, $J = 7.2$ Hz, Fmoc-H), 7.41 (t, 2H, $J = 7.3$ Hz, Fmoc-H), 7.32 (t, 2H, $J = 7.3$ Hz, Fmoc-H), 6.82 (m, 1H, CH_2-CH_2-NH), 5.67 (m, 1H, Fmoc-NH), 5.27 (m, 1H, C3), 5.08 (m, 1H, C4), 4.94 (t, 1 H, $J = 9.0$ Hz, H2), 4.70 (t, 1H, $J = 9$ Hz, H1), 4.54 (m, 1H, H^α), 4.41 (m, 2H, OCH_2-CH), 4.24 (t, 1H, $J = 6.5$ Hz, OCH_2CH), 3.96 (m, 1H, H5), 3.77 (m, 3.5H, Succinimide-CH/ OCH_3), 3.71 (m, 2H, CH_2-CH_2-NH), 3.59 (m, 1H, CH_2-CH_2-NH), 3.36 (m, 1H, CH_2-CH_2-NH), 3.20-3.24 (m, 2H, Succinimide- CH_2), 3.03 (m, 1H, H^γ), 2.75-2.87 (dm, 1H, H^γ), 2.49 (m, 0.5H, Succinimide-CH), 2.10-2.25 (dm, 2H, H^β), 2.00-2.08 (3s, 9H, CH_3 , 3 x OAc). **^{13}C NMR** (125 MHz, $CDCl_3$) δ 177.3 (C=O, Succinimide), 175.3 (C=O, Succinimide), 175.0 (C=O, Succinimide), 172.2 (C=O, CONH), 169.8 (C=O, OAc), 169.5 (C=O, OAc), 169.5 (C=O, OAc), 166.5 (C=O, CO $COOCH_3$), 156.1 (C=O, Fmoc), 143.8 (Fmoc Ar-C1), 141.3 (Fmoc Ar-C6), 127.8 (Fmoc Ar-C4), 127.1 (Fmoc Ar-C5), 125.1 (Fmoc Ar-C3), 120.0 (Fmoc Ar-C2), 87.8 (C1), 74.2 (C5), 71.8 (C3), 70.5 (C2), 69.1 (C4), 67.2 (OCH_2CH), 52.9 (C^α), 52.7 (OCH_3), 47.1 (OCH_2CH), 39.2 (Succinimide-CH), 38.9 (Succinimide-CH), 38.6 (CH_2-CH_2-NH), 38.3 (CH_2-CH_2-NH), 35.8 (Succinimide- CH_2), 32.0 (C^β), 27.8 (C^γ), 20.7 (CH_3 , OAc), 20.5 (CH_3 , OAc), 20.5 (CH_3 , OAc). **LRMS (ESI):** m/z 861 $[M + Na]^+$

***N*^α-(Fluorenylmethylcarbonyl)-*S*-(*N*-(1-(4'-(3''-hydroxypropyl)-1',2',3'-triazol-1'-yl)-2,3,4-tri-*O*-acetyl-β-D-glucuronoyl)-ethylenediamine succinimido)-*L*-homocysteine methyl ester (**138**)**



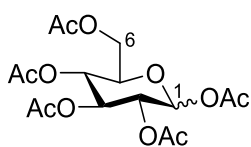
To a round bottom flask containing **137** (0.030 g, 0.036 mmol), 4-pentyn-1-ol (0.015 mL, 0.013 g, 0.143 mmol), CuOAc₂

(0.002 g, 0.010 mmol) and sodium ascorbate (0.003 g, 0.015 mmol) was added a 1:1 solution of *n*-BuOH:H₂O, (0.250 mL), with the solution stirred vigorously under an atmosphere of nitrogen at room temperature for 24 hours. Upon completion, the reaction mixture was diluted with CH₂Cl₂ (5 mL), and extracted with H₂O (1 mL), then brine (1 mL). Subsequent drying (MgSO₄) of the organic phase, and evaporation *in vacuo* resulted in a residue which was purified by flash column chromatography (1:3 Hexane: EtOAc) to yield **138** as a light yellow oil. (0.025 g, 76%). R_f 0.15 (1:3 Hexane: EtOAc). ¹H NMR (500 MHz, CD₃CN) δ 7.87 (m, 3H, Fmoc-H/Triazole-H), 7.72 (m, 2H, Fmoc-H), 7.46 (t, 4H, *J* = 7.3 Hz, Fmoc-H), 7.38 (t, 4H, *J* = 7.3 Hz, Fmoc-H), 7.01 (m, 1H, NH), 6.27 (m, 1H, Fmoc-NH), 6.05 (d, 1H, *J* = 8.5 Hz, H1), 5.51-5.60 (m, 2H, H3/H2), 5.33 (m, 1H, H4), 4.37 (m, 3H, H^α/OCH₂CH). 4.29 (m, 2H, OCH₂CH/H5), 3.80 (m, 0.5H, Succinimide-H), 3.73 (s, 3H, OCH₃) 3.49-3.62 (m, 4H, CH₂-CH₂-NH/CH₂-CH₂-CH₂-OH). 3.32 (m, 2H, CH₂-CH₂-NH), 3.10 (m, 2H, Succinimide-H), 2.93 (m, 1H, H^γ), 2.81 (m, 1H, H^γ), 2.77 (t, 2H, *J* = 7.1 Hz, CH₂-CH₂-CH₂-OH), 2.46 (m, 0.5H, Succinimide-H), 2.27 (m, 2H, H^β), 2.00-2.03 (2s, 6H, CH₃, 2 x OAc), 1.98 (m, 2H, CH₂-CH₂-CH₂-OH), 1.81 (s, 3H, CH₃, OAc). Exchangeable OH

not detected. ^{13}C NMR (125 MHz, CD_3CN) δ 177.2 (C=O, Succinimide), 175.3 (C=O, Succinimide), 175.3 (C=O, Succinimide), 172.6 (C=O, CONH), 170.0 (C=O, OAc), 169.7 (C=O, OAc), 169.0 (C=O, OAc), 166.6 (C=O, CONH), 156.4 (C=O, Fmoc), 148.4 (Triazole-C), 144.4 (Fmoc Ar-C1), 141.4 (Fmoc Ar-C6), 127.8 (Fmoc Ar-C4), 127.3 (Fmoc Ar-C5), 125.4 (Fmoc Ar-C3), 120.8 (Triazole-C), 120.2 (Fmoc Ar-C2), 84.8 (C1), 74.6 (C5), 72.1 (C3), 70.3 (C2), 69.2 (C4), 66.6 (OCH_2CH), 60.9 ($\text{CH}_2\text{-CH}_2\text{-CH}_2\text{-OH}$) 53.2 (C^a), 52.3 (OCH_3), 47.3 (OCH_2CH), 40.0 (Succinimide-CH), 39.7 (Succinimide-CH), 38.2 ($\text{CH}_2\text{-CH}_2\text{-NH}$), 36.7 ($\text{CH}_2\text{-CH}_2\text{-NH}$), 36.2 (Succinimide- CH_2), 32.6 ($\text{CH}_2\text{-CH}_2\text{-CH}_2\text{-OH}$), 32.2 (C^b), 30.2 ($\text{CH}_2\text{-CH}_2\text{-CH}_2\text{-OH}$), 27.8 (C^y), 20.1 (CH_3 , OAc), 20.0 (CH_3 , OAc), 19.6 (CH_3 , OAc). LRMS (ESI): m/z 945 $[\text{M} + \text{Na}]^+$

7.5 Chapter 5 Experimental Data:

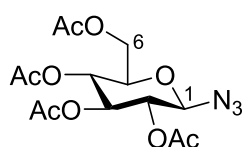
1,2,3,4,6-Penta-*O*-acetyl-D-glucopyranose (147)



To a round bottom flask containing D-glucose (2.54g, 14.1 mmol) was added pyridine (10 mL) and Ac_2O (7.00 mL, 7.52 g, 73.7 mmol), with the reaction mixture allowed to stir at room temperature for 72 hours. After which, the reaction mixture was diluted with CH_2Cl_2 (30 mL) and washed with 1% CuSO_4 solution (2 x 50 mL). The organic layers were further washed with water, dried with Na_2SO_4 and concentrated, with the resultant solid recrystallised from EtOAc to produce **147** as white crystals, present as a mixture of α/β anomers. (5.42 g, 96%). Mp 96-97°C (Lit 100-102°C),²²² R_f 0.65 (1:1 Hexane:EtOAc). ^1H NMR (500 MHz, CDCl_3) δ 6.31 (d, 1H, J = 3.9 Hz, H1 α), 5.72 (d, 1H, J = 8.2 Hz, H1 β) 5.47 (m, 1H, J = 9.8 Hz, H3 α) 5.26 (m, 1H, J = 9.6 Hz,

H3 β) 5.16-5.10 (m, 4H, H2 $\alpha\beta$ /H4 $\alpha\beta$) 4.30-4.25 (m, 2H) 4.14-4.09 (m, 3H, H5 α /H6 $\alpha\beta$), 3.84 (m, 1H, H5), 2.18 (s, 3H, OAc), 2.11-2.02 (5s, 15H, CH₃, 5 x OAc). ¹³C NMR (CDCl₃, 125 MHz): 170.4 (C=O, OAc), 170.1 (C=O, OAc), 169.5 (C=O, OAc), 169.3 (C=O, OAc), 168.6 (C=O, OAc), 92.0 (C1 β), 89.4 (C1 α), 73.2 (C3), 70.6 (C2 α), 70.2 (C2 β), 69.5 (C4), 68.2 (C5), 61.7 (C6), 21.0 (CH₃, OAc), 20.9 (CH₃, OAc), 20.8 (CH₃, OAc), 20.7 (CH₃, OAc). **LRMS (ESI):** m/z 413 [M + Na]⁺

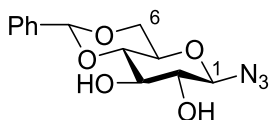
2,3,4,6-Tetra-*O*-acetyl- β -D-glucopyranosyl azide (**148**)



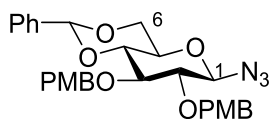
To a solution of **147** (1.17g, 2.99 mmol) in CH₂Cl₂ (30 mL) under a nitrogen atmosphere, were added sequentially TMSN₃ (0.500 mL, 0.458 g, 3.97 mmol) and SnCl₄ (0.200 mL, 0.444 g, 1.71 mmol), with the reaction mixture allowed to stir at room temperature for 24 hours. Upon completion, the reaction mixture was diluted further with DCM (50 mL), washed with aq. NaHCO₃ solution (50 mL) and H₂O (50 mL), dried with Na₂SO₄ and concentrated. The resultant solid was recrystallised from EtOH to produce **148** as a fine white powder. (0.728 g, 65%). Mp 128-130°C (Lit. 128.5°C),²⁵⁴ R_f 0.75 (1:1 Hexane:EtOAc). ¹H NMR (500 MHz, CDCl₃) δ 5.22 (t, 1H, J = 9.4 Hz, H3) 5.10 (t, 1H, J = 9.1 Hz, H4) 4.96 (t, 1H, J = 9.4 Hz, 9.1 Hz, H2) 4.66 (d, 1H, J = 8.8 Hz, H1) 4.27 (dd, 1H, J = 12.2 Hz, 4.8 Hz, H6) 4.16 (dd, 1H, J = 12.4 Hz, 2.5 Hz, H6') 3.79 (m, 1H, H5) 2.10-2.01 (4s, 12H, CH₃, 4 x OAc). ¹³C NMR (125 MHz, CDCl₃) δ 170.6 (C=O, OAc), 170.1 (C=O, OAc), 169.3 (C=O, OAc), 169.2 (C=O, OAc), 87.9 (C1), 73.6 (C3), 72.5 (C2), 70.6 (C4), 67.8 (C5), 61.6 (C6), 20.7 (CH₃, OAc), 20.6 (CH₃,

OAc), 20.5 (CH₃, OAc), 20.5 (CH₃, OAc). **LRMS (ESI):** m/z 396 [M + Na]⁺ **HRMS (ESI):** m/z calculated for C₁₇H₁₉N₃O₉Na [M + Na]⁺: 396.1019; Found 396.1026.

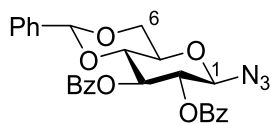
4,6-Benzylidene-β-D-glucopyranosyl azide (**150**)



According to the method of D'Onofrio *et al.*,¹⁵⁸ To a round bottom flask containing **148** (0.351 g, 940 μmol) in MeOH (9.50 mL) was added 0.500 mL of a 0.5M solution of NaOCH₃ in MeOH, with the reaction mixture allowed to stir at room temperature for 0.5 hours. The reaction mixture was neutralised with Dowex 50 x 4 [H⁺] resin, filtered and concentrated to dryness. The resultant residue (**149**) was dissolved in dry DMF (6 mL), treated with benzylidene dimethyl acetal (0.318 g, 0.320 mL, 2.09 μmol) and dry *p*-TsOH (0.020 g, 0.116 μmol), and allowed to stir under aspirator vacuum pressure at 60°C for 5 hours. Upon completion, the reaction mixture was concentrated, and purified using flash column chromatography (1:9 Acetone: CH₂Cl₂) to yield **150** as an amorphous white solid. (0.239 g, 87%) Mp 155-157°C (Lit. 152-153°C),²²⁵ R_f 0.27 (1:9 Acetone: CH₂Cl₂). **¹H NMR** (500 MHz, CD₃OD) δ 7.48 (m, 2H, Ar-H), 7.37 (m, 3H, Ar-H), 5.55 (s, 1H, PhCH), 4.68 (d, 1H, *J* = 8.9 Hz, H1), 4.30 (dd, 1H, *J* = 4.8 Hz, 9.2 Hz, H6), 3.81 (m, 1H, H3/H6'), 3.56 (t, 1H, *J* = 9.2 Hz, 8.5 Hz, H4), 3.55 (m, 1H, H5), 3.46 (t, 1H, *J* = 9.1 Hz, 8.8 Hz, H3), 3.25 (t, 1H, *J* = 8.8 Hz, 8.4 Hz, H2). **¹³C NMR** (125 MHz, CDCl₃) δ 137.1 (Ar-C1), 129.6 (Ar-C4), 128.6 (Ar-C3/5), 126.5 (Ar-C2/6), 102.2 (PhCH), 90.8 (C1), 80.4 (C4), 74.4 (C5), 73.8 (C3), 68.6 (C6), 68.6 (C2). **LRMS (ESI):** m/z 328 [M + Cl]⁻ **HRMS (ESI):** m/z calculated for C₁₃H₁₅N₃O₅Cl: 328.0700 [M + Cl]⁻; Found 328.0708.

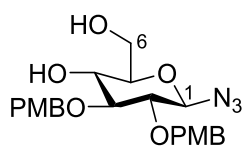
2,3-Di-*O*-*p*-methoxybenzyl-4,6-benzylidene- β -D-glucopyranosyl azide (151)

To a round bottom flask containing **150** (0.200 g, 0.682 mmol) was added *p*-methoxybenzyl chloride (0.530 mL, 0.614 g, 3.92 mmol), *tert*-butylammonium iodide (150 g, 0.406 mmol) and anhydrous DMF (10 mL). The reaction mixture was cooled to 0°C, before NaH – 60% dispersed in mineral oil (0.161 g, 3.93 mmol) was added portion wise. The reaction mixture was then allowed to warm to room temperature, and was left to stir for 24 hours. Upon completion, the reaction mixture was diluted with NH₃Cl and evaporated *in vacuo*. The residue was dissolved in CHCl₃ (20 mL), washed with water (2 x 20 mL), dried with Na₂SO₄ and evaporated. The resultant residue was purified using flash column chromatography (4:1 Hexane:EtOAc.), furnishing **151** as a fluffy white solid. (0.264 g, 73%). M.p. 132-133°C R_f 0.61 (4:1 Hexane:EtOAc.) **¹H NMR** (500 MHz, CDCl₃) δ 7.48 (d, 2H, *J* = 7.6 Hz, PhH₂/6), 7.36 (m, 3H, PhH₃/4/5), 7.26 (dd, 4H, *J* = 3.1 Hz, 5.5 Hz, PMB-H₃/5), 6.84 (dd, 4H, *J* = 8.5 Hz, 5.5 Hz, PMB-H₂/6), 5.54 (s, 1H, Ph-CH), 4.84 (d, 1H, *J* = 11.0 Hz, CH₂Ph), 4.74 (m, 2H, CH₂Ph), 4.71 (d, 1H, *J* = 11.0 Hz, CH₂Ph), 4.65 (d, 1H, *J* = 11.0 Hz, CH₂Ph), 4.34 (dd, 1H, *J* = 5.0 Hz, 10.5 Hz, H₆), 3.76 (m, 7H, 2 x OCH₃, H₃), 3.73 (dd, 1H, *J* = 4.4 Hz, 10.3 Hz, H_{6'}), 3.63 (t, 1H, *J* = 9.1 Hz, H₄), 3.45 (m, 1H, H₅), 3.34 (t, 1H, *J* = 8.5 Hz, H₂). **¹³C NMR** (125 MHz, CDCl₃) δ 159.8 (PMB-C₄), 159.6 (PMB-C_{4'}), 137.4 (Ph-C₁), 130.7 (PMB-C₁/C_{1'}), 130.2 (PMB-C₂/C₆), 130.0 (PMB-C_{2'}/C_{6'}), 129.3 (Ph-C₄), 128.6 (Ph-C₃/C₅), 126.3 (Ph-C₂/C₆), 114.2 (PMB-C₃/C₅), 114.1 (PMB-C_{3'}/C_{5'}), 101.5 (Ph-C-O), 91.0 (C₁), 81.5 (C₃), 81.3 (C₂), 81.1 (C₄), 75.5 (O-CH₂Ph), 75.1 (O-CH₂Ph), 68.7 (C₅), 68.4 (C₆), 55.5 (OCH₃). **LRMS (ESI):** *m/z* 556 [M + Na]⁺ **HRMS (ESI):** *m/z* calculated for C₂₉H₃₁N₃O₇Na [M + Na]⁺: 556.2060, Found: 556.2078.

2,3-Di-O-benzoyl-4,6-benzylidene-β-D-glucopyranosyl azide (152)

To a round bottom flask containing **150** (1.63 g, 5.54 mmol) was added pyridine (20 mL). The reaction mixture was cooled to 0°C, and benzoyl chloride (1.55 mL, 1.98 g, 13.33 mmol)

was added dropwise to the solution. The reaction mixture was subsequently allowed to warm to room temperature, and stirred for 3 hours. Upon completion, the reaction mixture was concentrated *in vacuo*, with the resulting residue recrystallized from EtOAc/Hexanes to produce **152** as a fine white solid. (2.79 g, 63%). M.p. 162-164°C (decomp.), R_f 0.90 (1:1 Hexane:EtOAc.). **¹H NMR** (500 MHz, CDCl₃) δ 7.96 (m, 4H, Bz-H₂/H₆), 7.47-7.53 (m, 2H, Bz-C₄). 7.31-7.40 (m, 9H, Ar-H), 5.81 (t, 1H, J = 9.5 Hz, H₃), 5.56 (s, 1H, PhCH), 5.42 (t, 1H, J = 9.2 Hz, H₄), 4.92 (d, 1H, J = 8.7 Hz, H₁), 4.48 (m, 1H, H₆), 3.88-3.97 (m, 2H, H₂/H₆'), 3.80 (m, 1H, H₅). **¹³C NMR** (125 MHz, CD₃OD) δ 165.5 (C=O), 165.2 (C=O), 136.5 (Ar-C₁), 133.6 (Ar-C₄), 133.3 (Ar-C₄), 129.9 (Ar-C₂/C₆), 129.8 (Ar-C₂/C₆), 129.2 (Ar-C₁), 128.7 (Ar-C₄), 128.5 (Ar-C₃/C₅), 128.4 (Ar-C₃/C₅), 128.2 (Ar-C₃/C₅), 126.1 (Ar-C₂/C₆), 101.6 (PhCH), 88.9 (C₁), 78.5 (C₄), 71.9 (C₃), 71.8 (C₅), 68.9 (C₂), 68.3 (C₆). **LRMS (ESI):** m/z 540 [M + K]⁺ **HRMS (ESI):** m/z calculated for C₂₇H₂₃N₃O₇K [M + K]⁺: 540.1173 Found 540.1173.

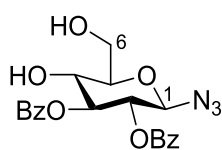
2,3-Di-O-*p*-methoxybenzyl-β-D-glucopyranosyl azide (153)

To a round bottom flask containing **151** (0.169 g, 0.318 mmol) in MeOH: CHCl₃ (5:1, 12 mL) was added dry *p*-TsOH (0.045 g, 0.261 mmol), with the reaction allowed to stir for 24 hours at

room temperature. Upon completion, solvent was removed and the resultant residue was purified using flash column chromatography (1:1 Hexane:EtOAc) providing **153** as a

waxy solid. (0.102 g, 72%), M.p 112-115°C R_f 0.31 (1:1 Hexane:EtOAc). **^1H NMR** (500 MHz, CD_3OD) δ 7.24 (m, 4H, $J = 8.5$ Hz, PMB-H3/H5), 6.84 (d, 4H, $J = 8.5$ Hz, PMB-H2/H6), 4.84-4.61 (m, 5H, $\text{CH}_2\text{-Ph}$, H1), 3.87 (dd, 1H, $J = 2.2$ Hz, 12.1 Hz, H6), 3.77 (s, 6H, $-\text{OCH}_3$), 3.68 (dd, 1H, $J = 5.1$ Hz, 12.2 Hz, H6'), 3.47-3.36 (m, 2H, H3/H5), 3.30 (m, 1H, H4), 3.20 (t, 1H, $J = 8.5$ Hz, H2). **^{13}C NMR** (125 MHz, CD_3OD) δ 159.6 (PMB-C4), 159.5 (PMB-C4'), 130.9 (PMB-C1), 130.3 (PMB-C1'), 129.5 (PMB-C2/C6), 129.5 (PMB-C2'/C6'), 90.2 (C1), 84.6 (C3), 81.0 (C2), 78.8 (C4), 74.9 ($\text{CH}_2\text{-Ph}$), 74.4 ($\text{CH}_2\text{-Ph}$), 70.1 (C5), 61.1 (C6), 54.4 (OCH_3). **LRMS (ESI):** m/z 479 $[\text{M} + \text{HCOO}]^-$

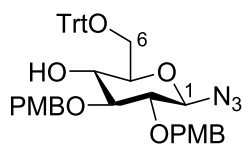
2,3-Di-*O*-benzoyl- β -D-glucopyranosyl azide (**154**)



To a round bottom flask containing **152** (0.528 g, 1.054 mmol), was added a solution of CH_2Cl_2 and CH_3OH (1:4, 5 mL). The resulting suspension was cooled to 0°C , and *p*-TsOH (0.091 g, 0.526 mmol) was added portionwise to the solution. The reaction mixture was then allowed to warm to room temperature, and stirred for 3 hours. Subsequently, the reaction mixture was quenched with sat. NaHCO_3 solution (5 mL), and extracted with CH_2Cl_2 (2 x 50 mL). The organic layers were pooled together, dried (MgSO_4) and concentrated *in vacuo*, with the resulting residue subject to flash column chromatography (1:1 Hexane:EtOAc), producing **154** as a clear oil. (0.320 g, 73%). R_f 0.25 (1:1 Hexane:EtOAc). **^1H NMR** (500 MHz, CDCl_3) δ 7.95 (t, 4H, 7.0 Hz, Ar-H2/H6), 7.51 (m, 2H, Ar-H4), 7.35 (m, 4H, Ar-H3/H5), 5.51 (t, 1H, $J = 9.5$ Hz, H3), 5.34 (t, 1H, $J = 9.0$ Hz, H2), 4.87 (d, 1H, $J = 8.9$ Hz, H1), 3.98 (m, 2H, H4/H6), 3.91

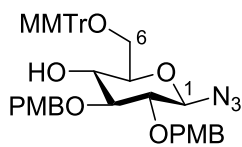
(dd, 1H, $J = 3.0$ Hz, 12.1 Hz, H6'), 3.90 (bs, 1H, OH), 3.69 (m, 1H, H5), 2.65 (bs, 1H, OH). ^{13}C NMR (125 MHz, CDCl_3) δ 167.3 (C=O), 165.5 (C=O), 133.9 (Ar-C4), 133.8 (Ar-C4), 130.1 (Ar-C2/C6), 130.1 (Ar-C2/C6), 129.0 (Ar-C1), 128.7 (Ar-C3/C5), 128.7 (Ar-C3/C5), 88.4 (C1), 78.4 (C3), 76.6 (C2), 71.3 (C5), 69.4 (C4), 62.1 (C6). **LRMS (ESI):** m/z 458 $[\text{M} + \text{HCOO}]^-$

2,3-Di-*O-p*-methoxybenzyl-6-trityl- β -D-glucopyranosyl azide (**155**)

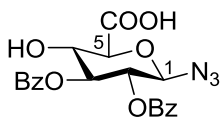


To a round bottom flask **153** (0.100 g, 0.145 mmol) was added trityl chloride (0.061 g, 0.218 mmol) and pyridine (5 mL), with the reaction allowed to stir at room temperature for 48 hours.

Upon completion, the reaction mixture was co-evaporated with toluene (2 x 25 mL). The resultant residue was purified using flash column chromatography (4:1 Hexane:EtOAc), producing **155** as a white amorphous solid. (0.048 g, 31%) R_f 0.28 (4:1 Hexane:EtOAc). ^1H NMR (500 MHz, CDCl_3) δ 7.45 (d, 4H, $J = 8.5$ Hz, PMB-H3/H5), 7.30-7.20 (m, 15H, Ar-H), 6.86 (m, 4H, $J = 8.5$ Hz, PMB-H2/H6), 4.82 (m, 2H, $J = 11.1$ Hz, $\text{CH}_2\text{-Ph}$, H1), 4.70 (d, 1H, $J = 5.7$ Hz, $\text{CH}_2\text{-Ph}$), 4.64 (d, 1H, $J = 6.3$ Hz, $\text{CH}_2\text{-Ph}$), 4.61 (d, 1H, $J = 8.1$ Hz, $\text{CH}_2\text{-Ph}$), 3.79 (s, 3H, OCH_3), 3.78 (s, 3H, OCH_3), 3.67 (t, 1H, $J = 5.5$ Hz, H3), 3.45-3.30 (m, 5H, H2/H4/H5/H6/H6'). ^{13}C NMR (125 MHz, CDCl_3) δ 159.8 (PMB-C4/C4'), 143.9 (Trt-C1), 130.8 (Ar-C), 130.3 (Ar-C), 130.2 (Ar-C), 130.0 (Ar-C), 129.0 (Ar-C), 128.2 (Ar-C), 127.5 (Ar-C), 114.3 (PMB-C3/C5), 114.2 (Ar-C3'/C5'), 90.2 (C1), 87.2 (Ph-C), 84.3 (C3), 81.4 (C2), 76.6 (C4), 75.5 ($\text{CH}_2\text{-Ph}$), 75.1 ($\text{CH}_2\text{-Ph}$), 71.5 (C5), 63.8 (C6), 55.6 (OCH_3). **LRMS (ESI):** m/z 710 $[\text{M} + \text{Na}]^+$

2,3-*O*-*p*-Methoxybenzyl-6-(*p*-methoxytrityl)- β -D-glucopyranosyl azide (156)

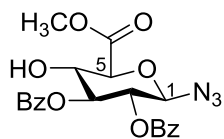
To a round bottom flask **153** (0.101 g, 0.146 mmole) was added 4-methoxytrityl chloride (0.068 g, 0.220 mmol) and pyridine (5 mL), with the reaction allowed to stir at room temperature for 48 hours. Upon completion, the reaction mixture was co-evaporated with toluene (2 x 25 mL). The resultant residue was purified using flash column chromatography (4:1 Hexane: EtOAc) producing **156** as a white amorphous solid. (0.099 g, 61%), R_f 0.35 (4:1 Hexane:EtOAc). $^1\text{H NMR}$ (500 MHz, CDCl_3) δ 7.45 (d, 6H, J = 8.5 Hz, PMB-H3/H5), 7.20-7.34 (m, 10H, Ar-H), 6.82-6.88 (m, 6H, PMB-H2/H6), 4.81 (d, 2H, CH_2 -Ph), 4.69 (m, 2H, CH_2 -Ph), 4.61 (d, 1H, J = 8.8 Hz, H1), 3.79 (3s, 9H, OCH_3), 3.67 (t, 1H, J = 9.0 Hz, H3), 3.33-3.45 (m, 5H, H2/H4/H5/H6/H6'). $^{13}\text{C NMR}$ (125 MHz, CDCl_3) δ 159.5 (PMB-C4) 159.4 (PMB-C4'), 158.7 (PMB-Trt-C4), 144.2 (Trt-C1/C1'), 135.3 (PMB-Trt-C1), 130.4 (Ar-C), 130.1 (Ar-C), 129.9 (Ar-C), 129.7 (Ar-C), 128.4 (Ar-C), 127.9 (Ar-C), 127.1 (Ar-C), 114.0 (PMB-C3/C5), 113.9 (PMB-C3'/C5'), 113.3 (PMB-Trt-C3'/C5'), 90.0 (C1), 86.7 (Ph-C), 84.0 (C3), 81.1 (C2), 76.3 (C4), 75.2 (CH_2 -Ph), 74.8 (CH_2 -Ph), 71.4 (C5), 63.6 (C6), 55.3 (OCH_3), 55.3 (OCH_3), 55.2 (OCH_3). **LRMS (ESI):** m/z 740 $[\text{M} + \text{Na}]^+$

2,3-Di-*O*-benzoyl-1-azido- β -D-glucuronic acid (161)

According to the method of van den Bos *et al.*,²²⁷ a round bottom flask containing **154** (0.120 g, 0.29 mmol), was added a solution of CH_2Cl_2 and H_2O (2:1; 1.50 mL). The biphasic solution was cooled to 0°C, and TEMPO (0.010 g, 0.640 mmol) and PhIOAc_2 (0.242 g, 0.751 mmol) was

added to the reaction mixture portion wise, after which the reaction mixture was warmed to room temperature, and stirred vigorously for 45 minutes. After this time, the reaction was diluted with 10% sodium thiosulphate solution (5 mL), and extracted with EtOAc (2 x 10 mL). The combined organic layers were washed with brine (5 mL), dried (MgSO_4) and evaporated *in vacuo*, with purification by flash column chromatography (5% AcOH in 1:1 Hexane:EtOAc) yielding the product **161** as a light yellow oil. (0.109 g, 88%). R_f 0.28 (5% AcOH in 1:1 Hexane:EtOAc). $^1\text{H NMR}$ (500 MHz, CD_3OD) δ 7.91 (t, 2H, 7.0 Hz, Ar-H2/H6), 7.51 (m, 2H, Ar-H4), 7.37 (m, 4H, Ar-H3/H5), 5.61 (t, 1H, $J = 9.3$ Hz, H3), 5.25 (t, 1H, $J = 9.0$ Hz, H2), 5.16 (d, 1H, $J = 8.7$ Hz, H1), 4.24 (d, 1H, $J = 9.7$ Hz, H5), 4.09 (t, 1H, $J = 9.6$ Hz, H4). $^{13}\text{C NMR}$ (125 MHz, CD_3OD) δ 169.7 (C=O, COOH), 165.9 (C=O), 165.2 (C=O), 133.3 (Ar-C4), 133.1 (Ar-C4), 129.3 (Ar-C2/C6), 129.3 (Ar-C2/C6), 128.8 (Ar-C1), 128.2 (Ar-C3/C5), 128.1 (Ar-C3/C5), 87.9 (C1), 77.0 (C3), 75.0 (C2), 71.4 (C5), 69.7 (C4). **LRMS (ESI):** m/z 426 $[\text{M} - \text{H}]^-$ **HRMS (ESI):** m/z calculated for $\text{C}_{20}\text{H}_{16}\text{N}_3\text{O}_8$ $[\text{M} - \text{H}]^-$: 426.0937; Found 426.0946

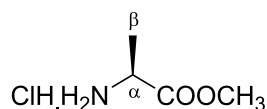
2,3-Di-*O*-benzoyl-1-azido- β -D-glucuronic acid methyl ester (**162**)



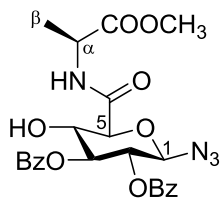
To a round bottom flask containing **161** (0.109 g, 0.255 mmol) in DMF (2 mL), was added K_2CO_3 (0.141 g, 1.02 mmol). The solution was stirred for 5 minutes, before being brought down to 0°C . MeI (0.024 mL, 0.054 g, 0.382 mmol) was subsequently added to the stirring solution dropwise, with the reaction mixture allowed to warm gradually to room temperature and stir for an additional 16 hours. Following completion, the reaction was diluted with H_2O (5 mL), and extracted with EtOAc (10 mL). The organic layers were collected, washed with brine (5 mL), dried (Na_2SO_4) and evaporated *in vacuo*, yielding

a residue that following flash column chromatography (2:1 Hexane:EtOAc.) resulted in the isolation of **162** as a clear oil. (0.072 g, 64%). R_f 0.35 (2:1 Hexane:EtOAc.). $^1\text{H NMR}$ (500 MHz, CDCl_3) δ 7.95 (m, 4H, Ar-H2/H6), 7.50 (m, 2H, Ar-H4), 7.37 (m, 4H, Ar-H3/H5), 5.60 (m, 1H, H3), 5.38 (t, 1H, $J = 9.5$ Hz, H2), 4.91 (d, 1H, $J = 8.7$ Hz, H1), 4.20 (m, 2H, H4/H5), 3.87 (s, 3H, OCH_3), 3.51 (bs, 1H, OH). $^{13}\text{C NMR}$ (125 MHz, CDCl_3) 168.5 (C=O, COOCH_3), 166.4 (C=O), 165.1 (C=O), 133.6 (Ar-C4), 133.6 (Ar-C4), 129.9 (Ar-C2/C6), 129.9 (Ar-C2/C6), 128.8 (Ar-C3/C5), 128.6 (Ar-C3/C5), 128.6 (Ar-C1), 128.5 (Ar-C1), 88.6 (C1), 76.2 (C3), 74.6 (C2), 70.5 (C5), 70.2 (C4), 53.1 (OCH_3). **LRMS (ESI):** m/z 464 $[\text{M} + \text{Na}]^+$ **HRMS (ESI):** m/z calculated for $\text{C}_{21}\text{H}_{19}\text{N}_3\text{O}_8\text{Na}$ $[\text{M} + \text{Na}]^+$: 464.1070; Found 464.1092. Data gained in the production of this compound was not consistent with that published elsewhere.²²⁶

L-Alanine methyl ester hydrochloride (**163**)



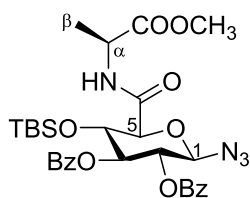
To a round bottom flask containing L-alanine (1.7 g, 19 mmol), was added MeOH (20 mL) and placed under an atmosphere of argon. The reaction mixture was cooled to 0°C, and thionyl chloride (1.45 mL, 2.37 g, 20 mmol) was subsequently added to the reaction mixture dropwise. After 30 minutes, the round bottom flask was allowed to warm to room temperature, and the reaction mixture was stirred for an additional 18 hours. Upon completion, the reaction mixture was concentrated *in vacuo*, producing **163** as an off-white crystalline solid. (2.64 g, 99%). M.p. 104-106°C (Lit. 107-110°C)²⁵⁵ $^1\text{H NMR}$ (500 MHz, $\text{DMSO}-d_6$) δ 8.54 (bs, 1H, NH_3), 4.05 (m, 1H, H^α), 3.73 (s, 3H, OCH_3), 1.43 (d, 3H, $J = 7.3$ Hz, H^β). $^{13}\text{C NMR}$ (125 MHz, $\text{DMSO}-d_6$) 170.4 (C=O, COOCH_3), 52.7 (OCH_3), 47.8 (C^α), 15.6 (C^β). **LRMS (ESI):** m/z 104 $[\text{M} - \text{Cl} + \text{H}]^+$

***N*-(1-Azido-2,3-di-*O*-benzoyl- β -D-glucopyranuronoyl)-L-alanine methyl ester (**164**)**

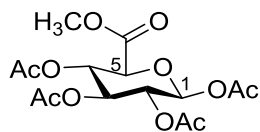
161 (0.100 g, 0.234 mmol), HBTU (0.178 g, 0.468 mmol) and L-alanine methyl ester hydrochloride (**163**, 0.049 g, 0.351 mmol) were placed in a round bottom flask. DMF (5 mL) was added to the flask, and the resulting solution was cooled to 0°C. DIPEA

(0.045 mL, 0.033 g, 0.257 mmol) was then added, and the reaction mixture was allowed to warm to room temperature, stirring for 24 hours. Upon completion, the reaction mixture was diluted with H₂O (5 mL), and the aqueous solution was washed with EtOAc (20 mL). The organic phases were pooled together and washed with brine (5 mL), dried (NaSO₄) and evaporated *in vacuo*. The resulting residue was then subjected to flash column chromatography (1:3 Hexane: EtOAc), resulting in the isolation of **164** as a clear oil. (0.060 g, 50%). *R*_f 0.05 (1:1 Hexane:EtOAc.). ¹H NMR (500 MHz, CDCl₃) δ 7.95 (m, 4H, Ar-H₂/H₆), 7.51 (m, 2H, Ar-H₄), 7.37 (m, 4H, Ar-H₃/H₅), 7.15 (d, 1H, *J* = 7.4 Hz, NH), 5.68 (t, 1H, *J* = 9.4 Hz, H₃), 5.36 (t, 1H, *J* = 9.5 Hz, H₂), 4.94 (d, 1H, *J* = 8.9 Hz, H₁), 4.64 (m, 1H, H^{*a*}), 4.11 (m, 2H, H₄/H₅), 3.80 (s, 3H, OCH₃), 1.51 (d, 3H, *J* = 7.5 Hz, H^{*b*}). ¹³C NMR (125 MHz, CDCl₃) 172.5 (C=O, COOCH₃), 168.9 (C=O, CONH), 165.7 (C=O), 165.1 (C=O), 133.6 (Ar-C₄), 133.3 (Ar-C₄), 129.9 (Ar-C₂/H₆), 129.8 (Ar-C₂/H₆), 129.0 (Ar-C₁), 128.6 (Ar-C₁), 128.5 (Ar-C₃/C₅), 128.3 (Ar-C₃/C₅), 88.3 (C₁), 74.4 (C₅), 73.9 (C₃), 70.6 (C₂), 70.4 (C₄), 52.8 (OCH₃), 47.9 (C^{*a*}), 18.1 (C^{*b*}). LRMS (ESI): *m/z* 547 [M + Cl]⁻. HRMS (ESI): *m/z* calculated for C₂₄H₂₄N₄O₉Cl [M + Cl]⁻: 547.1232; Found 547.1238.

***N*-(1-Azido-2,3-di-*O*-benzoyl-4-*t*-butyldimethylsilyl- β -D-glucopyranuronoyl)-L-alanine methyl ester (**165**)**



164 (0.105 g, 0.205 mmol) and imidazole (0.070 g, 1.03 mmol) were dissolved in dry DMF (1 mL) in a round bottom flask. The reaction mixture was cooled to 0°C, and *t*-butyldimethylsilyl chloride (0.077 g, 0.511 mmol) was added portion wise. The reaction mixture was then flushed with argon, warmed to room temperature and allowed to stir for 18 hours. Upon completion, the reaction mixture was diluted with H₂O (2 mL) and extracted with EtOAc (10 mL). The organic layers were washed with brine (2 mL), dried (Na₂SO₄) and evaporated *in vacuo*, with the resulting residue subjected to flash column chromatography (1:1 Hexane: EtOAc), producing **165** as a clear oil. (0.046 g, 36%). *R_f* 0.55 (1:1 Hexane:EtOAc.). ¹H NMR (500 MHz, CDCl₃) δ 7.92 (m, 4H, Ar-H₂/H₆), 7.50 (m, 2H, Ar-H₄), 7.37 (m, 4H, Ar-H₃/H₅), 6.87 (d, 1H, *J* = 7.4 Hz, NH), 5.48 (t, 1H, *J* = 9.4 Hz, H₃), 5.29 (t, 1H, *J* = 9.5 Hz, H₂), 5.09 (d, 1H, *J* = 8.9 Hz, H₁), 4.53 (m, 1H, H^{*a*}), 4.38 (t, 1H, *J* = 9.4 Hz, H₄), 4.17 (d, 1H, *J* = 6.5 Hz, H₅), 3.76 (s, 3H, OCH₃), 1.39 (d, 3H, *J* = 7.0 Hz, H^{*b*}), 0.79 (s, 9H, CH₃, Si-*t*-Bu), 0.04 (s, 3H, Si-CH₃), -0.08 (s, 3H, Si-CH₃). ¹³C NMR (125 MHz, CDCl₃) 172.9 (C=O, COOCH₃), 166.5 (C=O, CONH), 165.3 (C=O), 165.1 (C=O), 133.5 (Ar-C₄), 133.4 (Ar-C₄), 129.9 (Ar-C₂/H₆), 129.8 (Ar-C₂/H₆), 129.3 (Ar-C₁), 128.8 (Ar-C₁), 128.4 (Ar-C₃/C₅), 128.4 (Ar-C₃/C₅), 87.6 (C₁), 79.7 (C₅), 74.9 (C₃), 71.8 (C₂), 70.4 (C₄), 52.6 (OCH₃), 48.1 (C^{*a*}), 30.9 (Si-C), 25.6 (C(CH₃)₃), 18.4 (C^{*b*}), -4.6 (Si-C), -4.9 (Si-CH₃). LRMS (ESI): *m/z* 649 [M + Na]⁺. HRMS (ESI): *m/z* calculated for C₃₀H₃₈N₄O₉SiNa: 649.2306 [M + Na]⁺; Found 649.2302

1,2,3,4-Tetra-O-acetyl-β-D-glucopyranuronic acid methyl ester (52)

According to the method of Graff von Roedern *et al.*,¹⁵⁶

Glucuronolactone (**51**, 12.90 g, 72 mmol) was suspended in dry

MeOH (400 mL), and triethylamine (0.6 mL) was added. The

reaction mixture was stirred for 3 hours until the glucuronolactone was dissolved. The

solvent was evaporated and the resulting solid was used without further purification.

The solid was then suspended in Ac₂O (63.0 mL, 67.8 g, 660 mmol) and NaOAc

(6.30 g, 72.0 mmol) were added, and the suspension was stirred for 8 days. The reaction

mixture was then poured onto ice water (300 mL) and stirred overnight. The resulting

white solid was isolated by filtration, washed with water (50 mL), and recrystallized

from EtOAc/Hexanes to afford the desired product **52** solely present as the β anomer.

(10.59 g, 38%) Mp 179-180 °C. (Lit.179-180°C).¹⁶⁴ R_f 0.75 (1:1 Hexane:EtOAc).

¹H NMR (500 MHz, CDCl₃) δ 6.02 (d, 1H, *J* = 8.1 Hz, H1), 5.51 (dd, 1H *J* = 9.4 Hz,

H3), 5.01 (t, 1H, *J* = 9.6 Hz, H4), 4.97 (t, 1H, *J* = 8.2 Hz, H2), 4.67 (d, 1H, *J* = 9.8 Hz,

H5), 3.63 (s, 3H, OCH₃β), 2.08-1.97 (4s, 12H, OAc). ¹³C NMR (125 MHz, CDCl₃)

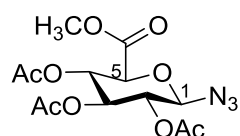
170.1 (C=O, OAc), 169.6 (C=O, OAc), 169.4 (C=O, OAc), 169.0 (C=O, OAc), 167.0

(C=O, COOCH₃), 91.6 (C1), 73.2 (C5), 72.0 (C4), 70.4 (C3), 69.1 (C2), 53.2 (OCH₃),

21.0 (CH₃, OAc), 20.8 (CH₃, OAc), 20.8 (CH₃, OAc), 20.7 (CH₃, OAc). LRMS (ESI):

m/z 399 [M + Na]⁺. HRMS (ESI): *m/z* calculated for C₁₅H₂₀O₁₁Na [M + Na]⁺:

399.0903; Found 399.0917.

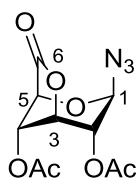
1-Azido-1-deoxy-2,3,4-tri-O-acetyl-β-D-glucuronic acid methyl ester (53)

To a solution of **52** (5.00g, 2.65 mmol) in CH₂Cl₂ (50 mL) under

a N₂ atmosphere, were added sequentially TMS-N₃ (2.50 mL,

2.290 g, 19.85 mmol) and SnCl_4 (1.00 mL, 2.22 g, 8.55 mmol), with the reaction mixture allowed to stir at room temperature for 3 hours. Upon completion, the reaction mixture was diluted further with CH_2Cl_2 (100 mL), washed with sat. NaHCO_3 solution (100 mL) and brine (100 mL), dried with Na_2SO_4 and concentrated. The resultant solid was recrystallised from EtOAc/Hexanes to produce **53** as a fine white powder. (3.89 g, 81%) Mp 154-157 °C (Lit. 152-153°C), $^{153}\text{R}_f$ 0.85 (1:1 Hexane:EtOAc). $^1\text{H NMR}$ (500 MHz, CDCl_3) δ 5.40 (dd, 1H, $J = 9.6$ Hz, H3), 5.19 (d, 1H, $J = 8.8$ Hz, H1), 5.05 (dd, 1H, $J = 9.8$ Hz, H4), 4.87 (dd, 1H, $J = 9.2$ Hz, H2), 4.57 (d, 1H, $J = 9.9$ Hz, H5), 3.66 (s, 3H, OCH_3), 2.04-1.98 (3s, 9H, OAc). $^{13}\text{C NMR}$ (125 MHz, CDCl_3) δ 170.2 (C=O, OAc), 169.4 (C=O, OAc), 169.3 (C=O, OAc), 167.1 (C=O), 88.1 (C1), 74.3 (C5), 72.0 (C4), 70.5 (C2), 69.1 (C3), 53.2 (OCH_3) 20.7 (CH_3 , OAc), 20.7 (CH_3 , OAc), 20.6 (CH_3 , OAc). **LRMS (ESI):** m/z 382 $[\text{M} + \text{Na}]^+$ **HRMS (ESI):** m/z calculated for $\text{C}_{13}\text{H}_{17}\text{N}_3\text{O}_9\text{Na}$ $[\text{M} + \text{Na}]^+$: 382.0862; Found 382.0867.

2,4-Di-*O*-acetyl- β -D-glucopyranuronyl azide-3,6-lactone (**166**)



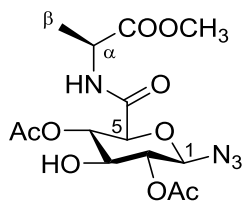
According to the method of Tosin *et al.*,¹⁵⁷ To a round bottom flask containing **53** (0.985 g, 2.74 mmol) was added a solution of LiOH (0.3 M, 60 mL) at 0°C, with the resulting suspension allowed to stir for 3.5 hours. Following this time, the pH of the solution was adjusted to 2 using Amberlite IR-120 resin, the solution was filtered, and concentrated *in vacuo*, before being subjected to lyophilisation overnight. The resulting white powder was suspended in Ac_2O (20.0 mL) and 4Å molecular sieves were added, with the reaction mixture placed under argon and allowed to stir at 85°C for 2 hours. After this time, filtration followed by concentration *in vacuo* and consecutive azeotropic distillation with toluene, resulted in the isolation of **166** as yellow oil that was directly used in the

next step without further purification. (0.586 g, 75%), R_f 0.31 (1:1 Hexane:EtOAc.).

$^1\text{H NMR}$ (500 MHz, CDCl_3) δ 5.44 (m, 1H, H1), 5.07 (m, 1H, H3), 4.93 (m, 2H, H2/H4), 4.36 (m, 1H, H5), 2.19 (s, 3H, CH_3 , OAc), 2.10 (s, 3H, CH_3 , OAc).

$^{13}\text{C NMR}$ (125 MHz, CDCl_3) δ 170.2 (C=O), 169.0 (C=O, OAc), 168.9 (C=O, OAc), 88.5 (C1), 71.4 (C5), 68.9 (C4), 68.6 (C3), 67.5 (C2), 20.7 (CH_3 , OAc), 20.7 (CH_3 , OAc).

N-(1-Azido-2,4-di-*O*-acetyl- β -D-glucopyranuronoyl)-L-alanine methyl ester (**169**)

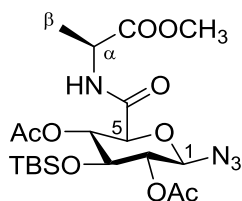


To a round bottom flask containing **166** (0.586 g, 2.05 mmol), was added L-alanine methyl ester hydrochloride (**163**, 0.430 g, 3.08 mmol) and dry CH_2Cl_2 (10 ml). The reaction mixture was cooled to 0°C , and NEt_3 (0.311 g, 0.430 mL, 3.08 mmol) was

added dropwise, with the resulting suspension allowed to warm to room temperature and stirred for 18 hours. Upon completion, the reaction mixture was diluted with CH_2Cl_2 (10 mL), and the organic phase was washed with H_2O (5 mL) and brine (5 mL). Drying (Na_2SO_4) and evaporation *in vacuo*, followed by flash column chromatography resulted in the isolation of **169** as a white solid. (0.447 g, 56%), M.p. $162\text{--}163^\circ\text{C}$ (decomp.) R_f 0.25 (1:1 Hexane:EtOAc.). $^1\text{H NMR}$ (500 MHz, CDCl_3) δ 6.93 (d, 1H, $J = 7.1$ Hz, NH), 5.04 (t, 1H, $J = 9.6$ Hz, H4), 4.87 (t, 1H, $J = 8.9$ Hz, H2), 4.69 (d, 1H, $J = 8.8$ Hz, H1), 4.54 (m, 1H, H^a), 3.94 (d, 1H, $J = 9.9$ Hz, H5), 3.83 (t, 1H, $J = 9.2$ Hz, H4), 3.76 (s, 3H, OCH_3), 2.16 (s, 3H, CH_3 , OAc), 2.13 (s, 3H, CH_3 , OAc), 1.43 (d, 3H, $J = 7.1$ Hz, H^b). $^{13}\text{C NMR}$ (125 MHz, CDCl_3) 172.9 (C=O), 170.3 (C=O, OAc), 170.2 (C=O, OAc), 165.8 (C=O, CONH), 87.9 (C1), 74.4 (C5), 72.9 (C4), 72.8 (C2), 71.5 (C3), 52.6 (OCH_3), 47.8 (C^a), 20.8 (CH_3 , OAc), 20.8 (CH_3 , OAc), 18.1 (C^b).

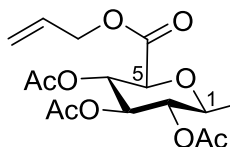
LRMS (ESI): m/z 411 $[M + Na]^+$ **HRMS (ESI):** m/z calculated for $C_{14}H_{20}N_4O_9Na$ $[M + Na]^+$: 411.1128; Found 411.1165.

***N*-(1-Azido-2,4-di-*O*-acetyl-3-*t*-butyldimethylsilyl- β -D-glucopyranuronoyl)-L-alanine methyl ester (**170**)**



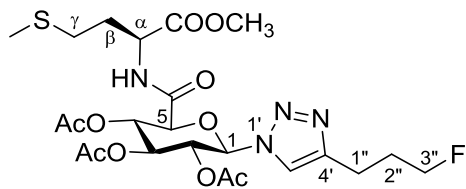
169 (0.400 g, 1.03 mmol) and imidazole (0.281 g, 4.12 mmol) were dissolved in dry DMF (10 mL) in a round bottom flask. The reaction mixture was cooled to 0°C, and *t*-butyldimethylsilyl chloride (0.310 g, 2.06 mmol) was added portionwise. The reaction mixture was then flushed with argon, warmed to room temperature and allowed to stir for 18 hours. Upon completion, the reaction mixture was diluted with H₂O (10 mL) and extracted with EtOAc (2 x 25 mL). The organic layers were pooled and washed with brine (10 mL), dried (Na₂SO₄) and evaporated *in vacuo*, with the resulting residue subjected to flash column chromatography, producing **170** as a white solid. (0.343 g, 66%), M.p. 152-153°C R_f 0.85 (1:1 Hexane:EtOAc.) **¹H NMR** (500 MHz, CDCl₃) δ 6.94 (d, 1H, J = 7.1 Hz, NH), 5.01 (t, 1H, J = 9.6 Hz, H₄), 4.93 (t, 1H, J = 8.9 Hz, H₂), 4.53 (m, 2H, H₁/H^{*u*}), 3.88 (m, 2H, H₄/H₅), 3.75 (s, 3H, OCH₃), 2.13 (s, 3H, CH₃, OAc), 2.10 (s, 3H, CH₃, OAc), 1.42 (d, 3H, J = 7.1 Hz, H^{*β*}), 0.81 (s, 9H, Si-*t*Bu), 0.05 (s, 6H, 2 x Si-CH₃). **¹³C NMR** (125 MHz, CDCl₃) 173.0 (C=O), 169.9 (C=O, OAc), 169.4 (C=O, OAc), 166.1 (C=O, CONH), 88.2 (C₁), 74.9 (C₅), 73.0 (C₄), 72.9 (C₂), 72.0 (C₃), 52.8 (OCH₃), 47.9 (C^{*u*}), 25.6 (C(CH₃)₃), 21.3 (CH₃, OAc), 21.2 (CH₃, OAc), 18.3 (C^{*β*}), 18.0 (C(CH₃)₃), -4.4 (Si-CH₃). **LRMS (ESI):** m/z 525 $[M + Na]^+$ **HRMS (ESI):** m/z calculated for $C_{20}H_{34}N_4O_9SiNa$ $[M + Na]^+$: 525.1993; Found 525.2014.

1-(4'-(3''-Fluoropropyl)-1',2',3'-triazol-1'-yl)-2,3,4-tri-*O*-acetyl- β -D-glucuronic acid allyl ester (173)



To a round bottom flask containing **74** (0.101 g, 0.215 mmol) dissolved in ACN (5 mL), was added $\text{C}_4\text{F}_9\text{SO}_2\text{F}$ (0.132 g, 0.080 mL, 0.433 mmol) $\text{NEt}_3 \cdot 3\text{HF}$ (0.069 g, 0.070 mL, 0.430 mmol) and NEt_3 (0.131 g, 0.180 mL, 1.30 mmol). Under an argon atmosphere, the reaction mixture was stirred at room temperature for 24 hours. Upon completion, the reaction mixture was filtered through a short silica plug. The resulting solution was then evaporated *in vacuo*, with purification by flash column chromatography (1:1 Hexane: EtOAc) producing the desired product **173** as a light yellow solid. (0.059 g, 58 %). R_f 0.15 (1:1 Hexane:EtOAc), M.p 114-116°C. $^1\text{H NMR}$ (500 MHz, CDCl_3) δ 7.65 (s, 1H, Triazole-H), 5.94-5.81 (m, 2H, H1/ $\text{CH}_2=\text{CH}-\text{CH}_2$), 5.48-5.27 (m, 5H, H4/H3/H2/ $\text{CH}_2=\text{CH}-\text{CH}_2$), 4.65 (m, 2H, $\text{CH}_2=\text{CH}-\text{CH}_2$), 4.51-4.42 (dt, 2H, $J = 6.1$ Hz, 47 Hz, $\text{CH}_2-\text{CH}_2-\text{CH}_2-\text{F}$), 4.36 (d, 1H, $J = 9.8$ Hz, H5), 2.87 (m, 2H, $\text{CH}_2-\text{CH}_2-\text{CH}_2-\text{F}$), 2.17 (m, 2H, $\text{CH}_2-\text{CH}_2-\text{CH}_2-\text{F}$), 2.05 (2s, 6H, OAc), 1.88 (s, 3H, OAc). $^{13}\text{C NMR}$ (125 MHz, CDCl_3) δ 170.0 (C=O, OAc), 169.6 (C=O, OAc), 169.1 (C=O, OAc), 165.8 (C=O), 147.9 (Triazole C), 131.0 ($\text{CH}_2-\text{CH}=\text{CH}_2$), 120.1 (Triazole C), 119.7 ($\text{CH}_2-\text{CH}=\text{CH}_2$), 85.6 (C1), 83.8-82.4 (d, $J = 164.9$ Hz, $\text{CH}_2-\text{CH}_2-\text{CH}_2-\text{F}$), 75.1 (C5), 72.1 (C4), 70.2 (C3), 69.2 (C2), 67.2 ($\text{CH}_2-\text{CH}=\text{CH}_2$), 30.0-29.8 (d, $J = 20.1$ Hz, $\text{CH}_2-\text{CH}_2-\text{CH}_2-\text{F}$), 21.5 ($\text{CH}_2-\text{CH}_2-\text{CH}_2-\text{F}$), 20.7 (CH_3 , OAc), 20.7 (CH_3 , OAc), 20.3 (CH_3 , OAc). **LRMS (ESI):** m/z 494 $[\text{M} + \text{Na}]^+$ **HRMS (ESI):** m/z calculated for $\text{C}_{20}\text{H}_{26}\text{FN}_3\text{O}_9\text{Na}$ $[\text{M} + \text{Na}]^+$: 494.1551; Found 494.1574.

***N*-(1-(4'-(3''-Fluoropropyl)-1',2',3'-triazol-1'-yl)-2,3,4-tri-*O*-acetyl- β -D-glucuronoyl)-L-methionine methyl ester (**174**)**



To a round bottom flask containing **86** (0.100 g, 0.174 mmol) dissolved in ACN (5 mL), was added $\text{C}_4\text{F}_9\text{SO}_2\text{F}$ (0.105 g, 0.063 mL, 0.348 mmol) $\text{NEt}_3 \cdot 3\text{HF}$ (0.059 g, 0.060 mL, 0.352 mmol) and NEt_3 (0.105 g, 0.145 mL, 1.04 mmol). Under an argon atmosphere, the reaction mixture was stirred at room temperature for 24 hours. Upon completion, the reaction mixture was filtered through a short silica plug. The resulting solution was then evaporated *in vacuo*, with purification of the residue by flash column chromatography (1:1 Hexane: EtOAc) producing the desired product **174** as a white solid (0.049mg, 49%). R_f 0.35 (1:1 Hexane:EtOAc), M.p 198-199°C. $^1\text{H NMR}$ (500 MHz, CDCl_3) δ 7.63 (s, 1H, Triazole-H), 7.06 (d, 1H, $J = 7.6$ Hz, NH), 5.94 (d, 1H, $J = 9.5$ Hz, H1), 5.55 (t, 1H, $J = 9.7$ Hz, H3), 5.49 (t, 1H, $J = 9.7$ Hz, H4), 5.35 (t, 1H, $J = 9.7$ Hz, H2), 4.64 (m, 1H, H^α), 4.27-4.25 (dt, 2H, $J = 5.8$ Hz, 52.9 Hz, $\text{CH}_2\text{-CH}_2\text{-CH}_2\text{-F}$), 4.25 (d, 1H, $J = 10.0$ Hz, H5), 3.73 (s, 3H, OCH_3), 2.89 (t, 2H, $J = 7.3$ Hz, $\text{CH}_2\text{-CH}_2\text{-CH}_2\text{-F}$), 2.51 (t, 1H, $J = 7.2$ Hz, H^γ), 2.17-2.15 (m, 2H, H^β), 2.09-2.04 (2s, 9H, 3 x OAc), 2.04-1.99 (m, 2H, $\text{CH}_2\text{-CH}_2\text{-CH}_2\text{-F}$), 1.89 (s, 3H, SCH_3). $^{13}\text{C NMR}$ (125 MHz, CD_3OD) δ 172.1 (COOCH_3), 169.9 (C=O, OAc), 169.7 (C=O, OAc), 169.1 (C=O, OAc), 165.4 (C=O), 148.0 (Triazole-C), 119.9 (Triazole-C), 85.3 (C1), 83.7-82.4 (d, $J = 164.6$ Hz, $\text{CH}_2\text{-CH}_2\text{-CH}_2\text{-F}$), 75.4 (C5), 72.2 (C2), 70.2 (C4), 69.2 (C3), 52.9 (C^α), 51.6 ($-\text{OCH}_3$), 31.2 (C^β), 30.0 (C^γ), 30.0-29.8 (d, $J = 20.5$ Hz, $\text{CH}_2\text{-CH}_2\text{-CH}_2\text{-F}$), 21.7 ($\text{CH}_2\text{-CH}_2\text{-CH}_2\text{-F}$), 20.8 (CH_3 , OAc), 20.7 (CH_3 , OAc), 20.3 (CH_3 , OAc), 15.5 (SCH_3). **LRMS (ESI):** m/z 599 $[\text{M} + \text{Na}]^+$ **HRMS (ESI):** m/z calculated for $\text{C}_{23}\text{H}_{33}\text{FN}_4\text{O}_{10}\text{SNa}$ $[\text{M} + \text{Na}]^+$: 599.1799; Found 599.1808.

Chapter 8 : References

- (1) Levy, D.; Fugedi, P. *The Organic Chemistry of Sugars*; CRC Press, Taylor and Francis, Boca Raton, Florida, USA, **2006**; pp. 25–52.
- (2) Miljkovic, M. *Carbohydrates - Synthesis, Mechanisms and Stereoelectronic Effects*; Springer, Hershey, Pennsylvania, USA, **2009**; pp. 1–24.
- (3) Kiessling, L. L.; Splain, R. A. Chemical Approaches to Glycobiology. *Annu. Rev. Biochem.* **2010**, 79, 619–653.
- (4) Dwek, R. A. Glycobiology: Toward Understanding the Function of Sugars. *Chem. Rev.* **1996**, 96, 683–720.
- (5) Lehninger, A. L.; Nelson, D. L.; Cox, M. M. *Lehninger: Principles of Biochemistry*; W.H. Freeman and Company, New York, USA; 5th Ed, **2008**; pp. 21–26.
- (6) Varki, A.; Cummings, R. D.; Esko, J.; Freeze, H. H.; Stanley, P.; Bertozzi, C. R.; Hart, G. W.; Etzler, M. *Essentials of Glycobiology*; Cold Spring Harbour Laboratory Press, New York, USA, **2009**; pp. 21–34.
- (7) Domozych, D. S.; Ciancia, M.; Fangel, J. U.; Mikkelsen, M. D.; Ulvskov, P.; Willats, W. G. T. The Cell Walls of Green Algae: A Journey through Evolution and Diversity. *Front. Plant Sci.* **2012**, 3, 82.
- (8) Zhao, H.; Kwak, J.; Conradzhang, Z.; Brown, H.; Arey, B.; Holladay, J. Studying Cellulose Fiber Structure by SEM, XRD, NMR and Acid Hydrolysis. *Carbohydr. Polym.* **2007**, 68, 235–241.
- (9) Tanthanuch, W.; Chantarangsee, M.; Maneesan, J.; Ketudat-Cairns, J. Genomic and Expression Analysis of Glycosyl Hydrolase Family 35 Genes from Rice (*Oryza Sativa* L.). *BMC Plant Biol.* **2008**, 8, 84.
- (10) Lenardon, M. D.; Munro, C. A.; Gow, N. A. R. Chitin Synthesis and Fungal Pathogenesis. *Curr. Opin. Microbiol.* **2010**, 13, 416–423.

- (11) Kurita, K. Chitin and Chitosan: Functional Biopolymers from Marine Crustaceans. *Mar. Biotechnol.* **2006**, 8, 203–226.
- (12) Teng, W. L.; Khor, E.; Tan, T. K.; Lim, L. Y.; Tan, S. C. Concurrent Production of Chitin from Shrimp Shells and Fungi. *Carbohydr. Res.* **2001**, 332, 305–316.
- (13) Winn, M.; Goss, R. J. M.; Kimura, K.; Bugg, T. D. H. Antimicrobial Nucleoside Antibiotics Targeting Cell Wall Assembly: Recent Advances in Structure-Function Studies and Nucleoside Biosynthesis. *Nat. Prod. Rep.* **2010**, 27, 279–304.
- (14) Gebel-Cook, O. Fungi <http://oliviagc.edublogs.org/2012/04/30/fungi/> (accessed Jan 5, 2014).
- (15) Flostro. Second-Generation Biofuels — Cellulosic Ethanol <http://planetsave.com/2012/05/07/second-generation-biofuels-cellulosic-ethanol-a-look-towards-sustainability-amongst-environmental-problems/> (accessed Jan 5, 2014).
- (16) Gershon, E. Human Presence Increases Indoor Bacteria <http://scitechdaily.com/human-presence-increases-indoor-bacteria/> (accessed Jan 5, 2014).
- (17) Baeurle, S. A.; Kiselev, M. G.; Makarova, E. S.; Nogovitsin, E. A. Effect of the Counterion Behavior on the Frictional–compressive Properties of Chondroitin Sulfate Solutions. *Polymer (Guildf)*. **2009**, 50, 1805–1813.
- (18) Gabius, H.-J.; Gabius, S. *Glycosciences: Status and Perspectives*; Wiley-VCH, Weinheim, Germany, **2008**; pp. 133–162.
- (19) Mouw, J. K.; Case, N. D.; Guldberg, R. E.; Plaas, A. H. K.; Levenston, M. E. Variations in Matrix Composition and GAG Fine Structure among Scaffolds for Cartilage Tissue Engineering. *Osteoarthr. Cartil.* **2005**, 13, 828–836.
- (20) Maeno, M.; Taguchi, M.; Kosuge, K.; Otsuka, K.; Takagi, M. Nature and Distribution of Mineral-Binding, Keratan Sulfate-Containing Glycoconjugates in Rat and Rabbit Bone. *J. Histochem. Cytochem.* **1992**, 40, 1779–1788.
- (21) Brandley, B. K.; Schnaar, R. L. Cell-Surface Recognition Carbohydrates and Response in Cell. *J. Leukoc. Biol.* **1986**, 111, 97–111.
- (22) Bertozzi, C. R.; Kiessling, L. L. Chemical Glycobiology. *Science* **2001**, 291, 2357–2364.
- (23) Spiro, R. G. Protein Glycosylation: Nature, Distribution, Enzymatic Formation, and Disease Implications of Glycopeptide Bonds. *Glycobiology* **2002**, 12, 43R – 56R.

- (24) Perez-Vilar, J.; Hill, R. L. The Structure and Assembly of Secreted Mucins. *J. Biol. Chem.* **1999**, *274*, 31751–31754.
- (25) Shylaja, M.; Seshadri, H. S. Glycoproteins: An Overview. *Biochem. Educ.* **1989**, *17*, 170–178.
- (26) Lis, H.; Sharon, N. Protein Glycosylation. *Eur. J. Biochem.* **1993**, *218*, 1–27.
- (27) Choppin, P. W.; Richardson, C. D.; Merz, D. C.; Hall, W. W.; Scheid, A. The Functions and Inhibition of the Membrane Glycoproteins of Paramyxoviruses and Myxoviruses and the Role of the Measles Virus M Protein in Subacute Sclerosing Panencephalitis. *J. Infect. Dis.* **1981**, *143*, 352–363.
- (28) Andersson, L. C.; Gahmberg, C. G. Surface Glycoproteins of Human White Blood Cells. Analysis by Surface Labeling. *Blood* **1978**, *52*, 57–67.
- (29) Perez-Vilar, J. Mucin Granule Intraluminal Organization. *Am. J. Respir. Cell Mol. Biol.* **2007**, *36*, 183–190.
- (30) Wright, A.; Morrison, S. L. Effect of Glycosylation on Antibody Function: Implications for Genetic Engineering. *Trends Biotechnol.* **1997**, *15*, 26–32.
- (31) Gala, F. A.; Morrison, S. L. V Region Carbohydrate and Antibody Expression. *J. Immunol.* **2004**, *172*, 5489–5494.
- (32) Nose, M.; Wigzell, H. Biological Significance of Carbohydrate Chains on Monoclonal Antibodies Immunology: *Proc. Natl. Acad. Sci. USA.* **1983**, *80*, 6632–6636.
- (33) Plum, M.; Michel, Y.; Wallach, K.; Raiber, T.; Blank, S.; Bantleon, F. I.; Diethers, A.; Greunke, K.; Braren, I.; Hackl, T.; Meyer, B.; Spillner, E. Close-up of the Immunogenic A-1,3-Galactose Epitope as Defined by a Monoclonal Chimeric Immunoglobulin E and Human Serum Using Saturation Transfer Difference (STD) NMR. *J. Biol. Chem.* **2011**, *286*, 43103–43111.
- (34) Xu, H.; Yin, D.; Naziruddin, B.; Chen, L.; Stark, A.; Wei, Y.; Lei, Y.; Shen, J.; Logan, J. S.; Byrne, G. W.; Chong, A. S.-F. The in Vitro and in Vivo Effects of Anti-Galactose Antibodies on Endothelial Cell Activation and Xenograft Rejection. *J. Immunol.* **2003**, *170*, 1531–1539.
- (35) Wagner, R.; Feldmann, A.; Wolff, T.; Pleschka, S.; Garten, W.; Klenk, H.-D. The Role of Hemagglutinin and Neuraminidase in Influenza Virus Pathogenicity. In *Structure-Function Relationships of Human Pathogenic Viruses SE - 12*; Holzenburg, A.; Bogner, E., Eds.; Springer US, **2002**; pp. 331–345.
- (36) Laver, W. G.; Colman, P. M.; Webster, R. G.; Hinshaw, V. S.; Air, G. M. Influenza Virus Neuraminidase with Hemagglutinin Activity. *Virology* **1984**, *137*, 314–323.

- (37) Danieli, T.; Pelletier, S. L.; Henis, Y. I.; White, J. M. Membrane Fusion Mediated by the Influenza Virus Hemagglutinin Requires the Concerted Action of at Least Three Hemagglutinin Trimers. *J. Cell Biol.* **1996**, *133*, 559–569.
- (38) Stegmann, T. Membrane Fusion Mechanisms: The Influenza Hemagglutinin Paradigm and Its Implications for Intracellular Fusion. *Traffic* **2000**, *1*, 598–604.
- (39) Agbandje-McKenna, M. Gripping Glycans
http://publications.nigms.nih.gov/findings/mar06/agbandje-mckenna_files/textmostly/slide4.html (accessed Jan 10, 2014).
- (40) Durocher, J. R.; Payne, R. C.; Conrad, M. E. Role of Sialic Acid in Erythrocyte Survival. *Blood* **1975**, *45*, 11–20.
- (41) Eylar, E. H.; Madoff, M. A.; Oncley, J. L. The Contribution of Sialic Acid to the Surface Charge of the Erythrocyte The Contribution of Sialic Acid to the of the Erythrocyte. *J. Biol. Chem.* **1962**, *237*, 1992–2000.
- (42) Razi, N.; Varki, A. Cryptic Sialic Acid Binding Lectins on Human Blood Leukocytes Can Be Unmasked by Sialidase Treatment or Cellular Activation. *Glycobiol.* **1999**, *9*, 1225–1234.
- (43) Crook, M. Sialic Acid: Its Importance to Platelet Function in Health and Disease. *Platelets* **1991**, *2*, 1–10.
- (44) Salhanick, A. I.; Amatruda, J. M. Role of Sialic Acid in Insulin Action and the Insulin Resistance of Diabetes Mellitus. *Am. J. Physiol. - Endocrinol. Metab.* **1988**, *255*, E173–E179.
- (45) Henricks, P. A. J.; Erne-van der Tol, M.; Verhoef, J. The Role of Sialic Acid in Phagocytic Cell Function. *Antonie Van Leeuwenhoek* **1982**, *48*, 191–192.
- (46) Czop, J. K.; Fearon, D. T.; Austen, K. F. Membrane Sialic Acid on Target Particles Modulates Their Phagocytosis by a Trypsin-Sensitive Mechanism on Human Monocytes. *Proc. Natl. Acad. Sci. U. S. A.* **1978**, *75*, 3831–3835.
- (47) Delorme, E.; Lorenzini, T.; Giffin, J.; Martin, F.; Jacobsen, F.; Boone, T.; Elliott, S. Role of Glycosylation on the Secretion and Biological Activity of Erythropoietin. *Biochemistry* **1992**, *31*, 9871–9876.
- (48) Wu, B.; Chen, J.; Warren, J. D.; Chen, G.; Hua, Z.; Danishefsky, S. J. Building Complex Glycopeptides: Development of a Cysteine-Free Native Chemical Ligation Protocol. *Angew. Chemie Int. Ed.* **2006**, *45*, 4116–4125.
- (49) Meléndez-Hevia, E.; Waddell, T.; Cascante, M. The Puzzle of the Krebs Citric Acid Cycle: Assembling the Pieces of Chemically Feasible Reactions, and Opportunism in the Design of Metabolic Pathways during Evolution. *J. Mol. Evol.* **1996**, *43*, 293–303.

- (50) Barnes, S. J.; Weitzman, P. D. Organization of Citric Acid Cycle Enzymes into a Multienzyme Cluster. *FEBS Lett.* **1986**, *201*, 267–270.
- (51) Veldhorst, M. A. B.; Westerterp-Plantenga, M. S.; Westerterp, K. R. Gluconeogenesis and Energy Expenditure after a High-Protein, Carbohydrate-Free Diet. *Am. J. Clin. Nutr.* **2009**, *90*, 519–526.
- (52) Kaferstein, H. Forensic Relevance of Glucuronidation in Phase-II-Metabolism of Alcohols and Drugs. *Leg. Med. (Tokyo)*. **2009**, *11 Suppl 1*, S22–S26.
- (53) Patrick, G. L. *An Introduction to Medicinal Chemistry*; Oxford University Press, Oxford, UK; 4th Ed., **2008**; pp. 156–157.
- (54) Fleet, G. W. J.; Estevez, J. C.; Smith, M. D.; Blcriot, Y.; Fuente, C. De; Kriille, T. M.; Besra, G. S.; Brennan, P. J.; Nash, R. J.; N, L.; Oikonomakos, N. G.; Stalmans, W. Sugar Mimics from Sugar Lactones. *Pure Appl. Chem.* **1998**, *70*, 279–284.
- (55) Ritter, J. K. Roles of Glucuronidation and UDP-Glucuronosyltransferases in Xenobiotic Bioactivation Reactions. *Chem. Biol. Interact.* **2000**, *129*, 171–193.
- (56) Levine, D. P. Vancomycin: A History. *Clin. Infect. Dis.* **2006**, *42 Suppl 1*, S5–S12.
- (57) Glupczynski, Y. Aminoglycosides : Activity and Resistance. *Antimicrob. Agents Chemother.* **1999**, *43*, 727–737.
- (58) Van Bambeke, F. Glycopeptides and Glycopeptide antibiotics in Clinical Development: A Comparative Review of Their Antibacterial Spectrum, Pharmacokinetics and Clinical Efficacy. *Curr. Opin. Investig. Drugs* **2006**, *7*, 740–749.
- (59) Sticherling, C.; Oral, H.; Horrocks, J.; Chough, S. P.; Baker, R. L.; Kim, M. H.; Wasmer, K.; Pelosi, F.; Knight, B. P.; Michaud, G. F.; Strickberger, S. A.; Morady, F. Effects of Digoxin on Acute, Atrial Fibrillation-Induced Changes in Atrial Refractoriness. *Circulation* **2000**, *102*, 2503–2508.
- (60) Von Itzstein, M.; Wu, W.-Y.; Kok, G. B.; Pegg, M. S.; Dyason, J. C.; Jin, B.; Phan, T. Van; Smythe, M. L.; White, H. F.; Oliver, S. W.; Colman, P. M.; Varghese, J. N.; Ryan, D. M.; Woods, J. M.; Bethell, R. C.; Hotham, V. J.; Cameron, J. M.; Penn, C. R. Rational Design of Potent Sialidase-Based Inhibitors of Influenza Virus Replication. *Nature* **1993**, *363*, 418–423.
- (61) Lew, W.; Chen, X.; Kim, C. . Discovery and Development of GS 4104 (oseltamivir): An Orally Active Influenza Neuraminidase Inhibitor. *Curr. Med. Chem.* **2000**, *7*, 663–672.

- (62) Bischoff, H.; Puls, W.; Krause, H. P.; Schutt, H.; Thomas, G. Pharmacological Properties of the Novel Glucosidase Inhibitors BAY M 1099 (miglitol) and BAY O 1248. *Diabetes Res. Clin. Pr.* **1985**, *1*, 53.
- (63) Shinozaki, K.; Suzuki, M.; Ikebuchi, M.; Hirose, J.; Hara, Y.; Harano, Y. Improvement of Insulin Sensitivity and Dyslipidemia with a New Alpha-Glucosidase Inhibitor, Voglibose, in Nondiabetic Hyperinsulinemic Subjects. *Metabolism.* **1996**, *45*, 731–737.
- (64) Kudchadkar, R.; Gonzalez, R.; Lewis, K. D. PI-88: A Novel Inhibitor of Angiogenesis. *Expert Opin. Investig. Drugs* **2008**, *17*, 1769–1776.
- (65) Johnstone, K. D.; Karoli, T.; Liu, L.; Dredge, K.; Copeman, E.; Li, C. P.; Davis, K.; Hammond, E.; Bytheway, I.; Kostewicz, E.; Chiu, F. C. K.; Shackelford, D. M.; Charman, S. A.; Charman, W. N.; Harenberg, J.; Gonda, T. J.; Ferro, V. Synthesis and Biological Evaluation of Polysulfated Oligosaccharide Glycosides as Inhibitors of Angiogenesis and Tumor Growth. *J. Med. Chem.* **2010**, *53*, 1686–1699.
- (66) Hollingsworth, M. A.; Swanson, B. J. Mucins in Cancer: Protection and Control of the Cell Surface. *Nat Rev Cancer* **2004**, *4*, 45–60.
- (67) Galan, M. C.; Dumy, P.; Renaudet, O. Multivalent Glyco(cyclo)peptides. *Chem. Soc. Rev.* **2013**, *42*, 4599–4612.
- (68) Stallforth, P.; Lepenies, B.; Adibekian, A.; Seeberger, P. H. 2009 Claude S. Hudson Award in Carbohydrate Chemistry. Carbohydrates: A Frontier in Medicinal Chemistry. *J. Med. Chem.* **2009**, *52*, 5561–5577.
- (69) Zhu, J.; Warren, J. D.; Danishefsky, S. J. Synthetic Carbohydrate-Based Anticancer Vaccines: The Memorial Sloan-Kettering Experience. *Expert Rev. Vaccines* **2011**, *8*, 1399–1413.
- (70) Ragupathi, G.; Koide, F.; Livingston, P. O.; Cho, Y. S.; Endo, A.; Wan, Q.; Spassova, M. K.; Keding, S. J.; Allen, J.; Ouerfelli, O.; Wilson, R. M.; Danishefsky, S. J. Preparation and Evaluation of Unimolecular Pentavalent and Hexavalent Antigenic Constructs Targeting Prostate and Breast Cancer: A Synthetic Route to Anticancer Vaccine Candidates. *J. Am. Chem. Soc.* **2006**, *128*, 2715–2725.
- (71) Harris, J. R.; Markl, J. Keyhole Limpet Hemocyanin (KLH): A Biomedical Review. *Micron* **1999**, *30*, 597–623.
- (72) Australian Institute of Health and Welfare (AIHW). *Cancer in Australia: An Overview, 2012.*; **2012**.
- (73) Agdeppa, E. D.; Spilker, M. E. A Review of Imaging Agent Development. *AAPS J.* **2009**, *11*, 286–299.

- (74) Ter-Pogossian, M. M.; Phelps, M. E.; Hoffman, E. J.; Mullani, N. A. A Positron-Emission Transaxial Tomograph for Nuclear Imaging (PETT). *Radiology* **1975**, *114*, 89–98.
- (75) Frankle, W. G.; Slifstein, M.; Talbot, P. S.; Laruelle, M. Neuroreceptor Imaging in Psychiatry: Theory and Applications. *Int. Rev. Neurobiol.* **2005**, *67*, 385–440.
- (76) Meisetchlager, G.; Poethko, T.; Stahl, A.; Wolf, I.; Scheidhauer, K.; Schotellius, M.; Herz, M.; Wester, H.; Schwaiger, M. Gluc-Lys([¹⁸F]FP)-TOCA PET in Patients with SSTR-Positive Tumors: Biodistribution and Diagnostic Evaluation Compared with [¹¹¹In] DTPA-Octreotide. *J. Nucl. Med.* **2006**, *47*, 566–573.
- (77) Fletcher, J. W.; Djulbegovic, B.; Soares, H. P.; Siegel, B. A.; Lowe, V. J.; Lyman, G. H.; Coleman, R. E.; Wahl, R.; Paschold, J. C.; Avril, N.; Einhorn, L. H.; Suh, W. W.; Samson, D.; Delbeke, D.; Gorman, M.; Shields, A. F. Recommendations on the Use of [¹⁸F]-FDG PET in Oncology. *J. Nucl. Med.* **2008**, *49*, 480–508.
- (78) Pacak, J.; Tocik, Z.; Cerny, M. Synthesis of 2-Deoxy-2-Fluoro-D-Glucose. *J. Chem. Soc. D Chem. Commun.* **1969**, 77.
- (79) Som, P.; Atkins, H. L.; Bandyopadhyay, D.; Fowler, J. S.; Macgregor, R. R.; Matsui, K.; Oster, Z. H.; Sacker, D. F.; Shiue, C. Y.; Turner, H.; Wan, C.; Wolf, A. P.; Zabinski, S. V; Macgregor, A. R. A Fluorinated Glucose Analog , 2-Fluoro-2-Deoxy-D-Glucose (Fluorine -18): Nontoxic Tracer for Rapid Tumor Detection. *J. Nucl. Med.* **1980**, *21*, 670–675.
- (80) Le Bars, D. Fluorine-18 and Medical Imaging: Radiopharmaceuticals for Positron Emission Tomography. *J. Fluor. Chem.* **2006**, *127*, 1488–1493.
- (81) Joensuu, H.; Ahonen, A. Imaging of Metastases of Thyroid Carcinoma with Fluorine- 18 Fluorodeoxyglucose. *J. Nucl. Med.* **1987**, *28*, 910–914.
- (82) Strauss, L. G. Fluorine-18 Deoxyglucose and False-Positive Results: A Major Problem in the Diagnostics of Oncological Patients. *Eur. J. Nucl. Med.* **1996**, *23*, 1409–1415.
- (83) Gulya, B.; Hallidin, C. New PET Radiopharmaceuticals: Beyond FDG for Brain Tumour Imaging. *Q. J. Nucl. Med. Mol. Imaging* **2012**, *56*, 173–190.
- (84) Chen, W. Clinical Applications of PET in Brain Tumors. *J. Nucl. Med.* **2007**, *48*, 1468–1481.
- (85) Kamel, E. M.; Thumshirn, M.; Truninger, K.; Schiesser, M.; Fried, M.; Padberg, B.; Stoeckli, S. J.; Schulthess, G. K. Von; Stumpe, K. D. M. Significance of Incidental [¹⁸F]-FDG Accumulations in the Gastrointestinal Tract in PET / CT : Correlation with Endoscopic and Histopathologic Results. *J. Nucl. Med.* **2004**, *45*, 1804–1810.

- (86) Kato, T.; Fukatsu, H.; Ito, K.; Tadokoro, M.; Ota, T.; Ikeda, M.; Isomura, T.; Ito, S.; Nishino, M.; Ishigaki, T. Fluorodeoxyglucose Positron Emission Tomography in Pancreatic Cancer: An Unsolved Problem. *Eur. J. Nucl. Med.* **1995**, 22, 32–39.
- (87) Mankoff, D. A.; Link, J. M.; Linden, H. M.; Sundararajan, L.; Krohn, K. a. Tumor Receptor Imaging. *J. Nucl. Med.* **2008**, 49, 149S – 63S.
- (88) Fani, M.; Maecke, H. R.; Okarvi, S. M. Radiolabeled Peptides: Valuable Tools for the Detection and Treatment of Cancer. *Theranostics* **2012**, 2, 481–501.
- (89) Hofland, L. J.; Lamberts, S. W. J. Review Somatostatin Receptor Subtype Expression in Human Tumors. *Ann. Oncol.* **2001**, 12, S31–S36.
- (90) De Herder, W. W.; Hofland, L. J.; Van Der Lely, A. J.; Lamberts, S. W. J. Somatostatin Receptors in Gastroentero-Pancreatic Neuroendocrine Tumours. *Endocr. Relat. Cancer* **2003**, 10, 451–458.
- (91) Kadekaro, A. L.; Chen, J.; Yang, J.; Chen, S.; Jameson, J.; Swope, V. B.; Cheng, T.; Kadakia, M.; Abdel-Malek, Z. Alpha-Melanocyte-Stimulating Hormone Suppresses Oxidative Stress through a p53-Mediated Signaling Pathway in Human Melanocytes. *Mol. Cancer Res.* **2012**, 10, 778–786.
- (92) Magni, P.; Motta, M. Expression of Neuropeptide Y Receptors in Human Prostate Cancer Cells. *Ann. Oncol.* **2001**, 12, 27–29.
- (93) Marenah, L.; Flatt, P. R.; Orr, D. F.; McClean, S.; Shaw, C.; Abdel-Wahab, Y. H. A. Skin Secretion of the Toad Bombina Variegata Contains Multiple Insulin-Releasing Peptides Including Bombesin and Entirely Novel Insulinotropic Structures. *Biol. Chem.* **2004**, 385, 315–321.
- (94) Brans, L.; Maes, V.; García-Garayoa, E.; Schweinsberg, C.; Daepf, S.; Bläuenstein, P.; Schubiger, P. A.; Schibli, R.; Tourwé, D. a. Glycation Methods for Bombesin Analogs Containing the (NalphaHis)Ac Chelator for [^{99m}Tc](CO)₃ Radiolabeling. *Chem. Biol. Drug Des.* **2008**, 72, 496–506.
- (95) Reubi, J. C.; Wenger, S.; Schmuckli-Maurer, J.; Schaer, J.-C.; Gugger, M. Bombesin Receptor Subtypes in Human Cancers : Detection with the Universal Radioligand [¹²⁵I]- [D-TYR6 , B -ALA11 , PHE13 , NLE14] Bombesin (6 – 14). *Clin. Cancer Res.* **2002**, 1139–1146.
- (96) Whiteman, M. L.; Serafini, a N.; Telischi, F. F.; Civantos, F. J.; Falcone, S. 111In Octreotide Scintigraphy in the Evaluation of Head and Neck Lesions. *AJNR. Am. J. Neuroradiol.* **1997**, 18, 1073–1080.
- (97) Vegt, E.; de Jong, M.; Wetzels, J. F. M.; Masereeuw, R.; Melis, M.; Oyen, W. J. G.; Gotthardt, M.; Boerman, O. C. Renal Toxicity of Radiolabeled Peptides and Antibody Fragments: Mechanisms, Impact on Radionuclide Therapy, and Strategies for Prevention. *J. Nucl. Med.* **2010**, 51, 1049–1058.

- (98) Fass, L. Imaging and Cancer: A Review. *Mol. Oncol.* **2008**, 2, 115–152.
- (99) Haubner, R.; Burkhart, F.; Senekowitsch-Schmidtke, R.; Weber, W.; Goodman, S. L.; Kessler, H.; Schwaiger, M. Glycosylated RGD-Containing Peptides: Tracer for Tumor Targeting and Angiogenesis Imaging with Improved Biokinetics. *J. Nucl. Med.* **2001**, 42, 326–336.
- (100) Ung, P.; Winkler, D. a. Tripeptide Motifs in Biology: Targets for Peptidomimetic Design. *J. Med. Chem.* **2011**, 54, 1111–1125.
- (101) Schottelius, M.; Reubi, J. C.; Senekowitsch-Schmidtke, R.; Schwaiger, M. Improvement of Pharmacokinetics of Radioiodinated Tyr 3 -Octreotide by Conjugation with Carbohydrates. *Bioconjug. Chem.* **2002**, 13, 1021–1030.
- (102) Schottelius, M.; Rau, F.; Reubi, J. C.; Schwaiger, M. Modulation of Pharmacokinetics of Radioiodinated Sugar-Conjugated Somatostatin Analogues by Variation of Peptide Net Charge and Carbohydration Chemistry. *Bioconjug. Chem.* **2005**, 16, 429–437.
- (103) Stahl, A.; Meisetschläger, G.; Schottelius, M.; Bruus-Jensen, K.; Wolf, I.; Scheidhauer, K.; Schwaiger, M. [¹²³I]Mtr-TOCA, a Radioiodinated and Carbohydrated Analogue of Octreotide: Scintigraphic Comparison with [¹¹¹In]octreotide. *Eur. J. Nucl. Med. Mol. Imaging* **2006**, 33, 45–52.
- (104) Wester, H. J.; Schottelius, M.; Scheidhauer, K.; Meisetschläger, G.; Herz, M.; Rau, F. C.; Reubi, J. C.; Schwaiger, M. PET Imaging of Somatostatin Receptors: Design, Synthesis and Preclinical Evaluation of a Novel [¹⁸F]-Labelled, Carbohydrated Analogue of Octreotide. *Eur. J. Nucl. Med. Mol. Imaging* **2003**, 30, 117–122.
- (105) Schwarz, S. B.; Thon, N.; Nikolajek, K.; Niyazi, M.; Tonn, J.-C.; Belka, C.; Kreth, F.-W. Iodine-125 Brachytherapy for Brain Tumours-A Review. *Radiat. Oncol.* **2012**, 7, 30–57.
- (106) Wester, H.-J.; Hamacher, K.; Stocklin, G. A Comparative Study of N . C . A . Fluorine-18 Labeling of Proteins via Acylation and Photochemical Conjugation. *Nucl. Med. Biol.* **1996**, 23, 365–372.
- (107) Beer, A. J.; Grosu, A.-L.; Carlsen, J.; Kolk, A.; Sarbia, M.; Stangier, I.; Watzlowik, P.; Wester, H.-J.; Haubner, R.; Schwaiger, M. [18F]galacto-RGD Positron Emission Tomography for Imaging of alphavbeta3 Expression on the Neovasculature in Patients with Squamous Cell Carcinoma of the Head and Neck. *Clin. Cancer Res.* **2007**, 13, 6610–6616.
- (108) Haubner, R.; Kuhnast, B.; Mang, C.; Weber, W. A.; Kessler, H.; Wester, H.-J.; Schwaiger, M. [18F]Galacto-RGD: Synthesis, Radiolabeling, Metabolic Stability, and Radiation Dose Estimates. *Bioconjug. Chem.* **2004**, 15, 61–69.

- (109) Haubner, R.; Wester, H.; Weber, W. A.; Mang, C.; Ziegler, S. I.; Goodman, S. L.; Senekowitsch-Schmidtke, R.; Kessler, H.; Schwaiger, M. Noninvasive Imaging of $\alpha\beta 3$ Integrin Expression Using [^{18}F]-Labeled RGD-Containing Glycopeptide and Positron Emission Tomography Advances in Brief. *Cancer Res.* **2001**, *61*, 1781–1785.
- (110) Littich, R.; Scott, P. J. H. Novel Strategies for Fluorine-18 Radiochemistry. *Angew. Chem. Int. Ed. Engl.* **2012**, *51*, 1106–1109.
- (111) Selivanova, S. V.; Mu, L.; Ungersboeck, J.; Stellfeld, T.; Ametamey, S. M.; Schibli, R.; Wadsak, W. Single-Step Radiofluorination of Peptides Using Continuous Flow Microreactor. *Org. Biomol. Chem.* **2012**, *10*, 3871–3874.
- (112) Ogawa, M.; Hatano, K.; Oishi, S.; Kawasumi, Y.; Fujii, N.; Kawaguchi, M.; Doi, R.; Imamura, M.; Yamamoto, M.; Ajito, K.; Mukai, T.; Saji, H.; Ito, K. Direct Electrophilic Radiofluorination of a Cyclic RGD Peptide for in Vivo $\alpha\beta 3$ Integrin Related Tumor Imaging. *Nucl. Med. Biol.* **2003**, *30*, 1–9.
- (113) McBride, W. J.; D'Souza, C. A.; Karacay, H.; Sharkey, R. M.; Goldenberg, D. M. New Lyophilized Kit for Rapid Radiofluorination of Peptides. *Bioconjug. Chem.* **2012**, *23*, 538–547.
- (114) Li, X.-G.; Dall'Angelo, S.; Schweiger, L. F.; Zanda, M.; O'Hagan, D. [^{18}F]-5-Fluoro-5-Deoxyribose, an Efficient Peptide Bioconjugation Ligand for Positron Emission Tomography (PET) Imaging. *Chem. Commun. (Camb).* **2012**, *48*, 5247–5249.
- (115) Li, X.-G.; Helariutta, K.; Roivainen, A.; Jalkanen, S.; Knuuti, J.; Airaksinen, A. J. Using 5-Deoxy-5- [^{18}F]fluororibose to Glycosylate Peptides for Positron Emission Tomography. *Nat. Protoc.* **2014**, *9*, 138–145.
- (116) Li, X.-G.; Autio, A.; Ahtinen, H.; Helariutta, K.; Liljenbäck, H.; Jalkanen, S.; Roivainen, A.; Airaksinen, A. J. Translating the Concept of Peptide Labeling with 5-Deoxy-5- [^{18}F]fluororibose into Preclinical Practice: ^{18}F -Labeling of Siglec-9 Peptide for PET Imaging of Inflammation. *Chem. Commun. (Camb).* **2013**, *49*, 3682–3684.
- (117) Kolb, H. C.; Finn, M. G.; Sharpless, K. B. Click Chemistry: Diverse Chemical Function from a Few Good Reactions. *Angew. Chem. Int. Ed. Engl.* **2001**, *40*, 2004–2021.
- (118) Rostovtsev, V. V.; Green, L. G.; Fokin, V. V.; Sharpless, K. B. A Stepwise Huisgen Cycloaddition Process: copper(I)-Catalyzed Regioselective “Ligation” of Azides and Terminal Alkynes. *Angew. Chem. Int. Ed. Engl.* **2002**, *41*, 2596–2599.
- (119) Tornøe, C. W.; Christensen, C.; Meldal, M. Peptidotriazoles on Solid Phase: [1,2,3]-Triazoles by Regiospecific Copper(i)-Catalyzed 1,3-Dipolar

- Cycloadditions of Terminal Alkynes to Azides. *J. Org. Chem.* **2002**, 67, 3057–3064.
- (120) Huisgen, R. 1,3-Dipolar Cycloadditions. *Proc. Chem. Soc.* **1961**, October, 357–396.
- (121) Boren, B. C.; Narayan, S.; Rasmussen, L. K.; Zhang, L.; Zhao, H.; Lin, Z.; Jia, G.; Folkin, V. V. Ruthenium-Catalyzed Azide-Alkyne Cycloaddition: Scope and Mechanism. *J. Am. Chem. Soc.* **2008**, 130, 8923–8930.
- (122) Himo, F.; Lovell, T.; Hilgraf, R.; Rostovtsev, V. V.; Noodleman, L.; Sharpless, K. B.; Fokin, V. V. Copper(I)-Catalyzed Synthesis of Azoles. DFT Study Predicts Unprecedented Reactivity and Intermediates. *J. Am. Chem. Soc.* **2005**, 127, 210–216.
- (123) Angell, Y. L.; Burgess, K. Peptidomimetics via Copper-Catalyzed Azide-Alkyne Cycloadditions. *Chem. Soc. Rev.* **2007**, 36, 1674–1689.
- (124) Moses, J. E.; Moorhouse, A. D. The Growing Applications of Click Chemistry. *Chem. Soc. Rev.* **2007**, 36, 1249–1262.
- (125) Kolb, H. C.; Sharpless, K. B. The Growing Impact of Click Chemistry on Drug Discovery. *Drug Discov. Today* **2003**, 8, 1128–1137.
- (126) Bertho, A. Nitrogen-Containing Sugars. I. Azido Derivatives of Glucose. *Berichte der Dtsch. Chem. Gesellschaft B* **1930**, 63B, 836.
- (127) Bräse, S.; Gil, C.; Knepper, K.; Zimmermann, V. Organic Azides: An Exploding Diversity of a Unique Class of Compounds. *Angew. Chem. Int. Ed. Engl.* **2005**, 44, 5188–5240.
- (128) Carroux, C. J.; Rankin, G. M.; Moeker, J.; Bornaghi, L. F.; Katneni, K.; Morizzi, J.; Charman, S. A.; Vullo, D.; Supuran, C. T.; Poulsen, S.; Fiorentino, S. A Prodrug Approach Toward Cancer-Related Carbonic Anhydrase Inhibition. *J. Med. Chem.* **2013**, 56, 9623–9634.
- (129) Carroux, C. J.; Moeker, J.; Motte, J.; Lopez, M.; Bornaghi, L. F.; Katneni, K.; Ryan, E.; Morizzi, J.; Shackelford, D. M.; Charman, S. a; Poulsen, S.-A. Synthesis of Acylated Glycoconjugates as Templates to Investigate in Vitro Biopharmaceutical Properties. *Bioorg. Med. Chem. Lett.* **2013**, 23, 455–459.
- (130) Wilkinson, B. L.; Innocenti, A.; Vullo, D.; Supuran, C. T.; Poulsen, S. Inhibition of Carbonic Anhydrases with Glycosyltriazole Benzene Sulfonamides. *J. Med. Chem.* **2008**, 51, 1945–1953.
- (131) Kuijpers, B. H. M.; Groothuys, S.; Keereweer, A. B. R.; Quaedflieg, P. J. L. M.; Blaauw, R. H.; Delft, F. L. Van; Rutjes, F. P. J. T. Expedient Synthesis of

- Triazole-Linked Glycosyl Amino Acids and Peptides. *Org. Lett.* **2004**, 6, 3123–3126.
- (132) Ning, X.; Guo, J.; Wolfert, M. a; Boons, G.-J. Visualizing Metabolically Labeled Glycoconjugates of Living Cells by Copper-Free and Fast Huisgen Cycloadditions. *Angew. Chem. Int. Ed. Engl.* **2008**, 47, 2253–2255.
- (133) Shieh, P.; Hangauer, M. J.; Bertozzi, C. R. Fluorogenic Azidofluoresceins for Biological Imaging. *J. Am. Chem. Soc.* **2012**, 134, 17428–17431.
- (134) Sletten, E. M.; Bertozzi, C. R. Bioorthogonal Chemistry: Fishing for Selectivity in a Sea of Functionality. *Angew. Chem. Int. Ed. Engl.* **2009**, 48, 6974–6998.
- (135) Jewett, J. C.; Sletten, E. M.; Bertozzi, C. R. Rapid Cu-Free Click Chemistry with Readily Synthesized Biarylazacyclooctynones. *J. Am. Chem. Soc.* **2010**, 132, 3688–3690.
- (136) Neves, A. A.; Sto, H.; Wainman, Y. A.; Kuo, J. C.; Fawcett, S.; Leeper, F. J.; Brindle, K. M. Imaging Cell Surface Glycosylation in Vivo Using “Double Click” Chemistry. *Bioconjug. Chem.* **2013**, 24, 934–941.
- (137) Kim, D. H.; Choe, Y. S.; Jung, K.-H.; Lee, K.-H.; Choi, J. Y.; Choi, Y.; Kim, B.-T. A (18)F-Labeled Glucose Analog: Synthesis Using a Click Labeling Method and in Vitro Evaluation. *Arch. Pharm. Res.* **2008**, 31, 587–593.
- (138) Sarowi, S. M. 18F Radiolabelling of Carbohydrates Using Click Chemistry for the Development of New Anticancer Imaging Agents for Positron Emission Tomography, University of Wollongong, **2010**.
- (139) Maschauer, S.; Prante, O. A Series of 2-O-Trifluoromethylsulfonyl-D-Mannopyranosides as Precursors for Concomitant 18F-Labeling and Glycosylation by Click Chemistry. *Carbohydr. Res.* **2009**, 344, 753–761.
- (140) Maschauer, S.; Haubner, R.; Kuwert, T.; Prante, O. F - Glyco-RGD Peptides for PET Imaging of Integrin Expression: Efficient Radiosynthesis by Click Chemistry and Modulation of Biodistribution by Glycosylation. *Mol. Pharm.* **2014**, 11, 505–515.
- (141) Maschauer, S.; Einsiedel, J.; Haubner, R.; Hocke, C.; Ocker, M.; Hübner, H.; Kuwert, T.; Gmeiner, P.; Prante, O. Labeling and Glycosylation of Peptides Using Click Chemistry: A General Approach to [¹⁸F]-Glycopeptides as Effective Imaging Probes for Positron Emission Tomography. *Angew. Chem. Int. Ed. Engl.* **2010**, 49, 976–979.
- (142) Lang, C.; Maschauer, S.; Hu, H.; Gmeiner, P.; Prante, O. Synthesis and Evaluation of a [¹⁸F]-Labeled Diarylpyrazole Glycoconjugate for the Imaging of NTS1-Positive Tumors. *J. Med. Chem.* **2013**, 56, 9361–9365.

- (143) Fischer, C. R.; Mu, C.; Reber, J.; Mu, A.; Kra, S. D.; Ametamey, S. M.; Schibli, R. [¹⁸F]Fluoro-Deoxy-Glucose Folate: A Novel PET Radiotracer with Improved in Vivo Properties for Folate Receptor Targeting. *Bioconjug. Chem.* **2012**, *23*, 805–813.
- (144) Boutureira, O.; D’Hooge, F.; Fernández-González, M.; Bernardes, G. J. L.; Sánchez-Navarro, M.; Koeppe, J. R.; Davis, B. G. Fluoroglycoproteins: Ready Chemical Site-Selective Incorporation of Fluorosugars into Proteins. *Chem. Commun. (Camb)*. **2010**, *46*, 8142–8144.
- (145) Buskas, T.; Ingale, S.; Boons, G.-J. Glycopeptides as Versatile Tools for Glycobiology. *Glycobiol.* **2006**, *16*, 113R – 136R.
- (146) Mehta, S.; Meldal, M.; Ferro, V.; Duus, J. Ø.; Bock, K. Internally Quenched Fluorogenic, A-Helical Dimeric Peptides and Glycopeptides for the Evaluation of the Effect of Glycosylation on the Conformation of Peptides. *J. Chem. Soc. Perkin Trans. I* **1997**, 1365–1374.
- (147) Plattner, C.; Höfener, M.; Sewald, N. One-Pot Azidochlorination of Glycals. *Org. Lett.* **2011**, *13*, 545–547.
- (148) Matesic, L.; Locke, J. M.; Vine, K. L.; Ranson, M.; Bremner, J. B.; Skropeta, D. Synthesis and Hydrolytic Evaluation of Acid-Labile Imine-Linked Cytotoxic Isatin Model Systems. *Bioorg. Med. Chem.* **2011**, *19*, 1771–1778.
- (149) Matesic, L. Development of Isatin-Based Compounds for Use in Targeted Anti-Cancer Therapy, University of Wollongong, **2011**.
- (150) Valeur, E.; Bradley, M. Amide Bond Formation: Beyond the Myth of Coupling Reagents. *Chem. Soc. Rev.* **2009**, *38*, 606–631.
- (151) O’Brien, C.; Poláková, M.; Pitt, N.; Tosin, M.; Murphy, P. V. Glycosidation-Anomerisation Reactions of 6,1-Anhydroglucopyranuronic Acid and Anomerisation of Beta-D-Glucopyranosiduronic Acids Promoted by SnCl₄. *Chem. Eur. J.* **2007**, *13*, 902–909.
- (152) Farrell, M.; Zhou, J.; Murphy, P. V. Regiospecific Anomerisation of Acylated Glycosyl Azides and Benzoylated Disaccharides by Using TiCl₄. *Chem. Eur. J.* **2013**, *19*, 14836–14851.
- (153) Gyorgydeak, Z.; Thiem, J. Synthesis of Methyl (D-Glycopyranosyl Azide) Uronates. *Carbohydr. Res.* **1995**, *268*, 85–92.
- (154) Wadouachi, A.; Kovensky, J. Synthesis of Glycosides of Glucuronic, Galacturonic and Mannuronic Acids: An Overview. *Molecules* **2011**, *16*, 3933–3968.

- (155) Haubner, R.; Wester, H.-J.; Weber, W. A.; Mang, C.; Ziegler, S. I.; Goodman, S. L.; Senekowitsch-Schmidtke, R.; Kessler, H.; Schwaiger, M. Noninvasive Imaging of A v B 3 Integrin Expression Using [^{18}F]-Labeled RGD-Containing Glycopeptide and Positron Emission Tomography Advances in Brief. *Cancer Res.* **2001**, *61*, 1781–1785.
- (156) Graf von Roedern, E.; Lohof, E.; Hessler, G.; Hoffmann, M.; Kessler, H. Synthesis and Conformational Analysis of Linear and Cyclic Peptides Containing Sugar Amino Acids. *J. Am. Chem. Soc.* **1996**, *118*, 10156–10167.
- (157) Tosin, M.; Brien, C. O.; Fitzpatrick, G. M.; Mu, H.; Glass, W. K.; Murphy, P. V. Synthesis and Structural Analysis of the Anilides of Glucuronic Acid and Orientation of the Groups on the Carbohydrate Scaffolding. *J. Org. Chem.* **2005**, *70*, 4096–4106.
- (158) D’Onofrio, J.; De Champdoré, M.; De Napoli, L.; Montesarchio, D.; Di Fabio, G. Glycomimetics as Decorating Motifs for Oligonucleotides: Solid-Phase Synthesis, Stability, and Hybridization Properties of Carbopeptoid-Oligonucleotide Conjugates. *Bioconjug. Chem.* **2005**, *16*, 1299–1309.
- (159) Kocienski, P. J. *Protecting Groups*; 3rd ed.; Georg Thieme Verlag, 2003; pp. 257–269.
- (160) Bergeon, J. A.; Chan, Y.-N.; Charles, B. G.; Toth, I. Oral Absorption Enhancement of Dipeptide L-Glu-L-Trp-OH by Lipid and Glycosyl Conjugation. *Biopolymers* **2008**, *90*, 633–643.
- (161) Conrow, R. E.; Dean, W. D. Diazidomethane Explosion. *Org. Process Res. Dev.* **2008**, *12*, 1285–1286.
- (162) Jeffrey, P. D.; McCombie, S. W. Homogeneous, palladium(0)-Catalyzed Exchange Deprotection of Allylic Esters, Carbonates and Carbamates. *J. Org. Chem.* **1982**, *47*, 587–590.
- (163) Vogel, C.; Jeschke, U.; Kramer, S.; Ott, A.-J. Galacturonic Acid Derivatives, VIII. Synthesis of N-(D-Galacturonoyl) Amino Acids and Dipeptides. *Liebigs Ann.* **1997**, *1997*, 737–743.
- (164) Pilgrim, W.; Murphy, P. V. SnCl_4 - and TiCl_4 -Catalyzed Anomerization of Acylated O- and S-Glycosides: Analysis of Factors That Lead to Higher A: β Anomer Ratios and Reaction Rates. *J. Org. Chem.* **2010**, *75*, 6747–6755.
- (165) Cronin, L.; Tosin, M.; Müller-Bunz, H.; Murphy, P. V. The Synthesis of Cyclic Imidates from Amides of Glucuronic Acid and Investigation of Glycosidation Reactions. *Carbohydr. Res.* **2007**, *342*, 111–118.
- (166) Haynes, P. A. Phosphoglycosylation: A New Structural Class of Glycosylation? *Glycobiol.* **1998**, *8*, 1–5.

- (167) Neises, B.; Steglich, W. Simple Method for the Esterification of Carboxylic Acids. *Angew. Chemie Int. Ed. English* **1978**, *17*, 522–524.
- (168) Ramamoorthy, P. S.; Gervay, J. Solution Phase Synthesis of Amide-Linked N - Acetyl Neuraminic Acid, A-Amino Acid, and Sugar Amino Acid Conjugates 1. *J. Org. Chem.* **1997**, *62*, 7801–7805.
- (169) Hu, K.-Z.; Wang, H.; Huang, T.; Tang, G.; Liang, X.; He, S.; Tang, X. Synthesis and Biological Evaluation of N-(2-[¹⁸F]Fluoropropionyl)-L-Methionine for Tumor Imaging. *Nucl. Med. Biol.* **2013**, *40*, 926–932.
- (170) Nuñez, R.; Macapinlac, H. A.; Yeung, H. W. D.; Akhurst, T.; Cai, S.; Osman, I.; Gonen, M.; Riedel, E.; Scher, H. I.; Larson, S. M. Combined 18F-FDG and 11C-Methionine PET Scans in Patients with Newly Progressive Metastatic Prostate Cancer. *J. Nucl. Med.* **2002**, *43*, 46–55.
- (171) Bourdier, T.; Shepherd, R.; Berghofer, P.; Jackson, T.; Fookes, C. J. R.; Denoyer, D.; Dorow, D. S.; Greguric, I.; Gregoire, M.-C.; Hicks, R. J.; Katsifis, A. Radiosynthesis and Biological Evaluation of L- and D-S-(3-[¹⁸F]fluoropropyl)homocysteine for Tumor Imaging Using Positron Emission Tomography. *J. Med. Chem.* **2011**, *54*, 1860–1870.
- (172) Geier, E. G.; Schlessinger, A.; Fan, H.; Gable, J. E.; Irwin, J. J.; Sali, A.; Giacomini, K. M. Structure-Based Ligand Discovery for the Large-Neutral Amino Acid Transporter 1, LAT-1. *Proc. Natl. Acad. Sci. U. S. A.* **2013**, *110*, 5480–5485.
- (173) Lattuada, L.; Demattio, S.; Vincenzi, V.; Cabella, C.; Visigalli, M.; Aime, S.; Crich, S. G.; Gianolio, E. Magnetic Resonance Imaging of Tumor Cells by Targeting the Amino Acid Transport System. *Bioorg. Med. Chem. Lett.* **2006**, *16*, 4111–4114.
- (174) Rajagopalan, K. N.; DeBerardinis, R. J. Role of Glutamine in Cancer: Therapeutic and Imaging Implications. *J. Nucl. Med.* **2011**, *52*, 1005–1008.
- (175) Qu, W.; Zha, Z.; Ploessl, K.; Lieberman, B. P.; Zhu, L.; Wise, D. R.; Thompson, C. B.; Kung, H. F. Synthesis of Optically Pure 4-Fluoro-Glutamines as Potential Metabolic Imaging Agents for Tumors. *J. Am. Chem. Soc.* **2011**, *133*, 1122–1133.
- (176) Weller, G. E. R.; Wong, M. K. K.; Modzelewski, R. A.; Lu, E.; Klivanov, A. L.; Wagner, W. R.; Villanueva, F. S. Ultrasonic Imaging of Tumor Angiogenesis Using Contrast Microbubbles Targeted via the Tumor-Binding Peptide Arginine-Arginine-Leucine. *Cancer Res.* **2005**, *65*, 533–539.
- (177) Herholz, K.; Hölzer, T.; Bauer, B.; Schröder, R.; Voges, J.; Ernestus, R. I.; Mendoza, G.; Weber-Luxenburger, G.; Löttgen, J.; Thiel, A.; Wienhard, K.;

- Heiss, W. D. ^{11}C -Methionine PET for Differential Diagnosis of Low-Grade Gliomas. *Neurol.* **1998**, *50*, 1316–1322.
- (178) Bourdier, T.; Fookes, C. J. R.; Pham, T. Q.; Greguric, I.; Katsifis, A. Synthesis and Stability of S⁻-(2-[^{18}F]fluoroethyl)-L-Homocysteine for Potential Tumour Imaging. *J. Label. Compd. Radiopharm.* **2008**, *51*, 369–373.
- (179) McConathy, J.; Yu, W.; Jarkas, N.; Seo, W.; Schuster, D. M.; Goodman, M. M. Radiohalogenated Nonnatural Amino Acids as PET and SPECT Tumor Imaging Agents. *Med. Res. Rev.* **2012**, *32*, 868–905.
- (180) Wilkinson, B. L.; Bornaghi, L. F.; Poulsen, S.-A.; Houston, T. a. Synthetic Utility of Glycosyl Triazoles in Carbohydrate Chemistry. *Tetrahedron* **2006**, *62*, 8115–8125.
- (181) Chan, T. R.; Hilgraf, R.; Sharpless, K. B.; Fokin, V. V. Polytriazoles as Copper(I)-Stabilizing Ligands in Catalysis. *Org. Lett.* **2004**, *6*, 2853–2855.
- (182) Auriemma, M.; Luger, T.; Loser, K.; Amerio, P.; Tulli, A. The Antinflammatory Effect of Alpha-MSH in Skin: A Promise for New Treatment Strategies. *Antiinflamm. Antiallergy. Agents Med. Chem.* **2009**, *8*, 14–21.
- (183) Brzoska, T.; Luger, T. a; Maaser, C.; Abels, C.; Böhm, M. Alpha-Melanocyte-Stimulating Hormone and Related Tripeptides: Biochemistry, Antiinflammatory and Protective Effects in Vitro and in Vivo, and Future Perspectives for the Treatment of Immune-Mediated Inflammatory Diseases. *Endocr. Rev.* **2008**, *29*, 581–602.
- (184) Van Well, R.; Ravindranathan Kartha, K.; Field, R. Iodine Promoted Glycosylation with Glycosyl Iodides: α -Glycoside Synthesis. *J. Carbohydr. Chem.* **2005**, *24*, 463–474.
- (185) Caballero, R. B.; Mota, J. F. A New Method for the Preparation of Acylated Glycosylamines and Their Transformations into Glycosyl Isothiocyanates and N,N'-Diglycosylthioureas. *Carbohydr. Res.* **1986**, *154*, 280–288.
- (186) Conroy, T.; Jolliffe, K. A.; Payne, R. J. Efficient Use of the Dmab Protecting Group: Applications for the Solid-Phase Synthesis of N-Linked Glycopeptides. *Org. Biomol. Chem.* **2009**, *7*, 2255–2258.
- (187) Jiménez Blanco, J. L.; Ortega-Caballero, F.; Ortiz Mellet, C.; García Fernández, J. M. (Pseudo)amide-Linked Oligosaccharide Mimetics: Molecular Recognition and Supramolecular Properties. *Beilstein J. Org. Chem.* **2010**, *6*, 20.
- (188) Jiménez Blanco, J. L.; Bootello, P.; Ortiz Mellet, C.; García Fernández, J. M. The Synthesis and Structure of Linear and Dendritic Thiourea-Linked Glycooligomers. *European J. Org. Chem.* **2006**, *2006*, 183–196.

- (189) Likhoshesterov, L. M.; Novikova, O. S.; Derevitskaja, V. A.; Kochetkov, N. K. A New Simple Synthesis of Amino Sugar P-D-Glycosylamines. *Carbohydr. Res.* **1986**, *146*, C1–C5.
- (190) Monrad, R. N.; Madsen, R. Rhodium-Catalyzed Decarbonylation of Aldoses. *J. Org. Chem.* **2007**, *72*, 9782–9785.
- (191) Fleet, W. J.; Ramsden, N. G.; David, R. A Practical Synthesis of Deoxymannojirimycin and of (2S, 3R, 4R, 5R)-3,4,5-Trihydroxypipicolinic Acid from D-Glucose. *Tetrahedron* **1989**, *4*, 327–336.
- (192) Hermanson, G. . *Bioconjugation Techniques*; 3rd ed.; Academic Press - Elsevier, **2013**; pp. 666–706.
- (193) Bracher, P. J.; Snyder, P. W.; Bohall, B. R.; Whitesides, G. M. The Relative Rates of Thiol-Thioester Exchange and Hydrolysis for Alkyl and Aryl Thioalkanoates in Water. *Orig. Life Evol. Biosph.* **2011**, *41*, 399–412.
- (194) Dawson, P. E.; Muir, T. W.; Clark-Lewis, I.; Kent, S. B. Synthesis of Proteins by Native Chemical Ligation. *Science* **1994**, *266*, 776–779.
- (195) Beekman, N. J. C. M.; Schaaper, W. M. M.; Langeveld, J. P. M.; Boshuizen, R. S.; Meloen, R. H. The Nature of the Bond between Peptide and Carrier Molecule Determines the Immunogenicity of the Construct. *J. Pept. Res.* **2001**, *58*, 237–245.
- (196) Nishimura, S.; Murakami, Y.; Yorimitsu, H. Novel [15O]-Labeled Monosaccharide and Method Thereof. PCT/JP2005/006547, 2004.
- (197) Zhu, J.; Hu, X.; Dizin, E.; Pei, D. Catalytic Mechanism of S-Ribosylhomocysteinase (LuxS): Direct Observation of Ketone Intermediates by ¹³C NMR Spectroscopy. *J. Am. Chem. Soc.* **2003**, *125*, 13379–13381.
- (198) McDonnell, C.; Cronin, L.; Brien, J. L. O.; Murphy, P. V. A General Synthesis of Iminosugars. *J. Org. Chem.* **2004**, *69*, 3565–3568.
- (199) Goswami, L. N.; Houston, Z. H.; Sarma, S. J.; Jalisatgi, S. S.; Hawthorne, M. F. Efficient Synthesis of Diverse Heterobifunctionalized Clickable Oligo(ethylene Glycol) Linkers: Potential Applications in Bioconjugation and Targeted Drug Delivery. *Org. Biomol. Chem.* **2013**, *11*, 1116–1126.
- (200) Crich, D. Mechanism of a Chemical Glycosylation Reaction. *Acc. Chem. Res.* **2010**, *43*, 1144–1153.
- (201) Schmidt, R. R.; Michel, J. Facile Synthesis of A- and B-O-Glycosyl Imidates; Preparation of Glycosides and Disaccharides. *Angew. Chemie Int. Ed. English* **1980**, *19*, 731–732.

- (202) Pellissier, H. Use of O-Glycosylation in Total Synthesis. *Tetrahedron* **2005**, *61*, 2947–2993.
- (203) Kelleman, A.; Mattern, R.-H.; Pierschbacher, M. D.; Goodman, M. Incorporation of Thioether Building Blocks into an $\alpha_v\beta_3$ -Specific RGD Peptide: Synthesis and Biological Activity. *Biopolymers* **2003**, *71*, 686–695.
- (204) Bousquet, E.; Spadaro, A.; Pappalardo, M. S.; Bernardini, R.; Romeo, R.; Panza, L.; Ronsisvalle, G. Synthesis and Immunostimulating Activity of A Thioglycolipopeptide Glycomimetic As A Potential Anticancer Vaccine Derived From Tn Antigen. *J. Carbohydr. Chem.* **2000**, *19*, 527–541.
- (205) Ludek, O. R.; Gu, W.; Gildersleeve, J. C. Activation of Glycosyl Trichloroacetimidates with Perchloric Acid on Silica ($\text{HClO}_4\text{-SiO}_2$) Provides Enhanced α -Selectivity. *Carbohydr. Res.* **2010**, *345*, 2074–2078.
- (206) Ranade, S. C.; Demchenko, A. V. Mechanism of Chemical Glycosylation: Focus on the Mode of Activation and Departure of Anomeric Leaving Groups. *J. Carbohydr. Chem.* **2013**, *32*, 1–43.
- (207) Almant, M.; Moreau, V.; Kovensky, J.; Bouckaert, J.; Gouin, S. G. Clustering of Escherichia Coli Type-1 Fimbrial Adhesins by Using Multimeric Heptyl α -D-Mannoside Probes with a Carbohydrate Core. *Chem. – A Eur. J.* **2011**, *17*, 10029–10038.
- (208) Hoyle, C. E.; Bowman, C. N. Thiol-Ene Click Chemistry. *Angew. Chem. Int. Ed. Engl.* **2010**, *49*, 1540–1573.
- (209) Chen, Y.-X.; Triola, G.; Waldmann, H. Bioorthogonal Chemistry for Site-Specific Labeling and Surface Immobilization of Proteins. *Acc. Chem. Res.* **2011**, *44*, 762–773.
- (210) Dondoni, A.; Marra, A. Recent Applications of Thiol-Ene Coupling as a Click Process for Glycoconjugation. *Chem. Soc. Rev.* **2012**, *41*, 573–586.
- (211) Richter, M.; Chakrabarti, A.; Ruttekolk, I. R.; Wiesner, B.; Beyermann, M.; Brock, R.; Rademann, J. Multivalent Design of Apoptosis-Inducing Bid-BH₃ Peptide-Oligosaccharides Boosts the Intracellular Activity at Identical Overall Peptide Concentrations. *Chem. - A Eur. J.* **2012**, *18*, 16708–16715.
- (212) *CRC Handbook of Chemistry and Physics*; Haynes, W. M., Ed.; 94th Editi.; CRC Press, Taylor and Francis, **2013**.
- (213) Glushchenko, A. V; Jacobsen, D. W. Molecular Targeting of Proteins by -Homocysteine: Mechanistic Implications for Vascular Disease. *Antioxid Redox Signal* **2010**, *9*, 1883–1898.

- (214) Tajc, S. G.; Tolbert, B. S.; Basavappa, R.; Miller, B. L. Direct Determination of Thiol pKa by Isothermal Titration Microcalorimetry. *J. Am. Chem. Soc.* **2004**, *126*, 10508–10509.
- (215) Gruner, S. A.; Kéri, G.; Schwab, R.; Venetianer, A.; Kessler, H. Sugar Amino Acid Containing Somatostatin Analogues That Induce Apoptosis in Both Drug-Sensitive and Multidrug-Resistant Tumor Cells. *Org. Lett.* **2001**, *3*, 3723–3725.
- (216) Lohof, E.; Planker, E.; Mang, C.; Burkhart, F.; Dechantsreiter, M.; Haubner, R.; Wester, H.; Schwaiger, M.; Hölzemann, G.; Goodman, S.; Kessler, H. Carbohydrate Derivatives for Use in Drug Design: Cyclic Alpha(v)-Selective RGD Peptides. *Angew. Chem. Int. Ed. Engl.* **2000**, *39*, 2761–2764.
- (217) Von Roedern, E. G.; Kessler, H. A Sugar Amino Acid as a Novel Peptidomimetic. *Angew. Chemie Int. Ed. English* **1994**, *33*, 687–689.
- (218) Gruner, S. A. W.; Locardi, E.; Lohof, E.; Kessler, H. Carbohydrate-Based Mimetics in Drug Design: Sugar Amino Acids and Carbohydrate Scaffolds. *Chem. Rev.* **2002**, *102*, 491–514.
- (219) Sicherl, F.; Wittmann, V. Orthogonally Protected Sugar Diamino Acids as Building Blocks for Linear and Branched Oligosaccharide Mimetics. *Angew. Chem. Int. Ed. Engl.* **2005**, *44*, 2096–2099.
- (220) Ying, L.; Gervay-Hague, J. Synthesis of N-(fluoren-9-Ylmethoxycarbonyl)glycopyranosylamine Uronic Acids. *Carbohydr. Res.* **2004**, *339*, 367–375.
- (221) Ying, L.; Gervay-Hague, J. General Methods for the Synthesis of Glycopyranosyluronic Acid Azides. *Carbohydr. Res.* **2003**, *338*, 835–841.
- (222) Bernardes, G. J. L.; Grayson, E. J.; Thompson, S.; Chalker, J. M.; Errey, J. C.; El Oualid, F.; Claridge, T. D. W.; Davis, B. G. From Disulfide- to Thioether-Linked Glycoproteins. *Angew. Chemie Int. Ed.* **2008**, *47*, 2244–2247.
- (223) Thomas, G. B.; Rader, L. H.; Park, J.; Abezgauz, L.; Danino, D.; DeShong, P.; English, D. S. Carbohydrate Modified Catanionic Vesicles: Probing Multivalent Binding at the Bilayer Interface. *J. Am. Chem. Soc.* **2009**, *131*, 5471–5477.
- (224) Zemplén, G.; Kunz, A. Über Die Natriumverbindungen Der Glucose Und Die Verseifung Der Acylierten Zucker. *Berichte der Dtsch. Chem. Gesellschaft (A B Ser.)* **1923**, *56*, 1705–1710.
- (225) Chong, P. Y.; Petillo, P. A. Synthesis of Allophanate-Derived Branched Glycoforms from Alcohols and P-Nitrophenyl Carbamates. *Org. Lett.* **2000**, *2*, 2113–2116.

- (226) Bera, S.; Linhardt, R. J. Design and Synthesis of Unnatural Heparosan and Chondroitin Building Blocks. *J. Org. Chem.* **2011**, *76*, 3181–3193.
- (227) Van den Bos, L. J.; Codée, J. D. C.; van der Toorn, J. C.; Boltje, T. J.; van Boom, J. H.; Overkleeft, H. S.; van der Marel, G. a. Thioglycuronides: Synthesis and Application in the Assembly of Acidic Oligosaccharides. *Org. Lett.* **2004**, *6*, 2165–2168.
- (228) Nooy, A. E. J. de; Besemer, A. C.; Bekkum, H. van. On the Use of Stable Organic Nitroxyl Radicals for the Oxidation of Primary and Secondary Alcohols. *Synthesis (Stuttg)*. **1996**, *1996*, 1153–1176.
- (229) Evier, E. I.; Nooy, A. E. J. De; Besemer, A. C.; Bekkum, H. Van. Highly Selective Nitroxyl Radical-Mediated Oxidation of Primary Alcohol Groups in Water-Soluble Glucans. *Carbohydr. Res.* **1995**, *269*, 89–98.
- (230) De Nooy, A. E. J.; Besemer, A. C.; van Bekkum, H. Selective Oxidation of Primary Alcohols Mediated by Nitroxyl Radical in Aqueous Solution. Kinetics and Mechanism. *Tetrahedron* **1995**, *51*, 8023–8032.
- (231) Ma, Z.; Bobbitt, J. M. Organic Oxoammonium Salts. 3. A New Convenient Method for the Oxidation of Alcohols to Aldehydes and Ketones. *J. Org. Chem.* **1991**, *56*, 6110–6114.
- (232) Semmelhack, M. F.; Schmid, C. R.; Carte, D. A. Mechanism of the Oxidation of Alcohols by 2,2,6,6-Tetramethylpiperidine Nitrosonium Cation. *Tetrahedron Lett.* **1986**, *27*, 1119–1122.
- (233) Van Den Bos, L. J.; Codée, J. D. C.; van der Toorn, J. C.; Boltje, T. J.; Van Boom, J. H.; Overkleeft, H. S.; Van Der Marel, G. A. Thioglycuronides: Synthesis and Application in the Assembly of Acidic Oligosaccharides. *Org. Lett.* **2004**, *6*, 2165–2168.
- (234) Tojo, G.; Fernandez, M. . TEMPO-Mediated Oxidations. In *Oxidation of Primary Alcohols to Carboxylic Acids - A Guide to Current Common Practice*; 2007; Springer; pp. 79–103.
- (235) Sims, J. W.; Schmidt, E. W. A Thioesterase-like Role for Fungal PKS-NRPS Hybrid Reductive Domains. *J. Am. Chem. Soc.* **2008**, *130*, 11149–11155.
- (236) Aspin, S.; Goutierre, A.; Larini, P.; Jazzar, R.; Baudoin, O. Synthesis of Aromatic Alpha-Aminoesters: Palladium-Catalyzed Long-Range Arylation of Primary C-H Bonds. *Angew. Chem. Int. Ed. Engl.* **2012**, *51*, 10808–10811.
- (237) Tosin, M.; Murphy, P. V. Synthesis of Structurally Defined Scaffolds for Bivalent Ligand Display Based on Glucuronic Acid Anilides. The Degree of Tertiary Amide Isomerism and Folding Depends on the Configuration of a Glycosyl Azide. *J. Org. Chem.* **2005**, *70*, 4107–4117.

- (238) Tosin, M.; Murphy, P. V. Synthesis of R-Glucuronic Acid and Amide Derivatives in the Presence of a Participating 2-Acyl Protecting Group. *Org. Lett.* **2002**, *4*, 3675–3678.
- (239) Bosco, M.; Rat, S.; Kovensky, J.; Wadouachi, A. Fast Synthesis of Uronamides by Non-Catalyzed Opening of Glucopyranurono-6,1-Lactone with Amines, Amino Acids, and Aminosugars. *Tetrahedron Lett.* **2010**, *51*, 2553–2556.
- (240) Nwe, K.; Brechbiel, M. W. Growing Applications of “Click Chemistry” for Bioconjugation in Contemporary Biomedical Research. *Cancer Biother. Radiopharm.* **2009**, *24*, 289–302.
- (241) Nicolaou, K. C.; Estrada, A. A.; Zak, M.; Lee, S. H.; Safina, B. S. A Mild and Selective Method for the Hydrolysis of Esters with Trimethyltin Hydroxide. *Angew. Chem. Int. Ed. Engl.* **2005**, *44*, 1378–1382.
- (242) Akiyama, S.; Olden, K.; Yamada, K. Fibronectin and Integrins in Invasion and Metastasis. *Cancer Metastasis Rev.* **1995**, *14*, 173–189.
- (243) Chigaev, A.; Wu, Y.; Williams, D. B.; Smagley, Y.; Sklar, L. A. Discovery of Very Late Antigen-4 (VLA-4, $\alpha 4 \beta 1$ Integrin) Allosteric Antagonists. *J. Biol. Chem.* **2011**, *286*, 5455–5463.
- (244) Blokhina, O.; Virolainen, E.; Fagerstedt, K. V. Antioxidants, Oxidative Damage and Oxygen Deprivation Stress: A Review. *Ann. Bot.* **2003**, *91*, 179–194.
- (245) Yin, J.; Zarkowsky, D. S.; Thomas, D. W.; Zhao, M. M.; Huffman, M. a. Direct and Convenient Conversion of Alcohols to Fluorides. *Org. Lett.* **2004**, *6*, 1465–1468.
- (246) Dann, S. G.; Selvaraj, A.; Thomas, G. mTOR Complex1-S6K1 Signaling: At the Crossroads of Obesity, Diabetes and Cancer. *Trends Mol. Med.* **2007**, *13*, 252–259.
- (247) Fuchs, B. C.; Bode, B. P. Amino Acid Transporters ASCT2 and LAT1 in Cancer: Partners in Crime? *Semin. Cancer Biol.* **2005**, *15*, 254–266.
- (248) Geier, E. G.; Schlessinger, A.; Fan, H.; Gable, J. E.; Irwin, J. J.; Sali, A.; Giacomini, K. M. Structure-Based Ligand Discovery for the Large-Neutral Amino Acid Transporter 1, LAT-1. *Proc. Natl. Acad. Sci. U. S. A.* **2013**, *110*, 5480–5485.
- (249) Fry, E. M. Tri-O-Acetyl-B-D-Glucopyranurono-6,1-Lactone. *J. Am. Chem. Soc.* **1955**, *77*, 3915–3916.
- (250) Cramer, F.; Otterbach, H.; Springmann, H. Eine Synthese Der 6-Desoxy-6-Amino-Glucose. *Chem. Ber.* **1959**, *92*, 384–391.

- (251) Zeggaf, C.; Poncet, J.; Jouin, P.; Dufour, M.-N.; Castro, B. Isopropenyl Chlorocarbonate (IPCC)1 in Amino Acid and Peptide Chemistry: Esterification of N-Protected Amino Acids; Application to the Synthesis of the Depsipeptide Valinomycin. *Tetrahedron* **1989**, *45*, 5039–5050.
- (252) Biron, E.; Voyer, N. Synthesis of Cationic Porphyrin Modified Amino Acids. *Chem. Commun. (Camb)*. **2005**, 4652–4654.
- (253) Moutevelis-Minakakis, P.; Sinanoglou, C.; Loukas, V.; Kokotos, G. Synthesis of Non-Natural Amino Acids Based on the Ruthenium-Catalysed Oxidation of a Phenyl Group to Carboxylic Acid. *Synthesis (Stuttg)*. **2005**, *2005*, 933–938.
- (254) Cagnoni, A. J.; Varela, O.; Gouin, S. G.; Kovensky, J.; Uhrig, M. L. Synthesis of Multivalent Glycoclusters from 1-Thio-B-D-Galactose and Their Inhibitory Activity against the B-Galactosidase from E. Coli. *J. Org. Chem.* **2011**, *76*, 3064–3077.
- (255) Malavašič, Č.; Grošelj, U.; Golobič, A.; Bezenšek, J.; Stanovnik, B.; Stare, K.; Wagger, J.; Svete, J. Synthesis and Structure of Novel (S)-1,6-Dialkylpiperazine-2,5-Diones and (3S,6S)-1,3,6-Trialkylpiperazine-2,5-Diones. *Tetrahedron: Asymmetry* **2011**, *22*, 629–640.